

Extracellular matrix associated proteins and processing enzymes as urinary biomarkers of Chronic Kidney Disease



By

Dr Michelle da Silva Lodge

MBChB, MMedSci

Academic Nephrology Unit, The Medical School

University of Sheffield

Thesis submitted for the degree of Doctor of Philosophy (PhD) in Nephrology

April 2015

Volume 1

**This thesis is dedicated to my mum, Jaci Nascimento da Silva, and my family
for their love, support and constant encouragement.**

“Omnia possum in eo qui me confortat”

Philippians 4:13

Acknowledgements

I would like to acknowledge the contribution of the following individuals and organisations to the completion of this PhD thesis:

Professor Timothy S Johnson: For teaching me all fundamental laboratorial skills to complete this project. For his guidance, encouragement and support at every step of this research, and for his invaluable supervision and assistance with the preparation of manuscripts and constructing this thesis.

Professor A Meguid El Nahas: For giving me the opportunity to carry out this study. For his inestimable supervision throughout this project and contribution to the discussion of this thesis.

Dr John L Haylor: For his surgical expertise in performing the UNx STZ model of Diabetic Nephropathy

Mr. Badri Shrestha: For his surgical expertise in performing the Fisher to Lewis model of Chronic Allograft Nephropathy

Dr. Linghong Huang: For her general help and for teaching me the basic techniques of confocal microscopy and the Masson's Trichrome staining.

Mrs Zoe Tazzyman: For her technical assistance in the first year of my PhD.

Dr Bisher Kawar, Dr Sarah Jenkins and Dr Alshami, Sheffield Kidney Institute nurses and study participants: For allowing me to attend their outpatients' clinics and helping me to collect all biological samples.

Pfizer Pharmaceuticals: For their invaluable financial support and funding the purchase of laboratory consumables and equipments, without which the completion of this research would not be possible.

Abstract

Background: Chronic Kidney Disease (CKD) is often progressive leading to End Stage Renal Disease (ESRD). Early detection of progressive CKD would almost certainly improve long term outcome. Current kidney function tests have serious limitations as they only can detect dysfunction after significant damage has occurred, provide limited help with diagnosis and are unhelpful in assessing early response to therapy or long term prognosis. Therefore there is a requirement for identification of early and reliable non invasive biomarkers of kidney disease and its progression. Regardless of the underlying disease, fibrosis drives movement to ESRD. Fibrosis is characterised by excessive accumulation of Extracellular Matrix (ECM). This thesis tests the hypothesis that mediators of the kidney fibrotic process are present in urine and would make good biomarkers of CKD and its progression.

Aims: To assess urine samples from three animal models of kidney fibrosis (5/6th Subtotalnephrectomy (SNx), Diabetic Nephropathy (DN) and Chronic Allograft Nephropathy (CAN) as well as 325 human urine samples (292 CKD and 33 controls) to determine if urinary ECM molecules, Transglutaminase 2 (TG2), ϵ (γ -glutamyl) lysine, Hydroxyproline, Metalloproteinases 1, 2 and 9, TIMPs 1, 2 and 3, TIMP-1/MMP-1 complex, PAI-1 and MMP activity have potential to act as an early biomarker of kidney scarring and if any of them could predict the rate of progression better than Albuminuria.

Experimental methods: Cation exchange chromatography was used to evaluate urine levels of ϵ (γ -glutamyl) lysine and Hydroxyproline. An in-house developed sandwich ELISA was used to analyse urine and blood levels of TG2 and commercially available immunoassays were used for determination of urine concentration of MMPs 1, 2 and 9, TIMPs 1, 2 and 3, TIMP-1/MMP-1 complex and PAI-1. MMP activity was measured by the EnzCheck Collagenase assay. One way ANOVA with Bonferroni correction was applied to estimate differences between groups. Area under the curve for Receiver Operating Characteristic (ROC) analysis was used to determine prediction accuracy. $p < 0.05$ was considered statistically significant.

Results: TG2 and ϵ (γ -glutamyl) lysine excretion were significantly increased as renal scarring developed in SNx and CAN models. However, in DN, increased levels were only observed as a 24 hour excretion at 8 months of study only due to the increased proteinuric state. TG inhibitor treated animals had a reduction in the measured levels of both TG2 and of ϵ (γ -glutamyl) lysine in the SNx study. Urine Hydroxyproline had increased levels as renal disease scarring progressed. MMP-1 was significantly increased in SNx and DN animals, with MMP-9 excretion undetectable in all control samples. Amongst the TIMPs, TIMP-1 gave the most promising response in the early stages of SNx and DN with a 6.4 fold increase at 7 days post SNx, $p=0.0025$ and 25 fold increase at 4 months post STZ injection, $p=0.0006$. Whereas in CAN, the TIMP2: CR ratio was double that in F-L Allografts than in L-L Isografts ($p=0.0095$) as early as 8 weeks post-transplant and remained elevated up to 33 weeks. Urine PAI-1 excretion was within the lower limits of detection and therefore was not used in human samples. In the human study, ROC curve analysis demonstrated that the TG2/CR ratio (86.4%) and TIMP1/CR ratio (75.7%) are better predictors of patients with progressive CKD than ACR (73.5%) indicating their potential as non-invasive biomarkers of progressive kidney scarring. The ROC curve analysis of ϵ (γ -glutamyl) lysine / CR ratio (73.3%) and TIMP2/ CR ratio (71.2%) presented similar levels of accuracy of prediction as ACR, whereas all other candidates were inferior to ACR. Measurement of MMP-1 activity had a remarkable predictive value in detecting rapid progressive patients, as very low levels were found in this subgroup of patients. A combo ROC

curve analysis using TG2CR, XLCR, TIMP1CR and ACR as prognostic tools of CKD progression generated a remarkable 87.7% risk prediction.

Conclusions: The data presented in this thesis demonstrates a potential benefit of using ECM molecules (especially TG2, TIMP-1 and ϵ (γ -glutamyl) lysine) detected in urine as biomarkers of CKD progression. Using a combined biomarker panel containing ACR, TG2/CR, TIMP/CR and XL/CR ratios may allow the earlier and more reliable detection of patients with more aggressive CKD that requires stronger treatment strategies to give better long term outcomes and facilitate shorter clinical trials in CKD.

Presentations from this study

Published papers:

1. **Inhibition of Thrombin-Activated Fibrinolysis Inhibitor Increases Survival in Experimental Kidney Fibrosis.** JM Atkinson, N Pullen, M Da Silva Lodge, L Williams, TS Johnson. Journal of the American Society of Nephrology (JASN), 2014 Nov 19. pii: ASN.2014030303
2. **Upregulation of transglutaminase and ϵ (γ -glutamyl)-lysine in the Fisher-Lewis rat model of chronic allograft nephropathy.** B Shrestha, I Butt, M Da Silva, A Sanchez-Lara, B Wagner, A Raftery, TS Johnson, J Haylor. BioMed Research International, 2014; 2014:651608. doi: 10.1155/2014/651608

Poster presentations:

1. **Urinary Transglutaminase 2 as a potential biomarker of chronic kidney disease detection and progression.** M da Silva Lodge, M El Nahas, TS Johnson. Spring Meeting for Clinician Scientists in Training, Royal College of Physicians, London, 2013.
2. **KIM-1 and MCP-1 do not predict CKD progression.** Z Abedin, B Kavar, M El Nahas, M da Silva Lodge, TS Johnson. Joint British Transplantation Society and Renal Association Congress, Bournemouth, 2013.
3. **Tissue Inhibitor of Matrix Metalloproteinase-1 as a potential biomarker in human Diabetic Nephropathy.** E Foteinopoulou, N Altemtam, N, M da Silva Lodge, TS Johnson. British Renal Society / Renal Association conference, Birmingham, 2011.
4. **Urinary Transglutaminase 2 as a potential biomarker of chronic kidney disease detection and progression.** M da Silva Lodge, M El Nahas, TS Johnson. Gordon Conference, North Carolina, USA, 2010.
5. **Urinary ϵ - γ (glutamyl) lysine: A novel biomarker of Chronic Kidney Disease.** M da Silva Lodge, M El Nahas, TS Johnson. British Renal Society / Renal Association Conference, Manchester, 2010.
6. **Increased Expression of Transglutaminase type 2 in the Fisher-to-Lewis Rat Model of Chronic Allograft Nephropathy.** B. M. Shrestha, M da Silva Lodge, TS Johnson, J L Haylor. British Renal Association Conference, Liverpool, 2009.

Oral Presentations:

1. **Urinary Hydroxyproline as a potential early biomarker of Diabetic Nephropathy.** M da Silva Lodge, M El Nahas, TS Johnson. Department of Infection and Immunity research day, Octagon Centre, University of Sheffield, Sheffield, 2011.
2. **Urinary ϵ - γ (glutamyl) lysine: A novel biomarker of Chronic Kidney Disease.** M da Silva Lodge, M El Nahas, TS Johnson. The Medical School research meeting, University of Sheffield, Sheffield, 2010.
3. **Can ϵ - γ (glutamyl) lysine be used as a non-invasive biomarker of Chronic Kidney Disease?** M da Silva Lodge, M El Nahas, TS Johnson. Department of Infection and Immunity research day, University of Sheffield, Sheffield, 2009.

ABBREVIATIONS

AAA	Amino Acid Analyser
ACE	Angiotensin converting enzyme
ADAM	A Disintegrin and metalloproteinase
ADAMTS	A Disintegrin and metalloproteinase with thrombospondin domains
ADPKD	Adult polycystic kidney disease
Alb	Albumin
α -SMA	alpha-smooth muscle actin
ANOVA	Analysis of variance
ASCVD	Atherosclerotic Cardiovascular Disease
ATP	Adenosine triphosphate
BCA	Bicinchoninic acid assay
bFGF	basic fibroblast growth factor
β -ME	beta mercaptoethanol
BMI	Body mass index
BP	Blood pressure
BSA	Bovine serum albumin
BUN	Blood urea nitrogen
CAD	Coronary Artery Disease
CAM	Cell adhesion molecules
CAN	Chronic allograft nephropathy
CGN	Chronic Glomerulonephritis
CIN	Chronic interstitial nephritis
CHD	Coronary Heart Disease
CHO	Aldehyde
CKD	Chronic kidney failure
Col	Collagen
Cr	creatinine
CrCl	Creatinine clearance

CTGF	Connective tissue growth factor
CVD	Cardiovascular Disease
DKD	Diabetic Kidney Disease
DM I	Diabetes Mellitus Type I
DM II	Diabetes Mellitus Type II
DMEM	Dulbecco's modified eagle's medium
DMSO	Dimethyl sulfoxide
DN	Diabetic Nephropathy
DNA	Deoxyribonucleic acid
DOQI	Dialysis Outcome Quality Initiative
DTT	Dithiothreitol
DW	Distilled water
ECL	Enhanced chemiluminescent
ECM	Extra cellular matrix
EDTA	Ethylene Diamine Tetra acetic Acid
EGF	Epidermal growth factor
eGFR	estimated Glomerular filtration rate
EM	electron microscopy
ESKD	End-stage kidney disease
ERA-EDTA	European Renal Association – European Dialysis and Transplant Association
FGF	Fibroblast growth factor
FSGS	Focal Segmental glomerulosclerosis
GAG	Glycosaminoglycan
GBM	Glomerular basement membrane
GFR	Glomerular filtration rate
GN	Glomerulonephritis
GS	Glomerulosclerosis
GTP	Guanidine triphosphate
HBP	High Blood Pressure

HD	Hemodialysis
HDL	High Density Lipoprotein
H&E	Hematoxylin and eosin
HIV	Human Immunodeficiency virus
HMW	High molecular weight
HPLC	High performance liquid chromatography
HRP	Horse-radish peroxidase
HTN	Hypertension
HYPRO	Hydroxyproline
IAP	Inhibitor of apoptosis proteins
IGF-I	Insulin-like growth factor-I
IGF-II	Insulin-like growth factor-II
IF	Interstitial fibrosis
IFN- γ	Interferon gamma
IL6	Interleukin 6
IN	Interstitial Nephritis
LAP	Leucine amino peptidase
LDL	Low Density Lipoprotein
LMW	Low Molecular Weight
MCs	Mesangial cells
Min	Minute (s)
MMP-1	Matrix metalloproteinases-1
MMP-2	Matrix metalloproteinases-2
MMP-3	Matrix metalloproteinases-3
MMP-9	Matrix metalloproteinases-9
mRNA	Messenger ribonucleic acid
MW	Molecular weight
MT	Masson's Trichrome
N	Number of subjects in sample or population
NKF	National Kidney Foundation

NO	Nitric oxide
NYN	Ninhydrin
NS	Non-significant
NSAID	Non-steroidal anti-inflammatory drug
OD	Optical density
PAI-1	Plasminogen activator inhibitor 1
PBS	Phosphate buffered saline
PBST	Phosphate buffered saline with 0.1% Tween 20
PCR	Polymerase chain reaction
PDGF	Platelet-derived growth factor
PLT	Platelets
Pmp	Per million population
PN	Pyelonephritis
PTH	Parathyroid hormone
RBCs	Red blood cells
RRT	Renal replacement therapy
SD	Standard deviation
SDS	Sodium dodecyl sulphate
SDS PAGE	Sodium dodecyl sulphate polyacrylamide gel electrophoresis
SEM	Standard error of mean
SLE	Systemic Lupus Erythematosus
SNc	Sham operated rats (controls of Subtotalnephrectomy)
SNx	Subtotalnephrectomy
STZ	Streptozotocin
TA	Tubular atrophy
TBS	Tris buffered saline
TBST	Tris buffered saline with 0.1% Tween 20
TEMED	Tetramethylethylenediamine
TG2	Tissue transglutaminase 2
TGF-β1	Transforming growth factor – beta 1

TIF	Tubulointerstitial fibrosis
TIMP-1	Tissue inhibitor of metalloproteinases 1
TIMP-2	Tissue inhibitor of metalloproteinases 2
TIMP-3	Tissue inhibitor of metalloproteinases 3
TIMP-4	Tissue inhibitor of metalloproteinases 4
TMB	Tetramethylbenzidine
TNF- α	Tumour necrosis factor - alpha
WBCs	White blood cells
WHO	World Health Organization
XL	Crosslink (ϵ (γ - glutamyl) lysine di peptide)

TABLE OF CONTENTS

Volume 1	Page
Acknowledgements	I
Abstract	II
Presentations from this study	IV
Abbreviations	V
Table of contents	X
List of figures	XVII
List of tables	XXIII
Chapter 1 Introduction	1
1.1. Chronic Kidney Disease	2
1.2. Causes of CKD	4
1.3. Epidemiology of CKD	8
1.4. Epidemiology of ESRD	9
1.5. Progression of CKD	12
1.5.1 Risk Factors for progressive CKD	12
1.6. Pathology of Kidney Fibrosis	17
1.6.1. Glomerulosclerosis	17
1.6.2. Tubulointerstitial Fibrosis	17
1.7. Mechanisms of Kidney Fibrosis	18
1.8. Models of Experimental renal scarring	21
1.8.1. 5/6 th Subtotal Nephrectomy	21
1.8.2. Diabetic Nephropathy	22
1.8.3. Chronic Allograft Nephropathy	23
1.9. Extracellular Matrix turnover	24
1.9.1. ECM deposition	24
1.9.2. ECM breakdown	28
1.10. ECM related molecules involved in the scarring process	28
1.10.1. Transglutaminase 2	28
1.10.2. Collagens	42
1.10.3. Matrix Metalloproteinases system	48
1.10.3.1. MMPs	48
1.10.4. Plasminogen-Plasmin system	56
1.11. Classical biomarkers of CKD progression	57
1.11.1. GFR	57
1.11.2. Proteinuria	58
1.12. Experimental biomarkers of kidney disease	60
1.12.1. Cystatin C	61
1.12.2. β -Trace protein	62
1.12.3. Neutrophil gelatinase-associated lipocalin (NGAL)	622
1.12.4. Kidney Injury Molecule-1 (KIM-1)	633
1.12.5. Urinary Nephryn, Podoxin and Podocalyxin	644
	X

1.12.6. Asymmetric dimethylarginine (ADMA)	644
1.12.7. Interleukin 18	655
1.12.8. TGF β 1	655
1.12.9. FGF-23 and Klotho	667
1.12.10. Oxidative stress molecules	688
1.12.11. Thesis rationale and hypothesis	69
Chapter 2 Aims	711
Chapter 3 Materials and Methods	733
3.1. <i>In Vivo</i> Experimentation	744
3.1.1. Experimental Animals	744
3.1.2. The 5/6 th Subtotal Nephrectomy model of renal scarring	744
3.1.3. The UNx STZ model of Diabetic Nephropathy	766
3.1.4. The Fisher to Lewis model of Chronic Allograft Nephropathy	777
3.1.5. Clinical Chemistry	788
3.1.6. Histopathology	80
3.2. Human prospective study	811
3.2.1. Study design	811
3.2.2. Ethics and Research governance	833
3.2.3. Patients recruitment	844
3.2.4. Protocol for Urine sample collection	855
3.2.5. Protocol for Blood collection	855
3.2.6. Bio-repository database	866
3.3. Determination of Protein concentration	90
3.3.1. Assays for estimation of protein concentration	90
3.4. Immunoassays	922
3.4.1. Rationale and principals of the Immunoassays	922
3.4.2. Sample preparation	933
3.4.3. Urine TG2 Enzyme-linked immunosorbent assay	933
3.4.4. Rat Immunoassays	977
3.4.5. Human Immunoassays	1055
3.5. Amino acid analysis by cation exchange chromatography	1144
3.5.1. Precipitation Methods	1144
3.5.2. Proteolytic digestion for ϵ (γ -glutamyl) lysine measurement	1144
3.5.3. Proteolytic hydrolysis for Hydroxyproline measurement	1155
3.5.4. Principles of the Biochrom 30 Amino Acid Analyser physiological system procedure	1166
3.5.5. Calibration of the Amino Acid Analyser	12020
3.5.6. Calculation of the results after calibration	1255
3.5.7. Quantitative estimation of amino acids and di amino acids	1266
3.6. <i>In vitro</i> crosslinking of TG2 substrates	1277
3.7. ECM proteolytic activity	1288
3.7.1. Rationale for using the ECM proteolytic activity assay	1288
3.7.2. Principal of EnzChek [®] Gelatinase/Collagenase Assay	1299
3.7.3. Materials	13030
3.7.4. Reagents preparation	13030

3.7.5. Assay procedure	13030
3.16. Statistical Analysis	1311
Chapter 4 The urine excretion of Transglutaminase type 2 and ϵ (γ glutamyl) lysine as biomarkers of renal fibrosis in animal models of Chronic Kidney Disease	1333
4.1 Introduction	1344
4.2. Transglutaminase type 2 measurement in urine from 5/6 th subtotal nephrectomised rats	1366
4.2.1. Experimental animals	1366
4.2.2. Measurement of Urine Transglutaminase type 2 using enzyme-linked immunosorbent assay (ELISA)	1377
4.2.3. 24 hour urine excretion of TG2 in the SNx Model	1388
4.2.4. Transglutaminase type 2/creatinine ratio in the SNx Model	1388
4.3. Transglutaminase type 2 measurement in urine from the streptozotocin induced model of diabetic nephropathy	14040
4.3.1. Experimental animals	14040
4.3.2. Urine Transglutaminase type 2 concentration in the UNx STZ model of DN	14040
4.3.3. 24 h urine excretion of TG2 in the UNx STZ model of DN	14040
4.3.4. Transglutaminase type 2/creatinine ratio in the UNx STZ model of DN	1422
4.4. Transglutaminase type 2 measurement in urine from the Fisher to Lewis transplant model of Chronic Allograft Nephropathy	1422
4.4.1. Experimental animals	1422
4.4.2. Urine Transglutaminase type 2 concentration in the Fisher to Lewis transplant model of CAN	1433
4.4.3. 24 h urine excretion of TG2 in the Fisher to Lewis transplant model of CAN	1444
4.4.4. Transglutaminase type 2/creatinine ratio in the Fisher to Lewis transplant model of CAN	1444
4.5. Correlation between urine Transglutaminase type 2 and clinical markers of renal function and damage	1466
4.5.1. 24h proteinuria	1466
4.5.2. Creatinine clearance	1466
4.5.3. Renal scarring levels	1466
4.6. ϵ (γ -glutamyl) lysine analysis in urine by cation exchange chromatography	1499
4.6.1. Optimisation of chromatography	1499
4.6.2. Validation of ϵ (γ Glutamyl) Lysine measurement in urines	15252
4.6.3. Determination of ϵ (γ glutamyl) lysine detection, sensitivity and range on a Biochrom 30 amino acid analyser	1533
4.7. ϵ (γ glutamyl) lysine measurement in urine from 5/6 th subtotal nephrectomised rats	1555
4.7.1. ϵ (γ glutamyl) lysine levels per mg of urine protein	1555
4.7.2. 24 hour urine excretion of ϵ (γ -glutamyl) lysine in the SNx Model	1588
4.7.3. ϵ (γ -glutamyl) lysine/creatinine ratio in the SNx Model	1588

4.8. ϵ (γ glutamyl)lysine measurement in urine from the streptozotocin induced model of diabetic nephropathy	16060
4.8.1 ϵ (γ glutamyl) lysine levels per mg protein	16060
4.8.2. 24 h urine excretion of ϵ (γ glutamyl) lysine	16161
4.8.3. ϵ (γ glutamyl) lysine/creatinine ratio	16161
4.9. ϵ (γ glutamyl) lysine measurement in urine from the Fisher to Lewis transplant model of Chronic Allograft Nephropathy	1633
4.9.1. ϵ (γ glutamyl) lysine levels per mg protein	1633
4.9.2. 24 h urine excretion of ϵ (γ glutamyl) lysine	1633
4.9.3. ϵ (γ glutamyl) lysine/creatinine ratio	1633
4.10. Correlation between urine ϵ (γ glutamyl) lysine and clinical markers of renal function and damage	1666
4.10.1. 24h proteinuria	1666
4.10.2. Creatinine clearance	1666
4.10.3. Renal scarring levels	1688
4.11. Discussion	1699
Chapter 5 Urinary Plasminogen activator inhibitor type 1, Matrix metalloproteinases and theirs inhibitors in experimental renal scarring	1733
5.1. Introduction	1744
5.2. Urine levels of Matrix Metalloproteinases in experimental CKD	1766
5.2.1. MMP-1 (Interstitial collagenase)	1766
5.2.1.1. Correlation between urine MMP-1 and clinical markers of kidney function and damage	18080
5.2.2. MMP-9 (Gelatinase-B)	18282
5.3. Urine levels of Tissue inhibitors of Metalloproteinases in experimental CKD	1866
5.3.1. Tissue inhibitor of metalloproteinase 1	1866
5.3.2. Correlation between urine TIMP-1 and clinical markers of kidney function and damage	1922
5.3.3. Tissue inhibitor of metalloproteinase 2	1944
5.3.4. Correlation between urine TIMP-2 and clinical markers of kidney function and damage	200
5.3.5. Tissue inhibitor of metalloproteinase 3	202
5.3.6. Correlation analysis for urine TIMP-3	2066
5.4. Plasminogen activator inhibitor type 1 (PAI-1)	2077
5.4.1. Measurement of PAI-1 in urine from the 5/6th Subtotal Nephrectomy model	2077
5.4.2. Measurement of PAI-1 in urine from the UNx STZ model of Diabetic Nephropathy	2099
5.4.3. Correlations between PAI-1 and clinical markers of renal function and damage	21111
5.5. Discussion	2133
Chapter 6 Urinary Hydroxyproline quantification in experimental renal scarring as a measure of total collagen levels	215

6.1. Introduction	2166
6.2. Optimization of Hydroxyproline measurement by cation exchange chromatography	2188
6.3 Hydroxyproline measurement in urine from 5/6 th subtotal nephrectomised rats	2199
6.3.1. 24 hour urine excretion of Hydroxyproline in the SNx Model	2199
6.3.2. Hydroxyproline/Creatinine ratio in the SNx model	2199
6.4. Hydroxyproline measurement in urine from the streptozotocin induced model of diabetic nephropathy	2222
6.4.1. 24 h urine excretion of Hydroxyproline in the UNx STZ model of DN	2222
6.4.2. Hydroxyproline/Creatinine ratio in the UNx STZ model of DN	2222
6.5. Hydroxyproline measurement in urine from the Fisher to Lewis transplant model of Chronic Allograft Nephropathy	2255
6.5.1. 24 h urine excretion of Hydroxyproline	2255
6.5.2. Hydroxyproline/creatinine ratio	2266
6.6. Correlations between Hydroxyproline and clinical markers of renal function and damage	2288
6.6.1. 24h proteinuria	2288
6.6.2. Creatinine Clearance	22828
6.7. Discussion	23030

Volume 2

Chapter 7 Human Chronic Kidney Disease and the urine excretion of Transglutaminase type 2 and ϵ (γ glutamyl) lysine 232

7.1. Introduction	2333
7.2. Study population & Clinical Sample Collection	2377
7.2.1. Study design	2377
7.2.2. Demographic and socio-economical characteristics of the study population	2377
7.2.3. Anthropomorphic data	2388
7.2.4. CKD diagnosis and co-morbidities	2399
7.2.5. CKD stages	24242
7.2.6. Clinical and Laboratorial assessment	2444
7.2.6. Rate of eGFR decline and CKD progression by aetiology	2444
7.2.7. Baseline demographic and clinical characteristics in different age groups	2555
7.2.8. Clinical and biochemical parameters of healthy volunteers	256
7.2.9. Renal biopsy from CGN patients	256
7.2.10. Clinical and biochemical parameters of healthy volunteers	258
7.3. Urine excretion of Transglutaminase type 2 in Human Chronic Kidney Disease	2599
7.3.1. Urine Transglutaminase type 2 measurement	2599
7.3.2. Urine Transglutaminase type 2 levels	2599
7.3.3. Urine Transglutaminase type 2 in different causes of CKD	26060
	XIV

7.3.4. Transglutaminase type 2: Creatinine ratio in urine of CKD patients	26161
7.3.5. Transglutaminase type 2: Creatinine ratio by CKD stage	2633
7.3.6. Comparison of Urine Transglutaminase type 2 levels in CKD patients by age and gender	2644
7.3.7. Relationship between Transglutaminase type 2: Creatinine ratio and CKD progression	265
7.3.8. Receiver Operating Characteristic curve for Urine Transglutaminase type 2 as a predictor of CKD progression	2666
7.4. Urine ϵ (γ glutamyl) lysine measurement in Human Chronic Kidney Disease	2688
7.4.1. Urine ϵ (γ glutamyl) lysine measurement by cation exchange chromatography	268
7.4.2. Urine ϵ (γ glutamyl) lysine concentration	2700
7.4.3. ϵ (γ glutamyl) lysine: Creatinine ratio relationship with the rate of CKD progression	270
7.4.4. Receiver Operating Characteristic curve for Urinary ϵ (γ glutamyl) lysine as a predictor of CKD progression	27272
7.5. Serum concentration of Transglutaminase type 2	2733
7.6. Correlation analysis for Transglutaminase type 2	2744
+ 7.6.1. Urinary Transglutaminase type 2 and ϵ (γ glutamyl) lysine association with histological changes	274
7.7. TG2 substrates	2767
7.8. Discussion	2799

Chapter 8 Urinary Matrix metalloproteinases and their inhibitors in Human Chronic Kidney Disease **282**

8.1. Introduction	2833
8.2 Urinary ECM collagenolytic activity	2866
8.2.1. Measurement of Collagenase activity	2886
8.2.2. Urine MMP activity of CKD patients and healthy volunteers	288
8.2.3. Urine MMP activity and CKD progression	29292
8.2.4. ROC curve analysis for urine MMP activity to predict CKD progression	2933
8.3. Urine levels of Matrix Metalloproteinases in Human CKD	2944
8.3.1. Measurement of urine MMP-1	294
8.3.2. Measurement of urine MMP-2	2966
8.3.3. Measurement of urine MMP-9	301
8.4. Urine levels of Tissue Inhibitors of Metalloproteinases in Human CKD	3066

8.4.1. Tissue inhibitor of metalloproteinase 1	3066
8.4.1.1. Tissue inhibitor of metalloproteinase 1 complexed with Interstitial collagenase C	306
8.4.2. Tissue inhibitor of metalloproteinase 2	3077
8.4.3. Tissue inhibitor of metalloproteinase 3	3077
8.4.4. Tissue inhibitors of MMPs in different CKD aetiologies and stages	31010
8.4.5. Tissue Inhibitors of Matrix Metalloproteinases in different demographic variables	31212
8.4.6. TIMPs excretion by rate of CKD progression	31212
8.4.7. Determination of the predictive potential of urine TIMPs 1, 2 and 3 for rate of disease progression by Receiver Operating Characteristic curve analysis	3155
8.5. Discussion	3166
Chapter 9 General Discussion	3188
9.1. Summary analysis	3199
9.2. General discussion	323
References	332
Appendix	362
10.1. 5/6th Subtotalnephrectomy study	363
10.2. Diabetic Nephropathy study	366
10.3. Chronic Allograft Nephropathy study	368
10.4. Consent forms, Patient Information sheets and GP letter	370

FIGURES

<i>Figure 1.1: Percentage of incident patients with ESRD due to Diabetes, 2010</i>	6
<i>Figure 1.2: Percentage distribution of primary renal diagnosis of ESKD</i>	7
<i>Figure 1.3: Geographic variations on the incidence and prevalence of ESRD</i>	11
<i>Figure 1.4: Development of kidney fibrosis</i>	18
<i>Figure 1.5: The involvement of cytokines in kidney fibrogenesis</i>	20
<i>Figure 1.6: Schematic structure of the ECM</i>	26
<i>Figure 1.7: The main molecular components of normal and fibrotic ECM</i>	27
<i>Figure 1.8: Biochemical activities of Transglutaminase 2</i>	30
<i>Figure 1.9: Transglutaminase 2 molecular structure</i>	32
<i>Figure 1.10: Binding of TIMPs to the active site of MMPs</i>	54
<i>Figure 3.1: 5/6th Subtotal Nephrectomy procedure</i>	75
<i>Figure 3.2: UNx STZ model of Diabetic Nephropathy</i>	76
<i>Figure 3.3: Renal Transplantation procedure</i>	77
<i>Figure 3.4: Jaffe colorimetric method</i>	78
<i>Figure 3.5: Rat Albuminuria Standard Curve</i>	80
<i>Figure 3.6: Overview of the Bio-Clinical assessment</i>	83
<i>Figure 3.7: SKI Bio-repository database</i>	88
<i>Figure 3.8: SKI Bio-repository database: Follow-up data</i>	89
<i>Figure 3.9: Protein Assay Standards Curves</i>	91
<i>Figure 3.10: Schematic representation of a sandwich immunoassay</i>	93
<i>Figure 3.11: Transglutaminase type 2 enzyme-linked immunosorbent assay standard curve</i>	97
<i>Figure 3.12: Gentaur Immunoassay Standard Curves</i>	101
<i>Figure 3.13: Quantikine Immunoassay Standard Curves</i>	105

<i>Figure 3.14:</i> Human Matrix Metalloproteinases Immunoassay Standard Curves	111
<i>Figure 3.15:</i> Human Tissue Inhibitors of Metalloproteinases Immunoassay Standard Curves	112
<i>Figure 3.16:</i> Human MMP-1/TIMP1 complex Standard Curve	113
<i>Figure 3.17:</i> The Biochrom 30 Amino Acid Analyser physiological system	116
<i>Figure 3.18:</i> The BioSys Manual operation window	118
<i>Figure 3.19:</i> The BioSys Program Control window	119
<i>Figure 3.20:</i> Simplified reaction between Ninhydrin, amino acids and imino acids	120
<i>Figure 3.21:</i> EZChrom Elite 96361 LiHP BioSys program	122
<i>Figure 3.22:</i> Physiological standard solution chromatogram	124
<i>Figure 3.23:</i> Graphical definition of peaks	125
<i>Figure 3.24:</i> Determination of crosslinking in Transglutaminase 2 substrates	128
<i>Figure 3.25:</i> Mechanism of Action from EnzChek® Gelatinase/Collagenase Assay	129
<i>Figure 4.1:</i> Representative Masson`s Trichrome stained sections of the SNx model	137
<i>Figure 4.2:</i> TG2 measurement in urine post SNx	139
<i>Figure 4.3:</i> TG2 measurement in urine from the UNx STZ model of DN	141
<i>Figure 4.4:</i> Representative Masson`s Trichrome of the Fisher to Lewis transplant model of CAN at 52 weeks	143
<i>Figure 4.5:</i> TG2 measurement in urine from the Fisher to Lewis model of CAN	145
<i>Figure 4.6:</i> Correlation plots of urine TG2 excretion with markers of kidney function and damage in experimental models of renal scarring	147
<i>Figure 4.7:</i> Correlation plots of 24hr TG2 excretion with scarring index	148
<i>Figure 4.8:</i> Physiological standard solution derivatised peaks	149
<i>Figure 4.9:</i> Determination of ϵ (γ glutamyl) lysine retention time	150
<i>Figure 4.10:</i> Clean fractionation of ϵ (γ -glutamyl) lysine di peptide from other amino acids on a Biochrom 30 analyser	151
<i>Figure 4.11:</i> Establishing accurate detention of ϵ (γ Glutamyl) Lysine in urines	152
<i>Figure 4.12:</i> ϵ (γ glutamyl) lysine standard curve	1533
<i>Figure 4.13:</i> ϵ (γ glutamyl) lysine multilevel calibration	154

<i>Figure 4.14:</i> Overall amino acid excretion in the SNx Model	156
<i>Figure 4.15:</i> Urine ϵ (γ Glutamyl) Lysine excretion in the SNx Model	157
<i>Figure 4.16:</i> Urine ϵ (γ Glutamyl) Lysine measurement in urine post SNx	159
<i>Figure 4.17:</i> Urine ϵ (γ Glutamyl) Lysine excretion in the UNx STZ model of DN	160
<i>Figure 4.18:</i> Urine ϵ (γ Glutamyl) Lysine measurement in urine from the UNx STZ model of DN	162
<i>Figure 4.19:</i> Urine ϵ (γ Glutamyl) Lysine excretion in the Fisher to Lewis Model of CAN	164
<i>Figure 4.20:</i> Urine ϵ (γ Glutamyl) Lysine measurement in urine from the Fisher to Lewis Model of CAN	165
<i>Figure 4.21:</i> Correlation plots of urine ϵ (γ glutamyl) lysine excretion with markers of kidney function and damage in experimental models of renal scarring	1677
<i>Figure 4.22:</i> Correlation plots of urine ϵ (γ glutamyl) lysine excretion and Scarring Index	168
<i>Figure 5.1:</i> MMP-1 measurement in urine post SNx	177
<i>Figure 5.2:</i> MMP-1 measurement in urine from the UNx STZ model of DN	179
<i>Figure 5.3:</i> Correlation plots of urine MMP-1 excretion with markers of kidney function and damage in experimental models of renal scarring	181
<i>Figure 5.4:</i> MMP-9 measurement in urine post SNx	183
<i>Figure 5.5:</i> MMP-9 measurement in urine from the UNx STZ model of DN	185
<i>Figure 5.6:</i> TIMP-1 measurement in urine post SNx	187
<i>Figure 5.7:</i> TIMP-1 measurement in urine from the UNx STZ model of DN	189
<i>Figure 5.8:</i> TIMP-1 measurement in urine from the in the Fisher to Lewis transplant model of CAN	191
<i>Figure 5.9:</i> Correlation plots of urine TIMP-1 excretion with markers of kidney function and damage in experimental models of renal scarring	193
<i>Figure 5.10:</i> TIMP-2 measurement in urine post SNx	195
<i>Figure 5.11:</i> TIMP-2 measurement in urine from the UNx STZ model of DN	197
<i>Figure 5.12:</i> TIMP-2 measurement in urine from the in the Fisher to Lewis transplant model of CAN	199
<i>Figure 5.13:</i> Correlation plots of urine TIMP-2 excretion with markers of kidney function and damage in experimental models of renal scarring	201
<i>Figure 5.14:</i> TIMP-3 measurement in urine post SNx	203
	XIX

<i>Figure 5.15:</i> TIMP-3 measurement in urine from the UNx STZ model of DN	205
<i>Figure 5.16:</i> Correlation plots of urine TIMP-3 excretion with markers of kidney function and damage in experimental models of renal scarring	206
<i>Figure 5.17:</i> PAI-1 measurement in urine post SNx	208
<i>Figure 5.18:</i> PAI-1 measurement in urine from the UNx STZ model of DN	210
<i>Figure 5.19:</i> Correlation plots for PAI-1	212
<i>Figure 6.1:</i> Validation of Hydroxyproline measurement in urines	218
<i>Figure 6.2:</i> Hydroxyproline detection in urine from 5/6th subtotal nephrectomised rats	220
<i>Figure 6.3:</i> Hydroxyproline measurement in urine post SNx	221
<i>Figure 6.4:</i> Hydroxyproline detection in Diabetic Nephropathy urines	223
<i>Figure 6.5:</i> Hydroxyproline measurement in urine from the UNx STZ model of DN	224
<i>Figure 6.6:</i> Hydroxyproline measurement in urine from the in the Fisher to Lewis model of CAN	227
<i>Figure 6.7:</i> Correlation plots for Hydroxyproline	229
<i>Figure 7.1:</i> Frequency distribution of CKD patients' demographic data	238
<i>Figure 7.2:</i> Anthropomorphic data from CKD patients and healthy volunteers	239
<i>Figure 7.3:</i> CKD Etiology	241
<i>Figure 7.4:</i> CKD stages	242
<i>Figure 7.5:</i> Frequency distribution of CKD stages according to CKD etiology	243
<i>Figure 7.6:</i> Regression analysis for estimation of eGFR decline	245
<i>Figure 7.7:</i> CKD progression in different aetiologies	257
<i>Figure 7.8:</i> TG2 measurement in urine from all cause CKD patients	260
<i>Figure 7.9:</i> Urine TG2 excretion in patients with different causes of CKD	262
<i>Figure 7.10:</i> TG2: Creatinine ratio in different CKD stages	263
<i>Figure 7.11:</i> TG2: Creatinine ratio by demographic data	264
<i>Figure 7.12:</i> Urine TG2 excretion in patients with different rates of CKD progression	266
<i>Figure 7.13:</i> Urine TG2 ROC curve	267
<i>Figure 7.14:</i> Urine ϵ (γ Glutamyl) Lysine excretion in Human CKD	269
<i>Figure 7.15:</i> ϵ (γ glutamyl) lysine (XL) excretion in urine from CKD patients	271
	XX

<i>Figure 7.16:</i> Urine ϵ (γ glutamyl) lysine ROC curve	272
<i>Figure 7.17:</i> Blood levels of Transglutaminase type 2	273
<i>Figure 7.18:</i> Urine TG2 excretion in patients with different causes of CKD	275
<i>Figure 7.19:</i> Correlation plots of urine TG2 and ϵ (γ glutamyl) lysine excretion with percentage of kidney fibrosis in patients with chronic glomerulonephritis	276
<i>Figure 7.20:</i> <i>In vitro</i> crosslinking of TG2 substrates	278
<i>Figure 8.1:</i> Example of a total MMP activity standard curve	287
<i>Figure 8.2:</i> Fluorescence gradient in CKD urine samples	290
<i>Figure 8.3:</i> MMP activity in CKD urine samples	291
<i>Figure 8.4:</i> Urine MMP activity by CKD progression	292
<i>Figure 8.5:</i> MMP activity ROC curve	293
<i>Figure 8.6:</i> Human Matrix Metalloproteinase 1 Immunoassay Standard Curve	294
<i>Figure 8.7:</i> MMP-2 measurement in urine from CKD patients	296
<i>Figure 8.8:</i> MMP-2:Creatinine ratio in CKD patients	298
<i>Figure 8.9:</i> MMP-2: Creatinine ratio and CKD progression	299
<i>Figure 8.10:</i> Urine MMP-2 ROC curve	300
<i>Figure 8.11:</i> MMP-9 measurement in urine from CKD patients	301
<i>Figure 8.12:</i> MMP-9:Creatinine ratio in CKD patients	303
<i>Figure 8.13:</i> MMP-9: Creatinine ratio and CKD progression	304
<i>Figure 8.14:</i> Evaluation by ROC curve analysis of MMP-9 ability to predict CKD progression	305
<i>Figure 8.15:</i> Urine TIMP levels in CKD patients	308
<i>Figure 8.16:</i> Measurement of MMP-1/TIMP-1 complex in 100 CKD patients	309
<i>Figure 8.17:</i> Urine TIMP levels in CKD patients by cause and stage	311
<i>Figure 8.18:</i> MMPs inhibitors by different demographic variables	313
<i>Figure 8.19:</i> Urine TIMPs 1, 2 and 3 levels by rate of CKD progression	314
<i>Figure 8.20:</i> TIMPs 1, 2 and 3 ability to predict CKD progression by ROC curve analysis	315
<i>Figure 9.1:</i> Albuminuria vs. CKD progression	320

<i>Figure 9.2: ACR, TG2CR, XLCR and TIMP1CR combo ROC curve</i>	322
<i>Figure 10.1: Assessment of kidney function and damage in the SNx Model</i>	365
<i>Figure 10.2: Assessment of kidney function and damage in the UNx STZ model of DN</i>	367
<i>Figure 10.3: Assessment of kidney function and damage in the Fisher to Lewis transplant model of CAN</i>	369

TABLES

<i>Table 1.1:</i> CKD classification by the K/DOQI guidelines	3
<i>Table 1.2:</i> Current CKD classification used by KDIGO	3
<i>Table 1.3:</i> Common causes of ESKD in the UK	5
<i>Table 1.4:</i> Prevalence (%) of CKD in the NHANES population within age, gender, race/ethnicity, & risk-factor categories	10
<i>Table 1.5:</i> Phases of kidney fibrogenesis	20
<i>Table 1.6:</i> Physiological Transglutaminases and respective functions	29
<i>Table 1.7:</i> TG2 Substrates in human diseases	38
<i>Table 1.8:</i> Structural characteristics of collagens	44
<i>Table 1.9:</i> Collagens types and their role in human diseases	47
<i>Table 1.10:</i> MMPs types, substrates specificity and domain composition	50
<i>Table 1.11:</i> General properties of human TIMPs	53
<i>Table 1.12:</i> Experimental CKD biomarkers according to the pathophysiological process	611
<i>Table 3.1:</i> Anti-transglutaminase 2 antibodies	94
<i>Table 3.2:</i> Urine TG2 Enzyme-linked immunosorbent assay reproducibility	96
<i>Table 3.3:</i> Accuracy % of rat MMP-1, TIMP-2, TIMP-3 and PAI-1 immunoassays	98
<i>Table 3.4:</i> Accuracy % of rat MMP-9 and TIMP-1 immunoassays	102
<i>Table 3.5:</i> Ion exchange process	117
<i>Table 3.6:</i> Main Amino acid and peptides classification and retention times	123
<i>Table 7.1:</i> Frequency distribution of main co-morbidities presented by CKD patients	240
<i>Table 7.2:</i> Clinical and laboratory characteristics of CKD patients, their subgroups and controls	246
<i>Table 7.3:</i> Clinical and laboratory characteristics of CKD patients, their subgroups and controls	247

<i>Table 7.4:</i> Main demographic and clinical characteristics of Diabetic Kidney Disease patients (n=91) analysed by CKD progression	248
<i>Table 7.5:</i> Main demographic and clinical characteristics of Chronic Glomerulonephritis patients (n=66) analysed by CKD progression	249
<i>Table 7.6:</i> Main demographic and clinical characteristics of patients with Hypertensive Nephrosclerosis (n=53) analysed by CKD progression	250
<i>Table 7.7:</i> Main demographic and clinical characteristics of patients with Atherosclerotic Renovascular disease (n=29) analysed by CKD progression	251
<i>Table 7.8:</i> Main demographic and clinical characteristics of patients with Chronic Interstitial Nephritis (n=15) analysed by CKD progression	252
<i>Table 7.9:</i> Main demographic and clinical characteristics of ADPKD patients (n=13) analysed by CKD progression	253
<i>Table 7.10:</i> Main demographic and clinical characteristics of patients with other causes of CKD (n=25) analysed by levels of CKD progression	254
<i>Table 7.11:</i> Comparison of main clinical parameters between different age groups	255
<i>Table 7.12:</i> Baseline clinical characteristics of healthy volunteers	258
<i>Table 8.1:</i> Detected Human Matrix Metalloproteinase 1 in urine	295
<i>Table 9.1:</i> Summary of human ECM biomarkers data	319
<i>Table 9.2:</i> ROC AUC values of ACR and Urinary ECM biomarkers	3201
<i>Table 10.1:</i> SNx study renal function data	363
<i>Table 10.2:</i> UNx STZ model of DN renal function data	366
<i>Table 10.3:</i> Fisher to Lewis transplant model of CAN renal function data	368

Chapter 1

Introduction

1.1. Chronic Kidney Disease

Chronic Kidney Disease (CKD) represents a major healthcare problem. It is defined by the persistence of kidney damage or reduced glomerular filtration rate (GFR) $< 60\text{ml}/\text{min}/1.73\text{m}^2$ for 3 months or longer regardless of its cause. In most cases, this damage is progressive and irreversible, leading to a reduction in kidney function (glomerular, tubular and endocrine) and later development of End Stage Kidney Disease (ESKD) and requirement for renal replacement therapy (RRT) (Floege 2013). According to the Kidney/Dialysis Outcome Quality Initiative (K/DOQI) guidelines, CKD can be subdivided into 5 stages (guidelines 2002) based on function, evidence of kidney damage (albuminuria or haematuria) and histology (table 1.1).

This classification from K/DOQI guidelines has evolved with time. In 2008, the U.K. National Institute of Health and Clinical Excellence (NICE) developed a guideline that recommended splitting the CKD stage 3 from the K/DOQI classification into 3a (estimated GFR between 45 and $59\text{ml}/\text{min}/1.73\text{m}^2$) and 3b (between 30 and $44\text{ml}/\text{min}/1.73\text{m}^2$). This subdivision is understood to improve clinical knowledge of prognosis and therefore enhance treatment (2008). The NICE guidelines also suggested the adoption of the suffix '(p)' for patients with significant proteinuria ($>0.5\text{g}/24\text{h}$) as this represents a major risk factor for disease progression.

In 2012, the Kidney Disease: Improving Global Outcomes (KDIGO) group suggested a new classification in which the prognosis of CKD is given by the association of six categories of GFR (G1 to G5, with G3 subdivided into G3a and G3b) and three levels of albuminuria; A1 (normal to mildly increased albuminuria $<30\text{mg}/\text{g}$ or albumin to creatinine ratio $<3\text{mg}/\text{mmol}$), A2 (moderately increased albuminuria $30\text{-}300\text{mg}/\text{g}$ or albumin to creatinine ratio $3\text{-}30\text{mg}/\text{mmol}$) and A3 (severely increased albuminuria $>300\text{mg}/\text{g}$ or albumin to creatinine ratio $>30\text{mg}/\text{mmol}$) (table 1.2) (KDIGO 2012).

CKD is associated with increased risk of development of Cardiovascular Diseases (CVD) (Ito 2012), Cerebrovascular Diseases (Bao *et al.* 2013), depression (Palmer *et al.* 2013), premature death (Tonelli *et al.* 2006), decreased quality of life (Cruz *et al.* 2011), reduced cognitive function (Davey *et al.* 2013), metabolic and nutritional disorders as well as increased health-care expenditures (Jha *et al.* 2012). Early detection is a key step to effective therapy, however, current kidney function and damage tests have several limitations as they can only detect dysfunction after significant damage had occurred, provide limited help with the disease stage and are also unhelpful in assessing early response to therapy. Hence, there is a requirement for identification of early and reliable biomarkers of kidney disease.

Table 1.1: CKD classification by the K/DOQI guidelines

CKD Stage	GFR (ml/min/1.73m ²)	Description
	>90 (with CKD risk factors)	At increased risk
1	>90	Normal renal function, but with other evidence of kidney damage, such as microalbuminuria, haematuria or histological changes
2	60-89	Mild reduction in GFR
3	30-59	Moderate reduction in GFR
4	15-29	Severe reduction in GFR
5	<15	ESKD, RRT needs to be considered

Table 1.1: Classification of CKD stages as defined in the K/DOQI guidelines. Data obtained from the National Kidney Foundation (NKF). Am J Kidney Disease 1, S1-S266

Table 1.2: Current CKD classification used by KDIGO

Prognosis of CKD by GFR and Albuminuria Categories: KDIGO 2012				Persistent albuminuria categories Description and range		
				A1	A2	A3
				Normal to mildly increased	Moderately increased	Severely increased
				<30 mg/g <3 mg/mmol	30-300 mg/g 3-30 mg/mmol	>300 mg/g >30 mg/mmol
GFR categories (ml/min/ 1.73 m ²) Description and range	G1	Normal or high	≥90			
	G2	Mildly decreased	60-89			
	G3a	Mildly to moderately decreased	45-59			
	G3b	Moderately to severely decreased	30-44			
	G4	Severely decreased	15-29			
	G5	Kidney failure	<15			

Green: low risk (if no other markers of kidney disease, no CKD); Yellow: moderately increased risk; Orange: high risk; Red, very high risk.

Table 1.2: Classification and prognosis of CKD according to the KDIGO guidelines 2012. Data obtained from the KDIGO 2012 Clinical Practice Guideline for the Evaluation and Management of Chronic kidney Disease. <http://kdigo.org/home/guidelines/ckd-evaluation-management/>

1.2. Causes of CKD

Numerous conditions can cause CKD. However, there is a distinct difference between the causes of CKD detected in the general population (Community CKD; cCKD) and those who are referred to nephrology centres (Referred CKD; rCKD). Community CKD is most common in the elderly population and is associated with an age-related decline in GFR. The majority of individuals that present cCKD die before reaching ESRD. On the other hand, rCKD mostly affects individuals that present acquired or inherited nephropathies. Referred CKD patients frequently present early kidney dysfunction and often progress to ESRD with time.

Community CKD is a condition mainly originated by the long lasting exposition suffered by the elderly individual to cardiovascular risk factors. This includes hypertension, diabetes, cardiovascular and atherosclerotic lesions which occur as a result of vascular aging. In developing countries, cCKD is also associated with socio-economic causes such as poverty, malnutrition, infectious diseases and exposition to environmental toxic factors (Floege 2013).

The commonest identifiable causes of rCKD are: diabetic nephropathy (Fox *et al.* 2005, Middleton *et al.* 2006, Whaley-Connell *et al.* 2008), hypertension (Andersen and Agarwal 2005, Barri 2008), glomerulonephritis (Kawasaki 2011), vascular diseases (Piecha *et al.* 2012), tubulointerstitial diseases (Hodgkins and Schnaper 2012), toxic nephropathy (De Broe 2012), cystic kidney disease (Grantham 1996), neoplasms and hereditary / congenital diseases and obstructive uropathy. In developed countries there is a bigger incidence of Glomerulonephritis (most common is IgA nephropathy) and diabetes whereas in the developing countries it is common to find causes of CKD such as hypertension, glomerulonephritis and interstitial nephritis due to infectious diseases as malaria, filariasis, schistosomiasis, tuberculosis, hepatitis C and others, all aggravated by undiagnosed conditions and social problems (El Nahas 2005, Weiner 2007). Less common causes of CKD include: vasculitis, dysproteinaemias and metabolic causes including cystinosis, cystinuria, hyperuricemia, oxalosis and nephrocalcinosis (Nestor Schor 2004).

Overall, diabetic kidney disease remains one of the most common causes of kidney failure worldwide, accounting for 24% of cases in the UK (table 1.3) although this number varies between countries (figure 1.1). Data is subdivided into age groups and shows that the incident rates of ESKD due to Diabetes increases with age, being significantly higher in individuals aged over 65 years old.

Comparative percentage distribution of primary renal diagnosis on patients starting RRT on two different developed countries (UK and USA) against two developing countries (Brazil and Singapore) - (SRR 2009) shows glomerulonephritis, hypertension and diabetes amongst the leading causes of CKD (figure 1.2).

Table 1.3: Common causes of ESKD in the UK

Causes	Percentage
Diabetes	24.2
Glomerulonephritis	11.6
Renal vascular disease	7.5
Pyelonephritis	7.4
Hypertension	6.7
Polycystic kidney disease	6.6
Other	16.2
Unknown aetiology	19.8

Table 1.3: Registry data of primary common causes of ESKD in the UK. Total Glomerulonephritis include presumed GN not biopsy proven. Data from UK Renal Registry 2011.

Figure 1.1: Percentage of incident patients with ESRD due to Diabetes, 2010

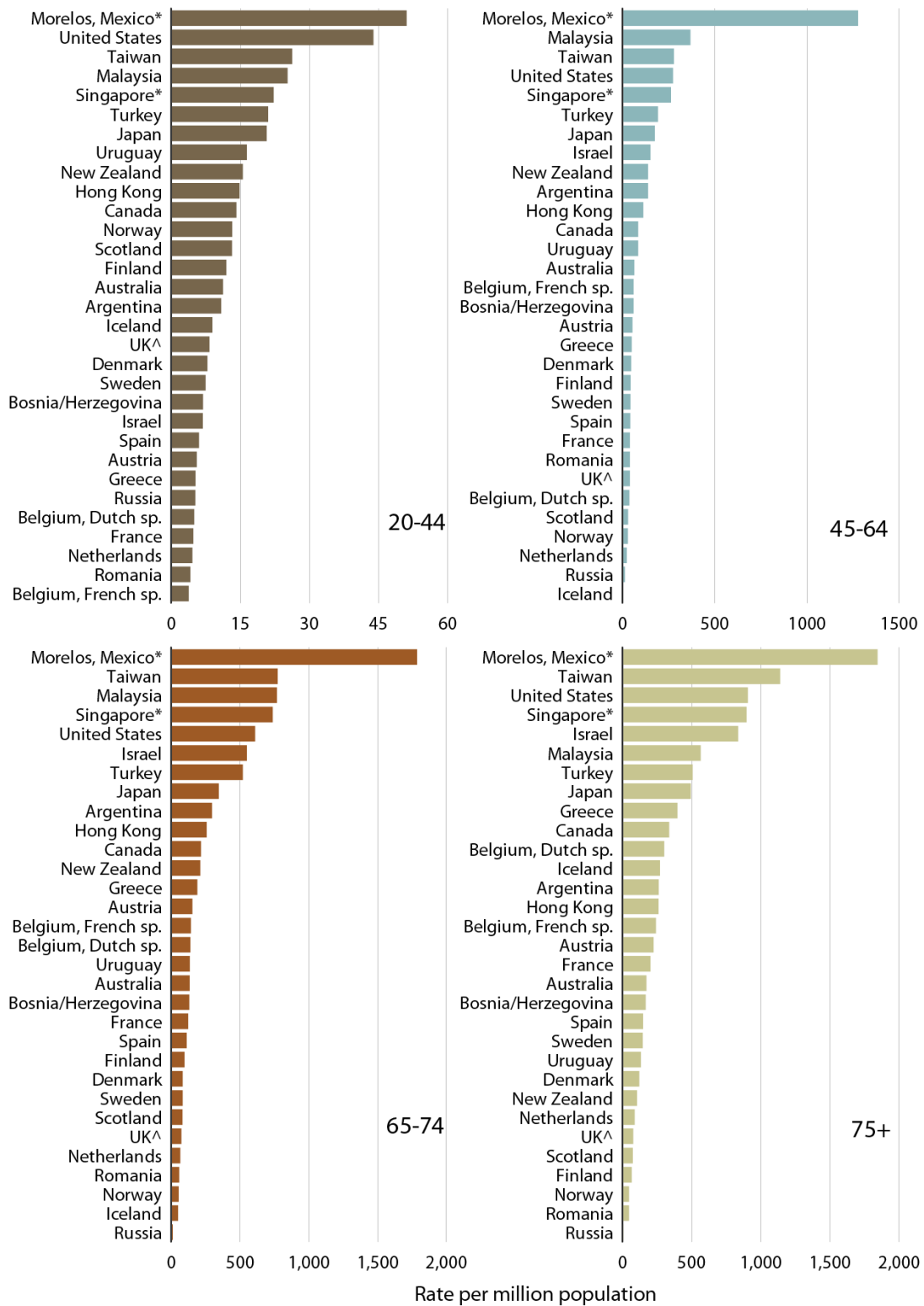


Figure 1.1: Incidence of patients with ESKD due to Diabetes in different countries in 2010. Data represents unadjusted rates of Diabetes divided by age groups from countries which relevant information was available. UK data includes England, Wales and Northern Ireland only. Adapted from *U.S. Renal Data System, USRDS 2012*

Figure 1.2: Percentage distribution of primary renal diagnosis of ESKD

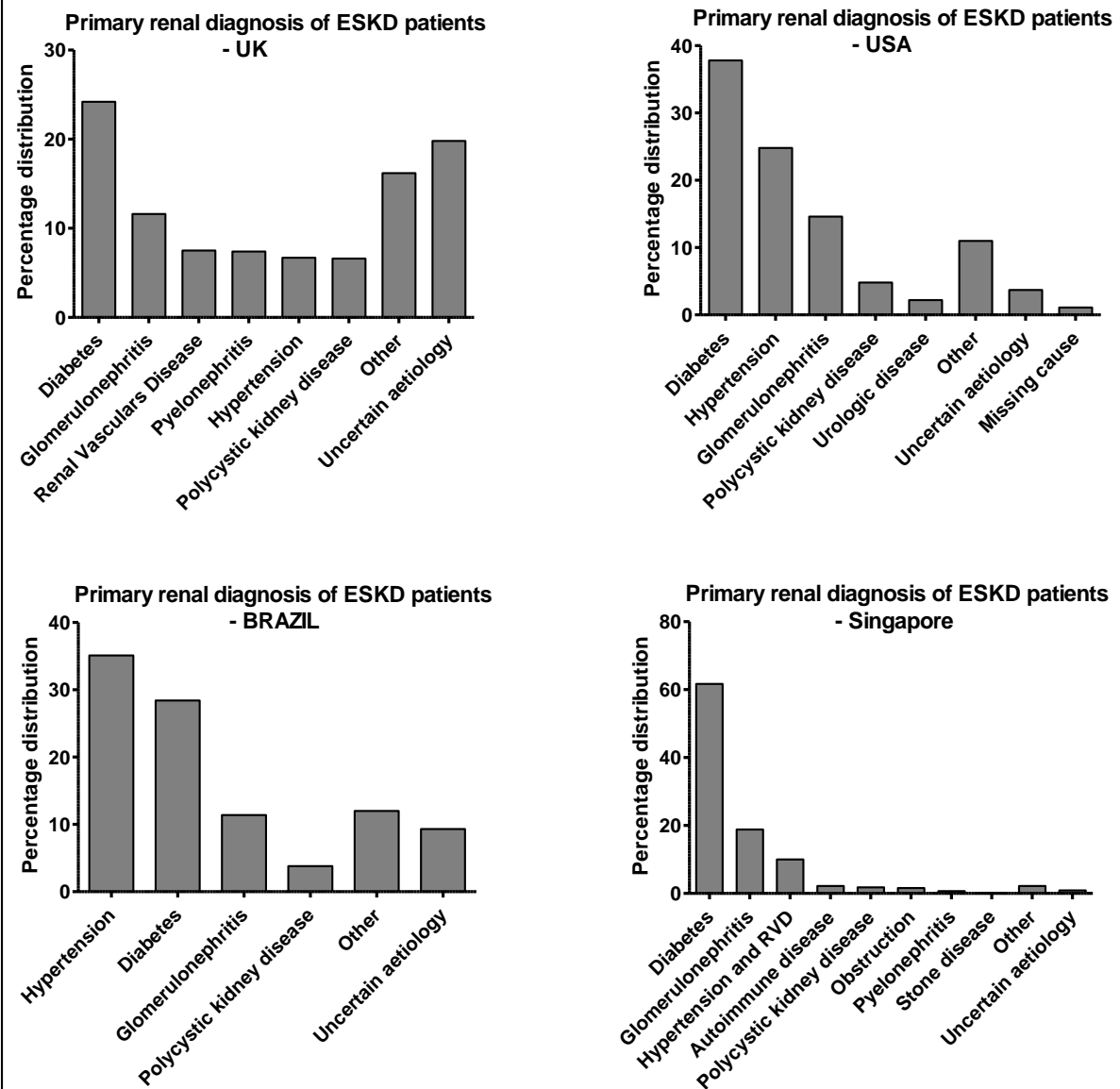


Figure 1.2: CKD aetiology of patients starting RTT in different countries. Data from local renal registries in 2009 (Singapore) and 2011 (UK, USA and Brazil). Total Glomerulonephritis include presumed GN not biopsy proven.

1.3. Epidemiology of CKD

It is difficult to assess the exact incidence and prevalence of CKD in the general population. According to a wide range of adult population screening studies, overall CKD prevalence is estimated to be >10% in the general population, with community prevalence screening ranging from 0.8% to 42.6% depending of the country of data collection (systematic review from (McCullough *et al.* 2012)). However, little data is available at the earlier stages of CKD when symptoms are mild, ignored or poor diagnosed. It is considered that the majority of patients at early and asymptomatic stages of CKD are undiagnosed and consequently untreated (Schieppati *et al.*, 2005; Levin *et al.*, 2001). This decreases the possibility of applying therapy to retard the progression of the disease early.

In the United States of America, according to the Third National Health and Nutritional Survey (NHANES III, 1988-1994), a report which analysed a sample of 15625 adults over 20 years old showed that the prevalence of CKD in adult Americans was estimated to be 10.8% (or approximately 19.2 million people) (Coresh *et al.* 2003). From this, 3.3% were estimated to be on stage 1 (or 5.9 million people), 3.0% on stage 2 (5.3 million), 4.3% on stage 3 (7.6 million), 0.2% on stage 4 (400 000 people) and less than 0.2% on stage 5 (300 000 people). This study also demonstrated that CKD prevalence increases with age as 11% of population aged above 65 years old were diagnosed with CKD 3, 4 or 5, even in the absence of Diabetes Mellitus (DM) or Hypertension (HTN) (table 1.4). The United States Renal Data System projects an increase of nearly 50% of the incidence and prevalence of ESKD in the American population by 2020 (System 2012).

Data from the Japanese annual health check program from 2000-2004 analysed 574,024 individuals over 20 years old and predicted a prevalence of around 13% (or 13.3 million) of the Japanese adult population had CKD in 2005 (Imai *et al.* 2009). The prevalence of CKD stages 1, 2, 3, and 4 plus 5 were estimated on 0.6, 1.7, 10.4 and 0.2% respectively.

A Southern Chinese study with 6101 subjects aged 20 years or older detected an overall 5.8% prevalence of low albuminuria with a general 12.1% prevalence of CKD (Chen *et al.* 2009), whereas some other studies have showed even higher CKD prevalence, such as 18.9% in Iran (Hosseinpanah *et al.* 2009). However, these high prevalence rates of CKD could be due either to an elevated ingress of older people in the study, or to the different type of equation applied to estimate GFR and also to the incorporation of low level albuminuria in the inclusion criteria despite the fact that this is not a specific marker of CKD.

1.4. Epidemiology of ESRD

Despite the rareness of accurate data on the epidemiology of CKD at early stages, there are numerous studies presenting information on moderate to advanced CKD as well as reports from renal registries in which focuses on ESRD. Overall, the incidence and prevalence of ESRD has increased globally over the past two decades leading to high health care expenditures (1999).

In Europe, the ERA – EDTA (European Renal Association – European Dialysis and Transplant Association) in 2010 took the data collected from 52 national or regional registries from 29 countries. The average incidence of ESKD on Europe was about 130 pmp and prevalence of 939 pmp (Registry 2012).

According to the United Kingdom (UK) Renal registry report from 2012, the incidence rate of ESKD in the UK in 2011 was stable at 108 pmp, with 25% of cases due to diabetic kidney disease (DKD). The overall prevalence of patients undergoing RTT was 842 pmp (Registry 2012). The prevalence rate was greater in males than females at all age groups, peaking in men aged between 75-79 years at 2918 pmp and for women aging between 65-69 years at 1460 pmp.

In 2011, the prevalence and the incidence of patients on RTT in Brazil corresponded to 475 pmp and 149 pmp respectively. 57.3% of individuals on RTT were male and 84.9% funded by the Brazilian Public Health System (SUS) (Nefrologia 2011, Sesso Rde *et al.* 2012). This represented less than half of the prevalence found on developed countries such as USA, which supports the presupposition that ESKD is underdiagnosed and/or undertreated in developing countries (Oliveira *et al.* 2005, Lugon 2009).

As well as the above renal registries, there is also diverse information on epidemiology of RTT in several worldwide registries. For instance, the Australia and New Zealand Dialysis and Transplantation Registry (ANZDATA), described an incidence of 110 pmp in Australia and 108 pmp in New Zealand, with a prevalence of 885 pmp in Australia and 877 pmp in New Zealand on 2011 (Report 2012). The Sociedad Latino-Americana de Nefrologia e Hipertension (SLANH), which aggregates data from twenty Latin American countries, showed an average of 604 pmp of prevalence and 198 pmp incidence in 2009. ((SLANH) 2012). A recent cross-sectional study in India analysed a cohort of 5588 people and reported a CKD prevalence of 17.2%. From this, 7%, 4.3%, 4.3%, 0.8% and 0.8% were estimated to be on CKD stages 1, 2, 3, 4 and 5 respectively (Singh *et al.* 2013).

In general we can observe an enormous increasing in the numbers related to CKD with an overall estimated increase of 6% per year. Differences on the incidence and prevalence data between countries may be related to the prevalence of the primary disease causes of the kidney injury as well as to ethnic and environmental reasons. Low rates displayed by developing countries could also be explained by an inadequate coverage by the registries, underdiagnosis and scant resources to detect and treat patients with CKD (figure 1.3).

Table 1.4: Prevalence (%) of CKD in the NHANES population within age, gender, race/ethnicity, & risk-factor categories

	All CKD		eGFR <60 ml/min/1.73m ²		ACR ≥30 mg/g	
	1988- 1994	2005- 2010	1988- 1994	2005- 2010	1988- 1994	2005- 2010
20-39	5.1	5.7	0.1	0.2	5.0	5.7
40-59	8.4	9.1	1.3	2.2	7.7	7.6
60+	32.2	35.0	19.5	24.1	18.3	18.4
Male	10.2	12.1	4.1	5.6	7.4	8.6
Female	14.2	15.8	5.6	7.7	10.2	10.2
Non-Hispanic White	12.3	14.3	5.5	7.9	8.2	8.6
Non-Hispanic Black Afro American	14.5	16.0	4.1	6.2	12.7	12.6
Other	10.5	11.9	2.2	2.6	9.2	10.6
Diabetes	43.1	40.1	15.6	19.3	36.3	29.9
Self-reported diabetes	42.7	41.6	16.4	20.4	35.9	30.8
Hypertension	22.2	23.2	10.4	12.9	15.4	14.8
Self-reported hypertension	25.3	26.8	12.9	15.6	17.1	16.7
Cardiovascular disease	25.4	40.8	14.5	27.9	16.6	24.3
Obesity (BMI ≥30)	16.6	16.8	6.2	7.4	12.3	11.7
All	12.3	14.0	4.9	6.7	8.8	9.4

Table 1.4: Percentage of CKD prevalence from 1988 to 2010 in the United States of America population. Data from the United States Renal Data System http://www.usrds.org/2012/view/v1_01.aspx

Figure 1.3: Geographic variations on the incidence and prevalence of ESRD

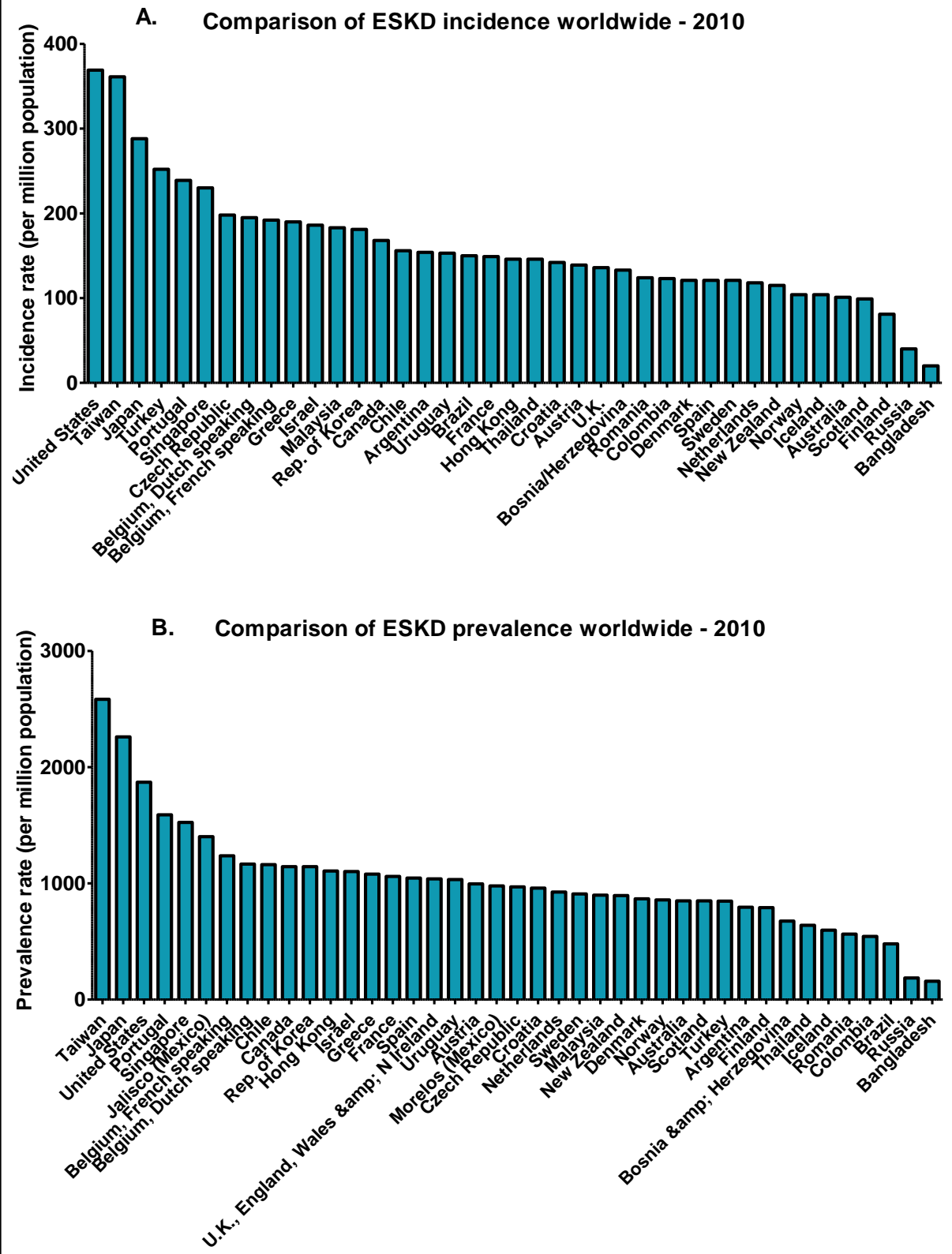


Figure 1.3: Worldwide ESRD epidemiology. A – Comparison of unadjusted ESKD incidence worldwide in 2010. Japan AND Taiwan are dialysis only. B – Prevalence rate of RRT per million population in different parts of the world. Adapted from *U.S. Renal Data System, USRDS 2012*

1.5. Progression of CKD

After the initial process of renal injury and irrespective of the cause, a progressive deterioration in renal function occurs that can lead to irreversible renal failure. Most cases of rCKD stages G3 to G5 progresses to ESKD with an estimated rate of decline in GFR that varies from -1 to -2 ml/min/year in patients with controlled blood pressure and glycaemia, to -10 ml/min/year in patients with Diabetic Nephropathy (DN) (Floege 2013). However, a portion of these patients can remain with stable CKD function and not develop ESKD or have a premature death caused by CVD or other causes (Floege 2013). The rate of progression to ESRD can vary spontaneously or according to internal and external factors such as uncontrolled blood pressure or glycaemia, infections, presence of proteinuria, haemodynamic status and others (reviewed by (Nahas 2000)).

Several experimental models and human trials have demonstrated that proteinuria is associated with tubulointerstitial damage and subsequent progression of kidney disease (McClellan and Flanders 2003, Remuzzi *et al.* 2006). Another pathway related to the progression of the initial kidney injury is the hyperfiltration that occurs in remaining nephrons after loss of renal mass; initially it is an adaptative effect to maintain GFR but subsequently would cause glomerular damage (Hostetter *et al.* 2001).

Interventions to prevent or slow CKD progression include control of blood pressure and cardiovascular risk factors as well as of the secondary hemodynamic and metabolic factors involved in the process of advancement of kidney disease. The eradication of all associated modifiable risk factors is a vital part of the treatment strategy for preventing the development and progression of CKD.

1.5.1 Risk Factors for progressive CKD

There is a considerable person-to-person variability on the rate of progression and loss of renal function. Such variation occurs not only between different diseases, but also in different individuals that share similar pathological processes (Schrier 2003). This can be consequence of the multifactorial nature of the biological mechanisms that are involved (Adler 2006). The factors that can influence the progression of CKD are as follow: non-modifiable - age, gender, race and genetics and modifiable risk factors, such as smoking, alcohol consumption, illicit drug use, use of nephrotoxic agents, presence of proteinuria, hyperphosphatemia, hypertension, uncontrolled blood glucose, dyslipidaemia, obesity, underlying disease activity, anaemia and others.

1.5.1.1. Non-modifiable risk factors

Age

Increased age is associated with increased risk for decline in renal function, although normally there is a loss of renal mass and function with aging. This normal alteration of kidney structure and function that occurs with aging has several reasons including the loss of self-renewing stem-cells (Lasagni and Romagnani 2010), decreased proximal tubular cell proliferation caused by an over expression of zinc-alpha-2 glycoprotein (Zag) (Schmitt *et al.* 2008), abnormal DNA methylation and modification of histones damaging the structure of renal cells (Dressler 2008) and the effects of telomere shortening and oxidative stress on cell senescence (Yang and Fogo 2010).

The incidence of CKD progression is higher in older people, especially those above 75 years old (Anderson *et al.* 2009). Aged-related glomerulosclerosis can be linked to atherosclerotic vascular disease as the arterial lumen narrowing could cause ischemia and/or thrombosis leading to subsequent glomerular damage (Schrier 2005, Abdelhafiz *et al.* 2008). Ageing is also associated with reduction in effective renal plasma flow with a preserved GFR. Systemic hypertension or intrinsic renal disease could contribute to the progression of the existent glomerulosclerosis on this group as there is an increased filtration fraction in those diseases. Another cause for CKD progression in elderly patients (above 65 years old) is linked to the occurrence of episodes of Acute Kidney Injury (AKI) which leads to a lower recovery of kidney function within this group when compared to younger patients (Schmitt *et al.* 2008).

Gender

Gender is also an additional risk factor for the progression of some renal disease (Carrero 2010). It is reported that males have a greater risk than females in certain types of nephropathies and this could be linked to the modulation of genes involved in ECM metabolism by Estrogen (Neugarten and Golestaneh 2013). Additional studies show slower progression rates of renal failure in females patients with hypertension, polycystic kidney disease, membranous glomerulopathy, IgA nephropathy, diabetes type I and some hereditary kidney diseases present a faster rate of decline in males that could be explained by differences in kidney sizes and in glomerular hemodynamics, different diet composition and by the effects of sex hormones in genetic pathways (Eriksen and Ingebretsen 2006, Silbiger and Neugarten 2008, Silbiger 2011).

Race

Race, ethnicity and genetics are correlated as factors associated with progression of kidney disease. There are numerous hypotheses to support this association. Examples include studies of familial aggregation of risk (Freedman *et al.* 1997), mutations in mitochondrial genes

(Watson *et al.* 2001), the reduced foetal growth theory which is associated with low nephrons mass and glomerular hypertrophy (Huxley *et al.* 2002) and polymorphisms of the gene UMOD which encodes the protein Uromodulin and in the gene encoding TGF β 1 (Tampe and Zeisberg 2013).

Overall, there is a higher predisposition to progressive kidney damage in blacks and in ethnic minority populations compared to Caucasians (Byrne *et al.* 1994, Tarver-Carr *et al.* 2002), especially those with increased proteinuria (Erickson *et al.* 2013). It has been demonstrated a higher prevalence and greater severity of diabetes and hypertension among black people than in white and that the response to some drugs such as the Angiotensin Converting Enzyme (ACE) inhibitors is lower in Blacks (Brenner *et al.* 2001, Lewis *et al.* 2001, Norris and Agodoa 2005).

1.4.1.2. Modifiable risk factors

Modifiable risk factors include: hypertension, presence of proteinuria, smoking, alcohol consumption, illicit drug use, chronic use of anti-inflammatory agents, unbalanced nutritional status, dyslipidaemia, anaemia, metabolic and mineral disturbances such as hyperparathyroidism and hyperuricemia, late referral to the nephrologist and socio-economic factors (Remuzzi *et al.* 2006, J Feehaly 2007, Turgut *et al.* 2007, Yamagata *et al.* 2007, Bello *et al.* 2008, Muntner *et al.* 2013).

Hypertension

Hypertension can act not only as the cause, but also in accelerating CKD. It is involved in the pathophysiology of CKD progression through the event of arteriolar nephrosclerosis and by its role on the divalent cation regulation system, which includes phosphate metabolism managed by the fibroblast growth factor 23 (FGF-23)/klotho system (John *et al.* 2011, Cozzolino *et al.* 2013). Poor blood pressure control can induce a faster GFR decline by increasing the glomerular filtration pressure and subsequently proteinuria levels that leads to higher degree of kidney injury. Furthermore, hypertension also accounts for increased cardiovascular risk. The Multiple Risk Factor Intervention Trial (MRFIT) studied 332 544 middle-aged men and revealed an elevated risk of progression to ESRD beginning at the third quintile of systolic and diastolic blood pressure (127/82 mm Hg)(Klag *et al.* 1996). Later on, similar findings were observed in the Okinawa mass screening program (n = 98 759) (Tozawa *et al.* 2003).

Proteinuria

Although the presence of proteinuria/albuminuria has been shown to be an independent risk factor for increased CVD events and progression of CKD in several studies (Martins *et al.* 2006, Foster *et al.* 2007, Ruggenenti *et al.* 2012), it has been also suggested that it acts more as a marker of CKD progression rather than its cause (Yusuf *et al.* 2008, Parving *et al.* 2012). In a meta-analysis of 10 cohorts involving 266 975 patients at increased risk of CKD, high albuminuria and low GFR predicted CVD and all-cause mortality independently of each other (van der Velde *et al.* 2011). Several other clinical studies correlate proteinuria and renal function decline in diabetic and nondiabetic kidney disease. It can accelerate kidney disease progression by multiple pathways such as complement activation, induction of tubular chemokine expression, inflammatory cell infiltration and subsequent glomerulosclerosis (Cravedi and Remuzzi 2013). The REIN (Ramipril Efficacy in Nephropathy) study showed that individuals in the highest tertile of baseline proteinuria (protein excretion ≥ 3.8 g/d) presented the highest rate of GFR decline (Ruggenenti *et al.* 1998). Likewise, the RENAAL (Reduction of Endpoints in NIDDM [Non-Insulin-Dependent Diabetes Mellitus] with the Angiotensin II Antagonist Losartan study reported that 85% of patients with proteinuria with protein excretion ≥ 3 g/d also were at higher risk of having increased serum creatinine levels and developing ESRD (de Zeeuw *et al.* 2004). Another study showing the association between higher baseline proteinuria and decreased GFR was the African-American study of kidney disease and hypertension (AASK) (Wright *et al.* 2002). Thereby proteinuria reduction by the use of ACE inhibitors/ARB and dietary protein restriction was considered to achieve renoprotective effects and improvement in renal function (Peterson *et al.* 1995, de Zeeuw 2004, Perico *et al.* 2005). However, new evidence shows that discontinuation of ACE inhibitors/ARB slows progression to RRT in advanced CKD patients (Ahmed *et al.* 2010). In addition, the ONTARGET study showed that a combination of an ACE inhibitor (Ramipril) and an ARB (Telmisartan) caused a reduction in albuminuria levels and worsening of kidney function (Yusuf *et al.* 2008). Comparable results were found in the ALTITUDE study where the addition of an ACE inhibitor (Aliskiren) did not improve kidney disease despite causing a reduction in the urinary albumin-to-creatinine ratio (Parving *et al.* 2012). Therefore, further studies are needed to prove or not the complete benefits of proteinuria reduction and better renal outcomes.

Smoking and alcohol consumption

Tobacco and alcohol consumption are associated with increased CV risk and with GFR decrease. Smoking-induced renal function impairment is stimulated by sympathetic activation, increased endothelin production and impaired endothelial cell-dependent

vasodilatation (Orth *et al.* 1997, Orth 2000, Ritz and Orth 2000, Orth 2004, Orth and Hallan 2008). In the United States, a prospective observational study of 20 years of duration analysed data from 23 534 people and identified a significantly high risk of CKD in individuals that smoked cigarettes with a hazard ratio of 2.9 in women and of 2.4 in men (Haroun *et al.* 2003). Cigarette smoking was also identified as an independent risk factor for diabetic nephropathy due to increased inflammation and microvascular dysfunction (Cignarelli *et al.* 2008). Therefore, CKD patients are strongly encouraged to quit this habit.

Nephrotoxicity

Use of illicit drugs along with nephrotoxic drugs such as NSAIDs can cause papillary necrosis and therefore haematuria. Intra-arterial infusion of radiocontrast agents causes initial vasodilation, followed by vasoconstriction resulting in medullary ischemia. Direct cytotoxicity to the tubular epithelial cells has also been observed (Solomon *et al.* 2009, Traub *et al.* 2013).

Obesity

The increasing rate of obesity in the world is a major problem. Overweight and obesity promote the development of insulin resistance, impaired glucose tolerance and consequent Diabetes Mellitus, metabolic syndrome, increased hypertension and cardiovascular risks. Histological changes comprise glomerulomegaly with or without focal segmental glomerulosclerosis (FSFS) (Kramer 2006, Hossain *et al.* 2007, Griffin *et al.* 2008, Goumenos *et al.* 2009, Kawar *et al.* 2009, Othman *et al.* 2009).

Malnutrition

Malnutrition is also a risk factor for the progression of CKD and it is associated with an increased risk of morbidity and mortality amongst those patients (Garg *et al.* 2001, Kuhlmann MK 2007). It can also be a consequence of CKD, especially at stages 4 and 5 where it is reported to affect roughly 40-50% of patients undergoing RRT as there is a spontaneous reduction of protein intake, poor appetite and fatigue in these patients. It can lead to the development of infections, MIA syndrome (Malnutrition Inflammation and Arteriosclerosis) and concomitant comorbidities that can worsen the prognosis of renal disease.

Later referral to the nephrologist

It was demonstrated that patients who are referred to a nephrologist at later stages of the disease are at an increased risk of CKD progression and premature death. Timely referral to the specialist is associated with better CKD management including modification of risk factors, more controlled haemoglobin levels and minimization of metabolic disturbances such as hyperuricemia and hyperparathyroidism (Levin 2001, Avorn *et al.* 2002, Kazmi *et al.* 2004, Jones *et al.* 2006).

Poverty

Several studies have revealed that a lower socioeconomic status is directly related to elevated incidence of ESRD (Young *et al.* 1994, Thamer *et al.* 1999, Cass *et al.* 2001, Forel *et al.* 2003, Maheswaran *et al.* 2003, Merkin 2008, Ward 2008). Diverse reasons can justify this inverse correlation between income level and ESRD incidence. These include: inequalities in the access of preventive health care and subsequently to dialysis treatment and renal transplantation, poor nutritional status, higher exposure to infectious diseases and to nephrotoxins and precarious urban environmental characteristics.

1.6. Pathology of Kidney Fibrosis

Despite this variety of factors that influence the progression of CKD to ESKD, its pathological mechanisms follows a final process characterised by the excessive accumulation of Extracellular Matrix (ECM) and consequent development of kidney fibrosis and scarring (el Nahas 1995, Liu 2006). Renal fibrosis is often characterized by glomerulosclerosis, tubulointerstitial fibrosis, vascular sclerosis, interstitial leukocyte infiltration and a reduction in the number of functioning nephrons. A representative microscopic photographs of progressive glomerulosclerosis (A-D) and Tubulointerstitium scarring (E-H) is shown in figure 1.4.

1.6.1. Glomerulosclerosis

Glomerular damage is usually initiated by localised loss of glomeruli, intracapillary hypertension, immunological injury, metabolic disorders and genetic defects (Schlondorff 2008). Subsequent expansion of the mesangial matrix and basement membrane is seen, often mediated by chemokines. Podocytes become hypertrophic with eventual apoptosis and glomerulosclerosis. Loss of podocytes leads to reduced vascular endothelial growth factor (VEGF) production and thereby glomerular endothelial apoptosis. Under these circumstances the glomeruli alter their permselectivity leading to proteinuria and the glomerular capillary flow is reduced causing tubular ischaemia and hypoxia.

1.6.2. Tubulointerstitial Fibrosis

The tubulointerstitial compartment plays a significant role in renal function and consequently the progression of renal disease as it accounts for over 90% of kidney cortical tissue (Nath 1998). Tubulointerstitial fibrosis can be initiated by an inflammatory process and is associated with tissue hypoxia resulting from reduced glomerular capillary flow and Angiotensin induced vasoconstriction, initiating the expression of cell adhesion molecules (ICAM-1 and VCAM-1) and upregulation of various chemokines, cytokines and growth factors such as Interleukins 1

and 8, Tumour Necrosis Factor α (TNF- α), Connective Tissue Growth Factor (CTGF), Bone Morphogenic protein 7, platelet-derived growth factor (PDGF) and Monocyte Chemoattractant protein-1 (MCP-1) (Boor and Floege 2011, Liu 2011). In addition, intracellular signal transduction pathways including the TGF β /Smad, integrin-linked kinase (ILK) and Wnt/ β -catenin signalling induce a concomitant epithelial mesenchymal transformation (EMT) which leads to the appearance of interstitial fibroblasts and *de novo* expression of α -smooth muscle actin (α SMA) with subsequent increased ECM deposition (Liu 2010).

Figure 1.4: Development of kidney fibrosis

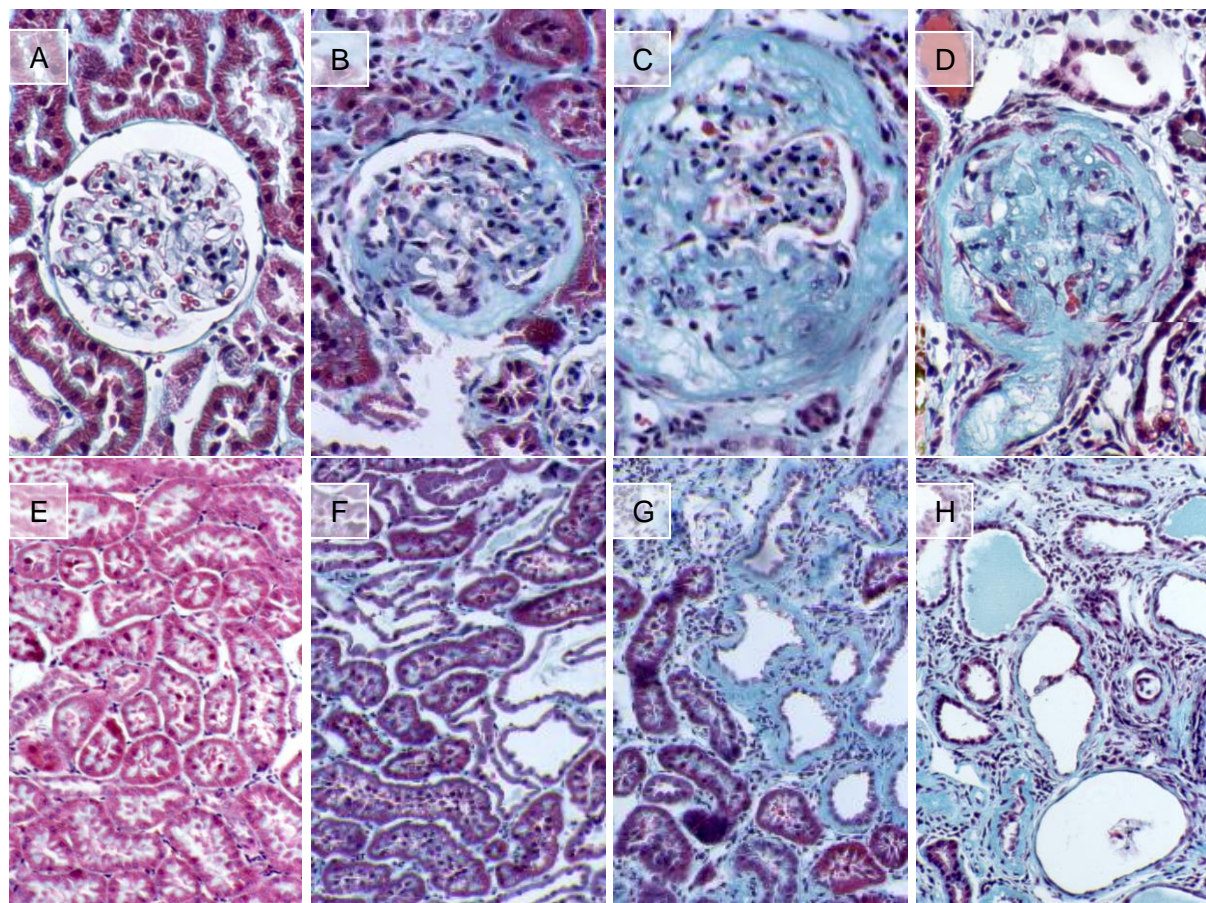


Figure 1.4: Histological development of glomerulosclerosis (A-D) and Tubulointerstitium scarring (E-H): Normal Glomerulus by light microscopy (A) showing thin capillary loops and endothelial and mesangial cells. (B), Mesangial hypercellularity. (C) and (D) progressive stages of sclerotic glomerulus. (E), normal tubules, surrounded by Tubular Basement Membrane (TBM) with small interstitium space. (F) shows dilated tubules and interstitium oedema. (G), segmental interstitial fibrosis and (H) development of diffuse interstitial fibrosis with deposition of Extracellular Matrix (ECM).

1.7. Mechanisms of Kidney Fibrosis

Kidney fibrosis is the common final outcome of most cases of progressive chronic kidney disease (Hewitson 2012). Following kidney damage, independently of the original nephropathy, there is a complex cascade of multiple cellular and molecular events (table 1.5).

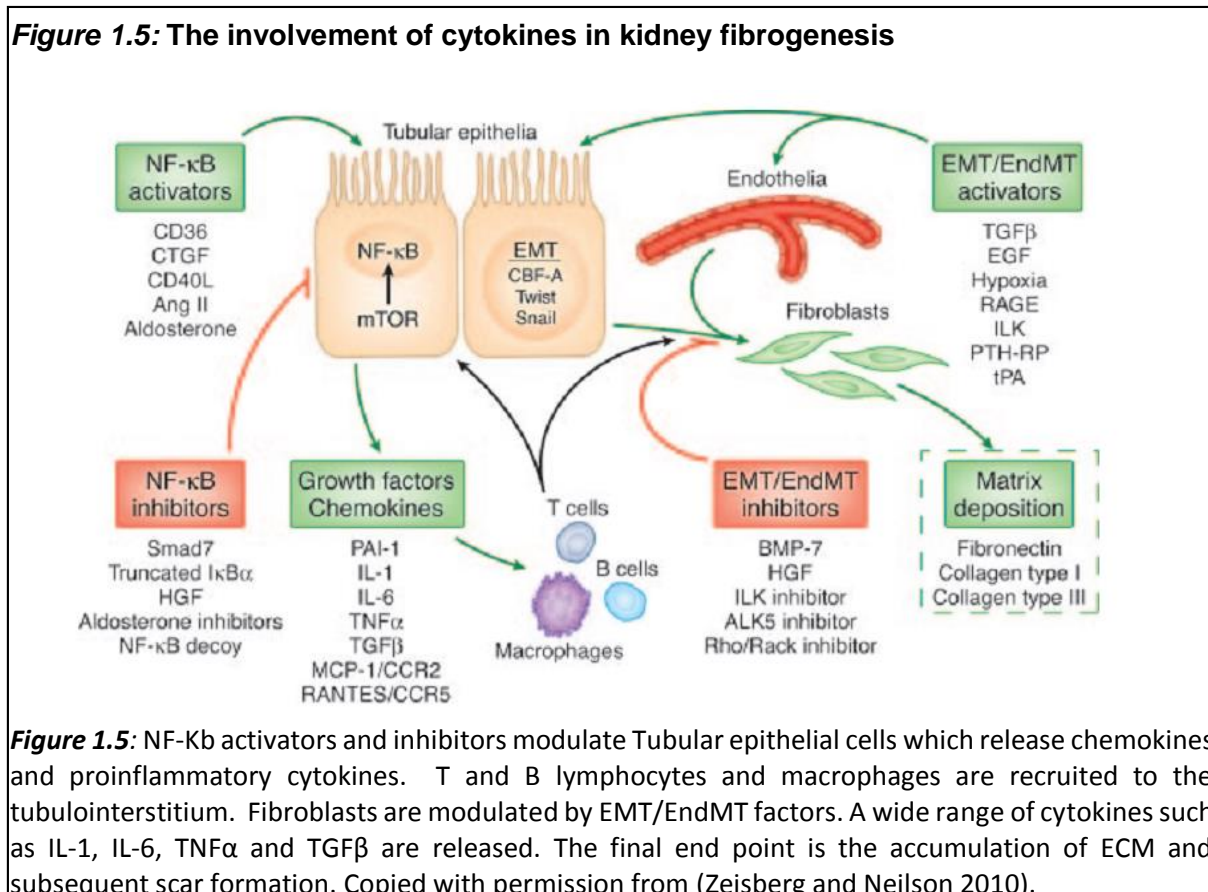
Briefly, this involves haemodynamic, immune and metabolic changes that injure endothelial cells, leading to the release of chemokines and cytokines initiating an inflammatory process (el Nahas and Coles 1997, Eddy 2000, Klahr and Morrissey 2003). In this process, mesangial and endothelial cells start to proliferate and dedifferentiate. This dedifferentiation is mediated by the action of several fibrogenic growth factors such as TGF- β 1, which can dedifferentiate epithelial and endothelial cells into a myofibroblast phenotype that produce ECM components, such as Types I and III Collagen (Boor and Floege 2011, Meran and Steadman 2011). Myofibroblasts can also result from activated residential fibroblasts, bone marrow fabrication, vascular pericytes, endothelial-to-mesenchymal transition (EndMT) or endothelial-fibroblast transition (He *et al.* 2013) via regulation of microRNAs (Srivastava *et al.* 2013).

TGF- β 1 can also promote podocyte apoptosis and consequential podocytopenia (Lopez-Hernandez and Lopez-Novoa 2012) as well as induce CTGF and bFGF production which are capable of inducing fibroblast proliferation and matrix protein synthesis (Liu 2011). Fibroblast activation and proliferation is mediated by numerous factors such as the hypermethylation of RASAL1 (RAS GTPase protein activator like 1) (Bechtel *et al.* 2010), hypoxia (Tanaka and Nangaku 2010), high glucose (Lam *et al.* 2004) and Angiotensin II (Faulkner *et al.* 2005). As a result of this inflammatory process, the fibrotic matrix becomes filled with fibrillar material such as fibronectin, collagens types I, III, IV and V, integrins and various fibrillins such as TGF β -binding proteins (LTBP) (Zeisberg and Neilson 2010) (figure 1.5). The increased synthesis of ECM components by fibroblasts associated with elevated deposition by Transglutaminase 2 and/or decreased breakdown by collagenolytic enzymes such as matrix metalloproteinases (MMPs) and Plasmin ultimately leads to ECM accumulation and subsequent formation of glomerulosclerosis, tubular atrophy and tubulointerstitial scarring (Johnson *et al.* 2007, Hewitson 2012).

Table 1.5: Phases of kidney fibrogenesis

<p>I – Induction phase</p> <ul style="list-style-type: none"> • A sustained injury sets up haemodynamic, immune and metabolic changes • Tubular epithelial cells release a wide range of chemokines and profibrogenic cytokines • Inflammatory response with infiltration of damaged kidneys by mononuclear cells • Mesangial cells proliferation and dedifferentiation • Activation and proliferation of interstitial fibroblasts and pericytes • Epithelial-mesenchymal transformation
<p>II – Inflammatory phase</p> <ul style="list-style-type: none"> • Increased synthesis and deposition of ECM • Continuous inflammatory response; release of neutrophils, T lymphocytes, macrophages, hematopoietic stem cells and other inflammatory cells
<p>III – Fibrosis phase</p> <ul style="list-style-type: none"> • Release of profibrogenic cytokines • Excessive ECM formation • Glomerular damage, tubular atrophy and microvascular rarefaction • Loss of podocytes, tissue hypoxia, apoptosis • Scar formation, progression to ESKD

Table 1.5: Irrespective of the initial causes, kidney fibrogenesis is a dynamic and complex process that consists of at least three overlapping phases: Induction, Inflammation and post-inflammation.



1.8. Models of Experimental renal scarring

Some of the best tools available to help understand the process of CKD and identify potential intervention sites are in vivo animal models. These allow us to follow the disease process from inception to ESKD with complete access to tissue and biofluids in a condensed timeframe. Several experimental models are commonly used such as the 5/6th Subtotal nephrectomy (SNx), the diabetic nephropathy (DN) and the chronic allograft nephropathy (CAN) models.

1.8.1. 5/6th Subtotal Nephrectomy (SNx)

This experimental model of renal scarring, also known as the remnant kidney model, consists of the development of chronic renal failure caused by a reduction in renal mass (Platt *et al.* 1952). The procedure involves the surgical removal of two-thirds of a kidney by either pole resection or selective ligation of renal arteries. This is followed by an unilateral Uninephrectomy which can occur at the same time or sometime later the partial resection (Gretz N 1993). This model has been used in a wide variety of animals including rats (Joo *et al.* 2013), mice (Kren *et al.* 1999), cats (Adams *et al.* 1994), dogs (Brown *et al.* 2013), rabbits and monkeys (Bourgoignie *et al.* 1994) (Adams *et al.* 1994, Bourgoignie *et al.* 1994, Kren and Hostetter 1999, Brown 2013, Joo *et al.* 2013).

The most common species to perform SNx is rat. Typically rats are subjected to a one step five-sixths nephrectomy procedure where the left kidney is removed and two-thirds of the right ligated and removed (Johnson *et al.* 2007). Following this reduction in the number of functioning nephrons, glomerular hemodynamic adaptive changes take place and leads to the development of hyperfiltration, proteinuria and systemic hypertension. Progressive increases in serum urea and creatinine concentration as well as reduced creatinine clearance are observed. Such metabolic changes produces a decrease in 5' adenosine monophosphate-activated protein kinase (AMPK) activity and subsequent hypercholesterolemia (Satriano *et al.* 2013).

These hemodynamic adaptations are associated with significant structural changes such as: glomerular and proximal tubular hypertrophy and at a late stage with progressive glomerulosclerosis and tubulointerstitial scarring. This experimental model of renal scarring typically evolves in three phases: the acute phase that develops after nephrectomy which is characterised by inflammation and hypertrophy of the remnant kidney, a stable renal function phase although there is increasing proteinuria and hypertension and a final stage where the animal develops end-stage renal failure due to focal segmental glomerular sclerosis (Kim *et al.*

et al. 2003). This progress to end-stage renal failure generally occurs within 60 to 180 days. Although this experimental model resembles several aspects of the development of human CKD, it lacks the association with further risk factors for CKD progression such as vascular damage. However, in a recent study, the use of a Nitric Oxide synthase inhibitor combined to a high salt diet after SNx improved this aspect as it promoted endothelial dysfunction (van Koppen *et al.* 2013).

1.8.2. Diabetic Nephropathy

A large number of animal models of Diabetic Nephropathy (DN) have been used to resemble either type I or type II human diabetes. Experimental Diabetic Nephropathy is most often induced in rodents (Brosius *et al.* 2009, Kong *et al.* 2013), but can also be done in monkeys (Liu *et al.* 2013), hamsters (Inenaga *et al.* 2002) and other animals. Type I diabetes is usually induced by the performance of pancreatectomy or administration of either alloxan or streptozotocin; agents that cause pancreatic β cell failure (Lenzen 2008). On the other hand, type II diabetes can be generated by mutations in the gene that encodes the leptin receptor, *agouti* mutations or a high-fat diet to induce obesity and insulin resistance (Soler *et al.* 2012). However, although these animal models exhibit many features in common with the development of diabetic nephropathy in humans, they also show some morphological and functional differences.

In humans with type I or II diabetes, the development of nephropathy can be subdivided into four categories (Class I - IV) according to the degree of severity of the glomerular lesions. Class I is observed at onset of diabetes and is characterised by glomerular hypertrophy and hyperfunction. Class II is characterised by glomerular alterations such as mild mesangial expansion, thickening of the capillary basement membranes and ECM expansion. This stage generally occurs 10-15 years after the disease is diagnosed and is characterised by the presence of microalbuminuria. In the Class III, patients develop clinical nephropathy which is marked by persistent proteinuria, Kimmelstiel-Wilson lesions, arteriolar hyalinosis and progressive decline of kidney function. As disease progresses, global glomerulosclerosis takes place (Class IV) and patients will develop end-stage renal failure (Tervaert *et al.* 2010).

Diabetic rats express similar early morphological alterations as well as increased glomerular filtration and proteinuria in the same way as diabetic patients in the first stage of nephropathy. They also produce comparable characteristics as in Class II. But, diabetic rats do not mimic late morphological features such as nodular Kimmelstiel-Wilson lesions, capillary occlusion and progressive decline in kidney function in the same extent as observed in advanced human

DN. Therefore, novel models of DN were developed to overcome this issue of inconsistent expression of late histopathological changes in diabetic rats. These include the knockout of endothelial nitric oxide synthase (eNOS3) model (Zhao *et al.* 2006), the development of a new inbred transgenic strain of mice (BTBR; black and tan, brachyuric) with the ob/ob leptin-deficiency mutation (Hudkins *et al.* 2010) and the GIPR(dn) transgenic mice model which express the mutated human glucose-dependent insulinotropic polypeptide receptor (GIPR) (Herbach *et al.* 2009).

The Animal Models of Diabetic Complications Consortium (AMDCC) established validation criteria for murine models of diabetic nephropathy so that these could try to replicate features of human nephropathy. These include: decline in GFR greater than 50% over the lifetime of the animal, increase in albuminuria greater than 10 fold compared with controls for that strain at the same gender and age, and renal pathology with advanced mesangial matrix expansion, nodular sclerosis, mesangiolysis, any degree of arteriolar hyalinosis, tubulointerstitial fibrosis and thickening of GBM by over 50% of baseline (Brosius *et al.* 2009).

One model of DN that is in accordance with the AMDCC criteria is based on the development of diabetes by the administration of streptozotocin but after an uninephrectomy. Following the induction of diabetes, renal vasodilation and glomerular hypertrophy occur as well as increased GFR and intraglomerular hypertension (Huang *et al.* 2009). These changes occur early in the disease before nephrons loss has occurred. Progressive mesangial expansion and subsequent proteinuria are observed within 1 to 3 months after streptozotocin administration. The development of glomerulosclerosis can take up to 18 months to develop without uninephrectomy as this causes systemic hypertension and thus reduces the development of glomerulosclerosis to 8 months.

1.8.3. Chronic Allograft Nephropathy

Chronic allograft nephropathy (CAN) is the major cause of kidney transplant failure. It is associated with the development of glomerulosclerosis, progressive interstitial fibrosis, tubular atrophy and obliterative arteriopathy. CAN is characterised by progressive loss of renal tissue and ECM deposition, culminating in kidney fibrosis and failure (Nankivell *et al.* 2001, Morales 2005). The pathogenesis of CAN is due to the interaction of both immune (acute rejection, alloantibody, allorecognition and viral infections) and non-immune risk factors (reduced renal mass, ischaemia-reperfusion injury, old donor age and calcineurin toxicity) leading to renal scarring (Joosten *et al.* 2004, Lutz *et al.* 2006, Akalin *et al.* 2007).

A typical experimental model of CAN is performed on male Fisher (F344) and Lewis (LEW) rats (Shrestha *et al*, 2014). In this model, donor kidneys obtained from Fisher rats (allograft) or Lewis rats (isograft) were transplanted into Lewis rats. Both isografts and allografts are given Cyclosporine for 10 days to prevent acute rejection. As the development of glomerulosclerosis is considerably prolonged, a nephrectomy of the right native kidney is carried out 10 days after transplantation to accelerate the kidney scarring process. CAN develops over a 12 month period.

1.9. Extracellular Matrix turnover

1.9.1. ECM deposition

All ECM is in a continuous state of turnover including that forming the interstitial matrix and basement membranes. The ECM acts to provide a complex three-dimensional structural support to the cells and regulates intercellular communication amongst many other vital cellular functions such as migration, polarity, adhesion, proliferation, differentiation and survival (Jarvelainen *et al*. 2009, Frantz *et al*. 2010). These ECM-cell interactions are modulated by a group of molecules named “matricellular proteins” which include thrombospondin-1 and -2, SPARC (secreted protein, acidic and rich in cysteine), tenascin-C, fibulin, CCN proteins (CYR61/CTGF/NOV), and osteopontin (Bornstein 2009). These signalling events are dependent on the interactions of such proteins with ECM adhesion receptors such as Integrins, growth factor receptors and proteoglycans (Kim *et al*. 2011). In the kidneys, the ECM forms the structural basis of the glomerular mesangium and the interstitium. Continuous turnover of ECM proteins is fundamental for tissue homeostasis and is kept by a balance between the deposition and degradation of its components (figure 1.7). Excessive ECM accumulation leads to scar formation and consequent distortion of the fine renal architecture, resulting in the collapse of its parenchyma and loss of kidney function.

ECM deposition is driven by intracellular synthesis of ECM proteins (as discussed above). These proteins include various Collagens types, Elastin, Non collagenous glycoproteins (such as Fibronectin, Tenascin, Osteonectin, Laminin and Thrombospondins) and Proteoglycans including hyaluronan (Jarvelainen *et al*. 2009). Numerous chemokines and profibrogenic cytokines (e.g. Fibroblast growth factor 23 (FGF23), Platelet-derived growth factor (PDGF), Epidermal growth factor (EGF), Connective tissue growth factor (CTGF), basic fibroblast growth factor (bFGF), IL-1, IL-6, IL-7, TNF α and TGF β 1) stimulate a myriad of intracellular signalling cascades that will lead to the transcription of matrix proteins (Boor and Floege 2011, Hsieh *et al*. 2012, Yang *et al*. 2012, Kovesdy and Quarles 2013, Staruschenko *et al*. 2013).

Fibronectin is one of the first proteins to be up regulated and is thought to form a scaffold for the deposition of other proteins in scarred tissue. Increased synthesis of Collagens type IV, V and VI in addition to Laminin has been observed in normal ECM homeostasis (figure 1.6). Furthermore, an additional synthesis of ECM components that are not normally found in the glomeruli under physiological conditions, such as Collagen type I and III, has also been demonstrated (Miyazaki *et al.* 2003).

Once secreted, ECM proteins need to be deposited by specific enzymes such as Tissue Transglutaminase and Lysyl Oxidase (Miyazaki *et al.* 2003, Eikmans *et al.* 2004). Tissue Transglutaminase has a decreased role in normal deposition pathways than that seen after insult, when it is linked to rapid ECM deposition (discussed in section 1.9.1). Lysyl Oxidase is involved in collagen biosynthesis and in the conversion of lysine and Hydroxyproline residues unto stable crosslinks between collagen fibrils (Kagan 2000). Different cell types have different capacities to synthesise and deposit ECM. Fibroblasts are the greatest producers of interstitial collagens for example, while tubular epithelial cells can synthesise considerable amounts of basement membrane proteins such as Collagen IV.

Figure 1.6: Schematic structure of the ECM

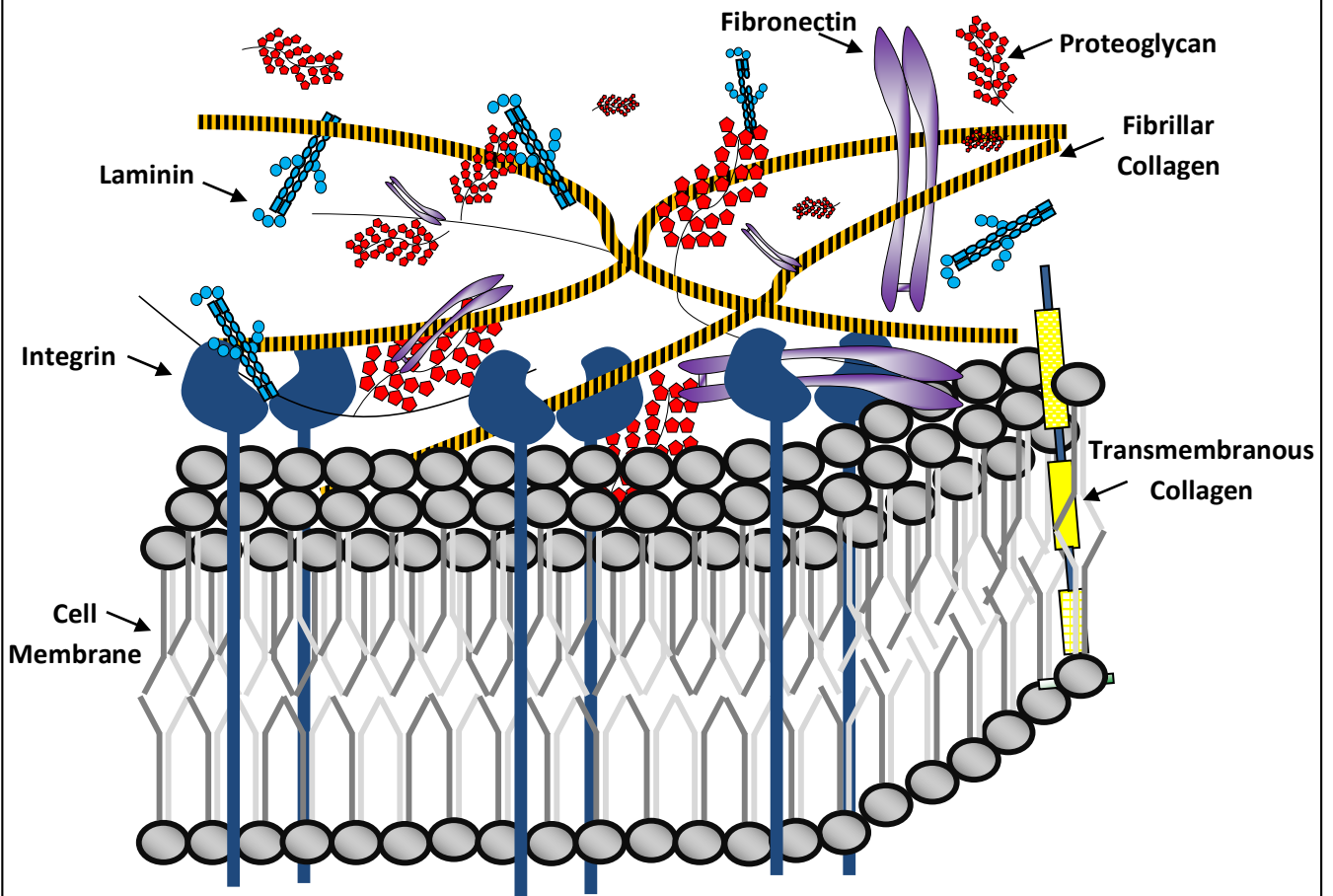
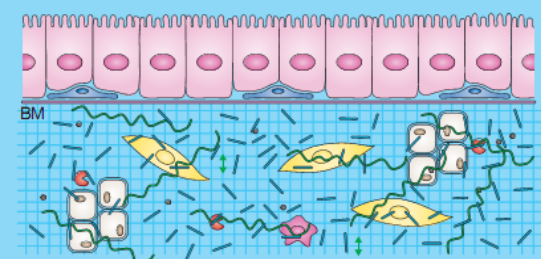


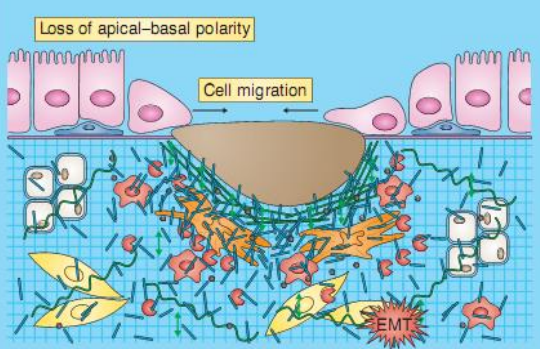
Figure 1.6: The ECM provides mechanical and structural support to cells and tissues as well as modulates major cell signalling processes. It is formed by numerous proteins including diverse Collagens types, Elastin, non-collagenous glycoproteins such as Fibronectin, Tenascin and Laminin, and Proteoglycans.

Normal



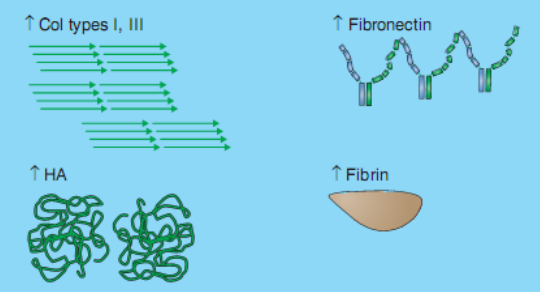
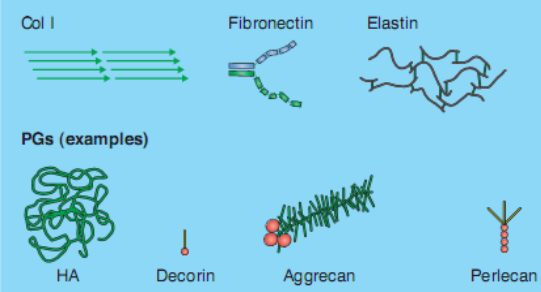
- Epithelial cell (apical-basal polarity)
- Fibroblast (secreting ECM precursors and reorganizing the ECM)
- Adipocyte (each surrounded by a secreted thick basal lamina)
- Myoepithelial cell (in contact with BM)
- Collagen-crosslinking enzymes
- Inflammatory cell (infiltration from blood and lymph vessels)
- MMP
- Proteoglycans (PGs) and glycosaminoglycan chains
- Col I
- Fibronectin

Wounded or fibrotic



- Fibrin blood clot
- Myofibroblast (differentiated fibroblast)
- Activated infiltrated inflammatory cell
- Epithelial-to-mesenchymal transition

Molecular composition



Biological and mechanical properties

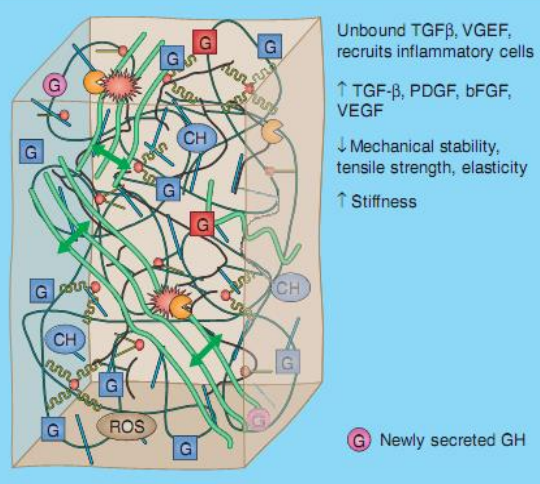
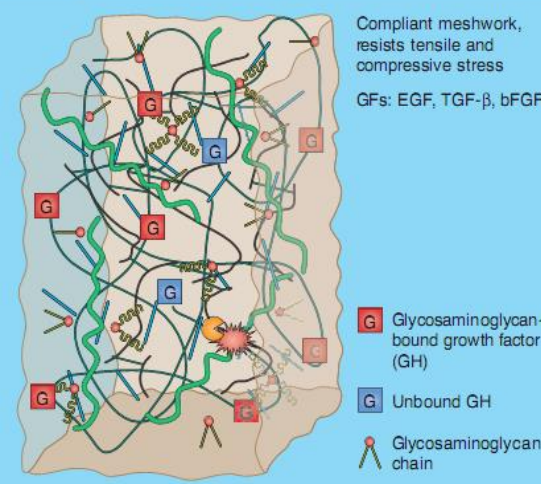


Figure 1.7: The main molecular components of normal and fibrotic ECM

1.9.2. ECM breakdown

ECM levels are also regulated through the degradation of its components. The degradation of the ECM is mediated by the activity of two collagenolytic systems, the Matrix Metalloproteinases (MMPs) (Page-McCaw *et al.* 2007) that can degrade most types of ECM proteins and the Plasminogen-Plasmin system (Eddy 2009), which also can degrade a variety of ECM substrates such as Proteoglycans, Laminin, Fibronectin, and Collagens III, IV and V. These enzymes are regulated by their inhibitors; Tissue Inhibitor of Metalloproteinases (TIMPs) and Plasminogen Activator Inhibitor (PAI) respectively. A loss of equilibrium ECM metabolism, such as an increased synthesis or deposition of its components and/or decreased breakdown causes an accumulation of ECM and consequently scar formation and fibrosis.

1.10. ECM related molecules involved in the scarring process

1.10.1. Transglutaminase 2

Transglutaminases (EC 2.3.2.13) are a family of proteins first described in 1957 by Clarke *et al.* (Clarke *et al.* 1957). So far there are nine characterised family members, one consists of a structural protein (protein 4.2) and eight encode active enzymes: Factor XIII (Fibrin Stabilizing factor), Keratinocyte transglutaminase, Transglutaminase 2, Epidermal Transglutaminase, Prostate Transglutaminase, TGM X, TGM Y and TGM Z (Lorand and Graham 2003, Iismaa *et al.* 2009). These enzymes catalyse at least five types of post-translational modification of proteins that can be subdivided into three categories: transamidation through acyl-transfer reactions by the formation of proteinase resistant ϵ (γ -glutamyl) lysine isopeptide bonds or through incorporation of primary amines at selected peptid-bound glutamine residues, esterification by the binding of an alcohol, and hydrolysis (Iismaa *et al.* 2009).

All members of this family have four structurally distinct domains: an NH₂-terminal β -sandwich, an α/β catalytic core containing a triad of Cys-His-Asp or Cys-His-Asn, and two COOH-terminal β -barrel domains that undertake a compressed conformation in the absence of calcium. They have been involved with a number of human disease states including celiac disease, cancer, abnormalities of coagulation, skin disorders, atherosclerosis and certain neurological diseases such as Huntington's and Parkinson's (Martin *et al.* 2006, Muma 2007, De Vivo and Gentile 2008). They are also implicated on tissue fibrosis including lung fibrosis (Olsen *et al.* 2011), liver fibrosis (Grenard *et al.* 2001) and renal scarring (Johnson *et al.* 1997, Johnson *et al.* 2003). The summary of their classification as well as their function can be seen on table 1.6.

Table 1.6: Physiological Transglutaminases and respective functions

NAME	GENE	CHROMOSOME	MW	FUNCTION
Factor XIII	F13A1	6p25-p24	83	Coagulation and wound healing
Keratinocyte transglutaminase (TG1)	TGM1	14q11.2	90	Terminal differentiation of keratinocytes
Transglutaminase 2 (TG2)	TGM2	20q11.2-q12	76	Ubiquitous, ECM stabilisation, Apoptosis
Epidermal transglutaminase (TG3)	TGM3	20q12	77	Terminal differentiation of keratinocytes
Prostate transglutaminase (TG4)	TGM4	3p22-p21.33	77	Semen coagulation
TGM X (TG5)	TGM5	15q15.2	81	Epidermal differentiation
TGM Y (TG6)	TGM6	20q11-15	Unknown	Unclear
TGM Z (TG7)	TGM7	15q15.2	81	Lung, testis
Erythrocyte protein band 4.2	EPB42	15q15-q21	77	ATP-binding protein

Transglutaminase 2 (tTG, TGase2; TG2) is a remarkably complex multifunctional protein associated with tissue stability and repair, ECM interactions, apoptosis, regulation of cell growth, differentiation, wound healing phases at multiple levels under normal and pathological situations and a wide range of biochemical functions (Verderio *et al.* 2004, Verderio *et al.* 2005). This includes the protein transamidation activity by incorporation of primary amines such as polyamines and histamine, the crosslinking of proteins via the formation of highly stable ϵ (γ glutamyl) lysine bonds, deamidation of glutamines, structural adhesion activity, GTP-binding/hydrolysing function, Ca^{+2} -dependent isopeptidase activity, and a recently found adenosine triphosphate (ATP) hydrolysis activity (Han *et al.* 2010, Gundemir *et al.* 2012). Outside the cells, TG2 promotes the interaction of integrins with fibronectin and also activates phospholipase C regulating transmembrane signalling through cell surface receptors (figure 1.8).

Figure 1.8: Biochemical activities of Transglutaminase 2

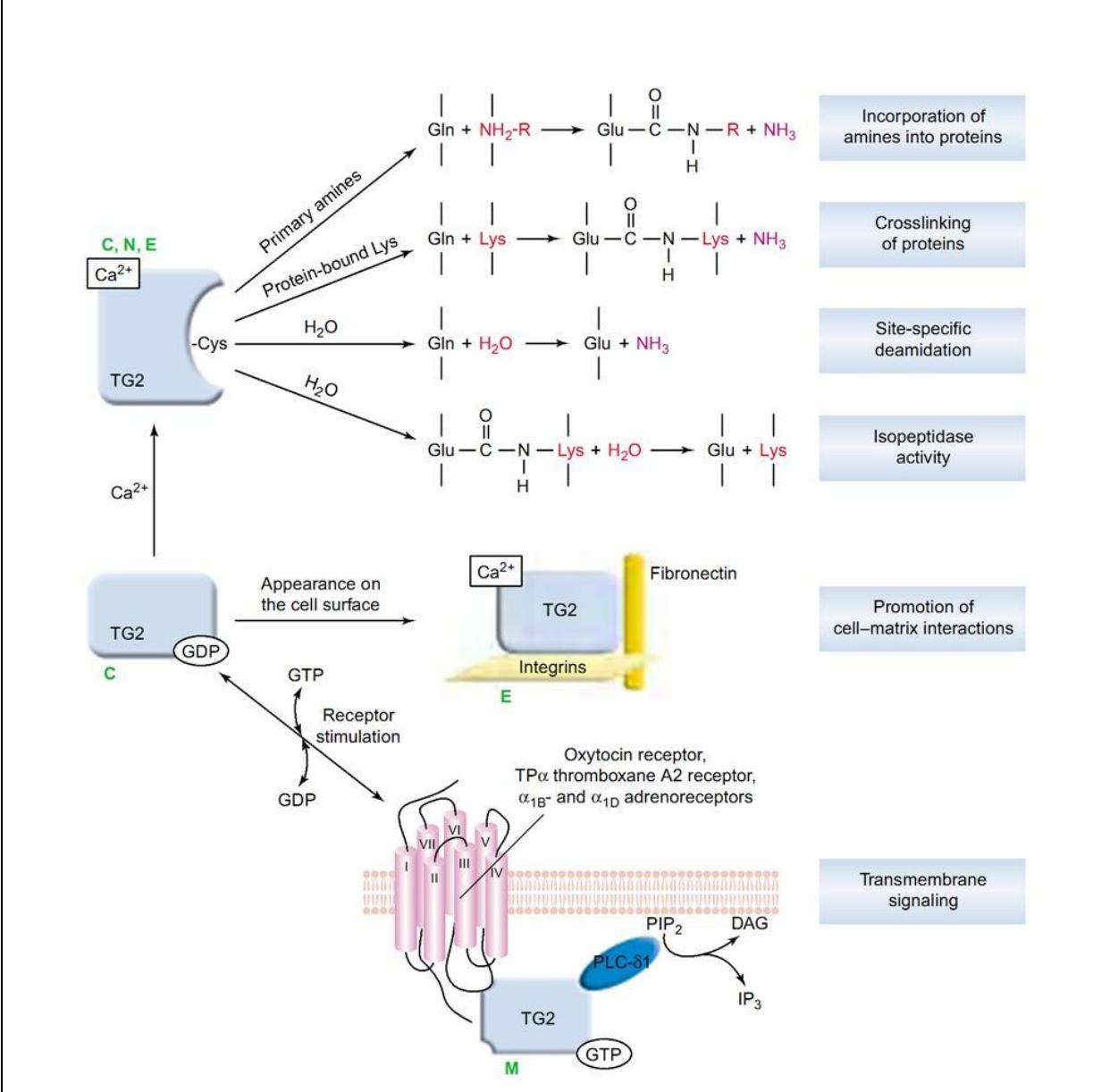


Figure 1.8: Biochemical functions of TG2. Adapted from Fesus and Piacentini: *TRENDS in Biochemical Sciences* V27, No. 10: 534-539. (Fesus and Piacentini 2002). C; cytosol, N; nucleus, E; extracellular space and M; cell membrane.

TG2 is the only member of the transglutaminase family which is ubiquitously expressed and it is notably released by epithelial cells, fibroblasts, endothelial cells, macrophages, osteoblasts and smooth muscle cells. It can be found in intracellular compartments, such as the cytosol, nucleus, endolysosomes and mitochondria, and extracellularly on the plasma membrane and in the ECM (Nurminskaya and Belkin 2012). Its extracellular release to the ECM increases in situations of tissue damage and cellular stress (Siegel *et al.* 2008).

1.10.1.1. TG2 structure

Human TG2 is a 76Kd protein, composed of 687 amino acids. It has a four-sequential domain structure: an N-terminal β sandwich (contains fibronectin and integrin binding sites), a core domain containing both the catalytic and regulatory sites and two C-terminal β -barrel domains (binds phospholipase C) (figure 1.9).

TG2 is characterised by a papain-like catalytic triad (Cys²⁷⁷, His³³⁵ and Asp³⁵⁸) on its transamidating active site (Kiraly *et al.* 2011). In addition to the catalytic triad, TG2 transamidating activity is also regulated by two conserved tryptophan residues (W241 and W332) which stabilize the enzyme-thiol intermediated formed during catalysis (Murthy *et al.* 2002, Pinkas *et al.* 2007). The catalytic activity of TG2 is positively regulated by calcium binding, which shifts TG2 to the “open” (extended) conformation by moving the β -barrel domains 3 and 4 apart from the catalytic domain 2, thus revealing the enzyme's active site (figure 1.9-B) (Pinkas *et al.* 2007). On the other hand, TG2 is negatively regulated by GTP/GDP, which inhibit it by converting it to the “closed” (compact) conformation (figure 1.9-C) (Han *et al.* 2010, Kiraly *et al.* 2011). Furthermore, a mutation of the tryptophan residue W241 to an alanine W241a knocks out TG2 transamidating activity without impacting on GTP/GDP binding (Pinkas *et al.* 2007). TG2 is kept in a latent state as a transamidase with an intracellular average GTP/ Ca⁺² ratio of ~ 150 μ M/~100nM (Gundemir *et al.* 2012) as well as in the absence of mechanical or chemical stress (Kiraly *et al.* 2011).

TG2/GDP bound structure has a unique guanidine nucleotide binding site situated between the catalytic core and the β -barrel domain 1; this is coded by exon 10 of TGM2. (Liu *et al.* 2002). When TG2 is complexed with GDP there is a blockage to the transamidation active site along with an attachment of a Tyr residue to hydrogen on the active site cysteine. Defective forms of TG2 where there is a loss of the GTP-binding site are more prone to mediate apoptosis (Datta *et al.* 2007). TG2/Ca⁺² bound structure shows conformational changes including the displacement of the hydrogen-bonded Tyr which enables the active site to be accessible (Mariani *et al.* 2000). It is believed that there are at least 5 (most probable 6) calcium binding sites and this confers different degrees of affinity of TG2 for calcium, however, the most important Ca²⁺ binding site is Cys²⁷⁷ located within the catalytic triad of the core domain (Kiraly *et al.* 2009, Gundemir *et al.* 2012).

Figure 1.9: Transglutaminase 2 molecular structure

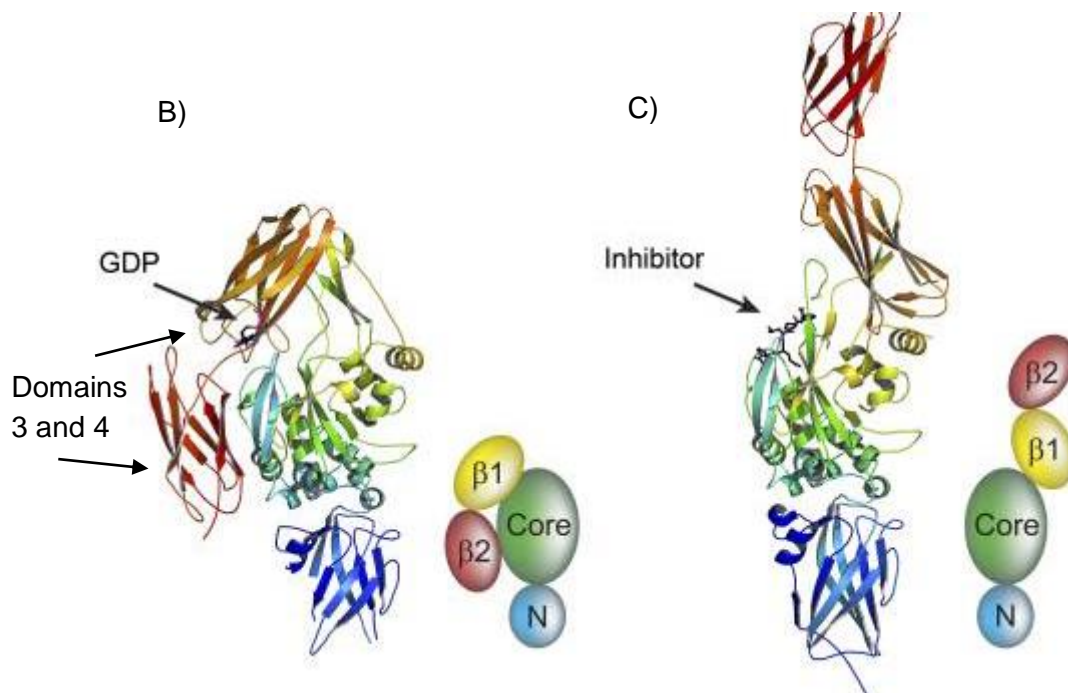
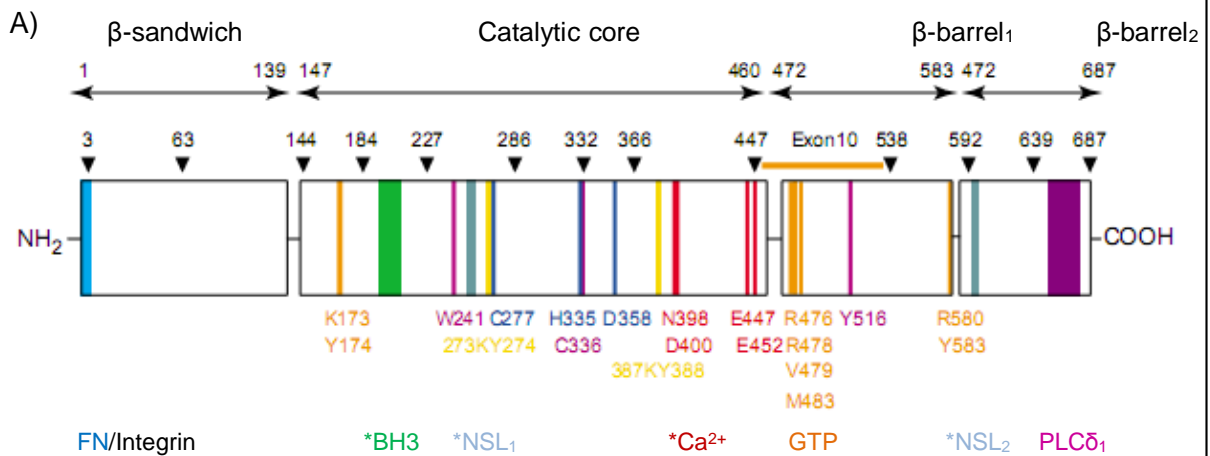


Figure 1.9: Representation of Transglutaminase 2 structure. A) Genomic organization of the four sequential protein domains. Three-dimensional ribbon structure of TG2: B) compact, inactive GDP-bound and C) extended, inhibitor-bound TG2 conformation. The four protein domains are colour-coded: the N-terminal β -sandwich is shown in blue (N), the catalytic domain (Core) in green, and the C-terminal β -barrels (β 1 and β 2) in yellow and red, respectively.

1.10.1.2 TG2 activity

It is well established that Ca^{2+} in the range of 3–100 μM is required for the activation of TG2 transamidating activity, with maximum activity seen at 5mM (Kiraly *et al.* 2011). However, the transglutaminase activity can be decreased by an interaction of TG2 with specific molecules such as sphingosylphosphocholine (Lai *et al.* 1997) and phosphoinositides (Zemskov *et al.* 2011) and increased by direct binding of TG2 to heparan sulphate proteoglycans such as syndecan-4 (Scarpellini *et al.* 2009, Verderio and Scarpellini 2010).

Transglutaminase activity is typically inhibited by GTP bounding, but can also be inhibited by nitrosylation of up to 15 of the 18 cysteine residues by nitric oxide (Telci *et al.* 2009, Santhanam *et al.* 2010). Nitrosylated TG2, without the presence of Ca^{+2} , was found to be 6-fold more susceptible to inhibition by Mg-GTP according to a study from Lai TS *et al.* 2001. Otherwise, the presence of Ca^{+2} can trigger the release of nitric oxide groups as well as regulate the S-nitrosylation and therefore activate TG2 activity (Lai *et al.* 2001). In addition, the formation of disulphide bonds between Cys370-Cys371 and Cys370-Cys230 can also result in the inactivation of the transglutaminase activity even in the presence of calcium (Stamnaes *et al.* 2010). Likewise, the generation of alternative protein spliced isoforms (Antonyak *et al.* 2006, Lai *et al.* 2007, Tee *et al.* 2010), an increased proteolytic cleavage of the molecule by trypsin (Fraij 2011), acetylation (Lai *et al.* 2010) and a highly oxidative state in the extracellular compartment in the absence of mechanical and/or chemical stresses (Siegel *et al.* 2008) were also reported to suppress the transamidating activity of TG2. On the other hand, the presence of Retinoic acid favours TG2 activity and this results in increased transamidation of RhoA and its binding to RhoA-associated kinase-2 (ROCK-2) with subsequent autophosphorylation of ROCK-2, increased kinase activity and phosphorylation of vimentin (Singh *et al.* 2001). RhoA transamidation also leads to platelet aggregation, exocytosis, modification of cytoskeleton organization and activation of MAP kinase pathway (Schoenwaelder *et al.* 2002, Singh *et al.* 2003).

1.10.1.3. TG2 transcription and externalization

The human TG2 gene is located on the 20th chromosome (20q11.2-q12). Multiple molecules can influence TG2 transcription, such as the retinoic acid (Chiocca *et al.* 1988, Nagy *et al.* 1996), histone deacetylase inhibitors (Liu *et al.* 2007), TGF β 1, TGF β 2 (Telci and Griffin 2006), TNF α (Collighan and Griffin 2009), Interferon γ (IFN γ) (Esposito *et al.* 2003), epidermal growth factor, interleukins (Aeschlimann and Thomazy 2000), corticosteroids (Johnson *et al.* 1998),

Hypoxia inducer factor (HIF) (Jang *et al.* 2010) and also DNA methylation (Lu and Davies 1997, Cacciamani *et al.* 2002).

A small portion of TG2 is exported to cell surface despite the absence of an export leader sequence. Recently, Chou *et al.* have used mutation and deletion analysis in three different renal tubular cell lines and were able to identify a vital sequence for TG2 externalization within the amino acids 88-106 in the N-terminal β -sandwich domain of TG2 (Chou *et al.* 2011).

1.10.1.4. Major TG2 functions

Transamidation function

One of the most recognized enzymatic functions of TG2 is its characteristic transamidating/protein cross-linking activity by the establishment of covalent bonds between epsilon-amino groups of primary amines such as lysine and the gamma-carboxamine group of glutamine residues (Nurminskaya and Belkin 2012) (figure 1.8). This reaction catalysed by TG2 leads to post-translational modifications of proteins such as fibrinogen/fibrin, fibronectin, collagens, dermatane sulphate proteoglycans, lipoprotein a, osteonectin, laminin, von Willebrand factor, Galectin-3, osteopontin, vitronectin and nidogen (Borth *et al.* 1991, Aeschlimann *et al.* 1992, Usui *et al.* 1993, Aeschlimann *et al.* 1995, van den Brule *et al.* 1998, Ritchie *et al.* 2000, Fisher *et al.* 2009). TG2 can also crosslink itself through its reactive lysine residues to a number of glutamine-containing substrates such as fibronectin, fibrinogen (Barsigian *et al.* 1991) and gluten peptides (Fleckenstein *et al.* 2004). The crosslinking of these proteins leads to the formation of highly stable ϵ (γ glutamyl) lysine (XL) bonds and this not only affects these protein's conformation, but also their molecular interactions, stability, and their capacity to undergo polymerization as such XL bonds are highly resistant to proteolytic degradation (Chen and Mehta 1999, Facchiano *et al.* 2006, Fisher *et al.* 2009).

Due to its protein crosslinking function, TG2 has been implicated in ECM-cell interaction and stabilization (Aeschlimann and Thomazy 2000, Fisher *et al.* 2009). Following tissue injury, accumulation of TG2 in the matrix leads to the intermolecular crosslinking of several ECM components, mainly collagens III and IV and fibronectin (Verderio *et al.* 2004). This increased rate of deposition of ECM polymers leads to increased mechanical stability and stiffness with subsequent organ scarring and fibrosis, such as pulmonary (Olsen *et al.* 2011), liver (Grenard *et al.* 2001), and kidney fibrosis (Johnson *et al.* 1999) as well as atherosclerosis (Van Herck *et al.* 2010). Johnson *et al.* (Johnson *et al.* 2007) studied the TG2 role in the rat SNx model of renal fibrosis and demonstrated that TG2 expression was increased in renal fibrotic cells and that pan transglutaminase inhibition could reduce the development of glomerulosclerosis and

tubulointerstitial fibrosis by diminishing the depositing of collagens I and III indicating its importance in the renal scarring process.

Fibronectin is one of several proteins that can be crosslinked by TG2. However, further to its crosslinking activity, plasma membrane TG2 also interacts with the gelatin-binding domain of fibronectin mediated by $\alpha 5\beta 1$ integrin and this contributes to fibrillogenesis (Akimov and Belkin 2001).

TG2 is also able to interact with microtubule-binding proteins and Tubulin- β , being linked to increased apoptosis in human neuroblastoma cells (Piredda *et al.* 1999). It was reported that TG2 can be translocated to the nuclear compartment of these cells through its interaction with the transport protein Importin $\alpha 3$ (Peng *et al.* 1999). Furthermore, it was shown that TG2 ablation decreases neuronal death (Mastroberardino *et al.* 2002).

Deamidation function

TG2 can also modify the structure of proteins by its deamidation function. TG-mediated deamidation is a variant of the transamidation reaction in which H_2O is used as a nucleophile in the absence of amine co-substrates (Lorand and Graham 2003, Facchiano and Facchiano 2009). As a result of the deamidation reaction, glutamine residues are modified to glutamic acid residues (figure 1.8). An example of TG2 deamidating function include the deamidation of peptides present in the wheat protein gliadin, causing them to become dominant epitopes for activating T cells in the pathogenesis of celiac disease (Shan *et al.* 2002, Sollid and Jabri 2005). Another example of TG2-induced protein deamidation is the deamidation of Gln15 in β -amyloid peptide what causes reduced solubility of this molecule and development of Amyloidosis (Schmid *et al.* 2011).

Protein Disulphide Isomerase function

In addition to the transamidation and deamidation functions, TG2 has also been implicated as a protein disulphide isomerase (PDI) and a regulator of mitochondrial function. The PDI activity of TG2 was shown in a study where TG2 was able to convert completely denatured / inactive RNaseA molecule into an active enzyme by the formation of disulphide bonds (Hasegawa *et al.* 2003). The same study showed that the PDI activity of TG2 is independent of calcium and not inhibited by nucleotides such as GTP. In another studies, the PDI activity of TG2 was confirmed by the formation of disulphide bridges in mitochondrial respiratory complexes I, II and V and also by configuration of the prohibitin complexes (Mastroberardino *et al.* 2006, Malorni *et al.* 2009).

Protein Kinase function

TG2 was also reported to have an intrinsic serine/threonine protein kinase activity as it was found that it can phosphorylate serine residues in a number of situations including; the insulin-like growth factor-binding protein-3 (IGFBP-3) on the surface of cancer cells (Mishra and Murphy 2004), residue Ser15 and Ser20 in the p53 tumour suppressor protein (Mishra and Murphy 2006), histones H1 and H3 (Mishra *et al.* 2006-A) and residue Ser780 in the retinoblastoma protein (Rb) in the nucleus (Mishra *et al.* 2007). Interestingly, TG2 can also phosphorylate itself by protein kinase A (PKA), and although this reaction decreases its transamidating activity, it increases the kinase activity of TG2 (Mishra and Murphy 2006-B).

GTPase and Transmembrane signaling

Another well established function of TG2 is linked to signal transduction across the plasma membrane (figure 1.8). TG2 acts as a non-canonical G protein (guanidine nucleotide-binding protein; Gh) and therefore is able to bind and hydrolyse GTP (Nakaoka *et al.* 1994). Thus, it alters the signaling function of several molecules including CD38 (Umar *et al.* 1996) and insulin-like growth factor binding protein 1 (Sakai *et al.* 2001).

TG2 also regulates other signaling pathways through its GTPase activity. It was shown that TG2 can mediate the adrenergic activation of extracellular signal-regulated kinases (ERK) and their regulatory kinases (MEK) in cardiomyocytes (Lee *et al.* 2003). Its GTPase activity was also found to promote cell proliferation induced by α_1 adrenergic receptors in hepatocytes (Wu *et al.* 2000) and myometrial cells (Dupuis *et al.* 2004) as well as in its binding with α_5 integrin subunit causing inhibition of vascular smooth muscle cell migration (Kang *et al.* 2004).

Cytoskeleton organization

A further TG2 function relates to its capacity of modifying the cytoskeleton organization by interaction with several cytoskeletal proteins such as Phospholipase C delta1 (PLCdelta1, PLC δ 1) (Iismaa *et al.* 2000), Integrins (Akimov and Belkin 2001), Tubulin- β (Piredda *et al.* 1999) and Importin α 3 (Peng *et al.* 1999).

PLC δ 1 is an enzyme that can accelerate TG2 binding to GTP γ S following an increased release of GDP from TG2. It also can mediate alpha1B-adrenoreceptor (alpha (1B) AR) – TG2 signalling (Baek *et al.* 2001). Through its GTPase activity, TG2 can form non-covalent complexes between PLC δ 1 and various transmembrane proteins such as thromboxane A2 (Veza *et al.* 1999), oxytocin (Park *et al.* 1998), the α_{1D} adrenergic (Im and Graham 1990) and follicle stimulating hormone receptors (Lorand and Graham 2003).

Apoptosis

In vitro experiments have shown that TG2 is upregulated in several cell types undergoing apoptosis. This could confer pro- or anti-apoptotic effects (Falasca *et al.* 2005, Fesus and Szondy 2005). Initial experiments showed that TG2 can crosslink major modulators of cell survival and death, such as retinoblastoma protein (Oliverio *et al.* 1997) and the pro-apoptotic enzyme DAP-like kinase (DLK) (Robitaille *et al.* 2004). One initial hypothesis was that the pro-apoptotic effect could be due to a TG2-dependent covalent polymerization of Bax throughnTG2 BH3 domain, which would induce a conformational change and translocation of Bax to the mitochondria, cytochrome-c releasing and subsequent cell death (Rodolfo *et al.* 2004). Some other studies have suggested that TG2 could exert an anti-apoptotic effect by binding to fibronectin and cell surface heparin sulphate chains (via $\alpha 5\beta 1$ integrins) promoting the activation of Rho and the adhesion-dependent survival signalling of cells (Verderio *et al.* 2003). In another study, TG2 capability to prevent apoptosis was found to be independent to its binding to fibronectin. Instead, TG2 could promote cell adhesion by regulation of PLC δ 1 (Baek *et al.* 2001).

Tissue repair

TG2 can potentially target the tissue repair process at multiple levels: incorporation of serum proteins such as Plasminogen activator inhibitor 2 (PAI-2), activation of TGF β 1 complex, post translational modification of sPLA2, phagocytic clearance, modulation of cell migration, RGD independent cell adhesion, fibril stabilisation, ECM homeostasis, apoptosis and modulation of angiogenesis (Douthwaite *et al.* 1999, Jones *et al.* 2006, Harrison *et al.* 2007).

Dermal wounding healing

TG2 was associated with increased skin strength in rats by the crosslinking of fucoprotein in the ECM. Its inhibition by the use of topical putrescine caused skin fragility and decreased wound firmness (Dolynchuk *et al.*, 1994).

Another biological function attributed to TG2 includes dermal wounding healing. It may play a role in keratinocyte basement membrane crosslinking. Pan Transglutaminase inhibitors, which also blocked TG1 and 3, were found to prevent keratinocyte terminal differentiation and consequently hyperproliferation, hyperproliferative epidermis with parakeratosis, loss of basement membrane collagen IV, enhanced expression of involucrin and cytokeratin 6 and 16 and reduction of cytokeratin 10 (Harrison *et al.* 2007).

1.10.1.5. The role of TG2 in human diseases

TG2 has been linked to a number of human diseases including coeliac disease, neurological diseases, cancer, metabolic and endocrinologic diseases, renal disease, along with other

autoimmune, inflammatory and related diseases. It can target a broad spectrum of different substrates and therefore, act on several pathologies (table 1.7).

Table 1.7: TG2 Substrates in human diseases

SUBSTRATE	REGULATION PROCESS	HUMAN DISEASE	REFERENCES
Amyloid beta A4 peptide	ND	Alzheimer	(Rasmussen <i>et al.</i> 1994)
Collagens I and III	ECM-S, PS	CKD	(Johnson, 1999 #765)
Fibrinogen A alpha	ECM-S, OTH	Amyloidosis	(Murthy <i>et al.</i> 2000)
Galectin 3	ECM-S, CB	Rheumatoid arthritis	(Mehul <i>et al.</i> 1995)
Glucagon	MED	Hypoglycaemia	(Molven <i>et al.</i> 2002)
Gluten	ECM-S, OTH	Coeliac disease	(Esposito <i>et al.</i> 2005)
Huntingtin	ND	Huntington disease	(Zainelli <i>et al.</i> 2004)
Insulin	MED	Diabetes Mellitus	(Bungay <i>et al.</i> 1984)
Keratin, type II cytoskeletal 5	DD, CR, MF	Epidermolysis bullosa	(Candi <i>et al.</i> 1998)
Myelin basic protein	ND	Multiple sclerosis	(Selkoe <i>et al.</i> 1982)
A-Synuclein	ND	Parkinson	(Andringa <i>et al.</i> 2004)
Tau protein	ND	Alzheimer	(Murthy <i>et al.</i> 1998)

Note: ND; neurological diseases, ECM-S; ECM interaction and stabilization, PS; protein stabilization, OTH; other autoimmune, inflammatory and related diseases, CB; cancer biology, MED; metabolic and endocrinology diseases, DD; dermatologic diseases, CR; cytoskeleton regulation, MF; membrane traffic and membrane structure/function.

1.10.1.5.1. TG2 in Coeliac disease

Coeliac disease (coeliac sprue, gluten-sensitive enteropathy) is an autoimmune disorder of the small intestine influenced by both environmental and genetic factors. The inflammatory injury of the small intestine mucosa occurs after the ingestion of wheat, gluten or related rye and barley proteins. It causes a malabsorption syndrome characterized by atrophy of villi in the jejunum. Following specific recognition by T cells, there is a binding of gluten peptides to HLA molecules (HLA-DQ2 and HLA-DQ8) (Dieterich *et al.* 1997, Sollid 2002, Vader *et al.* 2002). TG2 causes crosslinking of these proteins and also deamidation of glutamine side chains, creating covalent complexes via a thioester bond to the active site cysteine of TG2

(Esposito *et al.* 2005). Due to the TG2 modification on the gluten protein, the immune system cross-reacts with the small intestine causing inflammation and formation of autoantibodies anti-gliadin, anti-endomysial and IgA anti-TG2 (Vives-Pi *et al.* 2013). Recently, it was found that a materno-fetal transfer of anti-transglutaminase antibodies could cause a passive transfer model for coeliac autoimmunity (Baldassarre *et al.* 2012).

1.10.1.5.2. TG2 in Neurological diseases

Neurodegenerative disorders such as Alzheimer, Parkinson and Huntington disease have in common an elevated deposition of multimeric structures in the degenerative region of the brain, increased TG2 activity and intracellular calcium concentration (Jeitner *et al.* 2009). For instance, Alzheimer's disease is characterised by increased deposition of amyloid β aggregates and intracellular neurofibrillary complexes of tau protein. Parkinson's disease shows an accumulation of alpha-synuclein protein in the brain in the form of lewy bodies. Finally, in Huntington's disease there is a genetic mutation in which an expansion of CAG trinucleotide repeats in the gene encoding huntingtin. As a consequence, insoluble aggregates of huntingtin protein presenting polyglutamine repeats in its N-terminal domain makes it a good TG2 substrate and as a consequence are deposited in the striatum and cortex of Huntington's disease patients.

TG2 can act on several substrates in the neuron cellular compartment, including the microtubule-associated tau protein (Murthy *et al.* 1998), amyloid beta-A4 peptide (Rasmussen *et al.* 1994), alpha-synuclein (Jensen *et al.* 1995) and Huntingtin (Kahlem *et al.* 1998, Zainelli *et al.* 2004). It crosslinks these polypeptides resulting in the formation of ϵ (γ glutamyl) lysine bonds and also *bis*- γ -glutamylpolyamine bridges (Jeitner *et al.* 2008). Hence, the increased crosslinking activity of TG2 on these substrates and subsequent formation of protein aggregates is recognized to be a determinant factor on the pathogenesis of these neurological diseases.

1.10.1.5.3. TG2 in Cancer

Cancer formation and progression is a complex mechanism which includes modulation of programmed cell death, cell adhesion and motility, cytoskeleton assembly, ECM homeostasis, angiogenesis and metastatic dissemination (Kotsakis and Griffin 2007). TG2 has been implicated in all these molecular processes and so, has been related to the modulation of tumour formation and secondary metastatic progression (Di Giacomo *et al.*, 2009).

Several molecular targets associated with tumour development have been showed to be substrates for TG2. In fact, TG2 can crosslink as well as act as a non-covalent interactor with a variety of ECM proteins, integrins, galectin-3, TGF- β and nuclear proteins such as E2F and retinoblastoma protein (van den Brule *et al.* 1998, Esposito and Caputo 2005). However, TG2 has a controversial involvement in carcinogenesis. There is strong evidence that it can confer anti-apoptotic effects and subsequent chemotherapeutic resistance (Mehta 1994) as well as mediate metastasis and cancer cell progression (Mehta *et al.* 2004), but it was also described as a tumour suppressor (Mangala and Mehta 2005, Jones *et al.* 2006) and as critical for the execution of programmed cell death (Falasca *et al.*, 2005).

TG2 expression is up-regulated in a great variety of cancer types such as breast cancer (Mehta *et al.* 2004), ovarian (Satpathy *et al.* 2009, Cao *et al.* 2012), glioblastomas (Yuan *et al.* 2007), melanomas (Di Giacomo *et al.* 2009) and pancreatic ductal adenocarcinomas (Verma *et al.* 2008).

The involvement of TG2 in cancer development and progression could be due to a regulation at a transcriptional level of MMP-2 which is a major mediator of tissue invasiveness (Satpathy *et al.* 2009), integrin mediated signalling (Kotsakis *et al.* 2011), modulation of epithelial-to-mesenchymal transition (EMT) induced by TGF β , TNF α and NF- κ B (Cao *et al.* 2012, Brown 2013, Kumar and Mehta 2013), Akt phosphorylation (Verma *et al.* 2008), among other biological functions.

On the other hand, injection of TG2 in CT26 colon carcinoma tumour has shown to decrease tumour growth and even cause tumour regression in few cases (Jones *et al.* 2006). This effect was related to the fact that TG2 increased ECM proteins deposition and consequently angiogenesis inhibition. Decreased colon carcinoma growth was also related to TG2 interaction with integrin β 3, activation of TGF β 1 and subsequent increased matrix-deposited fibronectin, which promotes elevated cell adhesion and less migratory cells (Kotsakis *et al.* 2011). Notwithstanding, other different studies presented conflicting findings where TG2 could either inhibit or stimulate angiogenesis (Haroon *et al.* 1999, Haroon *et al.* 1999) and even inhibit metastasis (Mangala *et al.* 2005). Therefore, the role of TG2 in cancer biology represents a field that requires further investigation.

1.10.1.5.4. TG2 in Metabolic and Endocrinologic diseases

TG2 crosslinking and deamidation activities were observed in a number of hormones and hormone binding proteins including Insulin (Bungay *et al.* 1984, Lindsay *et al.* 1990), Glucagon (Molven *et al.* 2002), fatty acid synthase (Esposito and Caputo 2005), Glyceraldehyde 3-

phosphate dehydrogenase (GAPDH) and alpha-ketoglutarate (Schmidt *et al.* 1998). Therefore, it is an important mediator in metabolic homeostasis.

A TG2 knockout mice study showed impaired glucose-stimulated insulin secretion from pancreatic β cells (Bernassola *et al.* 2002). In addition to its role in the membrane-mediated events required for insulin release, TG2 has also been implicated in crosslinking insulin receptors in the area of clathrin-coated pits (Baldwin *et al.* 1980). It has also been demonstrated that TG2 is involved in the post-translational modification of Insulin-like growth factor-binding protein-1 (IGFBP-1) which binds and subsequently regulates cellular response to insulin-like growth factor-1 (IGF-1) (Sakai *et al.* 2001).

1.10.1.5.5. TG2 in Kidney disease

Regardless of the underlying disease, the final process of CKD is characterised by excessive accumulation of extracellular matrix what leads to fibrosis and scar formation (El Nahas 2005). TG2 has been strongly implicated in the kidney fibrotic process, being instrumental in scar tissue formation by catalysing the post-translational modification of ECM proteins by the formation of ϵ (γ -glutamyl) lysine bonds (Johnson *et al.* 1997).

A study done by Johnson *et al* using the rat 5/6th Subtotalnephrectomy (SNx) model of renal scarring demonstrated that tissue levels of TG2 and ϵ (γ -glutamyl) lysine correlate well with histological renal scarring (Johnson *et al.* 1997). Interestingly, in this study, the highest proportions of TG2 and ϵ (γ -glutamyl) lysine were found in the cytoplasm of renal tubular cells when compared to the extracellular renal interstitial space. This increased expression of TG2 is known to be modulated by many molecules, including TGF β 1 (Douthwaite *et al.* 1999).

In addition to its crosslinking activity on large latent TGF β 1 (Nunes *et al.*, 1997), TG2 can favour renal fibrosis by activation of TGF β 1. Increased TGF β 1 activation stimulates ECM deposition through the elevated synthesis of several polypeptides such as Collagen I, III and IV by mesangial cells, fibronectin by epithelial cells and proteoglycans biglycan and decorin by glomerular mesangial cells (Okuda *et al.* 1990). Conversely, a study on TG2 knockout (KO) mice showed diminished renal interstitial fibrosis due to a reduction on TGF β 1 activation and subsequent decreased deposition of fibrillar collagen and inflammation, as described on an unilateral ureteral obstruction (UUO) model of renal scarring (Shweke *et al.* 2008). Johnson *et al* demonstrated that administration of two irreversible inhibitors of TG2 (NTU281; acts mainly on the extracellular compartment, while NTU283; can also act on the intracellular compartment due to its high cell solubility) decreased the development of glomerulosclerosis

and tubulointerstitial fibrosis in rats submitted to SNx. In this study, immunohistochemical analysis showed reduced levels of collagens I and III in the remnant kidney. However, levels of active TGF β 1 were not reduced in rats treated with TG2 inhibitors in this study (Johnson *et al.* 2007).

In the rat streptozotocin model of Diabetic Nephropathy (DN), increased levels of TG2 in the peritubular interstitial space with consequential accelerated ECM crosslinking was linked to the development of DN (Skill *et al.* 2001). In a development of this model, treatment with TG2 inhibitor NTU281 was associated with reduction of myofibroblasts and collagens I, III and IV, resulting in reduced ECM deposition with improvement of kidney function (Huang *et al.* 2009) which was partly through increased active TGF β 1 levels. TG2 inhibition with NTU283 in renal proximal tubular epithelial cells (OK cells) reduced ϵ (γ -glutamyl) lysine, hydroxyproline and fibronectin levels, thus reducing ECM accumulation (Skill *et al.* 2004).

In human Diabetic Nephropathy, El Nahas *et al.* confirmed the presence of increased levels of TG2 and ϵ (γ -glutamyl) lysine by immuno-localisation in DN type 2 renal biopsies (El Nahas *et al.* 2004). Another study in human kidney disease showed a strong correlation between tissue levels of TG2 and its crosslink product and progressive renal scarring (Johnson *et al.* 2003). Thereby, TG2's role in renal fibrosis is related to increased crosslinking of the ECM that leads to its accumulation and elevated resistance to degradation by MMPs (Fisher *et al.* 2009).

1.10.2. Collagens

Collagens are the most abundant protein in the body and the major component of the extracellular matrix. They provide mechanical support in a variety of tissues including muscles, bone, cartilage, tendons, skin, heart valves, blood vessels and basement membranes (Pope and Nicholls 1987). So far 28 types subdivided into subfamilies based on their structures had been found in humans; Fibrillar, Fibril Associated Collagens with Interrupted Triple helices (FACITs), Network-forming, Anchoring fibrils, Transmembranous, Endostatin precursor and other collagens with distinct molecular assembly (Ricard-Blum 2011).

The common structural feature of collagens consists of three hydrogen bonded polypeptide α chains (662 up to 3152 amino acids) arranged in super triple helix that can range from most of their structure (96% for collagen I) to less than 10% (collagen XII) (Gordon and Hahn 2010, Ricard-Blum 2011). The most predominant are fibrillar collagens Type I (major component of tendon, ligament and, bones, corresponding to over 90% of the collagen in the body), Type II (cartilage), Type III (arteries, intestine, uterus and renal interstitium) and collagen IV (form

network-like structures including basal lamina of epithelia, glomerular and tubular basement membranes). Type V is a less common component and is present mainly in the hair, cell surfaces and placenta (Gordon and Hahn 2010). Collagen types I, II, III, V and XI self-assemble into D-periodic cross-striated fibrils (Kadler *et al.* 2007). The huge heterogeneity of the collagen family is a consequence of the existence of several different α chains, various distinct molecular isoforms and supramolecular structures for the same collagen type, and the use of alternative promoters and splicing variants. Numerous collagens (IX, XII, XIV, XV, XVIII) bear glycosaminoglycan chains (chondroitin sulphate and/or heparan sulphate chains) and therefore are considered also as proteoglycans (Ricard-Blum 2011).

Collagens are mainly synthesized by fibroblasts, osteoblasts, chondrocytes and mesangial cells, although epithelial cells can also synthesise them. Collagen types and their respective domain structures can be summarised into distinct families (table 1.8).

Table 1.8: Structural characteristics of collagens

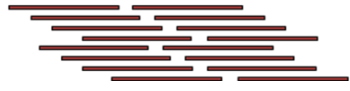
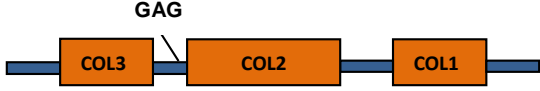
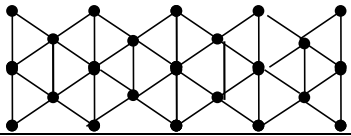
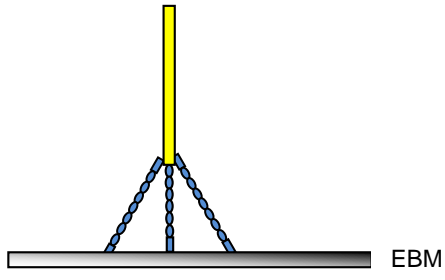
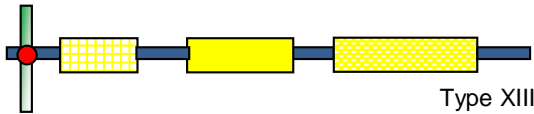






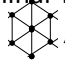

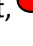
Collagen subfamily	Collagen types	α chains assembly
Fibrillar collagens	I, II, III, V, XI, XXIV, XXVII	
Fibril associated collagens with interrupted triple helices (FACITs)	IX, XII, XIV, XVI, XIX, XX, XXI, XXII, XXVI	 Type IX
Network-forming collagens	IV, VI, VIII, X	
Type VII collagen forming anchoring fibrils	VII	 EBM
Transmembranous	XIII, XVII, XXIII, XXV	 Type XIII
Endostatin precursor	XV and XVIII	 Type XV
Other collagens	XXVII, XXVIII	 Type XXVII

Table 1.8: Collagen types and their trimeric molecules. The collagen family comprises 28 members subdivided in subfamilies according to their domain composition and supramolecular assembly of α chains. GAG; glycosamino glycan side chain, EBM; epithelial basement membrane, TSP; thrombospondin N terminal repeat, ; fibrils,  and ; gly-X-Y domains, ; noncollagenous domain, ; hexagonal lattice, ; fibronectin type III repeat, ; transmembrane domain.

1.10.2.1. Collagen biosynthesis

Collagens are synthesised by a multistep process characterised by a large number of co and post-translational modifications mediated by highly specific enzymes (e.g. prolyl 3-hydroxylase, prolyl 4-hydroxylase, Lysyl Hydroxylase, n terminal collagen protease and lysyl oxidase amongst others). In a first step, a three dimensional stranded structure is assembled forming the precursor pre procollagen. This structure presents the amino acids glycine and proline as its principal components. Then, several molecules including vitamin C and Ascorbate modulate the conversion of pre procollagen to collagen (Myllyla *et al.* 1984, Boyera *et al.* 1998). This conversion involves a hydroxylation reaction that substitutes a hydroxyl group for a hydrogen atom in the proline residues at certain points in the polypeptide chains, converting those residues to hydroxyproline (C₅H₉O₃N). This hydroxylation reaction is catalysed by two different enzymes: prolyl-4-hydroxylase and lysyl-hydroxylase (Gorres and Raines 2010). In the folding step, the collagen's structure will consist of three hydrogen bonded polypeptide α chains forming a super helix containing non-collagenous sequences (NC domains) at their termini. In the final step, collagen fibers are formed by lysyl oxidase crosslinking. The resultant super helix structure is composed of polypeptide chains containing at least one domain with Gly-X-Y sequences (X; Proline and Y; 4-Hydroxyproline) and formed by the amino acids glycine, proline, Hydroxyproline and Hydroxylysine (Prockop and Kivirikko 1995, Shoulders and Raines 2009). Hydroxyproline constitutes a major component of the collagens, around 1/6th of its total structure. It is found in few proteins other than collagen (e.g.; elastin). Therefore, the presence of Hydroxyproline is a strong indicator of the presence of collagen.

1.10.2.2. Covalent crosslinking of Collagens

Collagens can undergo crosslinking by a range of different pathways. Transglutaminase 2 catalyses the formation of stable and insoluble ϵ (ν glutamyl) lysine isopeptide linkages in collagens I, III, IV, V, VI, VII, XI and XVI (Esposito and Caputo 2005, Collighan and Griffin 2009, Wang and Griffin 2012). Likewise, mature crosslinks of lysine, hydroxylysine, and histidine residues present in collagens I, II, III, V, IX and XI can be produced by the enzyme lysyl oxidase (Eyre and Wu 2005, Wu *et al.* 2009, Wu *et al.* 2010). Also, advanced glycation end-reaction products (AGEs) can form intermolecular crosslinking between two adjacent molecules such as lysine to lysine or lysine to arginine residues from collagen molecules within the fibre resulting in increased stiffness (Avery and Bailey 2006). A good example of AGEs crosslinking is the action of Glucosepan on ECM collagens (Sjoberg and Bulterijs 2009).

Furthermore, it was recently identified a sulfilimine bond (-S=N-) crosslink between hydroxylysine-211 and methionine-93 in collagen IV (Vanacore *et al.* 2009).

1.10.2.3. Collagen degradation

Collagen degradation occurs through a two-step process that involves an extracellular and an intracellular pathway. The extracellular pathway involves cleavage of collagen fibrils by proteolytic enzymes including the Matrix metalloproteinases (MMPs). All collagens can be degraded by most MMPs, however, this degradation is mediated by recognition of specific cleavage sites. Thus some MMPs had been shown to have preferential substrates for cleavage (Song *et al.* 2006). For example, fibril-forming collagens I, II, and III are cleaved by MMP-1 (interstitial collagenase), MMP-8 (neutrophil collagenase), MMP-13 (collagenase 3) and by membrane-anchored MMPs 14 and 16 (Ricard-Blum 2011). Collagen I is also degraded by MMP-2, whilst collagen II is a preferential substrate of MMP-13 and collagen IV can be cleaved by MMPs 2 and 9 (Klein and Bischoff 2011). Moreover, collagens can also be degraded by other membrane bound and soluble proteases such as subtilisin (Ran *et al.* 2013) as well as by urokinase/tissue type plasminogen activator (uPA/tPA) and plasmin (Ghosh and Vaughan 2012). The intracellular pathway involves binding and uptake of collagen fragments by fibroblasts and macrophages for lysosomal degradation by molecules such as cathepsins K and S which are two lysosomal cysteine proteases (Pietschmann *et al.* 2013).

1.10.2.4. The role of Collagens in human diseases

Collagen-related diseases are predominantly linked to genetic defects or mutations, nutritional deficiencies that alters their biosynthesis, unbalanced assembly into the matrix, changes in the posttranslational modification, secretion, or in other mechanisms implicated in collagen production (Gelse *et al.* 2003). Mutations in the collagens structure have been linked to a diverse range of human diseases, such as Osteogenesis imperfecta and Marfan's syndrome in collagen type I mutation (Gajko-Galicka 2002), Ehlers-Danlos Syndrome type IV in collagen type III mutation (Pope and Nicholls 1987, Kuivaniemi *et al.* 1991) and Leiomyomatosis in collagen type IV mutation (Hudson *et al.* 1993) (table 1.9).

Table 1.9: Collagens types and their role in human diseases

Collagen type	Genes	Human disease	References
I	COL1A1, COL1A2	Osteogenesis imperfecta, Marfan's syndrome, Ehlers-Danlos Syndrome	(Pope and Nicholls 1987, Gajko-Galicka 2002)
II	COL2A1	Chondrodysplasia	(Horton <i>et al.</i> 1989)
III	COL3A1	Ehlers-Danlos Syndrome	(Hamel <i>et al.</i> 1998)
IV	COL4A1, COL4A2, COL4A3, COL4A4, COL4A5, COL4A6	Leiomyomatosis, Alport syndrome, Goodpasture's syndrome	(Hudson <i>et al.</i> 1993, Kashtan 1993)
V	COL5A1, COL5A2, COL5A3	Ehlers-Danlos syndrome	(Kuivaniemi <i>et al.</i> 1991)
VI	COL6A1, COL6A2, COL6A3	Ulrich myopathy and Bethlem myopathy	(Bertini and Pepe 2002)
VII	COL7A1	Epidermolysis bullosa dystrophica	(Almaani <i>et al.</i> 2011)
VIII	COL8A1, COL8A2	Atherosclerosis	(Lopes <i>et al.</i> 2013)
IX	COL9A1, COL9A2, COL9A3	Multiple epiphyseal dysplasia	(Jackson <i>et al.</i> 2010)
X	COL10A1	Schmid-type metaphyseal dysplasia	(Woelfle <i>et al.</i> 2011)

1.10.2.4.1. Collagens in renal disease

Collagens types I, III and IV are the most abundant in the kidneys, however, low levels are found until damage has been established. Collagen type I is identified in smaller amounts in the interstitium and within the glomerular mesangium when compared to the collagen type III (Yoshioka *et al.* 1990). Type III collagen is highly expressed in the mesangial matrix as well as in the vascular pole of sclerosed glomeruli (Yoshioka *et al.* 1989). Collagen type IV is a major component of the GBM (Boutaud *et al.* 2000), being highly present in the mesangial and glomerular ECM. Interestingly, it was observed that whilst type I collagen promotes EMT, type IV renders protection to the epithelial phenotype in proximal tubular cells (Zeisberg *et al.* 2001).

Several studies have established that an increased synthesis and deposition of collagens on the ECM were directly involved with the development of renal fibrosis (Soylemezoglu *et al.* 1997, Skill *et al.* 2004, Johnson *et al.* 2007, Fisher *et al.* 2009, Huang *et al.* 2009, Liu 2011).

An overproduction and increased ECM accumulation, genetic mutations of collagens can also contribute to renal dysfunction.

Mutations of type I collagen are associated not only with Osteogenesis imperfecta and Marfan's syndrome (Gajko-Galicka 2002), but also with glomerular collagen deposition in the mesangial matrix as well as between the fenestrated endothelial cells of COL1A2 deficient mice. This fibrillar collagen deposition leads to the effacement of podocytes foot process and subsequent development of impaired kidney function (Brodeur *et al.* 2007). Mutations in collagen type IV have been related to the pathogenesis of Goodpasture's syndrome (carboxyl terminus of the NC1 domain of the $\alpha 3$ chain) and Alport syndrome (COL4A5 gene encoding the $\alpha 5$ chain) (Hudson *et al.* 1993).

Urinary collagen levels have been used as markers of progressive kidney fibrosis. Measurements of urinary amino terminal peptide of procollagen III (PIIINP) demonstrated a high correlation with the severity of kidney fibrosis (Soylemezoglu *et al.* 1997). Additionally, Hydroxyproline has been used to detect acute kidney injury in rats due to melamine and cyanuric acid nephrotoxicity (Schnackenberg *et al.* 2012).

1.10.3. Matrix Metalloproteinases system

1.10.3.1. MMPs

Matrix Metalloproteinases (matrixins, MMPs) are a group of at least 25 multidomain zinc-dependent endopeptidases (Iyer *et al.* 2012), secreted by a variety of cells such as macrophages (Hibbs *et al.* 1987), polymorphonuclear leukocytes (Murphy *et al.* 1982), fibroblasts (Wilhelm *et al.* 1989), osteoclasts (Reponen *et al.* 1994) and endothelial cells (Haas *et al.* 1998). The MMP family has been categorised into five subgroups: matrilynsins, collagenases, gelatinases, stromelysins, and membrane-type MMPs (MT-MMPs) (Iyer *et al.* 2012) (table 1.8). In order to be assigned as a member of the MMP family, there are five requirements that the enzyme should fulfil: 1) be able to cleave at least one ECM component, 2) be inhibited by ethylenediaminetetraacetic acid, 1,10-phenanthroline, and one of the TIMPs, 3) their catalysis function should be dependent on zinc at the active site, 4) activation by proteinases or organomercurials and 5) cDNA should have sequence homology to MMP-1 (Iyer *et al.* 2012).

Nearly all MMPs are capable of cleaving most components of the ECM and they can also process a number of bioactive molecules, like apoptotic ligands and growth factor receptors (Fingleton *et al.* 2001), pro-lysyl oxidase, IL-1 β and α_1 -proteinase inhibitor (Chakraborti *et al.*

2003, Varghese 2006). MMPs are also known to play a role on chemokine activation, cell localization, proliferation, differentiation, adhesion, apoptosis, angiogenesis and host defence (Clark *et al.* 2008, Manicone and McGuire 2008, Rydlova *et al.* 2008).

1.10.3.1.1. MMPs transcription and activity

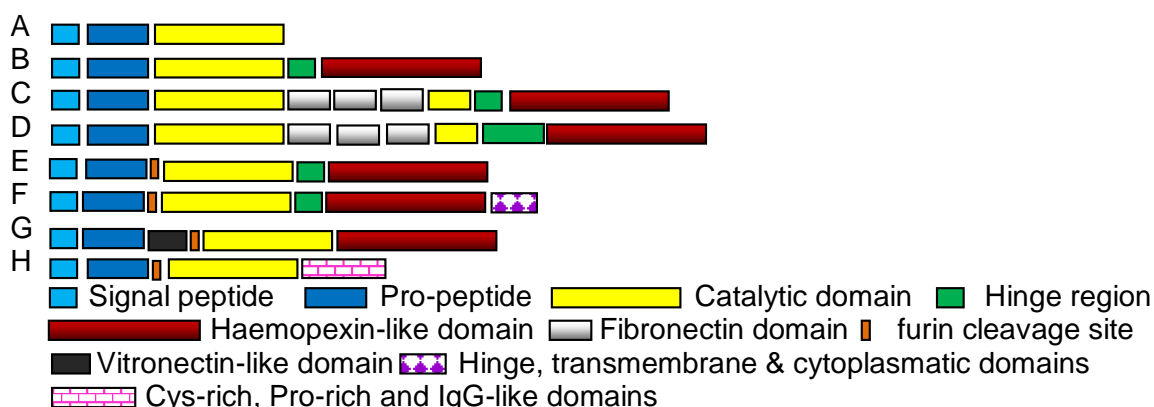
A large number of molecules can regulate MMPs transcription such as cytokines, growth factors, activating protein 2 (AP-2), NF-kappaB, Specificity protein1 (Sp1), proto-oncogenes and hormones (Matrisian 1990, Mohan *et al.* 1998). Their activity is strictly regulated at the level of transcription as well as by the activation of the precursor zymogens and through tight control from their endogenous inhibitors such as α 2 macroglobulin, trombospondin-1, trombospondin-2, tissue factor pathway inhibitor, the membrane-anchored glycoprotein RECK and specifically by tissue inhibitors of metalloproteinases (TIMPs) (Oh *et al.* 2001, Baker *et al.* 2002, Visse and Nagase 2003).

1.10.3.1.2. MMPs biosynthesis

Most MMPs are synthesized as prepro-enzymes and secreted in an inactive pro-form that requires zinc and proteolytic cleavage for activation (Nagase and Woessner 1999). However, MMPs 11 and 28 are intracellularly activated by furin and are secreted in active forms and MMP-14 is not always secreted (Osenkowski *et al.* 2004, Iyer *et al.* 2012). They share a primary three domain structure: the pro-peptide, the catalytic domain and the haemopexin-like C terminal domain (Bode *et al.* 1999, Nagase and Woessner 1999). The pro-peptide domain contains around 80 amino acids. It displays a cysteine switch motif PRCGXPD, where a cysteine residue inhibits binding and cleavage of substrates when interacting with zinc. This keeps MMPs in their pro-form. The catalytic domain has about 170 amino acids and contains the active site with a Zinc-binding motif HEXGHXXGXXH. This domain is composed of three α -helices, five-stranded β -sheet, and bridging loops (Dhanaraj *et al.* 1996). The haemopexin-like C terminal domain has around 210 amino acids and is connected to the catalytic domain by the Hinge region (around 75 amino acids). It presents a structure which consists of four antiparallel β -strands and an α -helix (Gomis-Ruth *et al.* 1996). Currently known MMPs, their correspondent domain composition and most common substrates are summarised in table 1.10.

Table 1.10: MMPs types, substrates specificity and domain composition

Subfamily	MMP	Protein name	Main substrates	Domain composition
Collagenases	MMP-1	Interstitial collagenase	Col I, II, III, VII, VIII, X,XI, gelatin	B
Gelatinases	MMP-2	Gelatinase-A	Gelatin, Col I, II, III, IV, VII, X	C
Stromelysins	MMP-3	Stromelysin 1	Col II, IV, IX, X, XI, gelatin	B
Matrilysins	MMP-7	Matrilysin	Fibronectin, laminin, Col IV, gelatin	A
Collagenases	MMP-8	Neutrophil collagenase	Col I, II, III, VII, VIII, X, aggrecan, gelatin	B
Gelatinases	MMP-9	Gelatinase-B	Gelatin, Col IV, V	D
Stromelysins	MMP-10	Stromelysin 2	Col III,IV,V laminin, fibronectin, elastin	B
Stromelysins	MMP-11	Stromelysin 3	Col IV, fibronectin, laminin, aggrecan	E
Metalloelastase	MMP-12	Macrophage metalloelastase	Elasin, fibronectin, Col IV	B
Collagenases	MMP-13	Collagenase 3	Col I, II, III, IV, IX, X, XIV, gelatin	B
Membrane-type	MMP-14	MT1-MMP	gelatin, fibronectin, laminin,aggrecan	F
Membrane-type	MMP-15	MT2-MMP	gelatin, fibronectin, laminin, tenascin	F
Membrane-type	MMP-16	MT3-MMP	gelatin, fibronectin, laminin	F
Membrane-type	MMP-17	MT4-MMP	fibrinogen, fibrin	F
Collagenases	MMP-18	Collagenase 4	Unknown	B
Other	MMP-19	RASI-1	Gelatin, tenascin	B
Enamelysin	MMP-20	Enamelysin	Amelogenin	B
Other	MMP-21	X-MMP	Unknown	G
Other	MMP-23A	CA-MMP	Casein, gelatin	B
Other	MMP-23B		Autoproteolysis	H
Membrane-type	MMP24	MT5-MMP	gelatin	F
Membrane-type	MMP-25	MT6-MMP	Pro-gelatinase A	F
Matrilysins	MMP-26	Matrilysin-2	Gelatin 1 α	A
Other	MMP-27	MMP-22, C-MMP	Unknown	B
Other	MMP-28	Epilysin	Unknown	E



1.10.3.3. TIMPs

Tissue inhibitors of metalloproteinases (TIMPs) are the main regulators of MMPs activities. They comprise a family of four protease inhibitors: TIMP1, TIMP2, TIMP3 and TIMP4 with molecular weights between 20-30 kDa (figure 1.11) and their expression is regulated during development and tissue remodelling (Clark *et al.* 2008). TIMPs structure consists of an N-terminal cysteine with an active site zinc dependent and has around 125 amino acids and a smaller C-terminal haemopexin domain, with around 65 amino acids. Each domain is characterized by parallel β strands (5 in the N-terminal and 2 in the C-terminal) and α helices secured by three disulfide loops (Brew and Nagase 2010) .

Tissue inhibitor of metalloproteinase 1 (TIMP-1) is a 184 amino acid residue glycoprotein that directly inhibits the action of most MMPs by binding to its catalytic site and consequently blocking the access of substrates. TIMP-1 only has a relatively low affinity for membrane-type MMPs 14, 16, 19 and 24 (Murphy and Nagase 2008). TIMP-1, on the other hand, is a potent inhibitor of MMPs 3 and 7 (Hamze *et al.* 2007) and ADAM10 (Amour *et al.* 2000) when compared to other TIMPs. It is widely secreted by many cell types, including fibroblasts and macrophages amongst other connective tissue cells, but new evidence shows that it is preferentially secreted by T helper cells 1 and 17 (Adamson *et al.* 2013) Besides its inhibitory action against MMPs, TIMP-1 also presents other distinct functions including an erythroid potentiating activity and inhibition of apoptosis in B cells (Stetler-Stevenson 2008).

Tissue inhibitor of metalloproteinase 2 (TIMP-2) is a 194 amino acid glycoprotein, which comprises 12 cysteine residues that forms six disulfide bonds, three of which are in the N- and C-terminal domain, respectively (Brew and Nagase 2010). It is secreted by Fibroblasts, macrophages, endothelial cells, VSMC and cardiomyocytes (Vanhouste *et al.* 2006). TIMP-2 is a stoichiometric inhibitor of collagenases which alongside TIMP-1 acts by blocking the MMP'S catalytic core. TIMP-2 has a distinct characteristic of promoting the binding of its C-terminal domain to the haemopexin-like domain of pro-MMP-2 (Wang *et al.* 2000). This interaction is essential in the cell-surface activation of pro-MMP-2 by active MMP-14 (Caterina *et al.* 2000). Apart from MMPs inhibition and the cell-surface activation mechanism of latent MMP-2, it can also suppress EGF-mediated mitogenic signalling by short-circuiting the epidermal growth factor cognate receptor (EGFR) activation (Hoegy *et al.* 2001) as well as bind to the integrin $\alpha 3\beta 1$ and inhibit cell migration (Stetler-Stevenson 2008). High levels of TIMP-2 have been associated with several diseases, such as cancer (Kachra *et al.* 1999, Remacle *et al.* 2000), systemic sclerosis (Yazawa *et al.* 2000) and CKD (Ahmed *et al.* 2007).

Tissue inhibitor of metalloproteinase 3 (TIMP-3) is a glycoprotein with a molecular mass of 30kDa produced by a wide variety of cells such as fibroblasts, macrophages, VSMC and cardiomyocytes (Vanhoutte *et al.* 2006). TIMP-3 has a peculiar property of presenting a high affinity for binding to the extracellular matrix. It forms a non-covalent binary complex with the MMP active site through its N-terminal; therefore it can protect the ECM from MMP attack. Also, TIMP-3 has the broadest inhibition spectrum of all TIMPs; it is an effective inhibitor of ADAM 17, also known as tumour necrosis factor α converting enzyme or TASCE (Amour A *et al.*, 1998 FEBS), ADAM 10 (Amour *et al.* 2000), ADAM 12 (Loechel *et al.* 2000, Mochizuki *et al.* 2004), ADAM 28 (Mochizuki *et al.* 2004) and ADAM 33 (Zou *et al.* 2004) and as it is the only known member of the TIMP family that can inhibit members of ADAMs that have a trombospondin-1-like domain (ADAMTS) family such as ADAMTS 1, 2, 4 and 5 (Brew and Nagase 2010). Mutations in the TIMP-3 gene have been reported to result in Sorsby's fundus dystrophy (Li *et al.* 2005). TIMP-3 has also been associated with accelerated apoptosis as well as decreased angiogenesis by blockage of VEGF binding to VEGF receptor-2 (Qi *et al.* 2003, Handsley and Edwards 2005). Amongst the TIMPs, TIMP3 possess a distinct role of binding to glycosaminoglycans (GAGs) such as heparin sulphate, heparin and chondroitin sulphate in the ECM (Yu *et al.* 2000).

Tissue inhibitor of metalloproteinase 4 (TIMP-4) is a 26 kDa glycoprotein, composed of 194 amino acids with a human gene located in the chromosome 3p25 (Olson *et al.* 1998). TIMP-4 is able to inhibit most MMPs, having high affinity to pro-MMP-2 (Bigg *et al.* 1997) alongside ADAM 17, ADAM 28 and ADAM 33 (Brew and Nagase 2010). TIMP-4 expression is greater in the brain, ovaries, skeletal muscles and heart (Lambert *et al.* 2004). Low plasma TIMP-4 levels has been associated with a higher cardiovascular risk due to an increased carotid artery intima-media (cIMT) thickness (Oikonen *et al.* 2012).

All TIMPs can bind in a stoichiometric 1:1 molar ratio to all MMPs. Their inhibitory effect on the enzymatic activity of MMPs is an aftermath of their binding to the catalytic domain of MMPs (Massova *et al.* 1998, Brew and Nagase 2010). However, they present varying affinity to specific MMPs. For instance, TIMP-1 can form tight complexes with MMP3 through a residue located between Cys¹ and Cys⁷⁰ on the first disulfide bond (Meng *et al.* 1999). However, TIMP1 has poor affinity to MMP-2, whereas TIMP-2 and TIMP-3 can form strong complexes with this MMP (Murphy *et al.* 1991, Will *et al.* 1996). There is evidence that TIMPs present higher affinity to some pro-MMPs. For example, TIMP-1 form specific complexes with pro-MMP9 (Vempati *et al.* 2007), whilst TIMP-2 (Morgunova *et al.* 2002) and TIMP-4 (Bigg *et al.* 1997) can bind to pro-MMP2.

In addition to being inhibiting MMP activity, TIMPs present a wide range of biological activities, including: induction of apoptosis (Smith *et al.* 1997, Ahonen *et al.* 1998), inhibition (Gomez *et al.* 1997, Hoegy *et al.* 2001) or promotion of tumour growth (Bourboulia and Stetler-Stevenson 2010) depending of the tumour model studied, stimulation of erythroid activity (Gasson *et al.* 1985, Stetler-Stevenson *et al.* 1992), stimulation of fibroblast proliferation along with the phenotypic differentiation into myofibroblasts (Lovelock *et al.* 2005), suppression of tyrosine kinase-type growth factor receptor activation (Hoegy *et al.* 2001) and modulation of myocardial remodelling (Vanhoutte and Heymans 2010).

Table 1.11: General properties of human TIMPs

Property	TIMP-1	TIMP-2	TIMP-3	TIMP-4
Molecular weight	23	21	30	26
Number of AA	184	194	188	194
Chromosomal location	X11p11.23-11.4	17q23-25	22q12.1-q13.2	3p25
MMP inhibition	Weak for MMPs 14,16,19 and 24	All	All	Most
Pro-MMP interactions	Pro-MMP-9	Pro-MMP-2	Pro-MMPs 9 & 2	Pro-MMP-2
Other MP inhibition	ADAM 10	ADAM 12	ADAM 10, 12, 17, 28 and 33; ADAMTS 1, 4, 5 and 2 (weak)	ADAM 17 and 28, ADAM 33 (weak)
Glycosilation	Yes	No	Partial	No
Apoptotic effects	Negative	Positive/ Negative	Positive	Unknown
Angiogenesis	Negative	Negative	Negative	Negative
Genetic disorder			Sorsby's fundus dystrophy	

Table 1.11: A summary of the general properties of human TIMPs 1, 2, 3 and 4 including their molecular structure characteristics, activity as inhibitors of Matrix and other Metalloproteinases, pro-MMP interactions and main biological functions.

Figure 1.10: Binding of TIMPs to the active site of MMPs

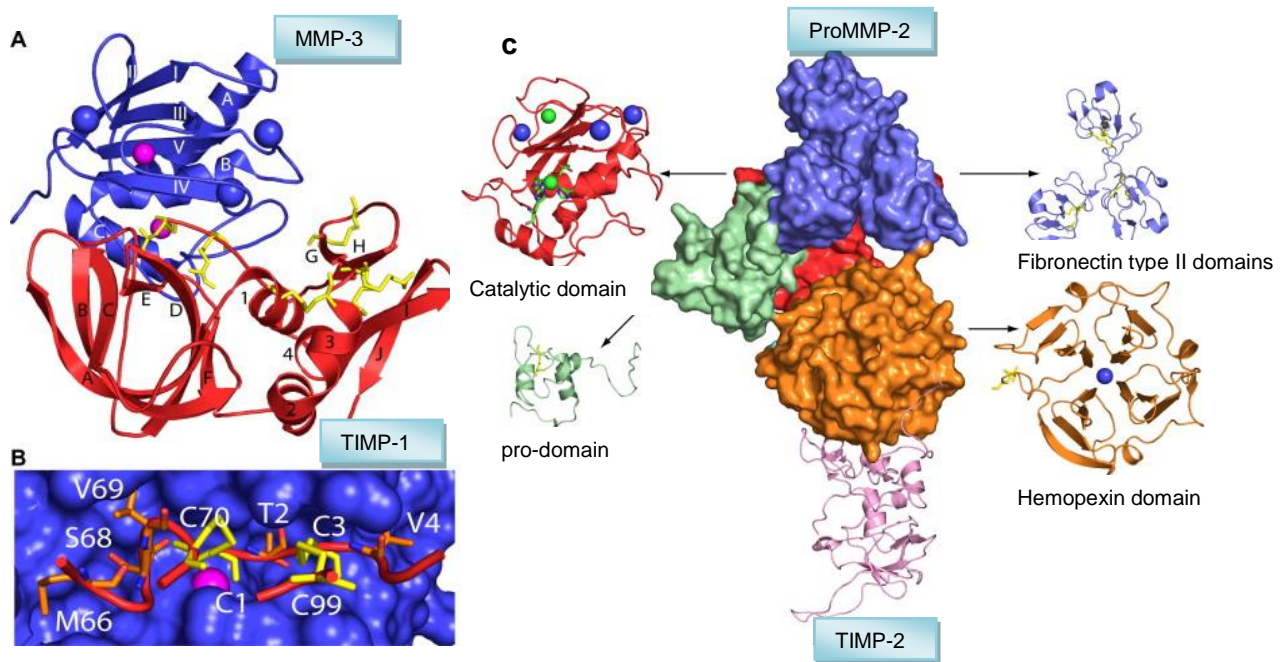


Figure 1.10: TIMPs bind to Pro-MMPs and to the active site of the MMPs in a stoichiometric 1:1 molar ratio, thereby blocking access to their extracellular substrates. **A)** Three-dimensional diagram of human TIMP-1 (in red) bound to the catalytic domain of MMP-3 (blue). **B)** Reactive centre residues of TIMP-1 in the active site of MMP-3. Disulfide bonds are shown in yellow, zinc ions in pink and calcium ions in blue. **C)** Three-dimensional diagram of human proMMP-2 and TIMP-2 complex. The catalytic domain is shown in red, fibronectin type II domains in blue, pro-domain in green, haemopexin domain in orange, and TIMP-2 in pink. Calcium ion is in blue sphere, Zinc ion in green sphere and disulfide bonds in yellow. Changed from (Murphy and Nagase 2008)

1.10.3.4. The role of MMPs and their inhibitors in human diseases

Degradation of ECM components is an important element of normal tissue remodelling, so reduced or inadequate ECM breakdown can result in a variety of pathologies. In addition to the matrix remodelling function, MMPs are also key regulators of cell homeostasis and of diverse signaling pathways, therefore, an altered expression and/or an uncontrolled modulation of MMP activities together with an imbalanced MMP/TIMP ratio have been associated with the development of a wide range of diseases (Rodriguez *et al.* 2010, Moore and Crocker 2012). Currently, there is ample evidence linking MMPs and their inhibitors to a wide range of pathological processes, amongst them arteriosclerosis (Galis and Khatri 2002), arthritis (Konttinen *et al.* 1999), aneurysms (Thompson and Parks 1996), cancer (Egeblad and Werb 2002, Ozden *et al.* 2013), systemic sclerosis (Young-Min *et al.* 2001), dermatitis herpiformis (Zebrowska *et al.* 2005), pulmonary fibrosis (Nagase and Woessner 1999)

kidney fibrosis (Ermolli *et al.*, 2003; Tashiro *et al.*, 2004; Catania *et al.*, 2007) and liver fibrosis (Arthur 2000).

1.10.3.4.1. MMPs and TIMPs in renal disease

Several studies have described the role of the MMP system in renal disease development. MMPs 1, 2, 3, 8, 9, 13, 14, 24, 25, 27, 28 and TIMPs 1, 2 and 3 are all expressed in the kidneys (Catania *et al.* 2007), however, , MMPs 1, 2, 3, 8, 9, 13 are the ones with higher and significant renal expression (Lenz *et al.* 2000). A variety of renal cells can express MMPs, including mesangial cells (Martin *et al.* 1994), glomerular epithelial cells (Knowlden *et al.* 1995), tubular epithelial cells and interstitial fibroblasts (Norman *et al.* 1995). Mesangial and glomerular epithelial cells predominantly produce MMPs 2 and 9 alongside TIMPs 1 and 2 (Martin *et al.* 1994, Knowlden *et al.* 1995), whereas tubular epithelial cells can produce MMPs 1, 2, 8, 9 and 13 (Norman *et al.* 1995). Interstitial fibroblasts have been shown to produce MMP2 as well as MMPs 1, 8 and 13 (Norman *et al.* 1995). MMP 14 is expressed in distal tubules and TIMP 2 in fibroblasts in a rat model of autosomal-dominant polycystic kidney disease (ADPKD) (Obermuller *et al.* 2001). MMPs 24, 25, 27 and 28 are also expressed in tubular epithelial cells (Romanic *et al.* 2001, Lemaitre and D'Armiento 2006).

Current evidence suggests that MMPs and their inhibitors are involved in a wide variety of acute and chronic renal pathologies including acute kidney injury (AKI) , CDK (Horstrup *et al.* 2002), CAN (Ahmed *et al.* 2012) and diabetic nephropathy (Thraillkill *et al.* 2009, Altemtam *et al.* 2012).

A recent study has shown a correlation between increased MMPs2 and 9 activities and the development of AKI (Kunugi *et al.* 2011). It seems that both MMPs are involved in the process of regenerating tubular epithelial cells and so the use of a MMP2/MMP9 inhibitor impaired the repair process of ischemic AKI (Kaneko *et al.* 2012). Interestingly, a previous study has also shown that MMP 9 levels were increased in an experimental model of acute kidney allograft rejection, however, MMP2 levels were decreased (Ermolli *et al.* 2003). Elevated pro-MMP 1 levels (Rodrigo *et al.* 2000) and reduced TIMP 1 (Caron *et al.* 2005) were also observed in different stages of acute ischemic injury.

The 5/6th subtotalnephrectomy model of renal scarring has provided some insightful information into the molecular mechanisms involving MMPs and their inhibitors in progressive kidney fibrosis. Ahmed *et al.* showed a reduction in MMP activity in the tubulointerstitium associated with increased glomerular expression of MMP1 and reduced TIMP3, with the

elevated levels of TIMP1 and TIMP2 with reduced tubular MMP3 was almost certainly being responsible for the lower MMP activity (Ahmed *et al.* 2007). Further evidence that they play a central role in the development of renal scarring includes the significant elevation of mRNA for MMPs 1 and 2 as well as TIMPs 1 and 2 mRNA in the remnant kidney (Johnson *et al.* 2002).

A number of studies have demonstrated a connection between altered MMP and TIMPs expression in CKD. For instance, urine and serum levels of TIMP1 were increased in CKD patients (Horstrup *et al.* 2002). TIMP1 in conjunction with MMPs 2, 3 and 9 were also overexpressed in patients with ANCA-associated Glomerulonephritis (Sanders *et al.* 2004). Downregulation of MMP activity has been linked to hypertensive glomerulosclerosis (Singhal *et al.* 1996) and cyclosporine nephrotoxicity (Duymelinck *et al.* 1998). There is also evidence that reduced expression of MMPs 1, 2, 3 and 9 together with an up regulation of TIMPs 2 and 3 play a central role in the development of CAN (Ahmed *et al.* 2012, Yan *et al.* 2012).

MMPs can also modulate ECM breakdown via the regulation of growth factors activity, such as the insulin-like growth factor-1 and therefore influence diabetes development (Fowlkes *et al.* 1995). The majority of studies show increased serum and urinary MMPs 2, 8 and 9 in diabetic patients (Romanic *et al.* 2001, Tashiro *et al.* 2004, Lauhio *et al.* 2008, Gharagozlian *et al.* 2009, Thrailkill *et al.* 2009, van der Zijl *et al.* 2010). Furthermore, *in vitro* studies reported decreased MMP activity in mesangial cells exposed to high glucose (McLennan *et al.* 1998). However, a more recent study analysing urine from diabetic nephropathy patients described elevated MMP activity in such individuals (Altemtam *et al.* 2012).

1.10.4. Plasminogen-Plasmin system

The Plasminogen-plasmin system is the second major pathway involved in ECM catabolism. Plasminogen is a pro-serine protease released from the liver and activated by tissue Plasminogen activator (tPA) and urokinase Plasminogen activator (uPA) to plasmin. The urokinase type can only cleave plasminogen to plasmin when it is bound to a urokinase type plasminogen activator receptor on the surface of the cells (Legrand *et al.* 2001). Plasmin can degrade multiple components of the ECM including collagens III, IV, V, Fibronectin, Laminin and Proteoglycans (Baricos *et al.* 1995). Plasmin also plays an important role in activating MMPs (Monea *et al.* 2002). Plasminogen activators (tPA and uPA) are regulated by growth factors, TNF- α , IL-1, PDGF, TGF- β 1 as well as some hormones and both are specifically inhibited by the Plasminogen Activator Inhibitor-1 (PAI-1) (Rerolle *et al.* 2000). PAI-2 function is

expressed more during pregnancy, where decreased levels were associated with placental dysfunction and intrauterine growth retardation (Astedt *et al.* 1998).

Alongside its role in ECM degradation, plasmin also plays a fundamental role in the clotting system. The clotting system can be divided into two distinct cascades; the coagulation cascade and the fibrinolytic cascade. Activation of the coagulation cascade results in the conversion of prothrombin to active thrombin, which in turn catalyses the conversion of soluble fibrinogen to fibrin (Nesheim 2003). Conversely, the fibrinolytic cascade modulates the formation of plasmin from plasminogen, which catalyses the solubilisation of fibrin.

1.11. Classical biomarkers of CKD progression

1.11.1. GFR

Among the functional biomarkers of CKD, the GFR is considered to be the gold standard method, with a prediction accuracy ranging from 65 to 74%. Measurement of the true GFR by the clearance of exogenous markers such as Inulin or radioisotopes of ⁵¹Cr-EDTA (Delanaye *et al.* 2008) or ^{99m}Tc-DTPA (Frennby and Sterner 2002) provide sensitive tests for overall kidney function, however, as a consequence of adaptation to nephron loss, this test may not indicate loss of kidney function reduction until around 60% of damage has occurred. Furthermore, such measurements require intravenous application and equilibration time which is difficult to achieve routinely.

The concentration of creatinine in the serum allows a mathematical estimate of the GFR, and provides the simplest and most common test used to measure kidney function in clinical practice. However, it is inaccurate at detecting mild kidney impairment as it is insensitive to changes in GFR within the range of normal or slightly impaired function and so in patients at an early stage of kidney damage a decrease in the GFR would not be reflected in the measurement of serum creatinine. Other limitations of creatinine-based equations to estimate the GFR are associated with non-GFR determinants such as muscle mass, age (especially among the elderly), gender and ethnicity (non-white populations). In addition, Creatinine clearance tends to overestimate the GFR by about 15% when the renal function is impaired as tubular secretion of creatinine accounts for a larger proportion of creatinine found in the urine. This overestimation can be inhibited by the use of cimetidine, which competitively inhibits the tubular secretion of creatinine (Agarwal 1993, Hilbrands *et al.* 1993, Payne 1993, Ixkes *et al.* 1997).

1.11.2. Proteinuria

The quantity of protein excreted in the urine is one of the strongest indicators of kidney disease progression and constitutes one of our “Classical” biomarkers of CKD progression (Lemley 2007). Currently, proteinuria is considered one of the strongest markers of CKD severity and constitutes the most used predictor of eGFR decline in diabetic and nondiabetic kidney disease (Cravedi and Remuzzi 2013). Moreover, proteinuria has been utilized as an useful surrogate end point in clinical trials with CKD patients and has been recognized as an important risk factor of cardiovascular disease.

Normal individuals excrete between 40 and 80mg of protein per day, with the upper range of normal being 150mg per day (Schrier 2005, J Feehaly 2007). Three main types of proteinuria can be seen: glomerular, due to an increased permeability of the glomerular capillary; tubular, due to an impairment in the tubular reabsorption; and overflow proteinuria, where an excessive production and filtration of low-molecular weight proteins such as monoclonal immunoglobulin light chains in Multiple Myeloma. Depending on the pattern of the excreted proteins, we are able to classify its origin (glomerular or non-glomerular) and also in some cases the length of the injury, like the increased excretion of tubular proteins such as β -2-microglobulin or retinol-binding protein reflects chronic damage characterized by interstitial fibrosis (Remuzzi and Bertani 1998). Several different proteins can be excreted in the urine. Tamm-Horsfall tubular mucoprotein or Uromodulin is the most common one and accounts for 30-50mg per day, whereas Albumin accounts for less than 20mg per day in normal subjects.

Urine protein excretion used to be measured by a 24 hour collection. However, this is neither convenient nor an accurate method of detecting it. Using a spot urine sample to obtain the protein concentration followed by normalization to a creatinine ratio gives a more adequate measurement as it rectifies for variation in the urine volume.

Studies have showed that elevated excretion of protein acts not only as an indicator of kidney damage, but it also plays a role in the progression of CKD. The mechanisms of proteinuria driving CKD include the increased ultrafiltered protein load in the proximal renal tubular cells (PTECs) activating the NF- κ B–dependent and NF- κ B–independent pathways and upregulating adhesive molecules (Donadelli *et al.* 2003) and chemoattractants IL-8 (Tang *et al.* 2003), MCP-1 (Wang *et al.* 1997) and RANTES (Zoja *et al.* 1998) for inflammatory cells such as macrophages, neutrophils and T lymphocytes.

In glomerular disorders such as Focal Segmental Glomerulosclerosis (FSGS) or IgA Nephropathy (IgAN) for example, there is an abnormal glomerular permeability with consequence being the presence of proteinuria (Woo *et al.* 1991, Shiiki *et al.* 1996). There is strong evidence that proteinuria is a factor inciting tubulointerstitial disease and this tubulointerstitial damage acts as a prime risk factor for subsequent kidney disease progression. It has also been demonstrated that patients with Nephrotic Syndrome (syndrome characterized by presence of $> 3.5\text{g proteinuria} / 1.73\text{m}^2 / \text{day}$ with hypoalbuminaemia, oedema, hyperlipidaemia and lipiduria) have worse prognosis than the patients without Nephrotic Syndrome.

Several experimental models and human trials show an association between the reduction of proteinuria and renoprotection (Kramer and Schweda 1997, Brenner *et al.* 2000, de Zeeuw *et al.* 2004). The MDRD study, for example, showed that patients who already had a baseline proteinuria were more likely to have further decline in GFR (Kopple *et al.* 1989). Follow on studies confirmed this finding by analysing the effects of a low protein diet on the progression of kidney disease and the results demonstrated that reduction in proteinuria was significantly associated with better kidney outcome (Kopple *et al.* 1989, de Zeeuw *et al.* 2006). Several other experimental models and human trials showed an association between the reduction of proteinuria by lowering glomerular pressure and subsequent renoprotection (Kramer and Schweda 1997, Brenner *et al.* 2000, de Zeeuw *et al.* 2004). Better kidney survival was associated not only with the reduction of proteinuria by diet, but also by the use of Angiotensin Converting Enzyme inhibitors (ACEi) or Angiotensin Receptor Blocker (ARB). However, it seems that proteinuria acts more as a marker rather than the cause of CKD progression. Even the RIEN trial, showed that although a greater survival was reached within the Ramipril group, no benefits were seen when proteinuria was reduced to under 1.5g per day. In addition, several recent large studies have shown that significant decreases in proteinuria did not reflect in slowing CKD progression. In the ALTITUDE study, for instance, the use of the direct renin inhibitor Aliskiren combined to ACE inhibitors or Angiotensin Receptor blockers although promoting decrease in albuminuria levels, it failed to promote a significant impact in loss of renal function in Diabetic Nephropathy (Parving *et al.* 2012). Similar results were also observed in the ONTARGET (Yusuf *et al.* 2008) and the ACCOMPLISH study (Jamerson *et al.* 2008). Interestingly, there is increasing evidence ACEi/ARB discontinuation on advanced CKD patients can slow down progression to RRT (Ahmed *et al.* 2010).

1.12. Experimental biomarkers of kidney disease

Nowadays, the measurement of eGFR and proteinuria provides the most sensitive way for identifying progression of CKD to ESRD in clinical practice (Hallan *et al.* 2009). However, these have limitations and as such early and more sensitive markers of CKD progression are required. There are several ongoing or recently completed studies on potential new biomarkers of kidney disease progression (Fassett *et al.*, 2011). Currently, none of these markers are ready for clinical use as large longitudinal, multicentre observational studies are necessary to investigate and validate them.

Proteomic studies may be very useful to identify potential candidates, especially in settings in which significant posttranslational modification of proteins occurs (phosphorylation, ubiquitination, methylation, acetylation, glycosylation, etc.) (Vivekanandan-Giri *et al.* 2011). Also, the use of metabolomics (the study the profile of large number of small metabolites) in the future is likely to reveal a better understanding of physiology of the cells as it can simultaneously identify multiple metabolic changes caused by a pathological process (Lemley 2007).

Continually being developed are tests involving a multiplex panel of biomarkers which searches through a more comprehensive panel of potential biomarkers of CKD such as the β -Trace protein, the connective tissue growth factor (CTGF), transforming growth factor β 1 (TGF β 1), podocyuria or β -2-microglobulin/creatinine ratio for example. This is a promising technique as it can give a multidimensional vision of the pathologic processes involved on CKD progression (Lemley 2007) especially as multiple mechanisms involved in the CKD mechanism can be assessed (table 1.12).

Table 1.12: Experimental CKD biomarkers according to the pathophysiological process

Main mechanism	Biomarker
Kidney function (GFR)	Cystatin C β-Trace protein
Tubulointerstitial injury	NGAL KIM-1 NAG
Glomerular injury	Nephrin Podoxin Podocalyxin
Endothelial dysfunction	ADMA
Inflammation	IL-18 Tenascin, others
Fibrosis	TGFβ1
Metabolic disorders	FGF-23 Adiponectin ApoA-IV
Oxidative stress	AGE Protein reduced thiols MDA TAS Urinary 8-hydroxydeoxy guanosine Superoxide dismutase, others

Table 1.12: Common experimental biomarkers in the kidney and their main mechanism of action.

1.12.1. Cystatin C

Cystatin C, a 13kDa serum protein encoded by the CST3 gene, is produced by all nucleated cells, freely filtered by the glomeruli and metabolized after tubular absorption (Madero *et al.* 2006). It has been shown as a better and more precise marker of kidney function than creatinine (Newman *et al.* 1994, Dharnidharka *et al.* 2002, Mussap *et al.* 2002), presenting a lower analytical and within-subject coefficient of variability (Delanaye *et al.* 2008). Its serum concentration is directly correlated with GFR and its levels are less dependent of muscle mass and other variables such as sex and weight (Filler *et al.* 2005, Herget-Rosenthal *et al.* 2005). It has been reported in several studies that using cystatin C as a marker of kidney damage shows earlier responses to therapy than creatinine as well as more precise description of disease severity (He *et al.* 2013, Liu *et al.* 2013). ROC curve analysis of 592 adult CKD patients showed that cystatin C presented a better ability to predict to predict the correct GFR than creatinine (91.6 and 84.1%, respectively) (Hojs *et al.* 2008). In addition, a combined creatinine-cystatin equation showed better GFR estimation than the calculations done by these individual markers by itself (Inker *et al.* 2012, Rule *et al.* 2013). A large meta-analysis of 16 studies done by Shilipak *et al.* including 90750 participants from the general population

and 2960 CKD patients, showed a correlation between creatinine-based and the combination-based (creatinine and cystatin C) eGFR with a reverse J-shaped risk prediction of death from any cause and from cardiovascular causes as well as development of ESRD in the general population. Conversely, no reverse J-shaped association was found for the creatinine-based eGFR measurements in the CKD group. In this study, across all groups, reclassification to a decreased eGFR based on cystatin C measurement presented an improved risk prediction of CKD progression to ESRD when compared to creatinine. Nevertheless, this improvement was not statistically significant (Shlipak *et al.* 2013). Furthermore, cystatin C concentration can be affected by different conditions such as use of ACE inhibitors (Filler *et al.* 2013), thyroid dysfunction (Ye *et al.* 2013), presence of asthma (Shigemura *et al.* 2012) and positivity for HIV (Inker *et al.* 2012).

1.12.2. β -Trace protein

β -Trace protein (BTP) is a 23-29kDa lipocalin glycoprotein, composed of 168 amino acids. BTP has shown to be a good predictor of CKD progression (Spanaus *et al.* 2010, Bhavsar *et al.* 2011) and it is a more sensitive marker of glomerular filtration rate than serum creatinine allowing earlier detection of loss of function (Donadio 2010). However, it was demonstrated that it is inferior to Cystatin C as an indicator of GFR (Filler *et al.* 2013).

1.12.3. Neutrophil gelatinase-associated lipocalin (NGAL)

One of the most interesting novel biomarkers is the Neutrophil gelatinase-associated lipocalin (NGAL), also known as neutrophil lipocalin (NL or HNL for the human form) (Xu *et al.* 1994), lipocalin-2, siderocalin, uterocalin (Liu *et al.* 1997) and oncogene protein 24p3 (Flower *et al.* 1991). Human NGAL consists of a single disulfide-bridged polypeptide chain of 178 amino-acid residues with molecular weight of 22kDa, but glycosylation raises its apparent molecular mass to 25kDa (Kjeldsen *et al.* 1993). NGAL belongs to the lipocalin iron-carrying family of proteins (Fassett *et al.* 2011). It was originally isolated from neutrophils (Xu *et al.* 1994), but it can be secreted by diverse tissues including the kidneys, prostate, liver, lungs, gastrointestinal tract, epithelial cells, vascular cells in the atherosclerotic plaques (Cowland and Borregaard 1997, Friedl *et al.* 1999, Hemdahl *et al.* 2006) and in carcinomas (Stoesz *et al.* 1998, Friedl *et al.* 1999, Lim *et al.* 2007, Chakraborty *et al.* 2012). Urine NGAL has been shown to be a useful early marker of Acute Kidney Injury (AKI) as it is freely filtered by the glomeruli and levels rises within 2 hours of injury (Devarajan 2007). In addition to AKI, kidney tissue expression of NGAL is also elevated in CKD patients where it directly increases the expression of epidermal growth factor receptor (EGFR), acting not only as a marker of kidney

fibrosis but also as an active cause for disease progression (Viau *et al.* 2010). Furthermore, it benefits from having multiple molecular forms in urine; it occurs as a monomer when produced by neutrophils and as a dimer or trimer when originated from kidney tubular epithelial cells (Cai *et al.* 2010). In kidneys, NGAL is secreted into urine by the thick ascending limb of loop of Henle and collecting ducts, with synthesis occurring in the distal nephrons (Bolignano *et al.* 2009). There is evidence that NGAL is over expressed in cases of renal impairment after kidney transplantation (Malyszko *et al.* 2009), contrast nephropathy (Schilcher *et al.* 2011), haemolytic uraemic syndrome (Lukasz *et al.* 2013) or in cases of CKD such as those caused by obstruction (Bolignano *et al.* 2008, Devarajan 2008), IgA nephropathy (Ding *et al.* 2007), polycystic kidney disease (Bolignano *et al.* 2007) and lupus nephritis (Sharifipour *et al.* 2013). Urinary NGAL was measured in eighteen patients with HIV-associated nephropathy (HIVAN) and presented a 88% capacity of correctly diagnose the disease when calculated by ROC curve analysis, compared to 80% by urinary liver fatty acid-binding protein (uL-FABP) and 71% of total proteinuria (Sola-Del Valle *et al.*, 2011). A prospective study with 96 CKD patients (stages 2 to 4) and 14 healthy subjects analysed the accuracy of prediction of CKD progression and showed a ROC AUC of 70% for serum NGAL, 78% for urine NGAL and 64% for eGFR (Bolignano *et al.* 2009). However, a larger study from the Chronic Renal Insufficiency Cohort (CRIC) with 3386 CKD patients concluded that although urine NGAL concentration had a strong correlation with risk of CKD progression to ESRD, its levels were not better in correctly identifying it than current biomarkers (24 hours proteinuria and eGFR), with area under the ROC curve (C-statistic) of 84.7% with and without the addition of NGAL to the final model (Liu *et al.* 2013).

1.12.4. Kidney Injury Molecule-1 (KIM-1)

The Kidney injury molecule-1 (KIM-1), a 104kDa type 1 transmembrane protein, is a marker of proximal tubular injury. KIM-1 has an ectodomain containing a six-cysteine immunoglobulin like domain, two N-glycosylation sites and a domain rich in threonine/serine and proline (Lim *et al.* 2013). There are two human homologues of KIM-1; KIM-1a, which lacks the tyrosine kinase phosphorylation motif and is predominant in the liver and KIM-1b, which is predominant in the kidneys and contains a highly conserved tyrosine kinase phosphorylation motif at position 350. KIM-1 is positively associated with kidney fibrosis and inflammation in many nephropathies (Bonventre 2008), progression to ESRD in IgA nephropathy patients (Peters *et al.* 2011) as well as with graft loss in kidney transplanted patients (van Timmeren *et al.* 2007) and nephrotoxicity (Vaidya *et al.* 2010). This assessment of KIM-1 as a predictor of drug toxicity revealed a better performance when compared to blood urea nitrogen, serum creatinine and urinary N-acetyl- β -D-glucosaminidase (NAG) (Vaidya *et al.* 2010). Although

KIM-1 expression and release are induced in proximal tubular epithelial cells (PTEC) upon injury (Lim *et al.* 2013), its expression is undetected in normal kidneys (van Timmeren *et al.* 2007). Despite having a potential great value in identifying kidney damage and repair process, urine levels of KIM-1 are currently used only as a specific indicator of tubular injury particularly in acute renal failure (Han *et al.* 2002).

1.12.5. Urinary Nephritin, Podoxin and Podocalyxin

Urinary Nephritin, Podoxin and Podocalyxin are markers of glomerular damage. Damaged podocytes detach from glomerular basement membrane, thus their presence in urine can be evaluated by the measurement of these three molecules. This detection can be done by Immunoassays or mRNA in urine sediment (Wang *et al.* 2007, Wang *et al.* 2008, Zheng *et al.* 2011, Hara *et al.* 2012). The presence of Nephritinuria was shown to be elevated in Diabetic Nephropathy (Patari *et al.* 2003, Yu *et al.* 2005). It has the advantage of being rapidly detected by Western Blot (185 kDa) using specific anti-nephritin antibodies. But, this detection has its limitations as just 1/3 of the patients with DN present damage to the filtration barrier of the glomerulus. In addition to the detection in DN patients, urine podoxin and podocalyxin are also elevated in active lupus nephritis (Wang *et al.* 2007, Wang *et al.* 2008) and the later was also observed in post-streptococcal Glomerulonephritis (Kanno *et al.* 2003) and in patients with IgA nephropathy (Asao *et al.* 2012).

1.12.6. Asymmetric dimethylarginine (ADMA)

Asymmetric dimethylarginine or 2-Amino-5 [(amino-dimethylaminomethylene) amino] pentanoic acid (ADMA) is an amino acid, closely related to L-arginine. ADMA is created through protein methylation by a reaction catalysed by an enzyme called S-adenosylmethionine protein N-methyltransferases (Rawal *et al.* 1995) and is measured using high-performance liquid chromatography. ADMA mechanism of action involves inhibition of nitric oxide synthase, thus decreasing nitric oxide production (Vallance *et al.* 1992). Raised levels of serum ADMA have been associated with development of nephropathy in patients with type 2 diabetes (Hanai *et al.* 2009), endothelial dysfunction and subsequent atherosclerosis (Ando *et al.* 2013, Eiselt *et al.* 2014), cardiorenal syndrome (Ueda *et al.* 2013) and CKD progression to ESRD (Baylis 2012). ROC curve analysis was used to evaluate the predictive potential of serum ADMA as a marker of inflammation in 142 CKD patients and compared to serum levels of symmetric dimethylarginine (SDMA), CRP, TNF- α and albumin, and as such was classified as an inferior biomarker giving only 66% prediction against 82% of CRP, 72% of albumin, 69% of SDMA and 57% of TNF- α (Schepers *et al.* 2011).

1.12.7. Interleukin 18

Interleukin-18 (IL18, also known as interferon-gamma inducing factor) is a pro-inflammatory cytokine that belongs to the IL-1 superfamily and is expressed in the intercalated cell of the late distal convolute tubule, the connecting tubule and the collecting duct of healthy human kidneys (Urbschat *et al.* 2011). It is a biomarker of proximal tubular injury in ischemic acute tubular necrosis (ATN) (Parikh *et al.* 2004) and has been shown to be a useful predictor of AKI (Nickolas *et al.* 2008, Liu *et al.* 2013) and of ESRD in patients with IgA nephropathy (Peters *et al.* 2011) and diabetic nephropathy (Miyachi *et al.* 2009)). Its plasma levels were also found elevated in cases of contrast-induced nephropathy (Ling *et al.* 2008, Duan *et al.* 2013) and in various pathophysiological states; such as systemic lupus, inflammatory arthritis and hepatitis (Urbschat *et al.* 2011). However, contrasting studies have showed low levels of prediction of tubule-interstitial damage in IgA nephropathy (64% by ROC-AUC analysis, n=76, (Shi *et al.* 2012), nephrotoxicity (65% by ROC-AUC analysis, n=85 children, (Zubowska *et al.* 2013) and even in dialysis patients when used in combination with other cytokines (IL-1 β , IL-6 and TNF- α , 59% by ROC-AUC analysis, n=217, (Zoccali *et al.* 2006). It looks like although this cytokine seems to be a good predictor of AKI severity and mortality, its application as a biomarker of CKD progression may be limited by the fact that it is upregulated in diverse inflammatory diseases. For instance, a study with 908 HIV-infected women showed that ACR was a better predictor of disease progression (based on eGFRcys decline) than IL-18, NGAL or KIM-1 (Shlipak *et al.* 2012), suggesting that it has no further beneficial value than the currently used standard biomarker.

1.12.8. TGF- β 1

Transforming growth factor-beta1 (TGF- β 1) is a 25kDa polypeptide member of the transforming growth factor beta superfamily of cytokines. It is mainly secreted by T and B cells, myofibroblasts, macrophages and tubular cells, however, podocytes have also been implicated in the up-regulation of TGF- β 1 (Abbate *et al.* 2002). TGF- β 1 conducts a variety of cellular functions, including the control of cell growth, proliferation, differentiation and apoptosis. It is extensively known as a potent fibrogenic renal growth factor (Douthwaite *et al.* 1999). The pro-fibrogenic effects of TGF- β 1 are associated with the activation of pericyte-myofibroblast transition induced by α smooth muscle actin (α -SMA) (Wu *et al.* 2013). TGF- β 1 has also been shown to modulate TG2 release and increase the synthesis of ECM polypeptides, such as fibronectin, heparan sulphate proteoglycan, laminin beta1 and collagen alpha1 (Douthwaite *et al.* 1999). Such actions increase deposition of ECM components and thereby promote scar formation.

Increases in TGF- β 1 have been observed in a variety of kidney scarring models including 5/6th nephrectomy (Coimbra *et al.* 1996, Junaid *et al.* 1997), diabetic nephropathy (Chen *et al.* 2001, Huang *et al.* 2010) and unilateral ureteral obstruction (Wu *et al.* 2013). In human kidney disease, there was an increase in urinary TGF- β 1 levels in DN (Fagerudd *et al.* 1997, Sato *et al.* 1998), chronic glomerulonephritis (Honkanen *et al.* 1997) and in CKD from different aetiologies (De Muro *et al.* 2004). Suthanthiran and colleagues were the first to report a positive association between TGF- β 1 and CKD progression in humans by activation of RAAS, affecting mostly African Americans (Suthanthiran *et al.* 2009). In fact, several other cross-sectional studies suggested a higher prevalence of CKD progression into ESRD in African Americans, but not in Caucasians, due to the effects of circulating TGF- β 1 (Lee *et al.* 2009; Suthanthiran *et al.* 1998). Levels of circulating total and active TGF- β 1 and its natural antagonist Bone morphogenetic protein-7 (BMP-7) were measured in 102 patients with DM type 2, presenting a combined total TGF- β 1 plus BMP-7 ROC-AUC prediction of renal progression of 88%, compared to 94% in the combination of total and active TGF- β 1 plus BMP-7 and 73% for the combination of the conventional markers ACR and eGFR (Wong *et al.* 2013). However, TGF- β 1 was added to a panel with other experimental biomarkers along with cystatin C, IL-6, high-sensitivity c-reactive protein (hsCRP) and fibroblast growth factor 23 (FGF-23) and screened in 2544 patients recruited from the Canadian CKD cohort (stages 4 and 3B) (Levin *et al.* 2014). In this large human study, TGF- β 1 failed to improve the prediction of progression to ESRD when compared to conventional markers such as ACR, phosphate and haemoglobin.

1.12.9. FGF-23 and Klotho

Fibroblast growth factor (FGF-23) is a 32kDa protein produced by osteoblasts and osteocytes which main function is the regulation of phosphate concentration in the plasma in response to elevated Calcitriol (1,25-dihydroxycholecalciferol or 1,25-dihydroxyvitamin D₃) levels (Shimada *et al.* 2004, Juppner 2011, Kovesdy and Quarles 2013). FGF-23 production is also upregulated by high phosphate intake as well as chronic hyperphosphatemia (Isakova *et al.* 2011, Vervloet *et al.* 2011), whereas the use of phosphate binders such as sevelamer decreases the circulating levels of this hormone (Oliveira *et al.* 2010, Adema *et al.* 2013, Chue *et al.* 2013). FGF23 acts on the kidneys, where it decreases the expression of NPT2a and NPT2c, two sodium-phosphate co-transporters in the proximal renal tubule (Juppner 2011). Thus, FGF23 reduces the reabsorption and increases urine excretion of phosphate (Olauson and Larsson 2013). In addition, FGF-23 directly suppresses 1 α -hydroxylase in the proximal

tubule leading to reduced conversion of 25-hydroxyvitamin D to its active metabolite (Liu *et al.* 2006). Further, FGF-23 can also regulate vitamin D metabolism through the stimulation of 24-hydroxylase (Cyp24) which increases vitamin D degradation and also by inhibiting the transcription and secretion of PTH (Ben-Dov *et al.* 2007, Krajsnik *et al.* 2007).

α -Klotho (Klotho) is a type-I membrane-bound protein that directly binds to FGF receptor 1c in a paracrine manner, converting it into a specific FGF-23 receptor (Olauson and Larsson 2013). Therefore, FGF-23 is dependent on Klotho to induce FGF-receptor signalling. Klotho has a short transmembrane domain and two large extracellular domains (Shiraki-Iida *et al.* 1998) and its expression in the kidneys is restricted to the distal tubules (Kovesdy and Quarles 2013). This limited distribution of Klotho in the kidneys leads to a restriction in the physiologic actions of FGF-23 (Kovesdy and Quarles 2013).

The phosphaturic action of FGF-23 increases dramatically as renal function declines (Pavik *et al.* 2013). However, it is possible that the increase in FGF-23 levels in the initial stages of CKD is an adaptive response to the reduction in vitamin D rather than a consequence of reduced kidney mass *per se* (Quarles 2012, Kovesdy and Quarles 2013). Blood concentration of FGF23 predicts adverse outcomes, particularly cardiovascular disease and CKD (Kendrick *et al.* 2011, Kovesdy and Quarles 2013, Zoccali *et al.* 2013). In the study from Kendrick *et al.* for example, plasma FGF-23 concentrations obtained from 1099 patients with advanced CKD were found to be strongly associated with progression to dialysis initiation, presenting a Hazard ratio of 1.68 (95% CI 1.38 to 2.05; $P < 0.0001$) per standard deviation increase in log FGF-23 concentrations (Kendrick *et al.* 2011).

Elevated circulating levels of FGF-23 had been associated with left ventricular hypertrophy (Gutierrez *et al.* 2009, Hsu and Wu 2009, Faul *et al.* 2011, Kirkpantur *et al.* 2011), bone-mineral disorders (Weber *et al.* 2003, Komaba and Fukagawa 2009), vascular calcification (Jimbo *et al.* 2013, Liabeuf *et al.* 2013), arterial stiffness (Houston *et al.* 2013) and renal fibrosis (Olauson and Larsson 2013). High serum FGF-23 levels were observed in 150 CKD patients at stages 3 to 5 and a ROC-AUC of 70.5% prediction for coronary calcification was found (Zhang *et al.* 2015). Conversely, tissue level of Klotho declines in early CKD and also contributes to an accelerated aging phenotype (Carracedo *et al.* 2012). Several studies outline the importance of FGF-23/Klotho complex to the progression of CKD to ESRD (Fliser *et al.* 2007, Gutierrez *et al.* 2008, Isakova *et al.* 2011). For example, in a recent prospective study with 3879 CKD patients from stage 2 to 4 study (median follow-up of 3.5 years) showed that elevated FGF-23 was an independent risk factor for CKD progression and mortality (Isakova *et al.* 2011). Also, in another study with 604 CKD patients, plasma FGF-23 was

positively correlated with proteinuria and smoking (Vervloet *et al.* 2012), major cardiorenal risk factors. Likewise, FGF-23 plasma concentrations (c-terminal and intact FGF-23) were measured in 227 nondiabetic CKD patients from The Mild to Moderate Kidney Disease (MMKD) study (Fliser *et al.* 2007). Prediction of renal disease progression was evaluated by ROC-AUC of 81% and 72% for c-terminal and intact FGF-23 respectively. However, eGFR remained the best prognostic tool for evaluating progressive CKD as it presented the highest area under the curve, with a predictive value of 84%.

1.12.10. Oxidative stress molecules

Oxidative stress refers to the *in vivo* oxidation of macromolecules such as lipids, carbohydrates and DNA (Fassett *et al.* 2011). It occurs as a result of an imbalance between the formation of reactive oxygen species (ROS) and anti-oxidant defence mechanisms. Formation of ROS such as hydrogen peroxide (H₂O₂) superoxide (O₂⁻) and hydroxyl radicals (OH) is mediated by both the mitochondrial respiratory chain and the NADPH oxidase systems. These are counteracted by the action of antioxidant enzyme systems such as superoxide dismutase, catalase and the oxidant scavenger glutathione peroxidase (Locatelli *et al.* 2003). Examples of oxidative stress molecules include AGE (Witko-Sarsat *et al.* 1996), protein reduced thiols, MDA, TAS, Urinary 8-hydroxydeoxy guanosine, Superoxide dismutase, amongst many others (Fassett *et al.* 2011).

Increased plasma levels of oxidative stress biomarkers (protein carbonyl group, free F₂-isoprostane and protein reduced thiol) have been observed in 60 CKD patients with stages 3 to 5 (Oberg *et al.* 2004). However, no significant relationship between those biomarkers and the MDRD eGFR was found. Circulating levels of oxidative stress molecules have been particularly elevated in patients presenting chronic glomerulonephritis (Shah 2004), diabetic nephropathy (Ha and Lee 2003) and in ischaemia-reperfusion injury (Dobashi *et al.* 2000). In addition, the predictive value of these markers has been studied in specific subsets of CKD patients, including 62 IgA nephropathy (ROC-AUC of 71% for predicting decline in renal function) (Camilla *et al.* 2011) and 626 Hypertensive individuals (ROC-AUC of 93.1% for plasma F₂-isoprostane). However, scant data on the predictive prognostic value is available in general CKD population and therefore, larger longitudinal studies are needed to investigate how well they can predict kidney disease progression.

1.12.11. Thesis rationale and hypothesis

Chronic Kidney Disease (CKD) affects up to 16% of the global population and is associated with significant morbidity and mortality, consuming a large proportion of health care resources (Stringer *et al.* 2013). It is often progressive leading to End Stage Renal Disease (ESRD) with the requirement for RRT (dialysis and transplantation). With the above in mind, it is imperative to tackle this disease by establishing early detection and prevention. However, current kidney function and damage tests have known limitations as they do not fully indicate diagnosis and its outcomes, provide low accuracy in predicting disease progression and are inadequate in assessing early response to therapy. Thus, there is a requirement for identification of early and reliable non-invasive biomarkers of progressive kidney disease. This would allow us to individualize patient care, improve long term outcomes and potentially lead to the development of new therapies capable of retarding CKD progression.

Current markers of kidney function include the estimation of GFR by measurement of urine creatinine, which does not provide an accurate evaluation, due to bias by race, sex, age, hydration status and muscle mass (Stevens *et al.* 2006; Wu *et al.* 2008). Alternatively, β -Trace protein or Cystatin C could be used for kidney function estimation. Cystatin C has proven to be more effective than creatinine for GFR assessment. However, results from a large meta-analysis conducted by Shlipak *et al.* revealed that the improvement in risk prediction of CKD progression to ESRD was not statistically different from that observed with creatinine (Shlipak *et al.* 2013). Furthermore, increase in cystatin C concentrations could also be affected by other inflammatory conditions such as thyroid dysfunction (Ye *et al.* 2013) and asthma (Shigemura *et al.* 2012). As for β -Trace protein, although it is a more sensitive marker than serum creatinine, it is inferior to cystatin C (Filler *et al.* 2013). Amongst the novel experimental biomarkers of CKD progression, raised levels of NGAL, ADMA, TGF- β 1 and FGF-23 were shown to be elevated in overall CKD. Nonetheless, distinct ROC curve analysis from such individual markers was performed in several different studies and reported that such biomarkers presented no significant improvement in accurately predicting CKD progression to ESRD when compared to conventional markers.

Regardless of the underlying disease, the final process of CKD is characterised by excessive accumulation of ECM what leads to fibrosis and scar formation. The pathology of this is well described and as such mediators of the process that are present in urine theoretically would make important biomarkers of CKD. Transglutaminase 2 (TG2) is well described as one of the mediators of kidney fibrosis, being instrumental in scar tissue formation by catalysing the post-translational modification of ECM proteins by the formation of ϵ (γ -glutamyl) lysine bonds

(Fesus *et al.* 2002). Previous studies demonstrated that tissue levels of TG2 and ϵ (γ -glutamyl) lysine correlate well with histological renal scarring (Fisher *et al.* 2009; Johnson *et al.* 2003; Johnson *et al.* 1997; Skill *et al.* 2001). Further studies have also established a good correlation between tissue levels of MMPs, TIMPs, PAI-1 and collagen with development of kidney fibrosis (Lauhio *et al.* 2008; Obermuller *et al.* 2001; Rodrigo *et al.* 2000; Tashiro *et al.* 2004; van der Zijl *et al.* 2010; Yan *et al.* 2012; Eddy *et al.* 2009). Hence, this study will evaluate if ECM related molecules in the urine could be used as potential non-invasive biomarkers of CKD progression and add prognostic value to current biomarkers.

This study therefore aims to test the hypothesis that proteins known to be involved in fibrotic remodelling are present in the urine, can be measured and that the levels of these may predict the status of the fibrotic pathway and thus predict the rate of disease progression.

Chapter 2

Aims

The main aims of this study are:

- 1) To obtain sequential urine and serum from three animal models of CKD which have progressive disease. These are the 5/6th SNx, DN and CAN models in the rat.
- 2) In these animal models evaluate urine levels of ECM related molecules known to be linked to fibrotic remodelling including TG2 and its crosslink product ϵ (γ -glutamyl) lysine, MMPs, TIMPs, MMP activity, total collagen and PAI-1.
- 3) To collect clinical samples (urine and blood) from >200 patients from all cause CKD at all stages of disease using the patient pool at the Sheffield Kidney Institute, NGH, UK.
- 4) Measure the best biomarker candidates from the animal models in the human patient samples. Determine their potential to predict progression by following these patients for 3 years post sampling.
- 5) Correlate urine measurements to histological changes using a set of patients with matched biopsies available.

Chapter 3

Materials and Methods

3.1. *In Vivo* Experimentation

3.1.1. Experimental Animals

Three animal studies were performed previously to the start of this study: The 5/6th Subtotal Nephrectomy model of renal scarring (SNx) (Johnson *et al.* 2007), the UNx STZ model of Diabetic Nephropathy (DN) (Huang *et al.* 2010) and the Fisher to Lewis model of Chronic Allograft Nephropathy (CAN) (Shrestha *et al.* 2014). Archival materials (kidney homogenate and urine samples) were available from these studies. In brief, male Wistar harn rats weighing 200-250g were used for the 5/6th Subtotal Nephrectomy model of renal fibrosis and for the UNx STZ model of Diabetic Nephropathy (University of Sheffield, UK). In both models, animals were aged between 8-10 weeks, weighing 200 to 250 g at the beginning of the experiment. For the Fisher to Lewis transplant model of Chronic Allograft Nephropathy, male Fisher (F334, RT1v1) and male Lewis (Lew, RT1) rats (Harlan, UK), weighing 200-300g and aged 8-12 weeks were used.

In all models, rats were housed 2-4 animals per cage in an environment of 45% humidity on a 12/12 hours light/dark cycle at 20-22°C. Animals were allowed free access to rat chow (protein/casein content 18%; LabSure Ltd, Cambridge, UK) and water. This represented a medium protein diet. All experiments were performed under and complied with the Animal Scientific Procedures Act 1986.

3.1.1.1. Anaesthesia

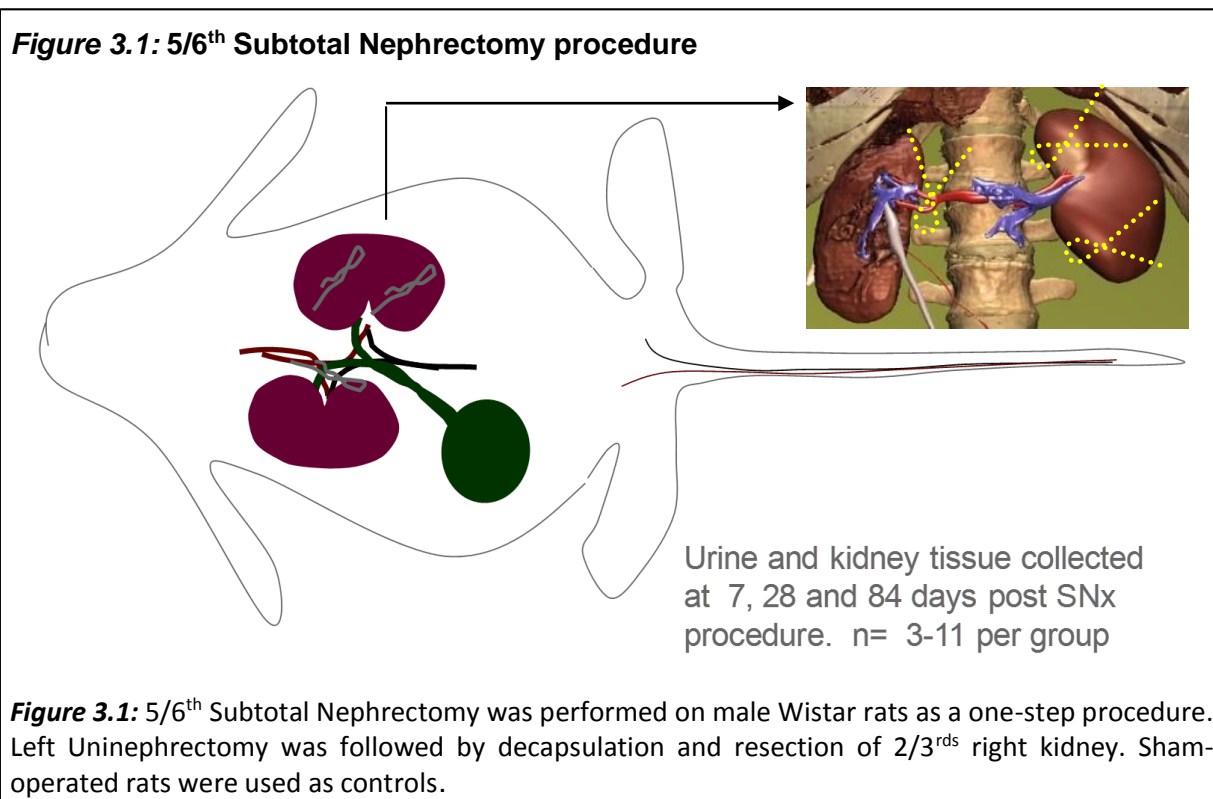
In all three animal models, anaesthesia was induced with 5% Halothane (Animalcare Ltd, York), 4L/min O₂ via inhalation in a sealed induction chamber and then maintained via nose cone at 3% Halothane, 1.5L/min O₂. The depth of anaesthesia was checked and confirmed by loss of both hind leg-withdrawal and corneal reflexes. Body temperature was maintained using a heat mat.

3.1.2. The 5/6th Subtotal Nephrectomy model of renal scarring

Subtotal Nephrectomy was conducted as a one-step procedure through excision of 5/6 of the kidney mass (Johnson *et al.* 2007). In this procedure, 2/3rds of the right kidney was resected following ligature (3/0 mersilk, Southern Syringe Services, London) of its lower and upper poles leaving the rat with only 1/3rd of the right kidney (figure 3.1). The degree of resection was calculated from the weights of the removed kidney poles:

$$\% \text{ Nephrectomy} = \frac{\text{left kidney (g)} + \text{right kidney poles (g)} + 0.1\text{g}}{2 \times \text{left kidney (g)}} \times 100$$

This procedure leads to the development of CKD over 3 months by the development of progressive glomerulosclerosis and tubule-interstitial fibrosis. Sham-operated rats (SNc) were used as controls. These rats had retro-peritoneal incisions on both the left and right side without manipulation of either kidney. Rats were sacrificed in groups at 7 (n=3-4), 28 (n=3-4) and 84 (n=3-11) days post surgery. Biochemical measurements (Creatinine clearance, Proteinuria, Albuminuria) and histopathology were analysed at these time points to evaluate kidney function and scarring process.



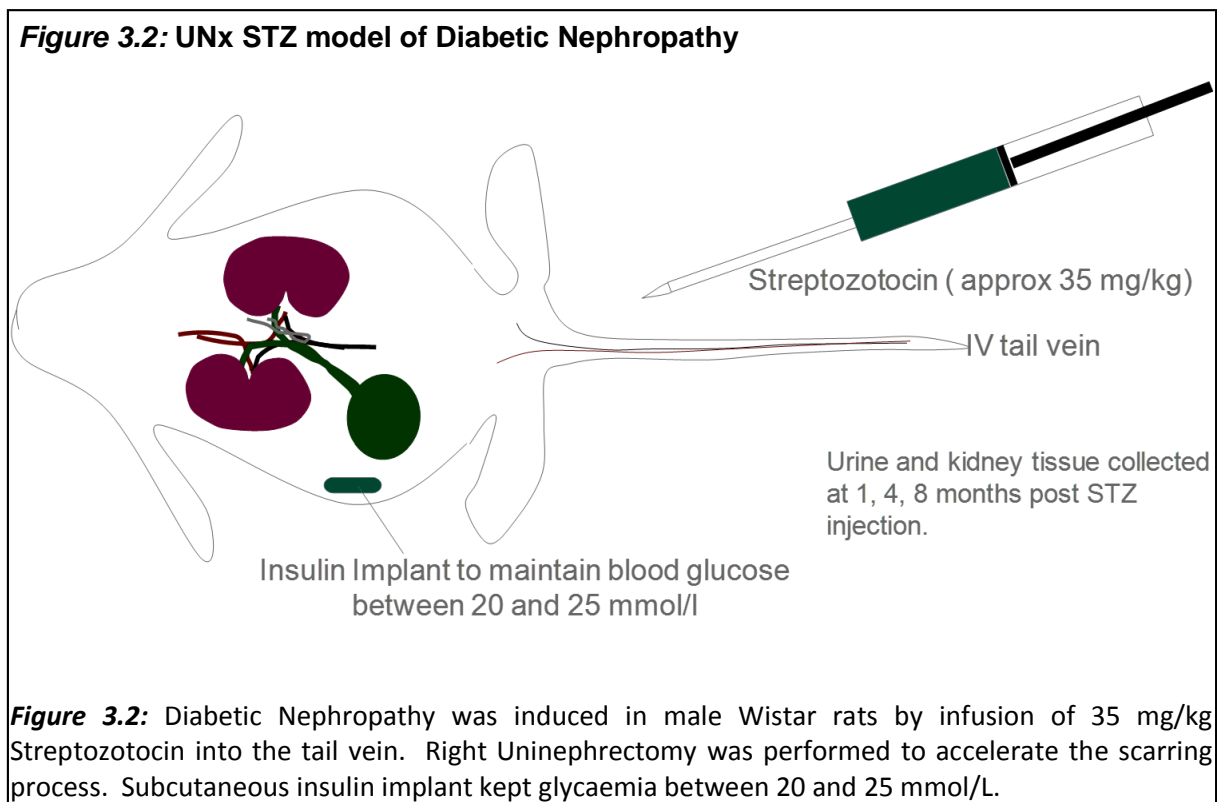
3.1.2.1. Pan Transglutaminase Inhibitors renal infusion in SNx

Two different types of pan TG inhibitors were used for direct infusion into the rat kidneys. Both compounds were site-directed and irreversible inhibitors of the enzyme, but with different properties. N-benzyloxycarbonyl-L-phenylalanyl-6-dimethyl-sulfonium-5-oxo-L-norleucine (NTU 281) was chosen as it acts predominantly in the extracellular compartment due to its poor permeability across cell membranes, while 1,Dimethyl-2 [(oxopropyl)thio] imidazolium (NTU 283) has high cell solubility and consequently its action is both extra and intracellular. TG inhibitors were made up in PBS (pH7.4) at 50mMol/L, loaded into a 2ML4 Azlet® mini-osmotic pump (Charles River, UK) which was inserted subcutaneously on the scruff and connected to a 9 cm long, 0.58 mm diameter polyethylene customised cannula placed into the

renal parenchyma, The cannula was secured in the kidney using a silk tie and tissue glue. TG2 inhibitors were delivered at a flow rate of 0.5ul/hour for 28 days at which point pumps were replaced.

3.1.3. The UNx STZ model of Diabetic Nephropathy

A total of 25 male Wistar rats had a right Uninephrectomy (UNx) performed. An infusion cannula was implanted in the lower pole of the left kidney and then connected to a mini-osmotic pump. 7 days post-surgery, 35 mg/kg of Streptozotocin (STZ) was administered in 0.1 mol/L Sodium Citrate buffer (pH 4.0) by IV injection into the tail vein using a 23G Butterfly Cannula (Venisystems, UK). After two days glycaemia was measured. Animals above 20mM/L glucose were considered diabetic. Glycaemia was controlled to between 20 and 25 mmol/L by titrating in quarters of a subcutaneous insulin implant (Linshin, Canada) to prevent animal wasting (figure 3.2). Sham operated rats (n=10) were used as controls. Control rats received 0.3ml of a 0.1mol/L sodium citrate (pH 4.0) solution. Creatinine clearance, albuminuria, glycaemia and histopathology were analysed at 1 (n=3-4), 4 (n=3-7) and 8 (n=3-5) months post Streptozotocin administration (Huang *et al.* 2009).



3.1.4. The Fisher to Lewis model of Chronic Allograft Nephropathy

In this model, donor rats; Lewis (isograft) or Fisher (allograft) received 2ml of 0.9% saline solution in bolus followed by a 6ml/h intravenous infusion. Testicular vessels, superior vesical artery, vessels supplying seminal vesicle, vas deferens and prostate, right ureter and urethra were ligated and divided. 300 units of Heparin were administered intravenously, the supra- and infrarenal aorta and the infrarenal IVC were ligated with 6/0 Vicryl (Southern Syringe Services, London) and the donor kidney was perfused with 2ml/min solution of cold University of Wisconsin (UW) for 10 minutes through the infrarenal aorta. The donor kidney was recovered and then stored in cold UW solution prior to transplantation. Recipient Lewis rats received an intravenous infusion of 2ml Succinylated fluid gelatine (Volplex, Maelor Pharmaceuticals Ltd, UK) in bolus followed by an administration of 6ml/h of this plasma volume expander prior to left nephrectomy. The donor kidney was transferred to the recipients. Blood vessels were anastomosed and the kidney reperfused. A cystotomy was performed and the donor bladder cuff anastomosed to the recipient bladder using continuous 6/0 Vicryl suture. The transplanted kidney was anchored to the retroperitoneum by suturing the perinephric fat to the psoas muscle. 5 rats were used on the Isograft group (Lewis to Lewis) and 7 on the Allograft group (Fisher to Lewis). Both isografts and allografts were given 5 mg/kg of Cyclosporine (Novartis, Basel, Switzerland) via intraperitoneal injection for 10 days to prevent acute rejection. Biochemical measurements (Creatinine clearance, Proteinuria, Albuminuria) were analysed at 2, 8, 17, 24, 33 and 52 weeks post transplantation and histopathology at the final time point.

Figure 3.3: Renal Transplantation procedure

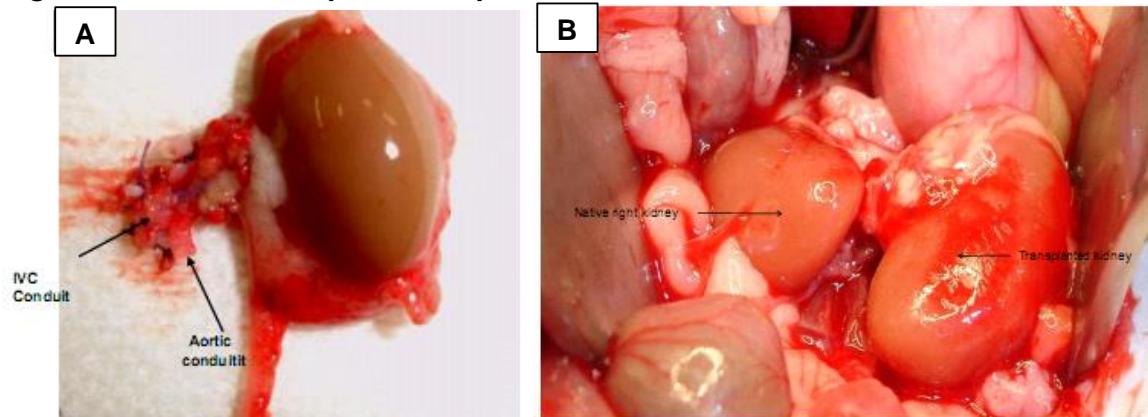


Figure 3.3: A) Left native kidney removed from a Lewis rat showing hilar vessels and ureter. After retrieval, donor kidney was perfused with UW solution. The infrarenal aorta and Inferior Venacaval (IVC) were mobilised. **B)** Recipient end-to-side anastomosis and re-perfusion (n = 5 L-L Isografts, n= 7 F-L Allografts).

3.1.5. Clinical Chemistry

Kidney function was assessed in order to monitor the progression of renal scarring in each animal model. All rats were subjected to twenty four hour urine collections at specific time points to determine creatinine clearance, total protein excretion and albuminuria. Blood samples were used to measure serum creatinine and glycaemia (UNx STZ model of Diabetic Nephropathy). Body weight and blood pressure (using a Model 229 blood pressure Amplifier/Pump; IITC, USA) were also measured at each time point.

3.1.5.1. Creatinine Clearance

Rats were placed in metabolic cages (Techniplast, Italy) for 24 hours for kidney function assessment. Urine was collect on chillers (Techniplast, Italy) to avoid protein denaturation and evaporation. After this, the volume of urine was measured, aliquoted and stored at minus 20°C. Blood samples were collected by either cardiac puncture at termination (SNx and DN models) or taken from the tail vein using a 23g venisystems butterfly cannula (Hospira, Ireland) (CAN model) and were left 30 minutes at room temperature to clot before centrifugation at 1500 X g, 4°C using a Sigma 3-18K centrifuge (SciQuip Ltd, UK) in order to collect serum. Urine and serum Creatinine were measured by the Clinical Chemistry Department at the Northern General Hospital (Sheffield, UK) using the Jaffe colorimetric method (figure 3.4). Creatinine Clearance was calculated using the equation below.

Figure 3.4: Jaffe colorimetric method

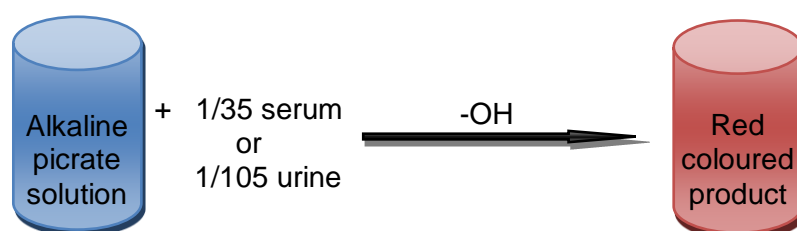


Figure 3.4: Urine or serum sample is placed in a reaction tube containing an alkaline picrate solution. The creatinine present in the sample reacts with picric acid to form a red-coloured product which is read by a Spectrophotometer at 520nm. The creatinine concentration will be directly proportional to the colour intensity.

$$\text{Creatinine Clearance} = \frac{\text{Urinary Creatinine } (\mu\text{mol/L}) \times \text{Urine flow rate (ml/min)}}{\text{Serum Creatinine } (\mu\text{mol/L})}$$

3.1.5.2. Proteinuria

Estimation of protein concentration was done on 24 hour urines collected from rats placed in metabolic cages. A modified Lowry protein assay (Lowry *et al.* 1951), the RC DC™ protein assay (Bio-Rad laboratories, UK), was used for this estimation, as described in section 3.2.2.1 and expressed as mg/24hrs.

3.1.5.3. Albuminuria

Rat Albuminuria was determined by a commercial Albumin ELISA kit (Bethyl Laboratories, Texas, USA). 100ul of Monoclonal sheep anti-rat albumin affinity purified capture antibody diluted in 1:100 in coating buffer (0.05M Carbonate-Bicarbonate, pH 9.6) was added to each well of a 96 well microplate (Costar 3590, Corning Incorporated, USA). The microplate was incubated at room temperature (20-25°C) for 1 hour and then washed five times with a solution containing 50mM Tris (Fisher Scientific, UK), 0.14 M NaCl, 0.05% Tween 20 (Fisher Scientific, UK) at pH 8.0. 200µl of a blocking solution (50mM Tris, 0.14M NaCl, 1% BSA, pH 8.0) was added to each well after washing. The microplate was incubated for 30 minutes at room temperature and then washed again for five times. A standard curve of 1.95-10,000ng/ml albumin was generated in 50mM Tris. Standards and urine samples were diluted in 50mM Tris, 0.14M NaCl, 1% BSA, 0.05% Tween 20 solution in a range of 1:2, 1:5, 1:10 and 1:50, and were coated in duplicates (100ul each well) on the microplate. Rat serum was used as internal control. After 1 hour incubation at room temperature, the microplate was washed a further 5 times. 100ul of 1:100 diluted Polyclonal Sheep anti-rat albumin HRP conjugated detection antibody was added to each well and incubated for another 1 hour. After 5 final washes, 100ul of Tetramethylbenzidine (TMB) (Sigma-Aldrich, UK) substrate solution was applied to the microplate which was then left in the dark for 15 minutes for reaction development. The reaction was stopped by addition of 0.18M Sulphuric Acid (H₂SO₄) (Analar Normarpar®, VWR International Ltd). Absorbance was measured on Labsystems Multiskan Ascent plate reader (Bio-Rad Laboratories, Hertfordshire, UK) at a wavelength of 450nm. Results were analysed by a Labsystems Genesis computer package (Bio-Rad Laboratories, Hertfordshire, UK). A typical standard curve is shown in figure 3.5.

Figure 3.5: Rat Albuminuria Standard Curve

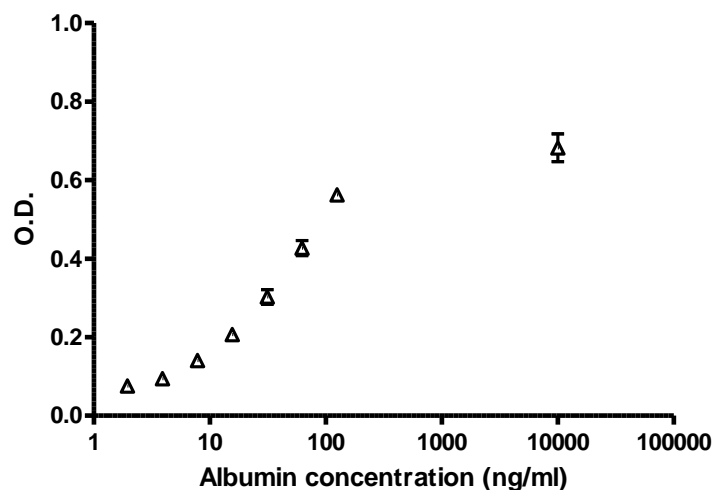


Figure 3.5: Rat Albumin ELISA standard curve generated with known concentrations of Albumin (1.95-10,000ng/ml). Data points are average of triplicates. Error bars showing standard error are smaller than symbols.

3.1.5.4. Glycaemia

Blood glucose was monitored in the morning using a One touch basic glucose monitor (Johnson & Johnson) and terminal glycaemia was determined by standard autoanalyser techniques by the Clinical Chemistry Department at the Northern General Hospital (Sheffield, UK) and expressed as mmol/L.

3.1.6. Histopathology

3.1.6.1. Proccession and fixation of kidney tissue

For estimation of the degree of kidney scarring, kidneys were harvested and placed in 10% neutral buffered formalin solution (Sigma-Aldrich, UK) for 24 hours at 4°C, then washed in autoclaved 1x Phosphate Buffered Saline (PBS) (8g Sodium Chloride (Fluka, Sigma-Aldrich, UK), 0.2g Potassium Chloride (Fisher Scientific, UK), 1.44g Disodium Hydrogen Orthophosphate (Fisher Scientific, UK), 0.24g Potassium Dihydrogen Orthophosphate (Analar Normarpur®, VWR International Ltd), dissolved in 1L H₂O, pH 7.4) and stored in PBS until embedded in paraffin blocks.

3.1.6.2. Masson's Trichrome staining

4µm paraffin embedded sections were de-waxed in xylene (Fisher Scientific, UK) for 10 minutes and rehydrated in a series of graded ethanol solutions (100%, 90%, 75%, 50%) (Analar Normarpur®, VWR International Ltd) for 5 minutes each and then washed with distilled H₂O prior to Masson's Trichrome staining which was performed by the Department of Histopathology, Northern General Hospital, Sheffield, UK. Briefly, this is a three-colour staining protocol which involves the immersion of the fixed kidney sample into Weigert's iron haematoxylin, and then in three different solutions: A or plasma stain (acid fuchsin, Xylidine Ponceau, glacial acetic acid, and distilled water), B (phosphomolybdic acid in distilled water) and C, also called fibre stain (Light Green SF yellowish).

Masson's Trichrome stains Collagenous fibers and Extracellular Matrix blue or green, cytoplasm red or pink and cell nuclei in dark red or purple. Glomerular and tubulointerstitial scarring levels were assessed by multiphase image analysis.

3.1.6.3. Multiphase Image Analysis

Multiphase image analysis of Masson's Trichrome stained kidney sections was performed using the Analysis™ 3.2 Software (Soft Imaging Systems, Germany) using an Olympus BX 61 fluorescent microscope. Sections were examined at 200 x magnification for tubulointerstitial fibrosis determination and at 400 x magnification for glomerulosclerosis. A minimum of 10 random non-overlapping cortical fields per sample were analysed. Three different phases were assigned to specific areas; Phase 1 (blue) covered all fibrotic areas, Phase 2 (pink) covered all stroma and cells, and Phase 3 (yellow) for blank areas (tubular lumen and vacuolation). The area covered by each phase was quantified to give a percentage area value. The combination of all 3 phases should show a minimum of 95% total phase coverage for accurate quantification. Levels of scarring presented on kidney samples were obtained by dividing the area of phase 1 by phase 2. Overall kidney scarring was determined by the average of the 10 scarring values (phase1/phase2) obtained from the 10 cortical fields selected.

3.2. Human prospective study

3.2.1. Study design

The study was conducted at the Sheffield Kidney Institute (SKI) located on the Northern General Hospital site of Sheffield Teaching Hospitals NHS Foundation Trust, UK. The SKI

covers a population in excess of 1.7 million in the North Trent region in England treating a large number of patients representing all different stages and forms of CKD. Therefore, it provides a suitable environment for this study.

This study consisted of a prospective observational cohort of adult CKD patients from stages 1 to 5 over a period of 3 years. Patients underwent a detailed bio-clinical assessment that included the measurement of blood pressure, pulse rate, BMI calculation, laboratory assessment (serum creatinine, blood urea nitrogen, eGFR, albuminuria, ACR, proteinuria, PCR, serum cholesterol, triglycerides, calcium, phosphorus and PTH), socio-economic status (employment type and household address), smoking habit, medications in use and collection of urine and blood samples for new biomarker analysis (figure 3.6). The full bio-clinical assessment took place at baseline, whereas the laboratory assessment was collected at every outpatient's clinical appointment for a period over 3 years in order to assess CKD progression and outcomes.

This study aimed to recruit CKD patients above 18 years old and of any CKD etiology attending the SKI outpatient clinic facilities to define the prognostic value of new urine CKD biomarkers with emphasis on ECM related molecules (TG2 and its crosslink product, total collagen, MMPs, TIMPs and PAI-1). This study also aimed to collect bio-samples (blood and urine) from healthy volunteers, diabetic controls and CKD patients undergoing renal biopsies to correlate these findings with histological changes as well as clinical parameters.

Figure 3.6: Overview of the Bio-Clinical assessment

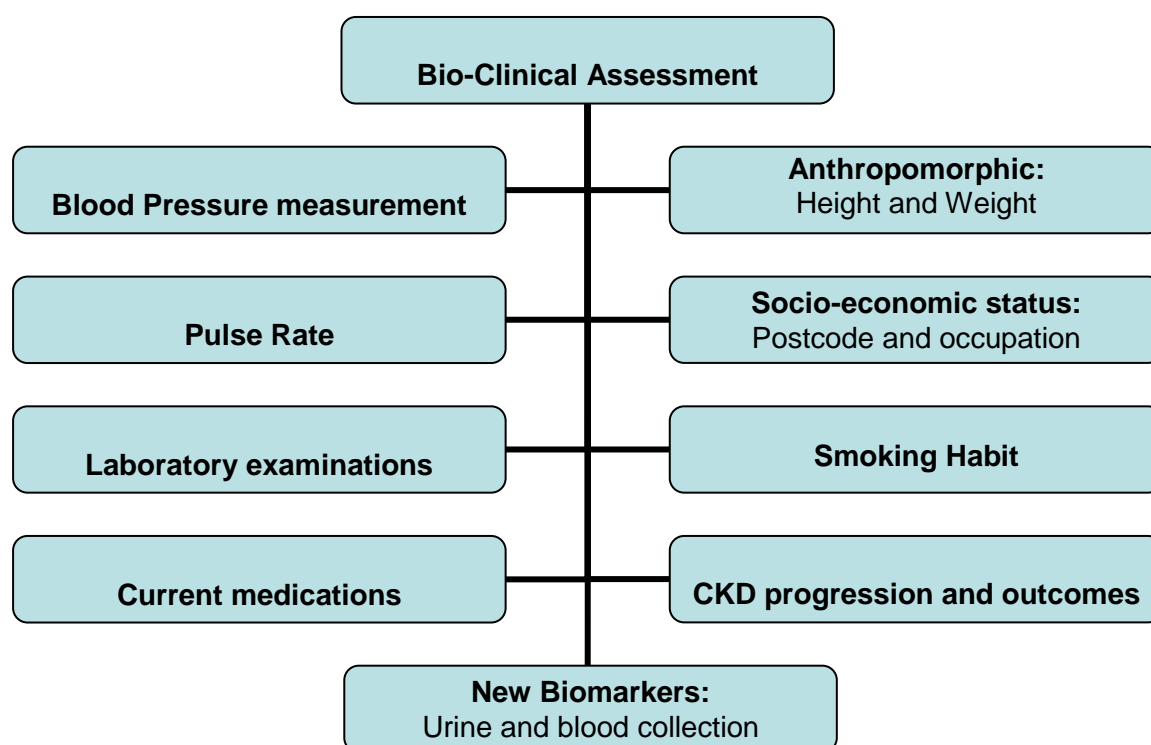


Figure 3.6: The structure of the Bio-Clinical assessment of patients recruited to the study

3.2.2. Ethics and Research governance

The study protocol has been approved by the South Humber Local Research Ethics Committee under the REC reference number 08/H1305/64 until October 2012 and 12/YH/0297 after this date. It was registered with the STH NHS Foundation Trust Research Department under the ethics reference application number STH 15004 and was sponsored by Pfizer pharmaceuticals. The research was conducted in accordance with the ethical principles set forth in the World Medical Association (WMA) Declaration of Helsinki and the International Conference on Harmonisation of Good Clinical Practice (ICH-GCP) guidelines in order to protect human subjects and to ensure collection of quality data. The chief investigator as well as the principal investigator possessed GCP training and accreditation. Patients received the Participants Information Sheet and Consent Forms before inclusion, having ample time before deciding whether or not they wished to take part in the study. Quality assurance procedures and research office inspections were performed at a regular basis during these 5 years of research. Copies of the Research Governance documents including the project registration forms, research department authorisation letter, the ethics committee approval letter, site

specific assessment, report of independent reviewers, letters of invitation to participants, Participants Information sheet and consent forms for healthy volunteers, CKD and kidney biopsy patients as well as the letter with information for GPs or consultants are attached in the thesis appendix.

3.2.3. Patient recruitment

3.2.3.1. Control group

A total of 33 adult healthy volunteers were included as a control group. This group consisted of subjects above 18 years old, without history of any type of kidney disease, hypertension, diabetes or any other chronic condition. Healthy volunteers had urine tests to ensure they were fit to participate in the study. These included the collection of mid-stream urine for albuminuria and creatinine (Microalbumin, Siemens, UK) and for sediment test with a Multistix urine test strip (Multistix 8SG, Siemens, UK) to verify the presence of proteins, glucose, ketones, haemoglobin, bilirubin, urobilinogen, acetone, nitrite and leucocytes as well as to test the pH, specific gravity and infection by different pathogens. Healthy volunteers' height, weight, blood pressure and pulse were also measured.

3.2.3.2. CKD patients

A total of 292 CKD patients from stages 1 to 5 were recruited at the SKI Outpatients Clinic. Major CKD causes were: diabetic kidney disease, chronic glomerulonephritis, hypertensive nephrosclerosis, atherosclerotic renovascular disease, chronic interstitial nephritis and ADPKD. From this total, 41 patients were recruited at the time of renal biopsy.

The inclusion criteria for this study were:

- ✚ Adult patients aged 18 or above
- ✚ CKD stages 1 to 5 from any aetiology

The exclusion criteria were:

- ✚ Patients on any form of RRT (Dialysis or Transplantation)
- ✚ Patients in a state of Acute Kidney Injury (AKI) at presentation
- ✚ Presence of UTI at presentation
- ✚ Mental incapacity

3.2.4. Protocol for Urine sample collection

3.2.4.1. Urine processing

220ml of fresh Mid-Stream Urine (MSU) were collected from every participant (CKD patients and Healthy volunteers) in the study. Urine samples were collected into a sterile container not containing any protease inhibitor and placed immediately on ice. 110ml of urine was removed and placed into a 175ml conical tip centrifuge tube. To ensure removal of cellular material, urines were centrifuged at 3000g for 10 minutes at 4⁰C using a Sigma 3-18K centrifuge (SciQuip Ltd, UK). The supernatant was removed and aliquoted into 5 x 20ml samples in universal tubes and 10 x 1ml in microfuge tubes to avoid protein degradation by freeze/thawing. Vials were labelled and stored at -80⁰C. These constituted the cell free urine (CFU) collection. The remaining 110ml of urine was aliquoted into 5 x 20ml samples in universal tubes and 10 x 1ml in microfuge tubes. All vials were labelled with SKI numbers, urine type and date of collection and then stored at -80⁰C. These constituted the complete urine collection (CU).

3.2.4.2. Initial screening

Initial screening of CKD patient's urines included the testing albuminuria and creatinine with a Microalbustix urine test strip (Microalbustix, Siemens, UK) and for sediment test with the Multistix (Multistix 8SG, Siemens, UK) to verify the presence of proteins, glucose, ketones, haemoglobin, bilirubin, urobilinogen, acetone, nitrite and leucocytes as well as to test the pH, specific gravity and infection. One patient presenting results compatible with UTI was excluded from the study.

3.2.4.3. Laboratory assessment

Serum creatinine, blood urea nitrogen, albuminuria, serum cholesterol, triglycerides, calcium, phosphorus and PTH were analysed by standard autoanalyser techniques by the Clinical Chemistry Department at the Northern General Hospital (Sheffield, UK). Total proteinuria was measured by the BCA assay (section 3.3.2.2). Retrieval of laboratory data was from patients' medical notes.

3.2.5. Protocol for Blood collection

10mls of blood were collected into 2 vacutainers; 1 containing EDTA for plasma and 1 containing clotting agent for serum. Both vacutainers were centrifuged at 400g for 10 minutes.

5ml of plasma and serum samples were aliquoted into 5x 1ml cryotubes, labelled and stored at -80°C.

3.2.6. Bio-repository database

The Sheffield Kidney Institute (SKI) bio-repository database was specially designed to store data from this and future studies. The database was constructed in Microsoft Access and was developed by the University of Sheffield Medical School Information technology support team. This electronic database enabled the automatic creation of a SKI patient (study) number which provided anonymity and therefore ensured the confidentiality of data collected from each subject. After generation of a SKI number, demographic details including gender, age, ethnicity and employment status; anthropometric data (height, weight and BMI), smoking habit, CKD diagnosis and co-morbidities, list of current medications as well as full clinical and laboratory results were entered and stored in the SKI database (figure 3.7). Glomerulosclerosis, tubulointerstitial fibrosis and vascular sclerosis score from each kidney biopsy patient were also recorded. In addition, 10 recordings of eGFR, serum creatinine and blood pressure collected during the follow-up period of 3 years were also recorded in the database (figure 3.8). All collected urine (CFU and CU) and blood (plasma and serum) samples were labelled (Avery LaserJet mini labels, Avery®, UK) with SKI numbers, sample type and date of collection and then stored in a dedicated racked -80°C upright Sanyo Freezer (MDF-U500VX, Sanyo-Biomedical, UK). This freezer had a dual cooling compressor system, an inbuilt temperature display with 24 temperature monitoring and an extensive alarm system in order to guarantee continuous maintenance of a temperature of -80°C. The SKI Bio-repository database is stored in a secure server designated by the University of Sheffield with exclusive access only by the investigators using onsite PCs only.

3.2.7.1. Data protection and confidentiality

All personal data collected in this study was processed in accordance with the rights of data subjects under the Data Protection Act 1998. All personal information about any participant was kept securely, confidential and processed in a fairly and lawful manner. Also, appropriate technical and organisational measures were taken to ensure the quality of the database and these included: undisclosed input of patients' details, anonymous labelling of samples with automatically generated SKI (study) numbers and administration documents marked with unique identifiers without participants' names recorded on them. The information revealing and connecting the identifiers to patients' names was kept separated from the rest of the data in a secure place where only authorised clinical investigators of this study had access. Finally,

standard procedure checks were regularly taken to ensure accuracy of data and adequate level of protection.

Figure 3.7: SKI Bio-repository database

The screenshot displays the 'patient_details - Microsoft Access' application. The interface is divided into several sections:

- Header:** The University of Sheffield logo and 'Academic Nephrology Unit Chronic Kidney Disease Study'.
- Navigation Pane:** A vertical sidebar on the left with a 'Navigation Pane' label.
- Form Fields:**
 - Find a Patient Record:** Search bar and buttons for 'Add Patient', 'Print Patient Record', 'Save Patient Record', and 'Patient Entered By' (Michelle da Silva).
 - Study ID:** SKI/37
 - Demographics:** Surname, Forenames, DOB (24/01/1957), Gender (Female), Employment Type (Unemployed), Job Title (Housewife), Patient Height (1.67m), Smoker? (Past Smoker), Current Medications (Doxazosin 2mg - OD, Quetiapine 200mg, Felodipine 10mg - OD, Quinine sulphate - 200mg, Atorvastatin 10mg -).
 - Addresses:** Address1, Address2, Address3, Postal Town (Clowne), Postcode (S43 4PJ), Telephone.
 - Diagnosis and Comorbidities:** CKD Diagnosis (Hypertensive Nephrosclerosis), co-morbidity 1 (Grade II hypertensive retinopathy), co-morbidity 2 (Asthma - 1997), co-morbidity 3 (Respiratory arrest - 1995), co-morbidity 4 (Depression - 1995), co-morbidity 5.
 - Date Patient Joined Study:** 20/03/2009
- Sample Details:**
 - Sample Date:** 20/03/2009
 - Sample ID:** 40
 - Anthropometric Data:** Patient Weight (69.20 kg), BMI (24.80), Blood Pressure (Systolic 134, Diastolic 66), Pulse (126 bpm).
 - Sample Locations:** Complete Urine 20ml (16.8), Complete Urine 1ml (3.8), Cell Free Urine 20ml (16.7).
 - Laboratory Data:**
 - urine?
 - EGFR (ml/min/kg): 24.00
 - serum_cholesterol (mmol/litre): 4.60
 - Diabetic?
 - 20ml Aliquots Complete Urine?: 4
 - EGFR Slope/Time?: 0.00
 - serum_triglycerides (mmol/litre): 1.60
 - ACE Inhibitors?
 - 1ml Aliquots Complete Urine?: 10
 - Rate of Decline of EGFR? (ml/min/year): -2.40
 - serum_calcium (mmol/litre): 2.26
 - ARBS?
 - 20ml Aliquots Cell Free Urine?: 5
 - serum_phosphorus (mmol/litre): 1.09
 - Statins?
 - 1ml Aliquots Cell Free Urine?: 10
 - Urine Albumin (pg/ml): 0.00
 - serum_ca_p (mg2 x dl2): 2.46
 - CKD Stage? (1-5): 4
 - Aliquots Urine Derived Cells?: 3
 - Urine Protein / Creatinine Ratio: 21.00
 - serum_PTH (pg/ml): 252.00
 - Total Cells Recovered: 17.00
 - Urine Albumin / Creatinine Ratio: 17.00
 - serum_creatinine (umol/litre): 187.00
 - Cell Conc in Urine (cells/ml): 0.15
 - Proteinuria (mg/ml): 0.15
 - 1/Creatinine Slope: 0.00
 - BUN (mmol/litre): 14.50
 - 24 Hour Proteinuria: 0.15
 - blood?
 - Serum Aliquots?: 4
 - Plasma Aliquots?: 3
 - biopsy?
 - SE - Glomerulosclerosis (From IIT): 0
 - SE - Tubulointerstitial (From IIT): 0
 - SE - Vascular Sclerosis (From IIT): 0
- Buttons:** 'Add New Sample', 'Save Sample Record', 'Print Sample Labels'.

Figure 3.7: The SKI Bio-repository database stored patients demographic details, anthropometric data, smoking habit, CKD diagnosis, past medical history, a full list of current medications as well as all relevant clinical and laboratory reports from each patient included in the study. Urine, blood and kidney biopsy samples locations in the -80°C freezer were also indicated in the files. Confidentiality was guaranteed by an anonymised input of data.

Figure 3.8: SKI Bio-repository database: Follow-up data

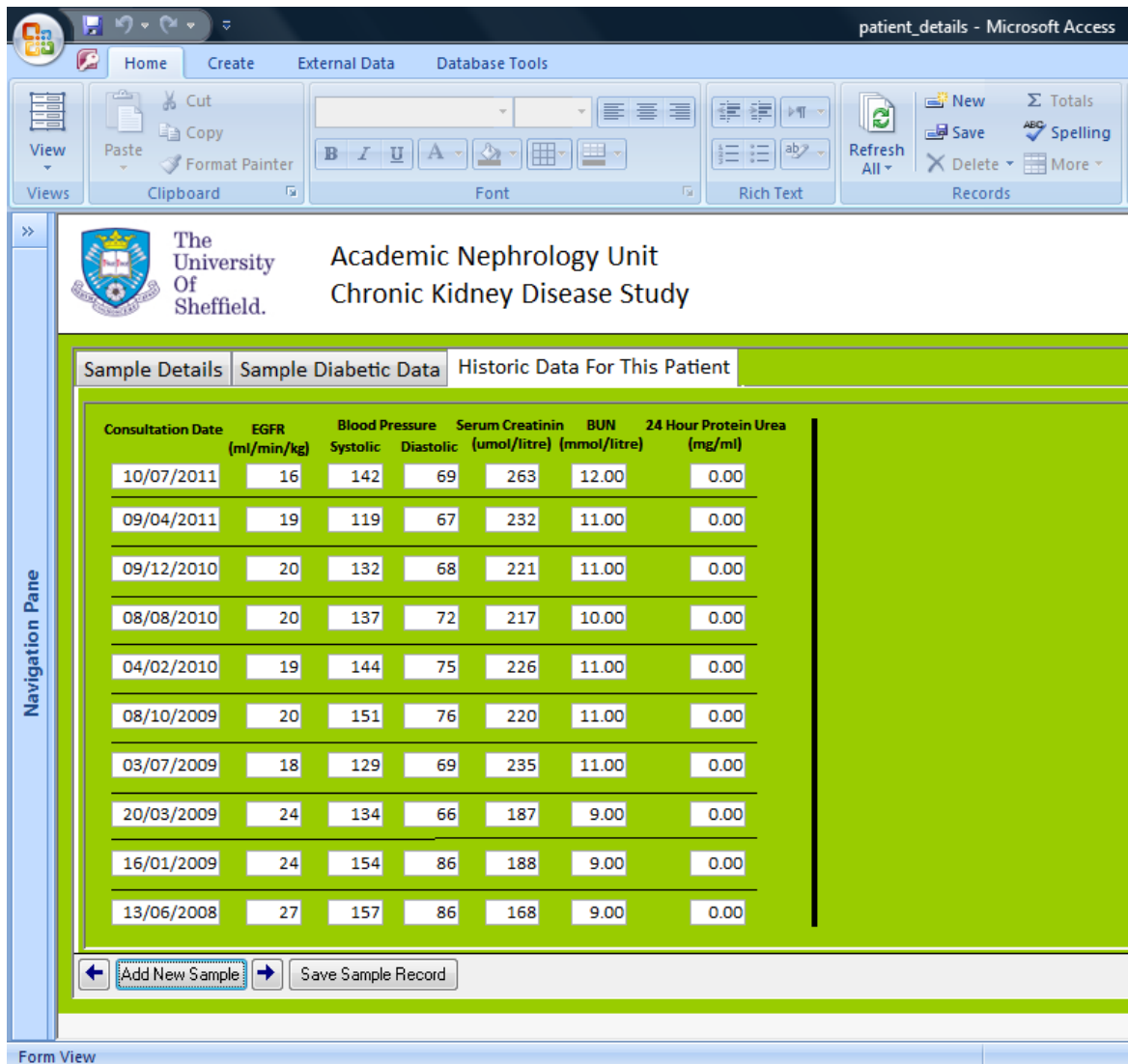


Figure 3.8: Historic data recording comprised of 10 measurements of eGFR, serum creatinine and blood pressure collected during the follow-up period of 3 years. This allowed us to assess the CKD progression status of subjects participating in the study cohort.

3.3. Determination of Protein concentration

3.3.1. Assays for estimation of protein concentration

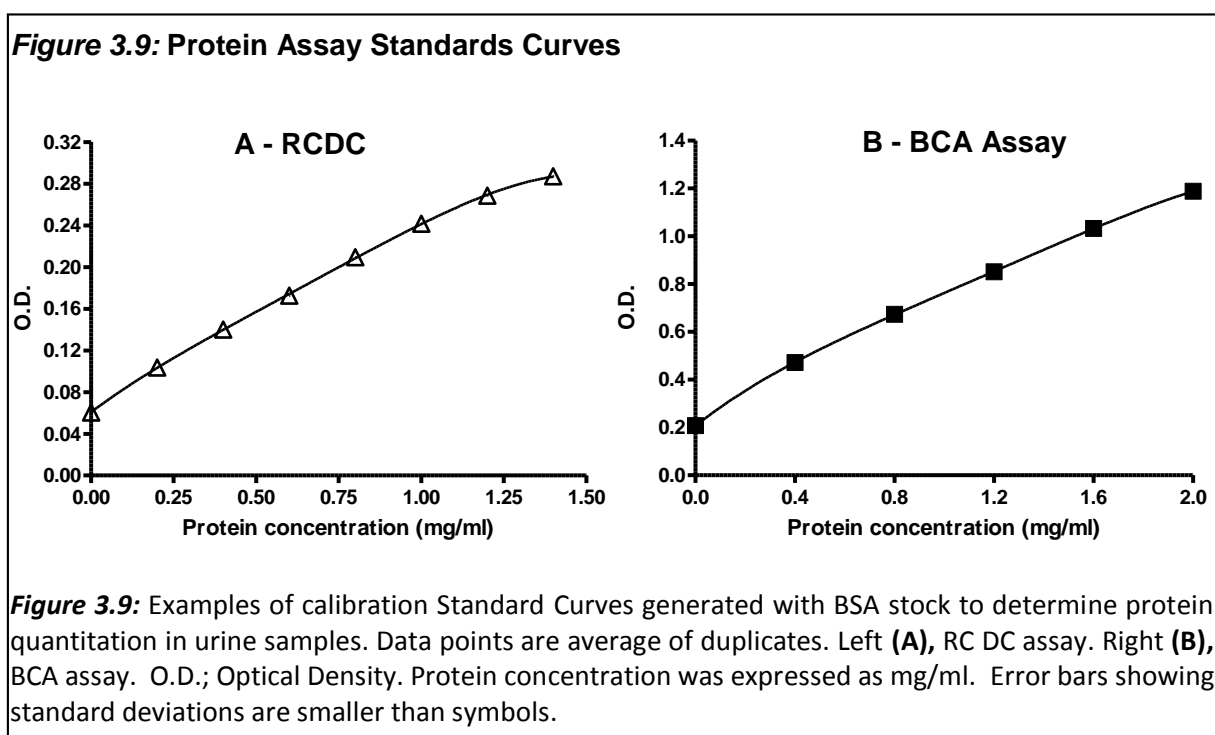
3.3.1.1. Reducing Compatible - Detergent Compatible (RC-DC) protein assay

This commercial protein assay was undertaken as per manufacturer's instructions (Bio-Rad Laboratories, UK). This assay is based on a modification of the Lowry protocol (Lowry *et al.* 1951). Albumin stock of 100 mg/ml was prepared by the addition of 0.1g of Bovine Serum Albumin (BSA) (VWR International Ltd) to 10 ml of distilled water. A standard curve of 0, 0.2, 0.4, 0.6, 0.8, 1.0, 1.2 and 1.4mg/ml BSA stock in Phosphate Buffered Saline (PBS) was used. Samples were diluted 1:2, 1:5 and 1:10 with PBS to ensure 1 dilution was on the standard curve. 125ul of RC reagent 1 (35% Sodium chloride, 10% Trichloroacetic acid, 55% H₂O) was added into each tube, vortexed and then incubated for 1 min at room temperature. 125ul of RC reagent 2 (3% acetone in H₂O) was added into each tube, vortexed and then centrifuged at 15000xg for 5 mins. Supernatant was discarded and again 125ul of RC reagent 1 was added into each tube, vortexed and then incubated for 1 min at room temperature and 125ul of RC reagent 2 was added into each tube, vortexed and then centrifuged at 15000xg for 5 mins. The supernatant was discarded. Reagent A1 was prepared by addition of 5ul of DC reagent S to each 250ul of reagent A (alkaline copper tartrate solution) that would be needed for use. 127ul of reagent A1 was added to each tube, vortexed and incubated at room temperature for 5 mins. Tubes were vortexed again and then 1 ml of DC reagent B (Folin Ciocalteu reagent) was added to each tube. After vortexing, tubes were incubated at room temperature for 15 mins. 200ul of each standard and sample was pipette into a 96 well plate and read by photo spectrometry using absorbance with wavelength 750nm (Labsystems Multiskan Ascent, UK) with curve generation and analysis undertaken using genesis light software. An example of a standard curve is shown in figure 3.9-A.

3.3.1.2. Bicinchoninic Acid (BCA) protein assay

A 100 mg/ml albumin stock was prepared by the addition of 0.1g of BSA (VWR International Ltd) to 10 ml of distilled water. A standard curve of 0, 0.4, 0.8, 1.2, 1.6 and 2.0mg/ml BSA in distilled water was used. 100ul of each sample was added to 100ul of 0.1M sodium hydroxide (NaOH) (Analar Normarpur®, VWR International Ltd) 2% (w/v) sodium dodecyl sulphate (SDS) (Fisher Scientific, UK) and then boiled at 100°C for 5 mins to facilitate solubilisation of proteins. Reagent A was prepared by addition of 1 g Bicinchoninic acid (Sigma-Aldrich, UK), 2g sodium carbonate (Fisher Scientific, UK), 0.16 g sodium tartrate (Sigma-Aldrich, UK), 0.4 g sodium hydroxide and 0.95 g sodium bicarbonate (Analar Normarpur®, VWR International

Ltd) brought to 100 ml with distilled water (the pH of the solution was adjusted to 11.25 with 10M NaOH). Reagent B was prepared by addition of 0.4 g cupric sulphate (5 x hydrated) (Analar Normarpur®, VWR International Ltd) to 10 ml of distilled water. The BCA working solution was then prepared by addition of 25 mls of Reagent A to 1ml of Reagent B. 1 ml of BCA working solution was added to each standard and sample and all tubes were vortexed before incubation at 37°C for 30 mins. 200ul of each standard and sample was pipette into a 96 well plate and read by photo spectrometry using absorbance with wavelength 562 nm (Labsystems Multiskan Ascent, genesis light software, UK). A typical standard curve is shown in figure 3.9-B.



3.4. Immunoassays

3.4.1. Rationale and principals of the Immunoassays

An Enzyme linked Immunosorbent Assay (ELISA) is a biochemical test that measures the concentration of an antigen in a sample through an immunological reaction with at least one antibody or immunoglobulin. Urine Transglutaminase 2 as well as MMPs 1, 2, 9, MMP-1/TIMP-1 complex, TIMPs 1, 2 and 3 were measured by this form of assay.

This assay involves the binding of a polyclonal capture antibody into a 96 well polystyrene microtiter plate, followed by blocking of any non-specific binding sites on this plate with a neutral protein, such as bovine serum albumin (BSA). Then, urine samples at determined dilutions were applied to the plate such that the desired antigen binds specifically to the primary antibody. The plate is washed with a mild detergent solution to remove unbound antigens. Then, a specific detection antibody from a different species to the capture antibody is applied so it can bind to the antigen forming a "sandwich" as the antigen is held between both antibodies. An Enzyme-linked secondary monoclonal antibody is then applied and the plate washed to remove the unbound antibody-enzyme conjugates. Following the use of the secondary antibody, Biotin conjugated to horse radish peroxidase (HRP) was applied. The HRP targets the anti-species of the Secondary Antibody. Finally, a TMB substrate is added and this will lead to changes in the solution colour upon reaction with the HRP enzyme (figure 3.10). The subsequent chemical reaction produces a detectable signal, most commonly a color change in the substrate. The color change can be read as a change in absorbance at a particular wavelength and is measured by a spectrophotometer. The change in absorbance is proportional to the amount of antigen binding to the capture antibody bound by the secondary antibody within a defined range. The optical density (OD) of the sample is compared to a standard curve, made by a serial dilution of a known-concentration solution of pure antigen.

Figure 3.10: Schematic representation of a sandwich immunoassay

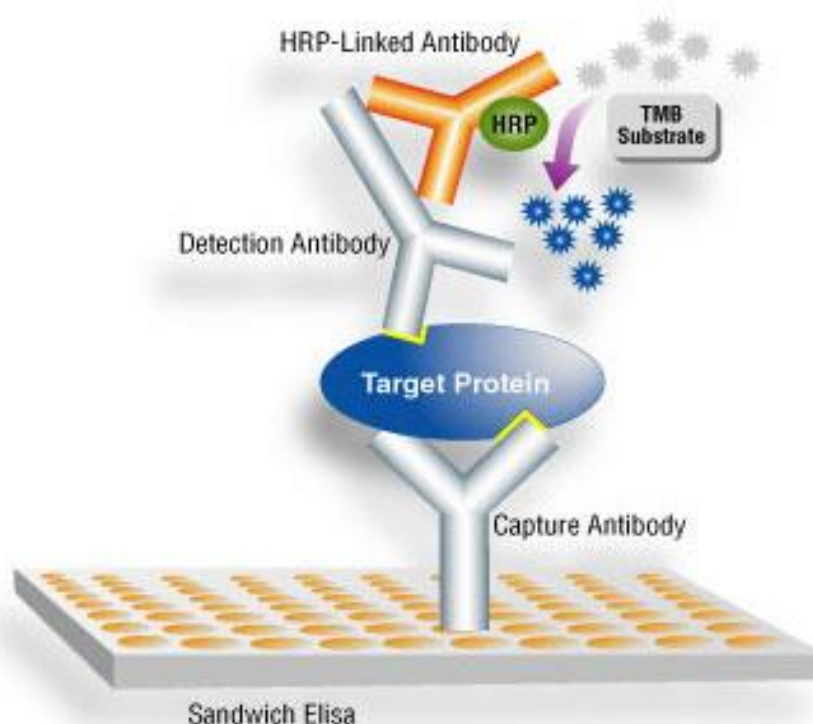


Figure 3.10: Principles of Sandwich ELISA. A microplate is coated with a capture antibody; then a sample containing the target protein is added, and any antigen present binds to the capture antibody. A detection antibody is added, and binds to antigen; an enzyme-linked tertiary antibody that recognises the species of the secondary antibody is added to that. A substrate is then added, that changes colour upon reaction with the enzyme. The absorbance of the plate wells is measured by a spectrophotometer to determine the presence and quantity of antigen.

3.4.2. Sample preparation

Aliquoted rat and human urine samples that have been previously stored at -80°C were thawed at 4°C to avoid protein denaturation. An appropriate assay dilution buffer was added to the samples according to the specific assay and the optimized dilution factor.

3.4.3. Urine TG2 Enzyme-linked immunosorbent assay

An in-house sandwich ELISA was developed for the quantification of TG2 in the urine.

3.4.3.1. Antibody selection

A number of antibodies anti-transglutaminase 2 was tested in order to optimize this immunoassay. Selected antibodies were also tested in several different concentrations to verify higher sensitivity and specificity against urine transglutaminase 2. After analysis, the

Goat polyclonal anti TG2 and the mouse monoclonal CUB7402 (both from AbCam) were selected as the Capture and Detection Antibody respectively. The main properties of both antibodies are shown on table 3.1.

Table 3.1: Anti-transglutaminase 2 antibodies

	Goat polyclonal to Transglutaminase 2: Capture ATB	Mouse monoclonal to Transglutaminase 2 (CUB7402): Detection ATB
Immunogen	Synthetic peptide C-ERDLYLENPEIKIR by a Cysteine residue linker	Purified guinea pig liver Transglutaminase 2
Epitope mapping	amino acids 579-592	amino acids 447-478
Species reactivity	Mouse, Rat, Guinea pig, Cow, Pig, Human	Mouse, Rat, Rabbit, Guinea pig, Dog, Human
Purity	IgG fraction	IgG fraction
Stock Concentration	0.5mg/ml	0.1mg/ml

3.4.3.3. Urine TG2 assay procedure

96 well microplates (Costar 3590, Corning Incorporated, USA) were coated for 4h at room temperature or overnight at 4°C with 100ul per well of goat anti-transglutaminase type II antibody (AbCam, UK) diluted 1/1000 in 50mM Carbonate Buffer (0.8g Sodium Carbonate anhydrous or 2.15g Sodium Carbonate Pentahydrated (Fisher Scientific, UK), 1.46g Sodium Hydrogen Carbonate (Analar GPR®, UK) 500 ml distilled water, pH 9.6). Plates were washed twice with PBS / 0.1% Tween 20 (8g Sodium Chloride (Fluka, Sigma-Aldrich, UK), 0.2g Potassium Chloride (Fisher Scientific, UK), 1.44g Disodium Hydrogen Orthophosphate (Fisher Scientific, UK), 0.24g Potassium Dihydrogen Orthophosphate (Analar Normarpur®, VWR International Ltd), 1L of distilled water, 1ml Tween 20 (Fisher Scientific, UK), pH to 7.4). Plates were then blocked for 1h at room temperature with 200ul of 5% (w/v) BSA in PBS and washed once with PBS / 0.1% Tween 20. A standard curve was prepared with a 7 point serial dilution from a stock solution of either rat or human recombinant TG2 (Zedira, UK), both at a concentration of 10ng/µl. Rat TG2 ELISA standard curve (SC) was made using a 2-fold dilution series: 31.25ng/ml, 62.5ng/ml, 125ng/ml, 250ng/ml, 500ng/ml, 1000ng/ml and 2000ng/ml, whilst human SC ranged from 15.6ng/ml to 1000ng/ml. Undiluted PBS served as the zero standard (0ng/ml). 100ul of Recombinant TG2 standards and of each urine sample (diluted in PBS) were added to each well of the microplate and incubated at room temperature for 2 hours. Rat urine samples were diluted in a 1:10, 1:50 and 1:100 ratio and human samples

in 1:1, 1:2 and 1:5. After this, plates were washed three times with PBS / 0.1% Tween 20. 100ul of 1ug/ml mouse anti-transglutaminase type II antibody (AB-2 clone TG100; AbCam) diluted in PBS (1:1000) was added and plates were left for 1h at room temperature. Plates were washed again three times with PBS / 0.1% Tween 20. 100ul of Biotinylated Goat anti Mouse IgG (H+L) (AbCam, UK) was added to each well and left for 1 hour at room temperature. This was followed by three washes with PBS / 0.1% Tween 20. 100ul of 1 ug/ml Streptavidin poly-HRP (horseradish peroxidase conjugated secondary antibody, Thermo Scientific, UK) diluted in 1:2000 in PBS was added to each well and left for 1 hour at room temperature. After final washes with PBS / 0.1% Tween 20, 100ul per well of the HRP substrate 1- Step Ultra TMB-ELISA (Pierce, USA) was added and left for 10 minutes. The reaction was stopped by the addition of 100ul 1N H₂SO₄ (Analar Normarpur®, VWR International Ltd) and absorbance values were read at 450nm using a Labsystems Multiskan Ascent spectrophotometer with genesis light software (Bio-Rad Laboratories, Hertfordshire, UK).

3.4.3.4. Determination of reproducibility and specificity

The ability of the urine TG2 assay to reproduce accurate results in urine was tested by adding three different known amounts of recombinant human TG2 (rhTG2, Zedira, UK) to twenty human urine samples (ten controls and ten CKD) . Each urine sample was spiked with 0.25, 0.5 and 1ug/ml of rhTG2, representing a low, medium and high TG2 concentration. Ten un-spiked control samples and ten un-spiked CKD samples were used to measure baseline values for TG2 concentration. Then, the percentage of spiked TG2 was calculated by using the equation below. The results showed a % of spike measured and ranged from 82.6 to 109.1% (table 3.2).

The specificity of the assay was evaluated by testing other potential cross-reactive molecules such as Factor XIII, but no cross-reactivity was observed with this or other Transglutaminases.

$$\% \text{ measured} = \frac{\text{Mean TG2 Spiked} - \text{un-spiked urine concentration (pg/ml)} \times 100}{\text{Mean total value from TG2 Spiked urine concentration}}$$

Table 3.2: Urine TG2 Enzyme-linked immunosorbent assay reproducibility

Tested Sample	% measured (low)	% measured (medium)	% measured (high)	% measured (average)
Controls	82.6	89.8	102.4	91.6
CKD	84.1	95.7	109.1	96.3

Table 3.2: The percent of spiked TG2 measured was calculated by dividing the average values of “spiked” samples with rhTG2 by “un-spiked” samples. The amount obtained was multiplied by 100 to express results in percentage.

3.4.3.5. Determination of Inter and Intra assay Coefficients of Variability

In order to obtain the precision, or repeatability, of our in-house TG2 immunoassay, two measures of the Coefficient of Variability (CV) were calculated: the inter- and the intra-assay CV. The inter-assay CV is an expression of plate-to-plate consistency and was calculated by adding two samples with known TG2 concentration in every plate run. The degree of precision was measured by the standard deviation of the two concentrations across all runs and converting it to the CV as below.

Urine TG2 immunoassay coefficient of variability calculation

$$\text{Coefficients of Variability} = \frac{\text{Standard Deviation}}{\text{Mean concentration}} \times 100\%$$

The intra-assay CV measures the precision of detection within the same plate. It was analysed by calculating the standard deviation of ten samples in multiple assay plates. The Inter- and Intra-Coefficients of Variability were 1.2% and 3.9% respectively.

A typical standard curve for the TG2 immunoassay is shown in figure 3.11. The lower limit of detection was 31.25pg/ml.

Figure 3.11: Transglutaminase type 2 enzyme-linked immunosorbent assay standard curve

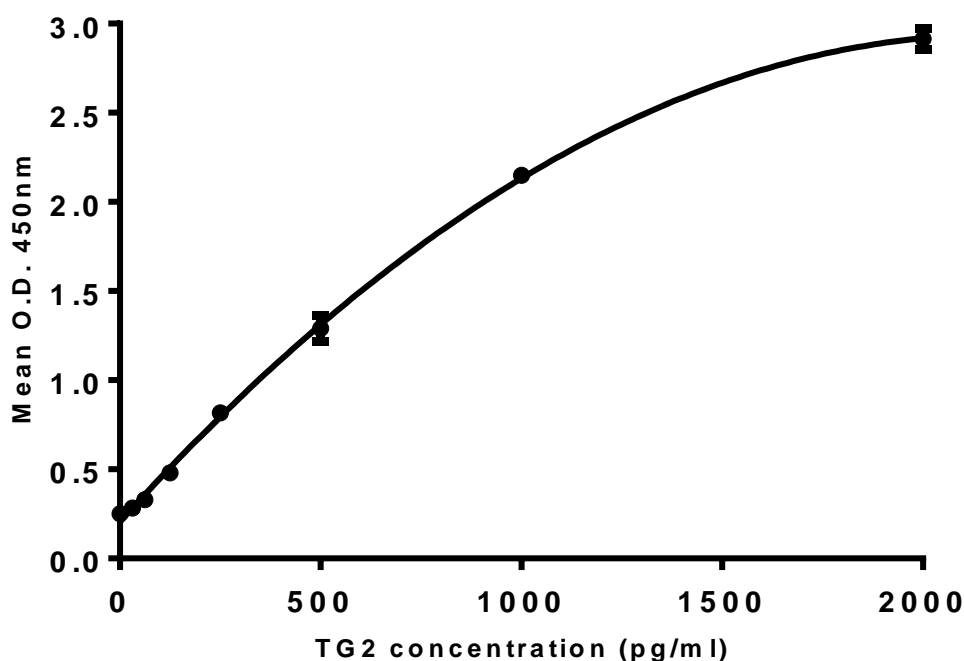


Figure 3.11: A TG2 standard curve generated using rrTG2 concentrations from 31.25 to 2000pg/ml. Colour development was allowed to proceed for 10 minutes and the plate read on a Labsystems Multiskan Ascent equipment using genesis light software to plot a curve using a cubic spline curve fit equation. Data points are average of duplicates.

3.4.4. Rat Immunoassays

Rat urine samples were analysed by two different commercially available sandwich enzyme-linked immunosorbent assay kits according to the availability and specificity of each assay in relation to the antigen to be measured. MMP-1, TIMPs 2 and 3 and PAI-1 were assayed using Gentaur kits (Uscn Life Science Inc., USA) whilst MMP-9 and TIMP-1 were assayed using the Quantikine system (R&D Systems, UK) as they provided accurate and highly sensitive detection of these analytes with minimal assay development.

3.4.4.1. Gentaur Enzyme-linked immunosorbent assay

3.4.4.1.1. Reproducibility and specificity of assays in urine

Four control samples and four SNx samples were spiked with either 250pg/ml of rat recombinant MMP-1 or 12.5ng/ml of TIMP-2 or 6.25ng/ml of TIMP-3 or 5ng/ml of rat recombinant PAI-1 and the spiked rates calculated by comparing the measured value to the

expected amount in samples (table 3.3). No significant cross-reactivity or interference between MMP-1, TIMP-2, TIMP-3, PAI-1 and analogues was observed.

Table 3.3: Accuracy % of rat MMP-1, TIMP-2, TIMP-3 and PAI-1 immunoassays

	Control (n=4)		SNx (n=4)	
	Recovery range (%)	Average (%)	Recovery range (%)	Average (%)
MMP-1	92-102	99	84-103	98
TIMP-2	83-104	93	87-101	94
TIMP-3	89-108	98	81-102	92
PAI-1	79-98	89	81-98	90

The minimum detectable doses were: 0.115ng/ml for rat MMP-1, 0.61ng/ml of rat TIMP-2, 0.094ng/ml for rat TIMP-3 and 0.18ng/ml for PAI-1.

3.4.4.1.2. Inter and Intra assay Coefficients of Variability

The Inter-assay CV (precision between assays) was tested by measuring two samples with low, middle and high levels of MMP-1, TIMPs 2 and 3 and PAI-1 on three different plates. The Intra-assay CV (precision within an assay) was calculated by assaying two samples, three times in duplicate on the same plate.

The inter- and intra-coefficients of variability of MMP-1 were 7.8% and 9.2% respectively. For TIMP-2 these values were 3.7% and 6.1%, TIMP-3, 5.4% and 7.2% and PAI-1 4.8% and 7.1% respectively.

3.4.4.1.3. Materials

The following reagents were used for measurement of MMP-1, TIMP-2, TIMP-3 and PAI-1 in rat urine:

Reagents	MMP-1	TIMP-2	TIMP-3	PAI-1
Capture Antibody (pre-coated)	Monoclonal AB anti-rat MMP-1	Monoclonal AB anti-rat TIMP-2	Monoclonal AB anti-rat TIMP-3	Monoclonal AB anti-rat PAI-1
Detection Reagent A	120µl Biotin-conjugated polyclonal AB anti-rat MMP-1	120µl Biotin-conjugated polyclonal AB anti-rat TIMP-2	120µl Biotin-conjugated polyclonal AB anti-rat TIMP-3	120µl Biotin-conjugated polyclonal AB anti-rat TIMP-3
Detection Reagent B	120µl Avidin conjugated to Horseradish Peroxidase	120µl Avidin conjugated to Horseradish Peroxidase	120µl Avidin conjugated to Horseradish Peroxidase	120µl Avidin conjugated to Horseradish Peroxidase
Standard	20ng/ml of recombinant rat MMP-1	100ng/ml of recombinant rat TIMP-2	10ng/ml of recombinant rat TIMP-3	80ng/ml of recombinant rat PAI-1
Standard Diluent	20ml of 0.01mol/L PBS (Ph 7.2)	20ml of 0.01mol/L PBS (Ph 7.2)	20ml of 0.01mol/L PBS (Ph 7.2)	20ml of 0.01mol/L PBS (Ph 7.2)
Wash Buffer	30 x concentrated Tween 20 in PBS, ph 7.4	30 x concentrated Tween 20 in PBS, ph 7.4	30 x concentrated Tween 20 in PBS, ph 7.4	30 x concentrated Tween 20 in PBS, ph 7.4
Substrate	9ml TMB solution	9ml TMB solution	9ml TMB solution	9ml TMB solution
Stop solution	6ml 2N H ₂ SO ₄	6ml 2N H ₂ SO ₄	6ml 2N H ₂ SO ₄	6ml 2N H ₂ SO ₄

3.4.2.1.4. Reagents preparation

- The standard, Detection Reagent A, Detection Reagent B and the 96-well strip plate were stored at -20°C upon being received. All the remaining reagents were stored at 4°C.
- All reagents were brought to room temperature and freshly reconstituted before use.
- The unused strips were kept in a sealed bag with the desiccant to minimize exposure to damp air.
- Rat MMP-1, TIMP-2, TIMP-3 and PAI-1 detection reagents A and B were diluted to a working concentration of 1:100 with their respective assay diluents.
- Standards were prepared minutes before assay. 20ng/ml of recombinant rat MMP-1 was reconstituted with 1ml of standard diluent to produce a stock solution of 20ng/ml. A seven point standard curve was prepared by a 2-fold serial dilution in standard

diluent: 20ng/ml, 10ng/ml, 5ng/ml, 2.5ng/ml, 1.25ng/ml, 0.625ng/ml and 0.312ng/ml (figure 3.12-A).

- 100ng/ml of Recombinant rat TIMP-2 was reconstituted with 1ml of standard diluent to produce a stock solution of 100ng/ml. A seven point standard curve was prepared by a 2-fold serial dilution in standard diluent: 100ng/ml, 50ng/ml, 25ng/ml, 12.5ng/ml, 6.25ng/ml, 3.12ng/ml and 1.56ng/ml (figure 3.12-B).
- 10ng/ml of Recombinant rat TIMP-3 was reconstituted with 1ml of standard diluent to produce a stock solution of 10ng/ml. A seven point standard curve was prepared by a 2-fold serial dilution in standard diluent: 10ng/ml, 5ng/ml, 2.5ng/ml, 1.25ng/ml, 0.625ng/ml, 0.312ng/ml and 0.156ng/ml (figure 3.12-C).
- 80ng/ml of Recombinant rat PAI-1 was reconstituted with 2ml of standard diluent to produce a stock solution of 40ng/ml. A seven point standard curve was prepared by a 2-fold serial dilution in standard diluent: 40ng/ml, 20ng/ml, 10ng/ml, 5ng/ml, 2.5ng/ml, 1.25ng/ml and 0.625ng/ml (figure 3.12-D).
- 20ml of wash solution concentrate (30x) was diluted with 580ml of deionized water to prepare 600ml of 1x wash solution.
- The reconstituted standards, detection reagent A and detection reagent B could be used only once.

3.4.4.1.5. Assay procedure

Rat urine samples, standards and reagents were prepared as per manufacture instructions (Gentaur, Uscn Life Science Inc., USA). A 96-well strip plate was pre-coated with a monoclonal capture antibody against either MMP-1, TIMP-2, TIMP-3 or PAI-1. 100µL of standards or rat urine sample (neat urine for MMP-1 and PAI-1 and 1:2, 1:5 and 1:10 dilution for TIMPs 2 and 3) was added to each well and incubated at 37°C for 2 hrs. After incubation, plates were aspirated and washed in PBS. Then, 100µL of Detection Reagent A (a biotin-conjugated antibody specific to each antigen) was added. Then, plates were incubated for one hour at 37°C after covering them with the plate sealer. Plates were washed thrice with 350µL/well of 1 X wash solution. After the last wash, plates were inverted and blotted against an absorbent paper to remove any remaining wash buffer. Next, 100µL of Detection Reagent B (Avidin conjugated to Horseradish Peroxidase (HRP) was added to each microplate well and incubated 30 minutes at 37°C. Plates were washed for five times. 90µL of TMB Substrate solution was added to each well and plates were incubated for 15-25 minutes at 37°C in the dark for blue colour to develop. The enzyme-substrate reaction is terminated by the addition of 50ul 2N sulphuric acid solution and the colour change was measured spectrophotometrically at a wavelength of 450nm using a Labsystems Multiskan Ascent spectrophotometer (Bio-Rad Laboratories, Hertfordshire, UK) using genesis light software.

The concentrations of MMP-1, TIMP-2, TIMP-3 and PAI-1 in the samples were then determined by comparing the O.D. of the samples to the standard curves (figure 3.12).

Figure 3.12: Gentaur Immunoassay Standard Curves

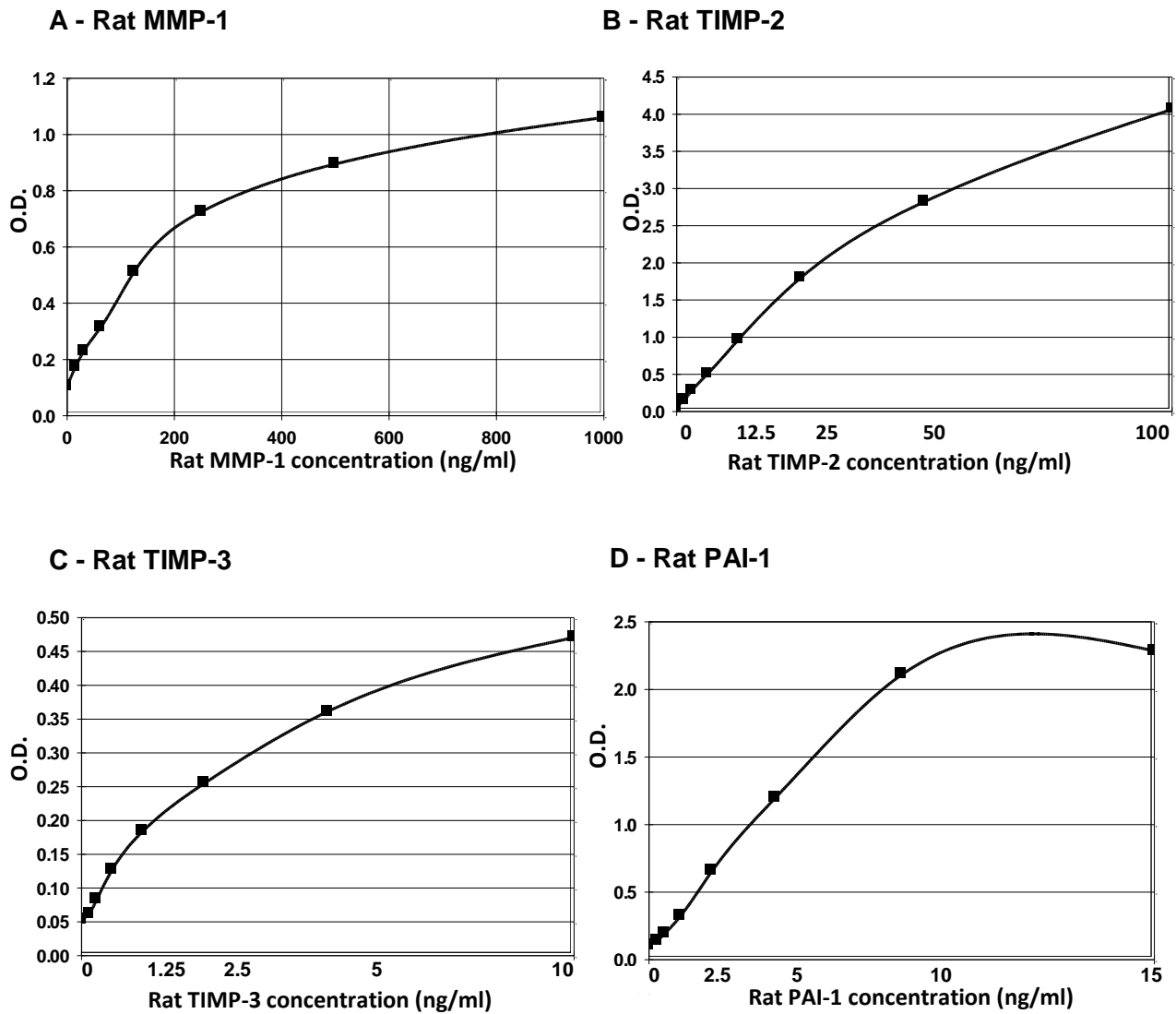


Figure 3.11: Gentaur Rat MMP-1 (A), TIMP-2 (B), TIMP-3 (C) and PAI-1 (D) ELISA standard curves were created using a Labsystems Genesis computer package which generated a four parameter logistic (4-pl) curve fit. Absorbance was measured on Labsystems Multiskan Ascent plate reader at a wavelength of 450nm. Optical density (O.D.) of each sample was plotted on the y-axis against the MMP-1 (pg/ml) or TIMP-2, TIMP-3, PAI-1 (ng/ml) on the x-axis. Data points are average of duplicates. Error bars showing standard deviations are smaller than symbols.

3.4.4.2. Quantikine Enzyme-linked immunosorbent assay

Total rat MMP-9 (Pro-, active, and TIMP-complexed MMP-9) and rat TIMP-1 in urine were measured by the Quantikine immunoassay (R&D Systems, UK).

3.4.4.2.1. Reproducibility and specificity of assays in urine

Four control samples and four SNx samples were spiked with either 1.25ng/ml of recombinant rat MMP-9 or 300pg/ml of recombinant rat TIMP-1. The recovery/accuracy percentage rates of rat MMP-9 ranged between 80-107% (table 3.4) and between 82-115% for TIMP-1. No significant cross-reactivity or interference between MMP-9 and related molecules was observed. In addition, no significant cross-reactivity or interference was observed between TIMP-1 and 50 to 500ng/ml of the following molecules: TIMP-2, TIMP-3, MMP-1, MMP-2 and MMP-9. However, rat recombinant TIMP-1 showed 0.015% cross-reactivity with TIMP-1 complexed with active MMP-9 at a 1:10 molar ratio.

Table 3.4: Accuracy % of rat MMP-9 and TIMP-1 immunoassays

	Control (n=4)		SNx (n=4)	
	Recovery range (%)	Average (%)	Recovery range (%)	Average (%)
MMP-9	87-107	94	80-103	92
TIMP-1	82-109	95	84-115	99

3.4.4.2.2. Inter and Intra assay Coefficients of Variability

Two samples of known rat MMP-9 (1ng/ml) and two samples containing a rat TIMP-1 concentration (450pg/ml) were tested on two plates to assess inter- and intra-assay precision and the coefficient of variability was 3.9% and 5.6% for MMP-9 and 3.2% and 6.0% for TIMP-1, respectively.

3.4.4.2.3. Materials

The following reagents were used for measurement of MMP-9 and TIMP-1 in rat urine:

Reagents	MMP-9	TIMP-1
Capture Antibody (pre-coated)	Monoclonal mouse anti-rat MMP-9	Monoclonal mouse anti-rat TIMP-1
Detection Antibody	12ml of a Polyclonal anti-rat MMP-9 conjugated to horseradish peroxidase	0.65ml of a 23-fold solution containing a Polyclonal anti-rat TIMP-1 conjugated to horseradish peroxidase
Standard	50ng of recombinant rat MMP-9 in a buffered protein base	12ng of recombinant rat TIMP-1 in a buffered protein base
Control	5ng of recombinant rat MMP-9 in a buffered protein base	600pg of recombinant rat TIMP-1 in a buffered protein base
Assay diluent	11ml of a buffered protein base with blue dye	12.5ml of a buffered protein base
Calibrator diluent	2 vials (21ml/vial) of a buffered protein base	2 vials (21ml/vial) of a buffered protein base
Wash Buffer	50ml of a 25-fold concentrated solution of buffered surfactant	50ml of a 25-fold concentrated solution of buffered surfactant
Color reagent A	12ml of stabilised hydrogen peroxide	12.5ml of stabilised hydrogen peroxide
Color reagent B	12ml of stabilised chromogen (TMB)	12.5ml of stabilised chromogen (TMB)
Stop solution	23ml of diluted hydrochloric acid	23ml of diluted hydrochloric acid

3.4.4.2.4. Reagents preparation

- All reagents were brought to room temperature and freshly reconstituted before use
- Rat MMP-9 control and rat TIMP-1 control were reconstituted with 1 ml of distilled water
- 0.5ml of rat TIMP-1 conjugate (detection antibody) was diluted in 11ml of conjugate diluent in a sterile container and protected from light.
- 25ml of wash buffer concentrate was added to 600ml of distilled water
- Substrate solution: color reagents A and B were mixed together in equal volumes within 15 minutes of use in a place protected from light.

- Rat MMP-9 standard was reconstituted with 5ml of calibrator diluents to produce a stock solution of 10ng/ml. The standard curve was prepared by a 2-fold dilution series: 10ng/ml, 5ng/ml, 2.5ng/ml, 1.25ng/ml, 0.625ng/ml, 0.313ng/ml and 0.156ng/ml (figure 3.13-A).
- Rat TIMP-1 standard was reconstituted with 5ml of calibrator diluents to produce a stock solution of 2400pg/ml. The standard curve was prepared by a 2-fold dilution series: 2400ng/ml, 1200ng/ml, 600ng/ml, 300ng/ml, 150ng/ml, 75ng/ml and 37.5pg/ml (figure 3.13-B).

3.4.4.2.5. Assay procedure

50µL of Assay Diluent was added to each well of the microplate pre-coated with a mouse monoclonal antibody specific for either rat MMP-9 or rat TIMP-1. 50µL/well of standards, control, and samples (all in duplicates) was added to each well to bind with the immobilized capture antibody. Rat urine samples were diluted 1:1, 1:2, 1:5 and 1:10 in both assays using the calibrator diluent. 50µL of standards, control, and samples (all in duplicate) was added to each well to bind with the immobilized capture antibody. The plate was then covered with an adhesive sealer and incubated at room temperature for 2 hours with gentle rocking (Stuart Digital Rocker SRT6, Geneflow, UK). Each well was aspirated and washed for a total of 5 washes with a buffer surfactant available in the kit. Complete removal of the wash buffer was achieved by inversion and blotting of the plate against clean paper towels. After washing away any unbound antibody-enzyme reagent, 100µL of an enzyme-linked polyclonal antibody specific for either rat MMP-9 or rat TIMP-1 conjugated to HRP, was added to each well. The plate was covered with a new sealer and incubated at room temperature for 2 hours. After incubation, the plate was aspirated and washed for 5 times. Following the washing, 100µL of Substrate solution (1:1 stabilised hydrogen peroxide and the chromogen TMB) was added to each well and incubated at room temperature for 30 minutes in a place protected from light. The enzyme reaction yields a blue product that turned yellow when 100µL of stop solution (hydrochloric acid) was added to each well. The samples values were then read at 450nm using a Labsystems Multiskan Ascent spectrophotometer (Bio-Rad Laboratories, Hertfordshire, UK) using genesis light software.

Figure 3.13: Quantikine Immunoassay Standard Curves

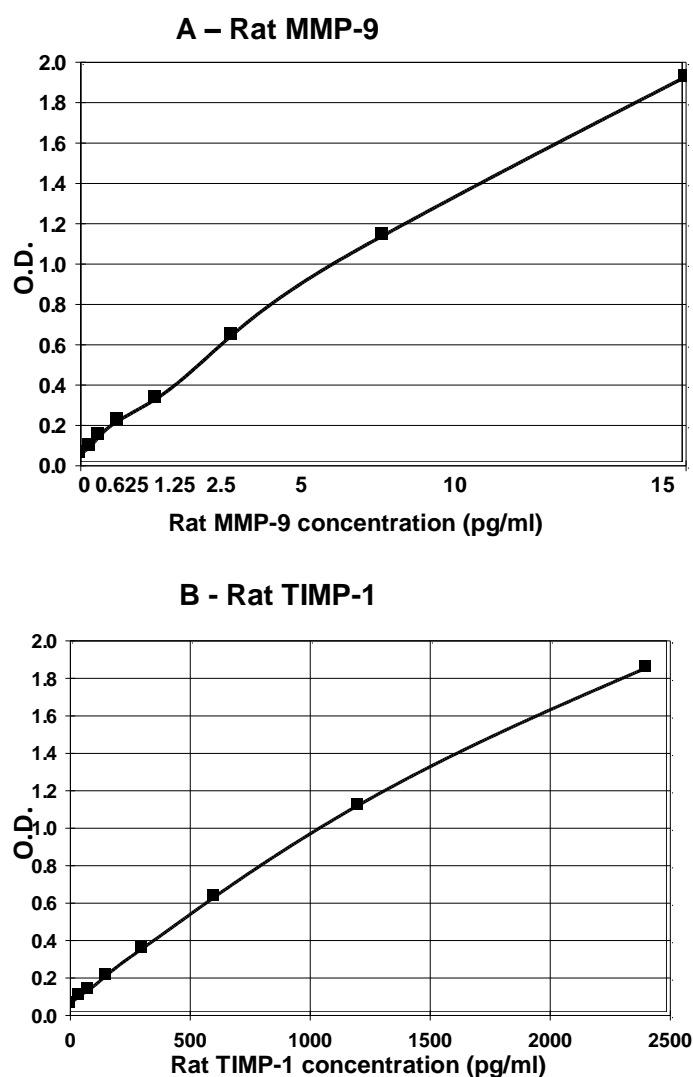


Figure 3.13: Quantikine Rat MMP-9 (A) and TIMP-1 (B) ELISA standard curves were obtained using either recombinant rat MMP-9 or TIMP-1 and calculated using a Labsystems Genesis computer package using a four parameter logistic (4-pl) curve fit. Absorbance was measured on Labsystems Multiskan Ascent plate reader at a wavelength of 450nm. Optical density (O.D.) of each sample was plotted on the y-axis against the MMP-9 or TIMP-1 concentration (ng/ml) on the x-axis. Data points are average of duplicates. Error bars showing standard deviations are smaller than symbols.

3.4.5. Human Immunoassays

Human urine samples were analysed for total (active and pro-) MMP-1, 2 and 9 as well as TIMP-1, TIMP-3, TIMP-3 and MMP-1/TIMP-1 complex by using the DuoSet immunoassay (R&D Systems, UK) as per manufacturer's instructions.

3.4.5.1.1. Reproducibility and specificity of assays in human urine

The accuracy of the total human MMP-1 DuoSet to quantify MMP-1 in urine was measured in four spiked samples with 625ng/ml recombinant human MMP-1 (R&D Systems, UK). The average percentage accuracy of MMP-1 ranged between 85-112%. No cross-reactivity was observed between MMP-1 and 100ng/ml of the following molecules: MMP-2, MMP-3, MMP-9, TIMP-1, TIMP-2 and TIMP-3.

Four spiked samples with 2.5ng/ml recombinant human MMP-2 (R&D Systems, UK) were used to calculate the recovery percentage of the assay. The average % recovery of MMP-2 ranged between 84-106%. No cross-reactivity was observed between MMP-2 and 200ng/ml of the following recombinant human molecules: MMP-1, MMP-3, MMP-9, TIMP-1, TIMP-2, TIMP-3 and TIMP-2 complexed with MMP-2.

The recovery of MMP-9 spiked with 250pg/ml recombinant human MMP-9 (R&D Systems, UK) was evaluated in four samples. The average % recovery of MMP-2 ranged between 74-108%. No cross-reactivity was observed between MMP-9 and 50ng/ml of the following recombinant human molecules: MMP-1, MMP-2, MMP-3, TIMP-1, TIMP-2 and TIMP-3.

The recovery of each human TIMP-1, TIMP-2 and TIMP-3 was measured in four different spiked samples (125pg/ml of recombinant human TIMPs 1 and 2 and 250pg/ml of TIMP-3) (R&D Systems, UK). The average % recovery of TIMP-1 ranged between 87-113, of TIMP-2; 89-108 and of TIMP-3; 81-102. No cross-reactivity was observed within any TIMPs or when assayed against MMP-1, MMP-2 and MMP-9 when prepared at 100ng/ml.

Human Samples (n=4)	Amount spiked	Recovery range (%)	Average (%)
MMP-1	625ng/ml	85-112	99
MMP-2	2.5ng/ml	84-106	97
MMP-9	250pg/ml	74-108	94
TIMP-1	125pg/ml	87-113	99
TIMP-2	125pg/ml	89-108	98
TIMP-3	250pg/ml	81-102	96
MMP-1/TIMP-1 complex	125pg/ml	83-109	97

3.4.5.1.2. Inter and Intra assay Coefficients of Variability

Four different samples of known concentrations of MMPs 1, 2 and 9, TIMPs 1, 2 and 3, and MMP-1/TIMP-1 complex were tested in duplicates on every run plate. The Inter- and Intra-Coefficients of Variability are as follows:

Human Samples (n=4)	Inter assay CV (%)	Intra assay CV (%)
MMP-1	3.9	6.2
MMP-2	5.4	9.8
MMP-9	2.9	6.9
TIMP-1	3.9	4.9
TIMP-2	4.4	7.3
TIMP-3	5.6	7.8
MMP-1/TIMP-1 complex	3.9	6.1

3.4.5.1.3. Materials

The following reagents were used for measurement of human MMPs 1, 2, 9, TIMPs 1, 2, 3 and the MMP-1/TIMP-1 complex in urine:

Reagents	MMP-1	MMP-2	MMP-9
Capture Antibody	360µg/ml of a goat monoclonal anti-human MMP-1	360µg/ml of a monoclonal mouse anti-human MMP-2	180µg/ml of a monoclonal mouse anti-human TIMP-3
Detection Antibody	18µg/ml of biotinylated goat anti-human MMP-1	90µg/ml of biotinylated mouse anti-human MMP-2	18µg/ml of biotinylated goat anti-human TIMP-3
Standard	180ng/ml of recombinant human MMP-1	1920ng/ml of recombinant human MMP-2	95ng/ml of recombinant human TIMP-3
Wash Buffer	0.05% Tween 20 in PBS, ph 7.4	0.05% Tween 20 in PBS, ph 7.4	0.05% Tween 20 in PBS, ph 7.4
Reagent Diluent	1% BSA in PBS, ph 7.4	1% BSA in PBS, ph 7.4	1% BSA in PBS, ph 7.4
Streptavidin-HRP	1ml of Streptavidin conjugated to horseradish-peroxidase	1ml of Streptavidin conjugated to horseradish-peroxidase	1ml of Streptavidin conjugated to horseradish-peroxidase
Substrate Solution	1:1 mixture of H ₂ O ₂ and Tetramethylbenzidine	1:1 mixture of H ₂ O ₂ and Tetramethylbenzidine	1:1 mixture of H ₂ O ₂ and Tetramethylbenzidine
Stop solution	2N H ₂ SO ₄	2N H ₂ SO ₄	2N H ₂ SO ₄

Reagents	TIMP-1	TIMP-2	TIMP-3
Capture Antibody	360µg/ml of a monoclonal mouse anti-human TIMP-2	360µg/ml of a monoclonal mouse anti-human TIMP-2	360µg/ml of a monoclonal mouse anti-human TIMP-3
Detection Antibody	9µg/ml of biotinylated goat anti-human TIMP-1	9µg/ml of biotinylated goat anti-human TIMP-2	360µg/ml of biotinylated mouse anti-human TIMP-3
Standard	80ng/ml of recombinant human TIMP-1	95ng/ml of recombinant human TIMP-2	90ng/ml of recombinant human TIMP-3
Wash Buffer	0.05% Tween 20 in PBS, ph 7.4	0.05% Tween 20 in PBS, ph 7.4	0.05% Tween 20 in PBS, ph 7.4
Reagent Diluent	1% BSA in PBS, ph 7.4	1% BSA in PBS, ph 7.4	1% BSA in PBS, ph 7.4
Streptavidin-HRP	1ml of Streptavidin conjugated to horseradish-peroxidase	1ml of Streptavidin conjugated to horseradish-peroxidase	1ml of Streptavidin conjugated to horseradish-peroxidase
Substrate Solution	1:1 mixture of H ₂ O ₂ and Tetramethylbenzidine	1:1 mixture of H ₂ O ₂ and Tetramethylbenzidine	1:1 mixture of H ₂ O ₂ and Tetramethylbenzidine
Stop solution	2N H ₂ SO ₄	2N H ₂ SO ₄	2N H ₂ SO ₄

3.4.5.1.4. Reagents preparation

- All reagents were brought to room temperature and freshly reconstituted before use
- Human MMP-1, MMP-2, MMP-9, TIMP-1, TIMP-2 and TIMP-3 capture antibodies were reconstituted with 1ml of sterile PBS without carrier protein, pH 7.4, 0.2µm filtered. After reconstitution, 55ul aliquots were stored at -80°C. The capture antibody was further diluted with PBS to a working concentration of 2.0µg/ml prior to coating the 96-well microplates.
- Human MMP-1, MMP-2, MMP-9, TIMP-1, TIMP-2 and TIMP-3 detection antibodies were reconstituted with 1ml of reagent diluent. After reconstitution, 55ul aliquots were stored at -80°C. MMP-1 detection antibodies were further diluted with reagent diluent to a working concentration of 100µg/ml, whilst MMP-2 was diluted to 500ng/ml, TIMP-1 and TIMP-2 to 50µg/m and TIMP-3 to 2.0µg/ml. MMP-9 detection antibody was diluted to a working concentration of 100ng/ml in reagent diluent with 2% heat inactivated normal goat serum (NGS) prepared 1-2 hours prior to use.
- 180ng/ml of Recombinant Human MMP-1 was reconstituted with 0.5ml of deionized water to produce a stock solution of 360ng/ml. Reconstituted standard were aliquoted and stored at -80°C for up to 6 months. A seven point standard curve was prepared by a 2-fold serial dilution in reagent diluent: 10000pg/ml, 5000pg/ml, 2500pg/ml, 1250pg/ml, 626pg/ml, 312pg/ml and 156pg/ml (figure 3.14-A).
- 1920ng/ml of Recombinant Human MMP-2 was reconstituted with 0.5ml of deionized water to produce a stock solution of 3840ng/ml. Reconstituted standard were aliquoted

and stored at -80°C for up to 6 months. A seven point standard curve was prepared by a 2-fold serial dilution in reagent diluent: 20ng/ml, 10ng/ml, 5ng/ml, 2.5ng/ml, 1.25ng/ml, 0.625ng/ml and 0.312ng/ml (figure 3.14-B).

- 95ng/ml of Recombinant Human MMP-9 was reconstituted with 0.5ml of deionized water to produce a stock solution of 190ng/ml. Reconstituted standard were aliquoted and stored at -80°C for up to 6 months. A seven point standard curve was prepared by a 2-fold serial dilution in reagent diluent: 2000pg/ml, 1000pg/ml, 500pg/ml, 250pg/ml, 125pg/ml, 62.5pg/ml and 31.25pg/ml (figure 3.14-C).
- 80ng/ml of Recombinant Human TIMP-1 was reconstituted with 0.5ml of reagent diluent to produce a stock solution of 160ng/ml. Reconstituted standard were aliquoted and stored at -80°C for up to 6 months. A seven point standard curve was prepared by a 2-fold serial dilution in reagent diluent: 2000pg/ml, 1000pg/ml, 500pg/ml, 250pg/ml, 125pg/ml, 62.5pg/ml and 31.25pg/ml (figure 3.15-A).
- 95ng/ml of Recombinant Human TIMP-2 was reconstituted with 0.5ml of reagent diluent to produce a stock solution of 190ng/ml. Reconstituted standard were aliquoted and stored at -80°C for up to 6 months. A seven point standard curve was prepared by a 2-fold serial dilution in reagent diluent: 2000pg/ml, 1000pg/ml, 500pg/ml, 250pg/ml, 125pg/ml, 62.5pg/ml and 31.25pg/ml (figure 3.15-B).
- 90g/ml of Recombinant Human TIMP-3 was reconstituted with 0.5ml of reagent diluent to produce a stock solution of 180ng/ml. Reconstituted standard were aliquoted and stored at -80°C for up to 6 months. A seven point standard curve was prepared by a 2-fold serial dilution in reagent diluent: 4000pg/ml, 2000pg/ml, 1000pg/ml, 500pg/ml, 250pg/ml, 125pg/ml and 62.5pg/ml (figure 3.15-C).
- For the MMP-1/TIMP-1 complex assay, 288 $\mu\text{g/ml}$ of goat anti-human MMP-1 was used as the capture antibody. This was reconstituted in 1ml of PBS. The capture antibody was further diluted with PBS without carrier protein to a working concentration of 1.6 $\mu\text{g/ml}$ prior to coating the 96-well microplates. For the detection antibody, 18 $\mu\text{g/ml}$ of biotinylated goat anti-human TIMP-1 was used. This was reconstituted in 1ml of reagent diluent (50mM Tris, 10Mm CaCl_2 , 0.15M NaCl, 0.05% Brij® 35, Ph 7.45). After reconstitution, 55 μl aliquots of both capture and detection antibodies, were stored at -80°C for up to 6 months. Then, the detection antibody was further diluted to a working concentration of 100ng/ml in reagent diluent prior to coating the 96-well microplates.
- 80ng/ml of Recombinant Human MMP-1/TIMP-1 complex was reconstituted with 0.5ml of reagent diluent (50mM Tris, 10Mm CaCl_2 , 0.15M NaCl, 0.05% Brij® 35, Ph 7.45) to produce a stock solution of 160ng/ml. Reconstituted standard were aliquoted and stored at -80°C for up to 2 months. A seven point standard curve was prepared by a 2-fold serial dilution in reagent diluent: 4000pg/ml, 2000pg/ml, 1000pg/ml, 500pg/ml, 250pg/ml, 125pg/ml and 62.5pg/ml (figure 3.16).
- 40 μl of Streptavidin-HRP was diluted in 9600 μl of reagent diluent for every microplate used.

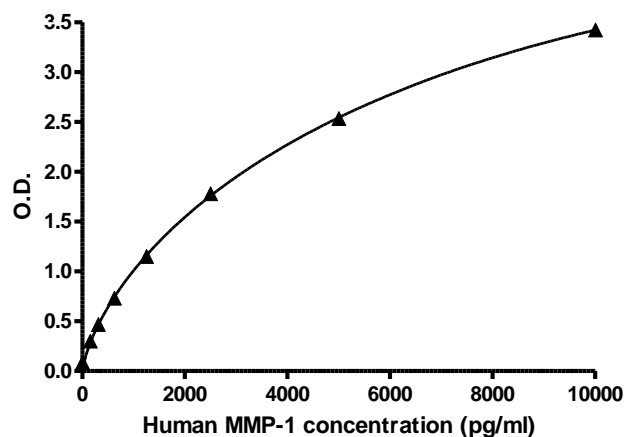
- The substrate solution was prepared by mixing equal volumes of H₂O₂ and Tetramethylbenzidine (e.g. 4800µl of each reagent for each microplate used) within 15 minutes of use in a place protected from light.

3.4.5.1.5. Assay procedure

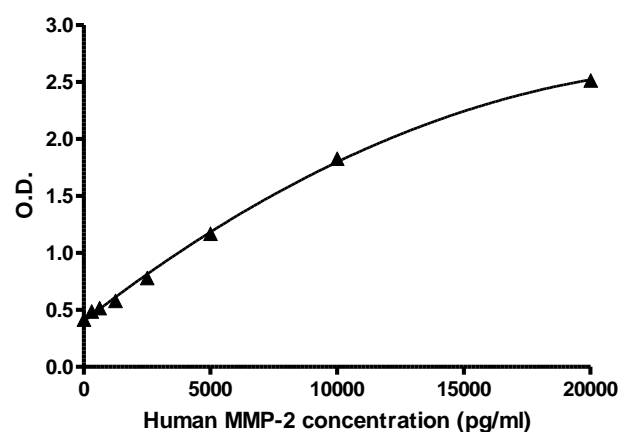
100µL per well of the diluted Capture Antibody (MMP-1 (for MMP-1 and MMP-1/TIMP-1 complex assays), MMP-2, MMP-9, TIMP-1, TIMP-2 or TIMP-3) was coated in 96 wells microplates (Costar 3590, Corning Incorporated, USA). Plates were sealed (Greiner multiwall plate sealer, Sigma-Aldrich, UK) and incubated overnight at room temperature with gentle rocking (Stuart Digital Rocker SRT6, Geneflow, UK). After this first incubation, wells were aspirated and the plate was washed three times with 0.05% Tween 20 in PBS, pH 7.4. Complete removal of wash buffer was obtained by inverting the plates and blotting against clean absorbent paper towels. 300ul per well of reagent diluent was used to block the plates for one hour at room temperature. Plates were again aspirated and washed three times with wash buffer. 100ul of standards or samples were added per well. All standards and samples tested were coated in duplicates. Plates were covered with a new adhesive strip and incubated two hours at room temperature with gentle rocking. Aspiration and wash of the wells were repeated. 100µl per well of the diluted Detection Antibody (MMP-1, MMP-2, MMP-9, TIMP-1 (for TIMP-1 and MMP-1/TIMP-1 complex assays), TIMP-2 or TIMP-3) was added to each well, plate was covered with a new adhesive strip and incubate two hours at room temperature at the rocker. The aspiration/washing process was repeated for three times and 100µl of Streptavidin-HRP 1:250 diluted in reagent diluent added to each well. Plates were incubated for 20 minutes at room temperature avoiding direct contact with light. The aspiration/washing process was repeated for a final time. Next, 100ul of Substrate Solution (1:1 mixture of H₂O₂ and TMB, R&D Systems, UK) was added to each well. Plates were incubated for another 20 minutes at room temperature, avoiding direct light. After colour development, 50ul of 2N H₂SO₄ (Analar Normarpur®, VWR International Ltd) was added to each well. Optical density was determined at 450nm using a Labsystems Multiskan Ascent spectrophotometer (Bio-Rad Laboratories, Hertfordshire, UK) using genesis light software.

Figure 3.14: Human Matrix Metalloproteinases Immunoassay Standard Curves

A - Human MMP-1



B - Human MMP-2



C - Human MMP-9

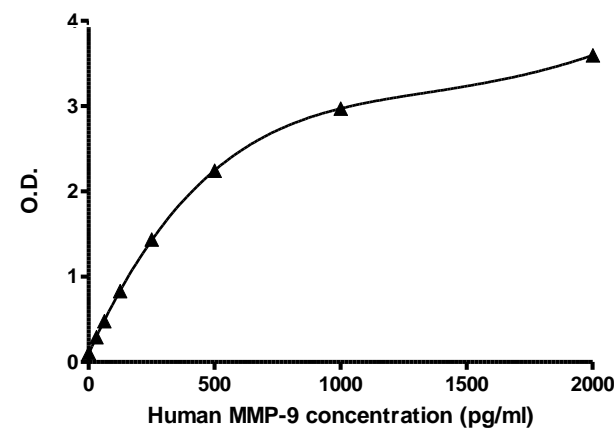
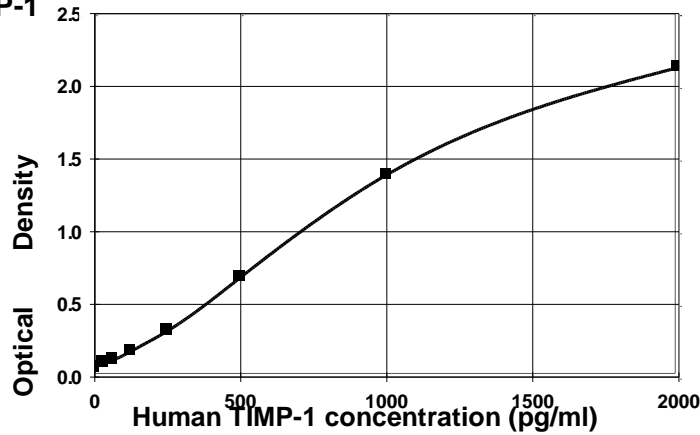


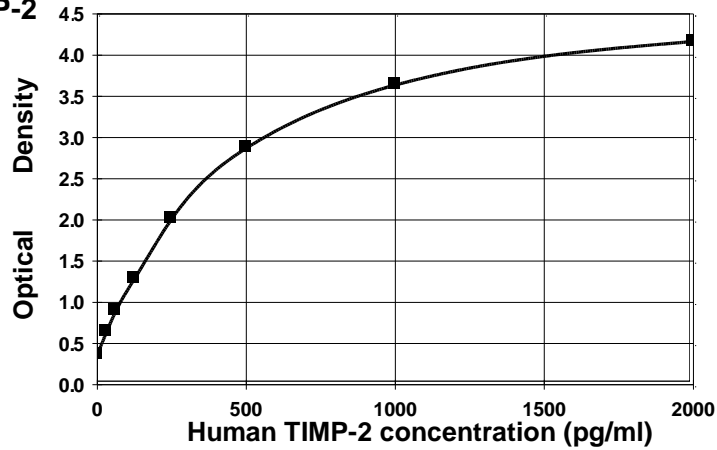
Figure 3.14: Human total MMP-1 (A), MMP-2 (B) and MMP-9 (C) immunoassay standard curves were obtained using recombinant human MMPS and calculated using a Labsystems Genesis computer package with a four parameter logistic (4-pl) curve fit. Absorbance was measured on Labsystems Multiskan Ascent plate reader at a wavelength of 450nm. Optical density (O.D.) of each sample was plotted on the y-axis against the MMP concentration (pg/ml) on the x-axis. Data points are average of duplicates.

Figure 3.15: Human Tissue Inhibitors of Metalloproteinases Immunoassay Standard Curves

A - Human TIMP-1



B - Human TIMP-2



C - Human TIMP-3

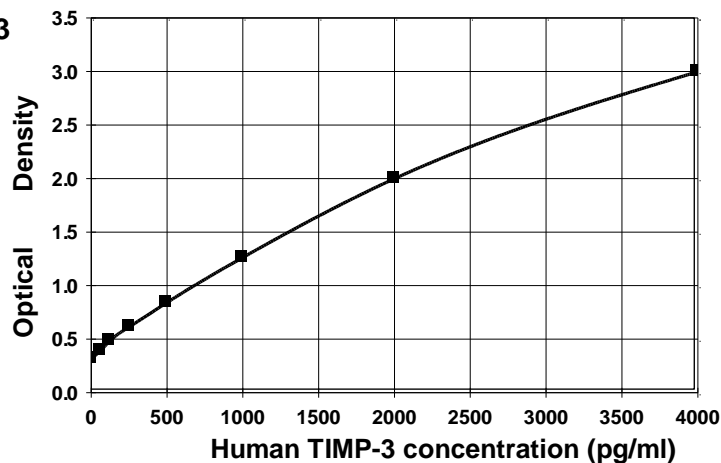


Figure 3.15: Human TIMP-1 (A), TIMP-2 (B) and TIMP-3 (C) immunoassay standard curves were obtained using recombinant human TIMPS and calculated using a Labsystems Genesis computer package using a four parameter logistic (4-pl) curve fit. Absorbance was measured on Labsystems Multiskan Ascent plate reader at a wavelength of 450nm. Optical density (O.D.) of each sample was plotted on the y-axis against the TIMP concentration (pg/ml) on the x-axis. Data points are average of duplicates.

Figure 3.16: Human MMP-1/TIMP1 complex Standard Curve

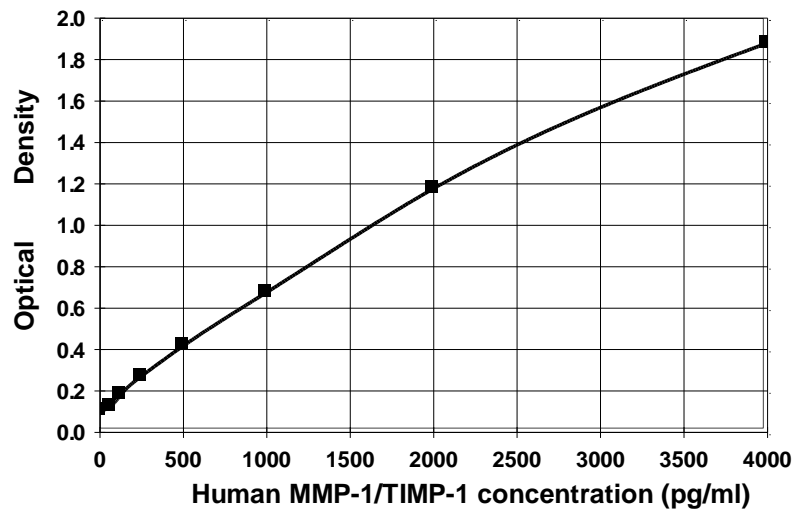


Figure 3.16: Human MMP-1/TIMP-1 complex immunoassay standard curve was obtained using a Labsystems Genesis computer package using a four parameter logistic (4-pl) curve fit. Absorbance was measured on Labsystems Multiskan Ascent plate reader at a wavelength of 450nm. Optical density (O.D.) of each sample was plotted on the y-axis against the MMP-1/TIMP-1 complex concentration (pg/ml) on the x-axis. Data points are average of duplicates.

3.5. Amino acid analysis by cation exchange chromatography

The analysis of amino acids and diamino acids in urine samples was performed on a Biochrom 30 Amino Acid Analyser physiological system (Biochrom, UK) after preparation of the samples.

3.5.1. Sample preparation

3.5.1.1. TCA / Acetone precipitation

5 mls of urine was added to 15 ml of 10% TCA / Acetone solution and left overnight at -20°C to precipitate the proteins in the solution. The precipitate was pelleted at 7000xg for 10 mins at 4°C using a Sigma 3-18K centrifuge (SciQuip Ltd, UK). The TCA / Acetone was poured off. The pellet was then washed with 15 ml of cold acetone and pelleted again at 7000xg for 10 mins at 4°C. The final pellet was resuspended in 100ul H₂O and 1900ul 0.1M NH₄CO₃ at room temperature. 50ul was taken off for protein measurement using BCA assay.

3.5.1.2. TCA precipitation with Ether extraction for ε (γ-glutamyl) lysine analysis

5 mls of urine was added to 1ml of 50% Trichloroacetic acid (TCA) (Sigma-Aldrich, UK) to make up a final concentration of 10% (w/v) TCA to precipitate the proteins in the solution. Precipitation occurred overnight at -20°C. Samples were centrifuged at 7000xg for 10 mins at 4°C using a Sigma 3-18K centrifuge (SciQuip Ltd, UK). TCA was poured off and 5 mls of 10% TCA was added to the pellet and homogenised to resuspend the pellet. Samples were centrifuged again at 7000xg for 10 mins at 4°C. TCA was poured off 5 mls of 1:1 diethylether: ethanol (Analar Normarpur®, VWR International Ltd), added to the pellet and then pelleted again at 7000xg for 15 mins at 4°C. This step was repeated three times. The diethylether: ethanol was poured off and 5 mls of diethylether was added to each sample. After homogenising, samples were centrifuged again at 7000xg for 10 mins at 4°C thrice. The final pellet was resuspended in 100ul H₂O and 1900ul 0.1M Ammonium carbonate (NH₄CO₃) (VWR International Ltd) at room temperature. 50ul was taken off for protein measurement using the RC-DC assay.

3.5.2. Proteolytic digestion for ε (γ-glutamyl) lysine measurement

A volume containing 10mg of protein from urine precipitate (TCA precipitation followed by ether extraction and resuspended in NH₄CO₃, section 3.5.1.2.) had a crystal of thymol (Fisher Scientific, UK) added to prevent bacterial decay. 2mg of Subtilisin (Sigma Aldrich, UK) dissolved in 10ul NH₄CO₃ (VWR International Ltd) was added to each tube and then incubated at 32°C for 12 hours with gentle shaking (Stuart Roller Mixer SRT9D, Geneflow, UK). The

addition of 2mg Subtilisin was repeated twice at 10 hours intervals. Samples were homogenised between each digest to ensure that there was no formation of particulate matter (Gallenkamp Spin Mix, Rigal Bennett, UK). 25ul of digest was removed for protein measurement (RC DC protein assay, section 3.2.2.1). 1.5 mg of Pronase E (Sigma Aldrich, UK) dissolved in 10ul NH_4CO_3 was added to each tube and then incubated at 32°C for 12 hours with gentle shaking. Samples were incubated at 100°C for 15 minutes to inactivate Pronase E. Leucine amino peptidase (LAP) (NBS Biologicals, UK) was activated by addition of 22.75U of it to 10ul 50Mm Magnesium chloride (Sigma-Aldrich, UK) and 90ul 10Mm Tris-HCL pH 8 (Sigma-Aldrich, UK) per sample and subsequent incubation at 37°C for 2 hours. The enzyme Prolidase (NBS Biologicals, UK) was activated by addition of 38.6U of it to 20ul 50 Mm MgCl_2 , 80ul 10 Mm Tris-HCL pH 8 and 80ul distilled water per sample. 180ul of activated LAP and 150ul of activated prolidase were added at the same time to each sample and then incubated at 37°C for 10 hours. The addition of 1.5mg of Pronase E (Sigma Aldrich, UK) dissolved in 10ul NH_4CO_3 per tube was then repeated with incubation at 32°C for 12 hours with gentle shaking.

The pH of the samples was measured using litmus paper (Full Range pH 1-14 test paper, Whatman®, UK) and then adjusted to 6.75-7.00 by the addition of a small volume of 1M HCL. 0.2mg of Carboxypeptidase Y (Sigma Aldrich, UK) dissolved in 10ul NH_4CO_3 was added to each sample and incubated at 30°C for 12 hours. Samples were placed overnight in a desiccator, under vacuum (Laboport Vacuum Pump, KNF Neuberger, USA), containing one beaker of 0.5M NaOH and 1M H_2SO_4 to remove ammonium carbonate. Then, samples were freeze dried for 18 hours and could be stored as this stage to await amino acid analysis. Samples were subsequently resuspended in 500ul 0.1M HCL and 500ul of Lithium citrate loading buffer (pH 2.2, 0.2M) (Biochrom, UK) and filtered (4mm PTFE, 0.2um pore size; Chromacol LTD - UK) into an appropriate chromatography vial (2.0ml Chromacol glass vial with PTFE screw-top sealer).

3.5.3. Proteolytic hydrolysis for Hydroxyproline measurement

10mg of protein from a urine precipitate (TCA / Acetone precipitation, resuspended in 100ul H_2O and 1900ul 0.1M NH_4CO_3 , section 3.2.1.2.) was hydrolysed in 2ml of 6M HCL in an incubator at 110°C for 18 hours. After hydrolysis, samples were centrifuged at 15000xg for 10 mins at 4°C using a Sigma 3-18K centrifuge (SciQuip Ltd, UK). The supernatant was transferred to a fresh 20ml universal tube, freeze dried for 18 hours, resuspended in 1ml Lithium citrate loading buffer (pH 2.2, 0.2M) (Biochrom, UK) and then filtered into a chromatography vial (4mm PTFE, 0.2um pore size; Chromacol LTD – UK).

3.5.4. Principles of the Biochrom 30 Amino Acid Analyser physiological system procedure

3.5.4.1. Biochrom 30 equipment preparation

To utilize the Biochrom 30 Amino Acid Analyser (AAA) physiological system (figure 3.17), previous set up of the Biochrom 30 instrument, the autosampler and the PC with the BioSys software are required.

Figure 3.17: The Biochrom 30 Amino Acid Analyser physiological system



Figure 3.17: The Biochrom 30 Amino Acid Analyser (AAA) physiological system consists of a Biochrom 30 instrument (in the middle), where the analytical column is present, the Autosampler Unit (right) and a PC with the BioSys and Ezchrom Elite softwares installed.

Biochrom 30 instrument set up:

The Biochrom 30 instrument requires a nitrogen supply with a pressure of 75-80 psi / 5-6 Bar. Also, 9 bottles containing different solutions should be connected and placed above the instrument: five lithium citrate buffers of varying pH and ionic strength and one with lithium hydroxide (regeneration buffer) (table 3.5), one containing Ultrapure water, one with the coil flush (50:50% methanol in ultrapure water) and one with the Ninhydrin reagent. The Ninhydrin reagent is prepared by bubbling 1750ml of Ultrasolve solution (Biochrom, UK) with nitrogen gas for 10 minutes (stirring) and addition of 250ml of Ninhydrin reagent. This solution should be stirred under nitrogen gas for a further 10 minutes.

Table 3.5: Ion exchange process

	Buffer	Molarity	pH
Buffer 1	Lithium A	0.20	2.80
Buffer 2	Lithium B	0.30	3.00
Buffer 3	Lithium CII	0.50	3.15
Buffer 4	Lithium DII	0.90	3.50
Buffer 5	Lithium pH 3.55	1.65	3.55
Buffer 6	Lithium Hydroxide	0.30	

Table 3.5: Five lithium citrate buffers of varying pH and ionic strength are pumped through a cation-exchange analytical column to release diverse amino acids which after reaction with Ninhydrin will form compounds that can be read in the photometer unit at 570nm and 440nm.

Autosampler:

The autosampler unit (MIDAS, Biochrom, UK) requires to be cooled down to a temperature of 4°C prior to use. After cooling the system, the equipment should be connected in serial mode with the Biochrom 30 and the PC, this will enable the AAA system to be controlled by the BioSys program. Also, the injection needle of the autosampler should be programmed to be washed with a solution containing 20% Isopropanolol (Analar Normapur®, VWR International Ltd) in ultrapure water and a waste bottle should be connected.

BioSys:

The BioSys software controls the injection of the samples (volume and appropriated separation program) in the autosampler as well as all other functions performed by the Biochrom 30 including the volumes of the lithium buffers, separation methods and timings, volume, speed and temperature of the ninhydrin reagent. The BioSys Manual operation window (figure 3.18) shows the flow rate and pressures of the lithium buffers (green) and ninhydrin (purple) as well as the temperature of the resin column, which should be above 50°C for optimal performance. All these functions are only possible to be performed when the reaction coil achieves a temperature above 100°C.

Figure 3.18: The BioSys Manual operation window

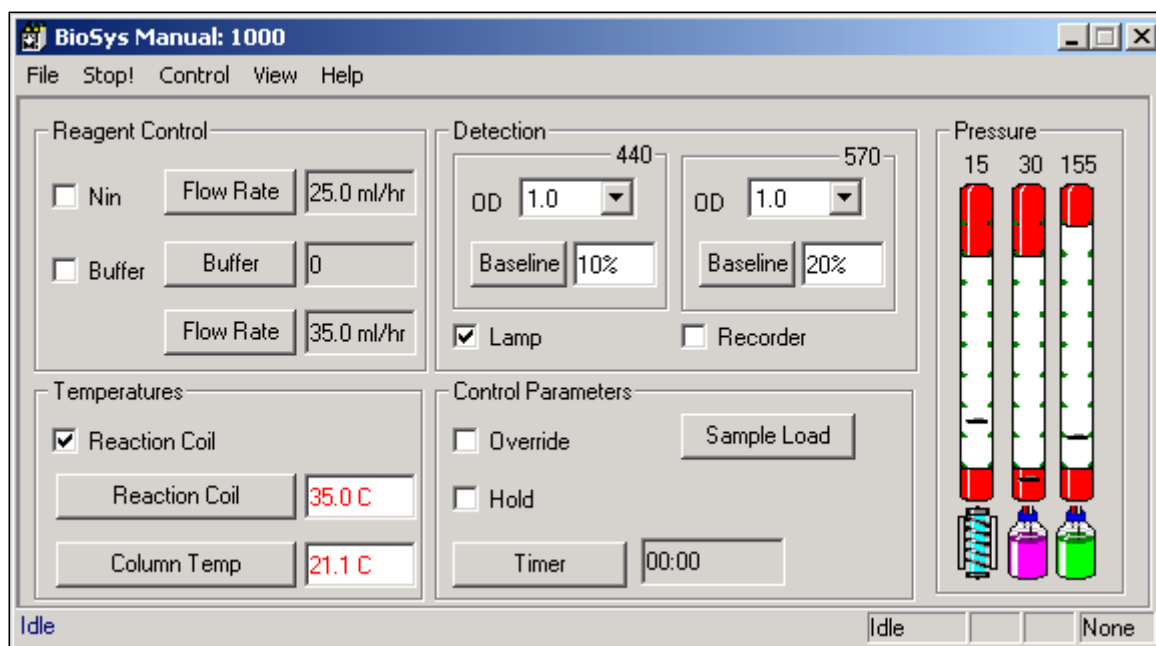


Figure 3.18: Injection of samples into the Autosampler is controlled by the BioSys software. Control parameters can be adjusted via this manual operation window.

3.5.4.2. Loading of the samples

To set up the instrument for running samples it is required to open the Program Control window (figure 3.19) from BioSys and create a list containing the samples required for the analyses to be performed. This will indicate the vial position in the autosampler as well as the volume used for injection in the system and the analytical separation program to be used. For ϵ (γ glutamyl) lysine and Hydroxyproline measurements, samples were fractionated using the 96361 LiHP control program using a partial fill loop. After each run, files will be saved in the Data directory and can be operated via a second software called EzChrom Elite.

Figure 3.19: The BioSys Program Control window

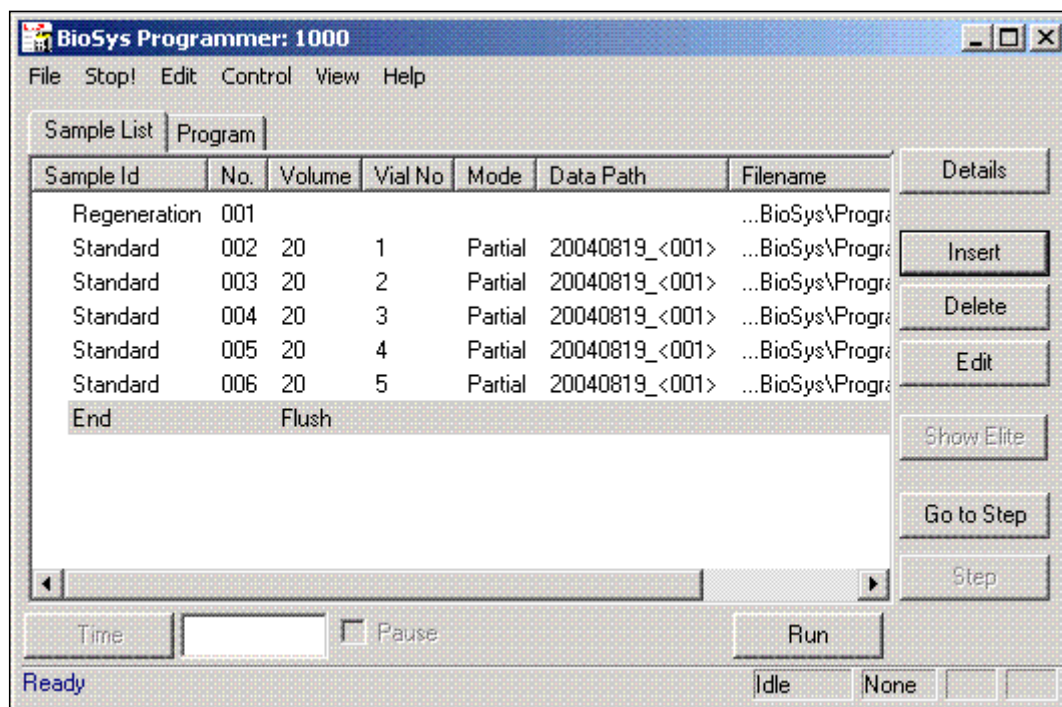


Figure 3.19: Running list is initiated by the regeneration program and contains the standard solution with aminoacids and re-suspended samples.

3.5.4.3. Fractionation of amino acids

After loading the samples in the autosampler, these are pumped to a cation-exchange column present in the Biochrom 30 AAA. The positively charged amino acids present in the sample are bound to the analytical resin present in the cation-exchange column, which is negatively charged. This resin consists of spherical beads of polystyrene which are crosslinked by the incorporation of divinylbenzene groups and are also sulphonated to give it a negative charge. The column is kept at a controlled high temperature (above 100°C), so that it can accommodate the influx of a series of Lithium Citrate buffer counter ions (Biochrom, UK) at increasing pH and concentrations (table 3.5) and allow ion exchange to take place between the positively charged groups in the Lithium buffers which are attached to the matrix by heteropolar bonds, and the amino acids which diffuse into it. When the isoionic point of an amino acid is reached, the ionic attraction to the resin is lost and the amino acid elutes from the column.

The eluent is then mixed with Ninhydrin (Biochrom, UK), a powerful oxidising reagent, in the reaction coil at 135°C to form coloured compounds through the Ruhemann's purple reaction (figure 3.20-A). The intensity of coloured compounds is directly proportional to the quantity of

amino acid present in the solution. Those compounds are read in the spectrophotometer unit at two wavelengths, 570 nm and 440 nm. α -amino groups will be better monitored at 570 nm and imino acids, such as proline and hydroxyproline, which do not have free α -amino groups are better monitored at 440 nm as their reaction with Ninhydrin will produce a bright yellow compound instead of purple (figure 3.20-B). The concentration of amino acids is recorded as a series of peaks read at EZChrom Elite software (Biochrom, UK). The retention time of each peak identifies the amino acid and the area under the peak indicates its concentration. This separation into individual peaks is determined by the ionic charge difference in the eluted amino acids caused by different pK values of their side chains and also by the hydrophobic interactions of these side chains with the polystyrene matrix.

Figure 3.20: Simplified reaction between Ninhydrin, amino acids and imino acids

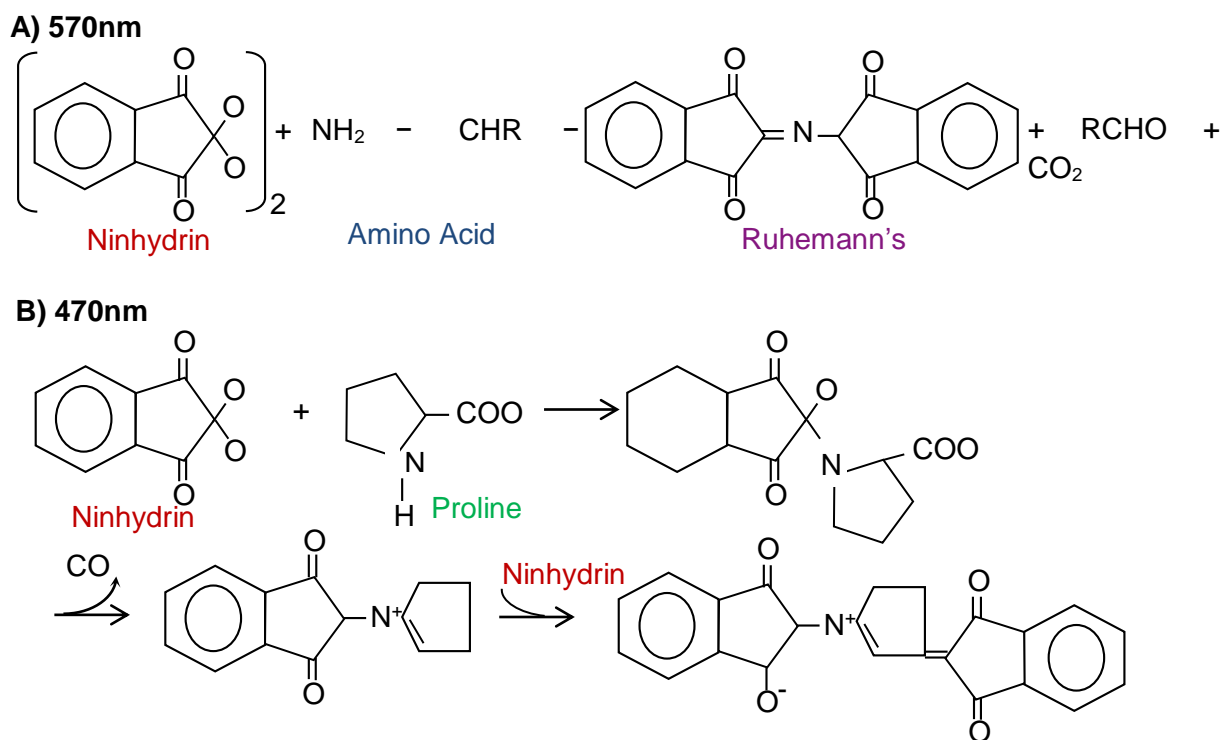


Figure 3.20: A) Reaction between ninhydrin and amino acids leads to the oxidative deamination of the alpha-amino group, liberating ammonia, carbon dioxide, an aldehyde and hydridantin. The reaction between ammonia and hydridantin yields a purple substance (Ruhemann's purple) that absorbs maximally around 570nm. **B)** The imino acids Proline and Hydroxyproline do not have free alpha-amino groups. Their reaction with ninhydrin forms a bright yellow compound monitored at 440nm.

3.5.5. Calibration of the Amino Acid Analyser

A physiological standard solution was prepared to calibrate the EZchrom Elite software by the addition of 100ul Basic amino acids (Sigma-Aldrich, UK) and 100ul Acidic and Neutral amino acids (Sigma-Aldrich, UK) to 300ul 0.2M Lithium Citrate loading buffer, pH 2.20 (Biochrom,

UK). 20ul of the standard solution was loaded using a partial fill loop onto the Biochrom 30 AAA and fractionation was controlled using the EZChrom Elite 96361 LiHP BioSys control program (figure 3.21). This solution contained a total of 56 amino acids and derivatives. However, ϵ (γ -glutamyl) lysine is not present in this composition. So, 10nmols ϵ (γ Glutamyl) Lysine in 20ul of physiological standard solution was prepared using a commercial lyophilised crosslink (H-Glu (H-Lys-OH)-OH, 250mg – MW=275.31, Bachem AG, Switzerland).

Following post column derivatization with Ninhydrin each amino acid elutes as an individual peak at specific retention times, with ϵ (γ Glutamyl) Lysine eluting between the amino acids Leucine and Tyrosine at approximately 77 minutes. All amino acids present in this standard solution are at a concentration of 10nmols/20ul. A typical chromatogram generated by a physiological standard solution spiked with 10nmols/20ul ϵ (γ Glutamyl) Lysine is shown on figure 3.22. Main amino acids, imino acids and peptides quantified by the amino acid analyser are listed on table 3.6.

Figure 3.21: EZChrom Elite 96361 LiHP BioSys program

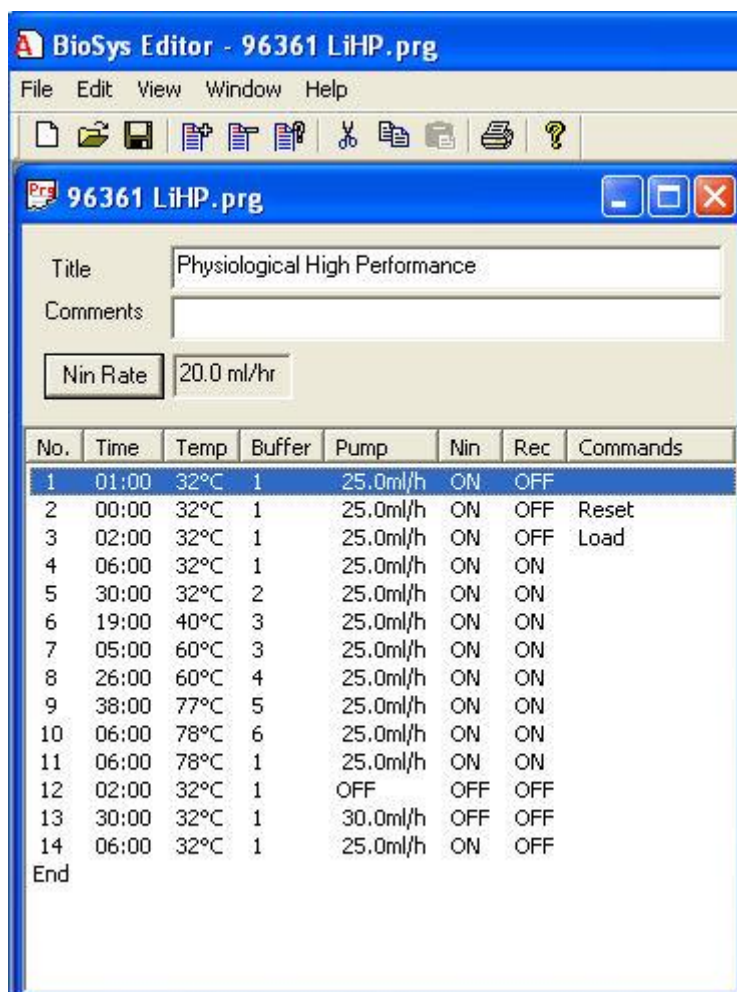


Figure 3.21: The EZChrom Elite 96361 LiHP BioSys control program regulates the fractionation of samples into individual amino acids by using 5 different Lithium Buffers and the Ninhydrin reagent. Buffers are sent at different rates of infusion to the analytical column, which is kept at varies temperatures.

Table 3.6: Main Amino acid and peptides classification and retention times

Amino Acid / Peptide	Abbreviation	Retention Time
Phosphoserine	Pser	4.2
Taurine	Taur	6.5
Urea	Ur	10.5
L-aspartate	Asp	21.3
Hydroxyproline	Hypro	24.9
L-threonine	Thr	27.6
Serine	Ser	29.8
Asparagine	Asn	34.2
Glutamate	Glu	36.5
Proline	Pro	47.0
Glycine	Gly	48.8
Alanine	Ala	50.4
Valine	Val	56.9
Cysteine	Cys	62.0
Methionine	Met	65.8
Isoleucine	Ileu	71.3
Leucine	Leu	75.7
Glutamyl-Lysine	Glu-Lys	77.0
Tyrosine	Tyr	79.4
Phenylalanine	Phe	81.9
Homocysteine	Homocyst	87.3
Gamma-aminobutyric acid	Gaba	89.5
Ethanolamine	Ethan	92.5
Lysine	Lys	105.7
Histidine	His	109.6
Arginine	Arg	124.2

Table 3.6: List of main amino acids and peptides detected by the AAA with their respective retention times. Adapted from “The Biochrom Handbook of amino acids”

3.5.6. Calculation of the results after calibration

To analyse the data results, it is necessary to access the EzChrom Elite server and first graphically define each peak and determine their retention times in both channels: 570nm and 440nm (figure 3.23). As the amino acid analyser is a comparative instrument, a calibration analysis must be performed before commencing a series of analyses at every run, thus producing a standard trace for comparison purposes. After this, the estimated concentration of each amino acid will be given and a report generated.

At the end of each sample analysis, the column is regenerated by pumping a strong base through the column followed by low pH Lithium buffer, which equilibrates the column prior to the next analysis.

Figure 3.23: Graphical definition of peaks

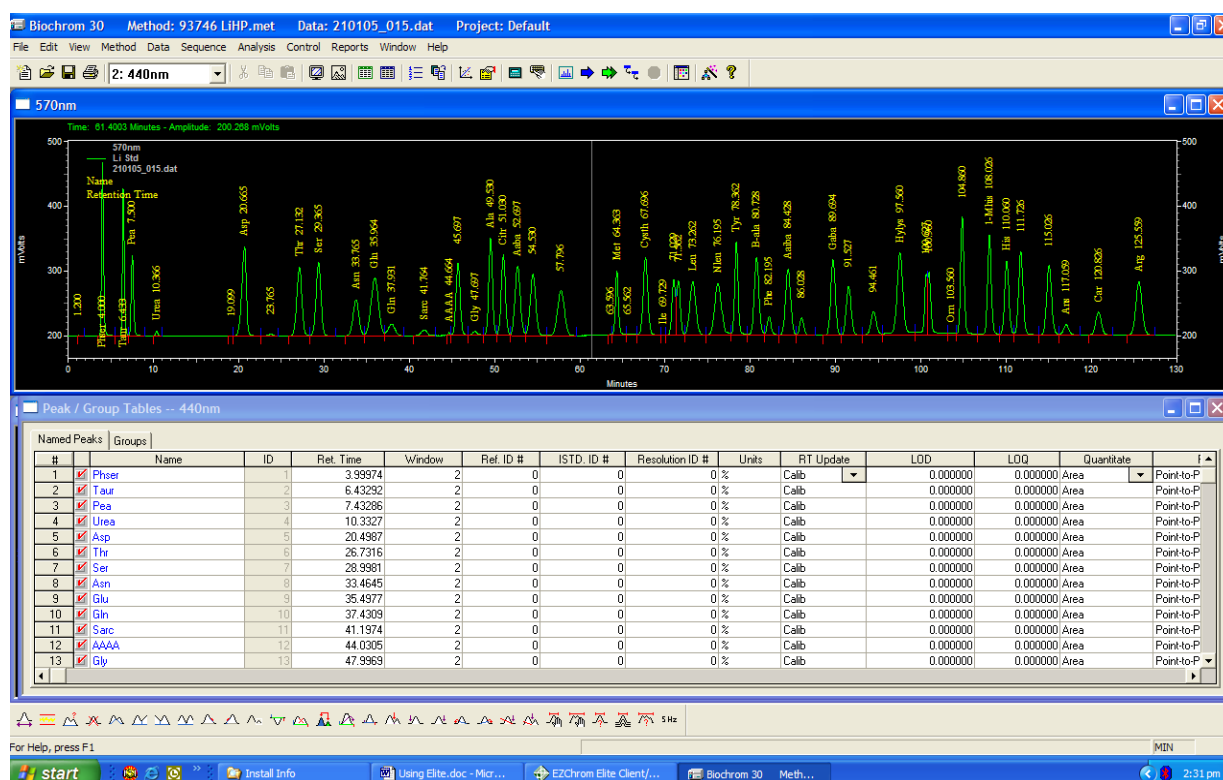


Figure 3.23: The full range of peaks generated by the end of the chromatography is graphically analysed for appropriated retention times. Then, the concentration of amino acids present in the samples can be estimated by reference to an amino acid solution used to calibrate the system in the beginning of every run.

3.5.7. Quantitative estimation of amino acids and di amino acids

Following exhaustive proteolytic digestion for ϵ (γ -glutamyl) lysine crosslink iso-dipeptide (section 3.5.2.) or hydrolysis for Hydroxyproline measurement (section 3.5.3.), 20ul of re-suspended sample containing a mixture of amino acids and di amino acids was placed into the autosampler unit (MIDAS, Biochrom, UK) and run on the cation-exchange Biochrom 30 Amino Acid Analyser (AAA) using a partial fill loop injection.

3.5.7.1. ϵ (γ -glutamyl) lysine crosslink iso-dipeptide

ϵ (γ -glutamyl) lysine crosslink peak ϵ (γ Glutamyl) Lysine clearly elutes as an individual peak between Leucine and Tyrosine using the 96361 LiHP program with a retention time of approximately 77 minutes. Estimated concentration of ϵ (γ -glutamyl) lysine crosslink iso-dipeptide in 20ul was calculated by reference to the 10nmols/20ul physiological standard solution (section 3.5.6.) taking reading of Ninhydrin derivatised peaks at 570nm (figure 3.22).

3.5.7.2. Hydroxyproline

Hydroxyproline peak elutes between the amino acids Aspartate and Threonine with a retention time of approximately 26 minutes. Estimated concentration of Hydroxyproline in 20ul was calculated by reference to the 10nmols/20ul physiological standard solution (section 3.5.6.) taking reading of Ninhydrin derivatised peaks at 440nm (figure 3.22).

3.6. *In vitro* crosslinking of TG2 substrates

250ug of Recombinant Human Tissue Transglutaminase (Zedira, UK) was reconstituted in 250ul of Ultrapure H₂O and 10ul Aliquots (1ug/ul) were stored at -80°C until required. TG2 in each aliquot was activated by the addition of 200mM Ca²⁺ in 50mM Tris, pH 7.4 (Sigma-Aldrich, UK) to a final Ca²⁺ concentration of 10mM and the addition of 100mM Dithiothreitol (DTT) (Sigma-Aldrich, UK) in 50mM Tris (pH 7.4) to a final concentration of 5mM (i.e. 0.5ul). A 1mg/ml solution of the following substrates was made in 5mM Tris pH 7.4 or ultrapure H₂O depending on the lyophilised material: Albumin from Human Serum, Human Collagen Type I, Human Collagen Type III, Human Collagen Type IV, Human Collagen Type V, Fibronectin from Human Plasma (FN) and Human Dimethyl casein (DMC) (all from Sigma-Aldrich, UK). Collagens were heated to 37°C for 30 mins to aid solubilisation. 10ul of activated rhTG2 was added to 100ul of 1mg/ml solution of Collagen I, III, IV, V, Albumin, FN and DMC and incubated overnight at 37°C. Protein was precipitated by addition of TCA (Trichloroacetic acid) to a final volume of 10% (w/v); i.e., 22ul of 50% TCA to 100ul TG2 substrate solution. Then, the precipitated solution was centrifuged at 7000xg for 15 minutes at 4°C using a Sigma 3-18K centrifuge (SciQuip Ltd, UK). Each sample was resuspended in 10ul H₂O, 190ul 0.1M NH₄CO₃ at room temperature with the release of ε(γ-glutamyl lysine di peptide in the potential TG2 substrates undertaken by exhaustive proteolytic digestion following the protocol described in section 3.5. Samples were re suspended in 200ul of 1:1 Solution of 0.1N (0.1M) HCl / Lithium Citrate Loading Buffer pH 2.2, 0.20M (Biochrom, UK). Separation and quantification of ε (γ-glutamyl) lysine was done by reverse phase HPLC (Biochrom 30 AAA). 40ul was loaded into the equipment using a partial fill loop. Fractionation and identification of ε (γ-glutamyl) lysine peak was performed as described in section 3.5.7.1. A schematic representation of the process involved in the detection of crosslink in TG2 substrates can be seen in figure 3.24.

Figure 3.24: Determination of crosslinking in Transglutaminase 2 substrates

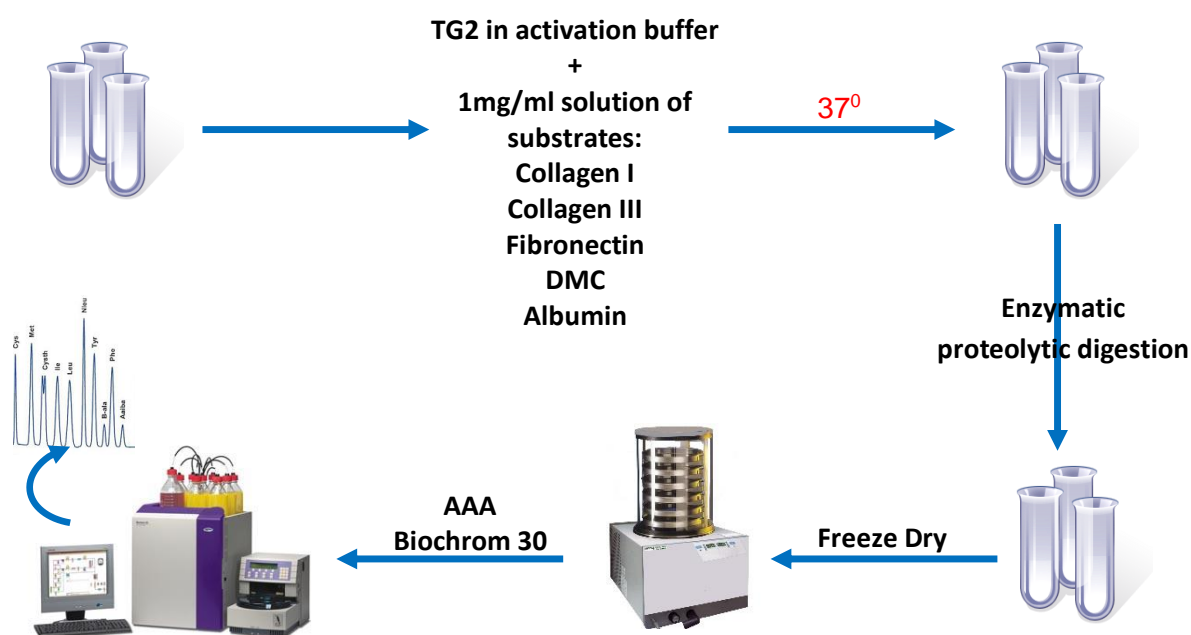


Figure 3.24: Schematic representation of the *In vitro* protocol for the measurement of ϵ (γ -glutamyl) lysine crosslinking in TG2 substrates. Briefly, this assay comprised: activation of Recombinant Human Transglutaminase 2, crosslinking of TG2 substrates, breakdown of TG2 substrates by exhaustive proteolytic digestion, samples freeze dry and separation and quantification of XL by reverse phase HPLC (Biochrom 30 Amino Acid Analyser).

3.7. ECM proteolytic activity

3.7.1. Rationale behind the MMP proteolytic activity assay

Matrix Metalloproteinases are able to digest collagen, gelatin (denatured collagen) and most ECM components. Each MMP can specifically digest a number of ECM molecules. For example, MMP-2 (gelatinase A) is primarily responsible for the breakdown of the helical domains of type IV collagen, whilst MMP-1 is more specific against to type I collagen. As MMPs can be found in latent forms and they have natural inhibitors (TIMPs) determining the true biological contribution of MMPs is difficult purely with antigen assays. Therefore, in order to analyse the overall ECM proteolytic activity in human urine due to MMPs, the Molecular Probes' EnzChek® Gelatinase/Collagenase Assay system was used (Invitrogen Corporation, EvoQuest™ Laboratory Services, USA) to measure overall MMP enzyme activity. The activity

of interstitial collagenase type MMPs (MMP-1, 7 and 13) was measured using a collagen 1 substrate, whereas the gelatinase type MMP activity (MMP-2, 9) was measured using a Collagen IV substrate. Overall MMP activity was measured using a gelatin substrate.

3.7.2. Principal of EnzChek® Gelatinase/Collagenase Assay

The EnzChek Gelatinase/Collagenase Assay Kit provides a fast and highly sensitive fluorometric method for measuring gelatinase or collagenase activity. In this assay, the substrate used is the fluorescein-labeled DQ™ gelatin or collagen conjugate, which are complete gelatin or collagen molecules (rather than peptides) that is highly labeled with fluorescein. The fluorescence signal is quenched by the protein itself until enzymatic digestion releases protein fragments containing the FITC which become highly fluorescent when released from the larger protein (figure 3.25). The Gelatin substrate is efficiently digested by all MMPs to yield highly fluorescent peptides. The increase in fluorescence is proportional to the MMP proteolytic activity and can be monitored with a fluorescent microplate reader, minifluorometer or standard fluorometer. Collagenase purified from *Clostridium histolyticum* can be used as a control enzyme to confirm proteolytic activity. A metal chelator and general inhibitor of metalloproteinases, 1,10-phenanthroline, can be used as a control for effective inhibition of the collagenase activity.

Figure 3.25: Mechanism of Action from EnzChek® Gelatinase/Collagenase Assay

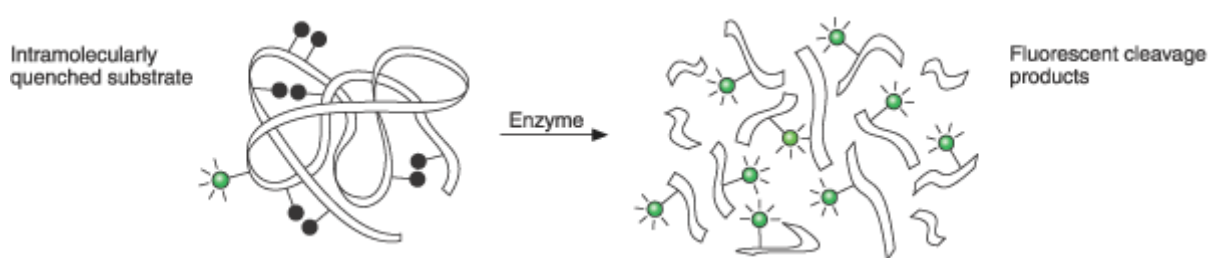


Figure 3.25: Principle of MMP activity detection via the disruption of intramolecular self-quenching. Enzyme-catalysed hydrolysis of the heavily fluorescein-labelled and almost totally quenched DQ™ gelatin substrate provided in the EnzChek Protease Assay, releases cleavage products which are highly fluorescent and can be analysed in a standard fluorescent microplate reader.

3.7.3. Materials

The following reagents were used for measurement of ECM proteolytic activity:

- DQ gelatin fluorescein conjugates. Gelatin was isolated from pig skin. Each vial containing 1mg of substrate lyophilized from 1ml of PBS, pH 7.2
- 10 X Reaction Buffer: 50ml of 0.5M Tris-HCL, 1.5M NaCl, 50Mm CaCl₂, 2mM sodium azide, pH 7.6.
- 30mg of 1,10-Phenanthroline, monohydrate (MW=198.2)
- 500U of type IV Collagenase from *Clostridium histolyticum*. One unit is defined as the amount of enzyme required to liberate 1µmole of L-leucine equivalents from collagen in 5 hours at 37°C, Ph 7.5.

3.7.4. Reagents preparation

- 1.0mg/ml stock solution of the DQ gelatin fluorescein conjugate was prepared by addition of 1.0ml of deionized water (dH₂O) directly to the vial containing the lyophilized substrate. After reconstitution the stock solution was aliquoted and stored at -80°C until use. The solution was left for 5 minutes in an ultrasonic water bath with agitation and heat to 50°C to facilitate dissolution prior to use.
- 1 X Reaction Buffer was prepared by dilution of 2ml of the 10 X Reaction Buffer in 18ml dH₂O
- 1000U/ml of *Clostridium histolyticum* stock solution was prepared by dissolving the 500U in 0.5ml dH₂O. After reconstitution, it was aliquoted and stored at -80°C until use.
- 9.9mg of 1,10-Phenanthroline was dissolved in 25µl ethanol. A 10mM working solution was prepared by adding 10µl of this solution to 2ml of 1 X Reaction Buffer.

3.7.5. Assay procedure

80µl per well of 1 X Reaction Buffer was added to half (48 wells) of a black polystyrene 96-well microplate for fluorescence (Corning® NBS™ 96 well plates, Corning Incorporated, USA). In the other half of the plate (48 wells), 70µl per well of 1 X Reaction Buffer and 10ul per well of the inhibitor solution (1,10-Phenanthroline) was added. The addition of this inhibitor enable the confirmation of the extent of the proteolytic activity due to the MMP action, as collagens and gelatins can be degraded to some degree by other proteases. A seven point standard curve was prepared by a 2-fold serial dilution using the collagenase from *Clostridium histolyticum*. The highest point was 0.2U/ml. 100µl of the diluted enzyme was added in

duplicates in both halves of the plate. 100ul of 1 X Reaction Buffer acted as a blank. 100µl/well of undiluted human urine was added in duplicates to both halves of the plate. Next, 20µl of the 1.0mg/ml stock solution of DQ gelatin or collagen conjugate was added to each well immediately prior to reading in a multi-well fluorescent plate reader equipped with standard fluorescein filters (Fusion Plate Reader, Packard BioScience Company, USA) with Excitation/Emission at 485/530nm, respectively. Samples were incubated for 48 hours at room temperature, protected from light. As the reaction is continuous, fluorescence intensity was read at multiple time points (every 15 minutes for the first 3 hours, then every hour for the following 6 hours, then a final time 48 hours after the addition of the DQ gelatin). This ensured the best linear reaction possible for each sample. For each time point, background fluorescence was corrected by subtracting the values derived from the no-enzyme control.

3.8. Statistical Analysis

Nominal categorical data such as gender, postal address, smoking habit and CKD etiology were expressed as a percentage of the total number of patients and graphically illustrated by either bar or pie charts.

Discrete numerical data such as the number of patients with anaemia or any other co morbidity and continuous numerical data such as patient's age, height, weight and all laboratorial results were expressed as mean \pm standard error of the mean (mean \pm SEM) or standard deviation (mean \pm SD) as appropriate. They were displayed either by dot plots, Histograms or Box and Whisker plots.

All generated laboratorial results were plotted to analysis of their shape of the distribution. Data which showed a bell shaped and symmetrical distribution with around 95% of the observations lying within two standard deviations (SD) was classified as having normal distribution, whilst other data results could be classified as skewed or ranked. The choice of statistical method of analysis was done according to the distribution pattern of the outcome data; parametric methods such as *t*-test, analysis of variance (ANOVA) and linear regression techniques were used to test normally distributed data. Comparison between two ordinal independent groups was performed by using Mann-Whitney U test.

The statistical significance of experimental CKD samples was assessed using either Mann-Whitney U test, Independent samples *t*-test or a single factor analysis of variance (ANOVA) with Bonferroni post test as appropriate.

Analysis of Human samples results were performed using two- way ANOVA with Bonferroni post test. Correlation analysis between variables was determined by performing Pearson's correlation. Multiple linear regression analysis was applied to determine the correlation and association among more than two parameters and also to select predominant impact factor. The null hypothesis (H_0) was set as the negation of the research hypothesis and therefore, that there was no difference in the average values of the urine ECM biomarkers between controls or healthy volunteers and diseased animals or CKD patients. The probability of obtaining results if the null hypothesis was true was defined as the p value. A p value >0.5 was taken as statistically significant difference and a p value of < 0.001 confirmed that it was very unlikely to observe the data if H_0 was true and thus there was a strong difference in the mean values (highly statistical significance difference). Receiver Operating Characteristic (ROC) curve analysis was used for all biomarkers to evaluate accuracy in prediction of CKD progression. ROC curve is a powerful instrument to measure the prognostic value of a molecule by determining the number of true positive cases (sensitivity) versus false positive cases (1-specificity). An area under the curve of 1 (or 100%) represents a perfect diagnostic test, whilst an area of 0.5 (50%) represents a worthless test. Statistical analysis was performed using Microsoft Excel 2013 software package, Graphpad prism 6 (Graphpad software Inc, California, USA) or SPSS version 21 (IBM, New York, USA).

Chapter 4

The urine excretion of Transglutaminase type 2 and ϵ (γ glutamyl) lysine as biomarkers of renal fibrosis in animal models of Chronic Kidney Disease

4.1 Introduction

Transglutaminase type 2 (tTG; TGase2; TG2) is a multifunctional enzyme associated with a wide range of biological processes including ECM stabilization (Johnson *et al.* 1997) , angiogenesis suppression (Jones *et al.* 2006), modulation of apoptosis (Fesus *et al.* 1987, Fesus *et al.* 1996, Oliverio *et al.* 1999), wound healing (Verderio *et al.* 2004), skin barrier formation (Harrison *et al.* 2007), TGF β 1 activation (Douthwaite *et al.* 1999, Huang *et al.* 2009) amongst a diversity of other cellular functions.

Out of all these biological functions, one of the most well established function of TG2 is its ability to promote ECM stabilization. TG2 catalyses the post-translational modification of ECM proteins by the formation of covalent bonds between epsilon-amino groups of peptide-bound lysine and the gamma-carboxamine group of glutamine residues (Folk and Finlayson 1977). This reaction is dependent of Ca²⁺ and can be inhibited by GTP (Achyuthan and Greenberg 1987, Zhang *et al.* 1998). Several ECM proteins such as collagens I, III, IV, fibronectin and dermatane sulphate proteoglycans can act as substrates for the formation of this highly stable ϵ (γ glutamyl) lysine crosslink (Aeschlimann and Thomazy 2000, Fisher *et al.* 2009, Verderio *et al.* 2009). For this reason, TG2 intermolecular crosslinking of ECM proteins leads to resistance to degradation by MMPs and subsequent ECM accumulation (Fisher *et al.* 2009).

Extensive studies have established that TG2 and its crosslink product play an important role in the development of kidney disease. In the rat 5/6th subtotalnephrectomy model of renal scarring, Johnson *et al.* demonstrated that increased matrix expansion and fibrosis was linked to elevated levels of TG2 and ϵ (γ glutamyl) lysine (Johnson *et al.* 1997). In addition, transglutaminase inhibition proved to reduce the development of glomerulosclerosis and tubulointerstitial fibrosis by decreasing the depositing of collagens I and III indicating the importance of TG2 in the renal scarring process (Johnson *et al.* 2007).

In the streptozotocin induced model of diabetic nephropathy, elevated levels of TG2 and its crosslink product were found in the peritubular interstitial space resulting in increased ECM deposition (Skill *et al.* 2001). In the same model, treatment with a TG inhibitor was associated with decreased levels of ϵ (γ -glutamyl) lysine, hydroxyproline and fibronectin with consequent reduction on ECM accumulation (Skill *et al.* 2004). In a further study using a different TG inhibitor it was shown a reduction of myofibroblasts, collagens I, III and IV, as well as decreased ECM deposition and improvement of kidney function (Huang *et al.* 2009).

Numerous others publications have also demonstrated the role of TG2 as one of the mediators of scarring and fibrosis in human renal disease. In human Diabetic Nephropathy, El Nahas *et*

al showed increased levels of TG2 and ϵ (γ -glutamyl) lysine in renal biopsies (El Nahas *et al.* 2004). In CKD patients, a strong correlation between tissue levels of TG2 and its crosslink product was associated with progressive renal scarring suggesting a role in the accumulation of renal matrix (Johnson *et al.* 2003).

There is clearly a strong relationship between fibrosis progression in the kidney and kidney TG2 levels, but to date no research has investigated if these changes in renal ϵ (γ glutamyl) lysine and TG2 are reflected in the urine. If this was possible, then this could be highly beneficial as it may provide a non-invasive biomarker of either the degree of fibrosis in the kidney or the rate at which the fibrotic program may be running. We have therefore hypothesised that TG2 and ϵ (γ -glutamyl) lysine crosslink are found in the urine and could be used as specific and non-invasive diagnostic markers of kidney fibrosis.

To test this hypothesis, this chapter aims to:

1. Determine TG2 and ϵ -(γ -glutamyl) lysine levels in urines obtained from 3 different animal models of CKD (SNx, DN and CAN model)
2. Relate these to the development of disease in these models
3. Determine if the changes in TG2 and ϵ -(γ -glutamyl) lysine have value as biomarkers of CKD progression that may be translated into clinical studies.

For this study an in-house Sandwich ELISA was developed to detect TG2 levels in the urine. An anti TG2 goat polyclonal was used as capture Antibody and anti TG2 monoclonal CUB7402 (both from AbCam, UK) as the detection antibody. For the urine excretion of ϵ (γ -glutamyl)-lysine a technique was developed to measure this in urine protein by cation-exchange HPLC using an amino acid analyser (Biochrom 30, Biochrom, UK).

4.2. Transglutaminase type 2 measurement in urine from 5/6th subtotal nephrectomised rats

4.2.1. Experimental animals

For this study archival material was used from a previous rat SNX study using TG inhibitors (Johnson *et al.* 2007). In brief, a total of 33 rats were subjected to SNx including 20 rats which were treated with 2 different irreversible pan TG inhibitors (NTU 281 and NTU 283). Sham operated rats (SNc, n = 19) were used as controls. Groups of rats were sacrificed at 7 (n=3-4), 28 (n=3-4) and 84 (n=3-11) days post SNx. Blood and urine samples were collected at all termination time points as well as recording of blood pressure. Renal function was assessed by analysing these samples for total proteinuria, serum creatinine and creatinine clearance (table 10.1 and figure 10.1 in Appendix). Kidney tissue was retrieved upon sacrifice & processed for histology and ECM protein immunohistochemistry

Quantification of Masson's Trichrome staining

For estimation of kidney scarring, the amount of fibrotic tissue and the cellular content were assessed by Masson's Trichrome as described in methods section 3.1.5.5.2. Degree of glomerulosclerosis was accomplished by Multiphase image analysis (figure 4.1).

By 7 days after surgery, few changes were noticed in the tubulointerstitium and glomeruli of SNx kidney samples (figure 4.1-B). Glomerulosclerosis and dilation in the tubules was observed at 1 month (figure 4.1-C). By day 84, there was clear ECM deposition associated with tubular atrophy and flattening of the tubular epithelial cells. At this time point, all SNx animals had developed significant glomerulosclerosis and advanced tubulointerstitial scarring (figure 4.1-D).

Figure 4.1: Representative Masson's Trichrome stained sections of the SNx model

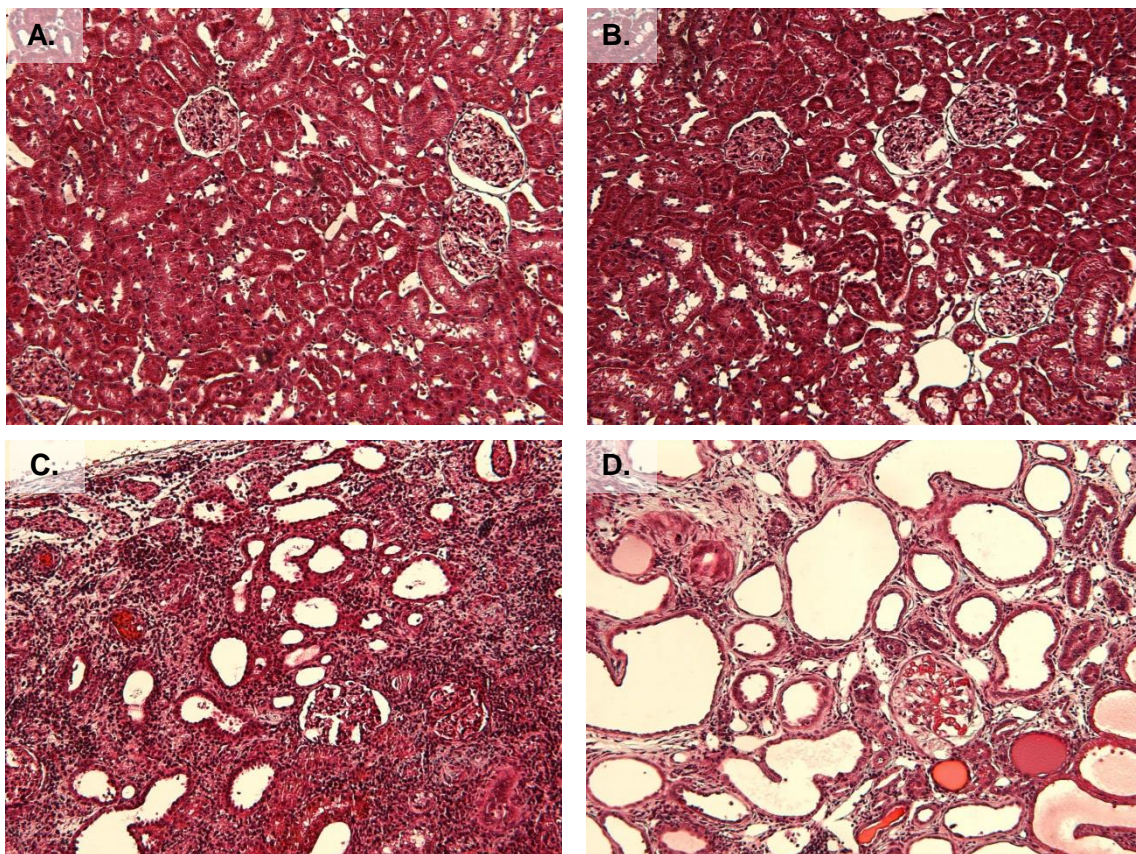


Figure 4.1: Multiphase image analysis of Masson's Trichrome stained SNx kidneys: A – Control. B – 1 week post SNx C – 1 month post SNx. D – 3 months post SNx (200X magnification).

4.2.2. Measurement of Urine Transglutaminase type 2 using enzyme-linked immunosorbent assay (ELISA)

To quantify the amount of TG2 present in urine, an in-house sandwich enzyme-linked immunosorbent assay (ELISA) was developed (see methods section 3.5.1 for full details). For this assay, commercially available antibodies were used. A goat Polyclonal anti TG2 antibody was used to capture and CUB7402 (both from AbCam) as a detection antibody. Rat recombinant TG2 was used to generate a standard curve (section 3.5.1). Inter and intra Assay Coefficients of Variability were 1.2% and 3.9% respectively. The limit of detection was 31.25pg/ml.

TG2 protein was readily detectable in rat urines. Urine TG2 concentration was elevated by 83% over control urines in the SNx group at 7 days, though this difference did not achieve statistical significance (figure 4.2-A). By day 28, the urine concentration of TG2 was 9.3 fold higher in the SNx when compared to the time matched control group ($p=0.0004$) and reached

a peak by day 84, where its average concentration ($522 \pm 135\text{ng/ml}$) was 38.5 fold higher ($p=0.0045$, 2 way ANOVA with Bonferroni post test).

Rats that were treated with TG inhibitors showed no difference in mean urine TG2 concentration to control animals at all time points. However, by 28 days post surgery, TG inhibitor treatment saw levels of urine TG2 significantly reduced in both groups compared to SNx ($p=0.0133$ for NTU C7 and $p=0.0436$ for NTU C56). By day 84, NTU C7 treated rats still had significantly lower levels of urine TG2 when compared to SNx ($p=0.0437$), but no statistical significance was found between NTU C56 treated animals and SNx ($p=0.0589$) (figure 4.2-A).

4.2.3. 24 hour urine excretion of TG2 in the SNx Model

To estimate total excretion of TG2 in 24 hours, its urine concentration was multiplied by the total volume of urine voided in 24 hours. Findings were similar to the ones found when expressed as a concentration, with TG2 excretion significantly increasing with disease progression (figure 4.2-B).

Interestingly, due to the high urine output in rats treated with TG inhibitors, there was no significant difference in estimated total TG2 excretion in 24 hours between these two groups and SNx animals at any time point (figure 4.2-B).

4.2.4. Transglutaminase type 2/creatinine ratio in the SNx Model

To address the problem of variability in the urine output, a correction for urine creatinine was applied. After correction, the urine TG2:creatinine ratio was 7.6 fold higher in the SNx compared to the controls as early as 1 week, 42.1 fold higher by 1 month and 130 fold higher at 3 months after surgery ($p<0.05$ at all time points) (figure 4.2-C).

Likewise, NTU C7 and NTU C56 treated animals also had TG2/creatinine measurements greater than controls. However, NTU C56 animals had significant lower levels of TG2/Creatinine than SNx at 28 days ($p=0.0345$). By 84 days after SNx, both groups of animals had a reduced TG2 creatinine ratio with NTU C7 reduced by 83% ($p=0.0340$) and NTU C56 by 81% ($p=0.0376$) (figure 4.2-C).

Figure 4.2: TG2 measurement in urine post SNx

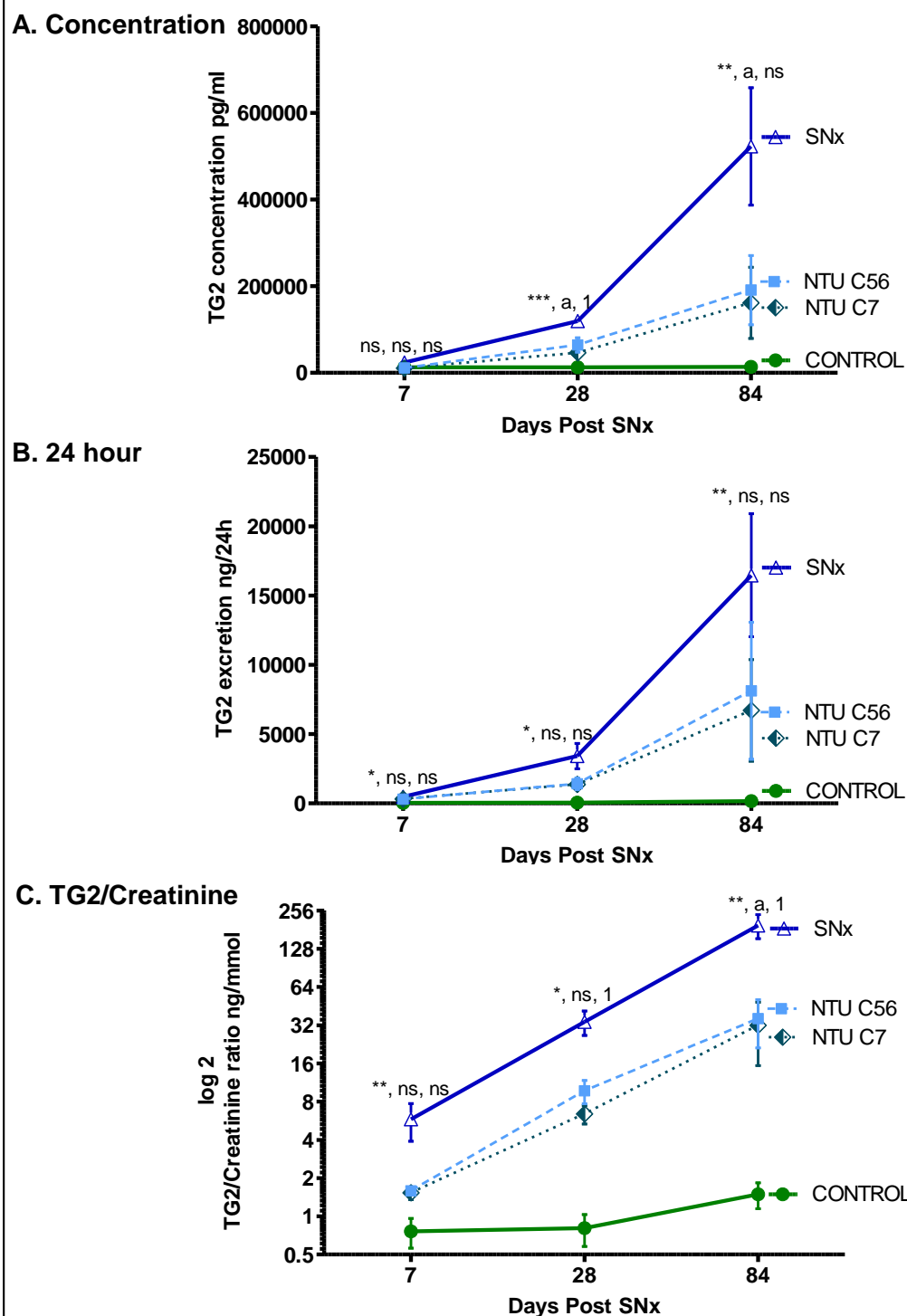


Figure 4.2: TG2 excretion in SNx urine samples was measured by ELISA at 7, 28 and 84 days post Subtotal nephrectomy in animals treated with 2 different TG inhibitors (NTU C56 and NTU C7). **A** - Urine TG2 concentration (mean \pm SEM, pg/ml) in control, SNx and samples treated with two different pan TG inhibitors, **B** - 24 hr urine TG2 excretion \pm SEM in the SNx model of CKD, **C** - TG2 / Creatinine ratio with y axis at log 2 scale. Statistical significance is shown by 2 Way ANOVA with Bonferroni post hoc test: NS= not statistically significant, * $p < 0.05$, ** $p < 0.01$, *** $p < 0.001$ between SNx and normal urine, a = $p < 0.05$, b = $p < 0.01$, c = $p < 0.001$ between NTU C7 and SNx and 1 = $p < 0.05$, 2 = $p < 0.01$, 3 = $p < 0.001$, between NTU C56 and SNx.

4.3. Transglutaminase type 2 measurement in urine from the streptozotocin induced model of diabetic nephropathy

4.3.1. Experimental animals

For this study an archived set of urines was used from a previously published diabetic study in the rat (Huang *et al.* 2009). A total of 25 rats subjected to diabetic nephropathy (DN) induction and 10 sham operated rats (DC) were used (full method is given on section 3.1.3). After 7 days post surgery, hyperglycaemia was induced by infusion of 35 mg/kg streptozotocin (STZ) in 0.1 mol/L Sodium Citrate buffer (pH 4.0) by injection into the tail vein. Two days after surgery, blood glucose was measured and a level above 15mM/L considered diabetic. Glycaemia was controlled between 20 and 25mmol/L by subcutaneous insulin implants to prevent animal wasting. Control rats received 0.3ml of a 0.1mol/L sodium citrate (pH 4.0) solution. Groups of rats were sacrificed at 1 (n=3-4), 4 (n=3-7) and 8 (n=3-5) months post STZ administration and creatinine clearance, total proteinuria, albuminuria and glycaemia were analysed at these time points (table 10.2 and figure 10.2 in Appendix).

4.3.2. Urine Transglutaminase type 2 concentration in the UNx STZ model of DN

Transglutaminase type 2 was measured in diabetic urines using the same in-house sandwich enzyme-linked immunosorbent assay described on section 4.1.2.

Across all time points, the urinary concentration of TG2 on DN samples was significantly higher than controls ($p=0.0006$, $p=0.0224$, $p=0.0335$, figure 4.3-A). Urine TG2 levels went up from $192 \pm 28\text{ng/ml}$ at 1 month to $450 \pm 142\text{ng/ml}$ at 4 months, reaching an average of $470 \pm 144\text{ng/ml}$ by 8 months. This represented a respective 18, 32.11 and 38.76 fold increase when compared to controls. Concentration in sham-operated rats ranged between 7 and 16ng/ml during the study.

4.3.3. 24 h urine excretion of TG2 in the UNx STZ model of DN

Total TG2 excretion in 24 hours was determined by adjustment to total volume of urine produced in 24 hours. At 1 month, total TG2 excretion had a massive 151 fold increase when compared to controls ($p=0.0328$). This impressive increment was maintained through the study time course, going up to 532 fold at 4 months ($p=0.0099$) and 551 fold by 8 months ($p=0.0179$) (figure 4.3-B).

Figure 4.3: TG2 measurement in urine from the UNx STZ model of DN

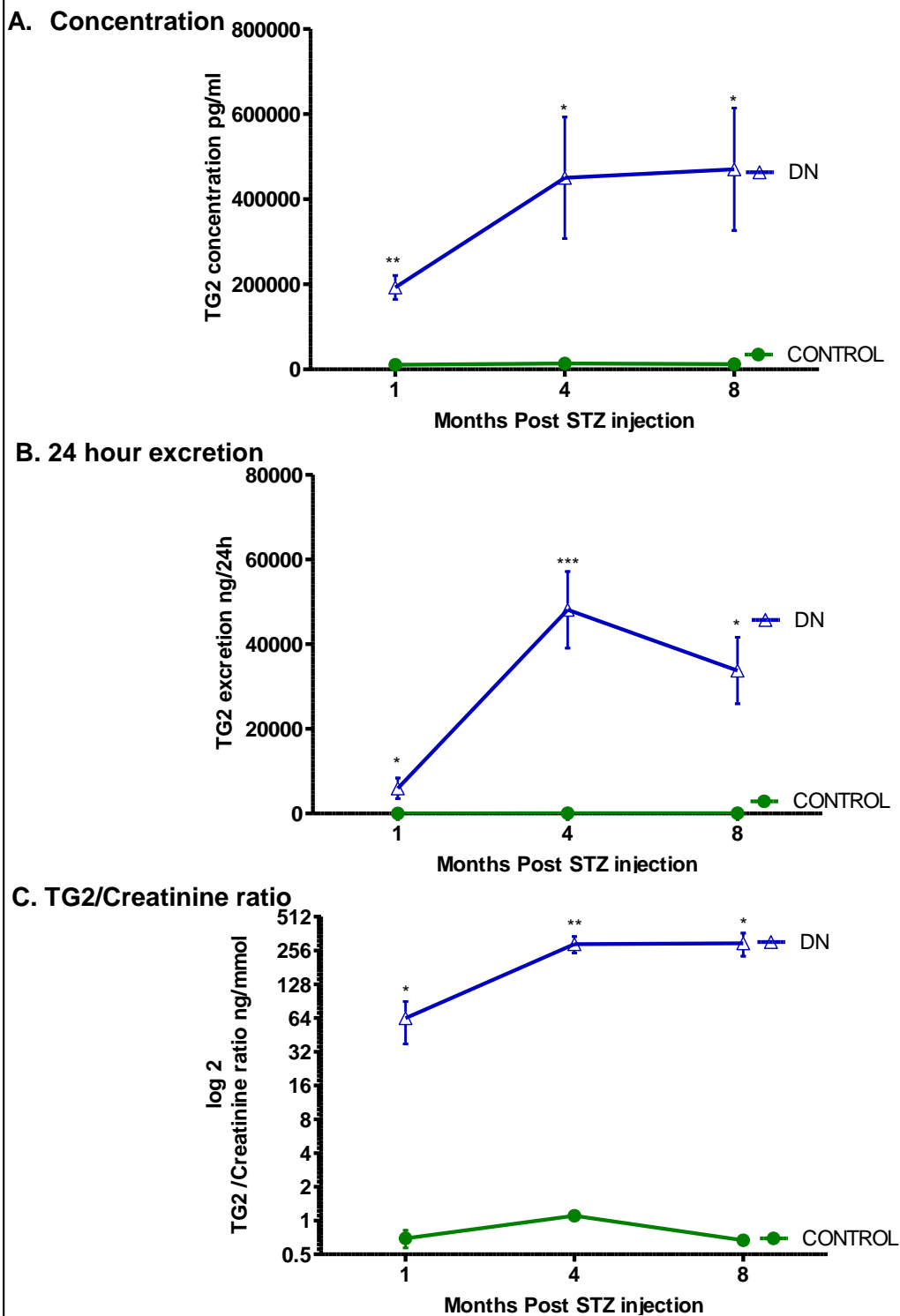


Figure 4.3: TG2 excretion in DN urine samples at 1, 4 and 8 months post UNx STZ induction shown as **A** - : Urine TG2 concentration in the UNx STZ model of DN, data represents mean TG2 in pg/ml \pm SEM. **B** - 24 hr urine TG2 excretion \pm SEM. **C** - TG2 / Creatinine ratio with y axis plotted as a log 2 scale. Statistical significance is shown by 2 Way ANOVA with Bonferroni post test: NS= not statistically significant * $p < 0.05$, ** $p < 0.01$, *** $p < 0.001$ between experimental groups and normal urine.

4.3.4. Transglutaminase type 2/creatinine ratio in the UNx STZ model of DN

Urinary TG2 concentration was adjusted by creatinine as described on section 4.1.5.

After correction, control samples displayed a TG2/creatinine ratio ranging from 0.32 to 1.20ng/mmol over the full length of the study. The TG2/Creatinine ratio steadily increased in DN animals throughout the time course showing 91.75, 265 and 443 fold increase at 1, 4 and 8 months respectively ($p=0.0345$, $p=0.0054$, $p=0.0181$, 2 way ANOVA with Bonferroni post test) when compared to sham-operated controls (figure 4.3-C).

4.4. Transglutaminase type 2 measurement in urine from the Fisher to Lewis transplant model of Chronic Allograft Nephropathy

4.4.1. Experimental animals

For this model of Chronic Allograft Nephropathy (CAN), male Fisher (F334, RT1v1) and male Lewis (Lew, RT1) rats, weighing 200-300g were used (Shrestha *et al.* 2014). Donor kidneys obtained from Lewis (L-L isograft, $n=12$) or Fisher (F-L allograft, $n=12$) rats were transplanted into Lewis rats. Twelve rats did not survive the transplant. A full description of the procedure is given in section 3.1.4. The surviving isografts ($n=5$) and allografts ($n=7$) were longitudinally studied at 2, 8, 17, 24, 33 and 52 weeks post transplantation. Biochemical measurements (serum and urine creatinine, creatinine clearance, proteinuria) were analysed at all these time points (table 10.3 in Appendix) and histopathology at the time of termination at 52 weeks (figure 4.4).

Quantification of Masson's Trichrome staining

Representative examples from sections of light microscopy are shown in figure 4.4. Renal scarring was estimated at 52 weeks by Masson's Trichrome staining (section 3.1.5.5.2). Terminal kidney tissue from the F-L allograft showed the development of glomerulosclerosis (b), obliterative arteriopathy and tubulointerstitial fibrosis with a marked increase in extracellular matrix protein (d) whereas the L-L isograft showed normal glomeruli with thin GBM (a), intact arterioles within the glomerular capillary and unexpanded mesangium (c).

Figure 4.4: Representative micrographs of the Fisher to Lewis transplant model of CAN at 52 weeks

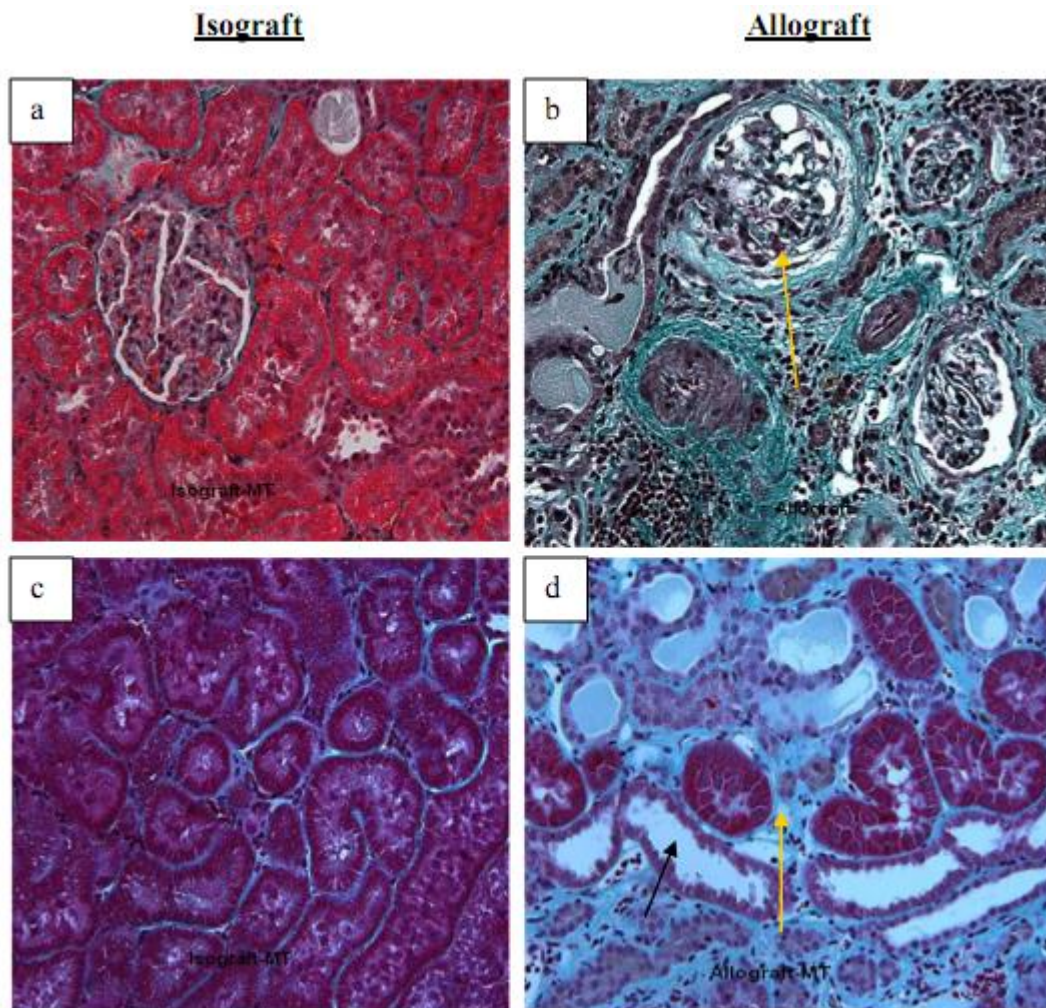


Figure 4.4: Representative photomicrographs of Masson's Trichrome stained kidney tissue. (A) Normal glomeruli and (C) tubulointerstitium from L-L isograft kidney, (B) glomerulosclerosis and (D) tubular atrophy (—→) and interstitial fibrosis (—→) from F-L allograft kidney. From Mr Badri Shrestha

4.4.2. Urine Transglutaminase type 2 concentration in the Fisher to Lewis transplant model of CAN

Urine TG2 excretion was markedly increased in the Fisher-to-Lewis transplanted animals from early after surgery (figure 4.5-A). At 2 weeks, L-L isografts had an average urine TG2 concentration of $12 \pm 1\text{ng/ml}$ compared to $22 \pm 1.9\text{ng/ml}$ of F-L allografts ($p=0.0043$).

By 17 weeks, F-L allografts had over a 5 fold increase in urine TG2 concentration in comparison to L-L allografts ($p=0.0381$). Maximum levels of TG2 in the urine were observed

6 months after transplantation (5.2 fold increase, $p=0.0095$). At termination, F-L allografts had an average urinary TG2 concentration of $45 \pm 8\text{ng/ml}$ whilst L-L isografts kept their baseline concentration at $11 \pm 0.3\text{ng/ml}$ ($p=0.0189$).

4.4.3. 24 h urine excretion of TG2 in the Fisher to Lewis transplant model of CAN

Twenty-four hour TG2 excretion was 119% higher on F-L allografts compared to L-L isografts at 2 weeks after the transplantation ($p=0.0198$, figure 4.5-B). Levels peaked by 6 months, with a total TG2 excretion 6.5 fold higher on allograft transplanted rats ($p=0.0366$) and were kept elevated until the end of the study (11.8 fold, $p=0.0231$).

4.4.4. Transglutaminase type 2/creatinine ratio in the Fisher to Lewis transplant model of CAN

The TG2/creatinine ratio was determined as reported in section 4.1.5.

Rats that received an allotransplantation had a significantly higher TG2/creatinine ratio through the whole study (figure 4.5-C). Average TG2/creatinine ratio were respectively $7.9 \pm 1.7\text{ng/mmol}$, $10.9 \pm 3.5\text{ng/mmol}$, $10.1 \pm 0.2\text{ng/mmol}$, $16.9 \pm 4.5\text{ng/mmol}$, $13.8 \pm 4.9\text{ng/mmol}$ and $15.1 \pm 4.5\text{ng/mmol}$ at 2, 8, 17, 24, 33 and 52 weeks after transplant ($p<0.05$ at all time points). L-L isografts presented a TG2/creatinine ratio varying between $2.7 \pm 0.4\text{ng/mmol}$ in the beginning of the study and $1.1 \pm 0.1\text{ng/nmol}$ at termination.

Figure 4.5: TG2 measurement in urine from the Fisher to Lewis model of CAN

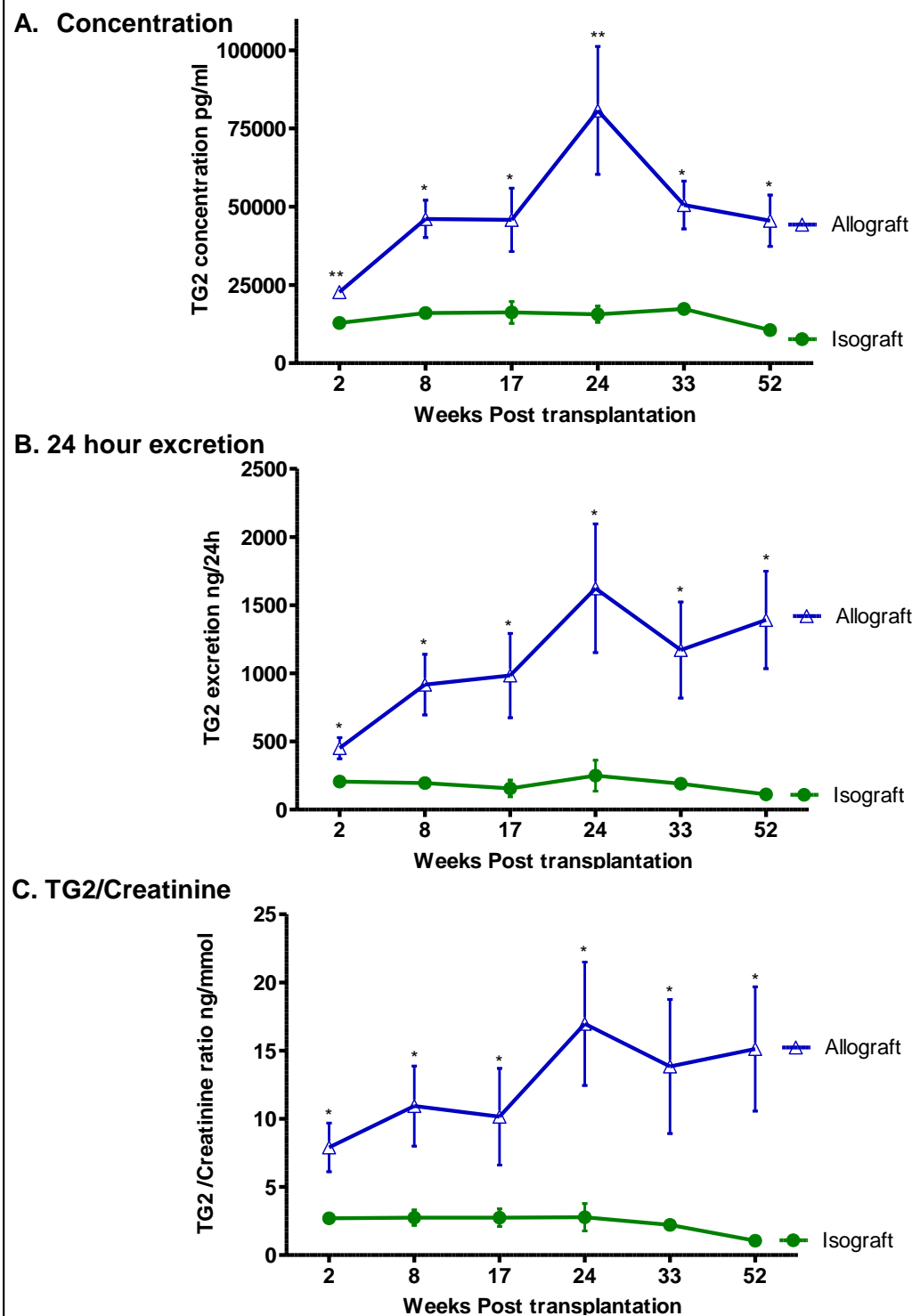


Figure 4.5: A - Urine TG2 concentration in the Fisher to Lewis transplant model of CAN over 12 months quantified by an in-house sandwich enzyme-linked immunosorbent assay. Data represents mean TG2 in pg/ml \pm SEM. **B** - 24 hr urine TG2 excretion \pm SEM, **C** - Average TG2 / Creatinine ratio in F-L allografts and L-L isografts. Statistical significance was shown by 2 Way ANOVA with Bonferroni post hoc test: NS= not statistically significant, * p<0.05, **p<0.01, ***p<0.001 between F -L allografts and L-L isografts.

4.5. Correlation between urine Transglutaminase type 2 and clinical markers of renal function and damage

4.5.1. 24h proteinuria

In the 5/6th subtotalnephrectomy model of renal scarring, correlation between 24 hour urine TG2 excretion and 24 hour proteinuria showed a strong positive association (Pearson's $r=0.8227$, 95% Confidence interval (CI): 0.6335 to 0.9191, $p<0.0001$) (figure 4.6-A).

TG2 excretion was also correlated with proteinuria in the UNx STZ model of DN ($n=25$, Pearson's $r = 0.5967$, 95% CI: 0.2637 to 0.8027 $p=0.0016$, figure 4.6-B).

A similar correlation was also found in the Fisher to Lewis model of CAN ($n=56$, Pearson's $r = 0.5739$, 95% CI: 0.3662 to 0.7271, $p<0.0001$, figure 4.6-C).

4.5.2. Creatinine clearance (CrCl)

To determine whether the urine excretion of TG2 was associated with changes in kidney function, a correlation of TG2 urine concentration with creatinine clearance was performed. In the SNx model, there was a negative association (Pearson's $r=-0.4533$, 95% CI: -0.7243 to -0.0609 $p=0.0261$) with CrCl, indicating that the higher the TG2 excretion the lower the creatinine clearance (figure 4.6-D). The same inverse correlation was found on CAN samples Pearson's $r = -0.4128$, 95% CI: -0.6080 to -0.1705, $p=0.0014$, figure 4.6-F).

Surprisingly, there was a positive correlation between TG2 excretion and creatinine clearance in diabetic samples (Pearson's $r=0.4829$, 95% CI: 0.1083 to 0.7374. $p=0.0145$, figure 4.6-E).

4.5.3. Renal scarring levels

SNx samples ($n=18$) were used to quantify kidney scarring. The presence of interstitial fibrosis and glomerulosclerosis was assessed by Masson's Trichrome staining as described in section 3.1.5.5.2. A positive association between scarring and elevated levels of 24 hour TG2 in SNx rat urines was seen (Pearson's $r = 0.6573$, 95% CI: 0.2746 to 0.8602, $p=0.0030$, figure 4.7-A).

DN samples ($n=25$) did not present a correlation between 24 hour urine TG2 and renal scarring (Pearson's $r = 0.1060$, 95% CI: -0.3018 to 0.4811, $p=0.6139$, figure 4.7-B).

Figure 4.6: Correlation plots of urine TG2 excretion with markers of kidney function and damage in experimental models of renal scarring

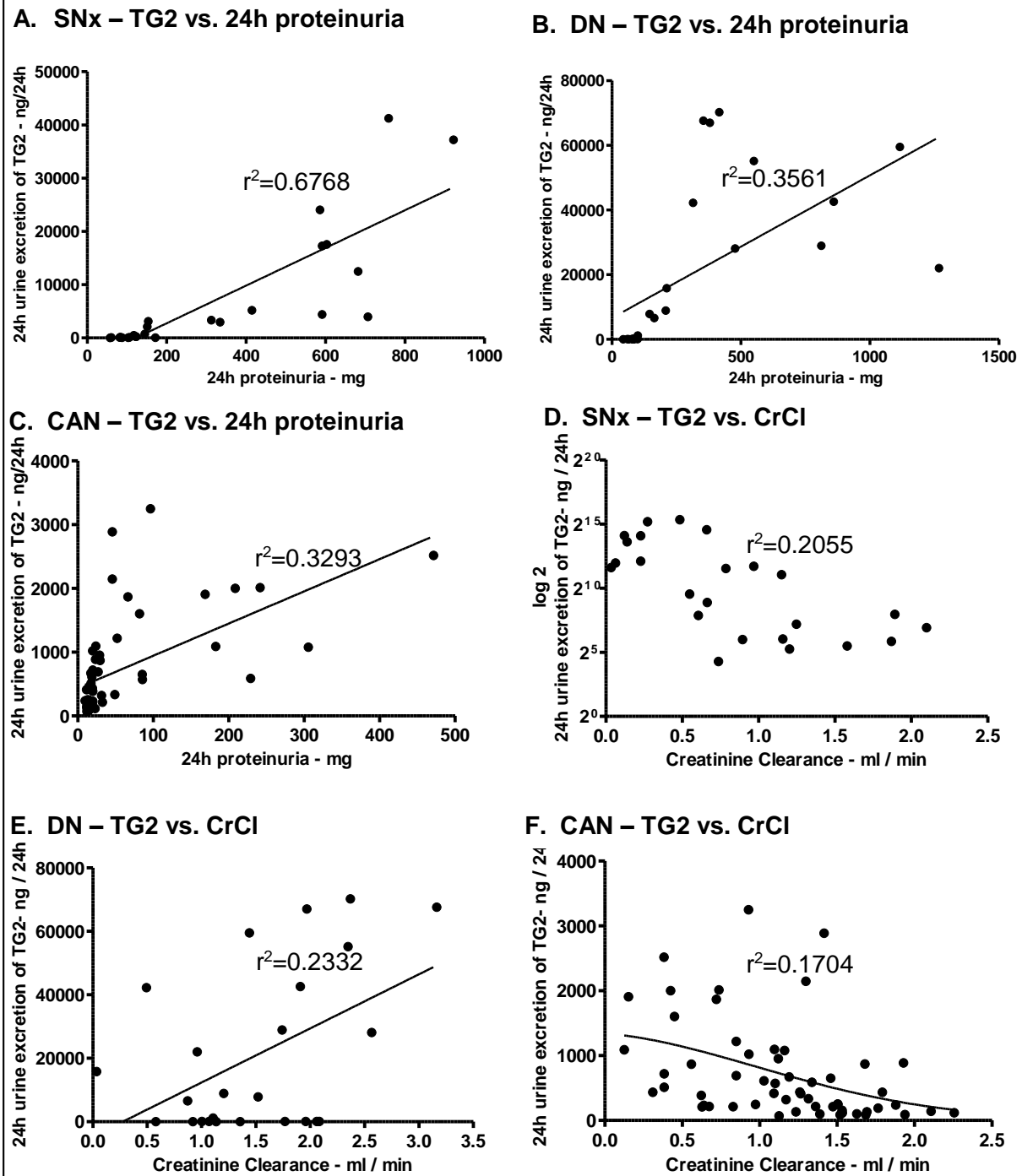


Figure 4.6: Pearson's correlations were performed for 24 hour urine TG2 excretion vs. 24 hour proteinuria in SNx (A), DN (B) and CAN (C) and then for 24 hour urine TG2 excretion vs. creatinine clearance in SNx (D), DN (E) and CAN (F). Statistical significance was shown by 2 Way ANOVA with Bonferroni post hoc test: NS= non statistical significant, * $p<0.05$, ** $p<0.01$, *** $p<0.001$. $n=25$ in SNx and DN and $n=56$ in CAN.

4.6. ϵ (γ -glutamyl) lysine analysis in urine by cation exchange chromatography

4.6.1. Optimisation of chromatography

To determine clean fractionation of peaks into individual amino acids by the AAA and to determine retention time of each amino acid and di amino acid, 20ul of a standard solution was loaded using a partial fill loop onto the Biochrom 30 AAA. Fractionation was controlled using the 96361 LiHP program (figure 4.8).

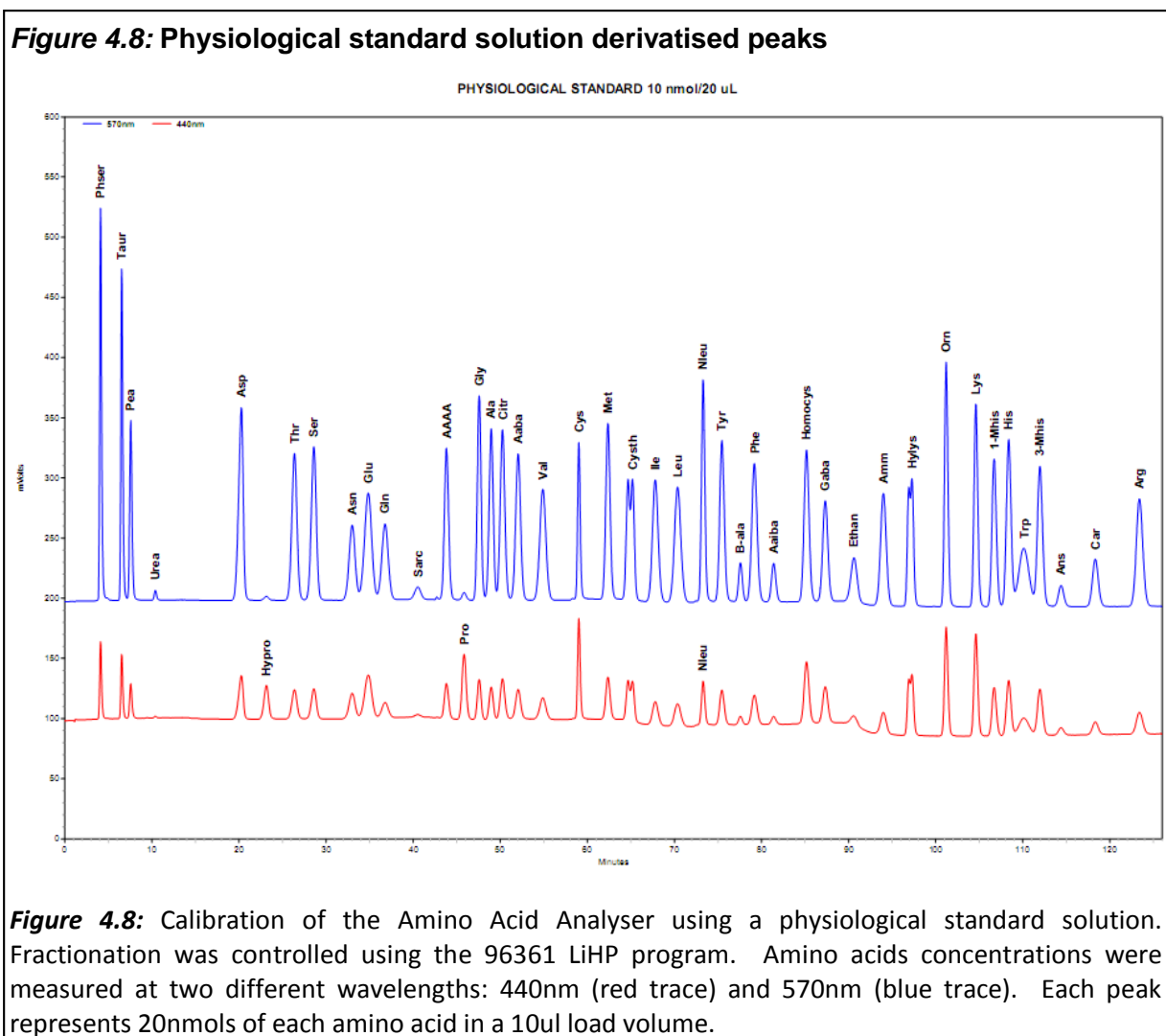


Figure 4.8: Calibration of the Amino Acid Analyser using a physiological standard solution. Fractionation was controlled using the 96361 LiHP program. Amino acids concentrations were measured at two different wavelengths: 440nm (red trace) and 570nm (blue trace). Each peak represents 20nmols of each amino acid in a 10ul load volume.

To establish the correct retention time for ϵ (γ Glutamyl) Lysine peak, a 20nmols/10 ul solution of ϵ (γ Glutamyl) Lysine was prepared using a commercial lyophilised crosslink (H-Glu (H-Lys-OH)-OH, 250mg – MW=275.31, Bachem AG, Switzerland). 20ul was loaded using a partial fill loop onto the Biochrom 30 AAA. A retention time of approximately 77 minutes was seen (figure 4.9).

Figure 4.9: Determination of ϵ (γ glutamyl) lysine retention time

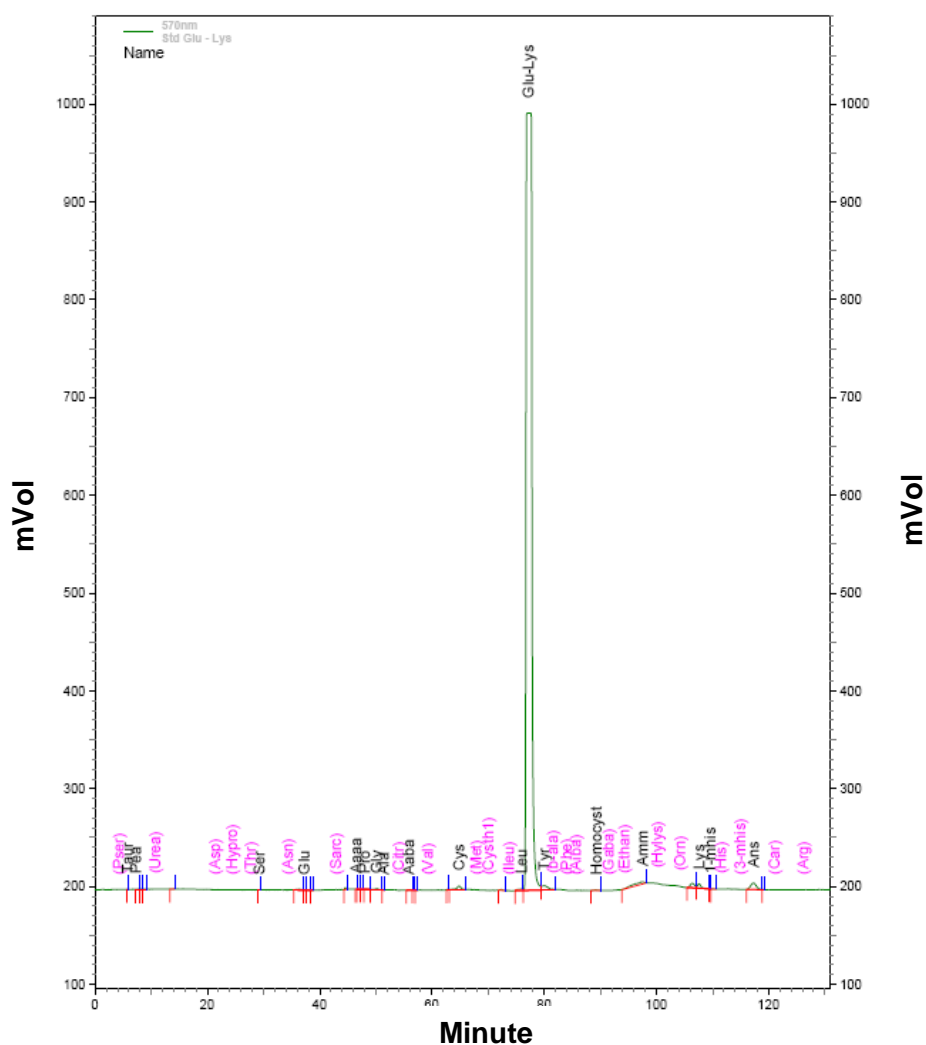


Figure 4.9: ϵ (γ glutamyl) Lysine solution (20nmols/10ul) was loaded onto the AAA and its retention time determined at around 77 minutes, trace at 570nm.

The physiological standard solution was then spiked with 10nmols / 10ul ϵ (γ Glutamyl) Lysine solution to check the ϵ (γ Glutamyl) Lysine peak could be distinguished from other amino acids. 20ul was loaded using a partial fill loop onto the Biochrom 30 AAA, at both 440nm and 570nm (figure 4.10). Adjustments to programming were done by increasing the loading time of buffer 3 in 2 minutes and also by raising the temperature settings in 1⁰C. ϵ (γ Glutamyl) Lysine clearly eluted as an individual peak between Leucine and tyrosine using Biochrom standard 96361 LiHP program.

Figure 4.10: Clean fractionation of $\epsilon(\gamma\text{-glutamyl})$ lysine di peptide from other amino acids on a Biochrom 30 analyser

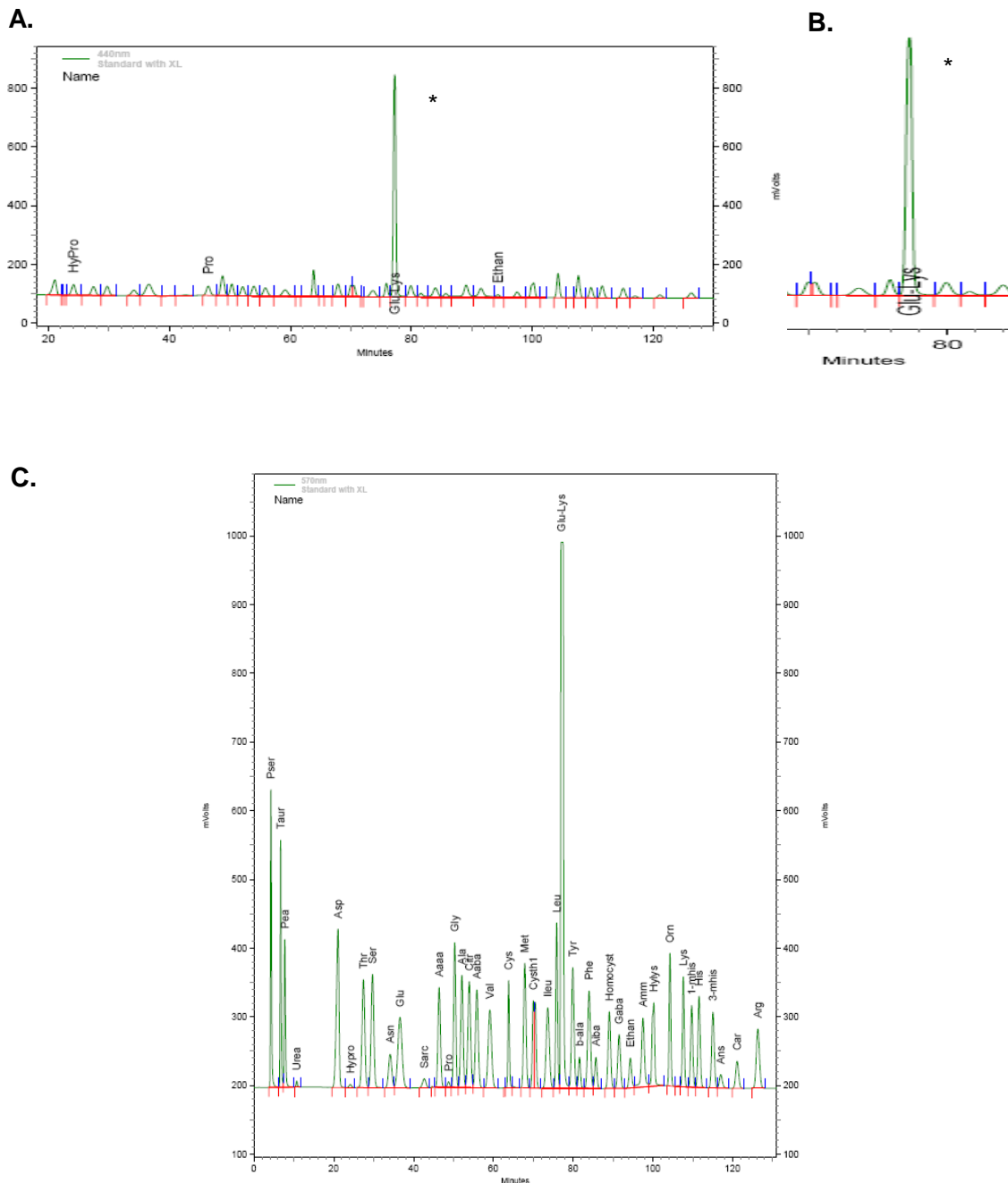


Figure 4.10: Physiological standard solution was spiked with 10nmols/10ul $\epsilon(\gamma\text{ Glutamyl})$ Lysine and fractionated using the Biochrom standard 96361 LiHP program **(A)** The $\epsilon(\gamma\text{ Glutamyl})$ Lysine peak eluting at 77 minutes on the 440nm trace. The same peak at a higher resolution **(B)** - The same $\epsilon(\gamma\text{ Glutamyl})$ Lysine peak produced a bigger peak at 570nm **(C)**.

4.6.2. Validation of ϵ (γ Glutamyl) Lysine measurement in urines

To confirm and validate the identification and measurement of ϵ (γ -glutamyl) lysine in urine, 2 proteolytic digested urine samples were spiked with 5nmols / 10ul of commercial ϵ (γ -glutamyl) lysine and 20ul was loaded onto the Biochrom 30 AAA and fractionated with the 96361 LiHP control program (figure 4.9). Overlay of urine spiked with ϵ (γ -glutamyl) lysine (green) with unspiked urine (blue) shows that the spiked ϵ (γ -glutamyl) lysine peak detected in figure 4.11 elutes at the same time point as the ϵ (γ -glutamyl) lysine in unspiked urine as the same peak is amplified. This confirms successful detection of ϵ (γ -glutamyl) lysine in urine.

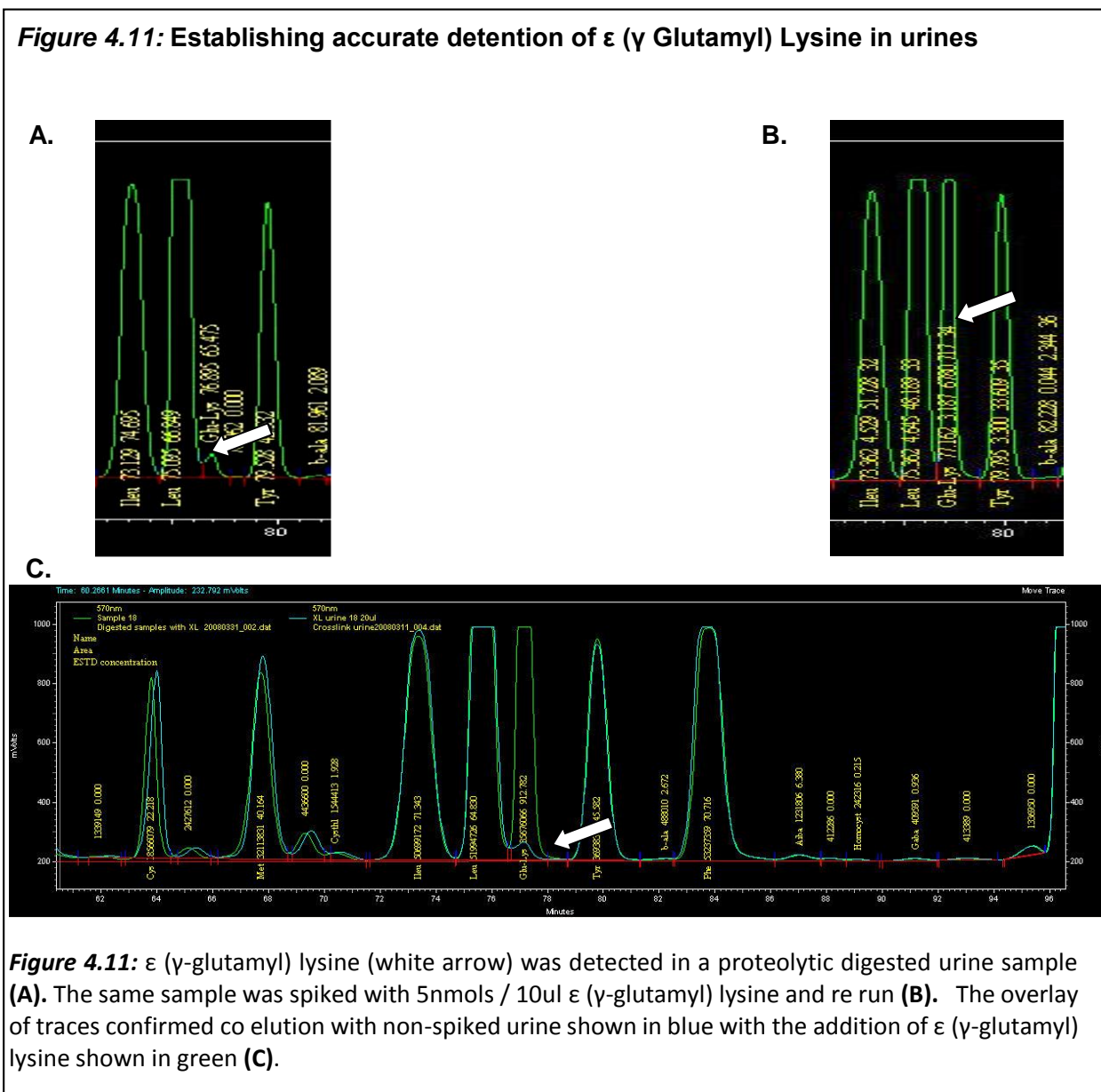


Figure 4.11: ϵ (γ -glutamyl) lysine (white arrow) was detected in a proteolytic digested urine sample (A). The same sample was spiked with 5nmols / 10ul ϵ (γ -glutamyl) lysine and re run (B). The overlay of traces confirmed co elution with non-spiked urine shown in blue with the addition of ϵ (γ -glutamyl) lysine shown in green (C).

4.6.3. Determination of ϵ (γ glutamyl) lysine detection, sensitivity and range on a Biochrom 30 amino acid analyser

Following optimisation of ϵ (γ glutamyl) lysine detection, a multilevel calibration of the AAA system was performed by measuring ϵ (γ glutamyl) lysine levels in physiological standard solutions spiked with 0.25, 0.5, 1, 2, 5, 10 and 15nmols/20ul solution of this dipeptide (figures 4.12 and 4.13).

Multiple samples containing known concentrations of ϵ (γ glutamyl) lysine were used to produce a standard curve (figure 4.12). Area under the curve (plotted on Y axis) was calculated and used to estimate concentrations (X axis). The curve started to saturate at 10nmols/20ul solution, therefore this was chosen as the upper concentration for ϵ (γ glutamyl) lysine detection. Minimum detection level was 500 mols/20ul.

Figure 4.12: ϵ (γ glutamyl) lysine standard curve

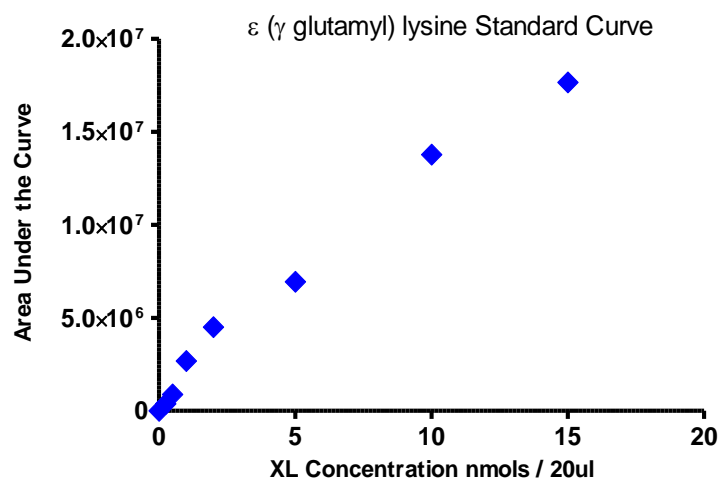


Figure 4.12: To determine the ϵ (γ glutamyl) lysine detection range on the Biochrom 30, an ϵ (γ glutamyl) lysine standard curve was generated by spiking buffer with commercial H-Glu(H-Lys-OH)-OH from Bachem at 0.25, 0.5, 1, 2, 5, 10 and 15nmols/20ul and then determining the AUC from the traces shown in Figure 4.16.

Figure 4.13: ϵ (γ glutamyl) lysine multilevel calibration

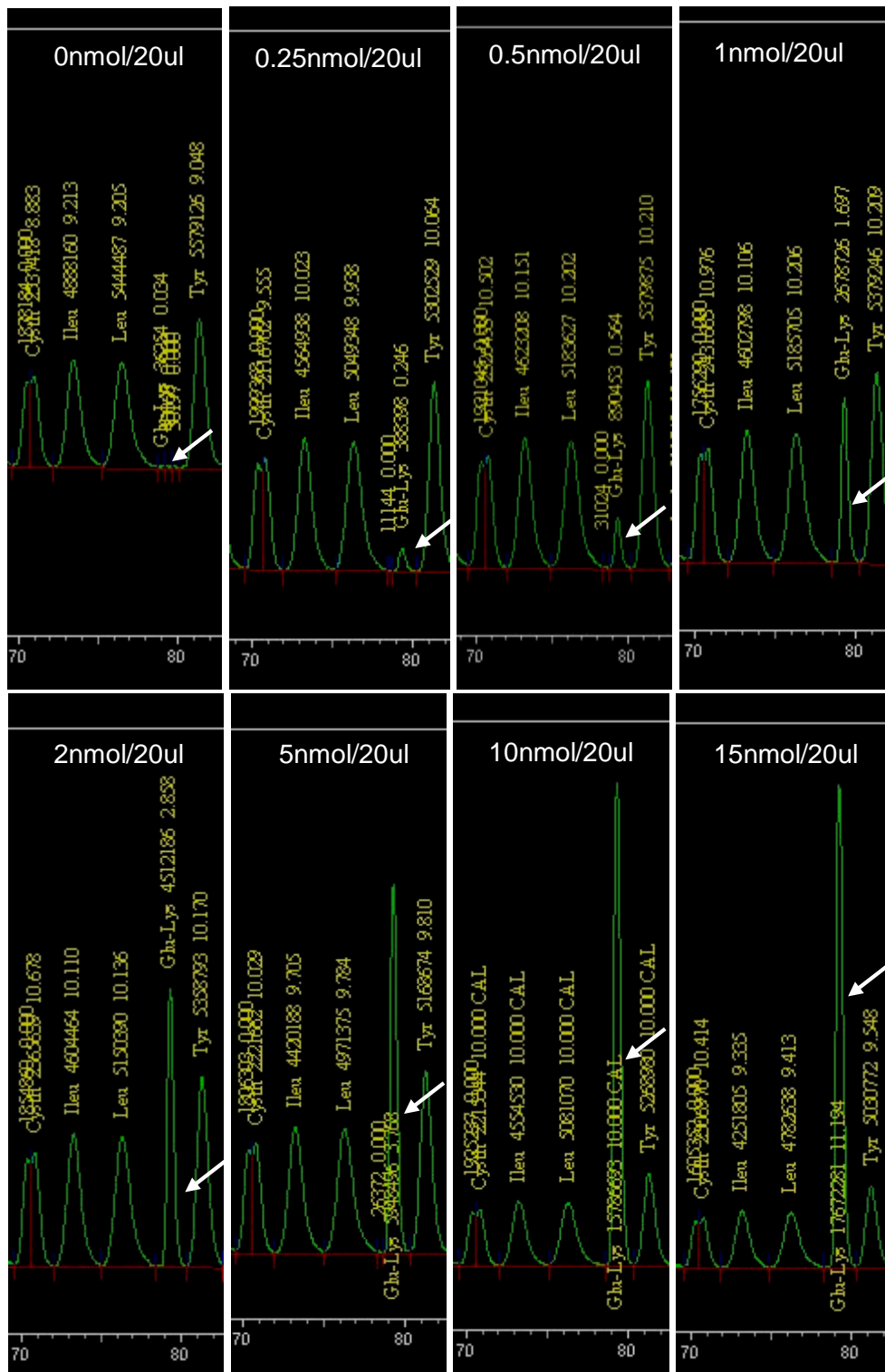


Figure 4.13: The range of ϵ (γ glutamyl) lysine quantitative detection was determined by using a physiological standard solution spiked with 0.25, 0.5, 1, 2, 5, 10 and 15nmols/20ul of ϵ (γ glutamyl) lysine. ϵ (γ Glutamyl) Lysine peaks eluted at 77 minutes on 570nm.

4.7. ϵ (γ glutamyl) lysine measurement in urine from 5/6th subtotal nephrectomised rats

4.7.1. ϵ (γ glutamyl) lysine levels per mg of urine protein

Having established and validated ϵ (γ -glutamyl) lysine measurement in urine, this was then applied to the same urine samples from an archived SNx model of CKD used in section 4.1.1.

Successful fractionation of amino acids from proteins collected from both normal and SNx urine was achieved. The ϵ (γ -glutamyl) lysine peak (77 mins) was visibly larger in late SNx urines compared to controls (figures 4.14 and 4.15) being clearly discernible by the software in samples 1 month post SNx and beyond.

Average concentration of ϵ γ -glutamyl) lysine in normal urine was stable at 1.63 ± 0.17 nmol/mg protein. Post SNx urine levels were unchanged at 1 week averaging 1.74 ± 0.44 nmol/mg protein ($p=0.7232$), but increased over 84 days reaching 3.69 ± 0.60 nmol/mg ($p=0.005$). The TG inhibitor treated urines had lower levels of urine XL as would have been predicted from the use of TG inhibitors, reaching only 2.52 ± 0.23 nmol/mg protein and 2.37 ± 0.41 nmol/mg protein levels for C7 and C56 respectively (figure 4.16-A). Despite this reduction, there was no statistical difference between SNx and SNx animals treated with TG inhibitor at all time points.

Figure 4.14: Overall amino acid excretion in the SNx Model

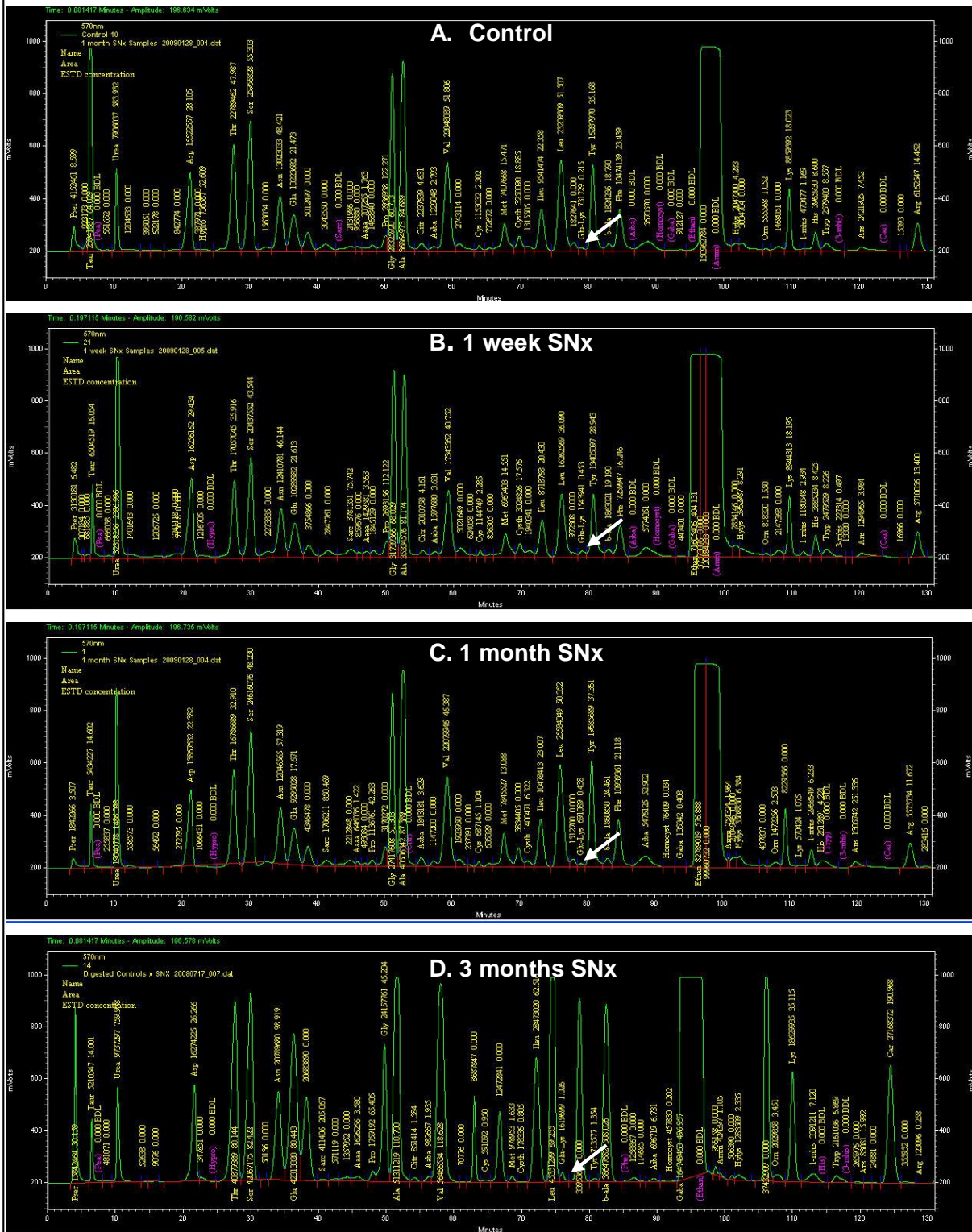


Figure 4.14: SNx urines were exhaustively digested as in section 3.6, freeze dried and reconstituted in 200ul of lithium loading buffer. 20ul was then loaded onto a Biochrom 30, fractionating using program 96361 LiHP. Full amino acids traces with Glu-Lys peak (white arrow) situated between Leucine and Tyrosine peaks in Control samples (A), 1 week (B), 1 month (C) and 3 months (D) post SNx.

Figure 4.15: Urine ϵ (γ Glutamyl) Lysine excretion in the SNx Model

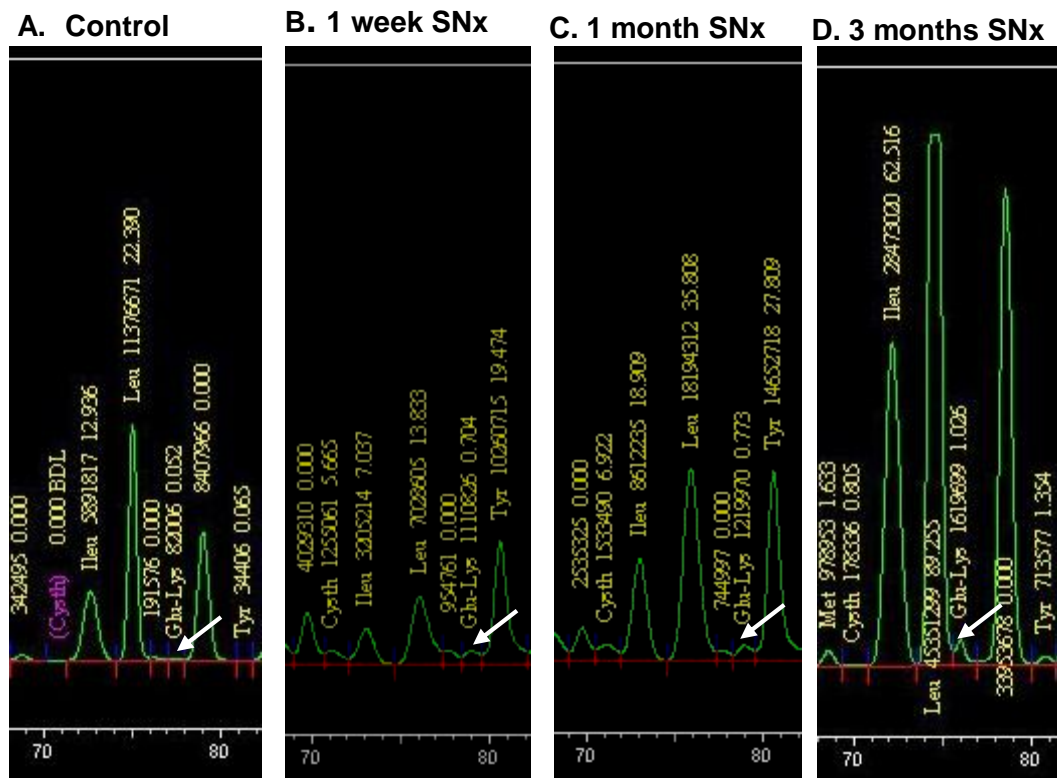


Figure 4.15: ϵ (γ Glutamyl) Lysine was measured in SNx urines by precipitating 2mg of protein from a 24 hour urine collection, exhaustively digesting this as in section 3.6, freeze drying and reconstituting in 200ul of lithium loading buffer. 20ul was then loaded onto a Biochrom 30, fractionating using program 96361 LiHP and the peak concentration calculated by the area under the curve. Control samples (SNc) showed a barely discernible Glu-Lys peak (white arrow) situated between Leucine and Tyrosine peaks (A). Glu-Lys peak at 1 week (B), 1 month (C) and 3 months (D) post SNx.

4.7.2. 24 hour urine excretion of ϵ (γ -glutamyl) lysine in the SNx Model

Twenty four hour ϵ (γ glutamyl) lysine excretion was estimated by adjustment of concentration with 24 hour urine volume to generate 24 hour ϵ (γ glutamyl) lysine measurements.

Urine excretion of ϵ (γ glutamyl) lysine in 24 hours was 2 fold higher in the SNx compared to the controls as early as 1 week, 2.4 fold by 1 month and 7 fold higher at 3 months, however this increase achieved statistical significance only at the latest time point ($p < 0.001$) (figure 4.16-B). Both groups of TG inhibitor treated animals did not show statistical difference in 24 hours ϵ (γ glutamyl) lysine measurements to either controls or SNx by 7 and 28 days, but were significantly reduced when compared to untreated SNx by 84 days post SNx ($p = 0.0053$ for NTU C7 and $p = 0.0031$ for NTU C56).

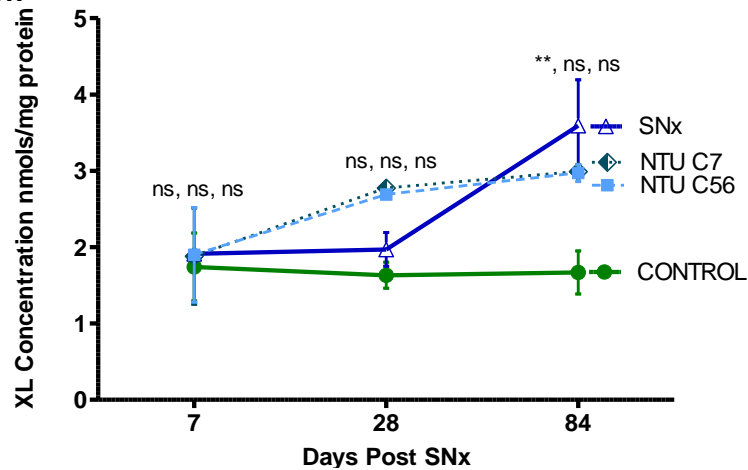
4.7.3. ϵ (γ -glutamyl) lysine/creatinine ratio in the SNx Model

ϵ (γ glutamyl) lysine measurements were corrected by urine creatinine in order to better reflect 24 hour excretion. After correction, urine levels of ϵ (γ glutamyl) lysine were significantly increased at all time points post SNx (figure 4.16-C).

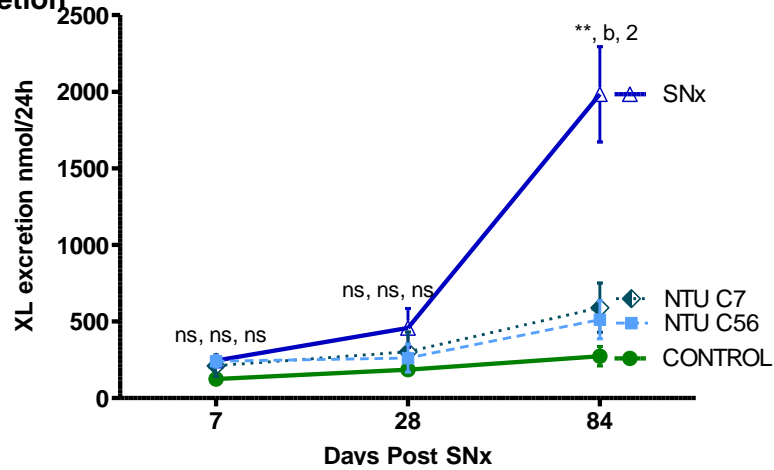
Seven days post SNx, ϵ (γ glutamyl) lysine/Creatinine ratio was significantly increased in the SNx group (0.4718 ± 0.011 mg/ml) compared to controls (0.1078 ± 0.032 mg/ml, $p = 0.0005$) and this increase remained unchanged over the duration of the study with a 4.5 fold increase at 1 month ($p = 0.0002$) and 15.2 at 3 months ($p < 0.0001$). Rats treated with TG inhibitors showed a significant reduction in urinary ϵ (γ glutamyl) lysine excretion when compared to SNx rats at all time points following surgery (1 week: NTU C7, $p = 0.0310$, NTU C56, $p = 0.0060$, 1 month: NTU C7, $p = 0.0084$, NTU C56, $p = 0.0011$ and 3 months: NTU C7, $p < 0.001$, NTU C56, $p = 0.0003$).

Figure 4.16: ϵ (γ glutamyl) lysine measurement in urine post SNx

A. Concentration



B. 24 hour excretion



C. XL/Creatinine

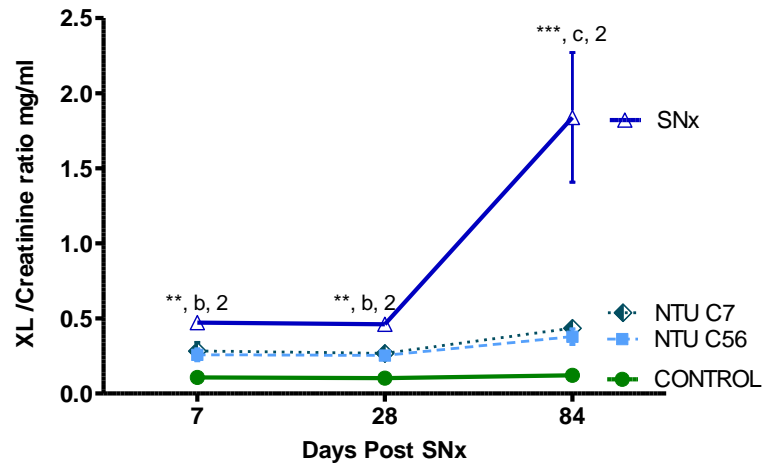


Figure 4.16: ϵ (γ glutamyl) lysine was measured in SNx urine samples at 7, 28 and 84 days post Subtotal nephrectomy as in figure 4.18 and displayed as concentration with mean ϵ (γ Glutamyl) Lysine given per mg urine protein \pm SEM (A). 24 hr urine ϵ (γ Glutamyl) Lysine \pm SEM calculated by adjustment to 24h urine protein and volume (B). The ϵ (γ glutamyl) lysine / Creatinine ratio was subsequently calculated. Statistical significance was calculated by 2 Way ANOVA with a Bonferroni post hoc test. NS= non statistical significant, * $p < 0.05$, ** $p < 0.01$, *** $p < 0.001$ between SNx and normal urine, a = $p < 0.05$, b = $p < 0.01$, c = $p < 0.001$ between NTU C7 and SNx and 1 = $p < 0.05$, 2 = $p < 0.01$, 3 = $p < 0.001$, between NTU C56 and SNx.

4.8. ϵ (γ glutamyl) lysine measurement in urine from the streptozotocin induced model of diabetic nephropathy

4.8.1 ϵ (γ glutamyl) lysine levels per mg protein

After establishing ϵ (γ -glutamyl) lysine measurement in SNx urines, 1, 4 and 8 months DN urines were used to assess ϵ (γ -glutamyl) lysine in the same way (figure 4.17). There was no significant change in ϵ (γ -glutamyl) lysine concentration between normal and disease animals when expressed per mg of urine protein (figure 4.18-A). Sham operated rats had XL levels ranging from 0.66 to 1.33nmol/mg protein. At 1 month, DN rats had an average XL concentration of 0.94 ± 0.16 nmol/mg protein ($n=3$, $p=0.4357$). Interestingly, there was a peak of XL excretion by 4 months ($n=7$, $\bar{x}=3.35 \pm 1.41$ nmol/mg protein). However, in spite of this elevated level, it failed to achieve significance ($p=0.1601$). At 8 months, XL excretion had fallen at 0.82 ± 0.11 nmol/mg protein ($n=5$, $p=0.3631$).

Figure 4.17: Urine ϵ (γ Glutamyl) Lysine excretion in the UNx STZ model of DN

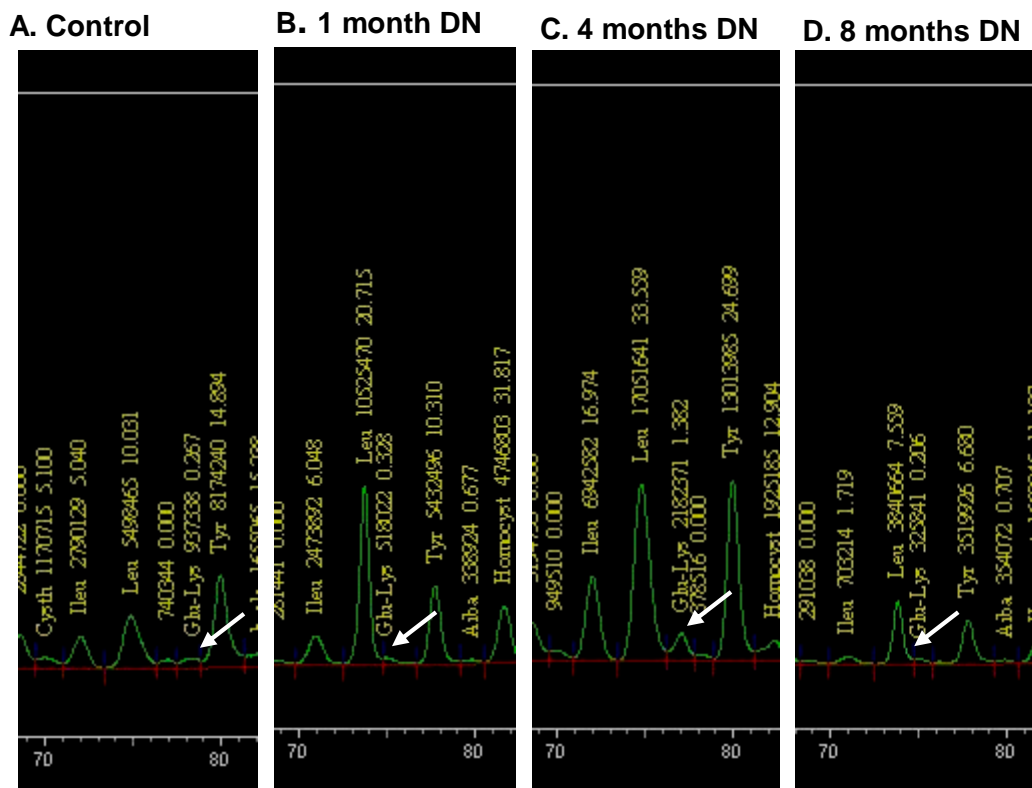


Figure 4.17: ϵ (γ Glutamyl) Lysine was measured in DN urines by precipitating 2mg of protein from a 24 hour urine collection, exhaustively digesting this as in section 3.6, freeze drying and reconstituting in 200ul of lithium loading buffer. 20ul was then loaded onto a Biochrom 30, fractionating using program 96361 LiHP and the peak concentration calculated by the area under the curve. **A** – Control sample (DC) showing the Glu-Lys peak (white arrow) situated between Leucine and Tyrosine peaks. Glu-Lys peak at 1 month (**B**), 4 months (**C**) and 8 months (**D**) after UNx STZ.

4.8.2. 24 h urine excretion of ϵ (γ glutamyl) lysine

To estimate 24 hours ϵ (γ glutamyl) lysine excretion, its concentration in mg/protein was multiplied by 24 hour urine volume.

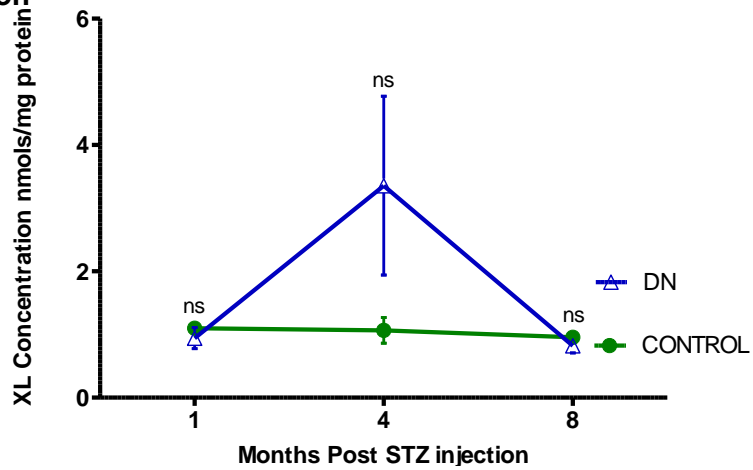
When expressed per 24h, ϵ (γ glutamyl) lysine increased significantly by 4 months with levels 15.6 fold higher than controls ($p=0.0167$). Furthermore, a 9.8 fold increase was observed at 8 months ($p=0.0357$). No statistical difference was found between controls and diabetic animals at 1 month ($p=0.867$). 24 hours ϵ (γ glutamyl) lysine measurements in sham-operated ranged between 72.88 and 82.46nmols/24h throughout the study (figure 4.18-B).

4.8.3. ϵ (γ glutamyl) lysine/creatinine ratio

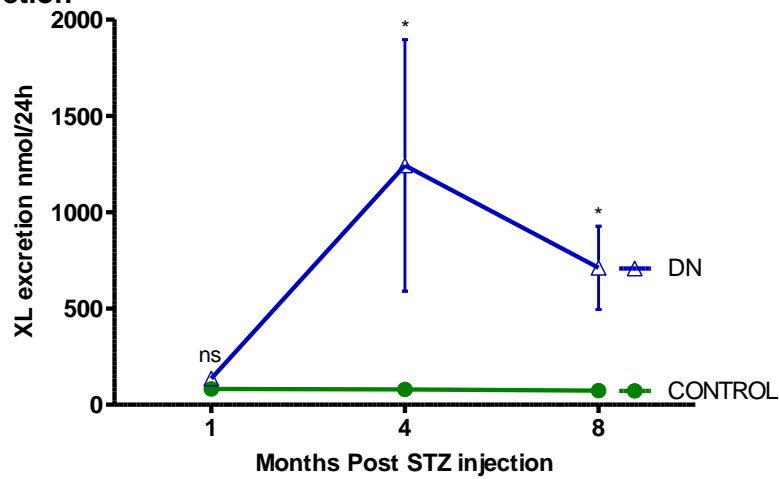
Urine XL excretion was calculated as a creatinine ratio as in section 4.2.3.4. Sham operated rats had a ϵ (γ glutamyl) lysine/ creatinine ratio ranging from 0.04 to 0.12mg/ml throughout the study. The XL/Creatinine ratio was 3.92, 20.84 and 11.89 fold higher on DN animals compared to controls at 1, 4 and 8 months post STZ injection respectively ($p=0.1413$, $p=0.0043$, $p=0.0292$, figure 4.18-C). The maximum ϵ (γ Glutamyl) Lysine to creatinine ratio was observed at 4 months where an average of 1.75 ± 0.37 mg/ml was seen.

Figure 4.18: ϵ (γ glutamyl) lysine measurement in urine from the UNx STZ model of DN

A. Concentration



B. 24 hour excretion



C. XL/Creatinine

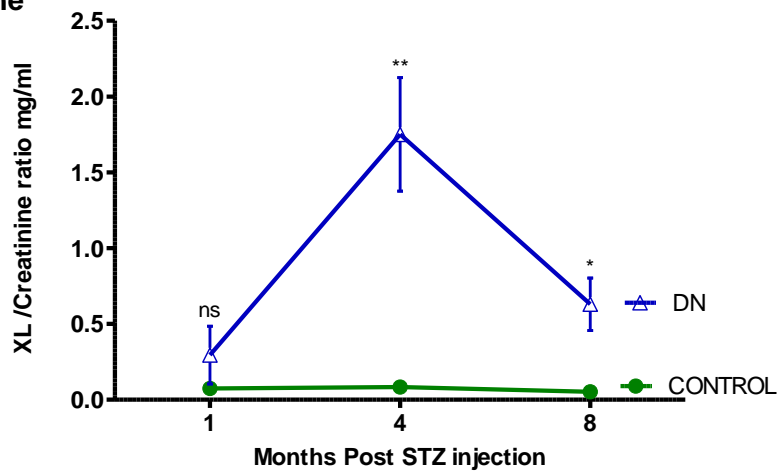


Figure 4.18: ϵ (γ glutamyl) lysine was measured in DN urine samples at 1, 4 and 8 months post STZ DN induction: **(A)** Mean ϵ (γ Glutamyl) Lysine per mg urine protein \pm SEM calculated by AUC of peaks as displayed in figure 4.19. **(B)** 24 hr urine ϵ (γ Glutamyl) Lysine \pm SEM calculated by adjustment to 24h urine protein and volume. **(C)** - XL/ Creatinine ratio. Statistical significance was calculated by 2 Way ANOVA with a Bonferroni post hoc test: NS= not statistically significant, * $p < 0.05$, ** $p < 0.01$, *** $p < 0.001$ between DN and normal urine.

4.9. ϵ (γ glutamyl) lysine measurement in urine from the Fisher to Lewis transplant model of Chronic Allograft Nephropathy

4.9.1. ϵ (γ glutamyl) lysine levels per mg protein

The urine concentration of ϵ (γ -glutamyl)-lysine in CAN samples was measured by cation-exchange HPLC using an amino acid analyser (Biochrom 30, Biochrom, UK) as described in section 4.5. Following derivatisation with ninhydrin, samples were read at 570nm with a retention time of 77 minutes and quantified from the area under the peak (figure 4.19). Urine crosslink concentration from L-L isografts (n=5), two weeks after transplantation was 1.89 ± 0.16 nmol/mg protein which remained unchanged for 52 weeks at 1.28 ± 0.08 nmol/mg protein. F-L allografts (n=7) had an initial crosslink concentration of 3.03 ± 0.25 nmol/mg protein (p=0.0066 to L-L isografts) and this peaked by 6 months at 4.67 ± 1.44 nmol/mg protein (p=0.0667). At termination, average ϵ (γ Glutamyl) Lysine levels at F-L isografts were 1.15 ± 0.07 nmol/mg protein (p=0.3230) (figure 4.20-A).

4.9.2. 24 h urine excretion of ϵ (γ glutamyl) lysine

Two weeks after transplantation, total urine ϵ (γ -glutamyl)-lysine excretion in 24 hours from L-L isografts was 28.61 ± 2.89 mmol/24h. Excretion on F-L allografts was significantly higher at 57.17 ± 4.06 mmol/24h (p=0.0004), and this gradually increased over 52 weeks to 534.2 ± 198.9 mmol/24h (p=0.0051), 10 fold higher than L-L isografts (49.13 ± 24.72 mmol/24h, figure 4.21-B).

4.9.3. ϵ (γ glutamyl) lysine/creatinine ratio

Urine crosslink excretion was corrected by creatinine as detailed in section 4.6.3. L-L isografts had a ϵ (γ glutamyl) lysine / Creatinine ratio ranging from 0.111 to 0.655mg/ml throughout the study. At 2 weeks post transplantation, F-L allografts had an average ϵ (γ glutamyl) lysine / Creatinine ratio 2.6 fold higher than L-L isografts (1.03 ± 0.220 mg/ml, p=0.0413). Crosslink/creatinine levels progressively increased until 6 months post kidney transplantation (4.6 fold higher than L-L isografts, p=0.0268) after which there was a reduction in ϵ (γ glutamyl) lysine / Creatinine ratio in the F-L allografts at 33 and 52 weeks post transplantation (0.4648 ± 0.1536 mg/ml and 0.3743 ± 0.070 mg/ml correspondingly). However, these were still significantly above values for L-L kidney transplants (p=0.0357 and p= 0.0369, figure 4.22-C).

Figure 4.19: Urine ϵ (γ Glutamyl) Lysine excretion in the Fisher to Lewis Model of CAN

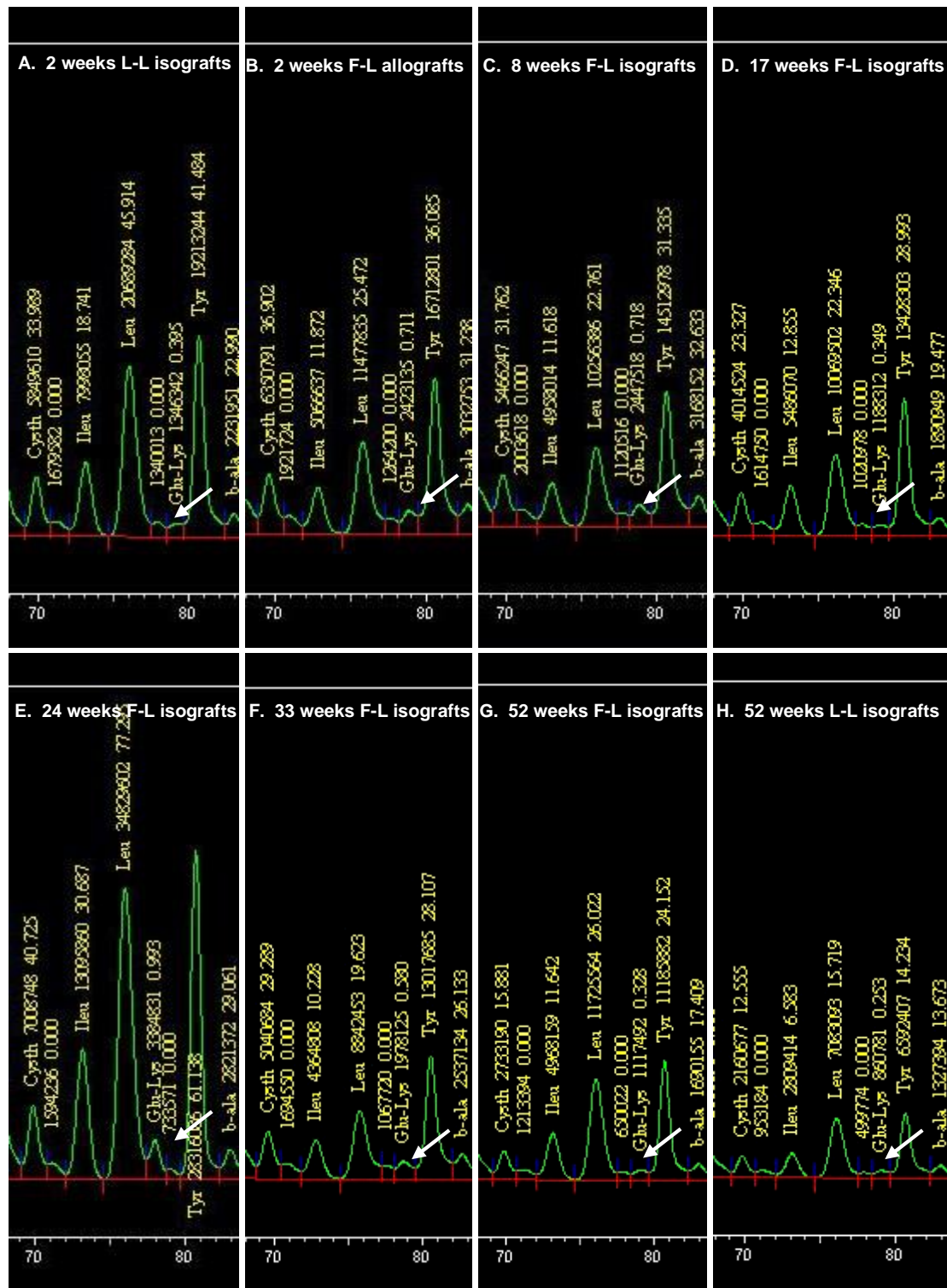
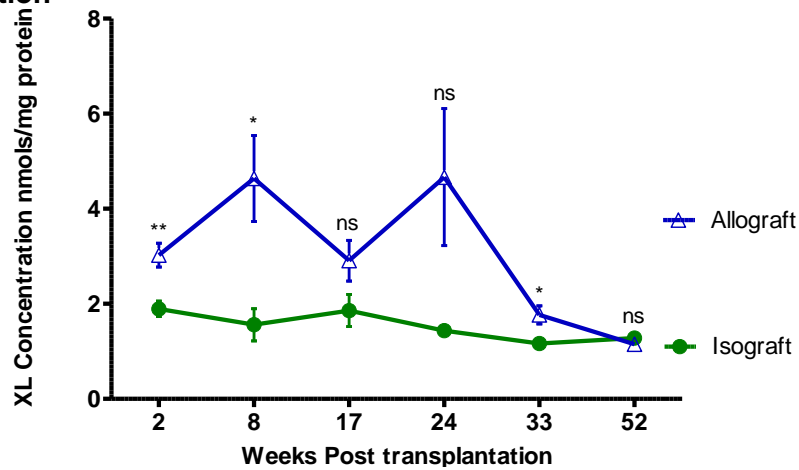


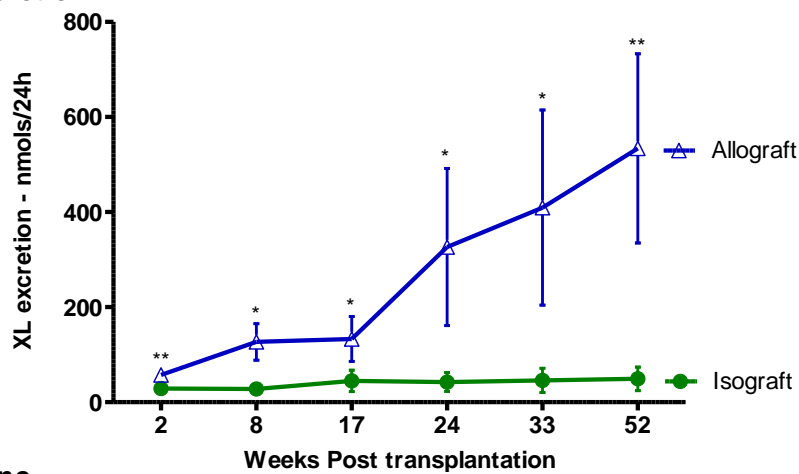
Figure 4.19: ϵ (γ glutamyl) lysine elution profile from L-L Isografts and F-L Allografts over 12 months. (A) Sample tracing of L-L Isograft at 2 weeks post kidney transplantation showing a 77 minute elution time for the crosslink peak (white arrow). F-L Allografts traces at: (B) 2 weeks, (C) 8 weeks, (D) 17 weeks, (E) 24 weeks, (F) 33 weeks and (H) 52 weeks. (G) Glu-Lys peak in a L-L Isograft urine sample at termination by 52 weeks.

Figure 4.20: ϵ (γ glutamyl) lysine measurement in urine from the in the Fisher to Lewis model of CAN

A. Concentration



B. 24 hour excretion



C. XL/Creatinine

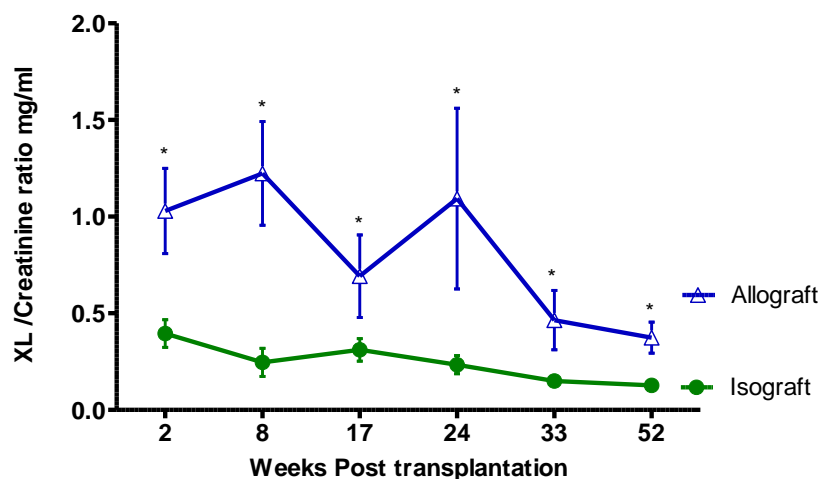


Figure 4.20: A – Mean urine ϵ (γ -glutamyl)-lysine concentration \pm SEM over a 12 month period in the L-L isograft (n=5) compared to the F-L allograft (n=7). **B** - 24 hr urine ϵ (γ glutamyl) lysine excretion \pm SEM, **C** - XL / Creatinine ratio in F-L allografts and L-L isografts transplanted rats. Statistical significance was shown by 2 Way ANOVA with Bonferroni post hoc test: NS= not statistically significant, * p<0.05, **p<0.01, ***p<0.001 between F -L allografts and L-L isografts.

4.10. Correlation between urine ϵ (γ glutamyl) lysine and clinical markers of renal function and damage

4.10.1. 24h proteinuria

To analyse the relationship between urinary excretion of ϵ (γ glutamyl) lysine and markers of disease progression, a series of correlations were performed. In the 5/6th subtotal nephrectomy model, twenty four hour urine excretion of ϵ (γ glutamyl) lysine from 30 SNx and TG inhibitors treated rats were plotted against 24 hour proteinuria (figure 4.21-A). A strong positive relationship between these two variables (Pearson's $r = 0.8979$, 95% CI: 0.7918 to 0.951, $p < 0.0001$) was seen.

Twenty five Diabetic urine samples were used to analyse the effects of protein excretion on ϵ (γ Glutamyl) Lysine output. Proteinuria levels had a steady increase throughout the study; XL levels peaked at 4 months, declining at 8 months. Urine ϵ (γ Glutamyl) Lysine was therefore not associated with changes in proteinuria in DN animals (Pearson's $r = 0.3897$, 95% CI: -0.0163 to 0.6854, $p = 0.0598$, figure 4.21-B).

Correlating 24 hour urine excretion of ϵ (γ glutamyl) lysine in 72 CAN samples and twenty four hours proteinuria revealed a strong linear positive relationship (Pearson's $r = 0.6483$, $p < 0.0001$, figure 4.21-C).

4.10.2. Creatinine clearance

Urine ϵ (γ glutamyl) lysine had a negative correlation with Creatinine Clearance in 30 SNx and TG inhibitors treated samples (Pearson's $r = -0.5355$, 95% CI: -0.7541 to -0.2102, $p = 0.0028$). Therefore, the lower the kidney function (low CrCl), the higher the excretion of ϵ (γ glutamyl) lysine dipeptide in this model of renal scarring (figure 4.21-D).

In the same way as urine TG2, its product ϵ (γ Glutamyl) Lysine, did not manifest a clear association with creatinine clearance in DN urine samples (Pearson's $r = 0.2210$, 95% CI: -0.2004 to 0.5733 $p = 0.2994$, figure 4.21-E).

In the Fisher to Lewis transplant model of CAN, 24 hour urine ϵ (γ -glutamyl)-lysine excretion showed a negative correlation (figure 4.21-F) with creatinine clearance (Pearson's $r = -0.5260$, 95% CI: -0.6881 to -0.3140 $p < 0.0001$), indicating that the higher the kidney damage and dysfunction, the higher will be the urinary crosslink output.

Figure 4.21: Correlation plots of urine ϵ (γ glutamyl) lysine excretion with markers of kidney function and damage in experimental models of renal scarring

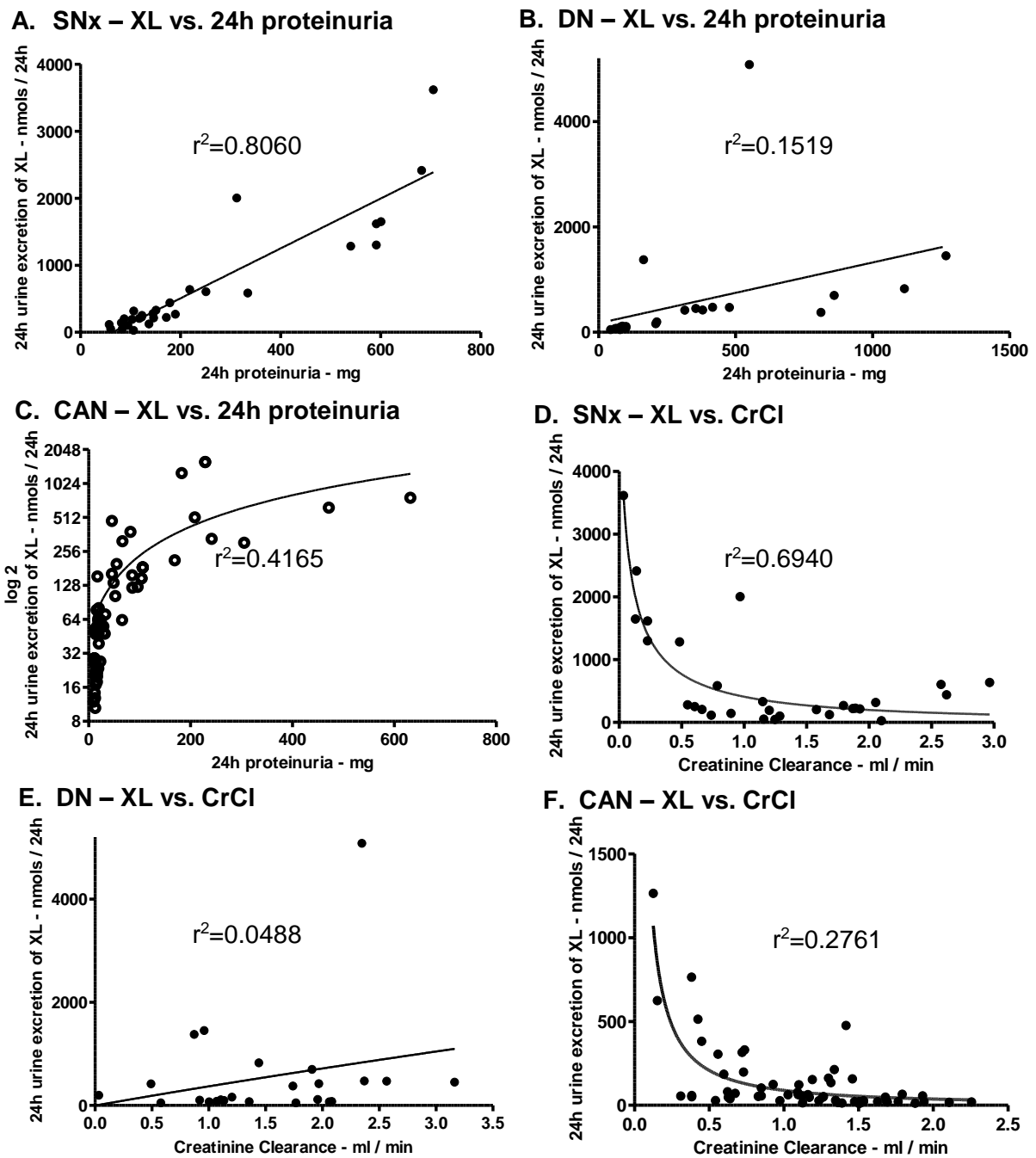
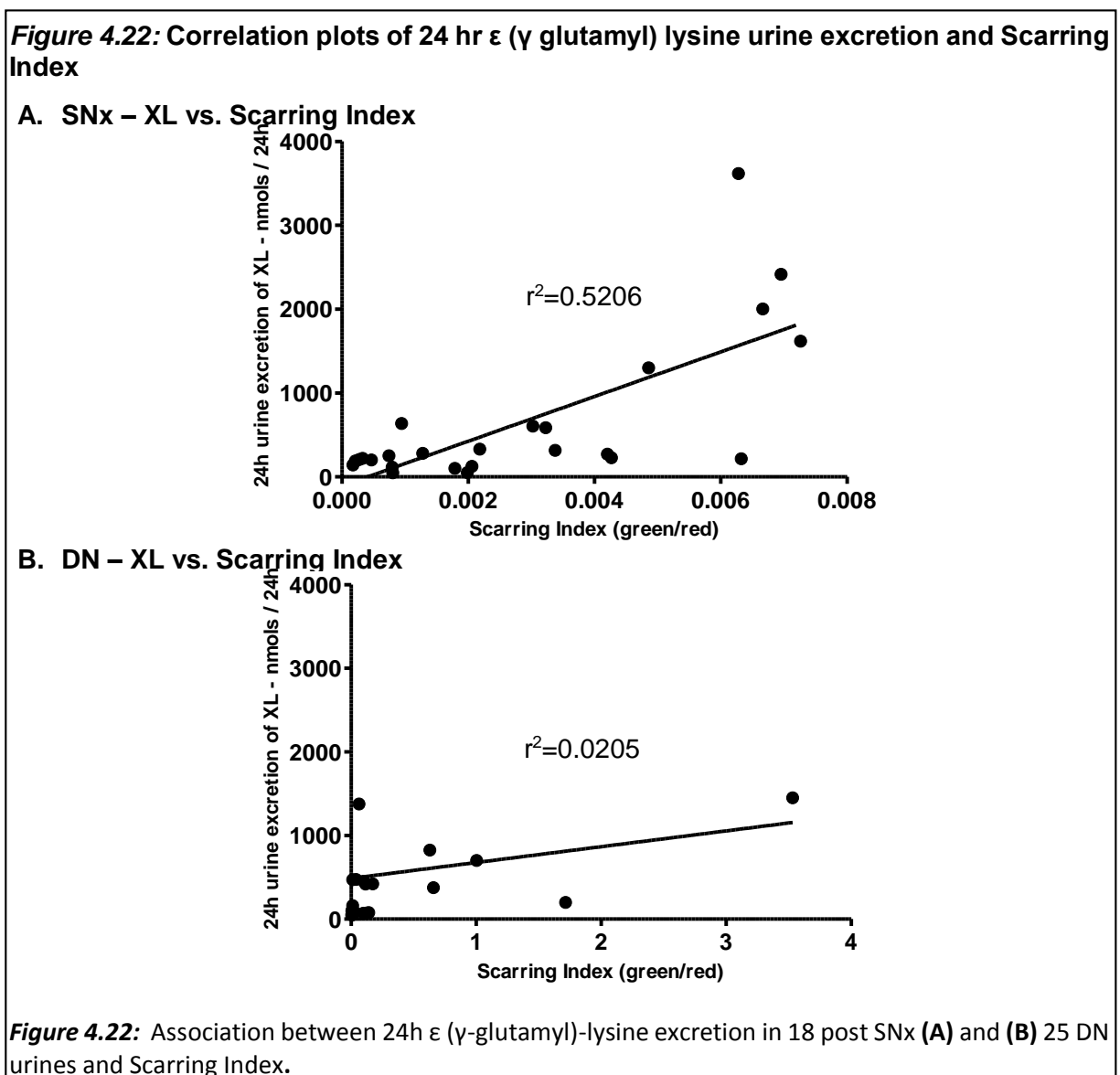


Figure 4.21: Pearson's correlations were performed for 24 hour urine ϵ (γ -glutamyl)-lysine excretion vs. 24 hour proteinuria in SNx (A), DN (B) and CAN (C) and then for 24 hour urine ϵ (γ -glutamyl)-lysine excretion vs. creatinine clearance in SNx (D), DN (E) and CAN (F). Statistical significance was shown by 2 Way ANOVA with Bonferroni post hoc test: NS= not statistically significant, * $p<0.05$, ** $p<0.01$, *** $p<0.001$. . $n=25$ in SNx and DN and $n=56$ in CAN.

4.10.3. Renal scarring levels

Scarring Index, obtained by Masson's Trichrome staining, was calculated by dividing the fibrotic areas (phase 1 - green) by all stroma (phase 2 - red) as described in methods section 3.1.5.5.2. Correlation analysis revealed a high level of association between total urinary crosslink excretion and scar formation in the SNx model of renal scarring (n=25, Pearson's $r = 0.7215$, 95% CI: 0.4565 to 0.8689, $p < 0.0001$), (figure 4.22-A). Hence, the higher the presence of fibrotic tissue in SNx kidney biopsy samples, the higher greater the excretion of crosslink in urine.

No correlation was observed between 24 hour urine ϵ (γ -glutamyl) lysine excretion in DN samples (n=25) and renal scarring (Pearson's $r = 0.1434$, 95% CI: -0.2760 to 0.5170, $p = 0.5037$, figure 4.22-B).



4.11. Discussion

In this study, assays have been established and validated to detect Transglutaminase type 2 and ϵ (γ glutamyl) lysine in urine. While it is possible to assess TG2, ϵ (γ glutamyl) lysine, collagens and other ECM related molecules in kidney tissue as well as study the histology (Johnson *et al.* 1997, Skill *et al.* 2001, Johnson *et al.* 2003, Johnson *et al.* 2007, Fisher *et al.* 2009, Huang *et al.* 2009), it is not ethical or practical to submit all patients to kidney biopsy. Therefore measurement of molecules involved in ECM regulation and scarring in the urine might represent an ideal non-invasive test to assess disease stage and its progression.

Following establishment of urine assays for TG2 and ϵ (γ glutamyl) lysine measurement, to assess if these molecules were of any potential value in CKD, measurements were undertaken in 3 animal models of renal scarring. An archived set of urines was obtained from the 5/6th subtotal nephrectomy (Johnson *et al.* 2007), the Streptozotocin Diabetic Nephropathy (Huang *et al.* 2009) and the Fisher to Lewis transplant model of CAN (Shrestha *et al.* 2014).

Quantification of TG2 protein was achieved using the developed sandwich enzyme-linked immunosorbent assay which showed no cross-reactivity with other molecules such as Factor XIII. This ensured we were not measuring other TGs in the urine. Analysis of TG2 activity was performed by assessment of its crosslink product, ϵ (γ glutamyl) lysine.

Measurement of ϵ (γ glutamyl) lysine can be done through indirect or direct methods (Griffin and Wilson 1984). Indirect methods include inhibition of ϵ (γ glutamyl) lysine by covalent incorporation of small molecular weight amine substrates such as histamine and cystamine into the ϵ (γ glutamyl) lysine groups of the protein, quantification of masked lysines within proteins and use of SDS-gel electrophoresis. Direct methods are done after release of ϵ (γ glutamyl) lysine from the sample by exhaustive proteolytic digestion with a series of endo and exopeptidases of broad specificity. It is a consensus that direct estimation of this dipeptide is the ultimate technique for analysing it as it gives better quantitative assessment of this crosslink. This is why it has been applied here.

There are several techniques used to analyse and separate amino acids and dipeptides from other components of the sample such as paper chromatography (involves the separation of amino acids on layers of cellulose paper), thin-layer chromatography (through the use of ready-coated systems), gas liquid chromatography (uses volatile derivatives such as trimethylsilyl), reversed phase HPLC (operates at high pressures and solvent flow rates), capillary electrophoresis (amino acids are separated by application of high voltages across

silica or coated polyamide tubing of 50-150 micron diameter), mass spectrometry (separation of molecules according to their atomic and molecular mass) and microbiological assays (using microorganisms such as *Lactobacillus casei* and *Tetrahymena pyriformis* to establish growth response under addition of samples containing specific amino acids). However, those techniques have several limitations. Amino Acid analysis uses highly specialised ion exchange chromatography to fractionate, identify and quantify directly amino acids. It is seen as the most accurate way to measure amino acids and again this is why this approach was selected for this study.

A key decision in presenting the data generated in this study was what to normalise data to. TG2 protein urine concentration was increased in 1 and 3 months SNx and at all time points in DN and F-L allografts which effectively means that TG2 measurements could be made on spot urine. On the other hand, rats that were treated with TG inhibitors showed reduced TG2 concentration when compared to SNx animals by 28 days in both NTU C7 and NTU C56 and by 84 days in NTU C7. Considering that these compounds should only block TG activity and not the production of this protein, we therefore realised that either twenty four urine excretion or a correction by urinary creatinine could provide a better way of expressing the urine measurement of this biomarker as changes to kidney physiology may affect urine flow and consequently its concentration.

Twenty four hour TG2 urine excretion was estimated by adjustment of concentration with 24 hour urine volume. Total TG2 was significantly elevated at all time points in SNx, DN and F-L allografts. But, as NTU C7 and NTU C56 treated animals had high urine production no difference was observed between these groups and SNx rats. So, one of the drawbacks to this way of expressing its measurement is the variability of the urine output. Also, twenty four hours urine collection is often impractical in a clinical outpatient environment with a random spot urine collection recommended more feasible option. For this reason, an adjustment of the concentration of the measured analyte by the level of urine creatinine was perceived as the most useful correction.

The crosslink product ϵ (γ -glutamyl) lysine was increased in the 3 months SNx and in the 2, 8 and 33 weeks F-L allografts when expressed per mg protein. In addition, 24 hour urine excretion of ϵ (γ -glutamyl) lysine was significantly elevated in late SNx and F-L allografts at all time points. However, in the DN group, no changes were detected per mg of protein. The reason for this could be down to the fact that the most common type of protein present in diabetic urines is albumin. The majority of DN patients typically progress with increased excretion of albumin and gradual decline in GFR until ESRD occurs (Ayodele *et al.* 2004,

Chang 2008, Jefferson *et al.* 2008, Woredekal 2008) and although a large number of substrates for TG2 have been identified, so far there is no published evidence that albumin could act as one of them. As concentrations given by the AAA are related to the amount of that amino acid or di amino acid present in 2mg of urine protein (amount used to digest), therefore the expression of ϵ (γ -glutamyl) lysine related to this amount of protein used to digest might not represent an ideal way to express it as in diseased urines most of the content would be due to the increased presence of albumin and not collagen, fibronectin, β_2 -microglobulin or other proteins of interest that could be crosslinked in the ECM. To investigate this we conducted an *in vitro* study which reported no crosslinking of albumin through TG2 (section 7.7). This could partially explain why diabetic rats with remarkable proteinuria showed reduced levels of ϵ (γ Glutamyl) Lysine.

Twenty four hour ϵ (γ glutamyl) lysine excretion was elevated at 4 and 8 months in diabetic samples. This was mostly caused by the increased proteinuric state observed at later stages of the disease. This is also in keeping with the fact that longstanding Diabetes Mellitus should be present before nephropathy develops. Gradual onset of diabetes leads to progressive kidney disease caused by angiopathy of capillaries in the kidney glomeruli. As diabetic nephropathy progresses, growing numbers of glomeruli are destroyed by progressive nodular glomerulosclerosis and this give rise to protein leakage.

In both groups of TG inhibitor treated animals lower levels of urine XL was observed as would have been predicted from the use of inhibitors. However, despite this reduction, there was no statistical difference between SNx and SNx animals treated with TG inhibitor when expressed per mg protein. After adjustment to 24 hour urine excretion ϵ (γ glutamyl) lysine was significantly reduced in both groups when compared to untreated SNx by 84 days.

ϵ (γ glutamyl) lysine measurements were also corrected by urine creatinine in order to better reflect XL excretion. After correction, urine levels of ϵ (γ glutamyl) lysine were significantly increased at all time points post SNx and allotransplantation. Furthermore, NTU C7 and NTU C56 treated animals showed reduced XL/Cr levels when compared to SNx animals throughout the study. In streptozotocin induced diabetic animals, XL/Cr levels were significantly elevated by 4 and 8 months with maximum ϵ (γ Glutamyl) Lysine to creatinine ratio observed at 4 months. This coincides with the clinical data which revealed increased glomerular hyperfiltration at this stage. The reduction in ϵ (γ Glutamyl) Lysine to creatinine ratio at 8 months DN and at late stages of the allotransplantation study could be due to the advanced level of disease which causes a lower glomerular filtration rate and therefore a decreased capability of the kidneys to excrete waste products.

SNx and CAN samples showed a positive correlation between both TG2 and ϵ (γ Glutamyl) Lysine with 24 hour proteinuria. However, highly proteinuric Diabetic animals did not present higher levels of ϵ (γ Glutamyl) Lysine. This could be due to the fact that albumin is not a preferential substrate for TG2 crosslinking (section 7.7). To minimise this effect of increased albuminuria steps could be added to remove albumin from samples. Application of albumin depletion methods could potentially improve ϵ (γ glutamyl) lysine detection as presence of high albuminuria impedes equivalent analysis of this molecule in diseased samples compared to samples where lower abundance of albumin occurs. Thus there is an increased concentration of other proteins when expressed per mg of total protein in disease urines. However, albumin depletion is costly and certainly not a “clean” technique, potentially removing proteins of interest.

Analysis of the correlation between 24 hour urine excretion of TG2 and ϵ (γ Glutamyl) Lysine indicated that both are negatively associated with creatinine clearance in the SNx and in the Fisher to Lewis transplant model of CAN. Also, Masson’s Trichrome staining of subtotal nephrectomised kidney samples revealed that the higher the presence of renal scarring and fibrosis the higher were the levels of 24 hr TG2 and its crosslink product in rat urines. This corroborates previous studies from our group (Johnson *et al.* 2007) where scarred rat kidneys presented high measurements of TG2 catalysed ϵ (γ glutamyl) lysine as well as high levels of in situ TG2 activity.

Overall, this chapter shows that TG2 and ϵ (γ Glutamyl) Lysine can be measured in urine, that overall this reflects the levels in the renal tissue and thus the degree of scar tissue formation. Further that correction for volume, either by 24 hour collection or by ratio to urine creatinine offers the most promising way to look at urine TG2 and ϵ (γ Glutamyl) Lysine levels.

Chapter 5

Urine plasminogen activator inhibitor type 1, matrix metalloproteinases and their inhibitors in experimental renal scarring

5.1. Introduction

Matrix Metalloproteinases are a group of more than 25 zinc-dependent endopeptidases secreted by a variety of cells that are capable of cleaving most of the components of the ECM, such as proteoglycans, laminin, fibronectin, and collagens III, IV and V. They can also process a number of bioactive molecules, such as apoptotic ligands, as well as being known to play a role in chemokine activation, cell proliferation, cell adhesion, differentiation, angiogenesis and host defence (Clark *et al.* 2008, Manicone and McGuire 2008, Rydlova *et al.* 2008). Previous studies have demonstrated that MMPs 1, 2, 3, 8, 9 and 13 are significantly expressed in the kidneys (reviewed by (Lenz *et al.* 2000)).

MMP activity is regulated at the level of transcription as well as by the activation of the precursor zymogens and through tight control from their endogenous inhibitors such as $\alpha 2$ macroglobulin and specifically by tissue inhibitors of metalloproteinases (TIMPs), which comprise a family of four protease inhibitors: TIMP1, TIMP2, TIMP3 and TIMP4 (Visse R, Circulation research 2003). From these, TIMPs 1, 2 and 3 are significantly expressed by the kidneys (Engelmyer *et al.* 1995, Norman *et al.* 1995). MMPs and TIMPs play a central role in the maintenance of ECM levels and thus, ECM remodelling and accumulation.

In addition to its major classical role in the coagulation and fibrinolysis cascades in the blood, the plasminogen/plasmin system also acts alongside the MMP system to degrade most ECM components. Although plasmin can directly degrade only part of ECM components such as fibronectin and laminin, it has an important function in ECM degradation as it contributes to the activation of several pro-MMPs including pro-MMP 2 and 9 (Galis and Khatri, 2002, Monea *et al.* 2002). Plasminogen activator inhibitor 1 (PAI-1) is the main regulator of tissue-type plasminogen activator (tPA) and urokinase-type plasminogen activator (uPA), the two main physiological activators of the precursor plasminogen into plasmin. Thus, an increase in PAI-1 levels is believed to contribute to fibrosis by decreasing plasmin production and therefore, ECM breakdown (Schaller and Gerber, 2011).

Recent data suggests that PAI-1, MMPs and their inhibitors are involved in many pathological processes, including the development of kidney scarring due to a decreased proteolytic activity leading to accumulation of ECM components (Ahmed *et al.* 2007). However, most of the published data about the pathological effects of PAI-1, MMPs and TIMPs in kidney disease were obtained from *in vitro* studies with cell lines and *in vivo* studies using tissue homogenates and circulatory levels of these molecules. In this chapter, we hypothesised that PAI-1, MMPs

and TIMPs are excreted in urine and therefore could predict the progression of renal fibrosis in a non-invasive way.

To test this hypothesis, this chapter aims to:

1. Validate measurements of MMP-1, MMP-9, TIMP-1, TIMP-2, TIMP-3 and PAI-1 in urine obtained from three experimental models of CKD (SNx, DN and CAN)
2. Correlate urine levels of MMPs and their inhibitors with the development of disease in these models
3. Determine if the changes in MMPs, TIMPs and PAI-1 levels could be used as indicators of CKD progression and if these could be applied to the human study.

Analyses of urine MMP-1, MMP-9, TIMP-1, TIMP-2, TIMP-3 and PAI-1 levels were performed by immunoassays as described in section 3.4.4.

5.2. Urine levels of Matrix Metalloproteinases in experimental CKD

5.2.1. MMP-1 (Interstitial collagenase)

Quantification of Matrix Metalloproteinase 1 (MMP-1; Interstitial collagenase) was done by the Gentaur immunoassay (Uscn Life Science Inc., USA) as described in section 3.10.4.1. The minimum detectable dose (M.D.D.) of rat MMP-1 was 1.7pg/ml.

MMP-1 levels were measured in two experimental models of renal scarring: the 5/6th Subtotalnephrectomy (SNx) and the UNx STZ model of Diabetic Nephropathy (DN). Archival urine samples from the Fisher to Lewis transplant model of Chronic Allograft Nephropathy were unavailable for use as they became exhausted during studies in chapter 4. Experimental animals and full methods are described in detail in chapter 3, sections 3.1.1.1, 3.1.2 and 3.1.3.

5.2.1.1. Measurement of MMP-1 in urine from the 5/6th Subtotal Nephrectomy model

In the SNx model, MMP-1 concentration in control animals (n=10) ranged between 3.61 to 35.75pg/ml (figure 5.1-A). SNx animals had a steady increase in urine MMP-1 concentration, with an average of 754.92 ± 255.18 pg/ml (n=3, p=0.0422), 1077.77 ± 65.94 pg/ml (n=3, p<0.001) and 1073 ± 28.22 pg/ml (n=6, p<0.001) at 7, 28 and 84 days after surgery respectively.

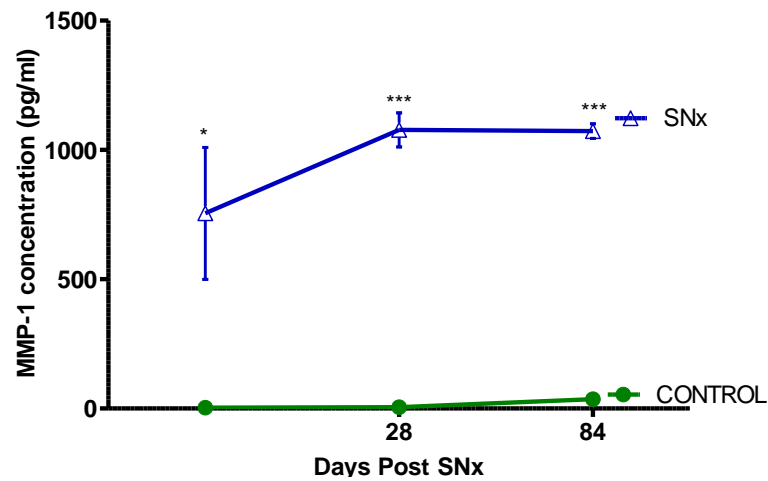
MMP-1 excretion over 24 hours (figure 5.1-B) was 12 fold higher in SNx animals at 7 and 28 days (p=0.0446 and p=0.0195 respectively), reaching an average of $35\ 676 \pm 4\ 115$ pg/24h by 3 months (p<0.0001, one way ANOVA with Bonferroni post test). Sham operated rats (n=10) displayed an average MMP-1 excretion in 24 hours ranging from 12.98 to 445.46pg/24h during the study.

Urine MMP-1 concentration was adjusted by creatinine as described in section 4.1.5.

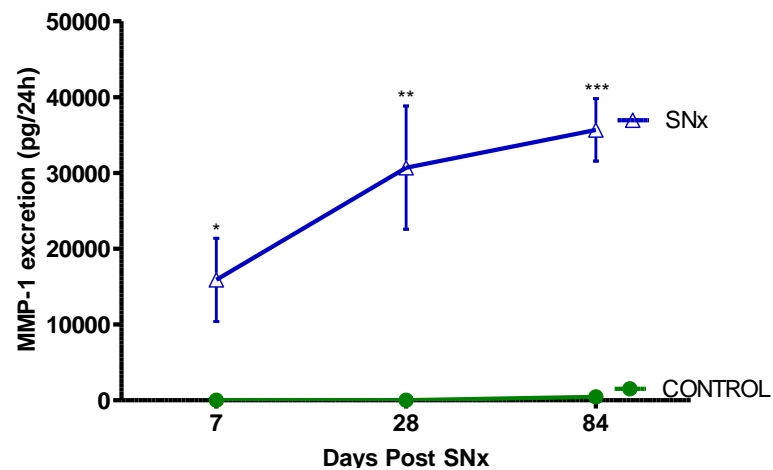
After correction, MMP-1: Creatinine ratio ranged between 0.22 to 3.86ng/mmol in sham operated rats. Average MMP-1: Creatinine ratio were respectively 85, 98 and 139 fold higher at 7, 28 and 84 days, respectively (p=0.0418, p=0.0074 and p=0.0098, one way ANOVA with Bonferroni post test) when compared to sham-operated controls (figure 5.1-C).

Figure 5.1: MMP-1 measurement in urine post SNx

A. Concentration



B. 24 hour



C. MMP-1/Creatinine ratio

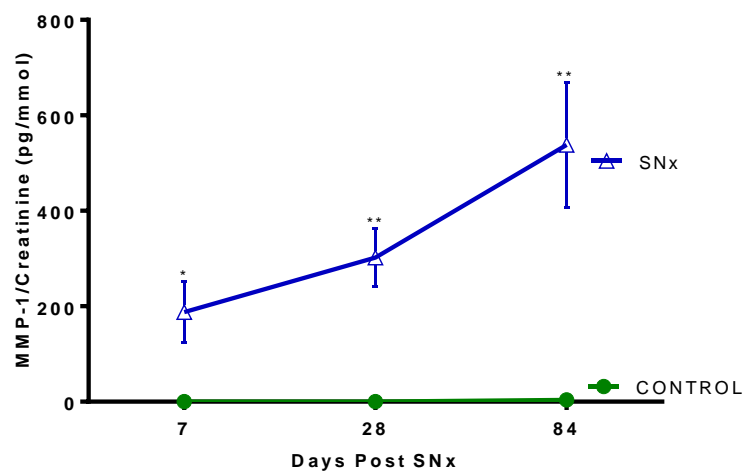


Figure 5.1: Urine MMP-1 levels were measured in SNx samples at 7, 28 and 84 days post Subtotal nephrectomy by the Gentaur rat MMP-1 Immunoassay and presented as concentration expressed in pg/ml (A) 24 hour excretion (B) and as a Creatinine ratio (C). Data represents mean \pm SEM. Statistical significance was tested using one way ANOVA with Bonferroni post test with NS= not statistically significant, * $p < 0.05$, ** $p < 0.01$, *** $p < 0.001$ between SNx and the time matched control.

5.2.1.2. Measurement of total MMP-1 in the UNx STZ model of Diabetic nephropathy

Sham operated rats (n=10) displayed a MMP-1 concentration ranging from 2.26 to 12.76pg/ml during the study (figure 5.2-A). MMP-1 concentration had a sustained rise in DN animals throughout the time course, with a 354% increase at 1 month after STZ administration (n=4, p<0.0001), to 429% (n=6, p<0.0001) at 4 months, peaking at 464% increase (n=4, p<0.0001, 2 way ANOVA with Bonferroni post test) at termination.

At 1 month, DN animals had a 24 hour MMP-1 excretion of 32.88 ± 14.44 pg/24h (n=3, p=0.0418), increasing to 181.17 ± 32.41 pg/24h (n=3, p=0.0066) by 4 months and then to 146.72 ± 51.57 pg/24h at termination. Although by 8 months, 24h MMP-1 concentration was 24 fold higher than controls, this difference failed to reach significance due to the variability of urine output (n=6, p=0.0614, 2 way ANOVA with Bonferroni post test). Total MMP-1 excretion in sham operated rats ranged 8.65-60.16pg/24hours throughout the study (figure 5.2-B).

To correct for the broad variability of urinary output within diabetic samples, MMP-1 excretion was converted to a creatinine ratio as described in details in section 4.2.3.4. Corrected MMP-1 excretion (MMP-1: Creatinine ratio) was elevated in DN animals when compared to sham operated animals at 1 month (357.6 ± 67.2 pg/mmol), but this difference was not significant (p=0.0509). However, MMP-1: Creatinine ratio showed a significant increase on DN animals by 4 and 8 months after DN induction (1099 ± 156 and 992 ± 180 pg/mmol, p= 0.0019 and p=0.0056 respectively) (figure 5.2-C).

Figure 5.2: MMP-1 measurement in urine from the UNx STZ model of DN

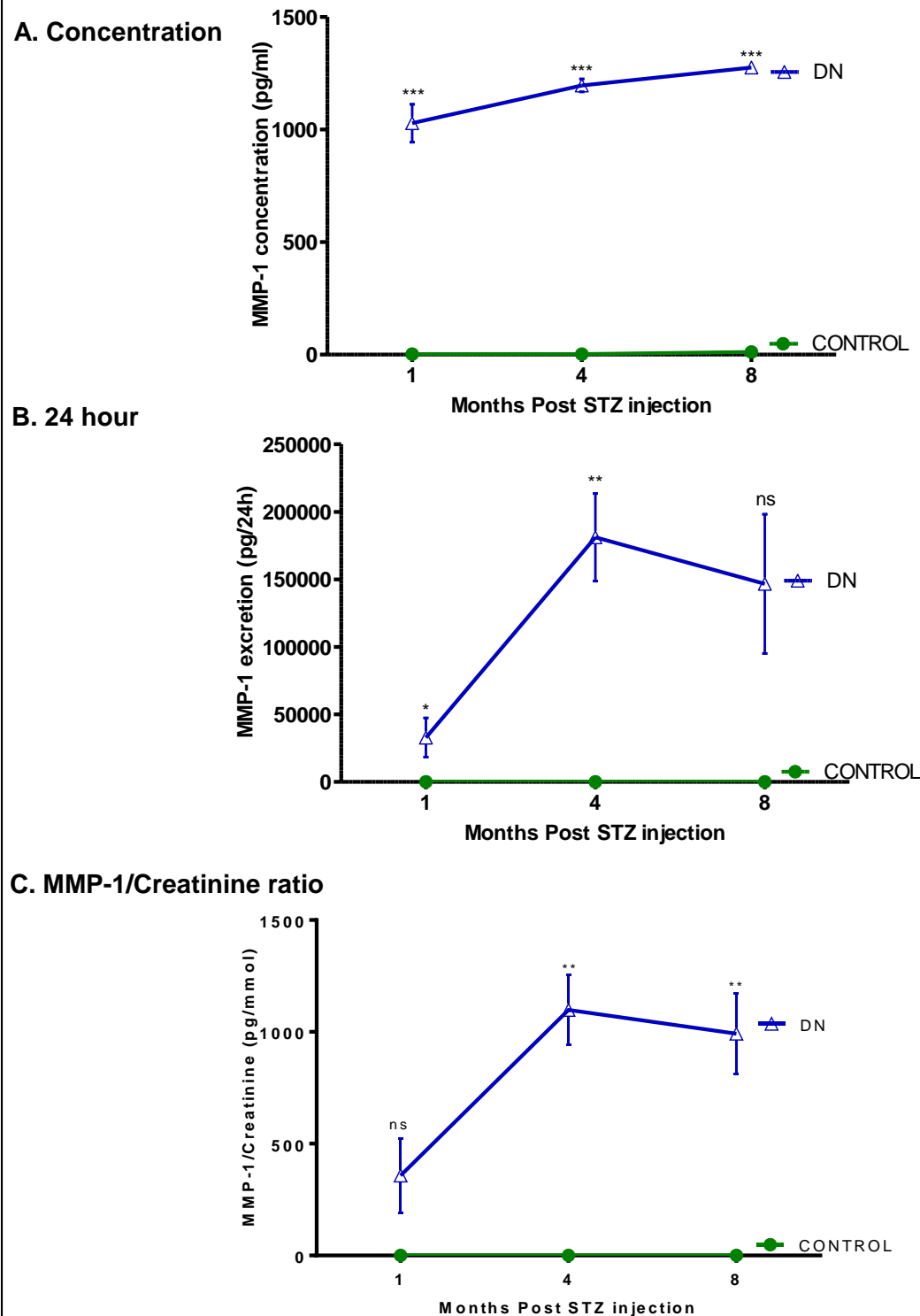


Figure 5.2: Urine MMP-1 levels in DN samples at 1, 4 and 8 months post DN induction were measured by Gentaur rat MMP-1 Immunoassay and presented as concentration expressed in pg/ml (A) 24 hour excretion, (B) and as a Creatinine ratio (C). Values are mean \pm SEM. Statistical significance was tested using one way ANOVA with Bonferroni post test with NS= not statistically significant, * $p < 0.05$, ** $p < 0.01$, *** $p < 0.001$ between DN and the time matched control.

5.3.2. Correlation between urine MMP-1 and clinical markers of kidney function and damage

5.3.2.1. 24h proteinuria

To determine whether the urine excretion of MMP-1 was associated with the presence of glomerular damage, a correlation of MMP-1 urine concentration with 24 hour proteinuria was performed. In the 5/6th subtotalnephrectomy model of renal scarring, there was a positive correlation between urinary MMP-1 excretion in 24 hours with twenty four hours protein excretion (Pearson's $r = 0.8658$, 95% Confidence interval: 0.6782 to 0.9474. $p < 0.0001$, $r^2 = 0.7495$, figure 5.3-A). A similar, but slightly weaker association was found in DN samples (Pearson's $r = 0.7488$, 95% Confidence interval: 0.4868 to 0.8872. $p < 0.0001$, $r^2 = 0.5607$, figure 5.3-B).

5.3.2.2. Creatinine Clearance

A strong negative association was observed when correlating urine MMP-1 with Creatinine clearance (CrCl) in the SNx model (figures 5.3-C), showing that MMP-1 excretion increased as disease progressed (Pearson's $r = -0.6860$. 95% CI: -0.8732 to -0.3223, $p = 0.0017$, $r^2 = 0.4706$). Conversely, Diabetic samples (figure 5.3-D) did not show any correlation between MMP-1 excretion and decreased kidney function (Pearson $r = 0.2991$, 95% CI: -0.1291 to 0.6333, $p = 0.1656$, $r^2 = 0.08947$).

Figure 5.3: Correlation plots of urine MMP-1 excretion with markers of kidney function and damage in experimental models of renal scarring

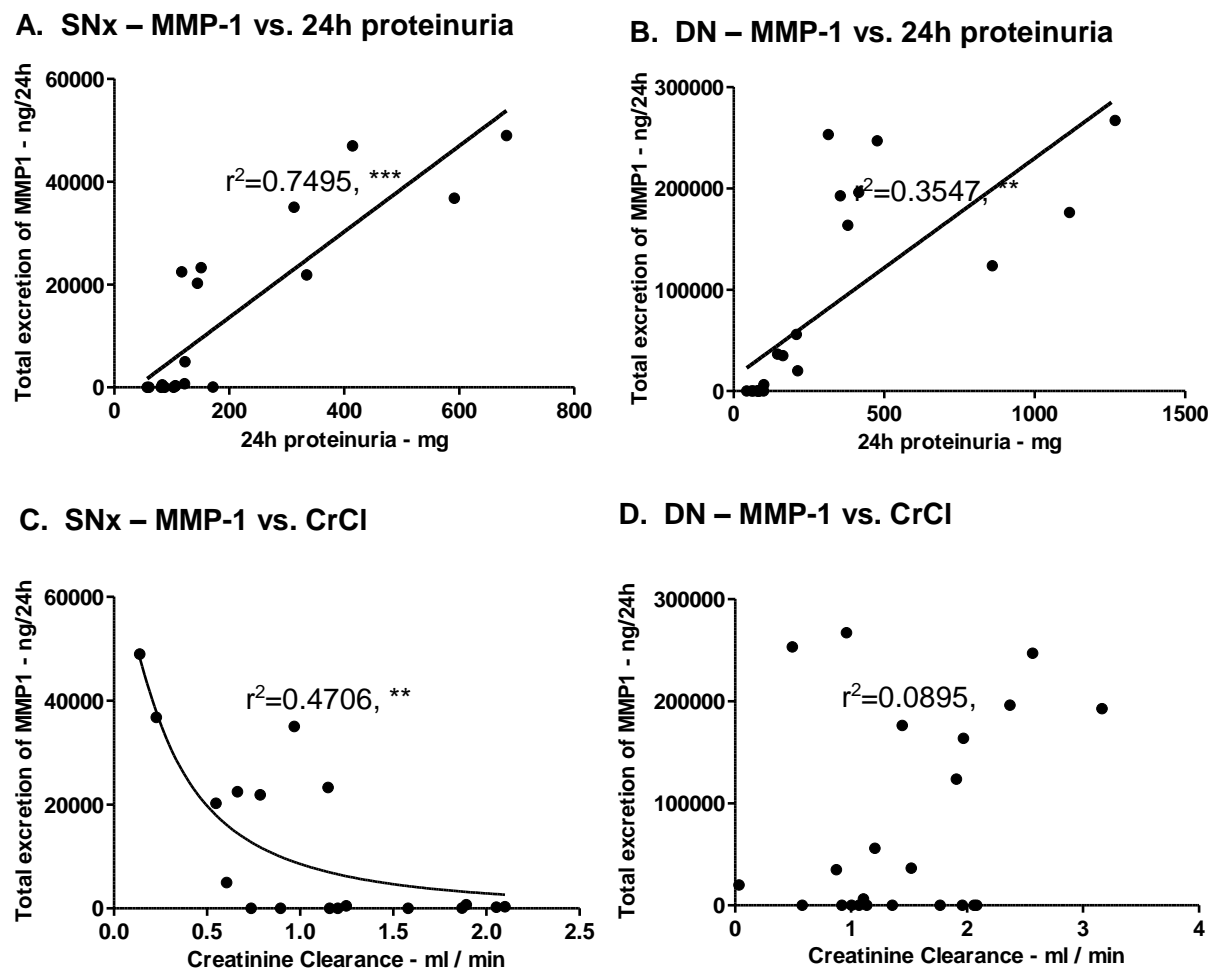


Figure 5.3: Pearson’s correlations were performed for 24 hour urine MMP-1 excretion vs. 24 hour proteinuria in SNx (**A**) and DN (**B**) and then for 24 hour urine MMP-1 excretion vs. creatinine clearance in SNx (**C**) and DN (**D**). NS= non statistical significant, * $p<0.05$, ** $p<0.01$, *** $p<0.001$. $n=20$ in SNx and 25 DN.

5.2.2. MMP-9 (Gelatinase-B)

Matrix metalloproteinase 9 (MMP-9), is a 92 kDa type IV collagenase. Levels were measured in rat urines by the Quantikine rat total MMP-9 Immunoassay as described in section 3.10.4.2. Total levels of the enzyme were measured, including its Pro-, active- and TIMP-complexed forms of the protein.

Total MMP-9 levels were measured in two experimental models of renal scarring: the 5/6th Subtotalnephrectomy (SNx) and the UNx STZ model of Diabetic Nephropathy (DN). Archival urine samples from the Fisher to Lewis transplant model of Chronic Allograft Nephropathy were unavailable for use as they became exhausted in studies performed in chapter 4. Experimental animals and full methods are described in detail in chapter 3, sections 3.1.1.1., 3.1.2 and 3.1.3.

5.2.2.1. Measurement of total MMP-9 in urine from 5/6th subtotal nephrectomised rats

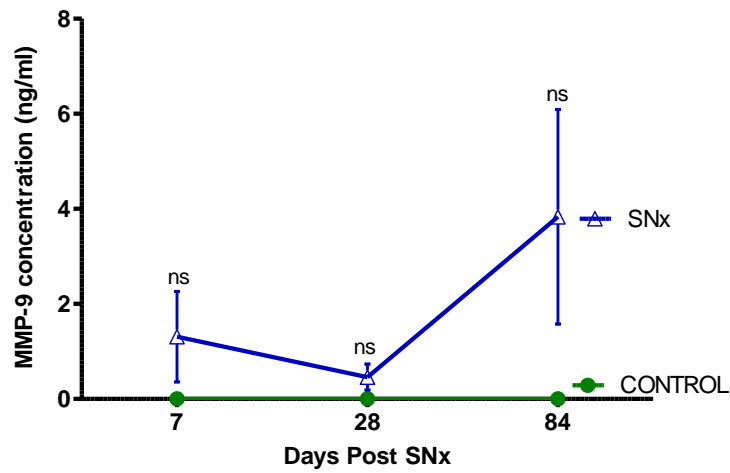
The Minimum Detectable Dose (MDD) of rat MMP-9 was 0.013ng/ml. However, MMP-9 levels were not detected in control animals (n=9) at any time points following sham operation and was very low in SNx samples (figure 5.4-A). At 7 day s, MMP-9 concentration was 1.31 ± 0.95 ng/ml (n=3), decreasing to 0.46 ± 0.27 ng/ml (n=3) by day 28 before rising to 3.83 ± 2.25 ng/ml at termination (n=7).

To calculate 24 hour MMP-9 excretion urine concentration was multiplied by total urinary volume. Total MMP-9 excretion was 24.9 ± 17.7 ng/24h at 7 days, compared to 12.2 ± 6.0 ng/24h and 103.7 ± 53.6 ng/24h at 28 and 84 days respectively (figure 5.4-B). No statistical difference was found between these groups.

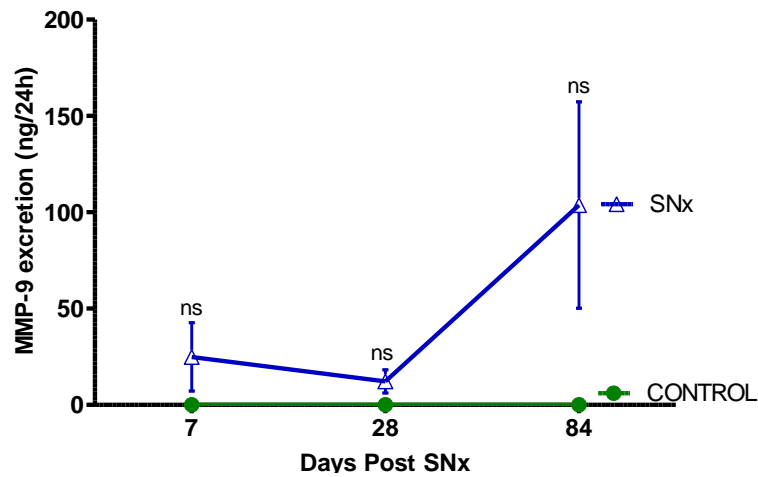
Conversion of MMP-9 to a creatinine ratio also showed an increase by 84 days (1.52 ± 0.63) when compared to 7 and 28 days (0.31 ± 0.22 and 0.12 ± 0.05), but this elevation also didn't reach significance (p= 0.1095 and p=0.0628) (figure 5.4-C).

Figure 5.4: MMP-9 measurement in urine post SNx

A. Concentration



B. 24-hour



C. MMP-9/Creatinine ratio

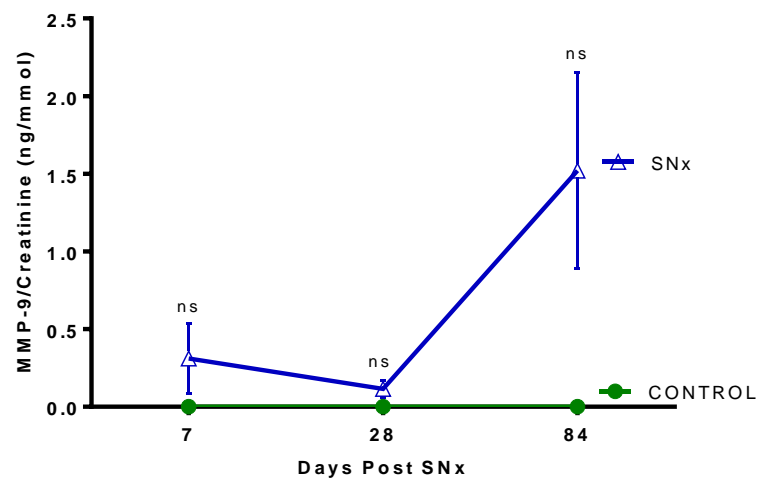


Figure 5.4: Urine MMP-9 levels were measured in SNx samples at 7, 28 and 84 days post Subtotal nephrectomy by the Quantikine rat total MMP-9 Immunoassay and presented as concentration **(A)** 24 hour excretion **(B)** and as a Creatinine ratio **(C)**. Values are mean \pm SEM. Statistical significance was tested using one way ANOVA with Bonferroni post test with NS= not statistically significant, * $p < 0.05$, ** $p < 0.01$, *** $p < 0.001$ between SNx and the time matched control

5.2.2.2. Measurement of total MMP-9 in the UNx STZ model of Diabetic nephropathy

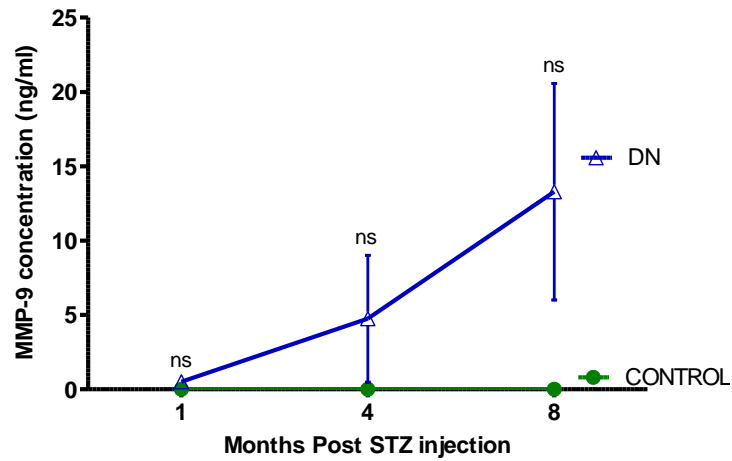
Similarly to the results seen in the SNx model, MMP-9 was undetectable in all control samples (n=10) (figure 5.5-A). Diabetic samples had a steady increase in urine MMP-9 concentration, although variability within sample groups was high. Average urine MMP-9 concentration was 0.51 ± 0.41 ng/ml (n=3), 4.75 ± 4.26 ng/ml (n=7) and 13.29 ± 7.28 ng/ml (n=5) at 1, 4 and 8 months post streptozotocin respectively.

When converted to MMP-9 excretion over 24 hours (figure 5.5-B) variability remained high. Total urine MMP-9 excretion was 25.39 ± 22.85 ng/24h at 1 month, rising to 743.55 ± 714.66 ng/24h by 4 months, and remaining elevated at termination at 1446.63 ± 835.40 ng/24h. One of the diabetic samples had persistent low MMP-9 levels through the study and this resulted in high standard error values.

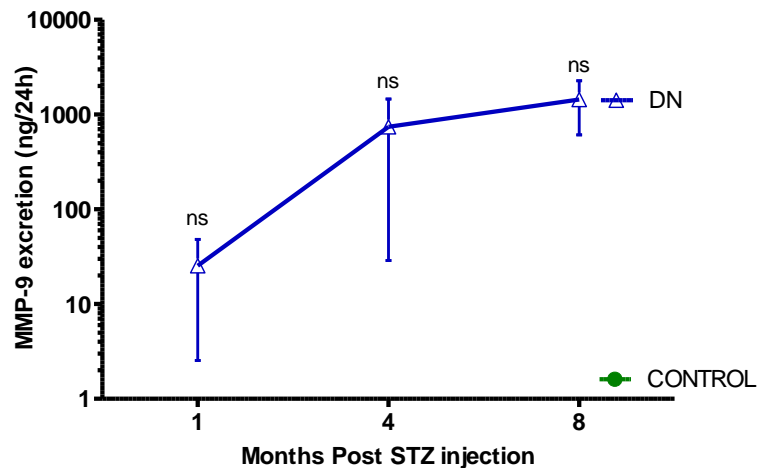
Once corrected to a creatinine ratio, MMP-9 was 0.30 ± 0.272 month after DN induction (figure 5.5-C). This had over a 15 fold increase by 4 months and subsequent 31 fold by 8 months. However, this difference was not significant due to the large variation that remained post volume correction.

Figure 5.5: MMP-9 measurement in urine from the UNx STZ model of DN

A. Concentration



B. 24-hour



C. MMP-9/Creatinine ratio

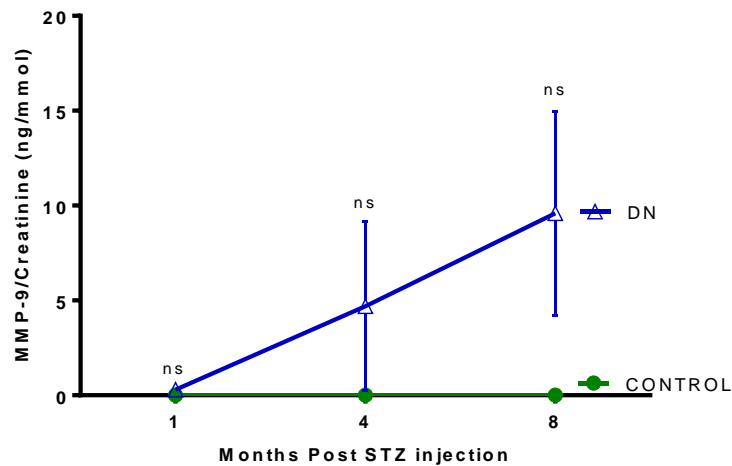


Figure 5.5: Urine MMP-9 levels in DN samples at 1, 4 and 8 months post DN induction were measured by Quantikine rat total MMP-9 Immunoassay and presented as concentration expressed in ng/ml **(A)** 24 hour excretion, plotted at log 10 scale for better visualization of differences **(B)** and as a Creatinine ratio **(C)**. MMP-9 was undetectable on controls and had a steady, but not significant rise in Diabetic animals. Values are mean \pm SEM. Statistical significance was tested using one way ANOVA with Bonferroni post test with NS= not statistically significant, * $p < 0.05$, ** $p < 0.01$, *** $p < 0.001$ between DN and the time matched control.

5.3. Urine levels of Tissue inhibitors of Metalloproteinases in experimental CKD

5.3.1. Tissue inhibitor of metalloproteinase 1

To investigate the urine expression of TIMP-1 and its subsequent potential as a non-invasive biomarker of kidney scarring progression, samples from three different animal models of renal scarring (SNx, DN and CAN) were used. TIMP-1 levels were analysed by an immunosorbent assay as described in section 3.11.1.1. Minimum detectable dose (MDD) of rat TIMP-1 was 3.5pg/ml.

5.3.1.1. Measurement of urine TIMP-1 in the 5/6th Subtotal nephrectomy model

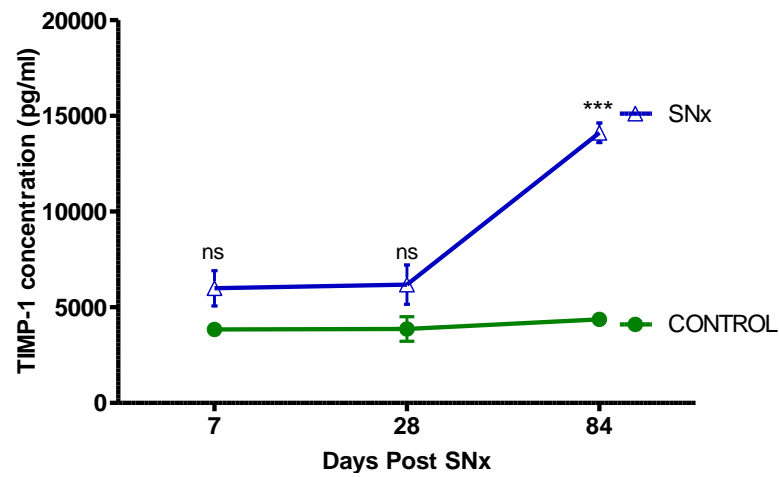
Urine TIMP-1 concentration on Sham operated rats ranged between 2.9 to 5.1ng/ml throughout the study (figure 5.6-A). SNx animals presented an average urinary TIMP-1 concentration of 6.0 ± 0.9 ng/ml (n=3) at 7 days and 6.2 ± 1.0 ng/ml (n=3) at 28 days after surgery. No statistical difference was found between SNx and control animals during these time points ($p=0.0858$ and $p=0.1283$, 2 way ANOVA with Bonferroni post test). By 84 days, urine TIMP-1 concentration was 233% higher than controls, with an average value of 14.1 ± 0.5 ng/ml (n=7, $p<0.0001$).

Total TIMP-1 excretion (figure 5.6-B) had a sustained rise in the SNx animals throughout the time course showing 849%, 881% and 841% increase at day 7, 28 and 84 respectively ($p=0.0007$, $p<0.0001$, $p<0.0001$, 2 way ANOVA) when compared to sham-operated controls. Total TIMP-1 excretion in sham operated rats ranged 8.9-56ng/24hours throughout the study.

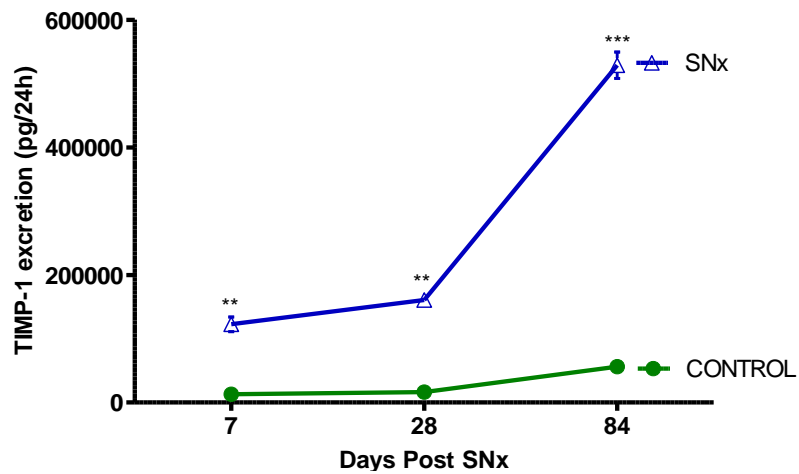
To correct for the wide difference in the variability of urine output within samples, an adjustment of TIMP-1 excretion was performed based on the levels of creatinine in the urine (as outlined in session 4.2.3.4). Corrected TIMP-1 excretion (TIMP-1/Creatinine ratio) was raised in SNx animals when compared to sham operated animals at all time points after subtotalnephrectomy: 6.4, 6.7 and 15.3 fold increase ($*p=0.0025$, $**p=0.0007$, $***p=0.0160$, two way ANOVA, figure 5.6-C). Sham-operated rats had an average TIMP-1/Creatinine ratio ranging from 0.230-0.480pg/mmol from 7 to 84 days after surgery.

Figure 5.6: TIMP-1 measurement in urine post SNx

A. Concentration



B. 24-hour



C. TIMP-1/Creatinine ratio

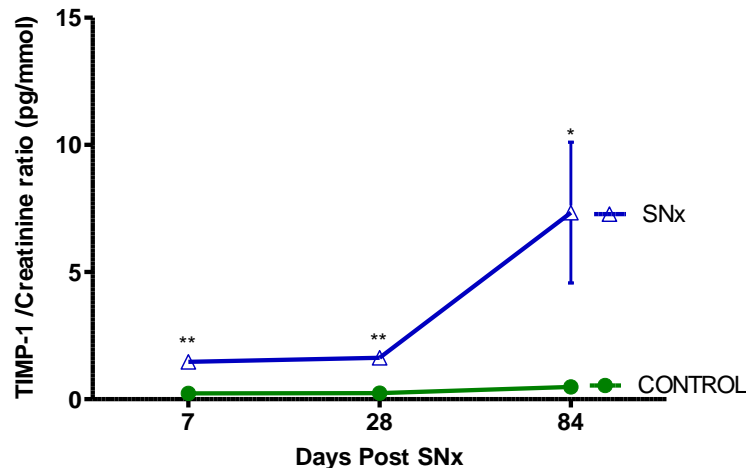


Figure 5.6: Urine TIMP-1 levels were measured in SNx samples at 7, 28 and 84 days post Subtotal nephrectomy by the Quantikine rat TIMP-1 Immunoassay and presented as concentration in pg/ml (A) 24 hour excretion (B) and as a Creatinine ratio (C). Values are mean \pm SEM. Statistical significance was tested with one Way ANOVA with Bonferroni post hoc test: NS= non statistical significant, * $p < 0.05$, ** $p < 0.01$, *** $p < 0.001$, between diseased samples and time matched control.

5.3.1.2. Measurement of urine TIMP-1 in the UNx STZ model of Diabetic nephropathy

Consistent with the SNx model, no difference could be found in urine TIMP-1 concentration in the early stages of the Diabetic disease (figure 5.7-A). At 1 month after DN induction, control animals (n=3) had an average TIMP-1 concentration of 1.8 ± 0.7 ng/ml against 3.5 ± 1.1 ng/ml of DN rats (n=3, p=0.2478). As disease progressed, TIMP-1 levels became significantly higher in DN urine samples (n=5, 4.1 ± 0.3 ng/ml, p=0.0047) when compared to controls at 4 months. At the time of termination, TIMP-1 levels remained elevated on urine from DN rats (n=5, 7.4 ± 3.3 ng/ml). However, it failed to achieve statistical significance (p=0.2106) at this point.

Total TIMP-1 excretion in Diabetic samples (figure 5.7-B) was elevated 1 month post STZ injection, showing a 15 fold increase compared to sham animals, however this difference was not significant (p=0.0571, 2 way ANOVA). At 4 months, this raised to a significant 50 fold increase in total urine TIMP-1 measurements between SNx and sham controls (p=0.0021, 2 way ANOVA). Between 4 and 8 months, although total TIMP-1 excretion in Diabetic urine samples had a decrease to 43 fold difference compared to control animals, it remained significantly elevated (p=0.0337).

After normalizing for urine creatinine concentration, corrected TIMP-1 excretion (TIMP-1/Creatinine ratio) was significantly increased in Diabetic samples at 4 and 8 months after DN induction (figure 5.7-C). At 4 months, TIMP-1/creatinine ratio was over 25 fold higher on Diabetic animals compared to controls (p=0.0006), whereas by termination this difference was elevated to 37 fold increase (p=0.0422).

Figure 5.7: TIMP-1 measurement in urine from the UNx STZ model of DN

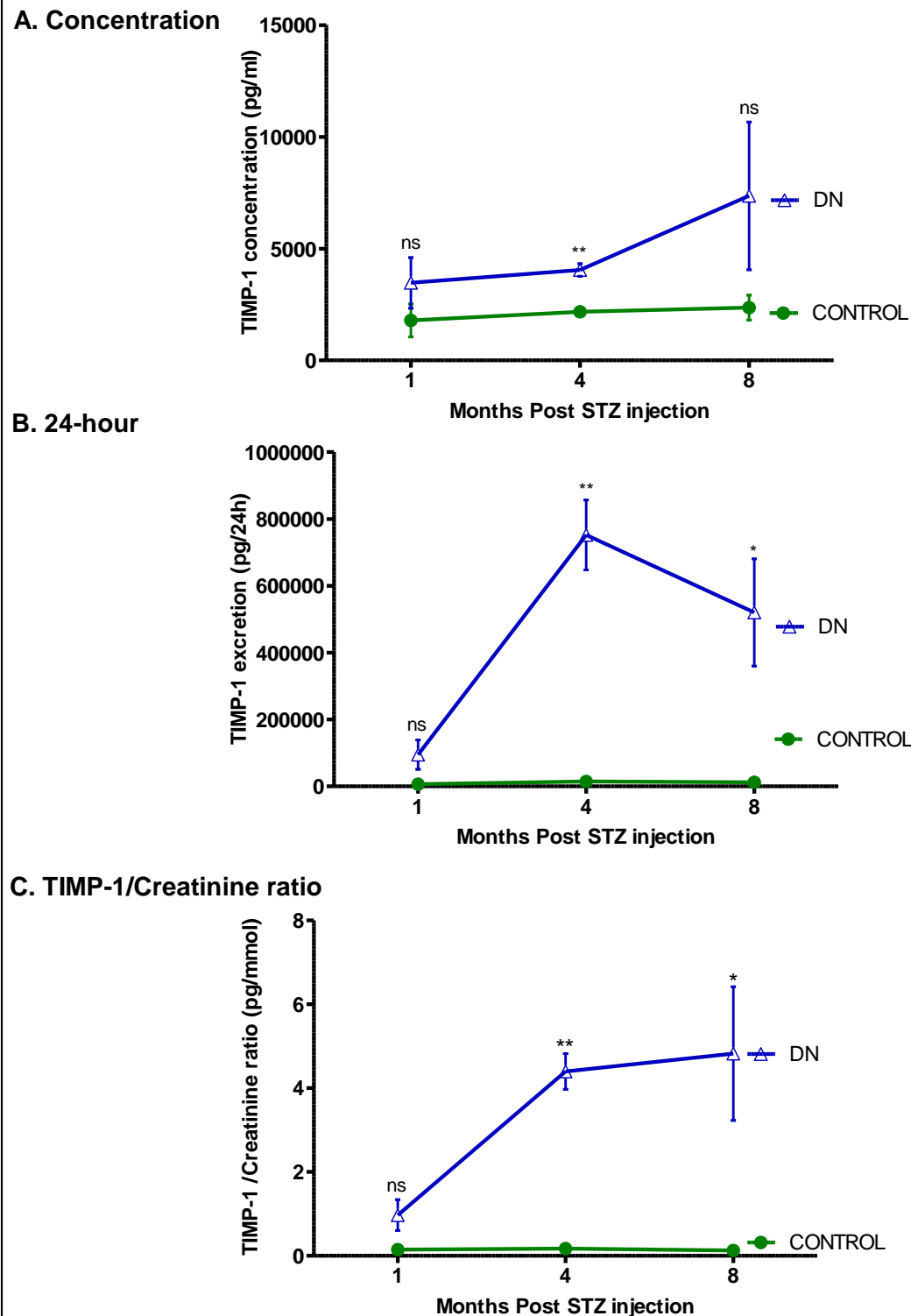


Figure 5.7: Urine TIMP-1 levels in DN samples at 1, 4 and 8 months post DN induction were measured by the Quantikine rat TIMP-1 Immunoassay and presented as concentration expressed in pg/ml (A), 24 hour excretion (B) and as a Creatinine ratio (C). Statistical significance was tested with one Way ANOVA with Bonferroni post hoc test: NS= non statistical significant, * p<0.05, **p<0.01, ***p<0.001, between diabetic samples and time matched control. Values are mean \pm SEM.

5.3.1.3. Measurement of urine TIMP-1 in the Fisher to Lewis transplant model of CAN

Similar urine concentrations of TIMP-1 were found between F-L allografts and L-L isografts during the entire study (figure 5.8-A). In the early phase of CAN, urine TIMP-1 concentration was 4.3 ± 0.4 ng/ml in isografts and 4.4 ± 0.8 ng/ml in allografts ($p=0.9051$) and remained unchanged over 33 weeks (isografts 4.5 ± 0.4 ng/ml and allografts 5.0 ± 0.9 ng/ml) $p=0.6255$. At 52 weeks, there was a slight increase in TIMP-1 concentration in the allograft group (6.5 ± 3.4 ng/ml), but this failed to achieve significance ($p=0.3097$).

As it can be seen in figure 5.8-B, there was no statistical difference in total TIMP-1 excretion between L-L isografts and F-L allografts in the initial stages of the study (2 and 8 weeks). Interestingly, it became significantly increased on F-L allografts at 17 (149% higher than L-L isografts, $p=0.0288$) and 24 weeks post transplantation (134% higher, $p=0.0360$). Nevertheless, by 33 weeks after surgery until termination, the difference in total TIMP-1 excretion between these two groups remained insignificant.

F-L allografts and L-L isografts showed similar urinary TIMP-1 levels, even when corrected by creatinine ratio (figure 5.8-C). No statistical difference was found between these two groups throughout the time course of this study despite a reduction on TIMP-1 levels noticed on L-L isografts. This interesting fact reflects the improvement on renal function observed on this group of animals towards the end of the study (figure 11.4-C appendix). F-L allografts had an average TIMP-1/creatinine ratio ranging from 0.984-2701pg/mmol, whilst in L-L isografts it was 0.231-0.945pg/mmol.

Figure 5.8: TIMP-1 measurement in urine from the in the Fisher to Lewis transplant model of CAN

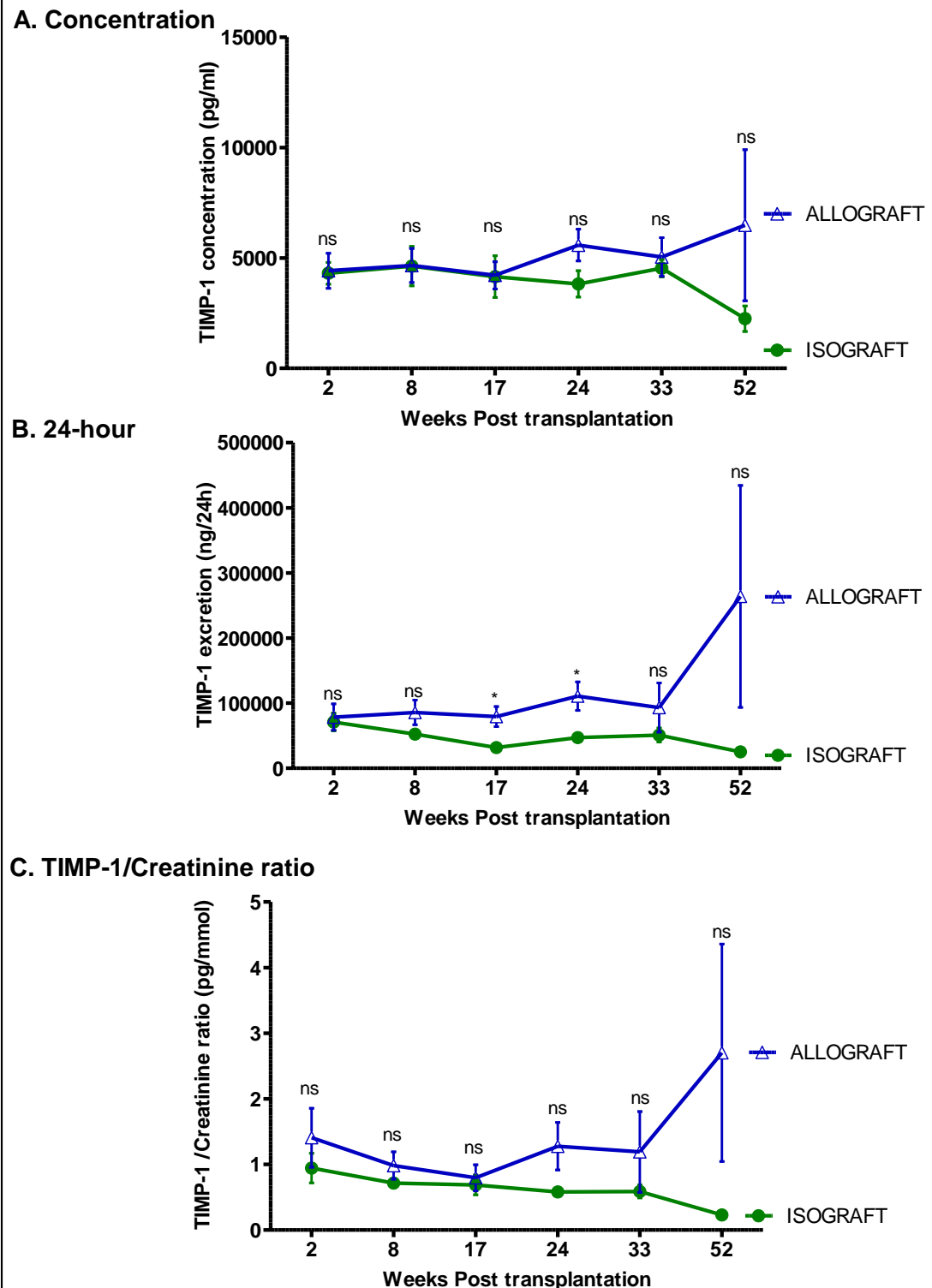


Figure 5.8: Urine TIMP-1 levels in the Fisher to Lewis transplant model of CAN over 12 months quantified by the Quantikine rat TIMP-1 Immunoassay and presented as concentration expressed in pg/ml (A), 24 hour excretion (B) and as a Creatinine ratio (C). Statistical significance was tested with 2 Way ANOVA with Bonferroni post hoc test: NS= non statistical significant, * p<0.05, **p<0.01, ***p<0.001, between F -L allografts and L-L isografts. Values are mean ± SEM.

5.3.2. Correlation between urine TIMP-1 and clinical markers of kidney function and damage

5.3.2.1. 24h proteinuria

Correlating total urinary TIMP-1 excretion in 24 hours with twenty four hours protein excretion showed a positive association in SNx samples (Pearson's $r = 0.8715$. 95% confidence interval: 0.6822 to 0.9513, $p < 0.0001$, $r^2 = 0.7596$, figure 5.9-A). The same association was observed on DN samples (Pearson's $r = 0.7556$. 95% confidence interval: 0.4806 to 0.8953. $p < 0.0001$, $r^2 = 0.5709$, figure 5.9-B) and in a smaller scale, with CAN samples (number of XL pairs=54, Pearson $r = 0.3490$. 95% confidence interval: 0.06523 to 0.5805. $p = 0.0174$, $r^2 = 0.1218$, figure 5.9-C).

5.3.2.2. Creatinine Clearance

When correlating total urine TIMP-1 with Creatinine clearance (CrCl), TIMP-1 excretion was inversely correlated with renal function in both SNx and CAN models (figures 5.9-D and 5.9-F). Therefore, the lower the kidney function, the higher the excretion of TIMP-1 in these models of renal scarring. SNx samples were negatively correlated with CrCl; Pearson's $r = -0.5837$. 95% CI: -0.8312 to -0.1430. $p = 0.0139$, $r^2 = 0.3407$ with CAN samples having a lower correlation (Pearson's $r = -0.3931$. 95% CI: -0.5980 to -0.1705. $p = 0.0033$, $r^2 = 0.1546$. Conversely, Diabetic samples (figure 5.9-E) did not demonstrate any relationship between TIMP-1 and reduced kidney function (Pearson $r = 0.3448$. 95% CI: -0.1022 to 0.6760. $p = 0.1258$, $r^2 = 0.1189$).

Figure 5.9: Correlation plots of urine TIMP-1 excretion with markers of kidney function and damage in experimental models of renal scarring

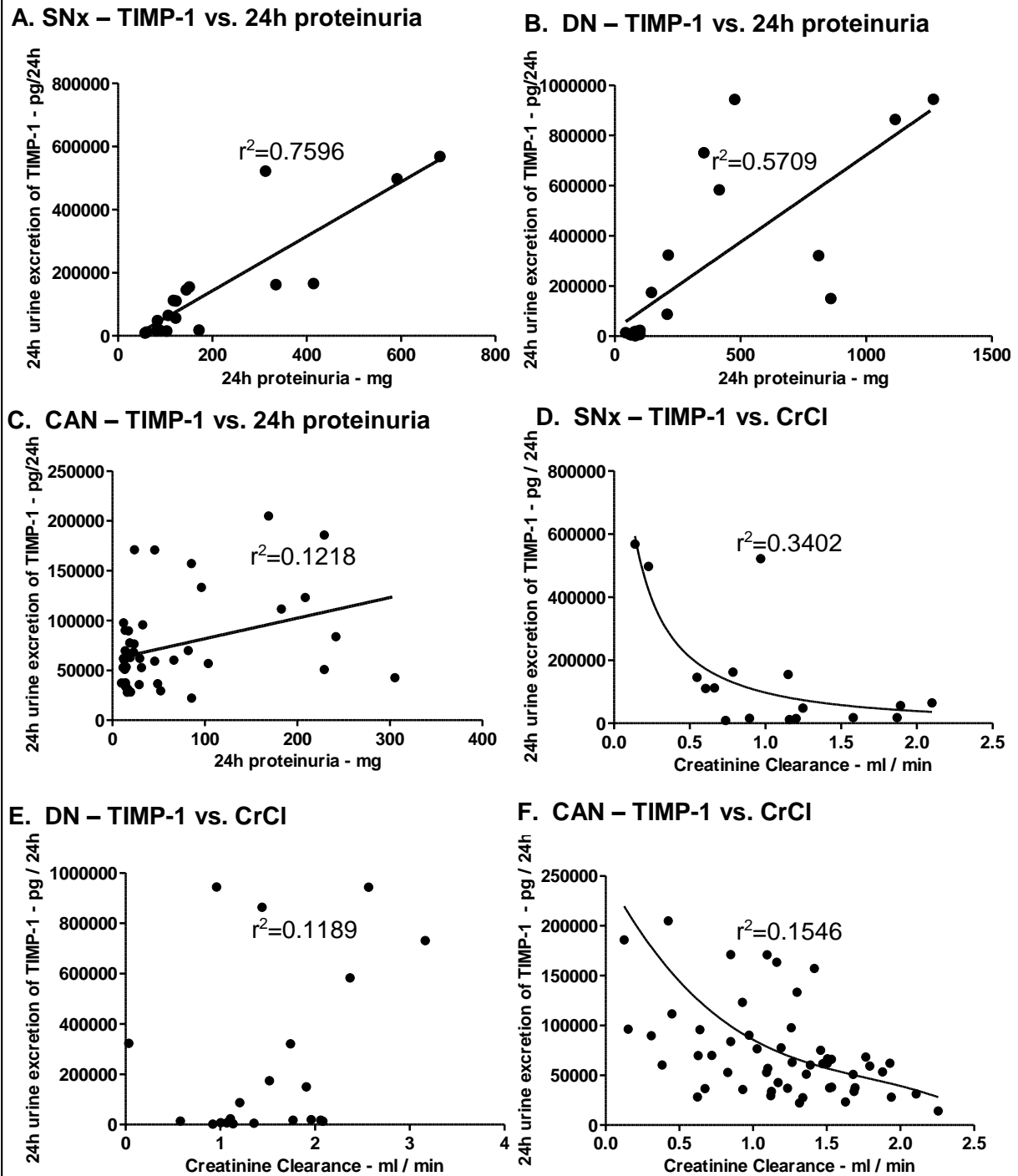


Figure 5.9: Pearson's correlations were performed for 24 hour urine TG2 excretion vs. 24 hour proteinuria in SNx (A), DN (B) and CAN (C) and then for 24 hour urine TG2 excretion vs. creatinine clearance in SNx (D), DN (E) and CAN (F). Statistical significance was shown as: NS= non statistical significant, * $p < 0.05$, ** $p < 0.01$, *** $p < 0.001$. $n=25$ in SNx and DN and $n=56$ in CAN.

5.3.3. Tissue inhibitor of metalloproteinase 2

In order to examine the presence of TIMP-2 in urines from rats submitted to experimental models of renal scarring (SNx, DN and CAN), TIMP-2 levels were analysed by the Gentaur Immunosorbent assay as described in section 3.11.1.2. Minimum detectable dose (MDD) of rat TIMP-2 was 0.36ng/ml.

5.3.3.1. Measurement of urine TIMP-2 in the 5/6th Subtotal nephrectomy model

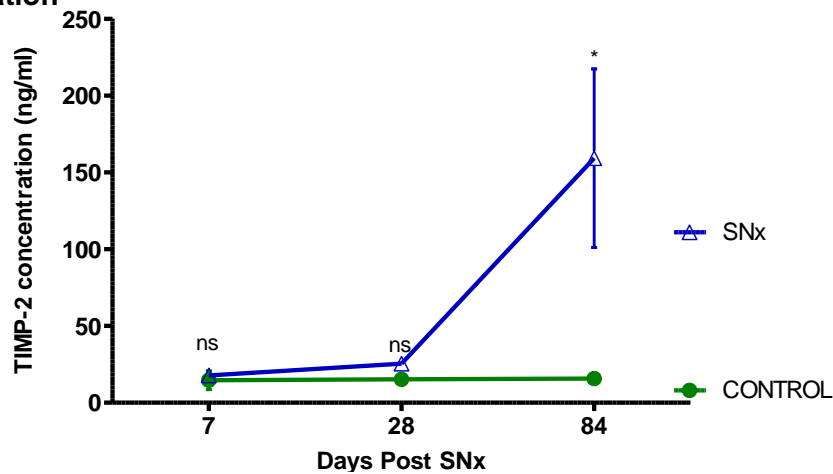
Urine TIMP-2 excretion on sham-operated rats was constant during the study (figure 5.10-A), ranging from 14.62ng/ml to 15.78ng/ml. Levels between controls and SNx rats was not different at 7 and 28 days after subtotal nephrectomy (*p=0.6446, **p=0.1160, one way ANOVA). However, increased urinary levels of TIMP-2 were observed in SNx samples by 3 months post subtotal nephrectomy, with a 10 fold increase in diseased animals (p=0.0390).

A comparison of 24 hour TIMP-2 excretion between SNx and sham-operated rats showed a significant increase from seven days after subtotal nephrectomy (figure 5.10-B). At one week, controls had an average TIMP-2 concentration of 52.76 ± 21.38 ng/24h whereas SNx was 370.1 ± 41.23 ng/24h (p=0.0024). By 1 month, SNx animals had a substantial increase to 727.0 ± 199.1 ng/24h (p=0.0279) and two months later, SNx animals had a 23 fold increase when compared to controls (p=0.0331).

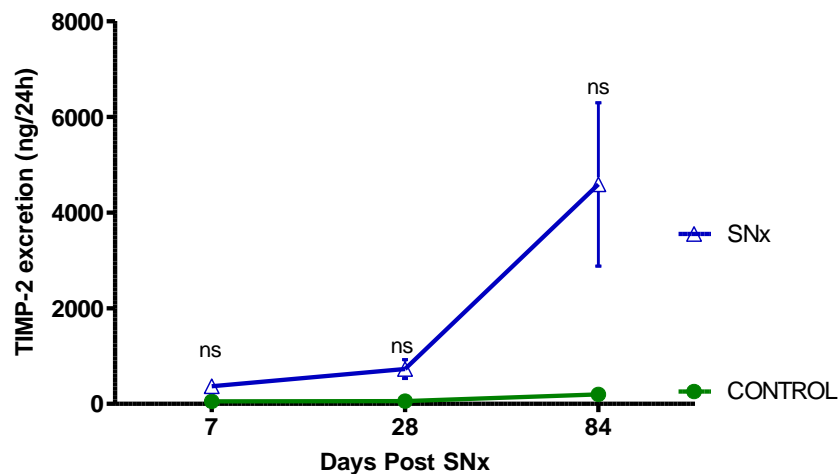
Normalising TIMP-2 excretion to creatinine showed progressive increases as renal scarring developed (figure 5.10-C). Early increases (1 week) are five times normal levels, p=0.0029. At 1 month, TIMP-2: Creatinine ratio was 7.6 fold greater than sham-operated rats, p =0.0379, while at 3 months this difference elevated to are 41.9 fold normal (p=0.0477) The TIMP-2: Creatinine ratio in sham operated rats ranged 0.87-1.90pg/mmol throughout the study.

Figure 5.10: TIMP-2 measurement in urine post SNx

A. Concentration



B. 24-hour



C. TIMP-2/Creatinine ratio

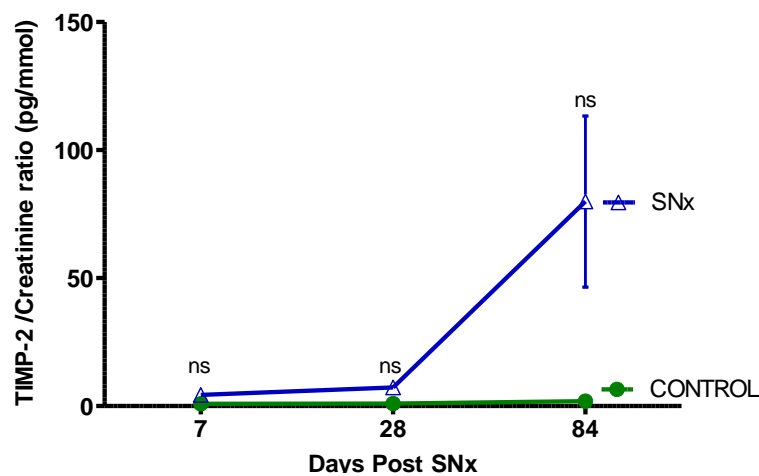


Figure 5.10: Urine TIMP-2 levels were measured in SNx samples at 7, 28 and 84 days post Subtotal nephrectomy by the Gentaur rat TIMP-2 Immunoassay and presented as concentration in pg/ml (A) 24 hour excretion (B) and as a Creatinine ratio (C). Statistical significance was tested with one Way ANOVA with Bonferroni post hoc test: NS= non statistical significant, * p<0.05, **p<0.01, ***p<0.001, between diseased samples and time matched control. Values are mean \pm SEM.

5.3.3.2. Measurement of urine TIMP-2 in the UNx STZ model of Diabetic nephropathy

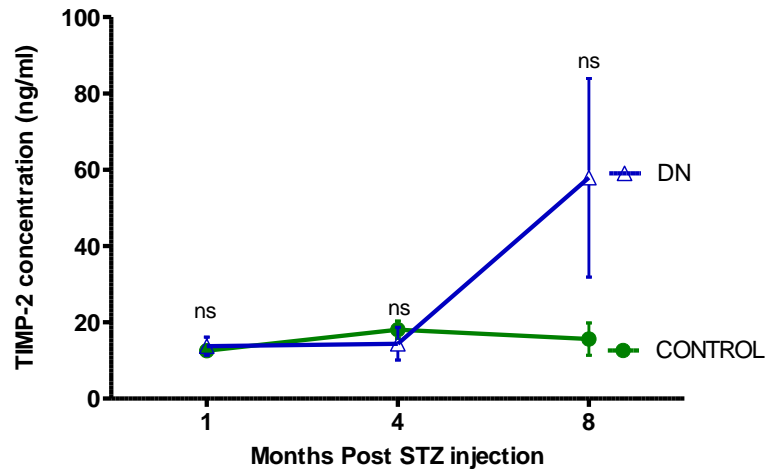
TIMP-2 concentration in diabetic urine samples followed a similar pattern to that in SNx samples, with controls rats' levels ranging from 12.56ng/ml to 18.04ng/ml (figure 5.11-A). At 1 month after STZ administration, urine TIMP-2 concentration was 13.77 ± 2.37 ng/ml, remaining at similar levels at 4 months (14.41 ± 4.27 ng/ml). By 8 months after hyperglycaemic induction, diseased animals had a mean urine TIMP-2 concentration 3.7 fold greater than controls. However, at no stage there was a significant difference between TIMP 2 levels in control and DN animals.

Sham-operated rats had a 24 hour TIMP-2 urine excretion varying from 43.45ng/24h to 123.32ng/24h, maximum excretion was noted at four months after surgery (figure 5.11-B). 24 hour TIMP-2 excretion steadily rose in the DN animals throughout the time course showing 10.9, 12.1 and 56.4 fold increase at month 1, 4 and 8 respectively (* $p=0.0571$, ** $p=0.0155$, *** $p=0.0365$, one way ANOVA) when compared to controls.

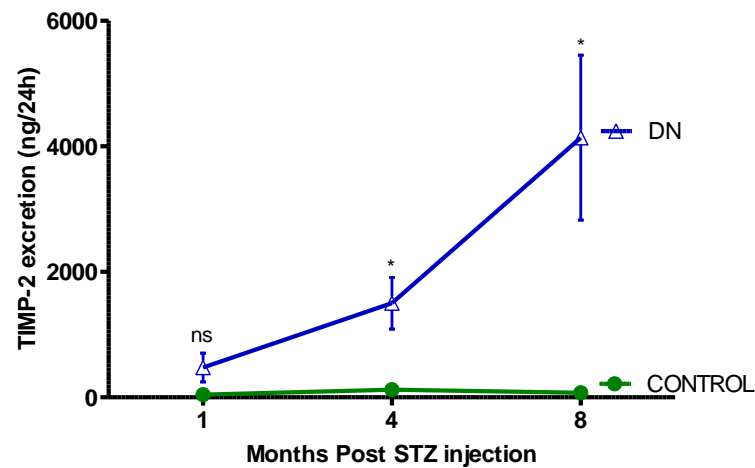
Urine TIMP-2 when corrected by creatinine was significantly elevated in 4 and 8 months diabetic animals only (figure 5.11-C). One month controls had an average TIMP-2: Creatinine ratio of $0.801 \pm 0.0.122$ pg/mmol, whilst in DN this was 5.178 ± 2.671 pg/mmol ($p=0.1081$). By four months, control rats had a slight increase to 1.449 ± 0.2459 pg/mmol, but diabetic animals were over six times higher at 9269 ± 2.299 pg/mmol ($p=0.0148$). At the end of the study, diabetic samples displayed an impressive 44.7 fold increase in the TIMP-2: Creatinine when compared to controls (37.90 ± 12.41 pg/mmol, $p=0.0405$).

Figure 5.11: TIMP-2 measurement in urine from the UNx STZ model of DN

A. Concentration



B. 24-hour



C. TIMP-2/Creatinine ratio

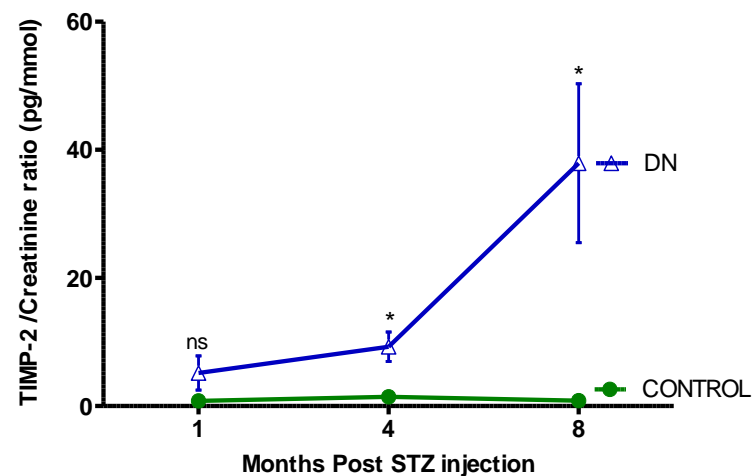


Figure 5.11: Urine TIMP-2 levels in DN samples at 1, 4 and 8 months post DN induction were measured by the Gentaur rat TIMP-2 Immunoassay and presented as concentration expressed in pg/ml (A), 24 hour excretion (B) and as a Creatinine ratio (C). Statistical significance was tested with one Way ANOVA with Bonferroni post hoc test: NS= non statistical significant, * p<0.05, **p<0.01, ***p<0.001, between diabetic samples and time matched control. Values are mean \pm SEM.

5.3.3.3. Measurement of urine TIMP-2 in the Fisher to Lewis transplant model of CAN

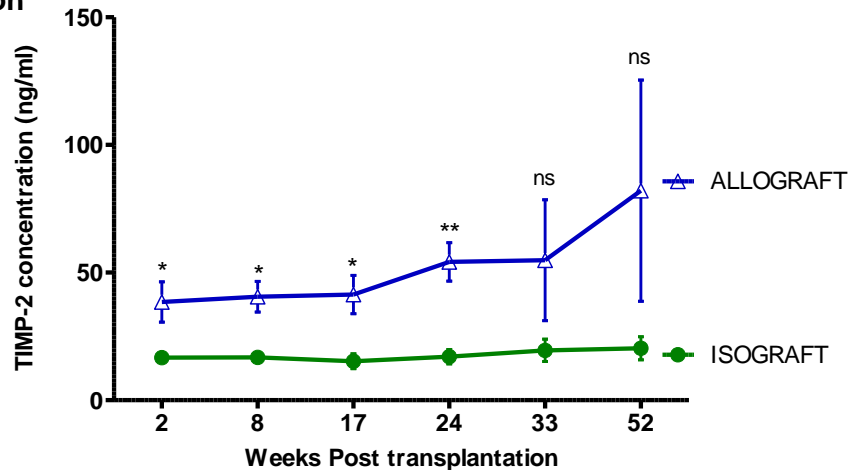
Urine TIMP-2 levels ranged between 16.69ng/ml to 20.36ng/ml on L-L isograft transplanted animals throughout the study (figure 5.12-A). F-L allografts showed significantly higher levels of TIMP-2 as early as two weeks after transplantation (38.45 ± 7.89 ng/ml, $p=0.0334$) and this gradually increased over 52 weeks to 82.10 ± 43.31 ng/ml, nonetheless this difference was significant only up to twenty four weeks (54.16 ± 7.51 ng/ml, $p=0.0036$).

24 hour urine excretion of TIMP-2 from L-L isografts, two weeks after transplantation was 286.3 ± 73.16 ng/24h ($n=5$) which remained unchanged for 52 weeks when the value was 231.7 ± 60.48 ng/24h (figure 5.12-B). F-L allografts progressively developed proteinuria, but they presented stable total volume of urine in twenty four hours. Two weeks after transplantation, total urinary TIMP-2 excretion from F-L allografts was significantly higher at 774.3 ± 260.1 ng/24h ($n=7$, $p=0.00242$), and this gradually increased over 52 weeks to 3347 ± 2160 ng/24h. In spite of this, again the difference was statistically significant only up to 24 weeks post transplantation.

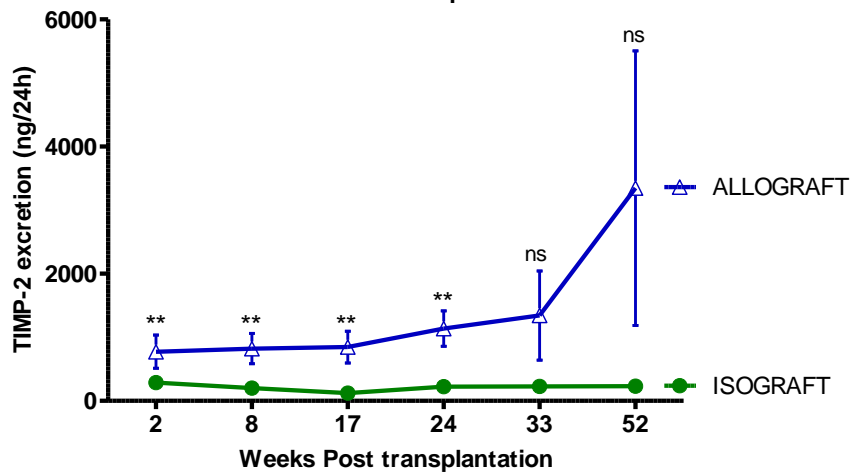
L-L isografts presented a slight decrease in the TIMP-2: Creatinine ratio during the study (figure 5.12-C). It declined from 3.81 ± 1.15 pg/mmol at two weeks to 2.10 ± 0.63 pg/mmol at termination by fifty two weeks. Interestingly, F-L allografts expressed significant increases in the TIMP-2: Creatinine ratio from week two up to 33 weeks of the study. However, it was not significant at termination. The TIMP-2: Creatinine varied from 12.21 ± 2.90 pg/mmol, $p=0.0311$ at the beginning of the study to 17.45 ± 10.76 pg/mmol, $p=0.0357$ at 33 weeks. By 52 weeks after kidney transplantation, F-L allografts had an average of 34.14 ± 21.02 pg/mmol of TIMP-2: Creatinine, $p=0.1143$ when compared to L-L isografts.

Figure 5.12: TIMP-2 measurement in urine from the in the Fisher to Lewis transplant model of CAN

A. Concentration



B. 24-hour



C. TIMP-2/Creatinine ratio

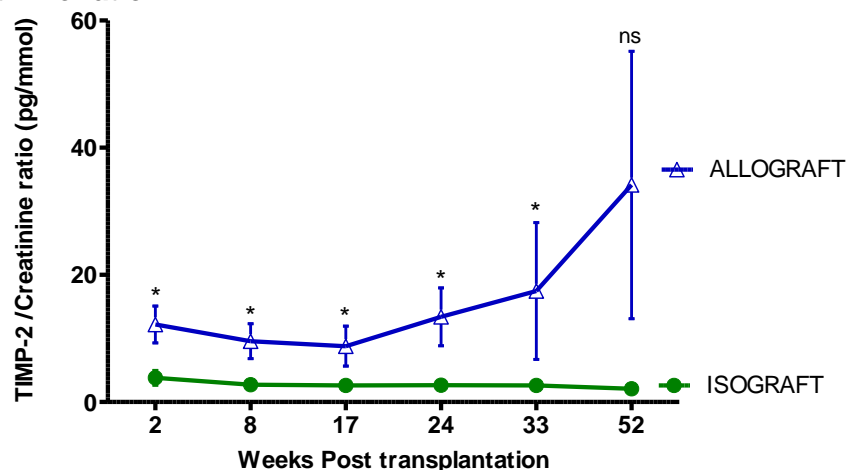


Figure 5.12: Urine TIMP-2 levels in the Fisher to Lewis transplant model of CAN over 12 months quantified by the Gentaur rat TIMP-2 Immunoassay and presented as concentration expressed in pg/ml (A), 24 hour excretion (B) and as a Creatinine ratio (C). Statistical significance was tested with one Way ANOVA with Bonferroni post hoc test: NS= non statistical significant, * p<0.05, **p<0.01, ***p<0.001, between F -L allografts and L-L isografts. Values are mean ± SEM.

5.3.4. Correlation between urine TIMP-2 and clinical markers of kidney function and damage

5.3.4.1. 24 hours proteinuria

24 hour urine TIMP-2 showed a positive linear association with twenty four hours proteinuria in all three models of renal scarring (figure 5.13-A, -B and -C). The strongest relationship was found with diabetic samples, where the higher the proteinuria excretion, the higher the total TIMP-2 levels (Pearson's $r = 0.8623$. 95% CI: 0.7085 to 0.9379. $p < 0.0001$, $r^2 = 0.7435$). A positive correlation was also found with CAN samples (Pearson's $r = 0.7799$. 95% CI: 0.6503 to 0.8654. $p < 0.0001$, $r^2 = 0.6083$) and in a smaller scale, with SNx samples (Pearson's $r = 0.6315$. 95% CI: 0.2859 to 0.8317. $p = 0.0016$, $r^2 = 0.3988$).

5.3.4.2. Creatinine Clearance

A correlation between 24 hour urine TIMP-2 and creatinine clearance demonstrated that the lower the kidney function, the higher the excretion of TIMP-2 in the SNx and CAN models of renal scarring. Animals submitted to SNx surgery presented a small, but significant negative relationship between urinary TIMP-2 and creatinine clearance (Pearson's $r = -0.4893$. 95% CI: -0.7604 to -0.07296. $p = 0.0244$, $r^2 = 0.2394$, figure 5.13-D). In the same way, transplanted animals had an inverse correlation between TIMP-2 excretion and kidney function (Pearson's $r = -0.4117$. 95% CI: -0.6088 to -0.1668. $p = 0.0016$, $r^2 = 0.1695$, figure 5.13-E). On the other hand, diabetic samples exhibited no correlation between urinary TIMP-2 and creatinine clearance (Pearson's $r = 0.003345$. 95% CI: -0.3666 to 0.4231. $p = 0.8739$, $r^2 = 0.0011$, figure 5.13-F).

Figure 5.13: Correlation plots of urine TIMP-2 excretion with markers of kidney function and damage in experimental models of renal scarring

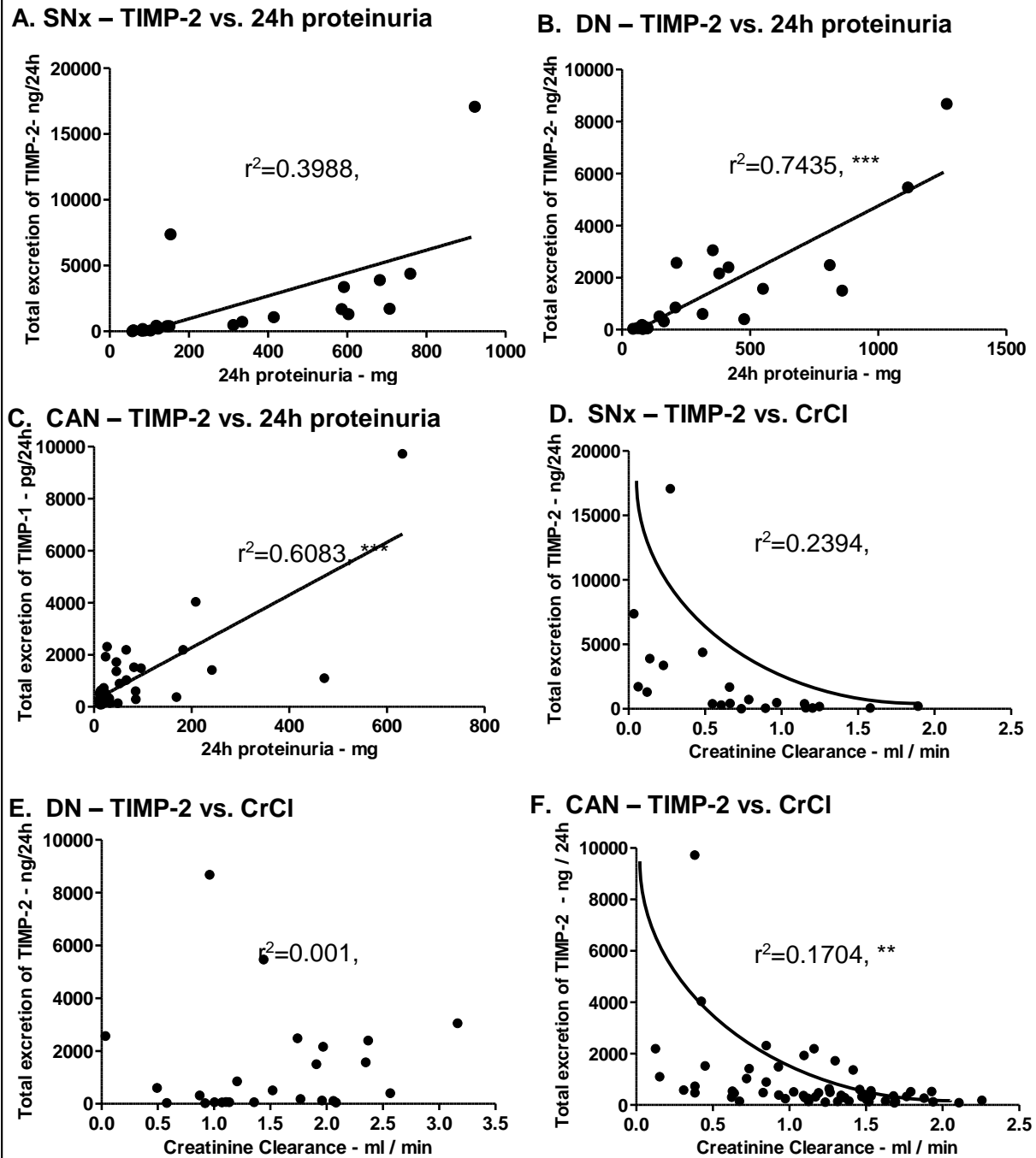


Figure 5.13: Pearson's correlations were performed for 24 hour urine TIMP-2 excretion vs. 24 hour proteinuria in SNx (A), DN (B) and CAN (C) and then for 24 hour urine TIMP-2 excretion vs. creatinine clearance in SNx (D), DN (E) and CAN (F) Statistical significance was shown as: NS= non statistical significant, * $p<0.05$, ** $p<0.01$, *** $p<0.001$. $n=25$ in SNx and DN and $n=56$ in CAN.

5.3.5. Tissue inhibitor of metalloproteinase 3

To evaluate the urine excretion of TIMP-3, we have used samples from two animal models of renal scarring (SNx and DN). Rat urine TIMP-3 was measured by an optimised Enzyme-linked immunosorbent assay from Gentaur Molecular products (section 3.11.1.2). Minimum detectable dose of rat TIMP-3 was 0.156ng/ml.

5.3.5.1. Measurement of urine TIMP-3 in the 5/6th Subtotal nephrectomy model

Urine TIMP-3 concentration on sham-operated rats varied between 0.18ng/ml to 0.56ng/ml throughout the study (figure 5.14-A). Oppositely to results for TIMP-1 and TIMP-2 levels, there was no statistical significance on uncorrected urine TIMP-3 concentration between controls and SNx rats at all time points of this study. Average urine TIMP-3 levels on SNx samples were 0.217 ± 0.116 ng/ml at seven days after surgery (* $p=0.8179$), then it had a slight increase at one month 0.370 ± 0.186 ng/ml (** $p=0.5289$), decreasing to a final concentration of 0.140 ± 0.026 ng/ml ($p=0.3893$) at 84 days post subtotalnephrectomy.

To quantify total urine TIMP-3 excretion, previously uncorrected TIMP-3 values were multiplied by the total volume of urine voided in twenty four hours (figure 5.14-B). Along with uncorrected TIMP-3 values, total TIMP-3 levels were not different between SNx and controls at 7, 28 and 84 days after SNx surgery (* $p=0.1738$, ** $p=0.0785$, *** $p=0.3925$, respectively

In contrast to TIMP-1 and TIMP-2, urine TIMP-3 to creatinine ratio was not significantly elevated on SNx samples even after correction by creatinine (figure 5.14-C). Average TIMP-3/Creatinine ratio ranged between 0.009 to 0.052pg/mmol on sham-operated rats during the three months of the study. On SNx animals, the TIMP-3: Creatinine ratio was 0.053 ± 0.002 pg/mmol, 0.090 ± 0.032 pg/mmol and 0.068 ± 0.018 pg/mmol at 7, 28 and 84 days respectively (* $p=0.2348$, ** $p=0.0817$, *** $p=0.2037$ to controls).

Figure 5.14: TIMP-3 measurement in urine post SNx

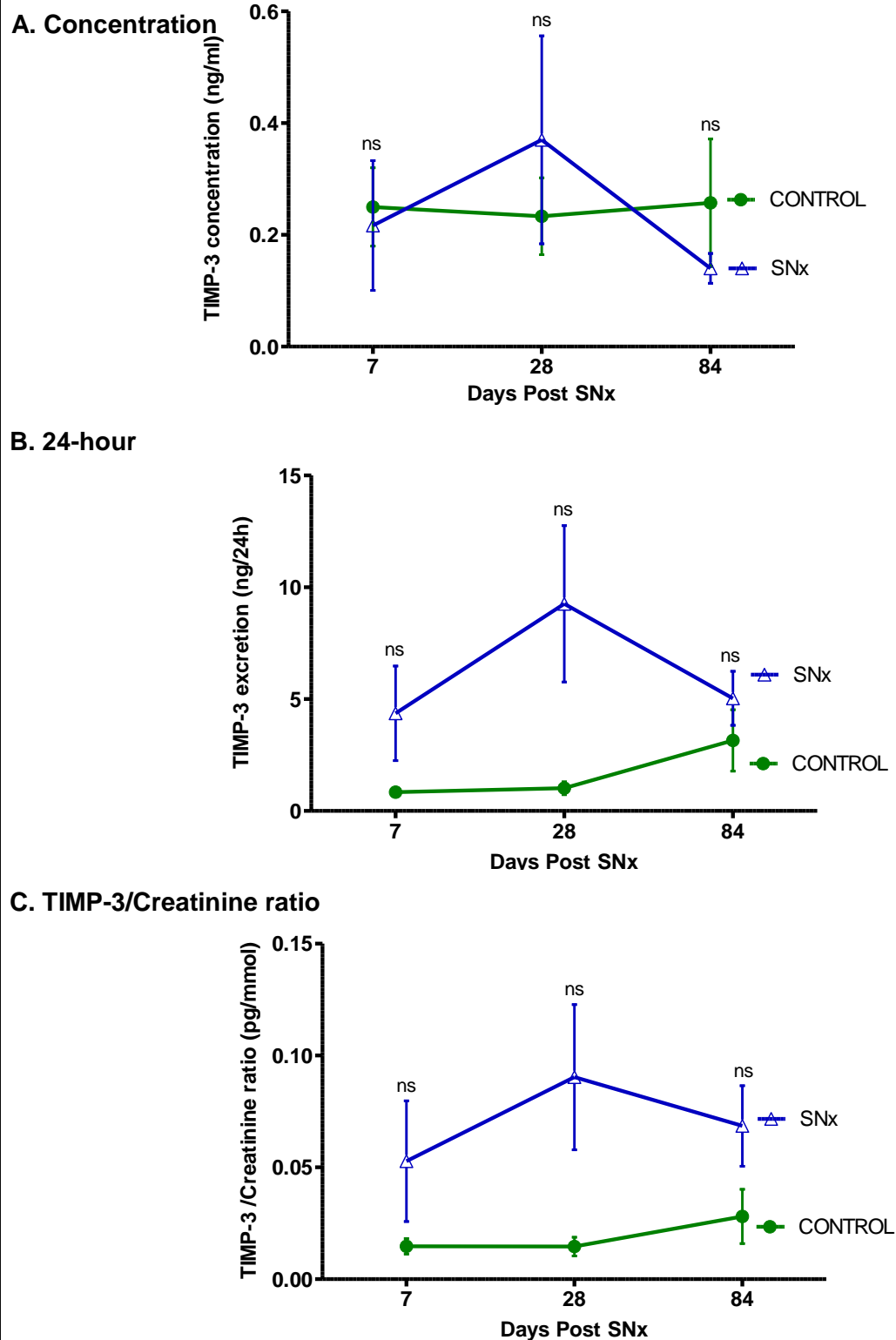


Figure 5.14: Urine TIMP-3 levels were measured in SNx samples at 7, 28 and 84 days post Subtotal nephrectomy by the Gentaur rat TIMP-3 Immunoassay and presented as concentration in pg/ml (A) 24 hour excretion (B) and as a Creatinine ratio (C). Statistical significance was tested with one Way ANOVA with Bonferroni post hoc test: NS= non statistical significant between diseased samples and time matched control. Data represents mean \pm SEM.

5.3.5.2. Measurement of urine TIMP-3 in the UNx STZ model of Diabetic nephropathy

Diabetic samples had significant urine levels of TIMP-3 at four and eight months after STZ injection (figure 5.15-A). At four months, urine TIMP-3 concentration was 63% higher in diabetic animals compared to controls ($p=0.0340$) and this difference increased to 142% by eight months ($p=0.0041$). Urine TIMP-3 concentration on controls was stable, with an average of 0.205ng/ml during the study.

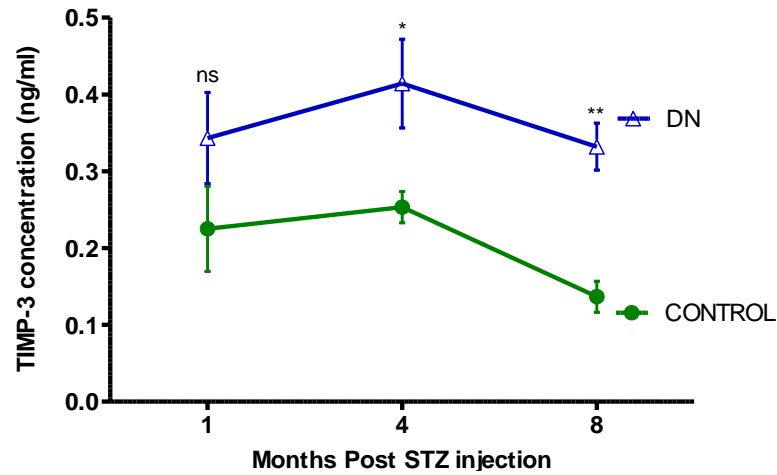
In diabetic animals, 24 hour TIMP-3 levels were much higher than in SNx (figure 5.15-B). This fact was due to the elevated volume of urine that diabetic animals produced. Nevertheless, sham-operated rats presented a similar range of total TIMP-3 excretion in both models of renal scarring (0.58 to 3.15ng/24h).

Total TIMP-3 excretion was markedly increased on diabetic rats at four months (29 fold higher than controls, $p=0.0032$, one way ANOVA with Bonferroni post test) and this persisted over the following four months reaching a 50 fold increase ($p=0.0224$) at termination time.

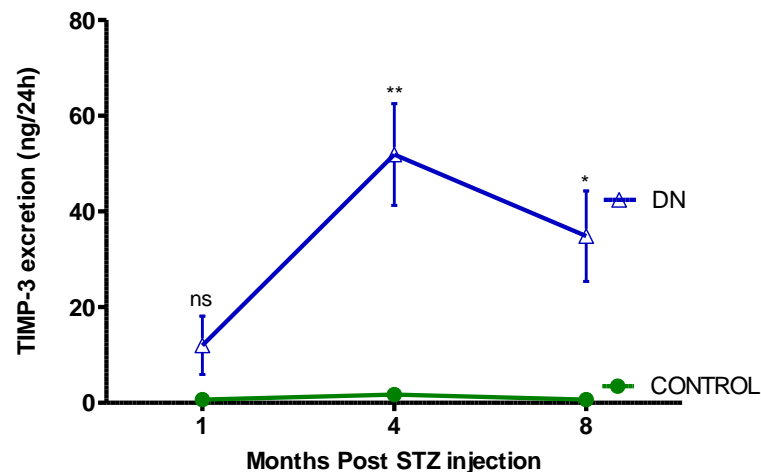
Diabetic animals showed progressive increase in the TIMP-3: Creatinine ratio, suggesting that the pattern on TIMP-3 excretion follows disease progression in this disease (figure 5.15-C). One month after STZ injection, the TIMP-3:creatinine ratio in diabetic rats was around nine times higher than controls, however due to the large spread of measurements it failed to achieve significance ($p=0.1082$, two way ANOVA with Bonferroni post test). Four months after DN induction, the TIMP-3: creatinine excretion from diabetic animals was significantly higher at 0.3236 ± 0.0527 pg/mmol ($p=0.0012$), and persisted at eight months with a 32 fold increase compared to controls.

Figure 5.15: TIMP-3 measurement in urine from the UNx STZ model of DN

A. Concentration



B. 24-hour



C. TIMP-3/Creatinine ratio

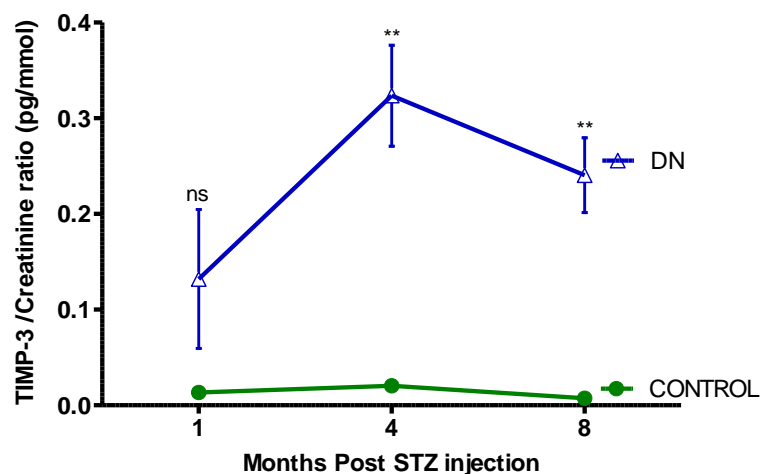


Figure 5.15: Urine TIMP-3 levels in DN samples at 1, 4 and 8 months post DN induction were measured by the Gentaur rat TIMP-3 Immunoassay and presented as concentration expressed in pg/ml **(A)**, 24 hour excretion**(B)** and as a Creatinine ratio **(C)**. Statistical significance was tested with one Way ANOVA with Bonferroni post hoc test: NS= non statistical significant, * p<0.05, **p<0.01, ***p<0.001, between diabetic samples and time matched control. Values are mean ± SEM.

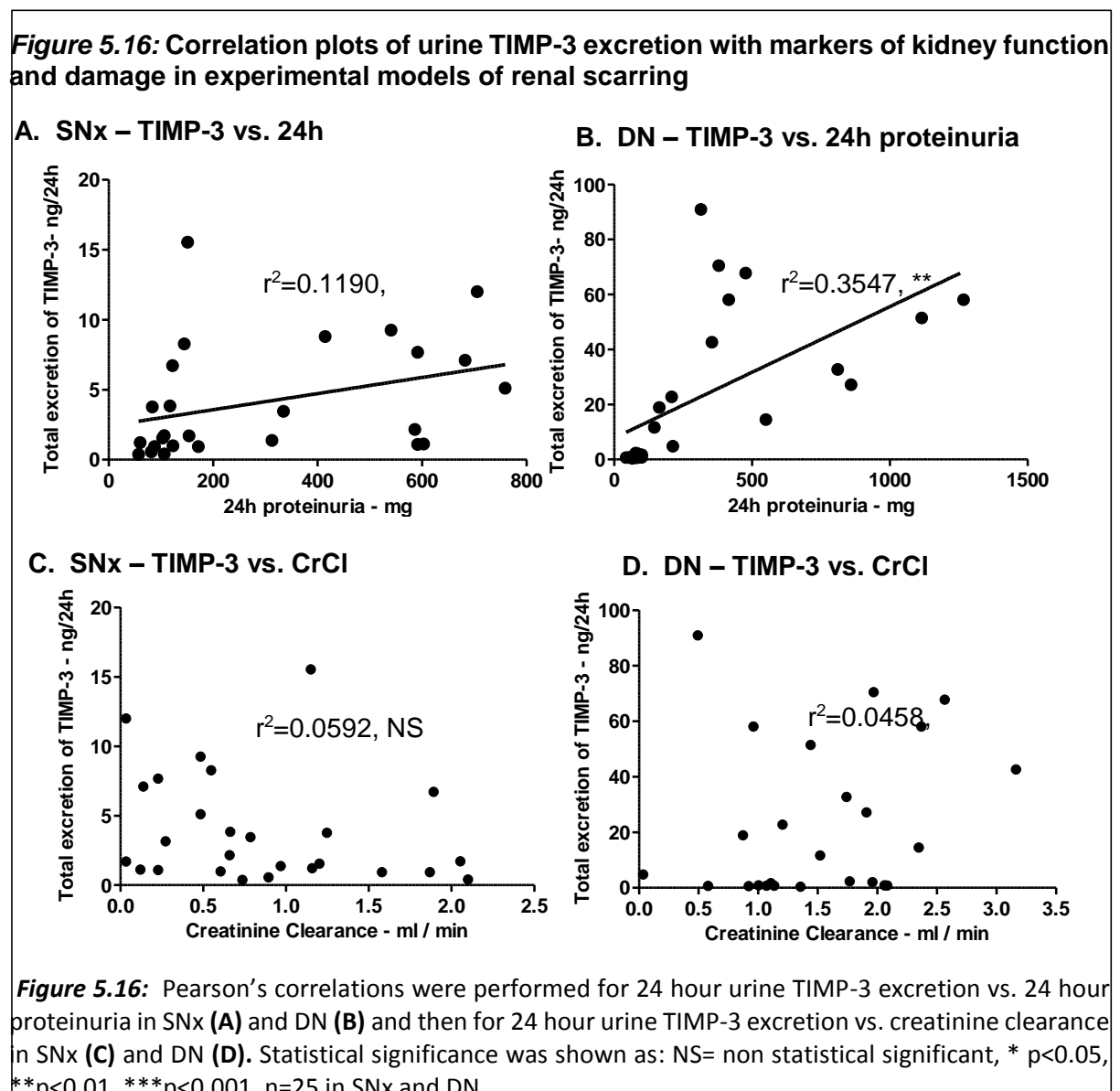
5.3.6. Correlation analysis for urine TIMP-3

5.3.6.1. 24h proteinuria

Total urinary TIMP-3 was not associated with twenty four hours proteinuria in the SNx model (Pearson's $r = 0.3449$. 95% CI: -0.0491 to 0.6460. $p=0.0844$, $r^2=0.1190$, figure 5.16-A). However, a linear positive correlation was observed in diabetic samples (Pearson's $r = 0.5955$. 95% CI: 0.2620 to 0.8020. $p=0.0017$, $r^2=0.3547$, figure 5.16-B).

5.3.6.2. Creatinine Clearance

Urine TIMP-3 was not correlated with variations in kidney function in the neither the SNx model (Pearson's $r = -0.2434$. 95% CI: -0.5765 to -0.1500. $p=0.2308$, $r^2=0.0592$, figure 5.16-C), nor the diabetic model (Pearson's $r = -0.2141$. 95% CI: -0.1979 to 0.5618. $p=0.3041$, $r^2=0.0458$ figure 5.16-D).



5.4. Plasminogen activator inhibitor type 1 (PAI-1)

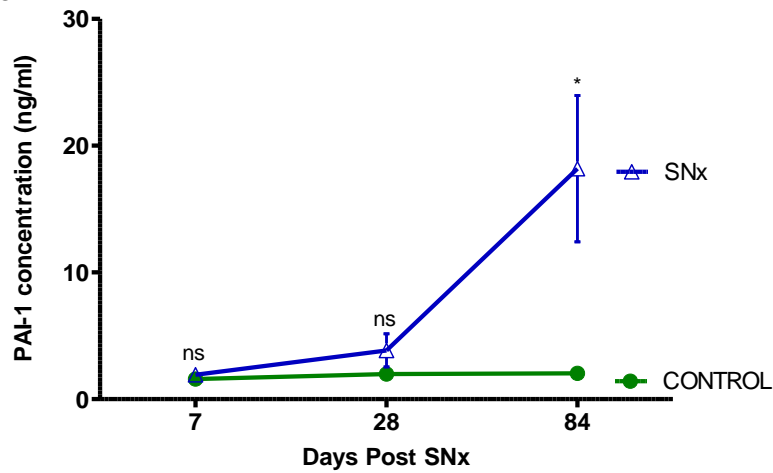
5.4.1. Measurement of PAI-1 in urine from the 5/6th Subtotal Nephrectomy model

Average concentration of PAI-1 in normal urine was 1.59 ± 0.19 pg/ml at 1 week after subtotal nephrectomy and remained stable at 2.04 ± 0.10 pg/ml until termination at 3 months. Post SNx urine PAI-1 levels were not significantly higher than controls at 1 week (1.93 ± 0.09 pg/ml, $p=0.1927$) and at 1 month (3.85 ± 1.31 pg/ml, $p=0.2385$). However, it increased by 84 days reaching 18.18 ± 5.77 pmol/mg ($p=0.0162$, figure 5.17-A).

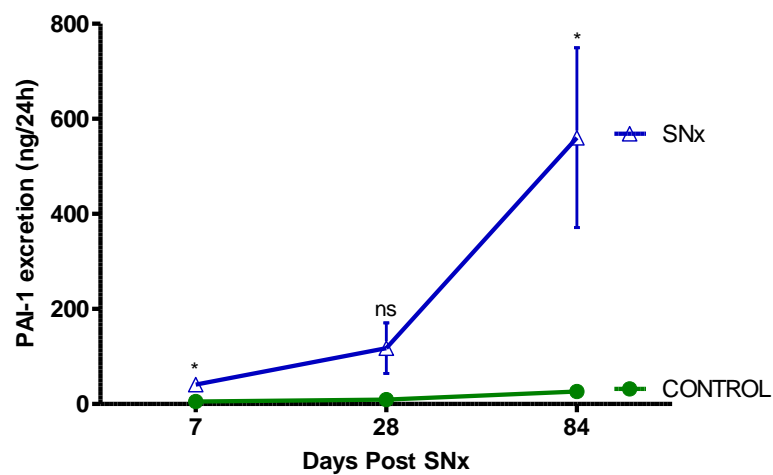
After adjustment of concentration with 24 hour urine volume, urine PAI-1 excretion in twenty four hours in control urines ranged between 5.38 to 26.17pg/24h (figure 5.17-B). Urine PAI-1 excretion in 24 hours was significantly increased in the SNx at 1 week and 3 months ($p=0.0211$ and $p=0.0154$ respectively), however this increase was not significant at 1 month post SNx ($p=0.1115$). Despite correction by creatinine ratio, figures were similar to 24 hour excretion where no statistical difference was observed between controls and SNx animals at one month ($p=0.0959$, figure 5.17-C).

Figure 5.17: PAI-1 measurement in urine post SNx

A. Concentration



B. 24-hour



C. PAI-1/Creatinine ratio

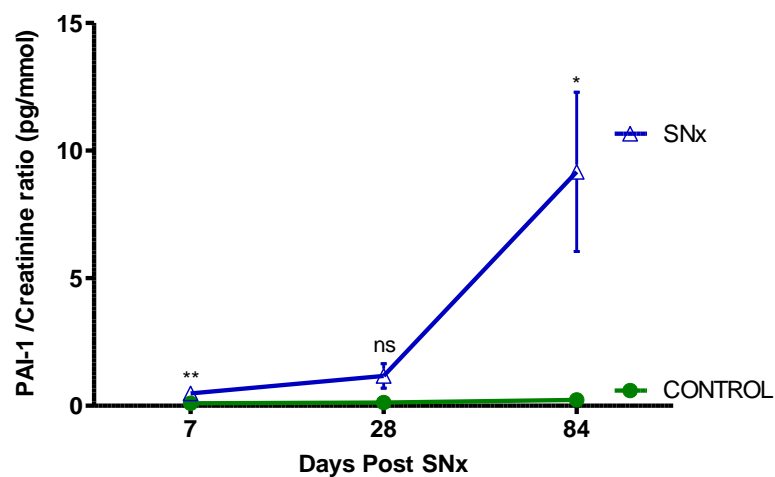


Figure 5.17: Urine PAI-1 excretion was measured in SNx samples at 7, 28 and 84 days post Subtotal nephrectomy by cation-exchange chromatography and presented as concentration in nmols/mg protein (A) 24 hour excretion (B) and as a Creatinine ratio (C). Statistical significance was tested with one Way ANOVA with Bonferroni post hoc test: NS= non statistical significant, * p<0.05, **p<0.01, ***p<0.001, between diseased samples and time matched control. Data represents mean SEM.

5.4.2. Measurement of PAI-1 in urine from the UNx STZ model of Diabetic Nephropathy

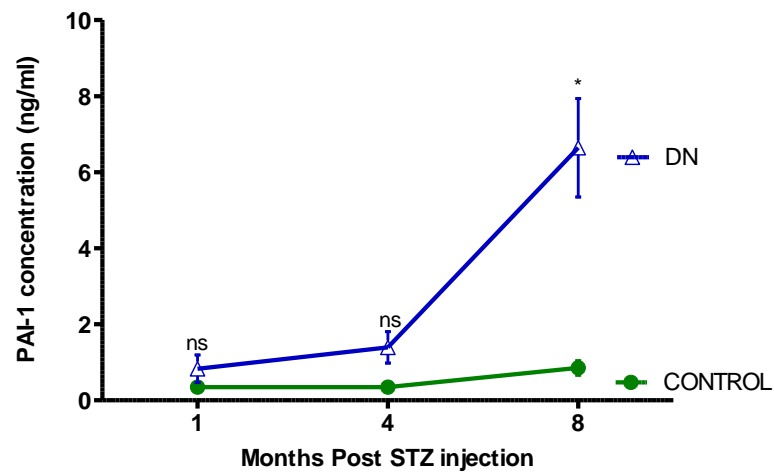
In a similar manner to the SNx model, urine samples from the UNx STZ model of Diabetic Nephropathy did not present increased levels of PAI-1 at early stages of the disease ($p=0.3425$ at 1 month after DN induction, figure 5.18-A). Urine PAI-1 concentration in DN samples was only significantly elevated by 8 months ($p=0.0114$) when levels reached 6.64 ± 1.29 ng/ml, whereas sham operated controls had urine PAI-1 concentration ranging from 0.35 to 0.85ng/ml throughout the study.

PAI-1 urine concentration was also adjusted to 24 hours excretion in DN samples. Interestingly, after adjustment to daily volume, values were significantly increased in 1 and 4 months diabetic animals ($p=0.0366$ and $p=0.0384$ respectively, figure 5.18-B). Nonetheless, despite the high PAI-1 levels by 8 months, it didn't reach significance when compared to controls ($p=0.0766$) to a large data spread.

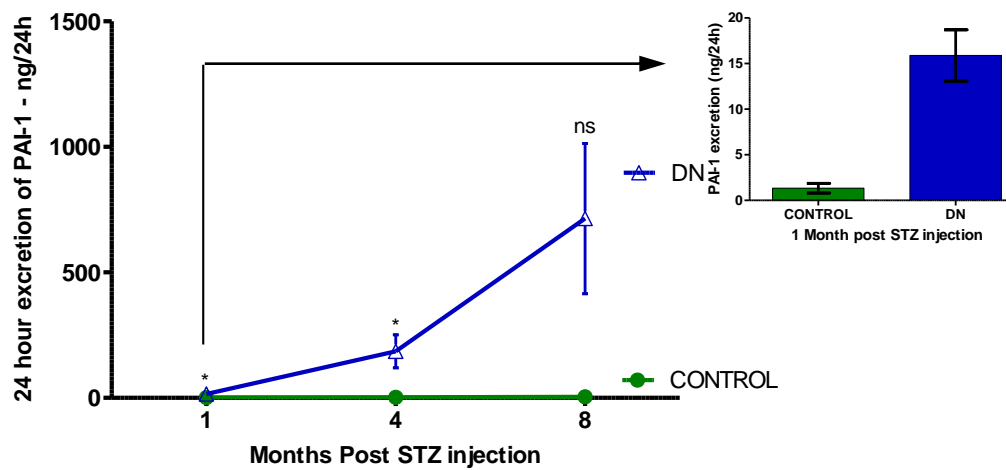
Expressing urine PAI-1 excretion as a creatinine ratio showed that it was significantly elevated at all time points (figure 5.18-C). Urine PAI-1 to creatinine ratio was 6, 41 and 108 fold higher than matched controls at 1, 4 and 8 months after STZ injection ($p=0.0022$, $p=0.0320$ and $p=0.0222$ respectively). Average values in controls ranged from 0.287 to 0.0467.

Figure 5.18: PAI-1 measurement in urine from the UNx STZ model of DN

A. Concentration



B. 24-hour



C. PAI-1/Creatinine ratio

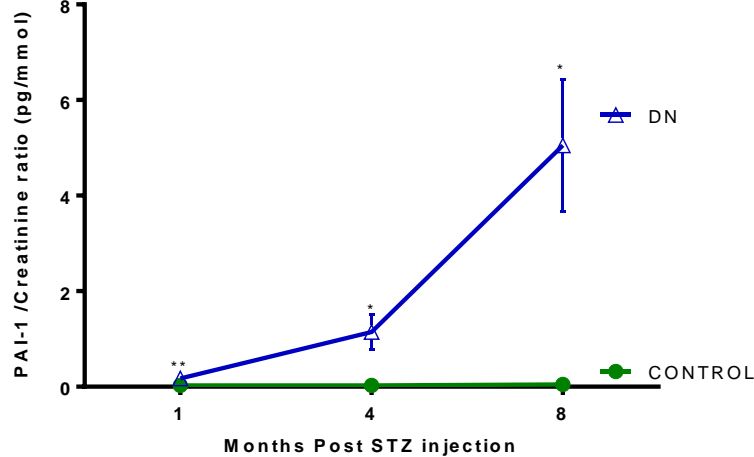


Figure 5.18: Urine PAI-1 excretion was measured in DN samples at 1, 4 and 8 months post STZ injection by cation-exchange chromatography and presented as concentration in nmols/mg proteins **(A)** 24 hour excretion **(B)** and as a Creatinine ratio, with in set paragraph showing differences at 1 month **(C)**. Statistical significance was tested with one Way ANOVA with Bonferroni post hoc test: NS= non statistical significant, * $p < 0.05$, ** $p < 0.01$, *** $p < 0.001$, between diabetic samples and time matched control. Data represents mean \pm SEM.

5.4.3. Correlations between PAI-1 and clinical markers of renal function and damage

5.4.3.1. 24h proteinuria

In the 5/6th subtotal nephrectomy model of renal scarring, correlation between 24 hour urine PAI-1 excretion and 24 hour proteinuria showed a strong positive association (n=28, Pearson's $r=0.5217$, 95% CI: 0.1848 to 0.7491, $r^2=0.2722$, $p=0.0044$) (figure 5.19-A).

A similar correlation was also found in the UNx STZ model of DN where PAI-1 excretion was highly correlated with proteinuria (n=25, Pearson's $r = 0.8816$, 95% CI: 0.7422 to 0.9479, $r^2=0.7773$, $p<0.0001$) (figure 5.19-B).

5.4.3.2. Creatinine clearance

To determine whether the urine excretion of PAI-1 was associated with changes in kidney function, a correlation of PAI-1 urine concentration with creatinine clearance was performed. In the SNx model, there was a negative association (Pearson's $r=-0.4475$, 95% CI: -0.7073 to -0.08121, $r^2=0.2003$, $p=0.0193$) with CrCl, indicating that the higher the PAI-1 excretion the lower the creatinine clearance (figure 5.19-C).

In the same way, there was a negative correlation between PAI-1 excretion and creatinine clearance in Diabetic samples. However, it did not reach any statistical significance (Pearson's $r=-0.02820$, 95% CI: -0.4268 to 0.3796, $r^2=0.0008$, $p=0.8959$, figure 5.19-D).

Figure 5.19: Correlation plots for PAI-1

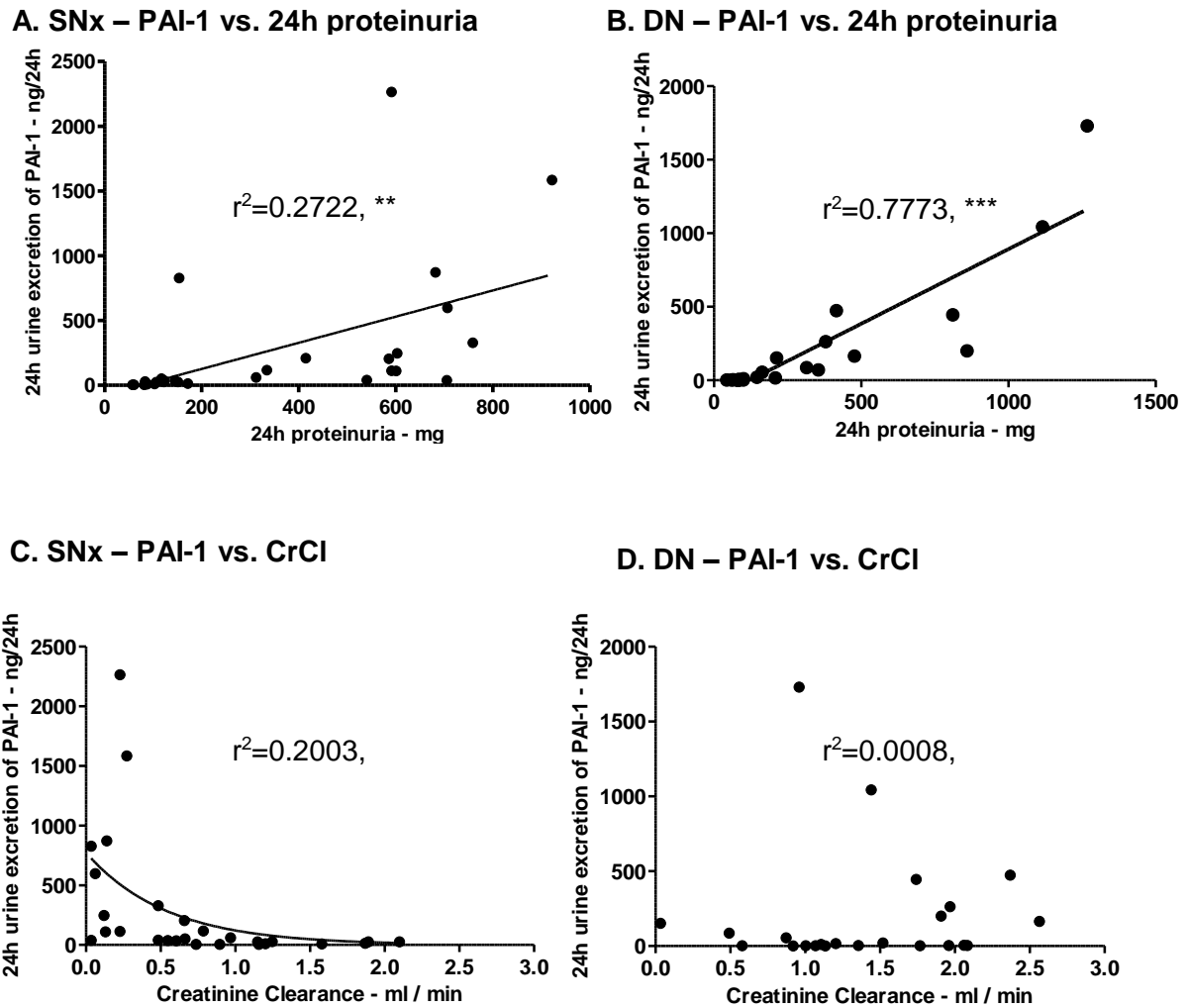


Figure 5.19: Pearson's correlations were performed for 24 hour urine PAI-1 excretion vs. 24 hour proteinuria in SNx (A) and DN (B) and then for 24 hour urine PAI-1 excretion vs. creatinine clearance in SNx (C) and DN (D). NS= non statistical significant, * $p<0.05$, ** $p<0.01$, *** $p<0.001$. $n=28$ in SNx and 25 DN.

5.5. Discussion

In this study, we have been able to quantify MMPs 1 and 9 as well as their inhibitors; TIMPs 1, 2 and 3 plus PAI-1 in rat urines obtained from three different models of kidney scarring. This was obtained by using commercially available immunoassays. We observed that urine MMP-1 when corrected to creatinine ratio was significantly increased in SNx animals at all time points and in 4 and 8 months diabetic animals. On the other hand, MMP-9 excretion was undetectable on all control samples and it had a steady, but not significant rise on SNx and Diabetic animals even when correcting by creatinine.

Urine TIMP-1 concentration showed no difference between diseased (SNx and DN) and control samples at early stages of the disease. However, diabetic samples presented a significantly higher excretion of TIMP-1 at 4 months. Reduction on this excretion by 8 months could be due to a decrease on glomerular filtration rate found on very late stages of the disease. After normalizing for urine creatinine concentration, corrected TIMP-1 excretion was significantly higher on SNx samples at all time points and on DN samples at 4 and 8 months. In the Fisher to Lewis transplant mode of CAN, urine concentrations of TIMP-1 were similar between F-L allografts and L-L isografts during the entire study, with significant increase on F-L allografts at 17 and 24 weeks only when values were expressed as total excretion in 24 hours. Overall, urine TIMP-1 excretion showed a very good correlation with disease progression in SNx and CAN samples. However, there was a lack of relationship with creatinine clearance in DN samples which also occurred with previous biomarkers (TG2 and ϵ (γ -glutamyl) lysine).

SNx, DN and CAN animals had a similar pattern in relation to urine TIMP-2 excretion. Urine TIMP-2 concentration in SNx samples was only elevated by 3 months post subtotal nephrectomy. However, by correcting to a creatinine ratio, TIMP-2 excretion showed a substantial increase in SNx animals as early as 7 days until the end of the study suggesting that it might have a good potential as a biomarker of kidney scarring caused by hypertension. F-L allografts also showed significantly higher levels of TIMP-2 as early as two weeks after transplantation when compared to L-L isografts, but not by the end of the study. Interestingly, TIMP-2: Creatinine ratio in F-L allografts was significantly increased from week two up to 33 weeks of the study. However, it was not significant at termination. In diabetic animals, TIMP-2: Creatinine ratio was significantly elevated at 4 and 8 months only. In addition, correlating urine TIMP-2 and creatinine clearance demonstrated that the lower the kidney function, the higher the excretion of TIMP-2 in the SNx and CAN models of renal scarring. Nevertheless, no relationship was observed between urine TIMP-2 and creatinine clearance in diabetic

animals. This discrepancy on diabetic samples may be due to hyperfiltration observed at initial stages of the disease and the prolonged onset until the disease has been established.

Urinary TIMP-3 excretion was not linked to decreased renal function on both models of renal scarring (SNx and DN). This indicates that urinary TIMP-3 measurements by itself have little value as a marker of kidney disease progression

The second part of this study is concerned with the measurement of Plasminogen Activator Inhibitor 1. PAI-1 was specifically quantified in SNx and DN samples as CAN archival samples became depleted. Its quantification was performed by using a commercially available ELISA kit. PAI-1 measurement was not significantly increased at earlier stages of both diseases, displaying a similar behaviour as TIMP-1 excretion which substantiates their action on ECM clearance. Urine PAI-1 concentration was especially elevated at 3 months SNx ($p=0.0162$) and 8 months DN ($p=0.0114$). Although the PAI-1/creatinine ratio became elevated as diseased progressed on DN samples, it did not follow the same pattern in SNx. This was an interesting outcome as previous research had showed an over expression of both TIMP-1 and PAI-1 in kidney tissue in CKD. This suggests that the TIMP-1 clearance system displays a much greater and earlier changes than PAI-1. Thus, as our main interest is to detect molecules that could act as better early biomarkers of all CKD causes, we excluded PAI-1 as a suitable candidate for pursuing further research in human urine samples.

From this chapter, the one point that is apparent is the current relationship between twenty four hours proteinuria and clinical markers of kidney scarring. Such outcome could suggest that the increase in the urine levels of the above markers might be a reflection of the protein excretion. However, correction to a creatinine ratio allowed control for variation in urine flow rate and better reflection on their truthful output. Furthermore, a strong negative relationship with CrCl was observed, which correlates with disease progression and agrees with previously published literature in tissue levels.

Of all measured biomarkers in this chapter, TIMPs 1 and 2 as well as MMP-1 have most potential to move forward to human studies as highly significant levels were observed in early stages of disease and such elevations were in line with disease progression. Whereas PAI-1 levels in the urine were either undetectable or close to limit of detection and therefore, unworthy of further investigations.

**Chapter 6 – Urine Hydroxyproline quantification
in experimental renal scarring as a measure of
total collagen levels**

6.1. Introduction

The progression of Chronic Kidney Disease is characterised by a relentless fibrosis of the kidneys due to an excessive accumulation of extracellular matrix. Histologically, this progressive accumulation of ECM is driven by the increased deposition of structural proteins such as collagen I, III and IV, laminin, nidogen, fibronectin and proteoglycans. As well as increased deposition of its components, a decrease in the activity of ECM degrading enzymes such as plasmin and MMPs, either due to increased expression of their respective inhibitors or reduced activation of the latent enzyme, can lead to ECM accumulation.

Collagens are the most abundant proteins in connective and interstitial tissues being the major component of the extracellular matrix. So far 27 types subdivided into 9 subfamilies based on their structures had been found in humans; the most important ones are the fibrillar collagens such as Type I (major component of tendon, ligament and, bones), Type II (cartilage) and Type III (arteries, intestine, uterus and renal interstitium), and basement membrane collagens such as Type IV that form network-like structures (basal lamina of epithelia, glomerular and tubular basements membranes) (Kadler *et al.* 2007). They are mainly synthesized by fibroblasts (especially collagen types I and III), osteoblasts, chondrocytes and mesangial cells, although epithelial cells (especially collagen IV) can also synthesise them. Collagen maturation is a multistep process characterised by a large number of co and post-translational modifications mediated by highly specific enzymes (e.g. prolyl 3-hydroxylase, prolyl 4-hydroxylase, & Lysyl Hydroxylase amongst others). The final collagen molecule will consist of three hydrogen bonded polypeptide α chains forming a super helix with non-collagenous sequences at their termini. Collagens are composed of polypeptide chains containing at least one domain with Gly-X-Y sequences (X; Proline and Y; 4-Hydroxyproline) (Prockop and Kivirikko 1995). They are formed by the amino acids glycine, proline, Hydroxyproline and Hydroxylysine. As Hydroxyproline ($C_5H_9O_3N$) is the major component of the collagens and found in few other proteins rather than collagen (e.g.; elastin), its measurement is commonly used an indicator of the presence of collagen.

Previous studies have established that an increased synthesis and deposition of collagen into the ECM underlies the development of CKD. However, most studies are limited to the investigation of *tissue* collagen, although there are some studies where urine and circulating levels of collagens III and IV respectively were also found to be increased in patients with nephropathies (Soylemezoglu *et al.* 1997). The limitations of these studies are both a small number of CKD cases studied and the fact that they had a very restricted subset of collagens

investigated which makes the robustness of the analysis difficult to interpret. Hydroxyproline has been used as a measure of total collagen successfully before, but this has been in acute kidney injury in rats due to melamine and cyanuric acid nephrotoxicity (Schnackenberg *et al.* 2012) rather than CKD. Given that CKD is characterised by an excessive accumulation of numerous collagens, there is therefore a strong reason to believe these increases in collagen can be measured in the urine of patients with CKD by hydroxyproline levels, and if so does the level of hydroxyproline reflects the rate of disease progression or stage. Therefore, this chapter will test the hypothesis that the measurement of urinary Hydroxyproline could be used as a non-invasive indicator of kidney scarring as its presence is an indicator of ECM deposition.

To test this hypothesis, this chapter aims to:

1. Establish if it is possible to detect hydroxyproline in urine robustly.
2. Determine the presence of the urinary collagen metabolite Hydroxyproline in urine samples obtained from three animal models of renal scarring: SNx, DN and CAN.
3. Determine whether changes in urine levels of Hydroxyproline are reflected by parallel changes in kidney function.
4. Determine if the analysis of the urinary levels of Hydroxyproline could provide a non-invasive tool for CKD assessment in clinical studies.

For Hydroxyproline measurement, samples containing 10mg of protein were submitted to complete hydrolysis in a 6M solution of HCl at 110°C for 18 hours followed by freeze drying and fractionation onto a Biochrom 30 Amino acid Analyser (AAA) using a standard lithium and pH gradient. The concentration of Hydroxyproline was obtained from a 440 nm profile by reference to a 10 nmols / 20ul standard (full method is described in section 3.5.3.).

6.2. Optimization of Hydroxyproline measurement by cation exchange chromatography

A Hydroxyproline peak is observed in the standard physiological solution at a retention time of approximately 24-26 minutes (full methodology in section 3.5.7.2) when fractionated on a AAA. However the initial run of hydrolysed urines from both normal and SNx containing 2mg of protein each, showed a Hydroxyproline peak just on the limit of detection for the AAA (figure 6.1-A) and thus it was necessary to establish if this was both the correct peak and the sensitivity of the system. Therefore, two samples were spiked with 1mg/ml Collagen type I (Sigma-Aldrich, UK) to confirm the hydroxyproline peak. Both spiked samples showed an amplified hydroxyproline peak at around 24-26 minutes, confirming its detection and correct retention time. Considering the amount of Collagen that was added to each sample (1mg) and the amount of hydroxyproline detected without its addition, it was possible to calculate a percentage recovery percentage of 77% and that hydroxyproline detection by the AAA could be optimised by decreasing the temperature in which the lithium citrate buffer 1, pH 2.80 runs from 31°C to 30°C and also by increasing the loading to 10mg protein (figure 6.1).

Figure 6.1: Validation of Hydroxyproline measurement in urines

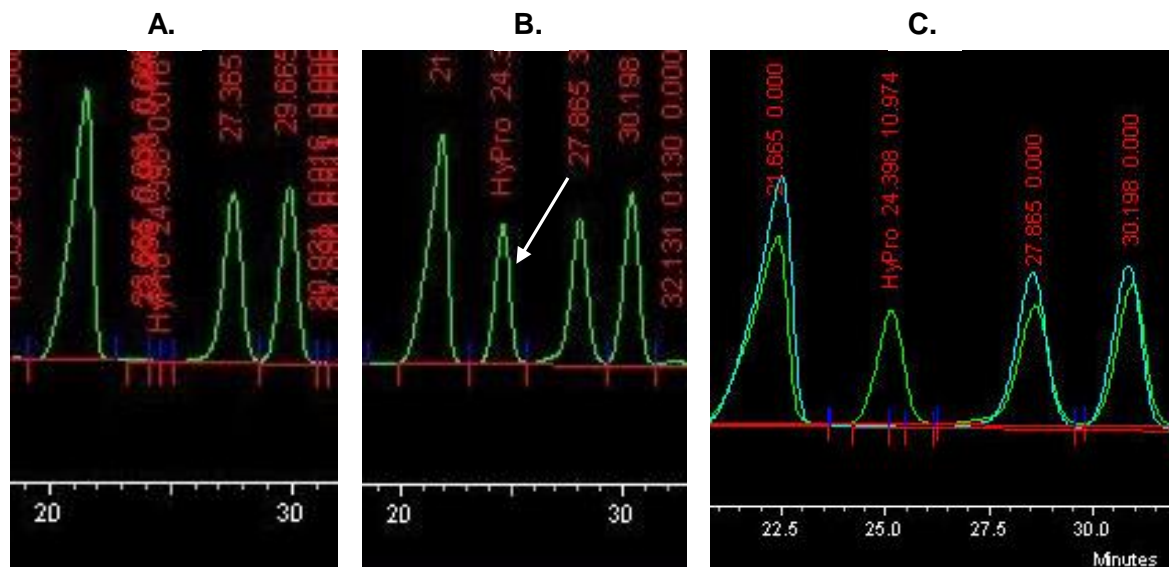


Figure 6.1: (A) The Hydroxyproline peak should be between Aspartate and Threonine, but it couldn't be detected in initial samples. **(B)**; the same sample spiked with 1mg Collagen type I. A Hydroxyproline peak is clearly detected (arrow) at around 25 minutes. **(C)**; overlay of both traces showing in Blue urine without and in Green, with addition of 1 mg Collagen type I. Peaks at 440 nm.

6.3 Hydroxyproline measurement in urine from 5/6th subtotal nephrectomised rats

Having established Hydroxyproline detection is possible in urine, this was then applied to analyse urine from SNx samples (19 SNx and 14 Controls) as used in previous chapters. Representative traces obtained from AAA analysis (figure 6.2)) show clear peaks for hydroxyproline which were greater in the earlier samples. The average concentration of Hydroxyproline was statically significant in SNx samples only at the beginning of the study (seven days after surgery) when it was expressed per mg protein ($11.92 \pm 3.86\text{nmol/mg}$ protein in the control group vs. $43.10 \pm 9.69\text{nmol/mg}$ protein in the SNx, ($p=0.0404$), figure 6.3-A). However, no difference was observed after this ($p=0.4337$ at 1 month and $p=0.1878$ at 3 months).

6.3.1. 24 hour urine excretion of Hydroxyproline in the SNx Model

Twenty four hours Hydroxyproline excretion was estimated by adjustment to total volume and proteinuria. Total excretion of Hydroxyproline in 24 hours was 6.8 fold higher in the SNx compared to the controls as early as one week ($p=0.0121$), 6.5 fold by one month ($p=0.0109$) and 8.1 fold higher at three months ($p=0.0003$) after subtotalnephrectomy (figure 6.3-B). Total Hydroxyproline excretion remained between 788.8 and 1838nmol/24h on sham operated rats.

6.3.2. Hydroxyproline/Creatinine ratio in the SNx model

Urine Hydroxyproline excretion was corrected for creatinine as described in section 4.2.3.4. Sham operated rats presented a Hydroxyproline/creatinine ratio ranging from 0.711 to 1.18ng/mmol throughout the study (figure 6.3-C). The Hydroxyproline/creatinine ratio was raised in SNx animals when compared to controls throughout the study time course showing a robust 15, 11 and 9.8 fold increases at day 7, 28 and 84 respectively ($p<0.05$, one-way ANOVA) was seen.

Figure 6.2: Hydroxyproline detection in urine from 5/6th subtotal nephrectomised rats

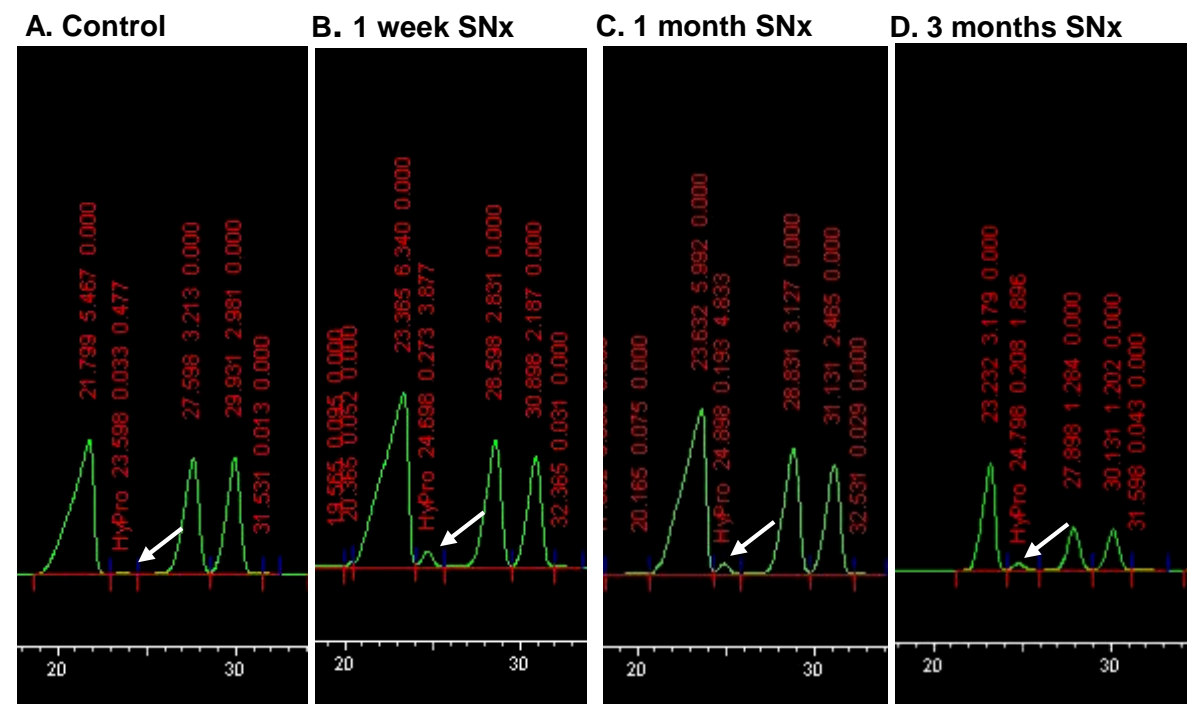
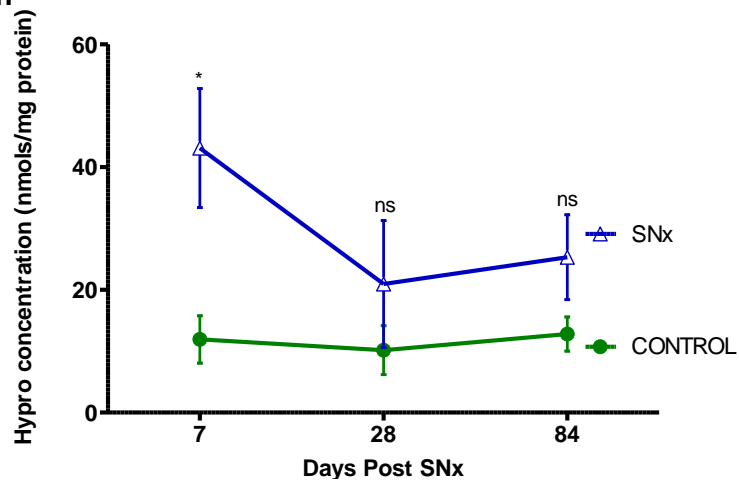


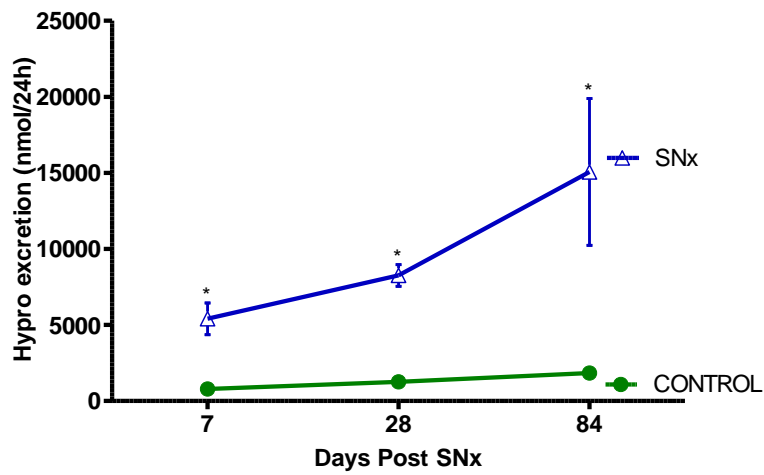
Figure 6.2: Measurement of Hydroxyproline in SNx samples was performed using a Biochrom 30 Amino acid Analyser. Hydroxyproline peak (white arrow) is situated between Aspartate and Threonine at around 24-26 minutes in **A** – Control Sample, **B** – 1 week, **C** – 1 month and **D** – 3 months after Subtotal Nephrectomy. Representative peaks at 440 nm.

Figure 6.3: Hydroxyproline measurement in urine post SNx

A. Concentration



B. 24-hour



C. Hydroxyproline/Creatinine ratio

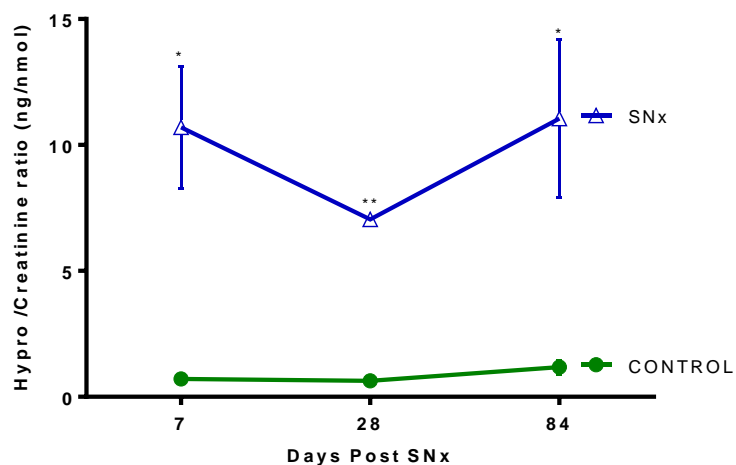


Figure 6.3: Urine Hydroxyproline excretion was measured in SNx samples at 7, 28 and 84 days post Subtotal nephrectomy by cation-exchange chromatography and presented as concentration in nmols/mg proteins (A) 24 hour excretion (B) and as a Creatinine ratio (C). Statistical significance was tested with one Way ANOVA with Bonferroni post hoc test: NS= non statistical significant, * p<0.05, **p<0.01, ***p<0.001, between diseased samples and time matched control. Values are mean \pm SEM.

6.4. Hydroxyproline measurement in urine from the streptozotocin induced model of diabetic nephropathy

Measurement of Hydroxyproline in diabetic samples was performed in the same way as in SNx (section 6.3). The concentration of Hydroxyproline was obtained from a 440 nm profile by reference to a 10 nmols/20ul standard. Hydroxyproline peak had at a retention time of around 25 minutes (figure 6.4).

Hydroxyproline excretion was increased by 190% in the DN group as early as one month when expressed per mg of urine protein ($p=0.0463$) and by 171% at four months ($p=0.0047$). However, there was surprisingly no increase at later stages of the disease (i.e. 8 months). Hydroxyproline peaks measured in eight months DN urines (3 normal, 5 DN) were very small and barely detectable (figure 6.5-A) with values lower than normal samples: controls – 10.35 ± 1.025 vs. 0.798 ± 0.251 nmol/mg protein in DN, ($p=0.0008$).

6.4.1. 24 h urine excretion of Hydroxyproline in the UNx STZ model of DN

Total excretion of Hydroxyproline in 24 hours was 5.7 fold higher in diabetic animals compared to the controls at one month ($p=0.0460$) and 12.3 fold by four months ($p<0.0001$) after STZ administration (figure 6.5-B). Notwithstanding, no difference was observed between diabetic and control rats at eight months ($p=0.9319$).

6.4.2. Hydroxyproline/Creatinine ratio in the UNx STZ model of DN

The Hydroxyproline/Creatinine ratio on sham-operated rats ranged between 0.57-0.69ng/ml (figure 6.5-C). One month after DN induction, Hydroxyproline/creatinine ratio from diabetic animals was significantly higher at 11.25 ± 1.65 ng/ml ($n=4$, $p=0.0246$) and steadily increased over four months to 18.87 ± 3.88 ng/ml ($p=0.0049$), higher than controls by over 30-fold. No significant difference was established at eight months ($p=0.942$).

Figure 6.4: Hydroxyproline detection in Diabetic Nephropathy urines

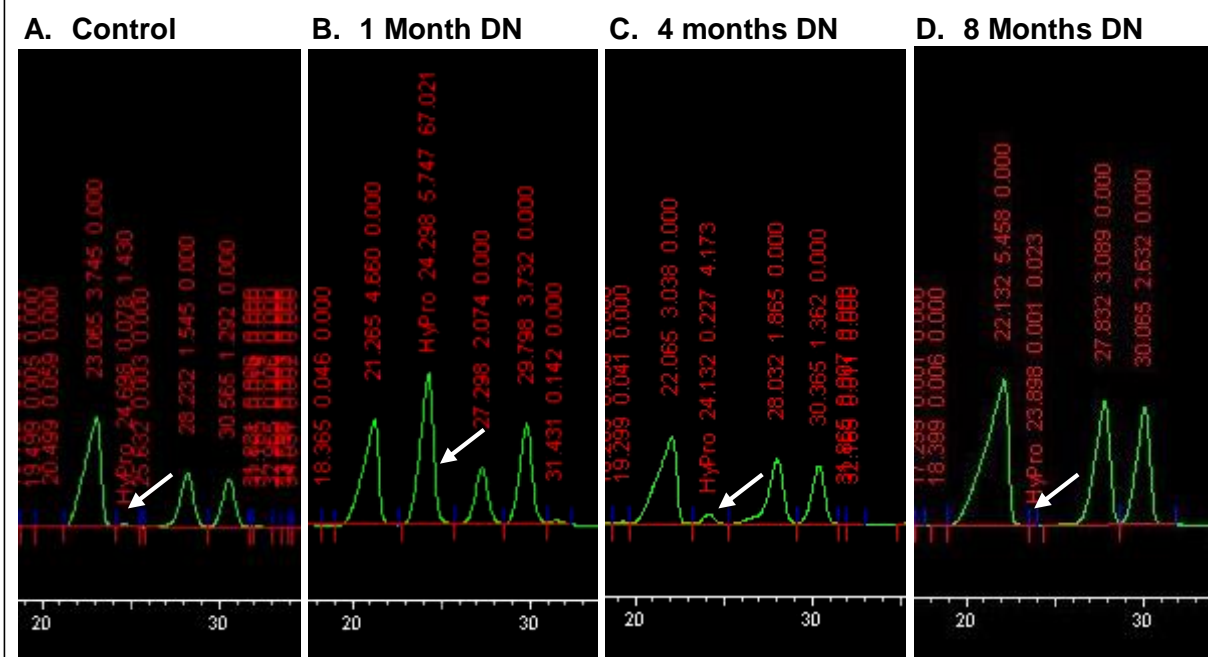


Figure 6.4: Representative traces of Hydroxyproline peaks (white arrow) in a Control sample (A) and DN samples at 1 month (B), 4 months (C) and 8 months after streptozotocin injection (D). Representative peaks at 440 nm.

Figure 6.5: Hydroxyproline measurement in urine from the UNx STZ model of DN

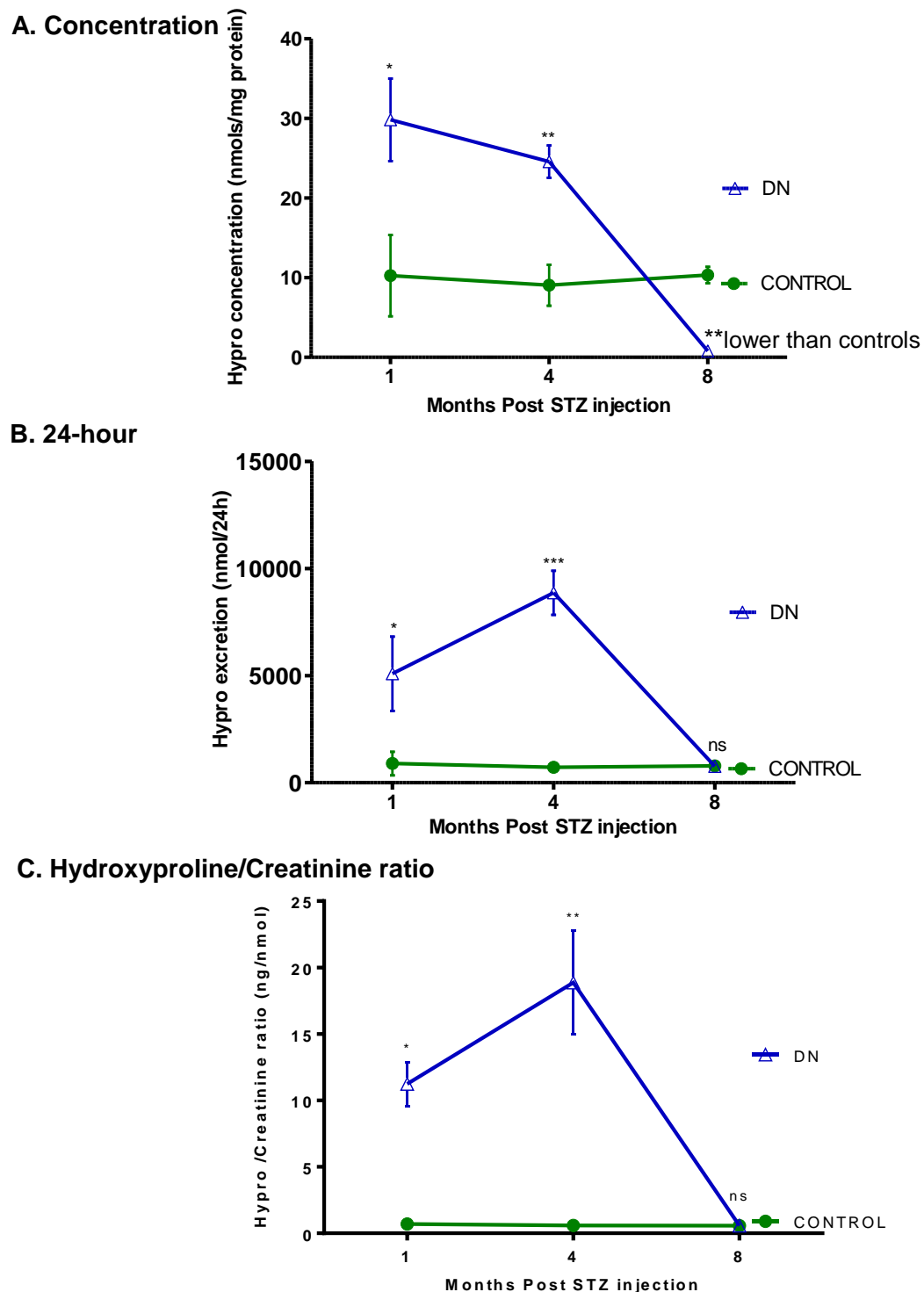


Figure 6.5: Urine Hydroxyproline excretion was measured in DN samples at 1, 4 and 8 months post STZ injection by cation-exchange chromatography and presented as concentration in nmols/mg proteins **(A)** 24 hour excretion **(B)** and as a Creatinine ratio **(C)**. Statistical significance was tested with one Way ANOVA with Bonferroni post hoc test: NS= non statistical significant, * $p < 0.05$, ** $p < 0.01$, *** $p < 0.001$, between diabetic samples and time matched control. Values are mean \pm SEM.

6.5. Hydroxyproline measurement in urine from the Fisher to Lewis transplant model of Chronic Allograft Nephropathy

47 urine samples urine from the Fisher to Lewis transplant model of Chronic Allograft Nephropathy were used to measure Hydroxyproline concentration. The full set of samples (n=72) as used in previous chapters was not available as archived samples became depleted. Therefore samples were only measured (for statistical evaluation) at weeks 8, 17, 24, 33 and 52 post Transplantation. Hydroxyproline levels per mg of urine protein were measured by cation-exchange HPLC using an amino acid analyser (Biochrom 30, Biochrom, UK) as described in section 3.5.7.2. Hydroxyproline retention time of 25 minutes was read at a wavelength of 440nm and quantified from the area under the peak (figure 3.22). No urine samples at the 2 weeks post transplantation sampling point were available for analysis in the L-L isografts. Eight weeks after transplantation, urine Hydroxyproline concentration from L-L isografts (n=5) was 4.77 ± 0.37 nmol/mg protein. This increased to 7.09nmol/mg protein (n=1) at 33 weeks. F-L allografts (n=7) had a Hydroxyproline concentration of 6.23 ± 0.99 nmol/mg protein at 8 weeks (p=0.2182 to L-L isografts), then 5.25 ± 1.18 nmol/mg protein at 17 weeks (n= 7, p=0.3762 to L-L isografts), 10.42 ± 2.84 nmol/mg protein at 24 weeks (n=5, p=0.2046 to L-L isografts), 13.83 ± 2.21 nmol/mg protein at 33 weeks (n=5) and this peaked at termination reaching 18.08 ± 2.94 nmol/mg protein. Statistical analysis was not performed in these two final points as there was insufficient number of L-L isografts (n=1 at 33 weeks and n=0 at 52 weeks) to make a comparison (figure 6.6-A). However a clear trend of increasing hydroxyproline can be seen.

6.5.1. 24 h urine excretion of Hydroxyproline

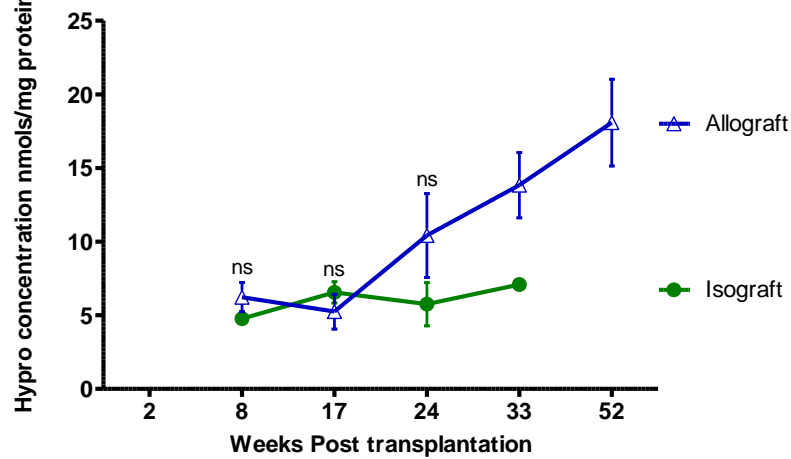
Eight weeks after transplantation, total urine Hydroxyproline excretion in 24 hours from L-L isografts was 75.59 ± 13.57 nmol/24h and this remained stable at 133.29nmol/24h by 33 weeks with no evidence of a rapidly increasing trend. Hydroxyproline excretion in 24 hours on F-L allografts showed a steady increase during the study time course (figure 6.6-B). It rose from 136.0 ± 27.46 nmol/24h at 8 weeks to 4569.69 ± 13.57 nmol/24h at 52 weeks. However, there was no statistical difference between L-L isografts and F-L allografts up to 33 weeks due to the large variability in the urine output of the latter.

6.5.2. Hydroxyproline/creatinine ratio

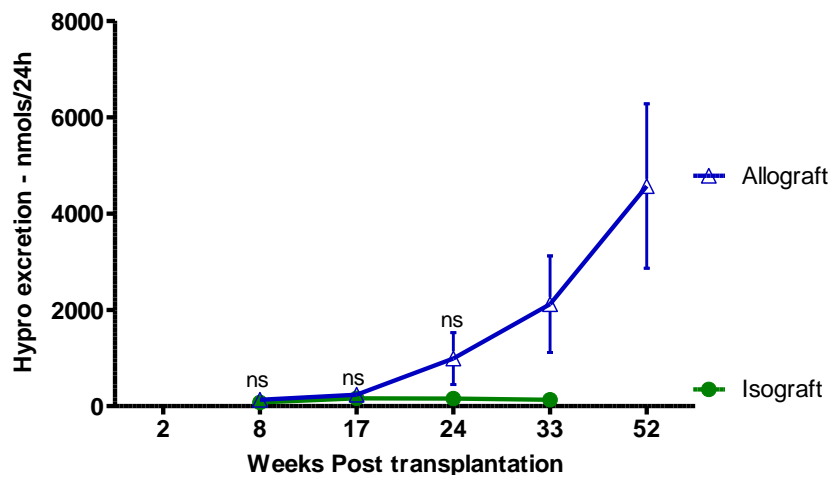
L-L isografts had a Hydroxyproline / Creatinine ratio ranging from 0.723 to 1.121 throughout the study. F-L allografts had a significantly increased Hydroxyproline / Creatinine ratio which was 1.8 fold higher than L-L isografts at 8 weeks post transplantation only (1.312 ± 0.212 , $p=0.0439$). It slightly dropped by 17 weeks to 1.213 ± 0.561 , $p=0.9010$). After this, Hydroxyproline/creatinine levels progressively increased until 52 weeks post kidney transplantation (2.9 fold higher than L-L isografts at 33 weeks, $p=0.3152$), but it failed to reach significance (figure 6.6-C).

Figure 6.6: Hydroxyproline measurement in urine from the in the Fisher to Lewis model of CAN

A. Concentration



B. 24-hour



C. Hydroxyproline/Creatinine ratio

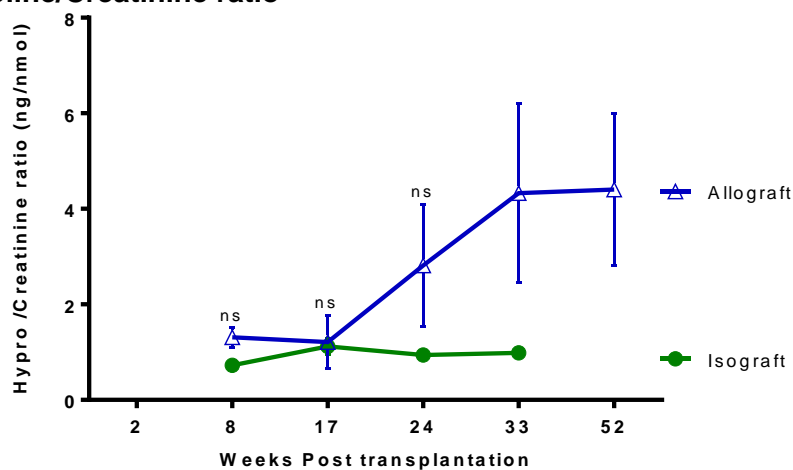


Figure 6.6: A – Mean urine Hydroxyproline concentration \pm SEM over a 12 month period in the L-L isograft (n=5) compared to the F-L allograft (n=7). **B** - 24 hr urine Hydroxyproline lysine excretion \pm SEM, **C** - Hydroxyproline / Creatinine ratio in F -L allografts and L-L isografts transplanted rats. Statistical significance was tested by 2 Way ANOVA with Bonferroni post hoc test: NS= not statistically significant, * $p < 0.05$, ** $p < 0.01$, *** $p < 0.001$ between F -L allografts and L-L isografts.

6.6. Correlation between Hydroxyproline and clinical markers of renal function and damage

6.6.1. 24h proteinuria

Total urine Hydroxyproline was associated with changes in proteinuria in thirty one urine samples from the SNx study (Pearson's $r = 0.5316$, $R^2 = 0.2826$, 95% CI: 0.2184 to 0.7456, $p=0.0021$) and in thirty nine samples from the Fisher to Lewis model of CAN (Pearson's $r = 0.5417$, $R^2 = 0.2934$, 95% CI: 0.2684 to 0.7342, $p=0.0004$), but not in diabetic samples (figures 6.7-A, 6.7-B and 6.7-C).

As albumin counts for the greatest amount of protein found on urines from diabetic patients, it was expected that an elevation in total proteinuria would not be a direct result of changes in urine Hydroxyproline excretion. As a consequence of this, total urine Hydroxyproline excretion showed very weak and not significant correlation with 24h proteinuria (Pearson's $r = 0.2184$, $R^2 = 0.0477$, 95% CI: -0.1685 to 0.5470, $p=0.2641$).

6.6.2. Creatinine Clearance

Urine excretion of Hydroxyproline was associated with changes in renal function in SNx samples (figure 6.7-D). A correlation between total urine Hydroxyproline and creatinine clearance has demonstrated that the lower the kidney function, the higher hydroxyproline excretion in the SNx model of renal scarring (Pearson's $r = -0.4240$, $R^2 = 0.1798$, 95% CI: -0.6804 to -0.0078, $p=0.0195$).

In diabetic samples, there was a poor positive correlation between Hydroxyproline excretion and creatinine clearance (Pearson's $r = 0.3835$, $R^2 = 0.1470$, 95% CI: 0.0120 to -0.6619, $p=0.0440$, figure 6.7-E). The high levels of Hydroxyproline excretion at early stages of the disease where kidney function had not deteriorated and the fall of hydroxyproline measurements at more advanced stages underlie this lack of association.

CAN samples did not present a correlation between 24 hour urine Hydroxyproline and CrCl (Pearson's $r = -0.07415$, 95% CI: -0.3848 to 0.2516, $R^2 = 0.0055$, $p=0.6582$, figure 6.7-F).

Figure 6.7: Correlation plots for Hydroxyproline

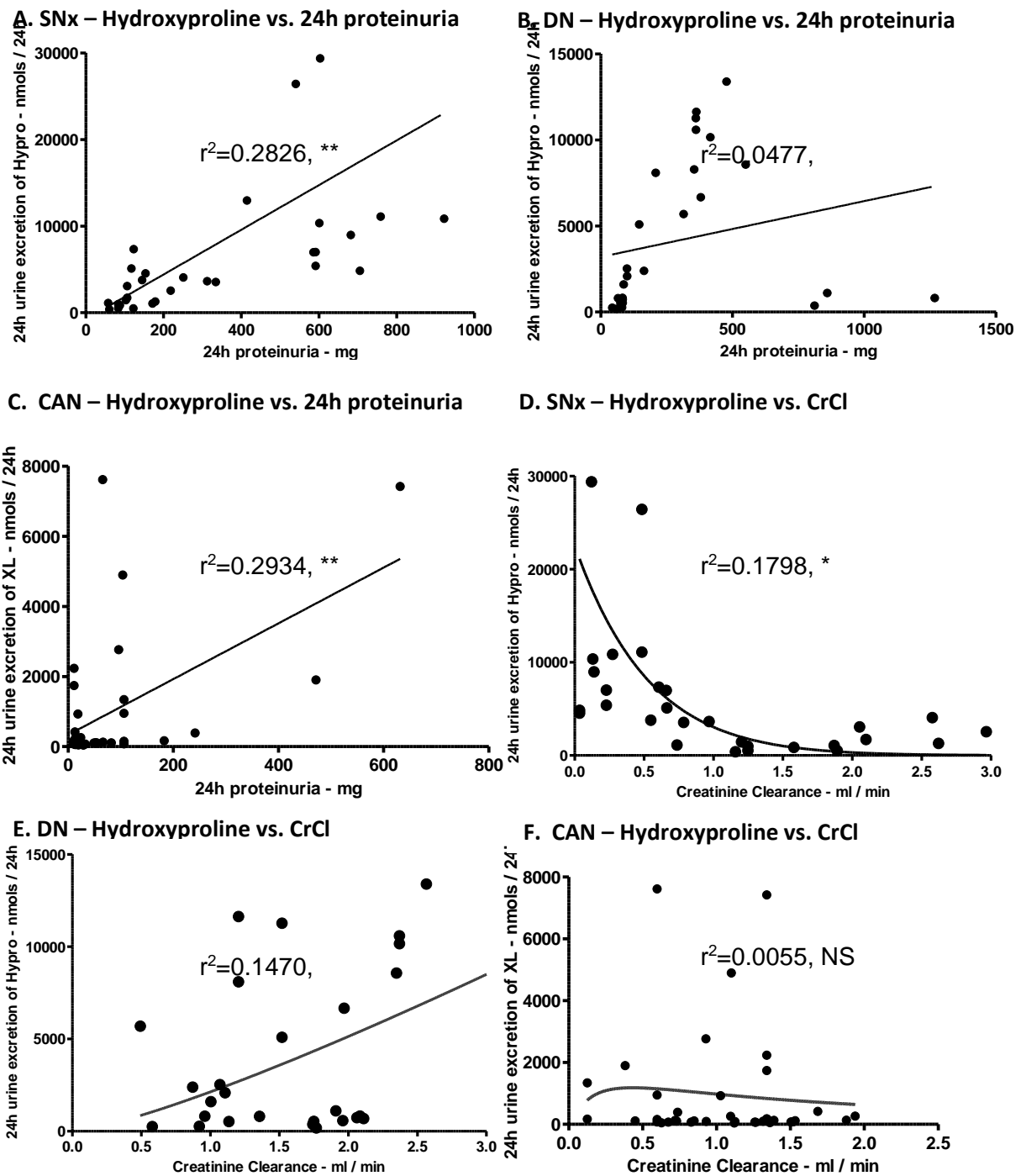


Figure 6.7: Pearson's correlations were performed for 24 hour urine Hydroxyproline excretion vs. 24 hour proteinuria in SNx (A), DN (B) and CAN (C) and then for 24 hour urine Hydroxyproline excretion vs. creatinine clearance in SNx (D), DN (E) and CAN (F). Statistical significance was shown by one Way ANOVA with Bonferroni post hoc test: NS= non statistical significant, * $p<0.05$, ** $p<0.01$, *** $p<0.001$. $n= 31$ in SNx, 25 DN and 39 in CAN.

6.7. Discussion

Urines obtained from the 5/6th Subtotal nephrectomy, the Streptozotocin Diabetic Nephropathy and the Fisher to Lewis transplant model of Chronic Allograft Nephropathy, which are well characterised and established models of kidney scarring, were used for hydroxyproline measurement. Assessment of Hydroxyproline in urines was undertaken as it has been widely reported in histopathological studies that development of scarring is correlated to increased synthesis and deposition of particularly fibrillar collagens with collagen acting as a key component of scar tissue. Measurement of urine collagen can be performed by commercially available immunoassays for individual collagen types or indirectly by the analysis of Hydroxyproline content. In our research, we chose to quantify hydroxyproline as it represents a measure of total collagen present in urine samples. Release of Hydroxyproline from the samples was achieved by hydrolysis followed by fractionation of amino acids by cation exchange chromatography.

To date, there are surprisingly few studies correlating the use of urine collagen as a possible marker of kidney scarring given its role in kidney fibrosis. Urine amino terminal peptide of procollagen III (PIIINP) was positively correlated to interstitial fibrosis in humans, although it was not correlated to increased serum creatinine (Soylemezoglu *et al.* 1997). The urine carboxy terminal fragment of type IV procollagen was found increased in Minimal Change disease, but again it was not correlated to increased serum creatinine and neither to CrCl or other nephropathies (Keller *et al.* 1992). Irrespective of the limitations of these early studies of urine collagen in CKD, we hypothesised that measurement of urinary Hydroxyproline could be used as a non-invasive indirect indicator of collagen presence and subsequently fibrosis.

In this study, initial assessment of Hydroxyproline showed increased concentration at initial stages of both SNx and DN groups when expressed per mg protein. But, no difference was observed at later stages of both diseased groups. However if Hydroxyproline secreted per 24 hours was calculated it increased markedly in the SNx group at all time points, indicating that pathological changes in the kidney were being carried through to the urine. In contrast, similar changes were surprisingly not seen in the DN animals despite an equivalent level of tissue scarring. Diabetic animals showed significantly increased levels of urine Hydroxyproline in 24 hours at 1 and 4 months only, but not at the last end point. Hydroxyproline peaks were very small and barely detectable at 8 months post STZ injection (figure 6.4) with values lower than normal samples expressed as either nmol per mg of urine or twenty four hours excretion. Also, no correlation was found between urine excretion of Hydroxyproline and 24 hour proteinuria. As discussed earlier, later stages of the diabetic disease are characterised by excessive

excretion of albumin in the urine. This albuminuria can vary from small amounts (30 to 300 mg/24h – Microalbuminuria) up to larger amounts (>300mg/24h – Macroalbuminuria). Biochemistry tests were performed in our samples and showed significant increased macroalbuminuria in diabetic rats by 8 months of study. Thus, the relative expression of hydroxyproline in such urines could be masked by the abundant amounts of albumin present in the urine. Another possible explanation for this, could be the fact that as ECM becomes increasingly crosslinked in the kidney (e.g. by TG2), this could prevent collagen on finding its way into the urine. Alternatively, it can also not be excluded that it could have been an artefact of the analysis given what occurs in the two other animal models.

On the other hand, in a further evaluation of the data, the Hydroxyproline/Creatinine ratio was calculated and it confirmed significant increase in the diseased samples in SNx at all time points and in DN at 1 and 4 months only. As to the CAN samples, although the set was incomplete, a trend was observed with increase in the Fisher-to-Lewis Allografts compared to the Lewis-to-Lewis Isograft group. However, no statistical difference was observed, mainly because there were not enough samples at the latter stages in order to draw a comparison. In SNX and CAN there was a similar trend of increased Hydroxyproline/Creatinine ratio at the late stages of disease. Thus in all models it is a good early indicator of the potential for CKD development, but not a late stage indicator in DN and this requires more studies to better understand why this occurred.

Chapter 7

Human Chronic Kidney Disease and the urine excretion of Transglutaminase type 2 and ϵ (γ glutamyl) lysine as biomarkers of CKD progression

7.1. Introduction

Chronic Kidney Disease (CKD) is recognised as a major public health problem with an estimated prevalence of approximately 10% of the adult population in Western Countries (McCullough *et al.* 2012). Novel CKD classification established by the KDIGO in 2012 divides it into 6 categories according to eGFR (G1 to G5) with G3 split into 3A (eGFR between 45 – 59ml/min/1.73m²) and 3b (eGFR between 30-44ml/min/1.73m²) and it is also based in three levels of albuminuria: A1 (normal to mildly increased albuminuria, <30mg/g), A2 (moderately increased albuminuria, 30-300mg/g) and A3 (severely increased albuminuria, >300mg/g) (KDIGO 2012). The new definition of CKD subdivides it into community CKD (cCKD) and referred CKD (rCKD). cCKD in Western countries is mainly a disease of old people due to age related abnormalities whilst in Eastern countries it is related to poverty, infections such as malaria, schistosomiasis and hepatitis, exposure to environmental pollution (air, water), use of traditional herbal remedies, malnutrition, low birth weight, drug toxicity and changes in life style (Westernisation). rCKD is associated with primary or secondary nephropathies including vasculitis, SLE, CGN, Interstitial Nephritis and PKD (Floege 2013).

Recent studies have stressed the importance of prevention, early detection and management of progressive kidney disease (Turner *et al.* 2012). Hence the crucial importance of developing tests for identification of CKD. Current kidney function and damage tests have several limitations including the delayed detection of dysfunction which happens only after significant damage has occurred and the inability to precisely establish disease stage. The limitations of these tests have instigated the search for early and reliable non invasive biomarkers of kidney disease.

CKD function is currently based on estimated GFR (eGFR), which is derived from the calculation of serum creatinine levels, or serum Cystatin C, or a combination of creatinine and Cystatin C (Delaine *et al.*, BMC nephrology 2013). The most used equation is derived from the Modification of Diet in Renal Disease (MDRD) study and this utilizes standardised serum creatinine, age, sex and race to estimate GFR adjusted for body surface area. However, it was found that this equation overestimates the measured GFR (mGFR) within individuals that have a mGFR above 60 ml/min/1.73m². This can lead to a misclassification of large number of patients with CKD 1, 2 and CKD3a. The Chronic Kidney Disease-Epidemiology Collaboration study (CKD-EPI) equation was recently developed and it also uses serum creatinine, age, sex and ethnicity (black) to estimate GFR. /it performs better than the MDRD when the GFR > 60ml/min/1.73m². CKD-EPI has less bias and it showed a mean measured

eGFR of 2.5ml/min/1.73m² in the CKD-EPI compared to 5.5ml/min/1.73m² in the MDRD (Delanaye *et al.* 2013). Although the CKD-EPI showed an improved precision and better risk prediction, it also had some limitations as this study used a low number of elderly and ethnic minorities to measure GFR. In addition, no difference was found in the ROC curves from both equations (Levey *et al.* 2009). The CKD-EPI cys (based on cystatin C) and the CKD-EPI mix (uses both creatinine and cystatin C) both use plasma cystatin C levels as it has shown good biomarker characteristics. Studies comparing the performance of these cystatin C based equations concluded that they present a better prediction of GFR, especially in individuals at CKD stage 3 (Delanaye *et al.*, 2013). Other molecules studied as alternative filtration biomarkers include beta-trace protein (BTP) and beta-2-microglobulin (B2M).

Microalbuminuria or low level albuminuria (mA, A2 category) has been used as the gold standard definer of CKD development and progression. However, it is a common feature of aging, obesity, extensive exercise, pregnancy, tobacco consumption, infections such as HIV, Scabies, Hepatitis C and H. Pylori, while it can also be associated with a large number of acute and chronic vascular as well as inflammatory pathologies including IBD, ATS, Psoriasis and periodontitis. Additionally, microalbuminuria is often regarded as an important risk factor for cardiovascular disease. Furthermore, mA is often transitory and irresolute thus not a specific and reliable marker of CKD, especially at early stages of the disease. So, although mA carries the title of the best CKD marker at the moment, it lacks specificity to kidney disease progression and therefore its sole use as such should be questioned.

Defining CKD progression is a point of ample controversy due to the issues raised by the eGFR equations when the GFR is greater than 60ml/min/1.73m². Also, the variability of serum creatinine levels represents a barrier for precise estimation of eGFR assessment and subsequent CKD progression. The KDIGO guidelines suggests classifying progressive kidney disease as a sustained decline in eGFR greater than 5 ml/min/1.73m² per year or a decline of over 25% in eGFR from baseline (KDIGO 2012), others have suggested a classification of progressive CKD when the eGFR decline is above 3 ml/min/1.73m² per year (Rosanski, *Am Journal of Nephrology* 2012). We have decided to extend this classification and subdivide it into two distinct categories: progressive CKD (eGFR decline above 2 ml/min/1.73m² per year) and rapidly progressive CKD (eGFR decline above 5 ml/min/1.73m² per year). The rationale for our sub classification is that a normal decline of eGFR in healthy individuals is below 1 ml/min/1.73m² per year from around 40 years of age, so we used a tighter definition of progression (double the normal loss of function), in order to potentially identify subjects at early stages of decline. Thus, earlier identification of individuals at potential risk for CKD

progression would enable clinicians to apply interventions aimed at slowing its progression and could decrease the number of patients reaching ESKD.

In previous chapters using urine samples obtained from three different animal models of kidney scarring (5/6th subtotal nephrectomy, the Streptozotocin Diabetic Nephropathy and the Fisher to Lewis transplant model of CAN (results chapter 4), effective assays for the detection of Transglutaminase type 2 and its crosslink product ϵ (γ glutamyl) lysine (Vass *et al.* 2012) were established. Urine expression of both molecules demonstrated a good correlation with disease status suggesting that they may have great potential as biomarkers of human chronic kidney disease. TG2 was remarkably increased in diseased urines when compared to time matched controls in all three animal models especially when converted to a TG2:creatinine ratio. Changes were detected in ϵ (γ glutamyl) lysine levels per mg of protein in SNx and CAN models, but surprisingly not in diabetic nephropathy samples.

Thus in this chapter it was hypothesised that similar changes in TG2 & ϵ (γ glutamyl) lysine also occurred in patients with CKD and may potentially have both diagnostic and prognostic value. To test this translational hypothesis this chapter aims to quantify Transglutaminase type 2 and its crosslink product ϵ (γ glutamyl) lysine in human urine samples. TG2 levels in the urine were quantified by an in-house Sandwich ELISA. For this assay, an anti TG2 goat polyclonal was used as capture antibody and anti TG2 monoclonal CUB7402 (both from AbCam, UK) as the detection antibody. A standard curve was generated by performing a serial dilution of human recombinant TG2 (methods section 3.4.3). In addition to the urine samples, serum and plasma samples were also collected in order to compare excretion and circulating levels. For the urine excretion of ϵ (γ -glutamyl)-lysine, a technique previously developed in the animal study was used. In this, 5 mg of urine protein was digested through a combination of five different proteolytic enzymes and products were analysed by cation-exchange HPLC using an amino acid analyser (AAA) (Biochrom 30, Biochrom, UK) (methods section 3.5.3).

Specifically, work in this chapter aimed to:

- Recruit CKD patients above 18 years old with any CKD etiology or stage attending the SKI outpatient clinic facilities
- Collect bio-samples (blood and urine) from all controls and CKD patients involved in this study, including the patients undergoing renal biopsies to correlate these findings with histological changes as well as clinical parameters
- Identify relevant demographic, social, and medical conditions in this group of patients

- Determine the prevalence of progressive and non-progressive CKD patients within this group and then to stratify subjects by levels of CKD progression
- Define the prognostic value of TG2 and ϵ (γ glutamyl) lysine in identifying patients with progressive CKD
- Determine the relative advantages of urine and circulating levels of TG2 as a prognostic marker

The first part of this chapter established a prospective observational cohort of adult CKD patients from stages 1 to 5. The investigation was performed under an ethics application entitled “The study of the natural history and biomarkers of Chronic Kidney Disease” (ethics reference application number STH 15004) and was conducted at the Sheffield Kidney Institute (SKI) located in the Northern General Hospital site of the Sheffield Teaching Hospitals NHS Foundation Trust. In this study, we collected urine and blood samples from 292 CKD patients and 33 Controls (section 3.2). The outcomes of the bio-clinical and laboratory assessment undergone by patients, as well as their anthropomorphic and socio-economic status are reported in this chapter.

7.2. Study population & Clinical Sample Collection

7.2.1. Study design

The study consisted of a prospective observational cohort of adult CKD patients over a period of 3 years. A total of 292 CKD patients from stages 1 to 5, including 41 which underwent kidney biopsy and 33 controls were included in this study. From this total of 292 CKD patients, 91 presented with Diabetic Nephropathy plus 201 patients which had non-diabetic CKD of various aetiologies. Full details of the study design are described in the methods chapter 3, section 3.2.1. Briefly, CKD patients above 18 years old with any type of CKD were recruited after appropriated consent procedures and initial screening of urine samples. Major CKD causes were: diabetic kidney disease (DKD), chronic glomerulonephritis (CGN), hypertensive nephrosclerosis (HTN), atherosclerotic renovascular disease (ARVD), chronic interstitial nephritis (CIN) and ADPKD. All patients underwent a detailed bio-clinical assessment at baseline and at every outpatient's clinical appointment for the period of enrolment in the study. Ten millilitres of blood (5ml of serum and 5ml of plasma) as well as a target of 220 ml of fresh Mid-Stream Urine (MSU) were collected at the time of recruitment. Recordings of eGFR and all clinical and laboratorial data were securely stored in the Sheffield Kidney Institute (SKI) CKD database.

7.2.2. Demographic and socio-economical characteristics of the study population

The CKD population consisted of: 38.69% Females and 61.31% Males, with 90.41% Caucasian and 9.59% from other ethnicities. The age range of these patients consisted of a median of 63.9 years with 25% percentile at 56.50 years and 75% at 75.70 years, with 61.9% aged above 65 years.

The control group consisted of: 30.30% Females and 69.70% Males, with 63.64% Caucasian and 36.36% from other ethnicities. The mean age of controls in this study was 38.48 ± 7.61 years.

As for the smoking habits; 11.30% of CKD patients were smokers, 36.99% past smokers and 51.71% non-smokers. In the control group only 3.03% were actual smokers, 6.06% were past smokers and 90.91% never smoked in their lives.

Majority of the CKD patients enrolled in this study were either retired (42.67%) or unemployed (14.68%), whilst only 42.65% were active workers (18.81% skilled/professionals and 23.84% manual workers). Most patients lived either in Sheffield (55.68%), Rotherham (22.29%) or in Barnsley (14.03%).

The overall demographic data is depicted in figure 7.1.

Figure 7.1: Frequency distribution of CKD patients' demographic data



Figure 7.1: Demographic data from 292 CKD patients enrolled in the study. The frequency distribution of their gender, race, age, employment status, residence location and smoking habits are displayed as a percentage of the total study population.

7.2.3. Anthropomorphic data

All patients had their weight, height and Body Mass Index (BMI) ascertained when bio-samples were collected. Body mass index was calculated as $\text{weight}/\text{height}^2$ (kg/m^2). A BMI below $18.5 \text{ kg}/\text{m}^2$ was used to classify patients as underweight, then between 18.5 and $24.9 \text{ kg}/\text{m}^2$ as normal weight, between 25 and $29.9 \text{ kg}/\text{m}^2$ as overweight and greater than $30 \text{ kg}/\text{m}^2$ for obesity.

Overall, the majority of CKD patients were either obese (46.47%) or overweight (34.85%). 17.17% of CKD patients had normal weight and only 1.51% were underweight, which included a patient suffering from anorexia nervosa (figure 7.2-B). The mean BMI \pm SD of the CKD study population was $30.83 \pm 6.07 \text{ kg}/\text{m}^2$ against $22.34 \pm 2.71 \text{ kg}/\text{m}^2$ in the healthy volunteer population. CKD patients had an average weight of 79.73 kg for females and 91.07 kg for males ($p < 0.0001$, figure 7.2-A) whilst male healthy volunteers also presented higher average

weight (75.09kg) than females (63.24kg, $p=0.0094$, figure 7.2-C). The vast majority of healthy volunteers had normal weight (58.06%), with 38.71% being overweight (figure 7.2-D).

Figure 7.2: Anthropomorphic data from CKD patients and healthy volunteers

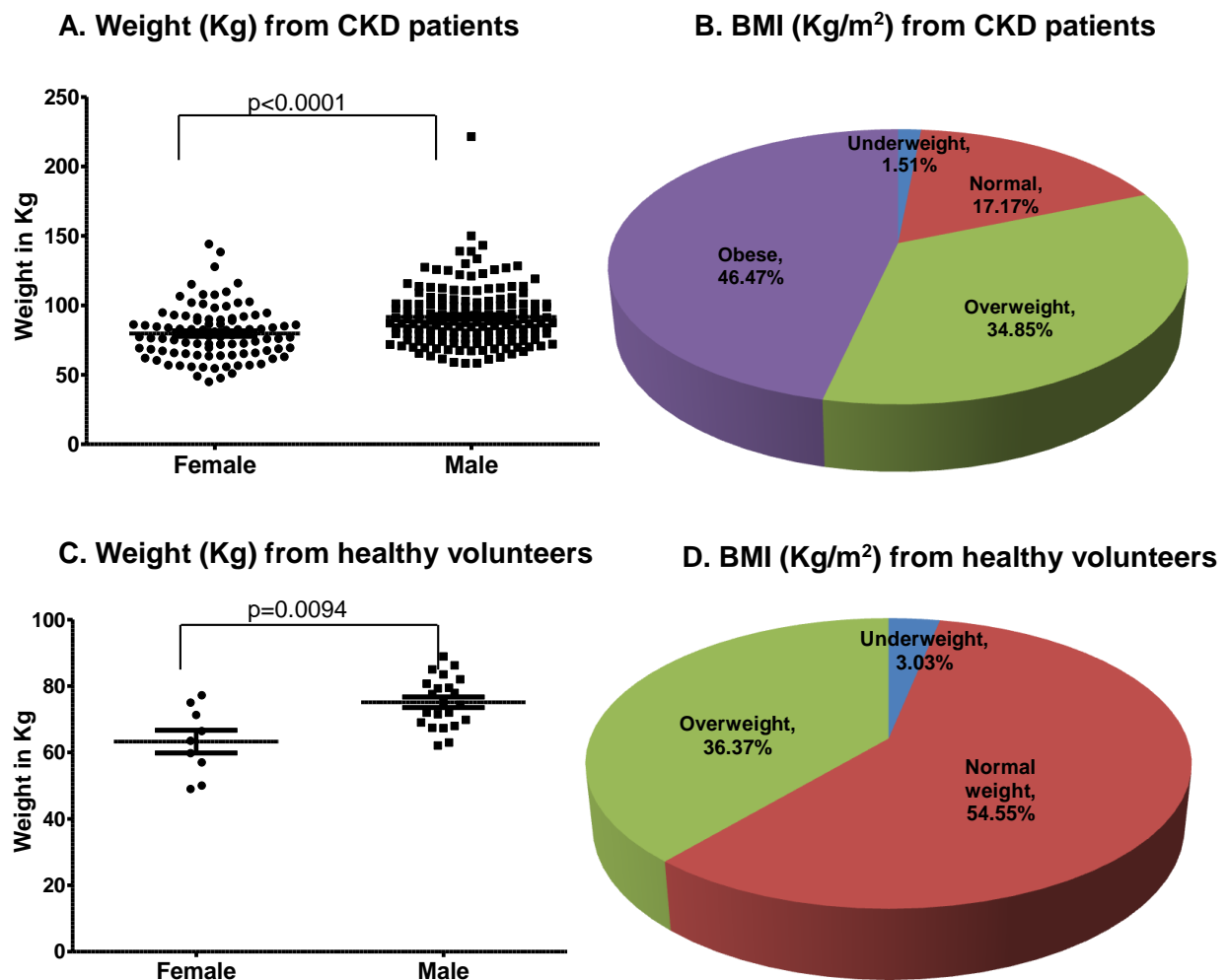


Figure 7.2: Anthropomorphic data from 292 CKD patients and 31 healthy volunteers (out of 33) enrolled in the study. Body weight of female and male participants (**A, C**) Body Mass Index (**B, D**). Underweight = <18.5 kg/m², Normal = 18.5-24.9 kg/m², Overweight = 25-29.9 kg/m² and Obese, BMI of 30 kg/m² or greater.

7.2.4. CKD diagnosis and co-morbidities

Primary aetiologies of CKD were: diabetic kidney disease (n=91, 31.17%), chronic glomerulonephritis (n=66, 22.60%), hypertensive nephrosclerosis (n=53, 18.15%), atherosclerotic renovascular disease (n=29, 9.93%), chronic interstitial nephritis (n=15, 5.14%) and ADPKD (n=13, 4.45%) (figure 7.3-A). Other causes of CKD (n=25, 8.56%) included cases of cast nephropathy (Multiple Myeloma), amyloidosis, idiopathic

thrombocytopenic purpura, Henoch Schölein purpura, monoclonal gammopathy of undetermined significance (MGUS), microscopic polyarteritis, familial renal disease, medullary sponge kidney, sarcoidosis, lupus nephritis, HIV-associated Nephritis, Tacrolimus toxicity and renal cell carcinoma. Patients with chronic glomerulonephritis had a biopsy diagnosis (n=41) of: Membranous nephropathy (36.59%), IgA nephropathy (34.15%), Focal and Segmental Glomerulosclerosis (FSGS) (12.20%), Membranoproliferative glomerulonephritis (7.32%), Minimal change (4.88%) and Rapidly Progressive glomerulonephritis (RPGN) (4.88%) (figure 7.3-B).

The main co-morbidities presented by CKD patients are displayed in table 7.1. Hypertension was the condition with highest prevalence amongst our study population, accounting for 81.16% of participants. Individuals were classified as having hypertension on the basis of receiving anti-hypertensive medication or by presenting high blood pressure measurements at the time of enrolment, this was done in accordance with the guidelines of the Eight Joint National Committee for Definition and Classification of Hypertension (JNC 8) (Chobanian *et al.* 2003). Hypercholesterolemia and obesity were present in nearly half of subjects (49.66% and 46.47% respectively). The presence of cardiovascular disease (CVD) was noted in over one third of this population (40.41%). Other important co-morbidities included: mineral bone disease (17.13%), peripheral vascular disease (16.44%), gout (14.04%) and anaemia (11.30%). Anaemia was classified as haemoglobin < 12 g/dl.

Table 7.1: Frequency distribution of main co-morbidities presented by CKD patients

Co-morbidity	Percentage
Hypertension	81.16%
Hypercholesterolemia	49.66%
Obesity	46.47%
Cardiovascular Disease	40.41%
Bone disease	17.12%
Peripheral vascular disease	16.44%
Gout	14.04%
Anaemia	11.30%
COPD	9.59%
Cerebral vascular disease	8.90%
Hypothyroidism	8.56%
Cancer *	8.22%
Psychological disease	4.11%
Recurrent UTI	1.71%

Table 7.1: The prevalence of the most common co-morbidities found in the study population is shown as a percentage of those affected. * Cases of cancer include the following organs: Lung, Prostate,

Penis, Testicular, Pancreas, Intestinal, Liver, Bladder, Kidney, Skin and Breast cancer. COPD = Chronic obstructive pulmonary disease.

Figure 7.3: CKD Etiology

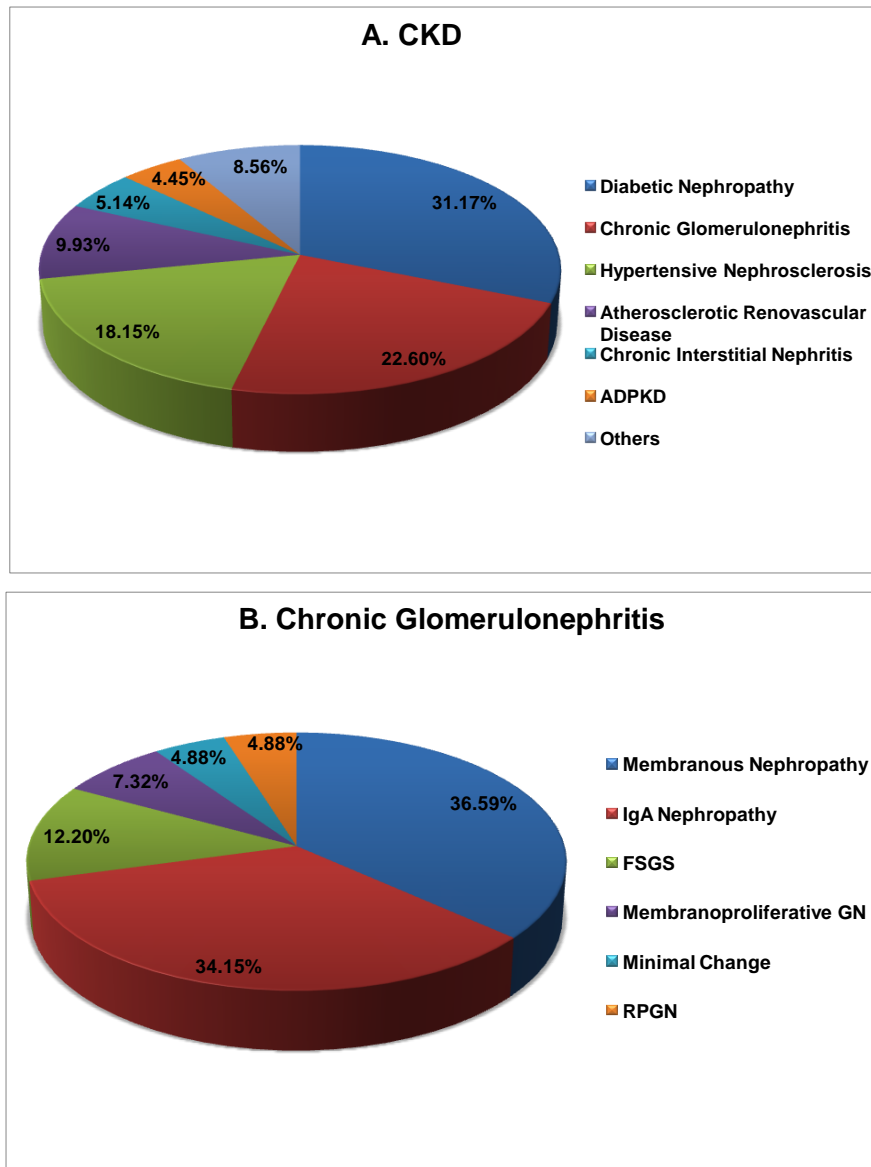


Figure 7.3: The pie charts illustrate the main CKD diagnosis presented as a percentage of the total study population (A) and the sub-classification of 41 Chronic Glomerulonephritis patients given by biopsy (B).

7.2.5. CKD stages

The mean follow up time for this study was 2.19 ± 0.68 years. The majority of patients were either at CKD stage 3 (38.36%) or stage 4 (45.21%) at recruitment. The full stratification into CKD stages, including the sub-division into stages 3A and 3B (figure 7.4) and the frequency distribution of CKD stages 1 to 5 in each cause of CKD (figure 7.5) demonstrated wide inclusion into the study.

Figure 7.4: CKD stages

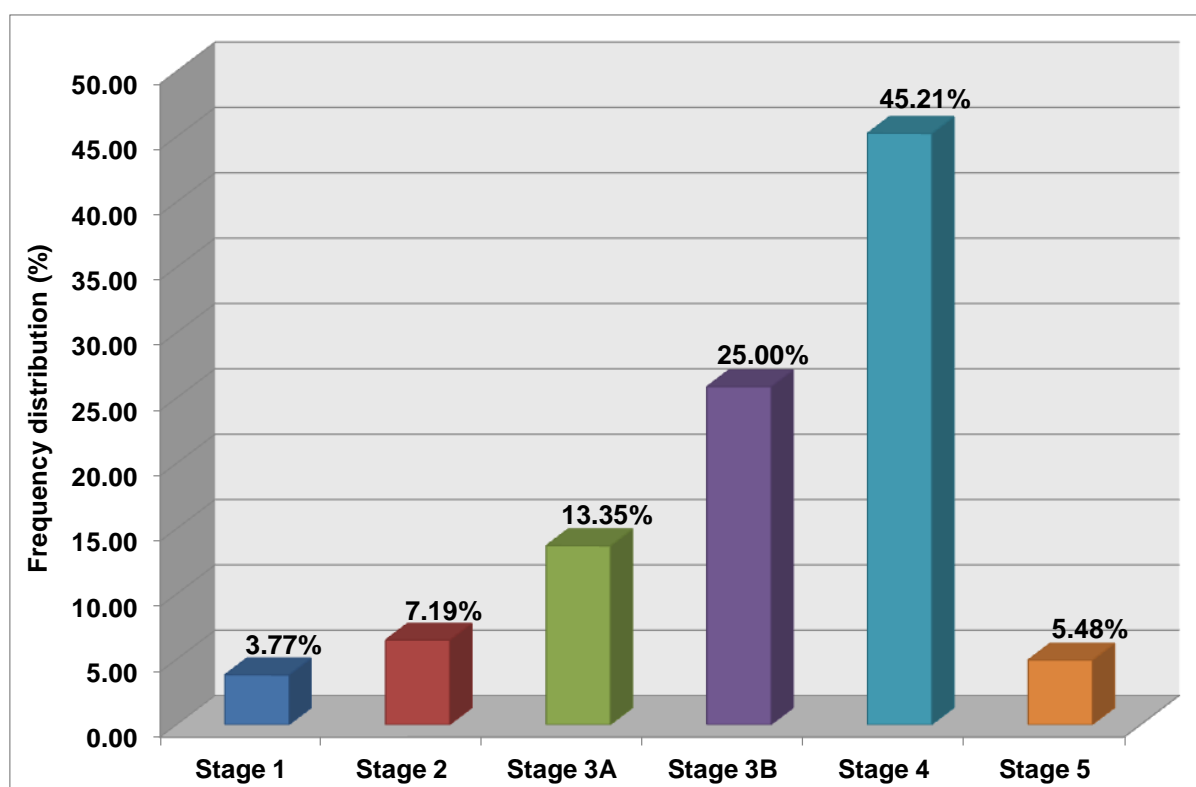


Figure 7.4: The bar chart shows the frequency distribution of the study population grouped by CKD stage. Classification of CKD stages is as defined in the K/DOQI guidelines: CKD stage 1, eGFR >90 ml/min/ 1.73m^2 , CKD stage 2, eGFR = 60-89 ml/min/ 1.73m^2 , CKD stage 3A, eGFR = 45-59 ml/min/ 1.73m^2 , CKD stage 3B, eGFR = 30-44 ml/min/ 1.73m^2 , CKD stage 4, eGFR = 15-29 ml/min/ 1.73m^2 and CKD stage 5, eGFR < 15 ml/min/ 1.73m^2 . Data represents the percentage of the total number of CKD participants in the study (n=292).

Figure 7.5: Frequency distribution of CKD stages according to CKD etiology

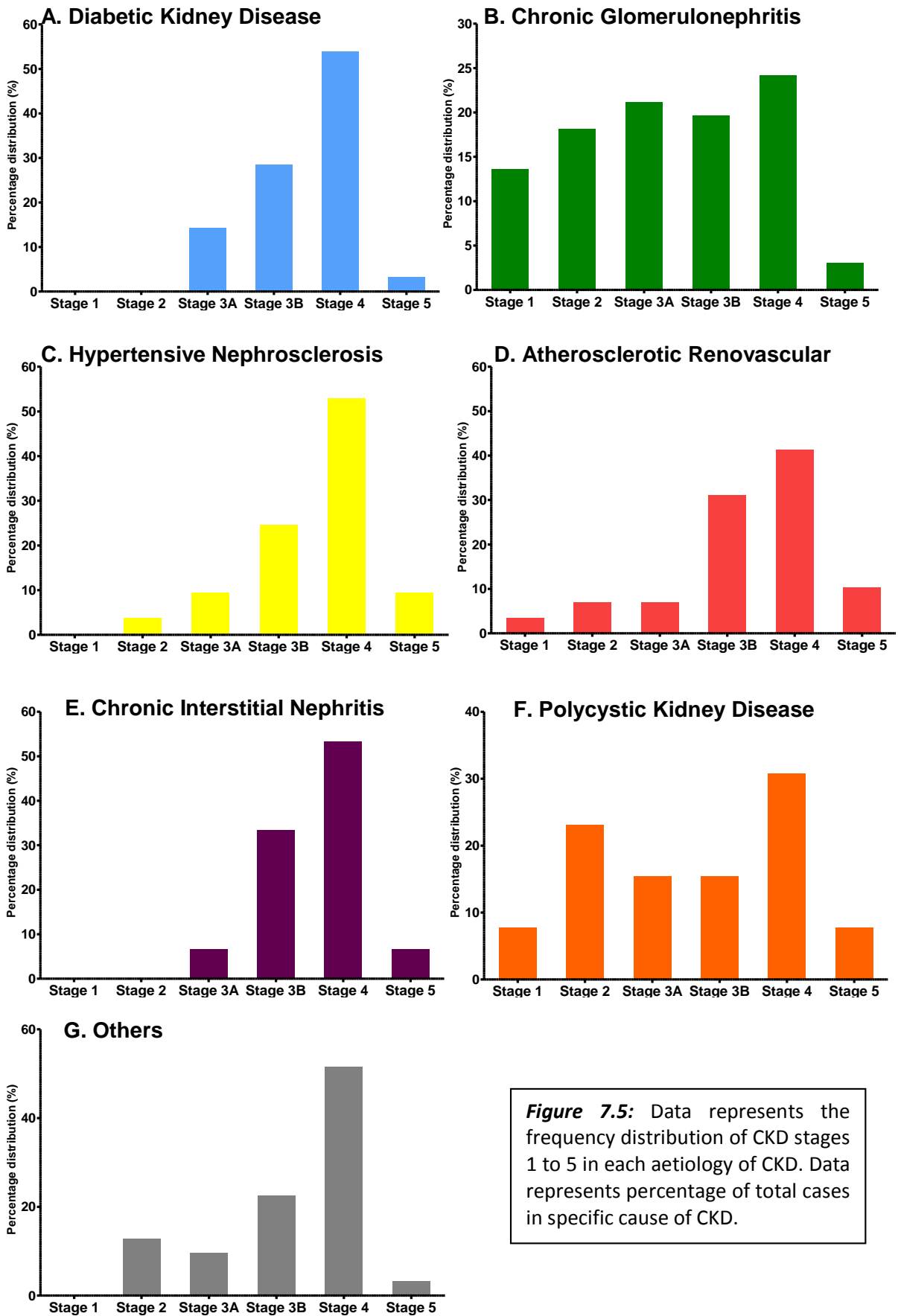


Figure 7.5: Data represents the frequency distribution of CKD stages 1 to 5 in each aetiology of CKD. Data represents percentage of total cases in specific cause of CKD.

7.2.6. Clinical and Laboratorial assessment

Serum creatinine, urine creatinine, blood urea nitrogen, albuminuria, serum cholesterol, triglycerides, calcium, phosphorus and PTH were analysed by standard autoanalyser techniques by the Clinical Chemistry Department at the Northern General Hospital (section 3.2.5.3). Total proteinuria was measured by the BCA assay (section 3.3.2.2) and urine sedimentoscopy was performed using a Microalbustix® urine test strip (section 3.2.5.2).

Tables 7.2 and 7.3 summarise the main biochemical as well as demographic characteristics from the study population.

7.2.6. Rate of eGFR decline and CKD progression by aetiology

The risk factors associated with CKD progression are described in section 1.5.1. CKD progression was evaluated by the rate of eGFR decline calculated by the regression analysis of 10 different eGFR values obtained over a period of approximately 3 years (figure 7.6). The mean rate of eGFR decline of the entire study population was $-0.79 \text{ ml/min/1.73m}^2$ ($n=292$). Overall, around one third of all CKD patients were classified as progressors (eGFR decline $> -2 \text{ ml/min/1.73m}^2/\text{year}$) and 184 patients were classified as stable or non-progressors (eGFR decline $< -2 \text{ ml/min/1.73m}^2/\text{year}$). The pathologies that caused the highest incidences of CKD progression were diabetic kidney disease (44.56%), chronic glomerulonephritis (42.42%) and hypertension (31.7%) (tables 7.2 and 7.3). Hypertensive patients presented the fastest rate of eGFR decline ($-1.25 \text{ ml/min/1.73m}^2$). Similar levels of kidney function reduction were observed in patients with CGN ($-1.22 \text{ ml/min/1.73m}^2$) and DKD ($-1.17 \text{ ml/min/1.73m}^2$). Interestingly, patients which presented chronic interstitial nephritis, atherosclerotic renovascular disease, polycystic renal disease and other causes of CKD showed lower levels of eGFR decline: -0.49 , 0.33 , -0.16 and $0.32 \text{ ml/min/1.73m}^2/\text{year}$, respectively (figure 7.7). Of note, around 17% of patients were classified as regressors as an improvement of kidney function was observed.

Figure 7.6: Regression analysis for estimation of eGFR decline

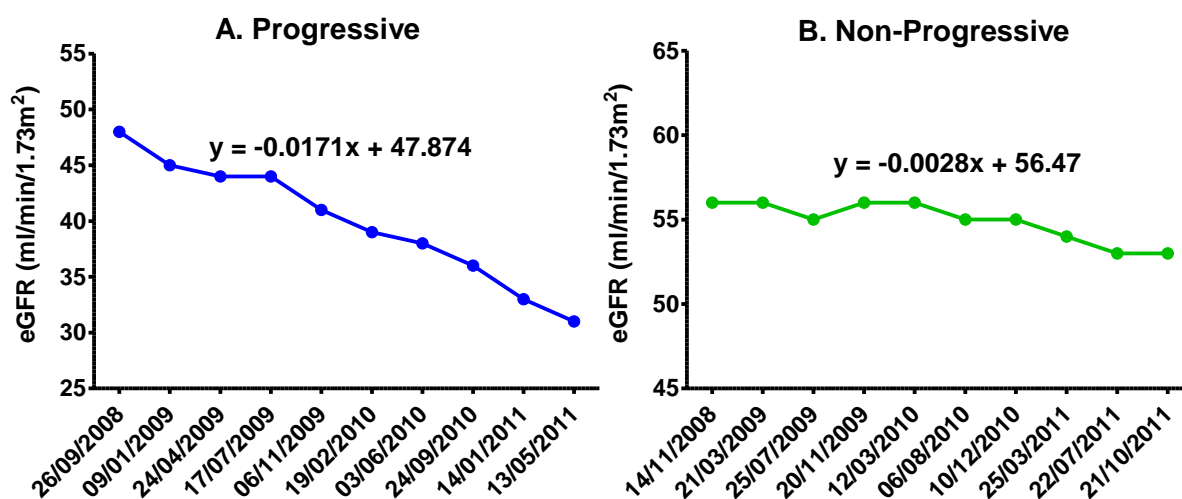


Figure 7.6: eGFR slope against time estimated by regression analysis showing in **(A)** an example of a CKD progressive patient with an estimated decline from 48 to 41.63 ml/min/1.73m² after a year ($x=365$ days, Δ eGFR = 41.63 – 48 = -6.37 ml/min/1.73m²/year) and **(B)** a non-progressive patient with eGFR ranging from 56 to 53 over a 3 years period and an estimated decline to 55.45 ml/min/1.73m² after a year ($x=365$ days, Δ eGFR = 55.45 – 56 = -0.55 ml/min/1.73m²/year), Y axis shows measured GFR and X axis when the test was performed.

The comparisons between the main demographic and clinical characteristics of the study population in each CKD aetiology were subdivided by levels of CKD progression (tables 7.4 to 7.10). Statistical analysis from contingency data was performed by Z-test for proportions and from biochemical measurements by Independent-samples T test. In DKD, the non-progressive group was significantly older and from white ethnicity, but not in any other aetiologies. Progressive DKD patients presented higher HbA1c (%), albuminuria, total proteinuria and co-morbidities at sampling. eGFR was lower in progressive patients at sampling in CGN and ADPKD only. Differences in CKD stage were only evident in patients with CGN (significantly more cases of CKD 1 and 2 in non-progressive), hypertensive (more cases of CKD 3B in non progressors), and ARVD (higher percentage of CKD 5 in progressive patients). In addition, both ADPKD patients with progressive CKD were at stage 4.

Table 7.2: Clinical and laboratory characteristics of CKD patients, their subgroups and controls

Variable	Controls	Total CKD patients	DKD	CGN	HTN	ARVD	CIN	ADPKD	Others
Number (n)	33	292	91	66	53	29	15	13	25
Gender:	23	179	57	41	31	22	7	7	14
Male, n (%)	(69.70%)	(61.31%)	(62.64%)	(62.12%)	(51.5%)	(75.86%)	(46.67%)	(53.85%)	(56%)
Age (years)	38.48 ± 7.6	63.9 ± 16.58	68.17 ± 11.61	49.81 ± 17.81	71.63 ± 12.04	75.41 ± 6.35	62.07 ± 13.05	47.23 ± 17.88	61.91 ± 19.05
Race:	21	264	83	57	46	27	15	13	23
Caucasians, n (%)	(63.64%)	(90.41%)	(90.22%)	(86.36%)	(86.79%)	(93.10%)	(100%)	(100%)	(92%)
BMI	22.34 ± 2.71	30.83 ± 6.07	31.81 ± 5.64	29.31 ± 5.72	31.18 ± 8.89	29.33 ± 4.04	27.94 ± 3.21	29.4 ± 6.64	25.89 ± 2.61
Smokers, n (%)	1 (3.03%)	33 (11.30%)	9 (9.89%)	3 (4.55%)	8 (15.09%)	6 (20.69%)	2 (13.33%)	2 (15.38%)	3 (12%)
CKD Stage 1, n (%)	NA	11 (3.77%)	0	9 (13.64%)	0	1 (3.35%)	0	1 (7.69%)	0
CKD Stage 2, n (%)	NA	21 (7.19%)	0	12 (18.18%)	2 (3.77%)	2 (6.90%)	0	3 (23.08%)	2 (8%)
CKD Stage 3A, n (%)	NA	39 (13.01%)	13 (14.29%)	14 (21.21%)	5 (9.43%)	2 (6.90%)	1 (6.67%)	2 (15.38%)	2 (8%)
CKD Stage 3B, n (%)	NA	73 (25.00%)	26 (28.57%)	13 (19.70%)	13 (24.53%)	9 (31.03%)	5 (33.33%)	2 (15.38%)	5 (20%)
CKD Stage 4, n (%)	NA	132 (45.55%)	49 (53.84%)	16 (24.24%)	28 (52.83%)	12 (41.38%)	8 (53.33%)	4 (30.77%)	15 (60%)
CKD Stage 5, n (%)	NA	16 (5.48%)	3 (3.30%)	2 (3.03%)	5 (9.43%)	3 (10.34%)	1 (6.67%)	1 (7.69%)	1 (4%)
eGFR at sampling (ml/min/1.73m²)	>90	36.70 ± 21.19	30.94 ± 11.01	55.05 ± 29.87	29.47 ± 14.36	30.20 ± 18.11	28.38 ± 9.66	46.25 ± 31.01	37.14 ± 20.16
CKD progression (%)	NA	108 (36.97%)	41 (44.56%)	28 (42.42%)	20 (37.74%)	6 (20.69%)	5 (33.33%)	2 (15.38%)	6 (22.58%)
Serum creatinine (µmol/L)	81.12 ± 12.49	183.39 ± 74.68	188.15 ± 63.55	143.43 ± 76.85	208.23 ± 87.94	207.32 ± 65.65	188.77 ± 66.52	177.64 ± 82.68	185.78 ± 68.35
Urine Creatinine (µmol/L)	11.4 ± 6.08	7.17 ± 4.94	6.45 ± 3.57	9.49 ± 6.60	7.76 ± 5.94	6.58 ± 4.05	6.01 ± 5.16	5.23 ± 4.23	6.81 ± 2.98
Albuminuria (mg/L)	1.8 ± 3.65	540.36 ± 1207.67	351.62 ± 633.21	1512.47 ± 2273.06	362.34 ± 611.79	296.83 ± 651.76	113.54 ± 218.64	165.35 ± 388.63	303.78 ± 505.92
Proteinuria (mg/L)	0.06 ± 0.03	0.92 ± 1.62	0.72 ± 0.95	1.97 ± 3.05	0.82 ± 0.87	0.52 ± 0.99	0.52 ± 0.56	0.43 ± 0.49	0.68 ± 1.08
BUN (mmol/L)	4.44 ± 1.16	13.86 ± 6.71	14.05 ± 6.66	12.69 ± 4.58	13.78 ± 4.91	13.24 ± 5.13	12.07 ± 4.89	13.15 ± 5.82	13.91 ± 6.94

Table 7.3: Clinical and laboratory characteristics of CKD patients, their subgroups and controls

Variable	Controls	Total CKD patients	DKD	CGN	HTN	ARVD	CIN	ADPKD	Others
Serum Cholesterol (mmol/L)	NA	4.51 ± 1.59	3.80 ± 1.07	5.95 ± 2.29	4.59 ± 1.29	4.38 ± 1.16	4.69 ± 1.40	4.32 ± 0.79	4.97 ± 1.22
Triglycerides (mmol/L)	NA	2.03 ± 1.44	1.86 ± 0.11	2.42 ± 1.82	2.14 ± 1.93	1.84 ± 1.18	1.68 ± 1.02	1.61 ± 1.00	2.19 ± 1.30
Serum calcium (mmol/L)	NA	2.33 ± 0.10	2.34 ± 0.11	2.35 ± 0.09	2.31 ± 0.09	2.32 ± 0.10	2.27 ± 0.10	2.34 ± 0.10	2.33 ± 0.11
Serum Phosphorus (mmol/L)	NA	1.20 ± 0.23	1.18 ± 0.25	1.21 ± 0.22	1.17 ± 0.20	1.28 ± 0.26	1.21 ± 0.17	1.25 ± 0.27	1.16 ± 0.20
Ca x P (mmol ² /L ²)	NA	2.78 ± 0.53	2.76 ± 0.54	2.86 ± 0.52	2.71 ± 0.45	2.96 ± 0.68	2.75 ± 0.45	2.88 ± 0.60	2.70 ± 0.47
PTH (pmol/L)	NA	146.58 ± 111.17	155.68 ± 112.01	93.12 ± 75.32	172.03 ± 131.04	148.79 ± 93.56	132.44 ± 94.01	149.83 ± 126.22	139.24 ± 109.92

Tables 7.2 and 7.3: The tables show the main clinical and biochemical characteristics of the participants of this study. Data is given as total number (n), percentage of total study population (%) and as mean ± SD, where applicable. Abbreviations: DKD = diabetic kidney disease, CGN = chronic glomerulonephritis, HTN = hypertensive nephrosclerosis, ARVD = atherosclerotic renovascular disease, CIN = chronic interstitial nephritis, ADPKD = adult polycystic kidney disease, BMI= Body Mass Index, eGFR = estimated glomerular filtration rate, BUN = blood urea nitrogen, Ca = calcium, P= = phosphorus, PTH = Para thyroid hormone. Other causes of CKD included cases of: cast nephropathy (Multiple Myeloma), amyloidosis, idiopathic thrombocytopenic purpura, Henoch Schölein purpura, monoclonal gammopathy of undetermined significance (MGUS), microscopic polyarteritis, familial renal disease, medullary sponge kidneys, sarcoidosis, lupus nephritis, HIV-associated nephritis, Tacrolimus toxicity and renal cell carcinoma. NA = not applicable.

Table 7.4: Main demographic and clinical characteristics of Diabetic Kidney Disease patients (n=91) analysed by CKD progression

Variables	Progressors	Non-Progressors	p-value
Number (n)	41	50	--
Gender: Male, n (%)	28 (68.29%)	29 (58%)	0.1563
Age (years)	64.89 ± 12.65	70.98 ± 10.04	0.0101
Race: Caucasians, n (%)	35 (85.37%)	48 (96%)	0.0376
Type of diabetes: T1DM	8 (19.51%)	7 (14%)	0.4777
T2DM	33 (80.49%)	43 (86%)	0.4777
BMI	31.05 ± 6.59	32.47 ± 4.64	0.2460
Co-morbidities, n (%)	41 (100%)	46 (92%)	0.0312
Systolic BP (mmHg)	147.18 ± 23.43	145.88 ± 16.48	0.7575
Diastolic BP (mmHg)	73.31 ± 12.33	73.87 ± 8.84	0.8025
CKD Stage 1, n (%)	0	0	--
CKD Stage 2, n (%)	0	0	--
CKD Stage 3A, n (%)	6 (14.63%)	7 (14%)	0.4641
CKD Stage 3B, n (%)	12 (29.27%)	14 (28%)	0.4483
CKD Stage 4, n (%)	21 (51.22%)	28 (56%)	0.3228
CKD Stage 5, n (%)	2 (4.88%)	1 (2%)	0.2207
eGFR at sampling (ml/min/1.73m ²)	31.09 ± 11.29	30.89 ± 10.65	0.9287
Serum creatinine (µmol/L)	192.42 ± 73.41	184.72 ± 53.58	0.5607
Urine Creatinine (µmol/L)	5.28 ± 2.27	7.38 ± 4.16	0.0021
Albuminuria (mg/L)	542.82 ± 745.02	186.15 ± 460.43	0.0063
Proteinuria (mg/L)	1.03 ± 1.16	0.45 ± 0.61	0.0017
BUN (mmol/L)	14.84 ± 6.96	13.43 ± 6.42	0.5313
HbA1c (%)	8.1 ± 1.9	7.0 ± 1.4	0.0109
Serum Cholesterol (mmol/L)	3.91 ± 1.03	3.71 ± 1.10	0.4305
Triglycerides (mmol/L)	1.82 ± 1.22	1.90 ± 0.92	0.3341
Serum calcium (mmol/L)	2.34 ± 0.09	2.34 ± 0.12	0.1255
Serum Phosphorus (mmol/L)	1.23 ± 0.28	1.15 ± 0.21	0.9169
Ca x P (mmol ² /L ²)	2.83 ± 0.54	2.71 ± 0.53	0.9040
PTH (pmol/L)	148.20 ± 114.30	161.94 ± 110.85	0.0008

Table 7.4: Baseline characteristics from diabetic kidney disease patients subdivided into progressors (eGFR decline > - 2 ml/min/1.73m²/year) and non-progressors (eGFR decline < - 2 ml/min/1.73m²/year). Data presented as percentage of the sub number of cases or as mean ± SD unless otherwise stated. p values marked in red represent statistically significant difference (p<0.05). Abbreviations: T1DM = Type 1 Diabetes Mellitus, T2DM = Type 2 Diabetes Mellitus, BP = Blood Pressure, HbA1c = glycosylated haemoglobin.

Table 7.5: Main demographic and clinical characteristics of Chronic Glomerulonephritis patients (n=66) analysed by CKD progression

Variables	Progressors	Non-Progressors	p-value
Number (n)	28	38	--
Gender: Male, n (%)	16 (57.14%)	25 (65.79%)	0.2358
Age (years)	55.13 ± 15.35	45.94 ± 18.98	0.0504
Race: Caucasians, n (%)	23 (82.14%)	34 (89.47%)	0.1949
BMI	27.78 ± 6.89	30.62 ± 4.32	0.2317
Membranous Nephropathy, n (%)*	5 (12.20%)	10 (24.39%)	0.2119
IgA Nephropathy, n (%)*	6 (14.63%)	8 (19.51%)	0.4483
FSGS, n (%)*	2 (4.88%)	3 (7.32%)	0.4721
Membranoproliferative GN, n (%)*	2 (4.88%)	1 (2.44%)	0.1788
Minimal Change, n (%)*	0	2 (4.88%)	0.1112
RPGN, n (%)*	2 (4.88%)	0	0.0427
Co-morbidities, n (%)	24 (85.71%)	25 (65.79%)	0.0672
Systolic BP (mmHg)	140.47 ± 18.47	137.96 ± 16.13	0.6356
Diastolic BP (mmHg)	79.37 ± 7.64	78.78 ± 9.39	0.8157
CKD Stage 1, n (%)	1 (3.57%)	8 (21.05%)	0.0202
CKD Stage 2, n (%)	2 (7.14%)	10 (26.32%)	0.0227
CKD Stage 3A, n (%)	7 (25%)	7 (18.42%)	0.2579
CKD Stage 3B, n (%)	5 (17.86%)	8 (21.05%)	0.3745
CKD Stage 4, n (%)	12 (42.86%)	4 (10.53%)	0.0012
CKD Stage 5, n (%)	1 (3.57%)	1 (2.63%)	0.4129
eGFR at sampling (ml/min/1.73m ²)	41.04 ± 20.99	65.90 ± 31.46	0.0009
Serum creatinine (µmol/L)	166.90 ± 65.15	126.04 ± 81.29	0.0624
Urine Creatinine (µmol/L)	7.75 ± 5.19	10.44 ± 7.29	0.1264
Albuminuria (mg/L)	2216.40 ± 2944.30	989.45 ± 1506.93	0.0897
Proteinuria (mg/L)	2.38 ± 4.32	1.62 ± 1.59	0.5067
BUN (mmol/L)	13.04 ± 6.18	12.34 ± 5.25	0.3732
Serum Cholesterol (mmol/L)	6.23 ± 1.92	5.71 ± 2.59	0.4775
Triglycerides (mmol/L)	2.27 ± 1.56	2.55 ± 2.04	0.6237
Serum calcium (mmol/L)	2.36 ± 0.09	2.35 ± 0.09	0.7778
Serum Phosphorus (mmol/L)	1.28 ± 0.19	1.15 ± 0.23	0.0429
Ca x P (mmol ² /L ²)	3.04 ± 0.49	2.71 ± 0.50	0.0306
PTH (pmol/L)	68.08 ± 39.76	120.25 ± 95.45	0.0999

Table 7.5: Baseline characteristics from patients with chronic glomerulonephritis subdivided into progressors (eGFR decline > - 2 ml/min/1.73m²/year) and non-progressors (eGFR decline < - 2 ml/min/1.73m²/year). Data is presented as percentage of the sub number of cases or as mean ± SD unless otherwise stated. p values marked in red represent statistically significant difference (p<0.05). Abbreviations: FSGS = Focal and Segmental Glomerulosclerosis, GN = glomerulonephritis, RPGN = Rapid and Progressive glomerulonephritis. *Total number of cGN cases = 66, with 41 biopsies done during the time of this study. Cases of * Calculated as a percentage of the number of biopsied cases (n=41).

Table 7.6: Main demographic and clinical characteristics of patients with Hypertensive Nephrosclerosis (n=53) analysed by CKD progression

Variables	Progressors	Non-Progressors	<i>p-value</i>
Number (n)	20	33	--
Gender: Male, n (%)	11 (55.56%)	20 (60.61%)	0.3446
Age (years)	70.67 ± 12.13	72.15 ± 12.14	0.6702
Race: Caucasians, n (%)	18 (88.89%)	28 (84.85%)	0.2946
BMI	31.71 ± 8.48	32.55 ± 9.52	0.8265
Co-morbidities, n (%)	17 (85%)	24 (72.73%)	0.3030
Systolic BP (mmHg)	138.18 ± 24.27	144.13 ± 18.29	0.4006
Diastolic BP (mmHg)	75.65 ± 12.98	73.75 ± 10.92	0.6264
CKD Stage 1, n (%)	0	0	--
CKD Stage 2, n (%)	2 (10%)	0	0.0322
CKD Stage 3A, n (%)	1 (5%)	4 (12.12%)	0.1949
CKD Stage 3B, n (%)	2 (10%)	11 (33.33%)	0.0281
CKD Stage 4, n (%)	12 (60%)	16 (48.48%)	0.2089
CKD Stage 5, n (%)	3 (15%)	2 (6.06%)	0.1401
eGFR at sampling (ml/min/1.73m ²)	29.00 ± 16.90	29.77 ± 12.79	0.8470
Serum creatinine (µmol/L)	215.76 ± 87.41	199.00 ± 90.63	0.5484
Urine Creatinine (µmol/L)	7.92 ± 7.36	7.57 ± 4.32	0.8974
Albuminuria (mg/L)	472.76 ± 631.69	337.91 ± 646.80	0.5305
Proteinuria (mg/L)	1.06 ± 1.08	0.70 ± 0.74	0.2414
BUN (mmol/L)	14.31 ± 4.63	11.85 ± 4.99	0.1094
Serum Cholesterol (mmol/L)	4.45 ± 2.06	4.12 ± 1.58	0.7347
Triglycerides (mmol/L)	2.62 ± 2.88	1.6 ± 0.94	0.2135
Serum calcium (mmol/L)	2.29 ± 0.10	2.32 ± 0.09	0.3746
Serum Phosphorus (mmol/L)	1.21 ± 0.22	1.16 ± 0.18	0.4268
Ca x P (mmol ² /L ²)	2.75 ± 0.49	2.71 ± 0.43	0.6982
PTH (pmol/L)	191.86 ± 189.75	133.70 ± 86.60	0.1818

Table 7.6: Baseline characteristics from patients diagnosed with hypertensive nephrosclerosis subdivided into progressors (eGFR decline > - 2 ml/min/1.73m²/year) and non-progressors (eGFR decline < - 2 ml/min/1.73m²/year). Data is presented as percentage of the sub number of cases or as mean ± SD unless otherwise stated. p values marked in red represent statistically significant difference (p<0.05). Abbreviations: see table 7.2.

Table 7.7: Main demographic and clinical characteristics of patients with Atherosclerotic Renovascular disease (n=29) analysed by CKD progression

Variables	Progressors	Non-Progressors	p-value
Number (n)	6	23	--
Gender: Male, n (%)	3 (50%)	19 (72.22%)	0.0485
Age (years)	74.83 ± 6.91	75.57 ± 6.35	0.8208
Race: Caucasians, n (%)	6 (100%)	19 (91.30%)	0.1357
BMI	30.90 ± 5.62	28.99 ± 3.81	0.8775
Co-morbidities, n (%)	4 (66.67%)	13 (56.52%)	0.3264
Systolic BP (mmHg)	149.60 ± 16.96	145.10 ± 15.66	0.6101
Diastolic BP (mmHg)	78.60 ± 18.20	72.65 ± 7.53	0.5107
CKD Stage 1, n (%)	0	1 (4.35%)	0.3015
CKD Stage 2, n (%)	1 (16.67%)	1 (4.35%)	0.1446
CKD Stage 3A, n (%)	0	2 (8.70%)	0.2266
CKD Stage 3B, n (%)	2 (33.33%)	7 (30.43%)	0.4443
CKD Stage 4, n (%)	2 (33.33%)	10 (43.48%)	0.3264
CKD Stage 5, n (%)	1 (16.67%)	2 (8.70%)	0.0217
eGFR at sampling (ml/min/1.73m ²)	24.60 ± 11.61	31.60 ± 19.38	0.3241
Serum creatinine (µmol/L)	219.60 ± 84.97	204.25 ± 62.24	0.7197
Urine Creatinine (µmol/L)	6.53 ± 2.02	6.59 ± 4.48	0.9669
Albuminuria (mg/L)	452.68 ± 832.93.17	254.32 ± 610.04	0.6039
Proteinuria (mg/L)	1.10 ± 2.12	0.38 ± 0.44	0.1499
BUN (mmol/L)	13.68 ± 6.12	10.18 ± 4.02	0.6906
Serum Cholesterol (mmol/L)	5.43 ± 0.59	4.13 ± 1.13	0.0351
Triglycerides (mmol/L)	1.63 ± 0.85	1.89 ± 1.26	0.6560
Serum calcium (mmol/L)	2.37 ± 0.10	2.30 ± 0.10	0.4917
Serum Phosphorus (mmol/L)	1.42 ± 0.31	1.27 ± 0.29	0.7678
Ca x P (mmol ² /L ²)	3.31 ± 0.67	2.89 ± 0.68	0.7586
PTH (pmol/L)	92 ± 20.70	163.93 ± 100.02	0.0331

Table 7.7: Baseline characteristics from patients with atherosclerotic renovascular disease subdivided into progressors (eGFR decline > - 2 ml/min/1.73m²/year) and non-progressors (eGFR decline < - 2 ml/min/1.73m²/year). Data presented as percentage of the sub number of cases or as mean ± SD unless otherwise stated. p values marked in red represent statistically significant difference (p<0.05). Abbreviations: see table 7.2

Table 7.8: Main demographic and clinical characteristics of patients with Chronic Interstitial Nephritis (n=15) analysed by CKD progression

Variables	Progressors	Non-Progressors	<i>p-value</i>
Number (n)	5	10	--
Gender: Male, n (%)	2 (40%)	5 (50%)	0.3557
Age (years)	62.2 ± 13.10	62 ± 13.74	0.9788
Race: Caucasians, n (%)	5 (100%)	10 (100%)	--
BMI	26.6 ± 1.22	28.95 ± 4.06	0.3401
Co-morbidities, n (%)	4 (80%)	7 (70%)	0.6818
Systolic BP (mmHg)	145.00 ± 22.11	141.25 ± 26.18	0.7882
Diastolic BP (mmHg)	75.40 ± 18.02	74.13 ± 12.73	0.8947
CKD Stage 1, n (%)	0	0	--
CKD Stage 2, n (%)	0	0	--
CKD Stage 3A, n (%)	0	1 (10%)	0.4654
CKD Stage 3B, n (%)	3 (60%)	2 (20%)	0.1211
CKD Stage 4, n (%)	1 (20%)	7 (70%)	0.0672
CKD Stage 5, n (%)	1 (20%)	0	0.1443
eGFR at sampling (ml/min/1.73m ²)	27.6 ± 10.14	28.88 ± 10.02	0.8298
Serum creatinine (µmol/L)	209.8 ± 94.88	192.63 ± 81.64	0.7469
Urine Creatinine (µmol/L)	8.34 ± 6.03	4.92 ± 4.58	0.3038
Albuminuria (mg/L)	248.98 ± 408.82	56.02 ± 66.73	0.3522
Proteinuria (g/L)	0.56 ± 0.50	0.47 ± 0.59	0.7805
BUN (mmol/L)	12.94 ± 4.57	11.13 ± 4.41	0.6905
Serum Cholesterol (mmol/L)	5.20 ± 2.09	4.25 ± 0.75	0.4384
Triglycerides (mmol/L)	2.48 ± 1.39	1.27 ± 0.18	0.1795
Serum calcium (mmol/L)	2.24 ± 0.15	2.29 ± 0.08	0.5378
Serum Phosphorus (mmol/L)	1.2 ± 0.16	1.22 ± 0.19	0.8693
Ca x P (mmol ² /L ²)	2.70 ± 0.48	2.78 ± 0.47	0.7710
PTH (pmol/L)	334.00 ± 128.01	93.14 ± 48.06	0.0018

Table 7.8: Baseline characteristics from patients with Chronic Interstitial Nephritis subdivided into progressors (eGFR decline > - 2 ml/min/1.73m²/year) and non-progressors (eGFR decline < - 2 ml/min/1.73m²/year). Data presented as percentage of the sub number of cases or as mean ± SD unless otherwise stated. Abbreviations: see table 7.2

Table 7.9: Main demographic and clinical characteristics of ADPKD patients (n=13) analysed by CKD progression

Variables	Progressors	Non-Progressors	p-value
Number (n)	2	11	--
Gender: Male, n (%)	1 (50%)	6 (54.55%)	0.9045
Age (years)	53.5 ± 20.51	46.09 ± 18.23	0.7005
Race: Caucasians, n (%)	2 (100%)	11 (100%)	--
BMI	25.05 ± 8.13	32.3 ± 4.85	0.4071
Co-morbidities, n (%)	2 (100%)	6 (54.55%)	0.2225
Systolic BP (mmHg)	128 ± 0	135.25 ± 10.96	0.2390
Diastolic BP (mmHg)	72.5 ± 6.36	81 ± 8.09	0.3567
CKD Stage 1, n (%)	0	1 (9.09%)	0.6599
CKD Stage 2, n (%)	0	3 (27.27%)	0.4009
CKD Stage 3A, n (%)	0	2 (18.18%)	0.5092
CKD Stage 3B, n (%)	0	2 (18.18%)	0.5092
CKD Stage 4, n (%)	2 (100%)	2 (18.18%)	0.0209
CKD Stage 5, n (%)	0	1 (9.09%)	0.6599
eGFR at sampling (ml/min/1.73m ²)	18.00 ± 0	51.9 ± 31.02	0.0072
Serum creatinine (µmol/L)	273.5 ± 28.99	156.33 ± 75.05	0.0160
Urine Creatinine (µmol/L)	3.4 ± 1.13	5.59 ± 4.56	0.2196
Albuminuria (mg/L)	23.00 ± 20.08	193.87 ± 423.25	0.2355
Proteinuria (g/L)	0.19 ± 0.02	0.38 ± 0.52	0.2821
Serum Cholesterol (mmol/L)	3.55 ± 0.21	3.98 ± 1.75	0.0186
Triglycerides (mmol/L)	1.65 ± 1.63	1.60 ± 0.94	0.9727
Serum calcium (mmol/L)	2.31 ± 0.20	2.34 ± 0.09	0.8566
Serum Phosphorus (mmol/L)	1.13 ± 0.36	1.28 ± 0.27	0.6581
Ca x P (mmol ² /L ²)	2.56 ± 0.61	2.96 ± 0.61	0.5168
PTH (pmol/L)	159.3 ± 207.47	146.67 ± 117.83	0.9461

Table 7.9: Baseline characteristics from patients Autosomal dominant Polycystic Renal Disease (ADPKD) subdivided into progressors (eGFR decline > - 2 ml/min/1.73m²/year) and non-progressors (eGFR decline < - 2 ml/min/1.73m²/year). Data presented as percentage of the sub number of cases or as mean ± SD unless otherwise stated. p values marked in red represent statistically significant difference (p<0.05). Abbreviations: see table 7.2

Table 7.10: Main demographic and clinical characteristics of patients with other* causes of CKD (n=25) analysed by levels of CKD progression

Variables	Progressors	Non-Progressors	p-value
Number (n)	6	19	--
Gender: Male, n (%)	4 (66.67%)	10 (52.63%)	0.2743
Age (years)	74.80 ± 6.65	58.33 ± 19.92	0.0077
Race: Caucasians, n (%)	6 (100%)	17 (89.47%)	0.2033
BMI	27.13 ± 1.65	25.52 ± 2.91	0.3917
Multiple Myeloma (cast nephropathy), n (%)	2 (33.33%)	2 (10.53%)	0.0918
Amyloidosis, n (%)	1 (16.67%)	0	0.0344
Lupus Nephritis, n (%)	1 (16.67%)	2 (10.53%)	0.3446
MGUS, n (%)	0	2 (10.53%)	0.2033
Familial renal disease, n (%)	0	2 (10.53%)	0.2033
Medullary sponge kidney, n (%)	0	2 (10.53%)	0.2033
Microscopic Polyarteritis, n (%)	1 (16.67%)	1 (5.26%)	0.1841
Sarcoidosis, n (%)	0	1 (5.26%)	0.2843
Idiopathic thrombocytopenic purpura, n (%)	0	1 (5.26%)	0.2843
Henoch Scholein purpura, n (%)	0	1 (5.26%)	0.2843
Renal stone disease, n (%)	0	2 (10.53%)	0.2033
Renal cell carcinoma, n (%)	1 (16.67%)	1 (5.26%)	0.1841
Tacrolimus toxicity, n (%)	0	1 (5.26%)	0.2843
HIV-associated nephropathy, n (%)	0	1 (5.26%)	0.2843
CKD Stage 1, n (%)	0	0	--
CKD Stage 2, n (%)	1 (16.67%)	1 (5.26%)	0.1841
CKD Stage 3A, n (%)	1 (16.67%)	1 (5.26%)	0.1841
CKD Stage 3B, n (%)	0	5 (26.32%)	0.081
CKD Stage 4, n (%)	3 (50%)	12 (63.16%)	0.2843
CKD Stage 5, n (%)	1 (16.67%)	0	0.0301
eGFR at sampling (ml/min/1.73m ²)	33.80 ± 20.71	38.12 ± 20.53	0.6945
Serum creatinine (µmol/L)	199.80 ± 114.45	168.69 ± 53.34	0.5843
Urine Creatinine (µmol/L)	9.50 ± 5.96	6.06 ± 3.23	0.2751
Albuminuria (mg/L)	645.22 ± 464.28	82.19 ± 82.56	0.0002
Proteinuria (g/L)	1.10 ± 0.99	0.30 ± 0.32	0.0136
Serum Cholesterol (mmol/L)	4.46 ± 0.46	5.19 ± 1.45	0.1131
Triglycerides (mmol/L)	1.70 ± 0.42	2.36 ± 1.70	0.1989
Serum calcium (mmol/L)	2.32 ± 0.08	2.33 ± 0.13	0.8491
Serum Phosphorus (mmol/L)	1.04 ± 0.20	1.18 ± 0.21	0.2087
Ca x P (mmol ² /L ²)	2.40 ± 0.42	2.74 ± 0.50	0.1713
PTH (pmol/L)	153.20 ± 177.43	131.29 ± 94.81	0.8033

Table 7.10: Baseline characteristics from patients diagnosed with other causes of CKD (for details see section 7.2.4) subdivided into progressors (eGFR decline > - 2 ml/min/1.73m²/year) and non-progressors (eGFR decline < - 2 ml/min/1.73m²/year). Data presented as percentage of the sub number of cases or as mean ± SD unless otherwise stated. p values marked in red represent statistically significant difference (p<0.05). Abbreviations: MGUS = monoclonal gammopathy of undetermined significance, and the rest in table 7.2.

7.2.7. Baseline demographic and clinical characteristics in different age groups

The mean age of CKD patients was 63.9 ± 16.58 years, with 61.9% of the study population aged above 65 years. The risk for decline in kidney function and subsequent incidence of CKD progression is higher in older people (section 1.5.1.1.). For this reason, an analysis of the demographic parameters of the study population by different age groups (above and below 65 years old) was performed (figure 7.11). This showed that older patients presented higher systolic and diastolic blood pressure, lower eGFR, lower albuminuria and proteinuria levels as well as lower cholesterol levels at sampling.

Table 7.11: Comparison of main clinical parameters between different age groups

Variables	< 65 years old	≥ 65 years old	p-value
Number (n)	111	181	--
Mean Age (years)	46.63 ± 13.82	74.40 ± 6.25	< 0.0001
Gender: Male, n (%)	67 (60.36%)	112 (61.88%)	0.3974
Race: Caucasians, n (%)	91 (81.98%)	173 (95.58%)	<0.0001
BMI	31.05 ± 6.99	30.69 ± 5.48	0.7147
Systolic BP (mmHg)	139.98 ± 18.26	145.26 ± 19.55	0.0371
Diastolic BP (mmHg)	77.66 ± 10.55	74.33 ± 10.43	0.0174
CKD Stage 1, n (%)	11 (9.91%)	0	<0.0001
CKD Stage 2, n (%)	17 (15.32%)	4 (2.21%)	<0.0001
CKD Stage 3A, n (%)	22 (19.82%)	17 (9.39%)	0.0055
CKD Stage 3B, n (%)	14 (12.61%)	59 (32.60%)	<0.0001
CKD Stage 4, n (%)	43 (38.74%)	89 (49.17%)	0.0409
CKD Stage 5, n (%)	4 (3.60%)	12 (6.63%)	0.1357
eGFR at sampling (ml/min/1.73m ²)	46.81 ± 27.80	30.05 ± 11.72	< 0.0001
CKD progression	39 (35.24%)	69 (38.12%)	0.3050
Serum creatinine (μmol/L)	167.64 ± 80.15	192.62 ± 69.90	0.0094
Urine Creatinine (μmol/L)	7.60 ± 6.13	6.96 ± 4.09	0.3060
Albuminuria (mg/L)	981.08 ± 1785.44	285.20 ± 539.96	<0.0001
Proteinuria (g/L)	1.38 ± 2.33	0.64 ± 0.82	0.0003
BUN (mmol/L)	13.59 ± 6.53	14.68 ± 7.31	0.4859
Serum Cholesterol (mmol/L)	5.11 ± 1.86	4.22 ± 1.21	<0.0001
Triglycerides (mmol/L)	2.17 ± 1.56	1.98 ± 1.35	0.3357
Serum calcium (mmol/L)	2.34 ± 0.10	2.32 ± 0.11	0.2884
Serum Phosphorus (mmol/L)	1.19 ± 0.22	1.20 ± 0.23	0.9280
Ca x P (mmol ² /L ²)	2.79 ± 0.53	2.78 ± 0.54	0.9597
PTH (pmol/L)	128.93 ± 109.61	155.15 ± 111.31	0.1135

Table 7.11: The main demographic and biochemical characteristics from patients under and above 65 years old. Data presented as percentage of the sub number of cases or as mean \pm SD unless otherwise stated. p values marked in red represent statistically significant difference ($p < 0.05$). Abbreviations: see table 7.2.

7.2.8. CKD progression by etiology

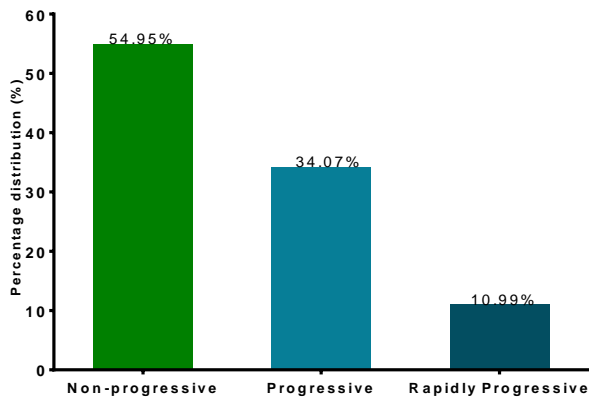
Patients from different CKD etiologies (diabetic kidney disease (n=91), chronic glomerulonephritis (n=66), hypertensive nephrosclerosis (n=53), atherosclerotic renovascular disease (n=29), chronic interstitial nephritis (n=15) and ADPKD (n=13) and other causes (n=25)) were also subclassified according to their levels of CKD progression (figure 7.7).

7.2.9. Renal biopsy from CGN patients

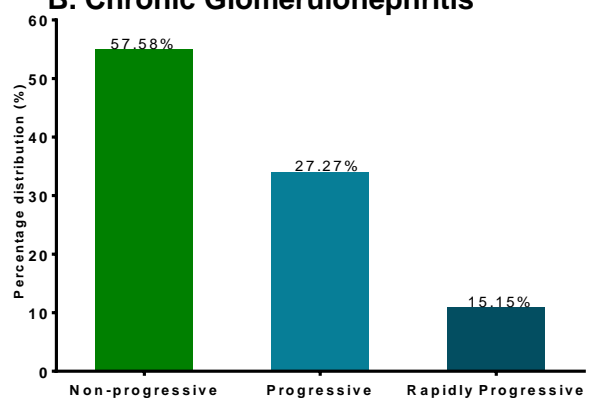
Forty one patients diagnosed with chronic glomerulonephritis were submitted to renal biopsy during the study. Recommendation for renal biopsy was made when CGN cause was not clear and upon presence of persistent haematuria, heavy proteinuria along with signs of kidney function deterioration. Main diagnosis were: membranous nephropathy (36.59%), IgA nephropathy (34.15%), focal and segmental glomerulosclerosis (FSGS) (12.20%), membranoproliferative glomerulonephritis (7.32%), minimal change (4.88%) and rapidly progressive glomerulonephritis (RPGN) (4.88%) (figure 7.3-B). Kidney tissue samples were analysed by light and electron microscopy by the Department of Renal Histopathology of the Northern General Hospital (Sheffield, UK). A fibrosis classification (mild, moderate or severe) was achieved by the estimation of a percentage score calculated through the evaluation of morphologic features of glomerulosclerosis and tubulointerstitial scarring. 46.34% (n=19) presented mild features of renal fibrosis, compared to 41.46% (n=17) which had moderate and 12.20% (n=5) with severe renal scarring. The average fibrosis percentage score for non-progressive patients was 16.41 ± 2.19 , whilst progressive and rapidly progressive presented 43.19 ± 5.24 and 73.07 ± 6.36 respectively.

Figure 7.7: CKD progression in different etiologies

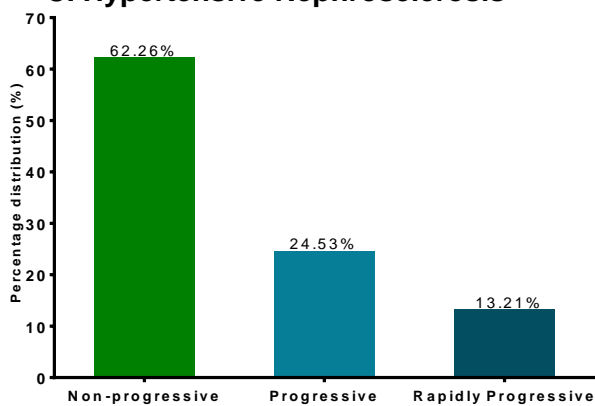
A. Diabetic Kidney Disease



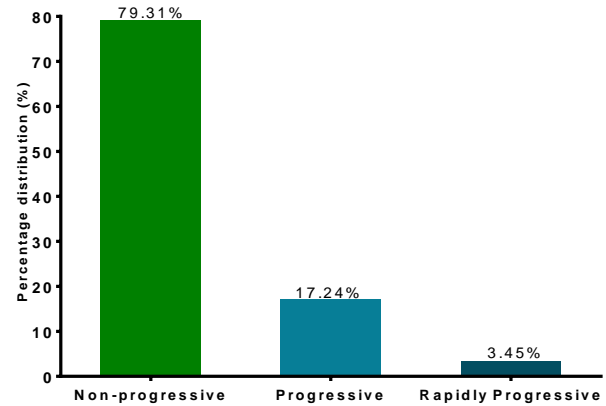
B. Chronic Glomerulonephritis



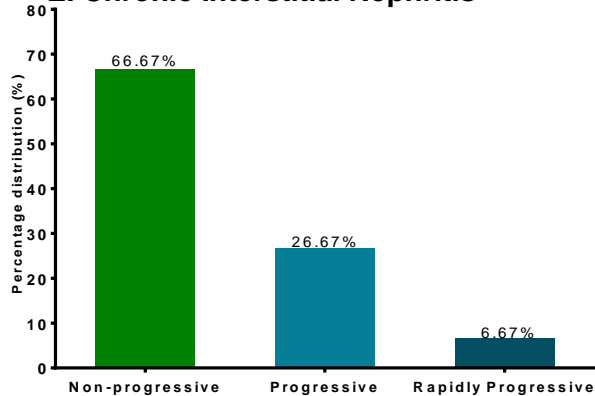
C. Hypertensive Nephrosclerosis



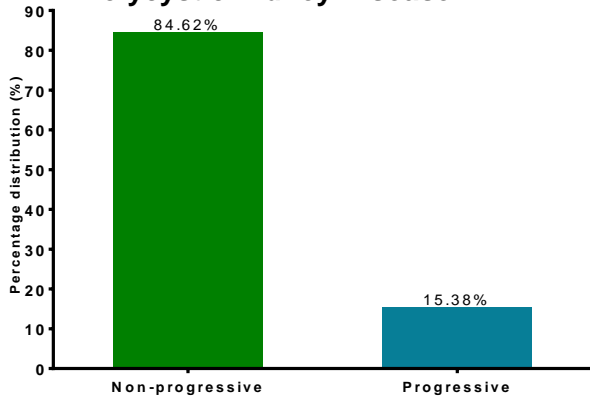
D. Atherosclerotic Renovascular



E. Chronic Interstitial Nephritis



F. Polycystic Kidney Disease



G. Others

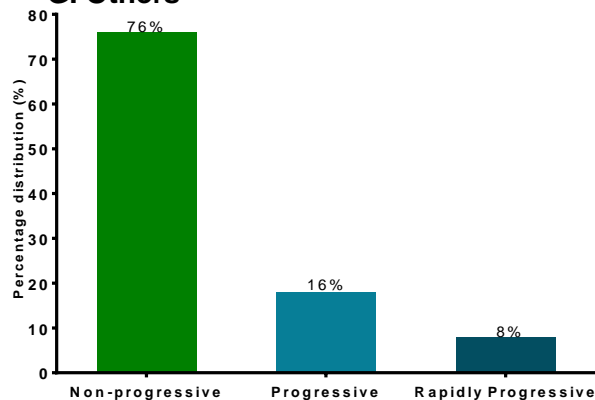


Figure 7.7: Percentage of CKD patients from different aetiologies classified as non-progressive (rate of eGFR decline < - 2 ml/min/1.73m²/year), progressive (eGFR decline between - 2 and -5 ml/min/1.73m²/year) and rapidly progressive (eGFR decline > - 2 ml/min/1.73m²/year)

7.2.10. Clinical and biochemical parameters of healthy volunteers

A total of 33 adult healthy volunteers were recruited as a control group. This group consisted of subjects above 18 years old, without history of any type of kidney disease, hypertension, diabetes or any other chronic condition (section 3.2.3.1). The control group consisted of 10 females and 23 males, with 63.64% caucasian and 36.36% from other ethnicities. The mean age of controls in this study was 38.48 ± 7.61 years, which was significantly lower than CKD patients. The main clinical and biochemical characteristics of healthy volunteers (table 7.12) indicated that albuminuria was below detectable levels in majority of healthy volunteers.

Table 7.12: Baseline clinical characteristics of healthy volunteers

ID	Age	Gender	Ethnicity	Albuminuria mg/L	Proteinuria	Urine Creatinine $\mu\text{mol/L}$	ACR	PCR
1	48	Female	Caucasian	0	0.02	6.0	0	0.003
2	28	Male	Caucasian	0	0.02	6.3	0	0.003
3	38	Female	Black	0	0.06	7.0	0	0.009
4	36	Male	Black	0	0.11	19.4	0	0.006
5	44	Male	Asian	0	0.06	6.5	0	0.009
6	45	Male	Asian	5.4	0.11	5.9	0.9	0.019
7	51	Male	Caucasian	0	0.02	11.8	0	0.002
8	27	Female	Caucasian	0	0.02	4.4	0	0.005
9	48	Male	Caucasian	4.0	0.10	4.9	0.8	0.02
10	49	Male	Caucasian	0	0.06	20.7	0	0.003
11	38	Female	Asian	0	0.06	13	0	0.005
12	32	Male	Black	0	0.06	19.6	0	0.003
13	43	Female	Asian	5.5	0.09	13.3	0.4	0.007
14	41	Male	Caucasian	0	0.04	10.8	0	0.004
15	50	Male	Caucasian	0	0.08	9.4	0	0.009
16	37	Male	Caucasian	0	0.03	2.2	0	0.014
17	47	Male	Caucasian	0	0.06	12.1	0	0.005
18	44	Male	Caucasian	0	0.06	9.6	0	0.006
19	43	Male	Caucasian	0	0.06	9.6	0	0.006
20	39	Male	Hispanic	12.8	0.10	24.7	0.5	0.004
21	39	Female	Hispanic	3.9	0.08	16.5	0.2	0.005
22	34	Male	Asian	0	0.06	5.9	0	0.01
23	25	Female	Caucasian	8.5	0.11	11.2	0.8	0.01
24	31	Male	Caucasian	0	0.07	25.7	0	0.003
25	44	Male	Caucasian	0	0.04	10.5	0	0.004
26	35	Male	Caucasian	5.8	0.09	18.9	0.3	0.005
27	38	Male	Caucasian	0	0.06	11.1	0	0.005
28	30	Male	Caucasian	0	0.06	10	0	0.006
29	28	Female	Hispanic	0	0.03	8.2	0	0.004
30	31	Female	Asian	0	0.02	5.8	0	0.003
31	31	Male	Caucasian	0	0.02	18.7	0	0.001
32	29	Male	Caucasian	0	0.02	4.2	0	0.005
33	47	Male	Caucasian	10.7	0.10	12.3	0.9	0.008

Table 7.12: The main demographic and biochemical characteristics from healthy volunteers (control group, n=33).

7.3. Urine excretion of Transglutaminase type 2 in Human Chronic Kidney Disease

7.3.1. Urine Transglutaminase type 2 measurement

Measurement of Transglutaminase type 2 was performed in urines from 292 CKD patients and 33 controls using an in-house sandwich ELISA where a goat polyclonal anti TG2 antibody was used to capture and CUB7402 (both from AbCam) as a detection antibody. In addition, 19 diabetic patients without clinical evidence of kidney disease (eGFR > 90ml/min/1.73m², normal serum creatinine and no proteinuria shown in dip sticks) were also used for comparison with DKD patients. Human recombinant TG2 was used to generate a standard curve (full method in section 3.5.1). One way ANOVA with Bonferroni correction was applied to estimate differences between healthy volunteers (n=33), diabetic controls (n=19), all CKD patients and those with different CKD aetiologies (diabetic kidney disease: n=91, chronic glomerulonephritis: n=66, hypertensive nephrosclerosis: n=53, atherosclerotic renovascular disease: n=29, chronic interstitial nephritis: n=15, ADPKD: n=13 and other causes of CKD: n=25). A p value < 0.05 was considered statistically significant.

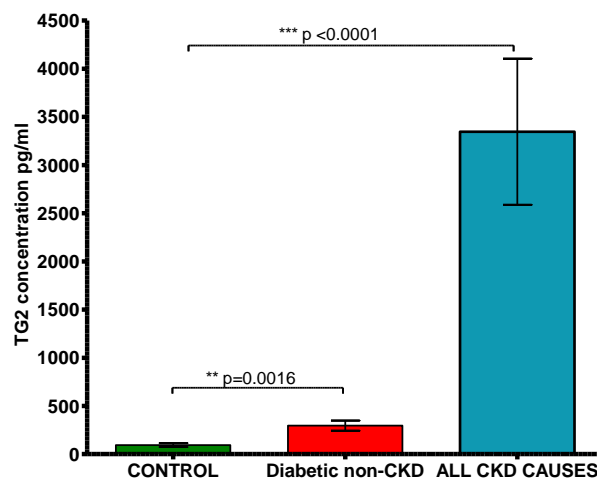
7.3.2. Urine Transglutaminase type 2 levels

TG2 concentration in the urine averaged 35 times higher in all cause CKD patients (3346 ± 758.5 pg/ml) compared to the control group (94 ± 19 pg/ml, p<0.0001) (figure 7.8-A). Diabetic controls (DM patients without kidney disease) presented an average concentration of TG2 in the urine of 295.5 ± 52.76 pg/ml. This was significantly higher than the control group (p=0.0016), but significantly lower than CKD patients (p<0.0001) (figure 7.8-A).

TG2 excretion was corrected to a creatinine ratio as described in section 4.1.4. to account for volume differences. This gave a 61 fold increase in all cause CKD patient (figure 7.8-B) with healthy volunteers having an average TG2:creatinine ratio of 9.72 ± 1.92 compared to 599.4 ± 118.9 in CKD, (p<0.0001).

Figure 7.8: TG2 measurement in urine from all cause CKD patients

A. Urine TG2 concentration including DM controls



C. TG2/Creatinine ratio

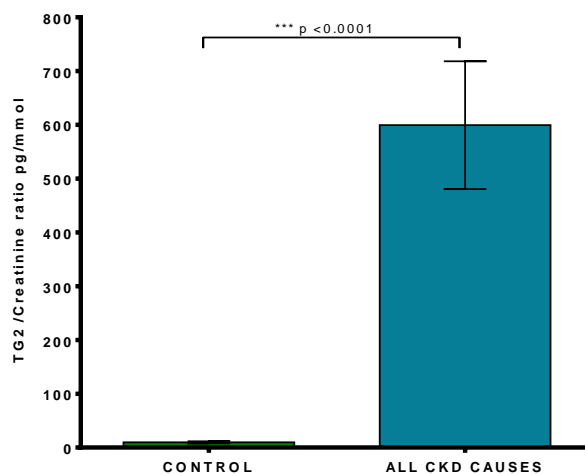


Figure 7.8: Urine TG2 was measured by an in-house ELISA in patients with CKD irrespective of cause (n=292), controls (n=33) and DM patients without CKD and expressed as a concentration (ng/ml) **(A)**. It was also expressed as TG2 / Creatinine ratio **(B)**. Results are displayed as mean \pm SD. Statistical significance is shown by Independent-samples T test: NS= not statistically significant, * p<0.05, **p<0.01, ***p<0.001 between CKD patients and healthy volunteers. Values are mean \pm SD.

7.3.3. Urine Transglutaminase type 2 in different causes of CKD

Healthy volunteers had an average urine TG2 concentration of 94 ± 19 pg/ml (n=33). Amongst CKD patients, the highest increase in urine TG2 concentration was observed on diabetic nephropathy patients (6071 ± 1989 pg/ml, p=0.0034) where 42.86% had CKD stage 3, 53.84% stage 4 and 3.30% stage 5. Hypertensive patients also presented significant levels of urine TG2 (2700 ± 1397 pg/ml, p=0.0167) as well all patients with chronic glomerulonephritis (2157

± 451.8 pg/ml, $p < 0.0001$), atherosclerotic renovascular disease (914.2 ± 298.9 pg/ml, $p = 0.0106$), CIN (2070 ± 912.9 pg/ml, $p = 0.0483$) and other CKD causes (1064 ± 434.7 pg/ml, $p = 0.0382$). ADPKD patients did not present a significant difference from controls due to its large variance (787.1 ± 561.9 pg/ml, $p = 0.2435$) (figure 7.9-A). Comparison of urine TG2 concentration between patients with diabetic kidney disease and all cause non-diabetic of CKD showed levels were higher in the diabetic cohort (figure 7.9-B). Furthermore, DKD patients had considerably higher values than diabetic controls ($p = 0.0046$, figure 7.9-C).

7.3.4. Transglutaminase type 2: Creatinine ratio in urine of CKD patients

TG2: Creatinine ratio was 9.72 ± 1.92 on healthy volunteers vs. 599.4 ± 118.9 in all CKD patient urine ($p < 0.0001$, figure 7.9-D). TG2: Creatinine ratio was massively increased in DKD patients (twice as much all CKD patients, $p = 0.0008$) and also significantly increased in CGN (40 fold increase compared to controls, $p = 0.0003$), HTN (45 fold increase, $p = 0.0117$), ARVD (14 fold increase, $p = 0.0060$), CIN (38 fold increase, $p = 0.0191$) and other causes of CKD (17 fold increase, $p = 0.0166$). ADPKD patients did not give a significant increase in TG2 excretion even when corrected to a creatinine ratio (268.4 ± 218.5 , $p = 0.2614$) (figure 7.9-D). The difference between DKD and non-diabetic CKD patients was also significant when TG2 was corrected for creatinine (figure 7.9-E).

Figure 7.9: Urine TG2 excretion in patients with different causes of CKD

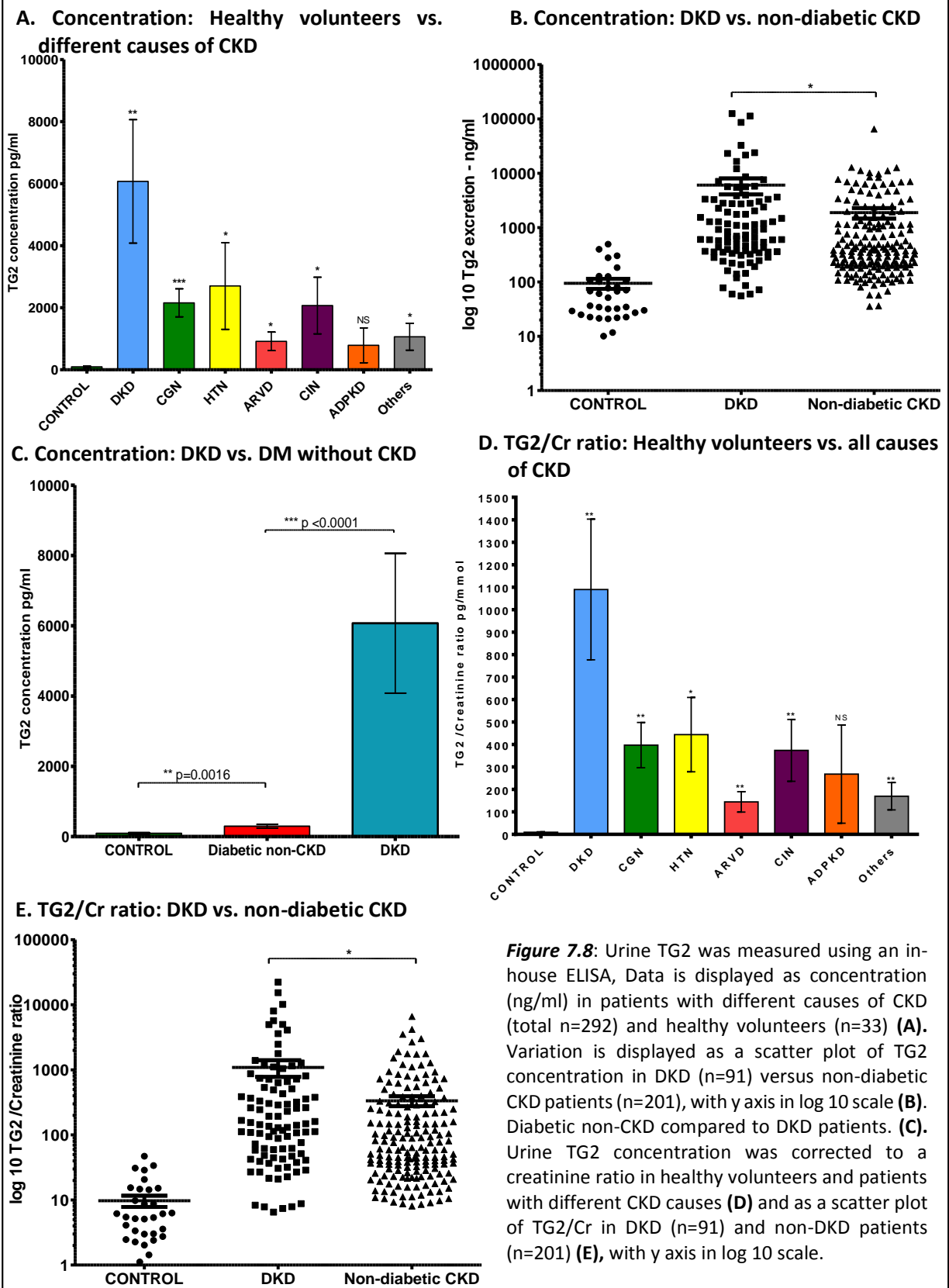


Figure 7.8: Urine TG2 was measured using an in-house ELISA, Data is displayed as concentration (ng/ml) in patients with different causes of CKD (total n=292) and healthy volunteers (n=33) (A). Variation is displayed as a scatter plot of TG2 concentration in DKD (n=91) versus non-diabetic CKD patients (n=201), with y axis in log₁₀ scale (B). Diabetic non-CKD compared to DKD patients. (C). Urine TG2 concentration was corrected to a creatinine ratio in healthy volunteers and patients with different CKD causes (D) and as a scatter plot of TG2/Cr in DKD (n=91) and non-DKD patients (n=201) (E), with y axis in log₁₀ scale.

7.3.5. Transglutaminase type 2: Creatinine ratio by CKD stage

TG2: Creatinine was significantly increased at early stages of the disease compared to healthy volunteers (figure 7.10). TG2: Creatinine ratio was 2.39 fold higher ($p=0.0029$) for CKD 1 ($n=11$) and 18.5 fold higher ($p=0.0181$) for CKD 2 patients ($n=21$). This increase became even more apparent at later stages of the disease; with a TG2: Creatinine ratio of 324.6 ± 119.7 ($p=0.0125$), 911.3 ± 290.2 ($p=0.0027$) and 635.0 ± 196.4 ($p=0.0018$) at CKD stage 3A, 3B and 4, respectively. Patients presenting CKD stage 5 had a reduction on TG2: Cr (374.0 ± 162.0) when compared to CKD stages 3 and 4, however it remained significantly higher than health volunteers ($p=0.0483$).

Figure 7.10: TG2: Creatinine ratio in different CKD stages

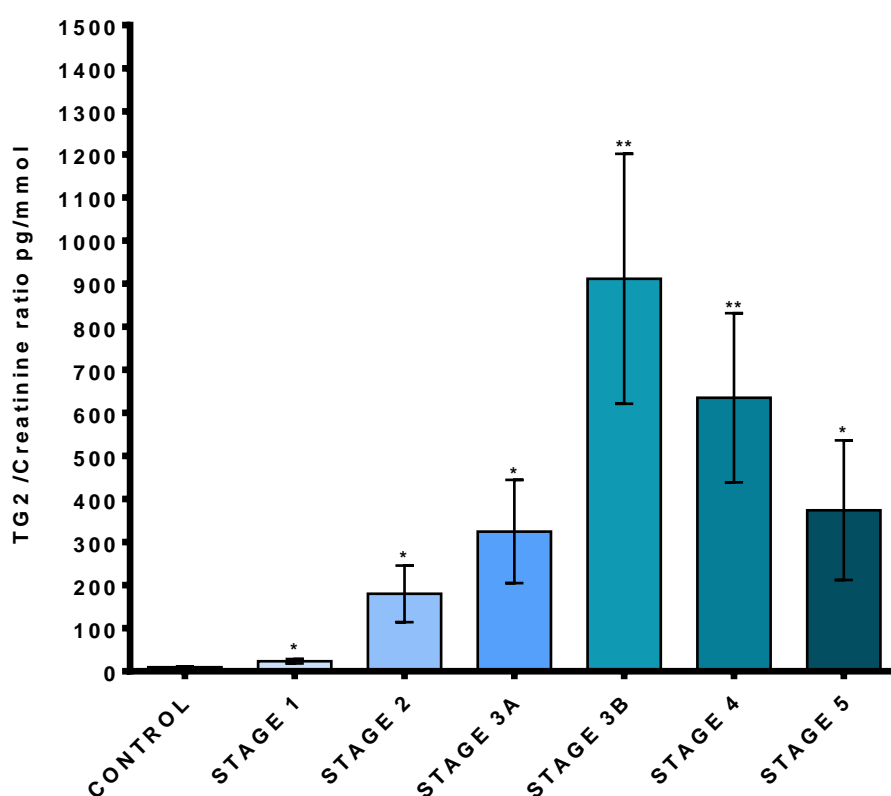


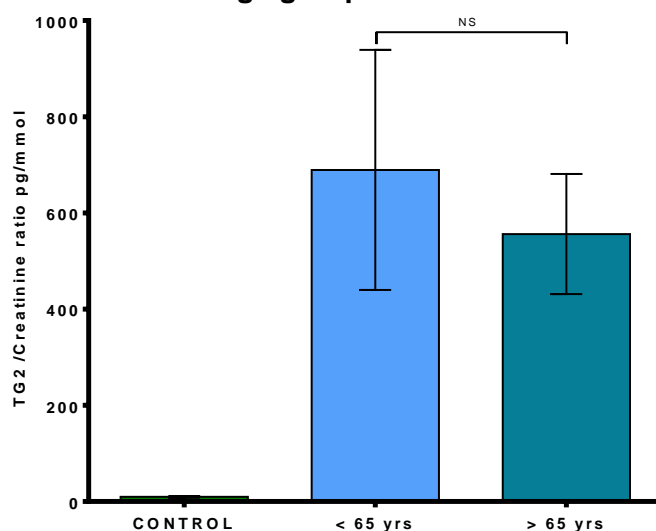
Figure 7.10: Average TG2: Creatinine ratio in all CKD patients subdivided by the disease stages. Control group, $n=33$; CKD 1, $n= 11$; CKD 2, $n=21$; CKD 3A, $n=39$; CKD 3B, $n=73$; CKD 4, $n=132$; CKD 5, $n=16$. Statistical significance is shown by One Way ANOVA with Bonferroni post test: NS= not statistically significant, * $p<0.05$, ** $p<0.01$, *** $p<0.001$ between CKD patients and healthy volunteers. Data represents mean \pm SD.

7.3.6. Comparison of Urine Transglutaminase type 2 levels in CKD patients by age and gender groups

No statistical difference was found between people aged above (n=181; 689.3 ± 249.6) or under 65 (n=111; 556.1 ± 124.7) years old (p=0.6339, figure 7.11-A) or between females (n=113; 400.4 ± 74.72) and males (n=179; 797.3 ± 262.3), (p=0.1480, figure 7.11-B) in terms of TG2: Creatinine ratio.

Figure 7.11: TG2: Creatinine ratio by demographic data

A. TG2/Creatinine ratio in different age groups



B. TG2/Creatinine ratio in females vs. males

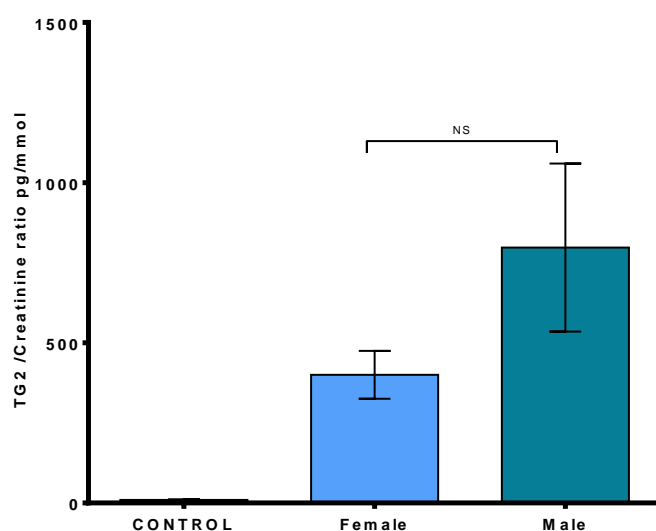


Figure 7.11: The average TG2: Creatinine ratio is shown in two different demographic subgroups: patients aged under or over 65 years (**A**) and by gender (**B**). Statistical significance is shown by One Way ANOVA with Bonferroni post test: NS= not statistically significant, * p<0.05, **p<0.01, ***p<0.001 between CKD patients and healthy volunteers. Data represents mean ± SD.

7.3.7. Relationship between Transglutaminase type 2: Creatinine ratio and CKD progression

CKD progression was determined by the rate of eGFR decline calculated through regression analysis of 10 different eGFR values obtained over a period of around 3 years as previously described. CKD patients who presented with a rate of eGFR decline below 2ml/min/1.73m² per year were classified as stable with non-progressive disease (or non-progressors). Patients with eGFR decline between 2 and 5ml/min/1.73m² were classified as having progressive disease (or progressors). Subjects with eGFR decline above 5ml/min/1.73m² per year were classified as having rapid disease progression (or rapid progressors).

TG2 excretion was higher in patients with progressive CKD compared to those with non-progressive disease. Non-progressive or stable patients (n=184) had an average TG2: Creatinine ratio of 113 ± 14, compared to 1244 ± 366 in those with progressive disease (n=79, p=0.0029) and 1898 ± 509 in rapidly progressive CKD patients (n=29, p=0.0017). Although the TG2: Creatinine was slightly more elevated in rapid progressive patients than in progressive, this difference did not reach any significance (p=0.3017, figure 7.12). In addition, stable, progressive and rapidly progressive CKD patients presented significantly higher TG2: Creatinine ratio compared to healthy volunteers: p<0.0001, p=0.0012 and p=0.0010 respectively.

Figure 7.12: Urine TG2 excretion in patients with different rates of CKD progression

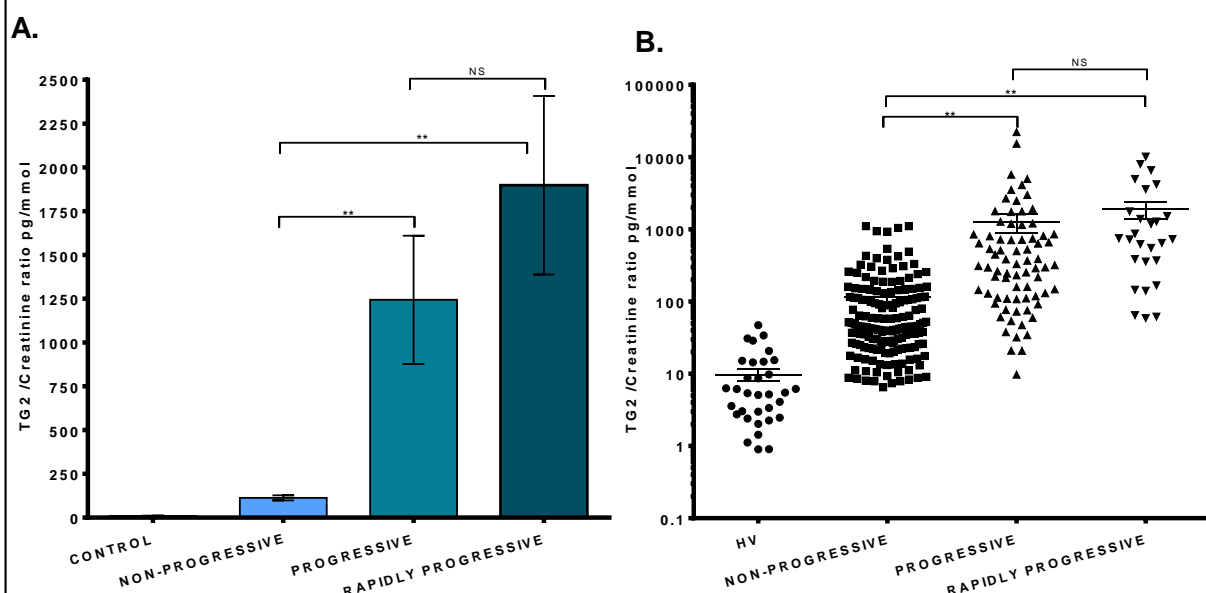


Figure 7.12: TG2: Creatinine ratio measurements in CKD patients were subdivided into groups according to their rate of disease progression: non-progressive (rate of eGFR decline <2ml/min/1.73m²/year, n=184), progressive (between 2-5ml/min/1.73m²/year, n=79) and rapidly progressive (>5ml/min/1.73m²/year, n=29) and data presented as a bar chart (A) and scatter plot (B), with y axis in log 10 scale. Statistical significance is shown by One Way ANOVA with Bonferroni post test: NS= not statistically significant, * p<0.05, **p<0.01, ***p<0.001 between non-progressive, progressive and rapidly progressive. HV = healthy volunteers. Data represents mean ± SD.

7.3.8. Receiver Operating Characteristic curve for Urine Transglutaminase type 2 as a predictor of CKD progression.

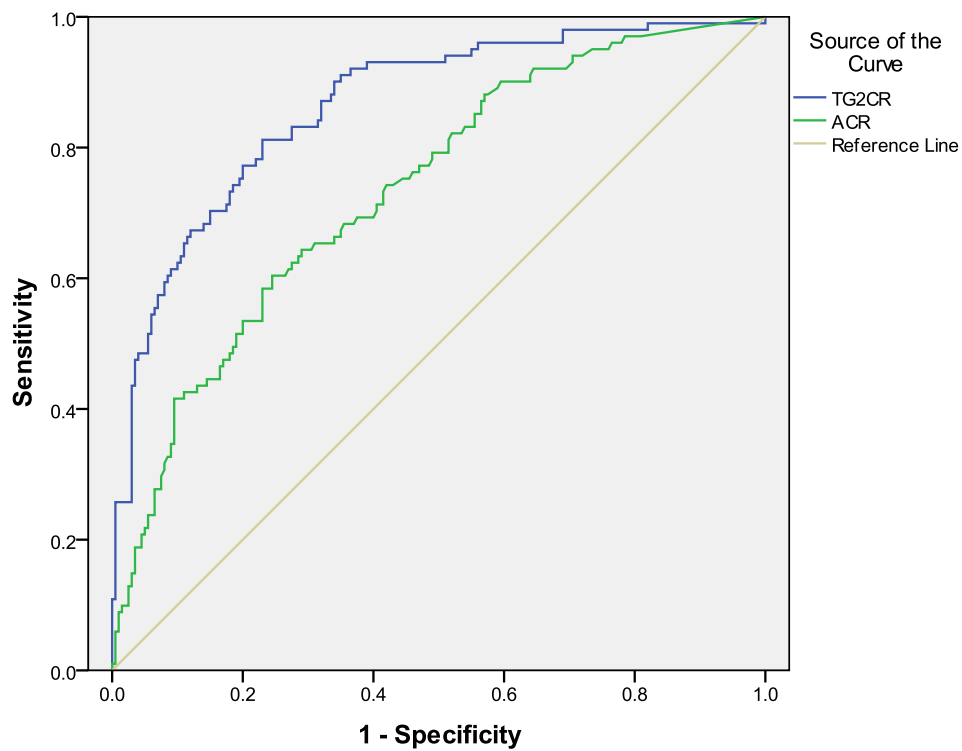
Receiver Operating Characteristic (ROC) curve analysis was used to evaluate the performance of TG2:Creatinine ratio (TG2CR) and Albumin:Creatinine ratio (ACR) in detecting CKD progression. Accuracy of prediction was determined by the Area Under the ROC curve (θ) using the following calculation:

$$\theta = \frac{1}{n_+ n_-} \sum_{\text{all possible combinations of } (x_+, x_-)} S(x_+, x_-),$$

where n_+ and n_- are the sample sizes of the two variables, x_+ denotes the number of values for cases with positive actual states, x_- denotes the number of values for cases negative with negative actual states and $S(x_+, x_-)$ is equal to 1 if $x_+ > x_-$, $\frac{1}{2}$ if $x_+ = x_-$ and 0 if $x_+ < x_-$.

Area under the ROC curve determined a 86.4% accuracy in CKD progression prediction of a spot measurement in a single prospective urine for TG2CR compared to 73.5% for ACR (figure 7.13).

Figure 7.13: Urine TG2 ROC curve



Diagonal segments are produced by ties.

Area Under the Curve

Test Result Variable(s)	Area	Std. Error ^a	Asymptotic Sig. ^b	Asymptotic 95% Confidence Interval	
				Lower Bound	Upper Bound
TG2CR	.864	.022	.000	.820	.908
ACR	.735	.030	.000	.676	.794

Figure 7.13: The TG2CR ROC curve with sensitivity (probability of correctly identifying a positive finding) plotted in the Y axis and 1-specificity (false positives) in the x axis. The higher the area under the curve the higher will be the accuracy of prediction of an event. a = under the nonparametric assumption, b = null hypothesis: true area = 0.5.

7.4. Urine ϵ (γ glutamyl) lysine measurement in Human Chronic Kidney Disease

7.4.1. Urine ϵ (γ glutamyl) lysine measurement by cation exchange chromatography

Human urine samples containing 5mg of protein each were precipitated with TCA followed by ether extraction. Samples were resuspended in NH_4CO_3 , submitted to exhaustive proteolytic digestion (Subtilisin, Pronase E, Leucine Aminopeptidase, Prolidase and Carboxypeptidase Y), freeze dried and fractionated on a Biochrom 30 Amino acid Analyser (AAA). Samples were read using the standard Biochrom 96361 LiHP control program as pre-programmed by the manufacturer. The estimated concentration of ϵ (γ glutamyl) lysine was given at 570 nm at a retention time of around 77 minutes (figure 7.14). Quantification was by reference to a 10 nmols / 20ul ϵ (γ -glutamyl) lysine standard (full methods in section 3.5.7.1. One way ANOVA with Bonferroni post test was applied to estimate differences between healthy volunteers (n=33) and CKD patients (n=292) and also from different CKD etiologies (diabetic kidney disease: n=91, chronic glomerulonephritis: n=66, hypertensive nephrosclerosis: n=53, atherosclerotic renovascular disease: n=29, chronic interstitial nephritis: n=15, ADPKD: n=13 and other causes of CKD: n=25). A p value < 0.05 was considered statistically significant.

Figure 7.14: Urine ϵ (γ Glutamyl) Lysine excretion in Human CKD

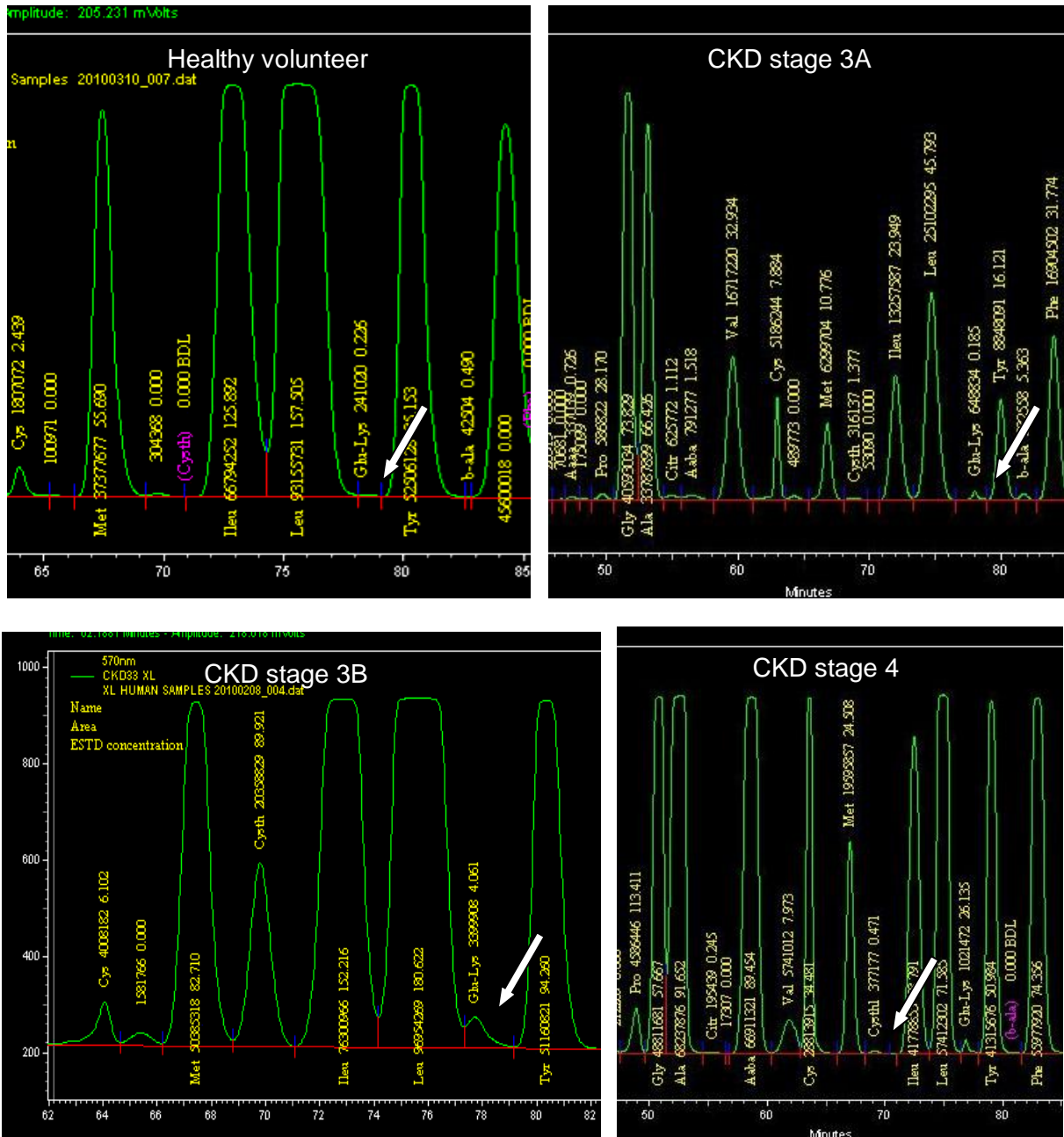


Figure 7.14:: Precipitated protein from human urine samples were exhaustively digested by a combination of five different proteases, freeze dried and reconstituted in 500ul of lithium loading buffer as described in section 3.6. ϵ (γ Glutamyl) Lysine was measured using a Biochrom 30 Amino Acid Analyser, fractionating using program 96361 LiHP and the peak concentration calculated by the area under the curve. Healthy volunteers showed a small Glu-Lys peak (white arrow) situated between Leucine and Tyrosine peaks (A). Maximum Glu-Lys peaks were observed on patients at CKD stage 3A (B), 3B (C) and CKD 4 (D).

7.4.2. Urine ϵ (γ glutamyl) lysine concentration

ϵ (γ glutamyl) lysine excretion was 6.7 fold higher in all cause CKD patient urines (1.304 ± 0.075 nmols per mg of protein) when compared to healthy volunteers (0.1945 ± 0.025 nmols per mg of protein) ($p < 0.001$, figure 7.15-A). When corrected to a creatinine ratio, this difference became 12.5 times higher in patients with all cause CKD (0.2796 ± 0.0285) than controls (0.0222 ± 0.004) ($p < 0.001$, figure 7.15-B).

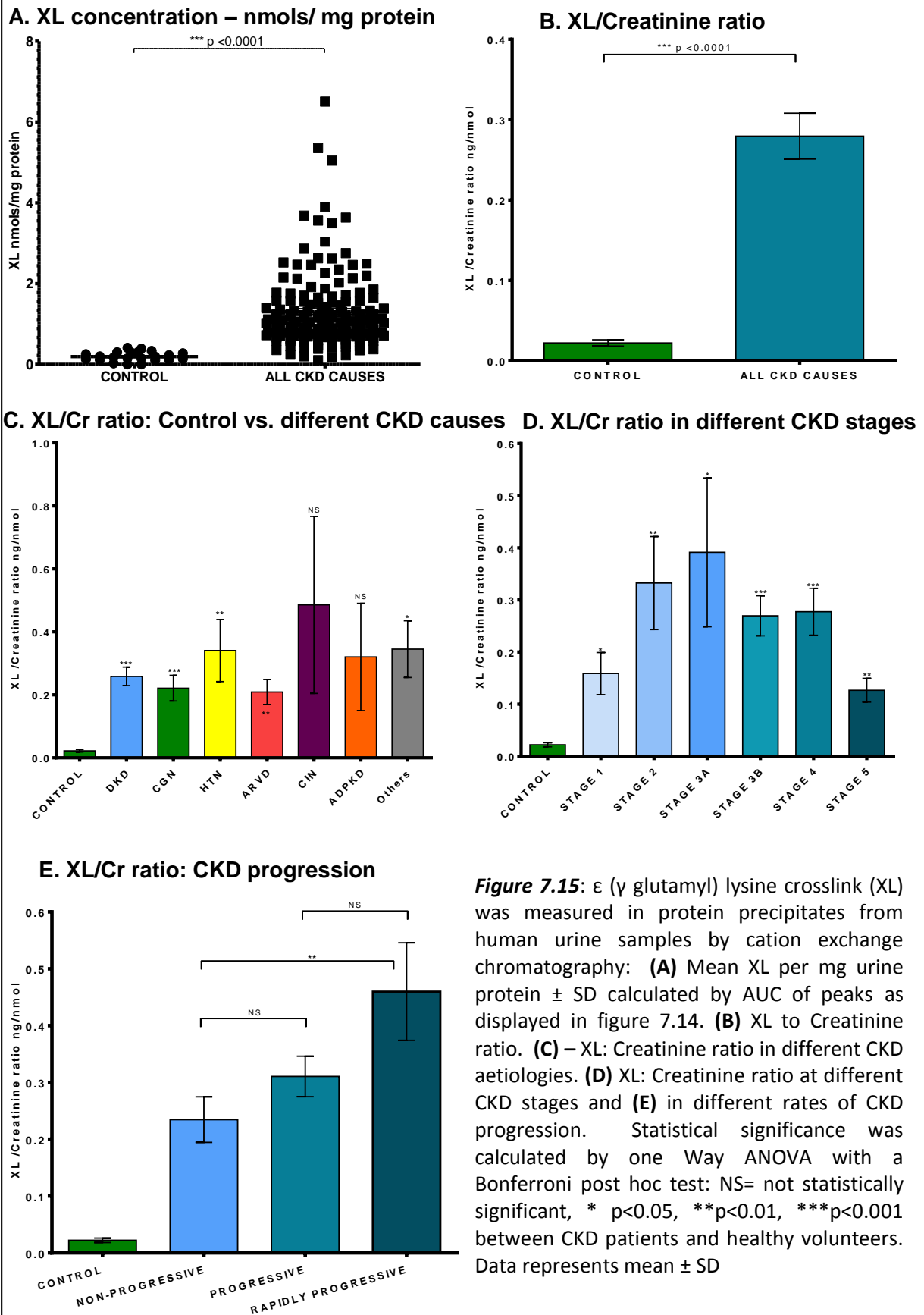
The highest levels of ϵ (γ glutamyl) lysine to creatinine ratio were observed in CIN patients (0.4857 ± 0.2810), however it failed to achieve significance when compared to healthy volunteers due to its large variance ($p = 0.1335$). Hypertensive patients also had a large ϵ (γ glutamyl) lysine:Cr (0.3405 ± 0.0986 , $p = 0.0034$) which is in line with the increased TG2 levels in this aetiology. In addition, patients with diabetic kidney disease (0.2586 ± 0.0293 , $p < 0.0001$), CGN (0.2211 ± 0.0407 , $p < 0.0001$), ARVD (0.2090 ± 0.0395 , $p = 0.0003$), and other CKD causes (0.3451 ± 0.0901 , $p = 0.0043$) also had significant levels of ϵ (γ glutamyl) lysine:Cr ratio. Similar to TG2, ADPKD patients did not present a significant difference from controls (0.3202 ± 0.1703 , $p = 0.1551$) (figure 7.15-C).

The ϵ (γ glutamyl) lysine: Creatinine ratio in patients at different CKD stages was significantly increased from CKD 1 to 5 (figure 7.15-D). At CKD 1, the ϵ (γ glutamyl) lysine:Cr ratio was 0.1588 ± 0.0403 ($p = 0.0120$ when compared to controls). This increased to 0.3325 ± 0.0892 at CKD stage 2 ($p = 0.0037$), then to 0.3913 ± 0.1429 ($p = 0.0183$) at CKD 3A and 0.2696 ± 0.03848 ($p < 0.0001$) at CKD 3B. Average ϵ (γ glutamyl) lysine:Cr levels were also highly elevated at stage 4 (0.2772 ± 0.0450 , $p < 0.0001$) and although it decreased at CKD stage 5, it remained significantly elevated (0.1268 ± 0.0228 , $p = 0.0028$) (figure 7.14-D). Such results mimicked urine TG2 levels.

7.4.3. ϵ (γ glutamyl) lysine: Creatinine ratio relationship with the rate of CKD progression

The ϵ (γ glutamyl) lysine: Creatinine ratio was significantly elevated in CKD patients with rapid progression when compared to those with stable disease. Non-progressors (eGFR decline < 2 ml/min/ 1.73 m² per year) had an average ϵ (γ glutamyl) lysine: Creatinine ratio of 0.2345 ± 0.0418 , compared to 0.3106 ± 0.0356 in progressive disease (eGFR decline between 2 and 5ml/min/ 1.73 m² per year, $p = 0.1591$) and 0.4598 ± 0.0858 in highly progressive disease (eGFR decline > 5 ml/min/ 1.73 m² per year, $p = 0.0262$). All CKD patients had a significantly higher urine ϵ (γ glutamyl) lysine: Creatinine ratio compared to healthy volunteers: $p < 0.0001$, $p < 0.0001$ and $p = 0.0001$ respectively (figure 7.15-E).

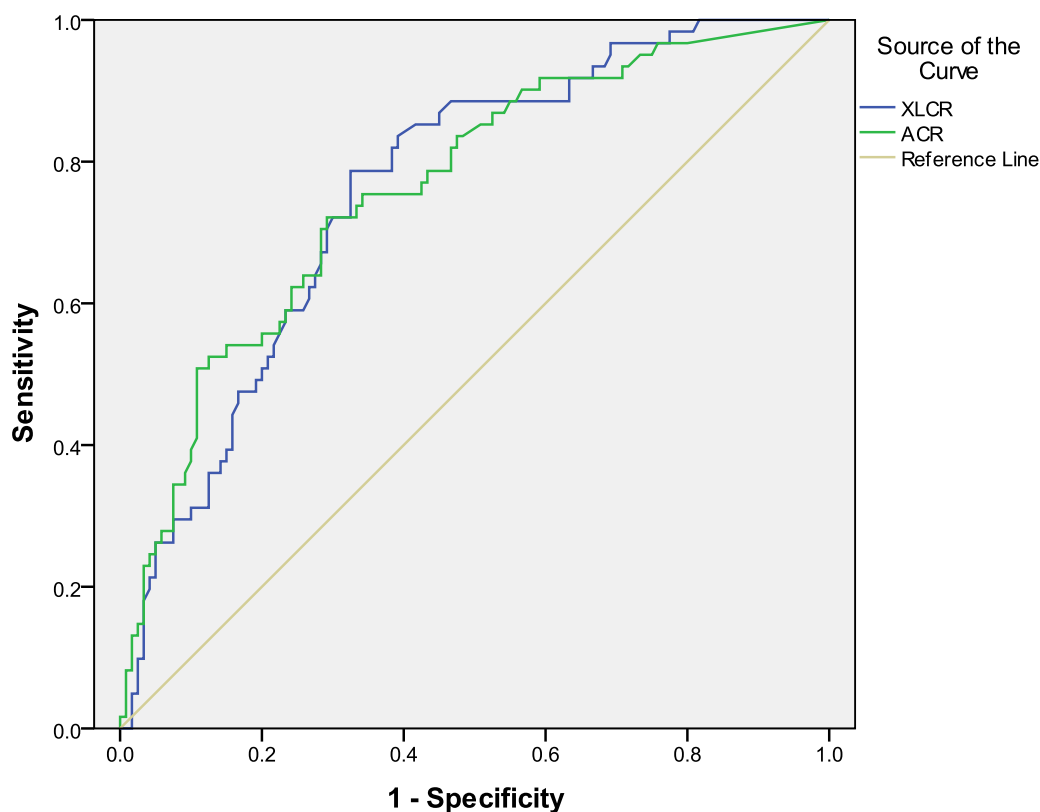
Figure 7.15: ϵ (γ glutamyl) lysine (XL) excretion in urine from CKD patients



7.4.4. Receiver Operating Characteristic curve for Urinary ϵ (γ glutamyl) lysine as a predictor of CKD progression

The ϵ (γ glutamyl) lysine to creatinine ratio (XLCR) presented a worse performance than TG2CR and ACR on predicting CKD progression. ROC curve analysis determined a 73.3% progression prediction to XLCR ratio compared to 73.5% ACR (figure 7.16).

Figure 7.16: Urine ϵ (γ glutamyl) lysine ROC curve



Area Under the Curve

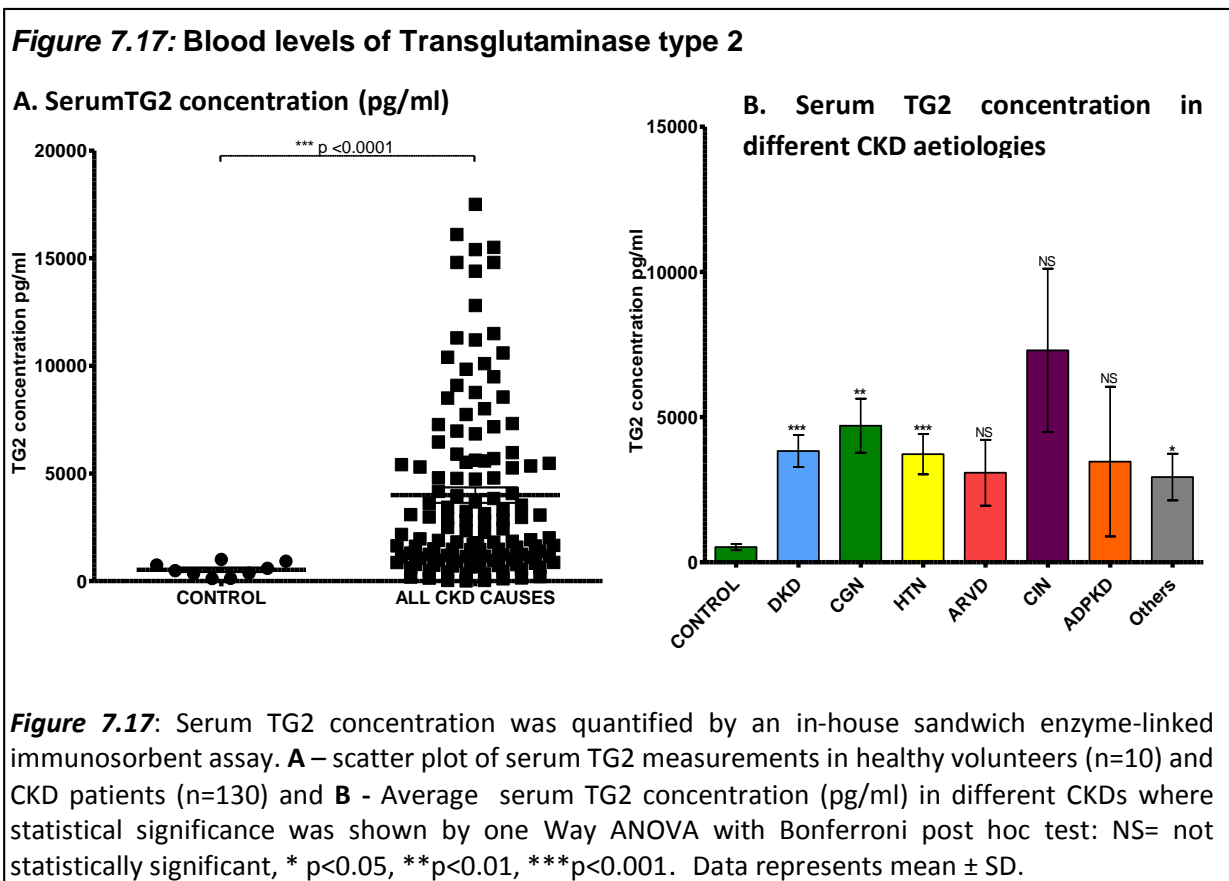
Test Result Variable(s)	Area	Std. Error ^a	Asymptotic Sig. ^b	Asymptotic 95% Confidence Interval	
				Lower Bound	Upper Bound
XLCR	.733	.036	.000	.689	.831
ACR	.735	.030	.000	.676	.794

Figure 7.16: The ϵ (γ glutamyl) lysine:CR (XLCR) ROC curve with sensitivity (probability of correctly identifying a positive finding) plotted in the Y axis and 1-specificity (false positives) in the x axis. The higher the area under the curve the higher will be the accuracy of prediction of an event. a = under the nonparametric assumption, b = null hypothesis: true area = 0.5.

7.5. Serum concentration of Transglutaminase type 2

Transglutaminase type 2 was measured in blood samples from 130 CKD patients and in 10 healthy volunteers in order to compare its levels in the circulation to urine excretion. Out of these 130 patients, 58 presented with DKD (44.62%), 24 CGN (18.46%), 23 HTN (17.69%), 8 ARVD (6.15%), 5 CIN (3.85%), 4 ADPKD (3.08%) and 8 had other CKD causes (6.15%). Full methods are described in section 3.4.3.

Average serum concentration of TG2 in healthy volunteers was 523 ± 107 pg/ml, which represented approximately 5 times their urine level ($n=33$). CKD patients had a significantly higher serum concentration of TG2 (3994 ± 358 pg/ml, $p<0.0001$) when compared to controls (figure 7.17). Amongst these, patients with DKD (3831 ± 5513 , $p<0.0001$), CGN (4704 ± 931 pg/ml, $p=0.0002$), HTN (3722 ± 692 pg/m, $p=0.0001$) and other CKD causes (2934 ± 803 pg/ml, $p=0.0207$) had significant higher serum TG2 levels than healthy volunteers. However, no significant difference was found in patients with ARVD (3085 ± 1133 pg/ml, $p=0.0591$), CIN (7300 ± 2813 pg/ml, $p=0.0738$) and ADPKD (3468 ± 2580 , $p=0.3371$) due to large variation within these groups.



7.6. Correlation analysis for Transglutaminase type 2

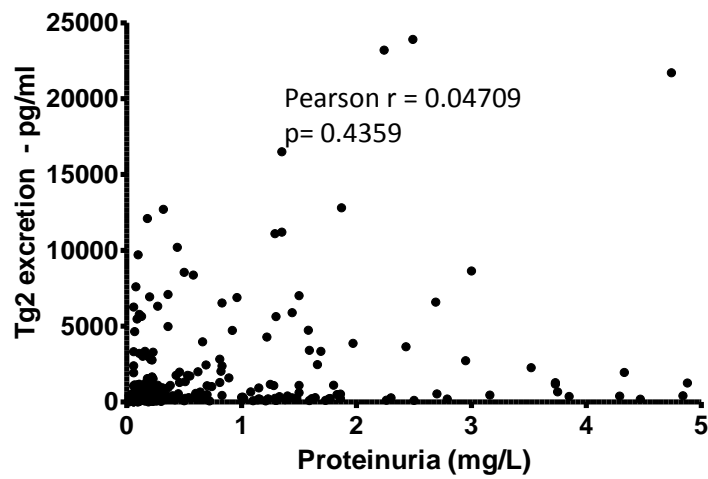
Correlation between serum concentration of TG2 (n=130) and excreted TG2 in the urine did not quite reach statistical significance ($r= 0.04788$, 95% CI = -0.1234 to 0.2164, $p = 0.0542$ (figure 7.18-C). However, urine levels of TG2 had a highly positive correlation with ϵ (γ glutamyl) lysine excretion in the urine ($r= 0.4913$, 95% CI = 0.3721 to 0.5946, $p < 0.0001$ (figure 7.18-B). There was no correlation with urine TG2 excretion and proteinuria ($r= 0.04709$, 95% CI = -0.07141 to 0.1643, $p = 0.4359$, figure 7.18-A) indicating the measurement of ϵ (γ glutamyl) lysine in urine was not simply a reflection of elevated proteinuria.

7.6.1. Urinary Transglutaminase type 2 and ϵ (γ glutamyl) lysine association with histological changes

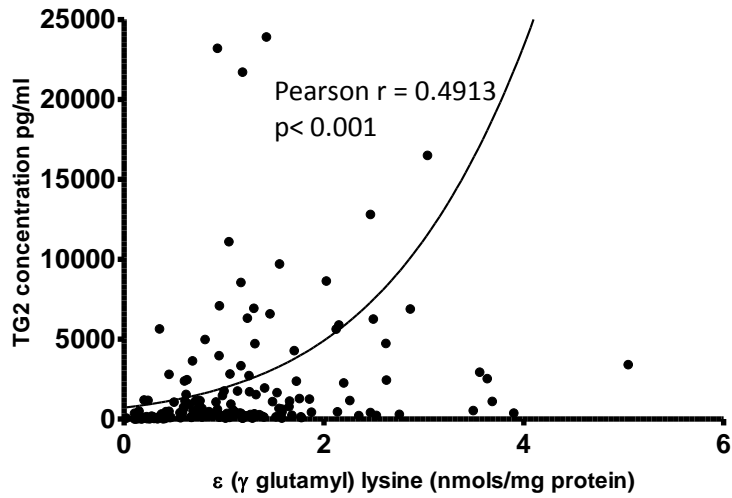
To determine if urine excretion of TG2 and its crosslink product of ϵ (γ glutamyl) lysine were associated with histological changes and scarring formation present in the kidneys, a correlation analysis between these molecules and percentage of renal fibrosis was performed in a subset of chronic glomerulonephritis patients (n=41) which undergone kidney biopsy during this study (figures 7-19-A and 7.19-B). Interestingly, both molecules presented a positive correlation with percentage of fibrosis (Pearson's $r=0.5496$, 95% CI: 0.2911 to 0.7332 $p=0.0002$ for TG2CR and Pearson's $r=0.3812$, 95% CI: 0.0094 to 0.6603, $p=0.0454$ for XLCR).

Figure 7.18: Urine TG2 excretion in patients with different causes of CKD

A. TG2 vs. proteinuria



B. TG2 vs. ϵ (γ glutamyl) lysine



C. Urinary TG2 vs. serum TG2

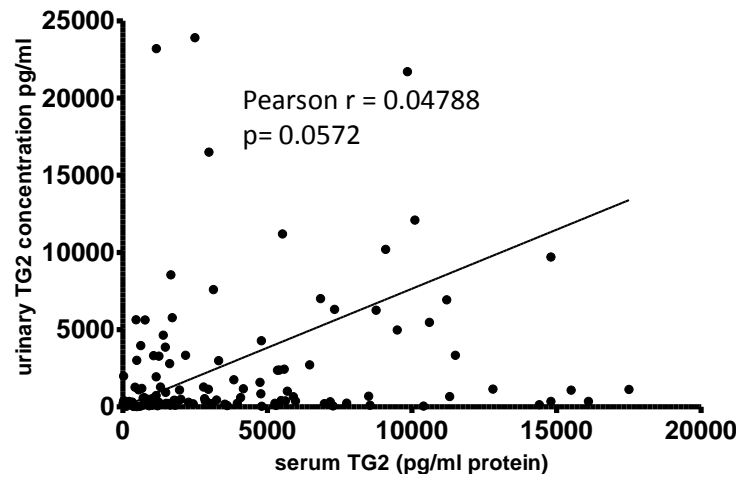
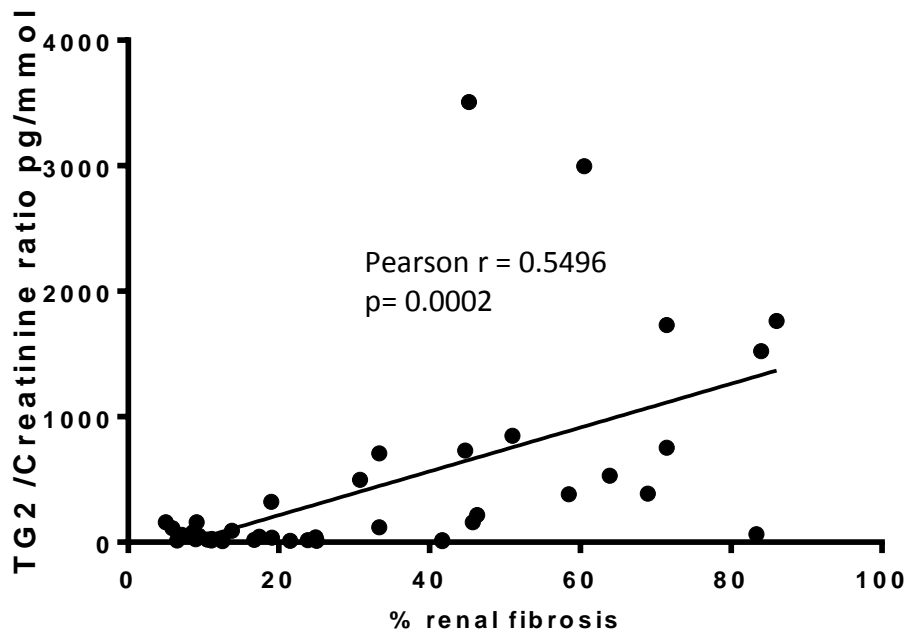


Figure 7.18: Correlation analysis of Urine TG2 with (A) proteinuria, (B) ϵ (γ glutamyl) lysine and (C) serum TG2.

Figure 7.19: Correlation plots of urine TG2 and ϵ (γ glutamyl) lysine excretion with percentage of kidney fibrosis in patients with chronic glomerulonephritis

A. TG2CR



B. XLCR

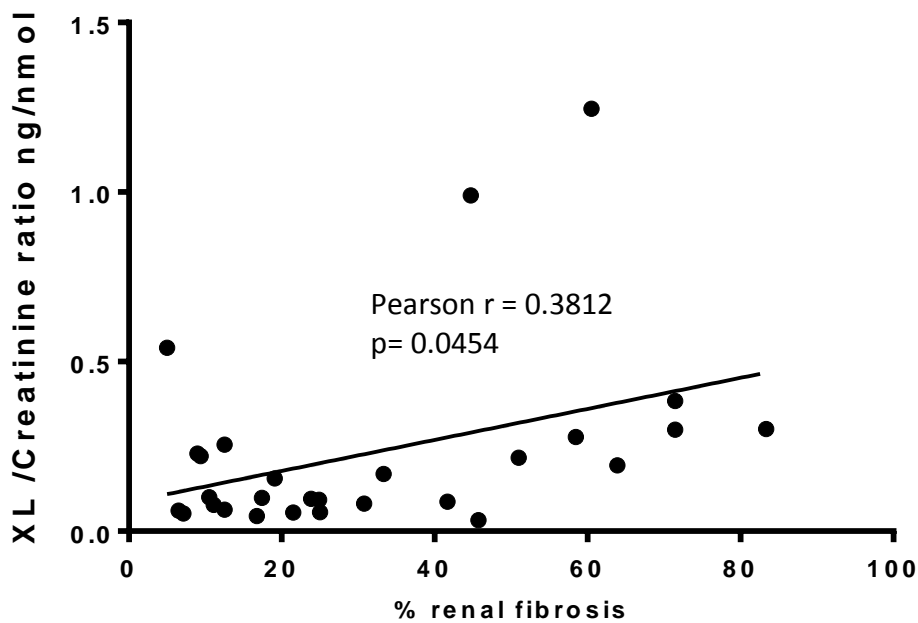


Figure 7.19: Pearson's correlations were performed for TG2CR (A) and XLCR (B) with percentage of kidney fibrosis in 41 CGN patients submitted to renal biopsy. Statistical significance was shown as, * p<0.05, **p<0.01, ***p<0.001.

7.7. TG2 substrates

To try and understand which proteins present in urine were substrates for TG2 crosslinking, several proteins found in urine including some ECM proteins were incubated with TG2 and the amount of ϵ (γ glutamyl) lysine crosslinking assessed as described in chapter 3, section 3.9. Briefly, this assay comprised of activation of 10ug recombinant human Transglutaminase 2 by a solution containing 2mM Ca^{2+} , followed by crosslinking a 1 mg/ml solution of the following proteins; Albumin from human serum, human Collagen type I, human Collagen type III, human Collagen type IV, human Collagen type V, fibronectin from human plasma (FN) and Dimethyl casein (DMC). Following incubation with TG2, each protein was subjected to exhaustive proteolytic digestion, freeze drying and separation with quantification of ϵ (γ -glutamyl) lysine by reverse phase HPLC on a Biochrom 30 Amino Acid Analyser.

Importantly, ϵ (γ -glutamyl) lysine was hardly detectable in human albumin (n=4, XL concentration of 0.001nmol/mg protein) (figure 7.18), whilst other proteins displayed higher levels of crosslinking: Human Collagen III (n=4, 0.026nmol/mg protein), DMC (n=4, positive control, 0.035nmol/mg protein), FN (n=4, 0.042nmol/mg protein) and Human Collagen I (n=4, 0.079nmol/mg protein). Human Collagen I without addition of TG2 was used as a negative control (figure 7.20).

Figure 7.20: In vitro crosslinking of TG2 substrates

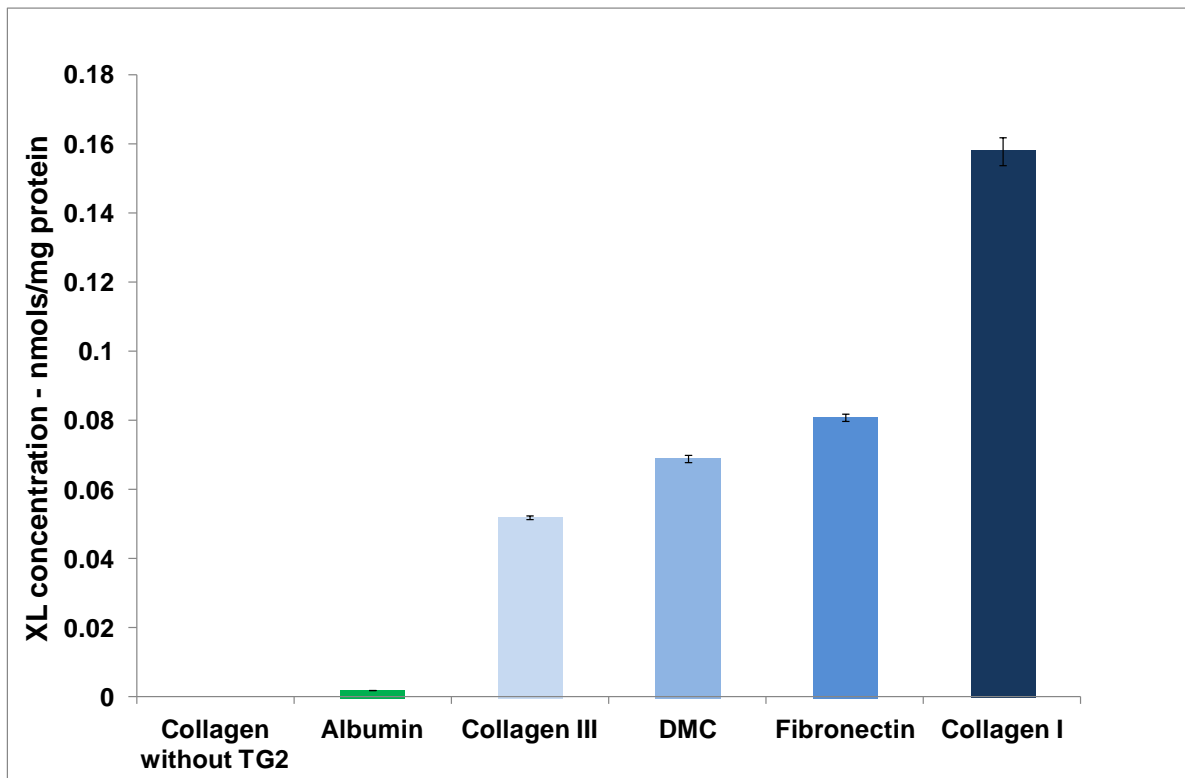


Figure 7.20: Establishing which urine proteins are good TG2 substrates. TG2 substrates: albumin from human serum, human collagen type I, human collagen type III, human collagen type IV, human collagen type V, fibronectin from human plasma (FN) and Dimethyl casein (DMC) were treated with 10ug rhTG2 for X hours and then subjected to exhaustive proteolytic digestion, and separation with reverse phase HPLC on a Biochrom 30 Amino Acid Analyser for quantification of ϵ (γ -glutamyl) lysine dipeptide. Collagen without TG2 was used as negative control.

7.8. Discussion

The overall aim of this chapter was to recruit a good number of CKD patients which would replicate routine clinical presentation and test the hypothesis that urine TG2 and its crosslink product ϵ (γ -glutamyl) lysine could be better predictors of CKD progression than ACR.

Our study consisted of a prospective observational cohort of 292 CKD adult patients from stages 1 to 5 followed over a period of 3 years. Nineteen patients with diabetes mellitus without any evidence of kidney dysfunction and 33 adult healthy volunteers were also recruited to this study.

The sample size of the population study had sufficient power (power of $0.80(1-\beta)$, with Type I error or α of 0.05 and Type II error or β of 0.20). It was representative of the breakdown of CKD patients attending the SKI and also matched with the national renal registry findings. Most groups were large enough and depictive of the CKD community. The number of patients present in each CKD stage group was also a reflection of what is observed daily at the outpatients' clinics.

Urine TG2 concentration was over 35 fold higher in patients with all CKD causes ($n=292$) when compared to healthy volunteers ($n=33$). Individuals with diabetic kidney disease presented the highest levels of urine TG2 when compared to all other groups, with nearly double the values found in the general CKD population. This was also significantly elevated when compared to patients presenting diabetes mellitus ($n=19$) without any evidence of kidney damage ($p<0.0001$). All other etiologies also presented significant urine levels of TG2, a part from ADPKD patients. Similar results were found when urine TG2 excretion was corrected to a creatinine ratio, with TG2 levels around 60 times greater than controls. Once again, no statistical significance was observed in ADPKD patients. This corroborates with the peculiarities of this disease which progression is more dependent on known risk factors such as PKD-1 gene mutation, hypertension (Schrier 2015), total kidney volume (Corradi *et al.* 2015) and urine copeptin levels (Nakajima *et al.* 2015).

There were significant urine levels of ϵ (γ -glutamyl) lysine (6.7 fold higher in patients with all CKD causes). When corrected to a creatinine ratio, ϵ (γ -glutamyl) lysine excretion was also substantially increased in all etiologies, excluding ADPKD and CIN, where a wide spread of values were observed. This could be due to a higher presence of patients at early stages of the disease in both groups and also to the prevalence of non-progressive cases.

An analysis by age groups revealed a slight increase of urine TG2 and ϵ (γ -glutamyl) lysine in patients above 65 years, however this was not statistically significant. In addition, males also presented higher urine levels of both molecules than females. But, once again no statistical difference was found.

TG2: Creatinine ratio was elevated in progressive and rapidly progressive CKD. Nonetheless, this was not reflected in terms of ϵ (γ -glutamyl) lysine excretion, where only rapid progressive patients displayed significant urine levels of the molecule. This suggests either a limitation in the types of proteins crosslinked to the ECM or that there is a need for more advanced kidney dysfunction to be translated into increased ϵ (γ -glutamyl) lysine excretion. To our knowledge, this is the first study to analyse human urine levels of both TG2 and ϵ (γ -glutamyl) lysine. Thus, no comparisons could be made with published data. Therefore, this prompted us to perform subsequent studies to determine serum TG2 levels and also to investigate what proteins were crosslinked in the matrix.

Serum TG2 levels were around five as much as urine levels. Significant amounts were found in all etiologies, excluding ARVD, CIN and ADPKD due to the large variability of values found in these groups. Moreover, a correlation analysis between TG2CR and XLCR with percentage of kidney biopsies from 41 CGN biopsies revealed a remarkable association with scar formation indicating that urine measurement of these molecules could indeed constitute a good non-invasive way of tracking disease progression. Notwithstanding, urinary TG2 presented a highly positive correlation with ϵ (γ glutamyl) lysine excretion in the urine, with no correlation to proteinuria ($r= 0.04709$, 95% CI = -0.07141 to 0.1643 , $p = 0.4359$) indicating that measurement of TG2 in urine was not simply a reflection of elevated proteinuria.

An *in vitro* investigation of which proteins present in human urine were substrates for TG2 crosslinking was performed. On this research, several proteins found in urine including some ECM proteins (albumin, collagens type I, III, IV and V, fibronectin, and DMC) were incubated with TG2 and the amount of ϵ (γ glutamyl) lysine determined by exhaustive proteolytic digestion with quantification by reverse phase HPLC (AAA). This showed that the most likely proteins being crosslinked were fibronectin and collagen type I, confirming previously published studies. However, ϵ (γ -glutamyl) lysine was hardly detectable in human albumin. Numerous studies have identified potential ECM substrates for TG2, for instance, fibronectin has been shown to be a major TG2 substrates both *in vivo* and *in vitro* (Jones *et al.* 1997), as well as fibronectin-collagen (Mosher 1984), collagens type III (Bowness *et al.* 1987), types V/XI (Kleman *et al.* 1995), lipoprotein(a) (Borth *et al.* 1991) and IGF-I (Sivaramakrishnan *et al.* 2013). However, no evidence of albumin crosslinking by TG2 has yet been published and

the data presented here suggests it is a very poor substrate in isolation. Structurally, it contains five to six internal disulfide bonds which could potentially suffer interaction with TG2. Interestingly, this supports our findings in terms of ϵ (γ glutamyl) lysine excretion in both experimental and human DKD. In both groups, although high amounts of TG2 were excreted in the urine, this was not translated into higher amounts of its crosslink product. This could be due to the fact that albumin is the major component found in both groups of diabetic subjects and as the proteolytic digestion of samples involved the breakdown of fixed amounts of protein (2-5mg in total, without albumin depletion), lower amounts of TG2 substrates were available for crosslinking and therefore ϵ (γ glutamyl) lysine levels were lower. This implies that large amounts of albumins, which is a poor substrate, dilute out the XL per mg of protein. Thus, moving forward depletion of albumin could improve sensitivity. However, this process would also lead to loss of other proteins of interest.

ROC curve analysis of TG2CR determined a 86.4% accuracy in CKD progression prediction, compared to 73.5% for ACR. This data suggests that TG2CR could be a better prognostic tool than the currently used standard method. On the other hand, XLCR did not display the same power of prediction, detecting 73.3% of cases. This could be a result of the selectivity for substrates by TG2 demonstrated in the *in vitro* study.

This is the first study to present urine measurements of TG2 and ϵ (γ -glutamyl)-lysine crosslink in human CKD caused by different etiologies. The collection and analysis of forty one kidney biopsy samples made possible the correlation of their excretion with development of kidney scarring. It was established that TG2 and ϵ (γ -glutamyl) lysine are significantly elevated in urine from CKD patients and that this fact was not only a result of increased proteinuria. In fact, the high serum levels of TG2 suggested that this molecule could be filtered, especially as levels were five times higher than the ones found in urine. ROC-AUC analysis determined a much higher prediction of CKD progression for TG2CR (86.4%), being superior to the best conventional marker currently used (ACR, 73.5%). A panel combining these biomarkers could represent a more effective way of predicting progressive CKD.

Chapter 8

Urine Matrix metalloproteinases and their inhibitors as prognostic markers in Human Chronic Kidney Disease

8.1. Introduction

Excessive Extracellular Matrix (ECM) accumulation is the final pathway in kidney fibrogenesis. Kidney basement membrane homeostasis results from a continual turnover of the ECM resulting from the balance between synthesis and degradation of ECM components. The renal ECM is formed by a complex framework of macromolecules which not only provides filtration and structural support to the kidneys, but also regulates cellular processes such as development, migration, differentiation and morphogenesis. It is comprised of structural proteins including various collagens and non collagenous glycoproteins such as fibronectin, elastin, laminin, tenascin, SPARC (Secreted Protein Acidic and Rich in Cysteine), thrombospondin and proteoglycans. Deposition onto the matrix occurs by up regulation of the transcription of these components by growth factors and cytokines such as TGF β 1, FGF and IGF-1. Activated fibroblasts increase their production of fibronectin and interstitial collagens (Zeisberg *et al.* 2000) whilst mesangial and epithelial cells synthesise abnormal glomerular collagens I and III during renal disease. In addition, there is the action of crosslinking enzymes such as TG2, LOXL2 and Lysyl oxidase, which also contribute to increased ECM accumulation by the crosslinking of proteins such as collagen and elastin (Kagan and Trackman 1991). ECM breakdown is mediated by specific enzymes such as the matrix metalloproteinases (MMPs; Matrixins), the cysteine/aspartic proteinases and the serine proteases. Therefore, increased deposition and/or a decreased breakdown of its components favors a reduction in ECM turnover and subsequent expansion of normal kidney matrix as well as the appearance of abnormal ECM components which is also associated with phenotypic changes to resident renal cells.

Studies suggest that decreased levels of MMPs or elevated levels of protease inhibitors are one of the major causes for this accumulation (Johnson *et al.* 2002). Fibrogenic cytokines such as TGF- β 1 can reduce the expression of these collagenolytic enzymes, as well as activate their endogenous inhibitors and up-regulate the integrin-mediated cell-matrix interactions. However, due to its action in a number of non-ECM proteins and their multiple biological activities, reduced MMP expression, not only leads to ECM accumulation, but also to complex changes in cellular behavior and phenotypes (Nagase *et al.* 2006, Giannandrea and Parks 2014). For instance, a decrease in MMP-1 mediated cleavage of type I collagen will affect keratinocyte migration and re-epithelization (Pilcher *et al.* 1997), a reduction in the E-cadherin cleavage by MMP-3 will affect EMT and cause disrupted cell aggregation and increased cell invasion (Lochter *et al.* 1997) and limited cleavage of IL-2R α by MMP-9 affecting IL-2 response (El Houda Aguezney *et al.* 2007).

Currently 25 MMP types have been identified in humans (Tan *et al.* 2012). They are subdivided into 6 groups according to their substrate specificity: Collagenases (MMPs 1, 8, 13, 18), Gelatinases (MMPs 2, 9), Stromelysins (MMPs 3, 10, 11), Matrilysins (MMPs 7, 26), Metalloelastase (MMP 12), Membrane-type (MMPs 14, 15, 16, 17, 24, 25), Enamelysin (MMP 20) and others (MMPs 19, 21, 23A, 23B, 27, 28) (Nagase *et al.* 2006). The mechanisms of activation of proMMPs as well as the complete domain structure of all MMPs can be found in section 1.10.3. MMPs are specifically inhibited by four TIMPs (TIMPs 1, 2, 3, 4) in a 1:1 stoichiometry way, so an increase in TIMP levels can directly decrease levels of MMP activity. Several other proteins can also inhibit MMPs, for example; α -macroglobulins, tissue factor pathway inhibitor-2, β -amyloid precursor protein and the GPI-anchored glycoprotein RECK (reviewed in (Murphy and Nagase 2008)).

Previous animal studies describing changes in protein and mRNA levels in kidney homogenates have showed that MMPs 1, 2, 3, 8, 9 and 13 as well as TIMPs 1, 2 and 3 have significant renal expression (Ahmed *et al.* 2007). In the same manner, studies in human kidney disease have highlighted the renal expression of such molecules, however, majority of these studies are restricted to histological measurements of such molecules. For instance, a recent study has performed an Immunohistochemistry examination of MMP-2 and TIMP-1 in kidney biopsy samples from transplanted patients with chronic allograft dysfunction (CD4+ antibody-mediated rejection) and reported increased expression in tubular interstitial cells from AMR patients when compared to health kidneys from controls (Yan *et al.* 2012). Another study in ANCA-associated glomerulonephritis has showed an increase in glomerular and tubule-interstitial expression of MMPs 2, 3 and 9 and TIMP1 (Sanders *et al.* 2004). However, there is a lack of studies showing if these changes are reflected in urine levels of these molecules, especially in human CKD as they could potentially give us an insight into the status of the renal fibrosis.

In Chapter 5, MMPs 1 and 9 as well as their inhibitors TIMPs 1, 2 and 3 were quantified in rat urines obtained from three different models of kidney scarring (SNx, Streptozotocin induced DN and CAN). Results showed increased MMP1:Creatinine ratio in SNx animals and at later stages of disease in Diabetic animals. However, MMP-9 excretion did not present higher levels than controls. The TIMP-1:Creatinine and TIMP-2:Creatinine ratio were significantly higher at all time points tested in SNx samples and at 4 and 8 months DN animals. 24 hour TIMP-1 excretion was markedly increased in F-L Allografts at 17 and 24 weeks post transplantation when compared to L-L Isografts, whilst the TIMP-2:Creatinine ratio was

significantly higher in F-L Allografts as early as two weeks post transplantation. However, this difference was not observed at the termination of the study when kidneys were completely scarred. Urinary TIMP-3 excretion did not present a good correlation with disease progression in experimental kidney scarring. Based on this there was good evidence to study MMPs 2, 9, TIMPs 1 and 2 in human patient samples

It is therefore hypothesized that the changes seen in the MMPs and TIMPs in the aforementioned 3 animal models of CKD would also be altered in human urines from CKD patients and that the levels of these would correlate to the activity of fibrotic modeling and hence rate of loss of kidney function.

To test this hypothesis the aim in this chapter is to use urine samples from the 292 CKD patients with different etiologies and 33 healthy volunteers collected and characterised in chapter 7 to:

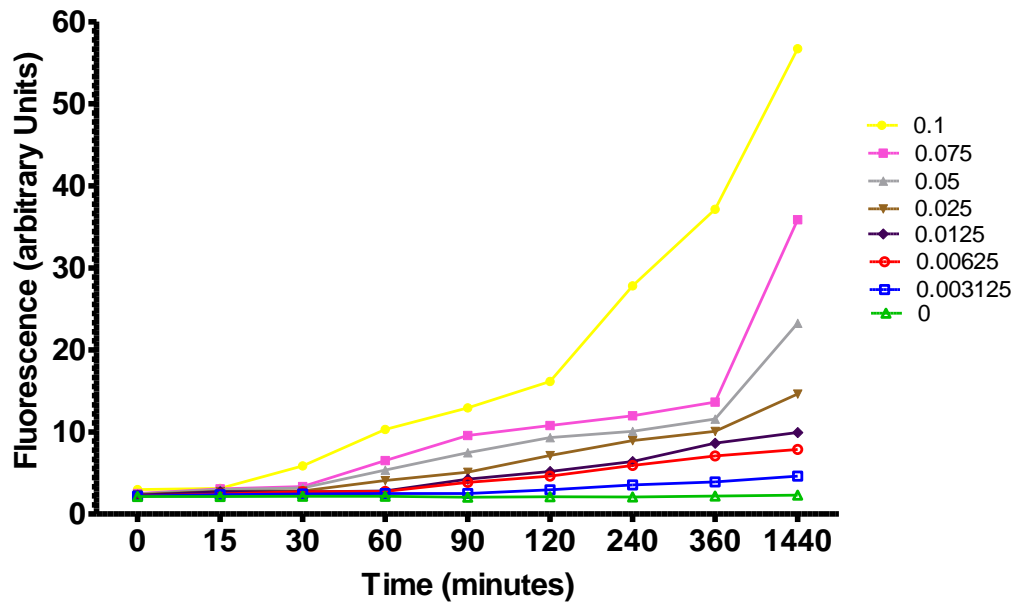
1. Measure the total urinary ECM collagenolytic activity in cell free urines using DQ gelatin cleavage.
2. Quantify MMPs 1, 2 and 9 as well as TIMPs 1, 2 and 3 and the complex formed between MMP-1 with TIMP-1 in these urine samples by using commercially available immunoassays.
3. To evaluate the potential value of overall MMP-activity, MMPs 1, 2 and 9 as well as TIMPs 1, 2 and 3 in accurately predicting CKD progression and compare these outcomes with ACR by ROC curve analysis. MMP-9 was included in this panel as parallel work done by cytokine array analysis indicated that this molecule had a potential as a CKD biomarker.

8.2 Urinary ECM collagenolytic activity

The Molecular Probe's EnzChek® Gelatinase/Collagenase Assay is a highly sensitive fluorometric method used to analyze total gelatinase and interstitial collagenase activity. Full methods for measurement of urinary MMP activity are described in section 3.14.2. Briefly, whole molecule gelatin pre-labeled with fluorescein (DQ™-gelatin conjugate), was incubated with undiluted human urine samples. DQ gelatin is digested by MMPs in the urine to yield highly fluorescent peptides by cleavage of the molecule. The intensity of the fluorescence is proportional to the MMP proteolytic activity, being read in a fluorescent Plate reader equipped with standard fluorescein filters. Collagenase IV purified from *Clostridium histolyticum* was used to produce a seven point standard curve (figure 8.1). Microplates were incubated at room temperature, protected from light, and read for 48 hours.

Figure 8.1: Example of a total MMP activity standard curve

A: Changes in Fluorescence with time at different collagenase concentrations



B: Standard curve generated from linear rates of enzyme activity in A

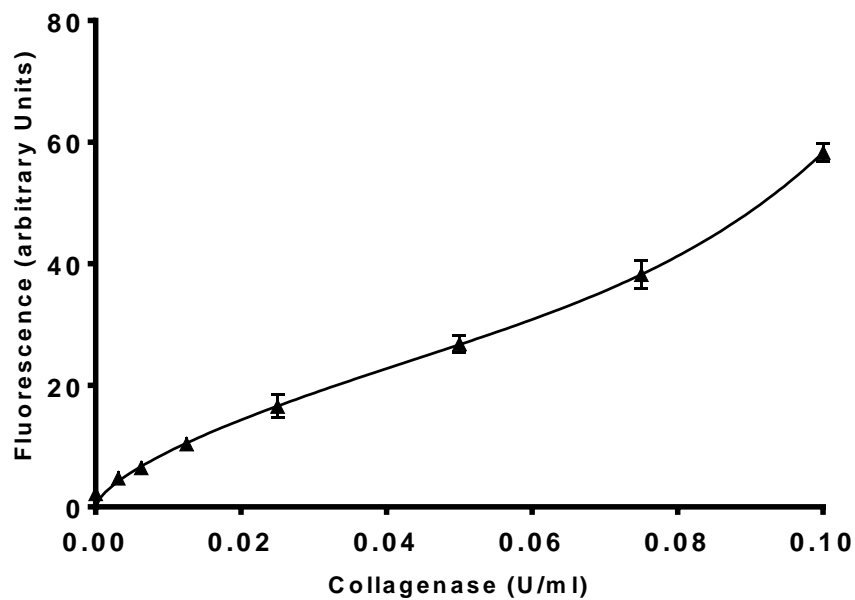


Figure 8.1: The EnzCheck Gelatinase/ Collagenase assay Standard Curve.

A - Collagenase from *Clostridium histolyticum* in a seven point serial dilution (0.1-0U/ml) was used to digest 100µg/ml DQ™-gelatin. Microplates were incubated at room temperature and protected from light. Incubation times were set for every 15 minutes for 4 hours, then every hour for the following 4 hours. Final incubation at 12, 24 and 48 hours were also used during this assay. Fluorescence was measured using a Fluorescent microplate reader set for excitation at 485 ± 10nm and emission detection at 530 ± 15nm. Background fluorescence defined by a control sample without Collagenase was subtracted from each value.

B - The change in Fluorescence (arbitrary Units) of each control sample was plotted in the y-axis against the Collagenase concentration (U/ml) in the x-axis. Data points are average of duplicates. Values are mean ± SEM.

8.2.1. Measurement of Collagenase activity

After validation and optimisation of the assay protocol, undiluted CFU were selected for measurement of the absolute urinary ECM proteolytic activity. Collagenase IV purified from *Clostridium histolyticum* was used as a control enzyme to produce a seven point standard curve (figure 8.1). DQ™-gelatin (denaturated collagen) is a substrate which is efficiently digested by all MMPs. 50 ul of a 100ug/ml of substrate was added to each well and the increase in fluorescence used to estimate the amount of collagenase present in the urine sample. A 48 hours incubation period was used, with readings every 15 minutes for the first 4 hours, then every hour for the following 4 hours and final recordings at 12, 24 and 48 hours. The assay could detect collagenase activity down to a final concentration of 2×10^{-3} U/ml, where one unit of collagenase was defined as the amount that can breakdown 1µmole of L-Leucine equivalents from collagen within 5 hours at 37°C, pH 7.5.

Different patterns of MMP activity were observed in CKD patients. Most patients presented a fluorescence level increasing steadily with time (figure 8.2-A). However, some did not show significant changes during the 48 hour incubation period (figure 8.2-C) and some even had a decrease in activity over the time (figure 8.2-E) which is most likely an assay artefact. Linear regression analysis was used to analyse fluorescence levels with time in every sample and used to calculate the gradient (Δ FI / hr) and therefore indicate the proteolytic activity of each urine sample (figures 8.2-B, 8.2-D and 8.2-F).

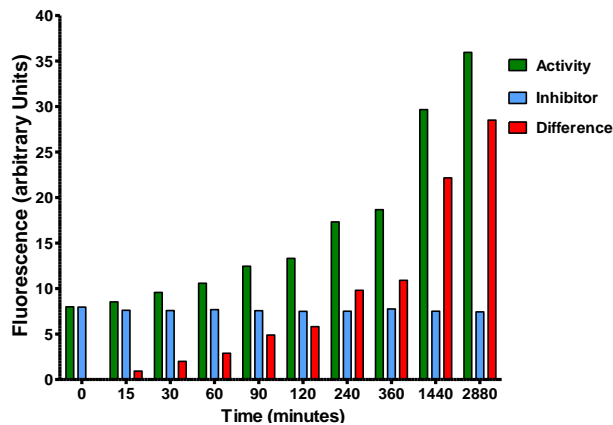
8.2.2. Urine MMP activity of CKD patients and healthy volunteers

To determine the urine MMP activity of healthy volunteers and CKD patients, undiluted CFU were measured in duplicate with and without the addition of 1,10 phenanthroline and the proteolytic gradient calculated by linear regression analysis. The rate of MMP specific activity was calculated by subtraction of the inhibitor containing sample rate from just the CFU rate. Healthy volunteers presented an overall MMP activity of $0.4997 \pm 0.076 \Delta$ FI / hr, whilst patients with all CKD causes presented a substantial 4.7 fold increase ($2.376 \pm 0.191 \Delta$ FI / hr, $p < 0.0001$, figure 8.3-A). When corrected to a creatinine ratio, this difference increased to a 7.2 fold higher average values in the group of patients with all CKD causes ($0.5394 \pm 0.058 \Delta$ FI / hr per µmol of creatinine, $p < 0.0001$) when compared to healthy volunteers ($0.0741 \pm 0.019 \Delta$ FI / hr per µmol of creatinine, figure 8.3-B). Amongst the CKD group, hypertensive patients presented the highest elevation in the MMP activity: Creatinine ratio when compared to healthy volunteers (10.7 fold increase; $0.7919 \pm 0.226 \Delta$ FI / hr per µmol of creatinine, $p = 0.0028$) followed by CIN (8.3 fold increase; $0.6144 \pm 0.193 \Delta$ FI / hr per µmol of creatinine,

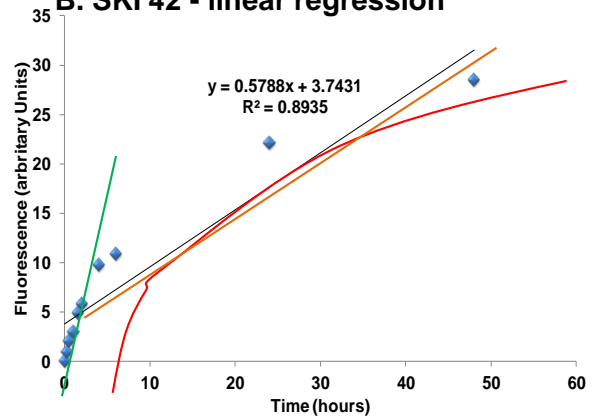
p=0.0147) and diabetic kidney disease (7 fold increase; $0.5144 \pm 0.08 \Delta \text{FI} / \text{hr per } \mu\text{mol}$ of creatinine, $p < 0.0001$). Patients with ARVD and CGN also had significant increases in the MMP activity: creatinine ratio ($p = 0.0142$ and $p = 0.031$ respectively). However, ADPKD patients presented a wide range of values (average of $0.6408 \pm 0.4408 \Delta \text{FI} / \text{hr per } \mu\text{mol}$ of creatinine) and consequently did not differ statistically from controls ($p = 0.2311$, figure 8.3-C).

Figure 8.2: Fluorescence gradient in CKD urine samples

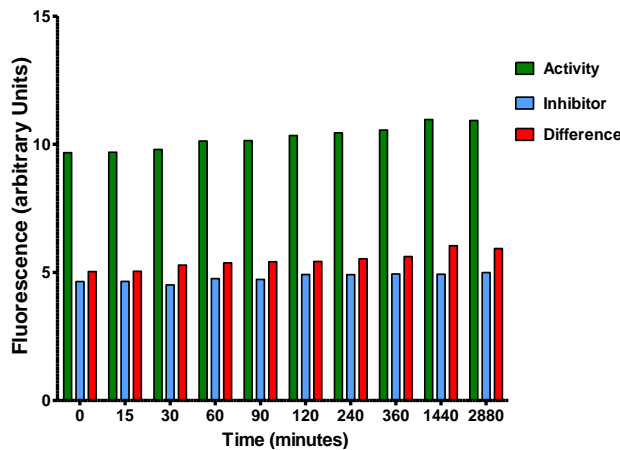
A. SKI 42 - fluorescence gradient



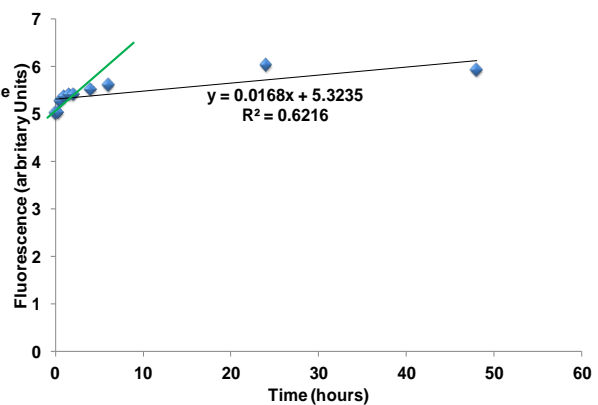
B. SKI 42 - linear regression



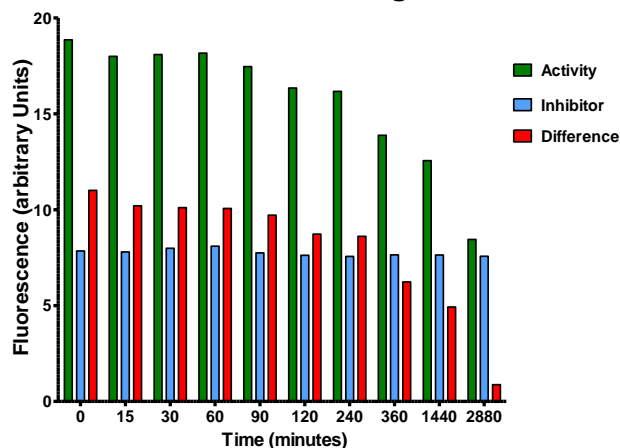
C. SKI 56 - fluorescence gradient



D. SKI 56 - linear regression



E. SKI 314 - fluorescence gradient



F. SKI 314 - linear regression

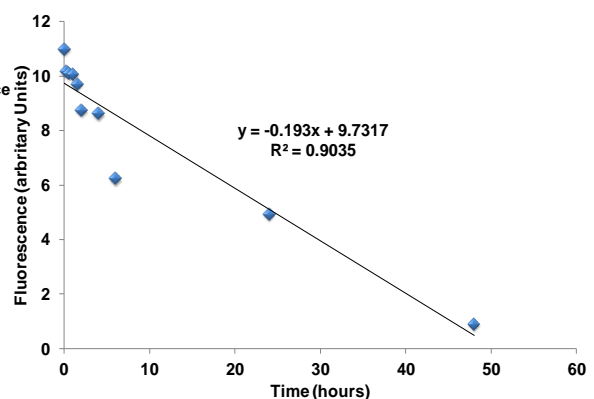
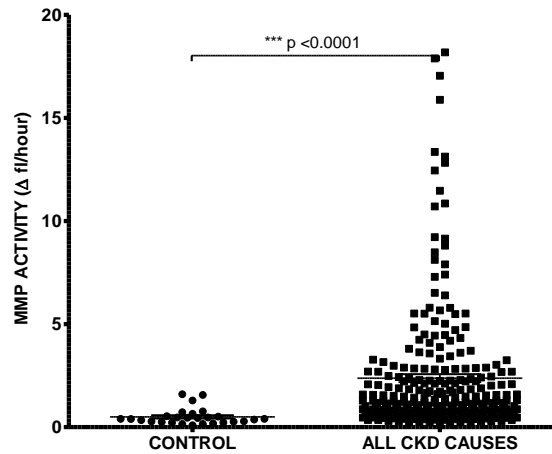


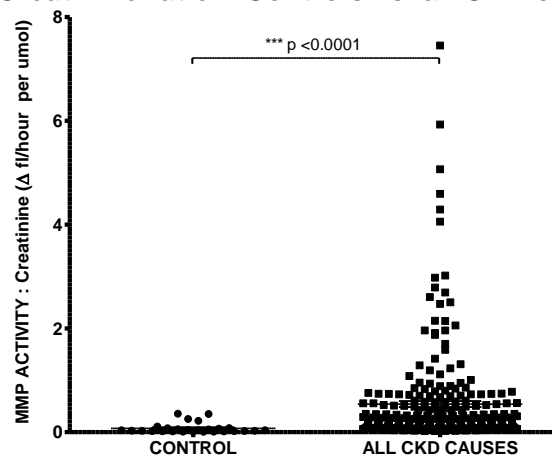
Figure 8.2: Urinary MMP activity of CKD samples was performed by using the EnzCheck Gelatinase/ Collagenase assay and measured by plotting the fluorescence gradient which evaluated proteolytic activity over 48 hours. Different profiles of MMP activity could be observed: A (SKI 42); shows a typical pattern of increase in activity, B (SKI 56) a stable profile and C (SKI 314) shows an uncommon decrease of activity over time. The calculation of the gradient for each sample ($\Delta FI / hr$) was done by linear regression analysis (D, E, F) of all readings done over the 48 hours period.

Figure 8.3: MMP activity in CKD urine samples

A. MMP Activity – Controls vs. all CKD causes



B. MMP Activity: Creatinine ratio – Controls vs. all CKD causes



C. MMP Activity: Creatinine ratio – Different CKD etiologies

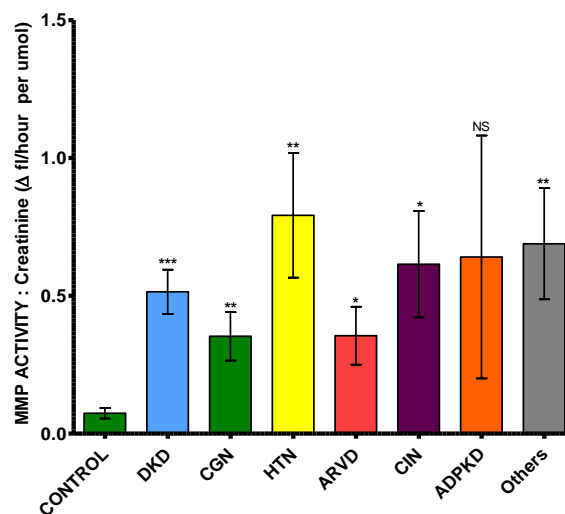


Figure 8.3: MMP activity in human urine samples was measured by the EnzChek® Gelatinase/Collagenase Assay and presented as MMP activity expressed in Δfl/h (A), as a creatinine ratio (B) and further sub classified by different CKD etiologies (C). Statistical significance was tested with one Way ANOVA with Bonferroni post hoc test: NS= non statistical significant, * p<0.05, **p<0.01, ***p<0.001, between controls and CKD patients. Values are mean ± SD.

8.2.3. Urine MMP activity and CKD progression

Interestingly, CKD non-progressive and progressive patients had notably higher MMP activity (0.5567 ± 0.069 and $0.5749 \pm 0.133 \Delta \text{Fl} / \text{hr}$ per μmol of creatinine, respectively) than rapidly progressive ($0.2158 \pm 0.06 \Delta \text{Fl} / \text{hr}$ per μmol of creatinine, $p=0.0172$, figure 8.4). In addition, all three groups of CKD patients had considerably more MMP activity than healthy volunteers ($p<0.001$).

Figure 8.4: Urine MMP activity by CKD progression

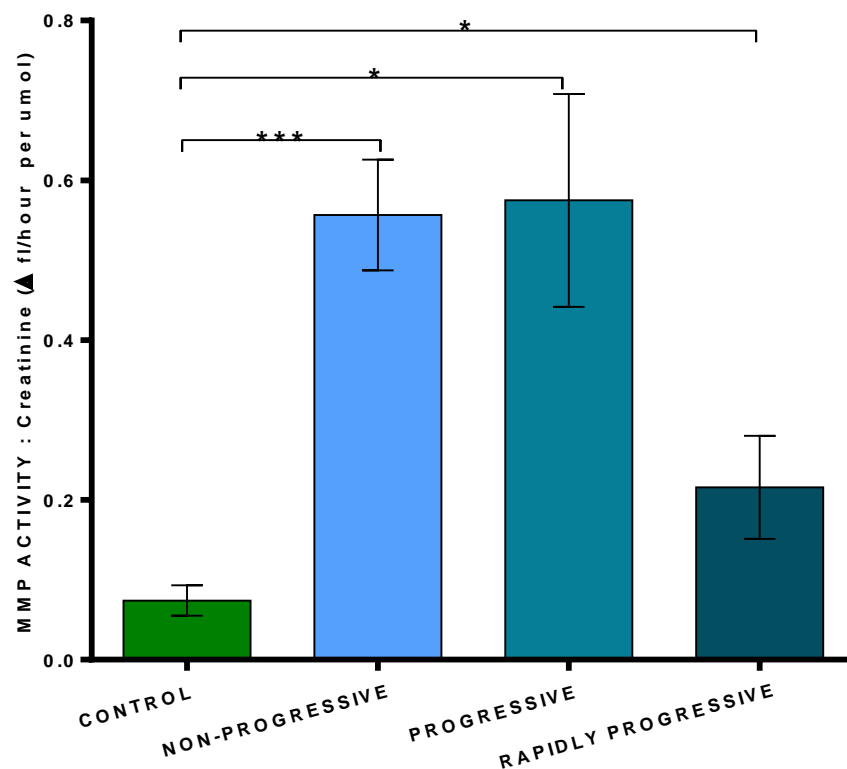
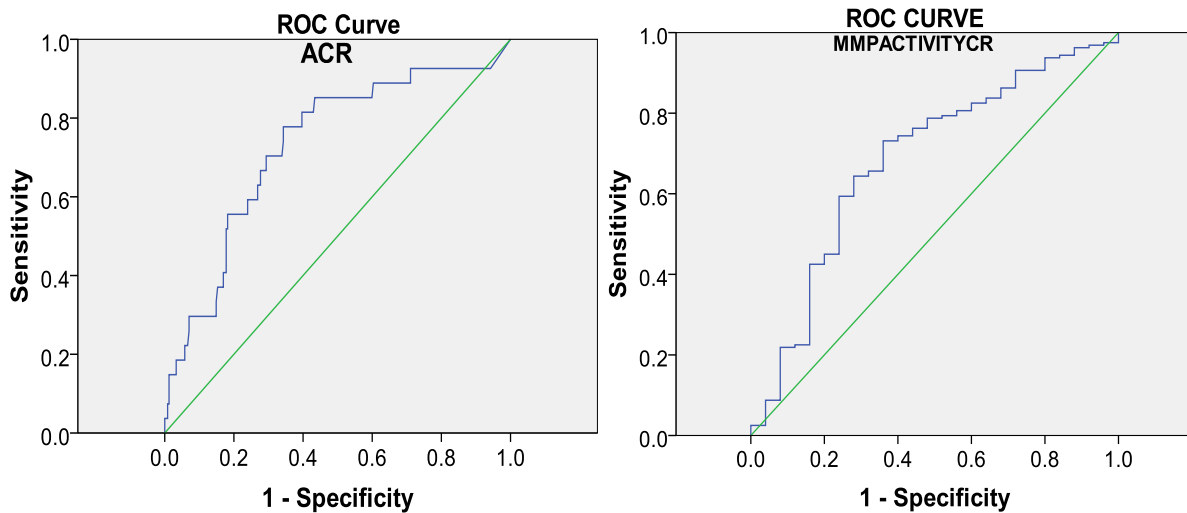


Figure 8.4: MMP activity: Creatinine ratio measurements in CKD patients were subdivided into groups according to their rate of disease progression: non-progressors (rate of eGFR decline $<2\text{ml}/\text{min}/1.73\text{m}^2/\text{year}$, $n=184$), progressors (between $2\text{--}5\text{ml}/\text{min}/1.73\text{m}^2/\text{year}$, $n=79$) and rapidly progressors ($>5\text{ml}/\text{min}/1.73\text{m}^2/\text{year}$, $n=29$). Statistical significance is shown by One Way ANOVA with Bonferroni post test: NS= not statistically significant, * $p<0.05$, ** $p<0.01$, *** $p<0.001$ between non-progressors, progressors and rapidly progressors. Data represents mean \pm SD.

8.2.4. ROC curve analysis for urine MMP activity to predict CKD progression

A ROC curve analysis was used to evaluate the accuracy of ACR and MMP activity over creatinine ratio in predicting the annual decline of kidney function in rapid progressive CKD patients (eGFR decline > 5ml/min/1.73m²). Overall, ACR presented a 73.0% prediction in this subgroup of patients when compared to 68.3% of urinary MMP activity (figure 8.5).

Figure 8.5: MMP activity ROC curve



Area Under the Curve

Test Result Variable(s):ACR

Area	Std. Error ^a	Asymptotic Sig. ^b	Asymptotic 95% Confidence Interval	
			Lower Bound	Upper Bound
.730	.053	.000	.626	.834

Test Result Variable(s):MMPACTIVITYCR

Area	Std. Error ^a	Asymptotic Sig. ^b	Asymptotic 95% Confidence Interval	
			Lower Bound	Upper Bound
.683	.060	.003	.566	.800

Figure 8.5: The MMP activity:CR ROC curve with sensitivity (probability of correctly identifying a positive finding) plotted in the Y axis and 1-specificity (false positives) in the x axis. The higher the area under the curve the higher will be the accuracy of prediction of an event. a= Under the nonparametric assumption. b= Null hypothesis: true area = 0.5.

8.3. Urine levels of Matrix Metalloproteinases in Human CKD

8.3.1. Measurement of urine MMP-1

Urinary MMP-1 was measured in human samples using a DuoSet immunoassay (section 3.10.5). Four randomly selected urine samples were spiked with 6.25ng/ml recombinant human MMP-1 to validate the assay protocol and evaluate the recovery of total human MMP-1 (active and pro-MMP-1). The average % recovery of MMP-1 ranged between 85-102% by reference to a MMP-1 standard curve (figure 8.6).

MMP-1 levels were below limit of detection in the majority of human CKD urines (n= 277, 94.86%), even after 10X concentration using a centrifugal evaporator. Of note were 15 CKD urine samples with detectable MMP-1 concentrations (7 with significant amounts). The samples with measurable MMP-1 were rather random, being regardless of their CKD etiology, gender, age or rate of CKD progression. The characteristics of these 15 remaining samples (5.14%) are displayed in table 8.1.

Figure 8.6: Human Matrix Metalloproteinase 1 Immunoassay Standard Curve

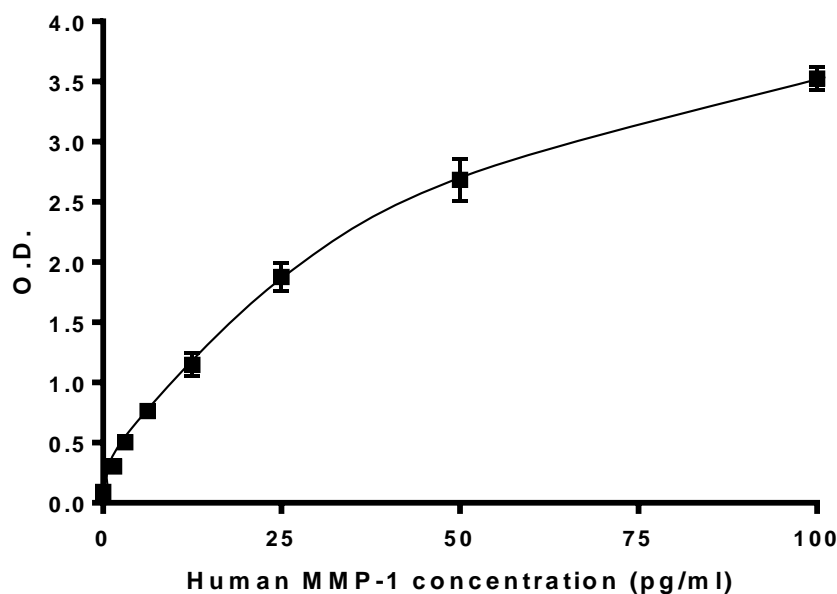


Figure 8.6: Human total MMP-1 immunoassay standard curve was obtained using recombinant human MMP-1 in duplicates and a R&D antibody DuoSet kit. Absorbance was measured on a Labsystems Multiskan Ascent plate reader at a wavelength of 450nm using the Labsystems Genesis computer package. Optical density (O.D.) of each sample was measured, plotted on the y-axis against the MMP concentration (pg/ml) on the x-axis. Curve fit used was a four parameter regression model. Data points are average of duplicates.

Table 8.1: Detected Human Matrix Metalloproteinase 1 in urine

ID	CKD DIAGNOSIS	AGE	GENDER	CKD STAGE	PROGRESSION	MMP-1 (pg/ml)
SKI 97	CGN	50	FEMALE	3A	RAPIDLY PROGRESSIVE	6611.9
SKI 105	HTN	63	MALE	3A	RAPIDLY PROGRESSIVE	624.3
SKI 108	ARVD	77	FEMALE	3B	PROGRESSIVE	166.4
SKI 121	DKD	69	FEMALE	4	PROGRESSIVE	13300
SKI 135	CGN	68	MALE	3B	NON-PROGRESSIVE	168.3
SKI 156	DKD	74	FEMALE	4	NON- PROGRESSIVE	585.2
SKI 182	CGN	60	FEMALE	2	RAPID PROGRESSIVE	1203.8
SKI 221	CGN	43	FEMALE	4	PROGRESSIVE	358.9
SKI 222	CGN	50	MALE	2	NON-PROGRESSIVE	17600
SKI 235	ADPKD	39	FEMALE	4	PROGRESSIVE	517.0
SKI 238	CGN	74	MALE	4	PROGRESSIVE	6304.2
SKI 241	CGN	43	FEMALE	3A	PROGRESSIVE	332.9
SKI 251	CGN	22	MALE	3B	NON- PROGRESSIVE	5987.1
SKI 304	OTHERS	68	MALE	3B	NON- PROGRESSIVE	690.2
SKI 305	CGN	61	MALE	4	PROGRESSIVE	25200
SKI 319	HTN	63	MALE	3A	NON-PROGRESSIVE	17600

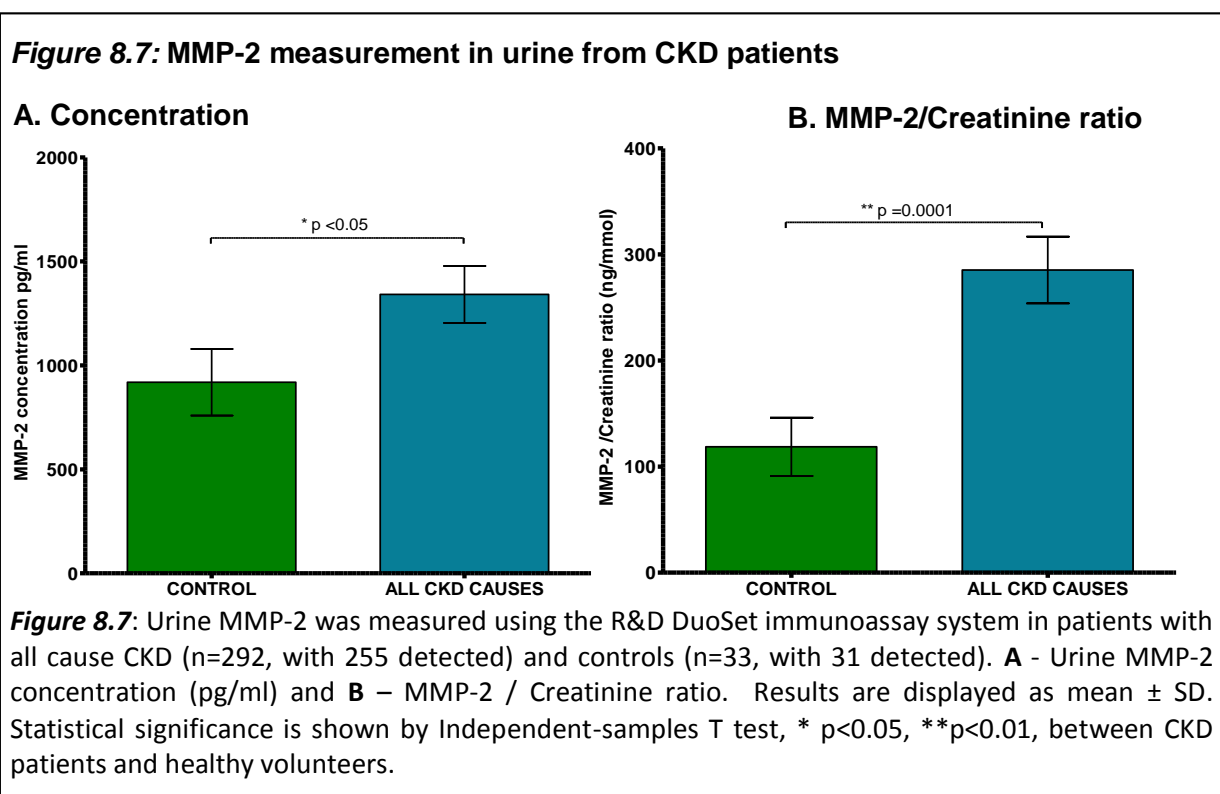
Table 8.1: Demographic and clinical characteristics of 15 CKD patients (out of 292) which had detectable MMP-1 levels in the urine. CGN= chronic glomerulonephritis, HTN = hypertensive nephrosclerosis, ARVD = arterosclerosis renovascular disease, DKD = diabetic kidney disease, ADPKD = adult polycystic kidney disease. Patients subdivided into rapidly progressive (eGFR decline > - 5ml/min/1.73m²/year), progressive (eGFR decline between - 2 and 5ml/min/1.73m²/year) and non-progressive CKD (eGFR decline < - 2 ml/min/1.73m²/year).

8.3.2. Measurement of urine MMP-2

To establish the levels of total Matrix metalloproteinase 2 (active and pro-MMP-2) in human CKD urine, the total MMP-2 DuoSet Immunoassay was used, as described in section 3.10.6.1. Reproducibility and specificity tests for this assay are shown in section 3.10.6.1.1.

Initial analysis showed that urine MMP-2 concentration was 45.9% higher in patients with all CKD causes (n=292, 1341 ± 136pg/ml) when compared to health volunteers (n=33, 919 ± 160, p=0.0481, figure 8.7-A). However, MMP-2 concentration was below the levels of detection in 37 CKD patients and 2 controls. These patients belonged to the same group of patients with undetectable urine MMP-1.

To address the issue of urine volume variability, the MMP-2 concentration was corrected to a creatinine ratio. MMP-2: Creatinine ratio was 2.4 fold higher in CKD patients (p<0.0001, figure 8.7-B). Healthy volunteers presented an average MMP-2: Creatinine ratio of 118.6 ± 27.45 ng/mmol.



8.3.2.1. MMP-2: Creatinine ratio in different CKD etiologies and stages

Hypertensive patients showed the highest increase in the MMP-2: Creatinine ratio with an average 290 ± 61 ng/mmol, $p=0.0136$ when compared to healthy volunteers (figure 8.8-A). Patients with chronic glomerulonephritis (275 ± 50 ng/mmol, $p=0.0079$) and diabetic kidney disease (265 ± 57 ng/mmol, $p=0.0223$) also had significantly increased MMP-2: Creatinine ratios. Although patients which presented with other CKD causes also had elevated levels of MMP-2: Creatinine (atherosclerotic renovascular disease = 237 ± 83.96 ng/mmol, $p=0.1893$), CIN (335.7 ± 185 ng/mmol, $p=0.2663$), ADPKD (425 ± 214 ng/mmol, $p=0.1836$) and other CKD causes (352 ± 141 ng/mmol, $p=0.1209$), they failed to achieve significance.

The MMP-2: Creatinine ratio was not elevated in early CKD stages (CKD 1, 2, 3B) nor advanced disease (CKD 5). *p values* were 0.2989, 0.0631, 0.0503 and 0.5270 respectively. But, significant levels were found in patients with CKD stage 3A, which had an average 406 ± 124 ng/mmol ($p=0.0296$), and at stage 4 with an average MMP-2: Creatinine ratio of 296 ± 48 ng/mmol ($p=0.0018$), these values represented a 3.4 and 2.5 fold increase, respectively, when compared to controls (figure 8.8-B).

8.3.2.2. Urine MMP-2 excretion vs. demographic variables

Although the MMP-2: Creatinine ratio was higher in females (average: 327 ± 51 ng/mmol), there was no statistical significance when compared to males (260 ± 40 , $p=0.3088$, figure 8.8-C).

CKD patients aged below 65 years presented significantly elevated levels of MMP-2: Creatinine (415 ± 65 ng/mmol), compared to patients above 65 years of age (216 ± 31 ng/mmol, $p=0.0081$, (figure 8.8-D).

Figure 8.8: MMP-2:Creatinine ratio in CKD patients

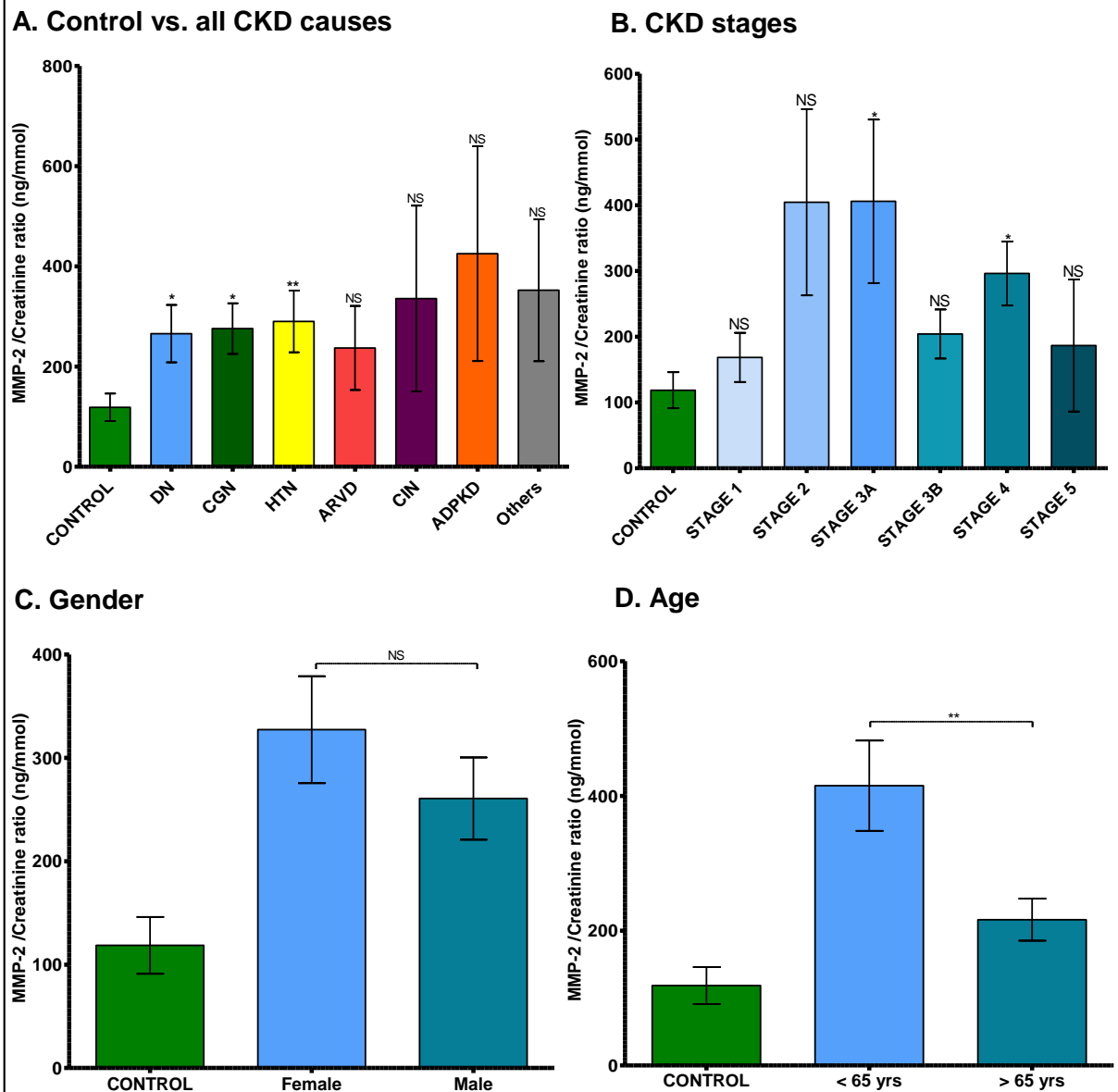


Figure 8.8: Urine MMP-2 excretion was corrected to a creatinine ratio in 33 healthy volunteers and 292 CKD patients. Data is presented by **(A)** CKD cause (n=292), **(B)** CKD stage, **(C) gender** – Females (n=113) vs. Male (n=179) and **(D) age** – patients below (n=111) and above (n=181) 65 years old. Results are displayed as mean \pm SD. Statistical significance is shown by One Way ANOVA with Bonferroni post test: NS= not statistically significant, * p<0.05, **p<0.01, ***p<0.001 between CKD patients and healthy volunteers. Abbreviations: see figure 7.2.

8.3.2.3. MMP-2: Creatinine ratio by rate of CKD progression

Overall, CKD patients presented with higher urine MMP-2: Creatinine ratios than healthy volunteers, regardless of their rate of eGFR decline (figure 8.9). However, non-progressors ($189.6 \pm 36.12 \text{ ng/mmol}$) and progressors ($343.6 \pm 110.8 \text{ ng/mmol}$) were not significantly higher ($p=0.1222$ and $p=0.0575$, respectively). Rapid progressors exhibit considerably higher MMP-2: Creatinine ratio $705.0 \pm 268.3 \text{ ng/mmol}$ ($p=0.0425$) when compared to healthy volunteers.

No difference was found between non-progressors and progressors ($p= 0.1949$), but in patients presenting a rate of eGFR decline above $5 \text{ ml/min/1.73m}^2/\text{year}$ (rapid progressors) had considerably higher MMP-2 levels than non-progressors ($p=0.0129$) and progressors ($p=0.0372$) (figure 8.9).

Figure 8.9: MMP-2: Creatinine ratio and CKD progression

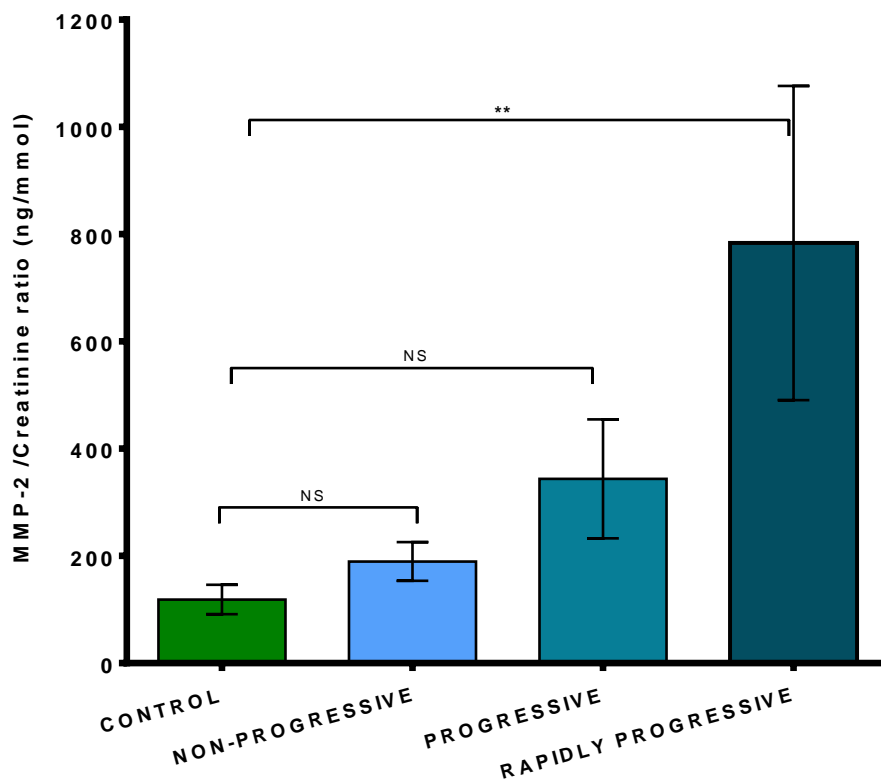
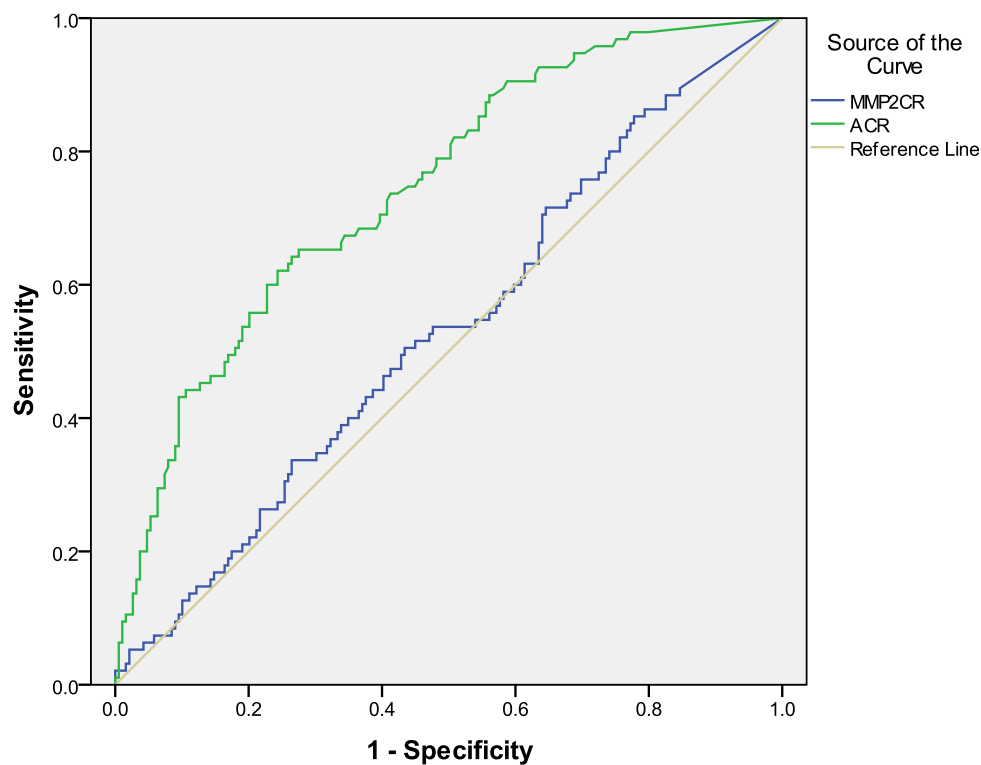


Figure 8.9: The average MMP-2: Creatinine ratio in CKD patients was subdivided by rate of eGFR decline: non-progressive (eGFR decline $< 2 \text{ ml/min/1.73m}^2/\text{year}$, $n=184$); progressive (eGFR decline between $2-5 \text{ ml/min/1.73m}^2/\text{year}$, $n=79$) and rapidly progressive (eGFR decline above $5 \text{ ml/min/1.73m}^2/\text{year}$, $n=29$). Statistical significance between groups is shown by One Way ANOVA with Bonferroni post test: NS= not statistically significant, * $p<0.05$. Data represents mean \pm SD.

8.3.2.4. Receiver Operating Characteristic curve for Urine MMP-2 as a predictor of CKD progression

ROC curve analysis was used to compare the accuracy of the MMP-2: Creatinine ratio (MMP2CR) and Albumin: Creatinine ratio (ACR) to predict CKD progression. MMP2CR had a lower predictive potential compared to ACR, with an area under the ROC curve showing a 53.2% prediction of CKD progression by MMP2CR compared to 73.5% of ACR, figure 8.10.

Figure 8.10: Urine MMP-2 ROC curve



Area Under the Curve

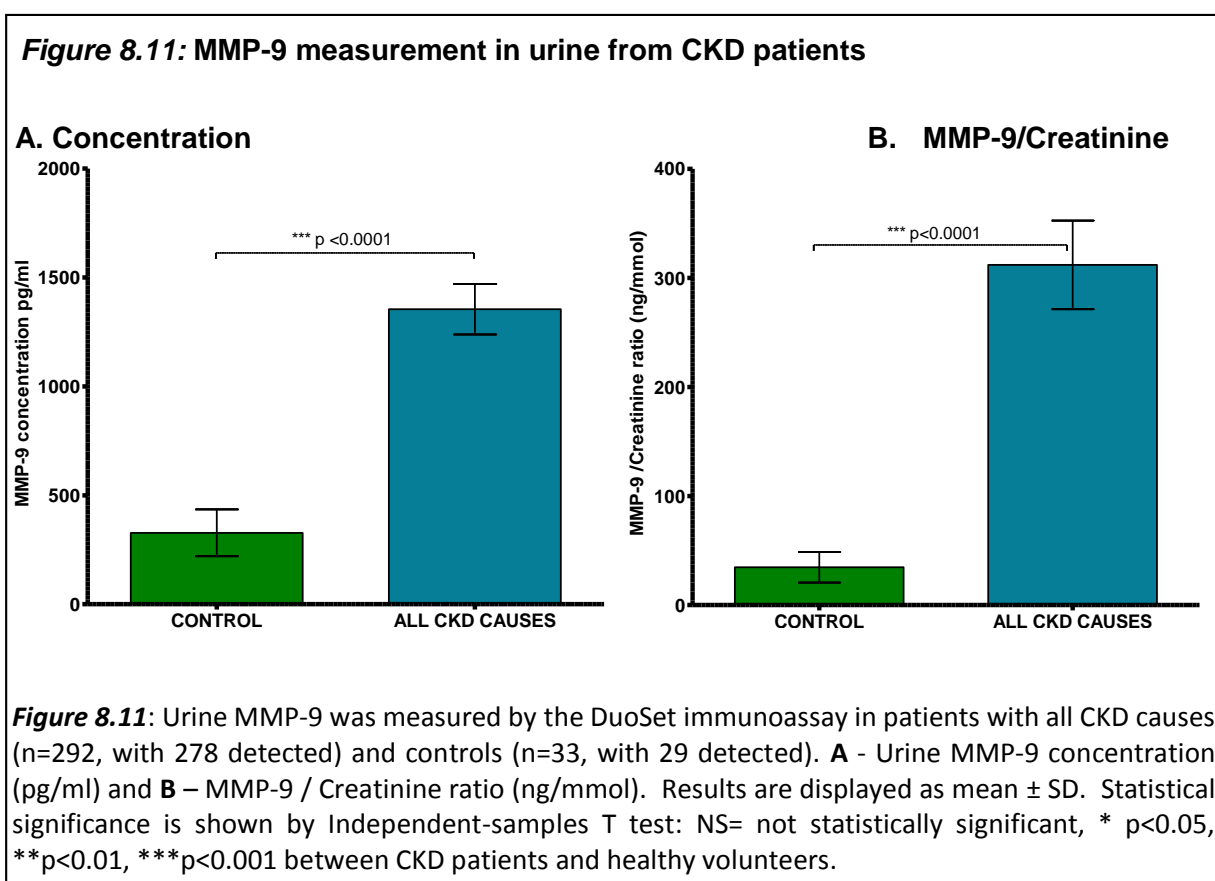
Test Result Variable(s)	Area	Std. Error ^a	Asymptotic Sig. ^b	Asymptotic 95% Confidence Interval	
				Lower Bound	Upper Bound
MMP2CR	.532	.036	.385	.461	.602
ACR	.735	.030	.000	.676	.794

Figure 8.10: The MMP2CR ROC curve with sensitivity (probability of correctly identifying a positive finding) plotted in the Y axis and 1-specificity (false positives) in the x axis. ACR presented a higher area under the curve (73.5%) and therefore a higher accuracy of CKD progression prediction when compared to MMP2CR (53.2%). a = under the nonparametric assumption, b = null hypothesis: true area = 0.5.

8.3.3. Measurement of urine MMP-9

Measurement of total MMP-9 (pro- and active MMP-9) in patient urine was performed using the DuoSet immunoassay as described in section 3.7.10.1.3. Reproducibility and specificity tests are shown in section 3.7.10.1.1.

MMP-9 urine levels had the highest percentage of detection amongst all MMPs analysed in this study: CKD patients (n= 278, 95.21%) and healthy volunteers (n=29, 87.88%). MMP-9 concentration was significantly elevated in patients with all CKD causes (1354 ± 116 .pg/ml, $p<0.0001$) when compared to controls (327 ± 107.4 pg/ml, figure 8.11-A). This difference became even higher when urine MMP-9 excretion was corrected to a creatinine ratio (35 ± 14 ng/mmol in controls and 312 ± 40 ng/mmol in CKD patients, $p<0.0001$, figure 8.11-B).



8.3.3.1. MMP-9: Creatinine ratio in different CKD aetiologies and stages

An analysis of the data from different CKD aetiologies showed that ADPKD patients presented the highest variability in the MMP-9: Creatinine ratio (716 ± 405 ng/mmol, $p=0.1208$). Patients with all other CKD causes had significant increase in the MMP-9: Creatinine ratio when compared to healthy volunteers: DKD (274 ± 62 ng/mmol, $p=0.0004$), CGN (201.8 ± 50.22 ng/mmol, $p=0.0023$), HTN (337.1 ± 109.5 ng/mmol, $p=0.0093$), ARVD (345.0 ± 106.5 ng/mmol, $p=0.0083$), CIN (367.2 ± 115.8 ng/mmol, $p=0.0146$) and other causes of CKD (327.6 ± 117.8 ng/mmol, $p=0.0245$) (figure 8.12-A).

The MMP-9: Creatinine ratio was not elevated at either CKD stage 1 or at CKD 5. However, significant increased levels of MMP9:Cr were observed in CKD patients from stage 2 to 4 (figure 8.12-B).

8.3.3.2. Comparison of Urine MMP-9 levels in different demographic variables

Interestingly, female patients presented a 2.5 fold higher MMP9:Cr levels than males ($p<0.0001$, figure 8.12-C). In addition, elderly patients aged above 65 years old had a 1.96 fold increase in MMP9: Cr levels when compared to younger patients ($p=0.0227$, figure 8.12-D).

Figure 8.12: MMP-9:Creatinine ratio in CKD patients

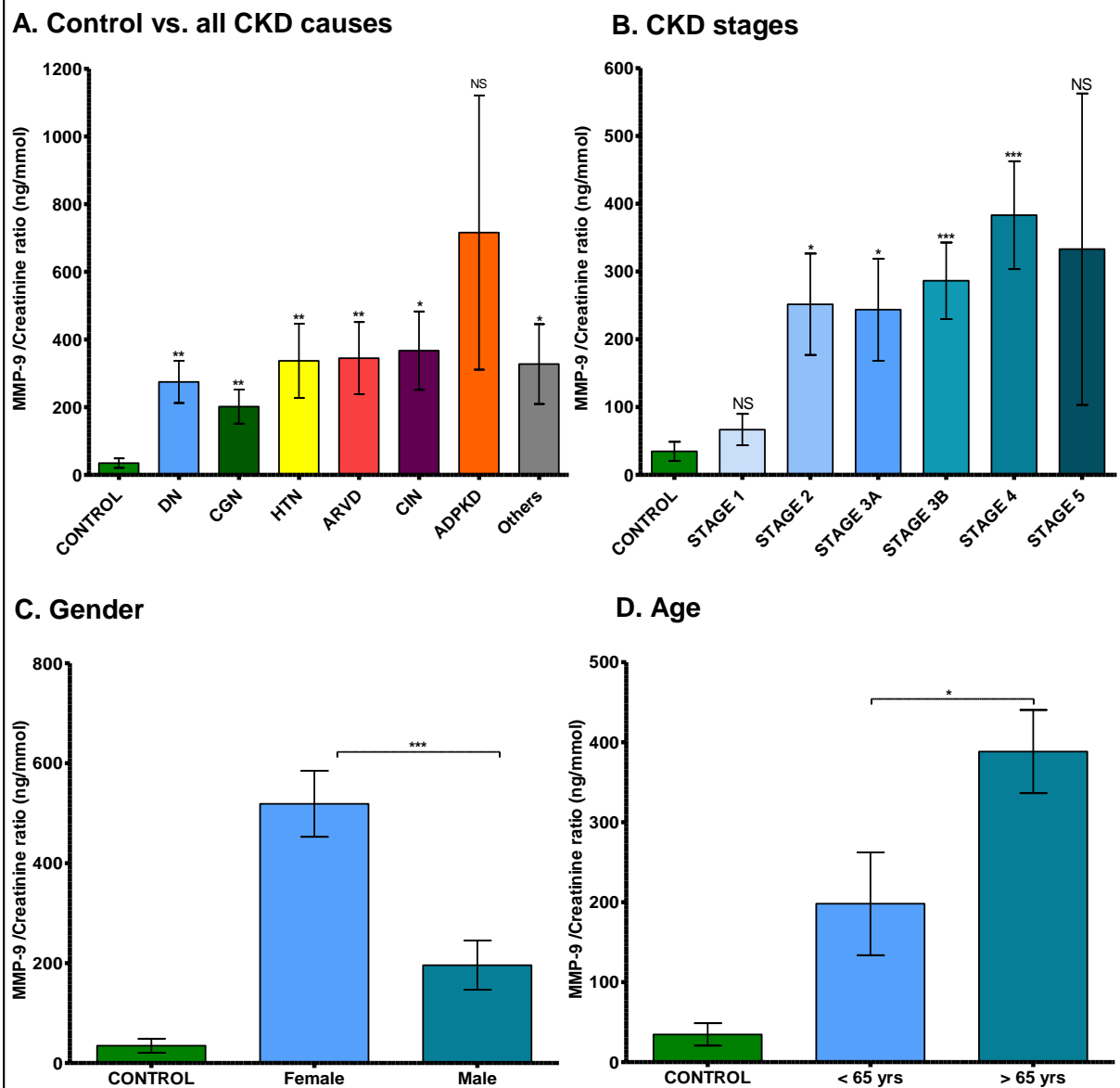


Figure 8.12: Urine MMP-9 excretion was corrected to a creatinine ratio and is displayed as: **(A)** healthy volunteers (n=33) and patients with different CKD causes (n=292), **(B)** – CKD stages 1 to 5, **(C)** – Females (n=113) vs. Male (n=179) and in **(D)** – patients below (n=111) and above (n=181) 65 years old. Results are displayed as mean \pm SD. Statistical significance is shown by One Way ANOVA with Bonferroni post test: NS= not statistically significant, * p<0.05, **p<0.01, ***p<0.001 between CKD patients and healthy volunteers. Abbreviations: see figure 7.2.

8.3.3.3. MMP-9: Creatinine ratio by rate of CKD progression

Patients classified into non-progressive (average MMP9:Cr = 303 ± 53 ng/mmol), progressive (329.7 ± 71.22 ng/mmol) and rapidly progressive (328.0 ± 122.0 ng/mmol) groups and had approximately an 8.6, 9.4 and 9.3 fold increase compared to healthy volunteers ($p < 0.0001$, $p = 0.0002$ and $p = 0.0288$ respectively). However, no difference was found between these groups: ($p = 0.7645$ between non-progressive and progressive, $p = 0.8525$ between non-progressive and rapidly progressive and $p = 0.9906$ between progressive and rapidly progressive, figure 8.13).

Figure 8.13: MMP-9: Creatinine ratio and CKD progression

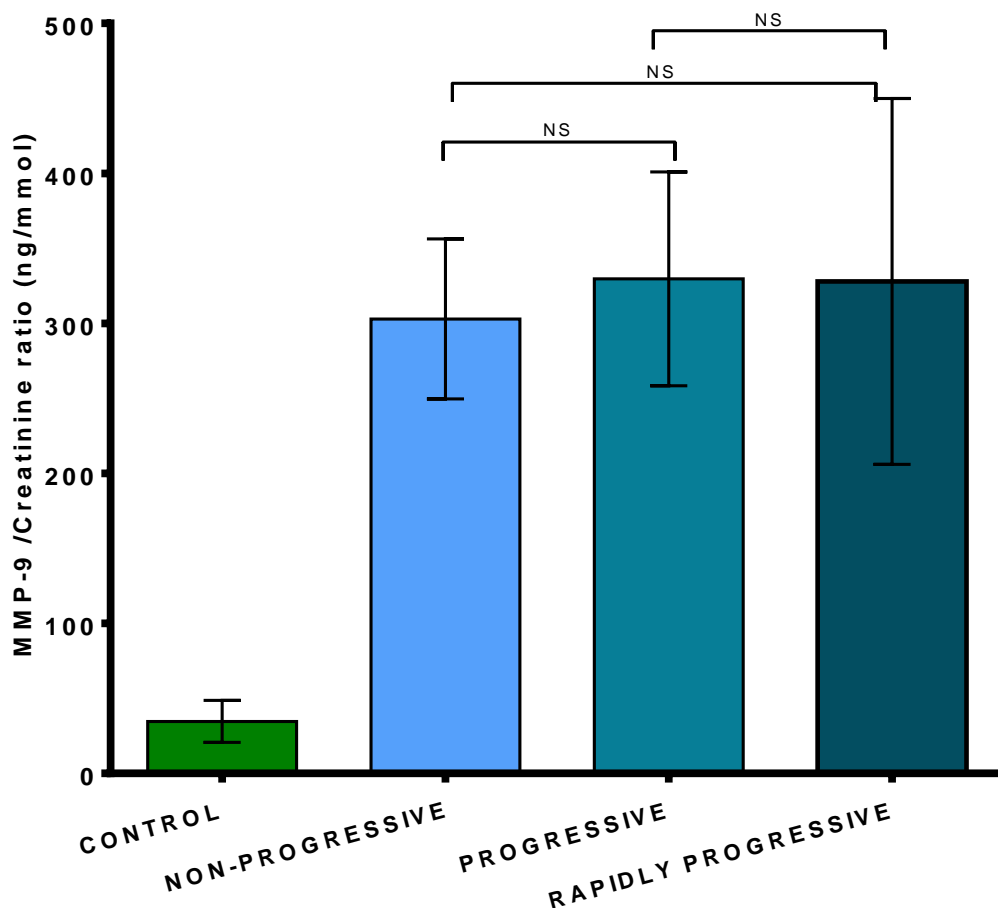
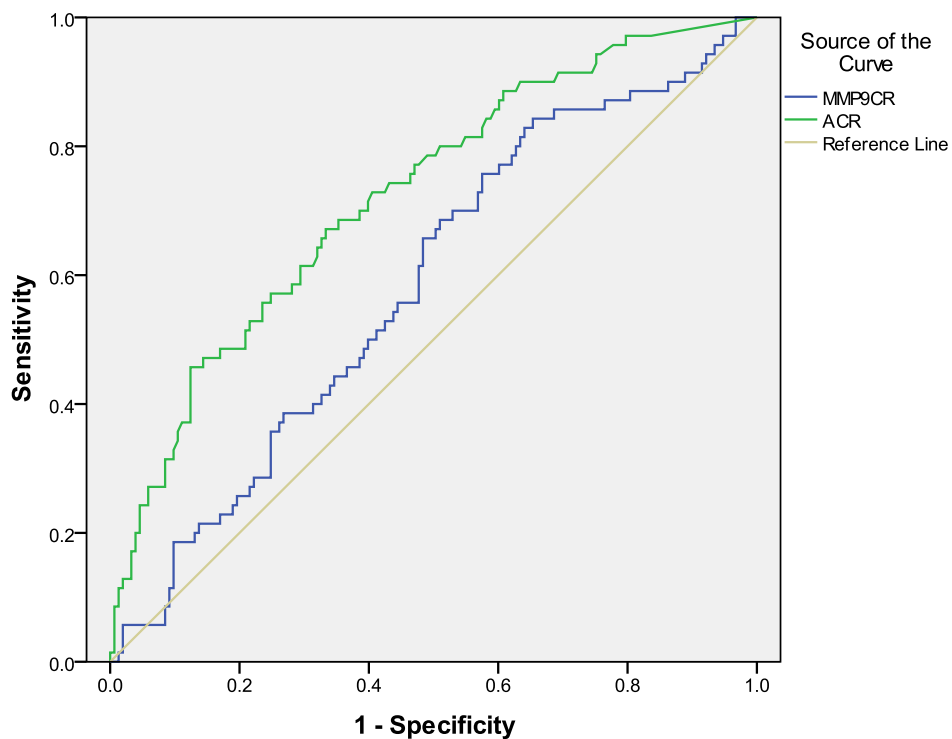


Figure 8.13: The bar chart shows the average MMP-9: Creatinine ratio in CKD patients subdivided by rate of eGFR decline: non-progressive (eGFR decline < 2 ml/min/ 1.73 m²/year, $n = 184$); progressive (eGFR decline between $2-5$ ml/min/ 1.73 m²/year, $n = 79$) and rapidly progressive (eGFR decline above 5 ml/min/ 1.73 m²/year, $n = 29$). Statistical significance between groups is shown by One Way ANOVA with Bonferroni post test: NS= not statistically significant. Data represents mean \pm SD

8.3.3.4. Receiver Operating Characteristic curve for Urinary MMP-9

MMP-9:Creatinine ratio (MMPCR) and Albumin:Creatinine ratio (ACR) accuracy in predicting CKD progression were evaluated by ROC curve analysis. ACR presented a superior performance (73.5% prediction of CKD progression) when compared to MMP9:CR (58.3%), figure 8.14.

Figure 8.14: Evaluation by ROC curve analysis of MMP-9 ability to predict CKD progression



Diagonal segments are produced by ties.

Area Under the Curve

Test Result Variable(s)	Area	Std. Error ^a	Asymptotic Sig. ^b	Asymptotic 95% Confidence Interval	
				Lower Bound	Upper Bound
MMP9CR	.583	.040	.046	.504	.663
ACR	.735	.030	.000	.676	.794

Figure 8.14: The MMP9:CR ROC curve with sensitivity (probability of correctly identifying a positive finding) plotted in the Y axis and 1-specificity (false positives) in the x axis. ACR presented a higher area under the curve (73.5%) and therefore a higher accuracy of CKD progression prediction when compared to MMP9: CR (58.3%). a = under the nonparametric assumption, b = null hypothesis: true area = 0.5.

8.4. Urine levels of Tissue Inhibitors of Metalloproteinases in Human CKD

Midstream urine samples from 292 patients with Chronic Kidney Disease stages 1-5 and 33 healthy volunteers were used to measure TIMPs 1, 2, 3 and the MMP-1/TIMP-1 complex, using a modification of the R&D systems duo set ELISA system (methods section 3.4.5). Results were obtained using optimised dilutions and data was analysed with SPSS and Graph Pad prism software.

8.4.1. Tissue inhibitor of metalloproteinase 1

TIMP-1 is strongly elevated in the urine of CKD patients. Mean TIMP-1 concentration was 12.75 fold higher in the urine of patients with all CKD causes ($2383 \pm 206\text{pg/ml}$, $p < 0.0001$) when compared to healthy volunteers ($185 \pm 37\text{pg/ml}$, figure 8.15-A). To account for volume variability, TIMP-1 values were corrected to a creatinine ratio as done previously. Average TIMP-1: Creatinine ratio in healthy volunteers was $19 \pm 3\text{ng/mmol}$ and with a 23 fold increase at $426 \pm 42\text{ng/mmol}$ in CKD patients ($p < 0.0001$, figure 8.15-B).

8.4.1.1. Tissue inhibitor of metalloproteinase 1 complexed with Interstitial Collagenase

To study the amount of MMP-1 complexed with TIMP-1, an immunoassay was performed pairing a recombinant human anti MMP-1 as a capture antibody with a recombinant human anti TIMP-1 as a biotinylated detection antibody (full methods in section 3.4.5). Assay optimisation as well as reproducibility and specificity tests are shown in section 3.4.5.1.

MMP-1/TIMP-1 complex was undetectable in all urine samples obtained from healthy volunteers. Assays were repeated twice (samples in quadruplicates) and using undiluted urines to confirm results. Limit of detection for MMP-1/TIMP-1 was 62pg/ml . In CKD patients, MMP-1/TIMP-1 complex was detected in 100 urine samples (34.25% of total number of samples) and had an average value of 491pg/ml (range from 62.13 to 8014pg/ml , figure 8.17-A). MMP-1/TIMP-1 complex was also corrected to a creatinine ratio and its average in CKD samples was $76 \pm 16\text{ng/mmol}$ (range from 2.99 to 917.91ng/mmol). Further comparison by CKD aetiology showed no statistical difference between the average MMP1TIMP1: Creatinine ratio in urine samples from different CKD causes (figure 8.17-B): DKD ($95 \pm 31\text{ng/mmol}$, $n=35$), CGN ($116 \pm 36\text{ng/mmol}$, $n=21$), HTN ($61 \pm 27\text{ng/mmol}$, $n=17$), ARVD ($179 \pm 2\text{ng/mmol}$, $n=5$), CIN ($39 \pm 8\text{ng/mmol}$, $n=6$), ADPKD ($71 \pm 50\text{ng/mmol}$, $n=4$) and other CKD causes ($16 \pm 2\text{ng/mmol}$, $n=12$).

An analysis by stages of CKD did not show any statistical differences (figure 8.17-C): CKD 1 (n=1, 152ng/mmol), CKD 2 (498 ± 365 ng/mmol, n=9), CKD 3A (635 ± 235 , n=20), CKD 3B (264 ± 79 ng/mmol, n=23), CKD 4 (584 ± 224 ng/mmol, n=43) and CKD 5 (142 ± 22 ng/mmol, n=4).

8.4.2. Tissue inhibitor of metalloproteinase 2

Oppositely to TIMP-1, no difference was found between the average urine TIMP-2 concentration in healthy volunteers (2726 ± 363 pg/ml) and CKD patients (2857 ± 196 pg/ml, $p=0.7516$, figure 8.15-C). Nonetheless, TIMP-2 corrected to a creatinine ratio in CKD patients was nearly double the value of controls (259 ± 44 ng/mmol, $p<0.0001$, figure 8.15-D).

8.4.3. Tissue inhibitor of metalloproteinase 3

Considerably lower levels of TIMP-3 were detected in human urines when compared to TIMPs 1 and 2 levels. Urines were assayed undiluted and each sample run in quadruplicate (in two different microplates). However, TIMP-3 was below detectable levels in 8% of healthy volunteers and in 20.74% of CKD patients' urine samples. Mean urine TIMP-3 concentration was higher in controls (302 ± 86 pg/ml) compared to patients with all CKD causes (199 ± 16 pg/ml, $p=0.2532$, figure 8.15-E) and even after rectification to a creatinine ratio, no difference was found between healthy volunteers (33 ± 7 ng/mmol) and CKD patients (38 ± 3 , $p=0.5150$, figure 8.15-F).

Figure 8.15: Urine TIMP levels in CKD patients

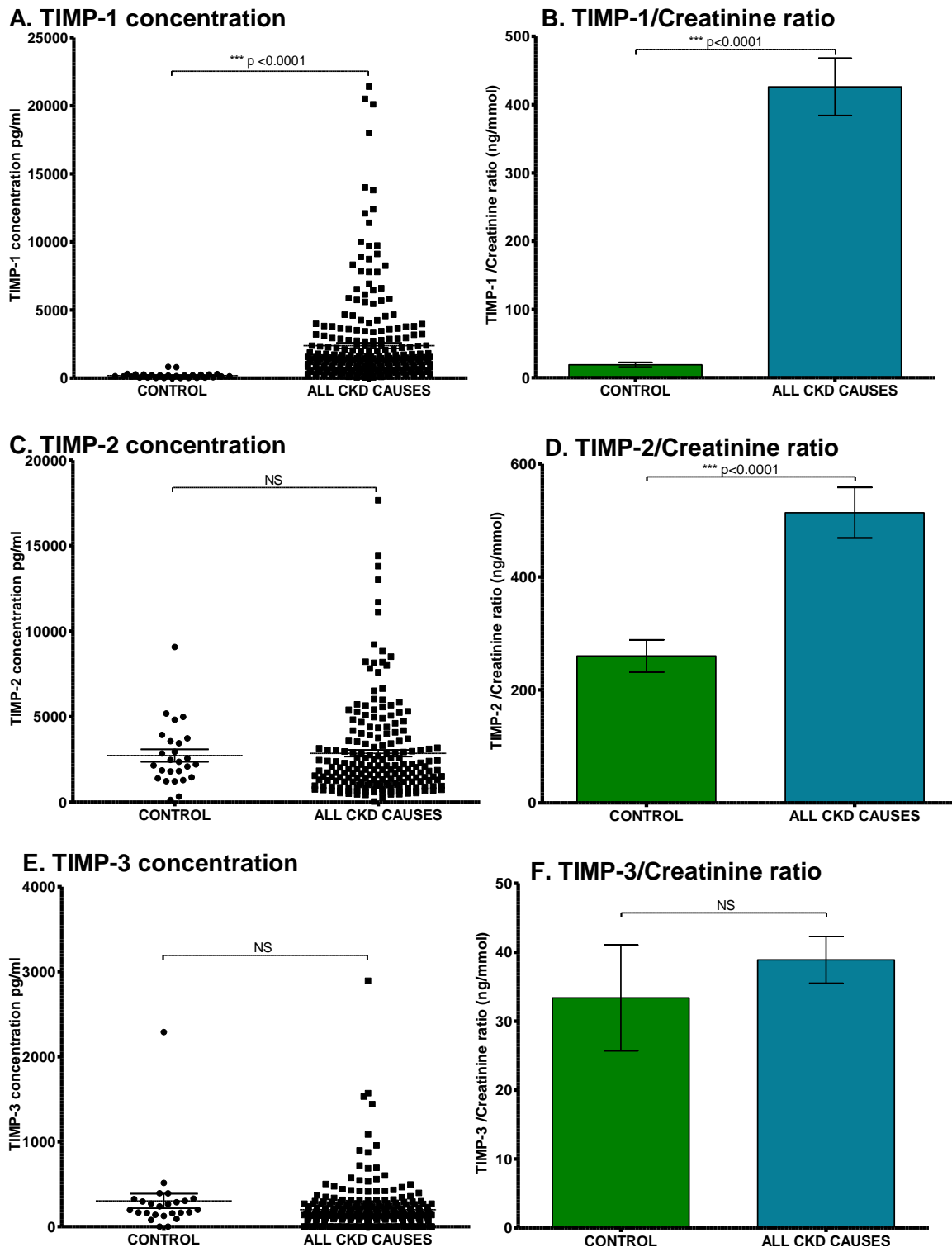


Figure 8.15: Urine TIMPs were measured by the DuoSet immunoassay in patients with all CKD causes (n=292) and controls (n=33). Scatter plots showing the concentration (pg/ml) of: **A** - TIMP-1, **C** –TIMP-2 and **E** – TIMP-3 and bar graphs showing their concentrations corrected to a creatinine ratio (ng/mmol): **B** – TIMP-1:Creatinine, **D** – TIMP-2:Creatinine and **F** – TIMP-3:Creatinine. Statistical significance is shown by Independent-samples T test: NS= not statistically significant, * p<0.05, **p<0.01, ***p<0.001 between CKD patients and healthy volunteers. Data represents mean \pm SD.

Figure 8.16: Measurement of MMP-1/TIMP-1 complex in 100 CKD patients

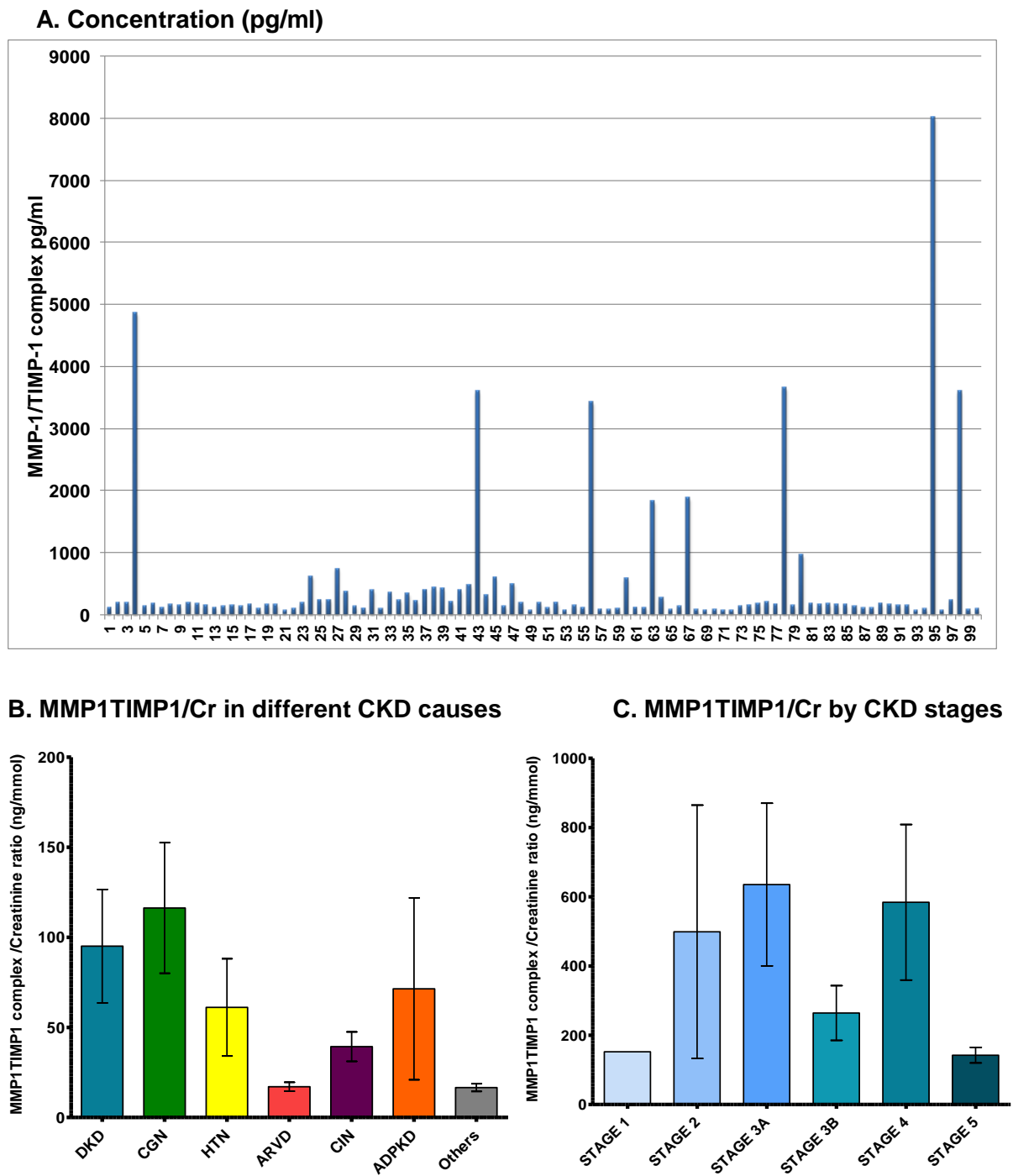


Figure 8.16: MMP-1/TIMP-1 complex was measured by the DuoSet immunoassay in CKD patients (n=292) and health volunteers (n=33). However, it was detectable in only 100 urine samples obtained from CKD patients (A). The MMP-1/TIMP-1 complex was corrected to a creatinine ratio and is shown in different CKD etiologies (B) and stages (C). Data represents mean \pm SD.

8.4.4. Tissue inhibitors of MMPs in different CKD aetiologies and stages

Urine TIMP-1 was significantly increased in nearly all causes of CKD when expressed as a creatinine ratio, excluding only patients with CIN (610.7 ± 474.4 ng/mmol, $p=0.2362$). All other diseases had impressive increases in TIMP:CR when compared to healthy volunteers: DKD had a substantial 28 fold (533 ± 76 ng/mmol, $p<0.0001$), whilst CGN (400 ± 75 ng/mmol, $p<0.0001$), 21 times higher. HTN and ARVD patients presented similar figures (380 ± 74 ng/mmol, $p<0.0001$ and 328 ± 75 ng/mmol, $p=0.0003$, respectively), whereas ADPKD (233 ± 85 ng/mmol, $p=0.0295$) and others (211 ± 32 ng/mmol, $p<0.0001$) presented 12 and 11 times more TIMP1CR levels. Healthy volunteers presented an average TIMP1CR of 19 ± 3 ng/mmol; figure 8.17-A).

Changes in TIMP2: CR were less consistent across diseases where only patients with DKD (605 ± 98 ng/mmol, $p=0.0012$), CGN (512 ± 61 ng/mmol, $p=0.0005$) and HTN (491 ± 90 ng/mmol, $p=0.0199$) having a significant TIMP2:CR increase compared to controls (figure 8.17-B).

In contrast with previous TIMP results, patients with CIN (52 ± 16 ng/mmol, $p=0.2949$) and ADPKD (77 ± 44 ng/mmol, $p=0.1336$) had apparently higher TIMP3CR levels amongst patients. However, no statistical difference in TIMP3:CR values was found between these and any other type of CKD compared to healthy volunteers (33 ± 7 ng/mmol; figure 8.17-C).

Average TIMP1:CR was significantly higher as early as in CKD stage 1 (158.5 ± 40 ng/mmol, $p=0.0113$) and gradually increased to stage 4 (523.7 ± 67.71 ng/mmol, $p<0.0001$). There was a slight reduction in the TIMP1:CR at stage 5, but this remained significantly elevated (441 ± 173 ng/mmol, $p=0.0347$; figure 8.17-D). TIMP2:CR was significantly elevated only at CKD stages 3A (378 ± 41 ng/mmol, $p=0.0228$), 3B (521 ± 83 ng/mmol, $p=0.0042$) and 4 (587 ± 85 ng/mmol, $p=0.0004$; figure 8.17-E). No statistical difference was found in the average TIMP3CR between CKD patients and healthy volunteers at any stage of the disease (figure 8.17-F).

Figure 8.17: Urine TIMP levels in CKD patients by cause and stage

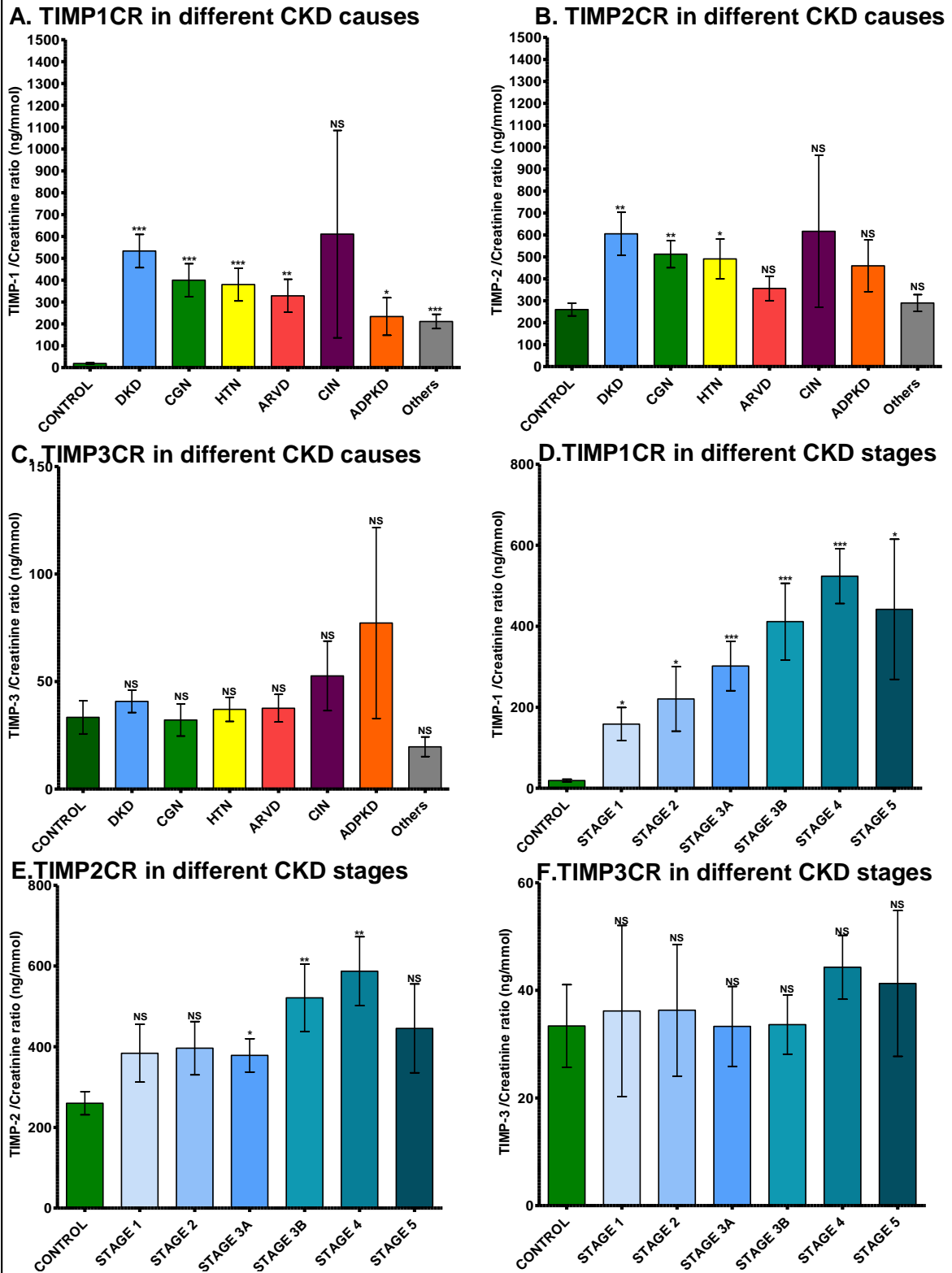


Figure 8.17: Urine TIMP-1 (A; D), TIMP-2 (B; E) and TIMP-3 (C; F) excretion was corrected to a creatinine ratio and presented in patients with different CKD causes and stages respectively. Results are displayed as mean \pm SD. Statistical significance is shown by One Way ANOVA with Bonferroni post test: NS= not statistically significant, * $p < 0.05$, ** $p < 0.01$, *** $p < 0.001$ between CKD patients and healthy volunteers. Abbreviations: see figure 7.2.

8.4.5. Tissue Inhibitors of Matrix Metalloproteinases in different demographic variables

Overall, there were slightly higher values of TIMP1:CR, TIMP2:CR and TIMP3:CR in females than in males (figures 8.18-A, 8.18-B and 8.18-C, respectively). However, no statistical difference was found in any of these groups: $p=0.5980$, $p=0.1668$ and $p=0.3039$.

Additionally, younger people (aged under 65 years old) presented higher figures of TIMP1:CR, TIMP2:CR and TIMP3:CR than people aged above 65 years. Notwithstanding, it only reached significance in TIMP1CR, where values were nearly double in the younger group ($p=0.0239$, figure 8.18-D-F).

8.4.6. TIMPs excretion by rate of CKD progression

As described in section 7.2.6, patients with CKD were sub classified according to their rate of eGFR decline. Patients classified into non-progressors, progressors and rapid progressors had significantly higher TIMP1:CR ($p<0.0001$, $p<0.0001$ and $p=0.0032$) and TIMP2:CR ($p=0.0150$, $p=0.0010$ and $p=0.0355$, respectively) values than healthy volunteers. However, no difference was seen in relation to TIMP3:CR values ($p=0.6949$, $p=0.3025$, $p=0.7377$).

Despite a clear mean elevation of the TIMP1:CR and TIMP2: CR ratios from non-progressive to rapidly progressive patients, no statistical difference was observed within these three groups when using Bonferroni post test (figures 8.19-A and 8.19-C, respectively). Opposing, TIMP3CR values did not increase as the rate of disease progression increased. Rather, there was a drop of around 37% in rapidly progressively patients (figure 8.19-B). Nevertheless, no statistical difference was seen.

Figure 8.18: MMPs inhibitors by different demographic variables

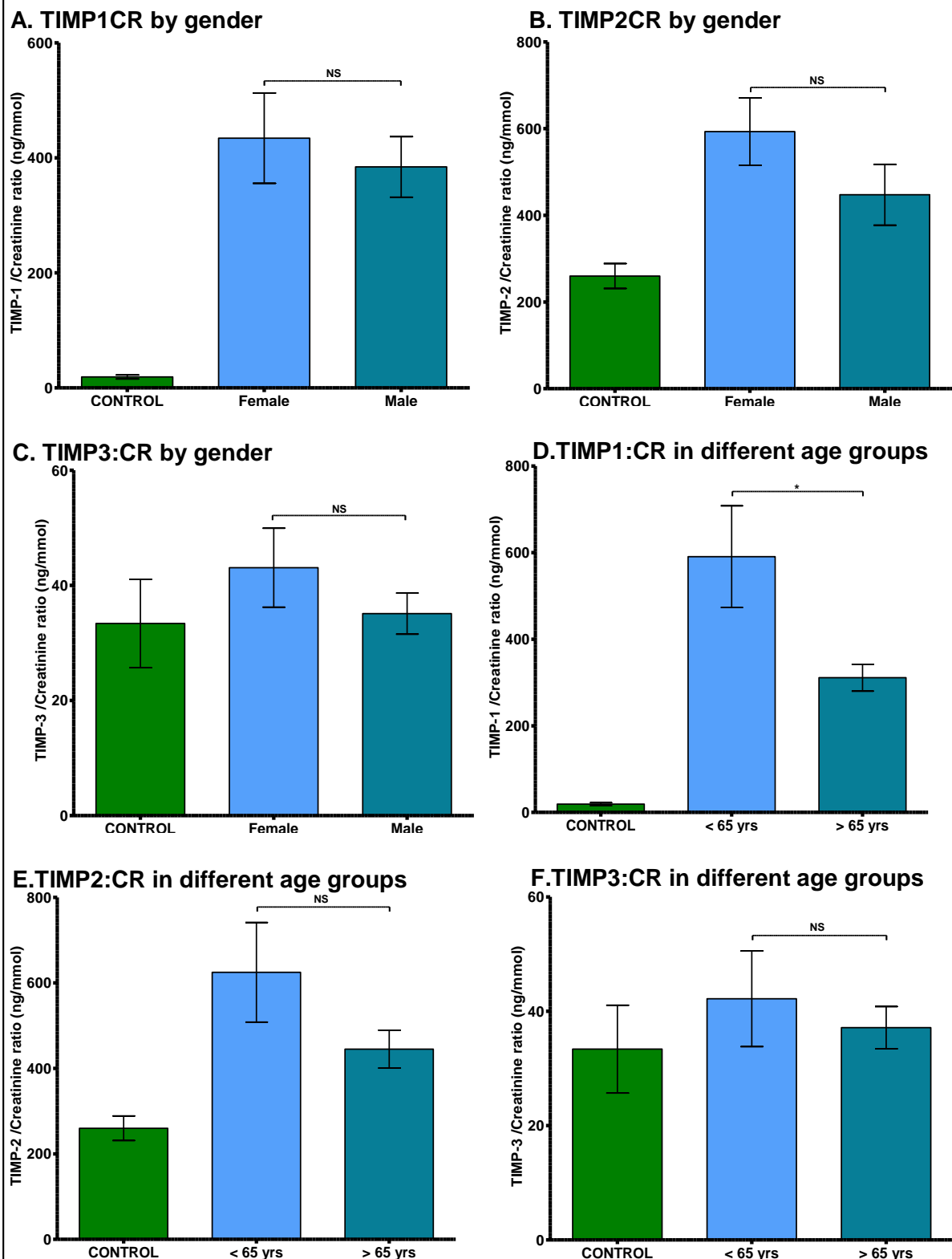
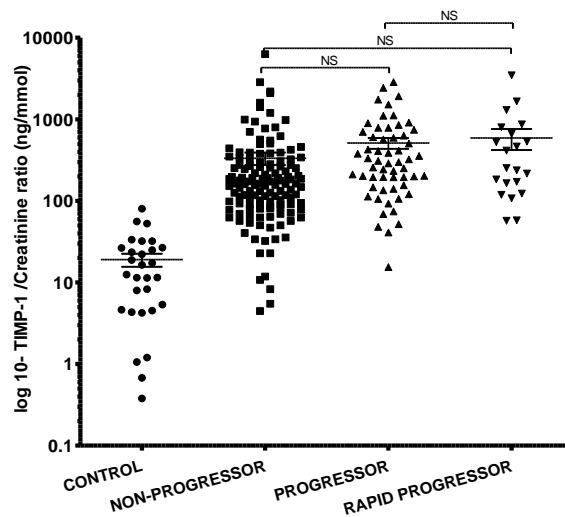


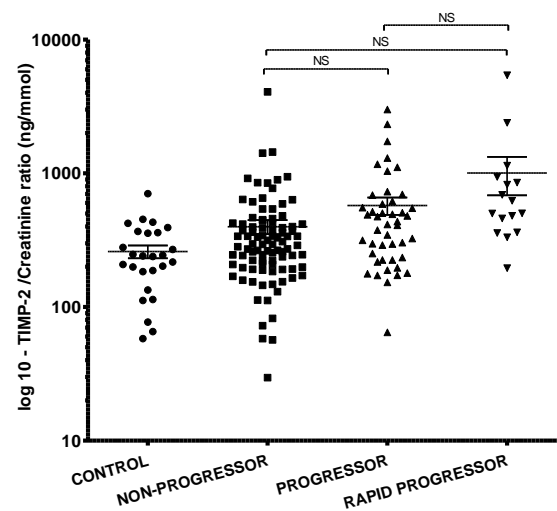
Figure 8.18: Urine TIMP-1 (A; D), TIMP-2 (B; E) and TIMP-3 (C; F) excretion was corrected to a creatinine ratio and is presented in patients by gender and age (< and >65 years), respectively. Results are displayed as mean \pm SD. Statistical significance is shown by One Way ANOVA with Bonferroni post test: NS= not statistically significant, * $p < 0.05$, ** $p < 0.01$, *** $p < 0.001$ between CKD patients and healthy volunteers. Abbreviations: see figure 7.2.

Figure 8.19: Urine TIMPs 1, 2 and 3 levels by rate of CKD progression

A. TIMP-1



B. TIMP-2



C. TIMP-3

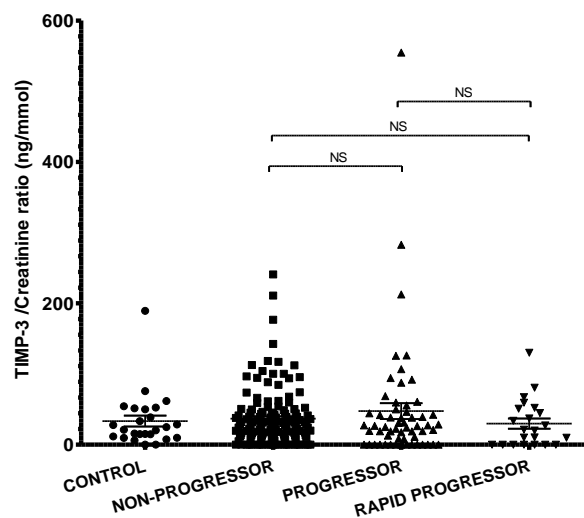
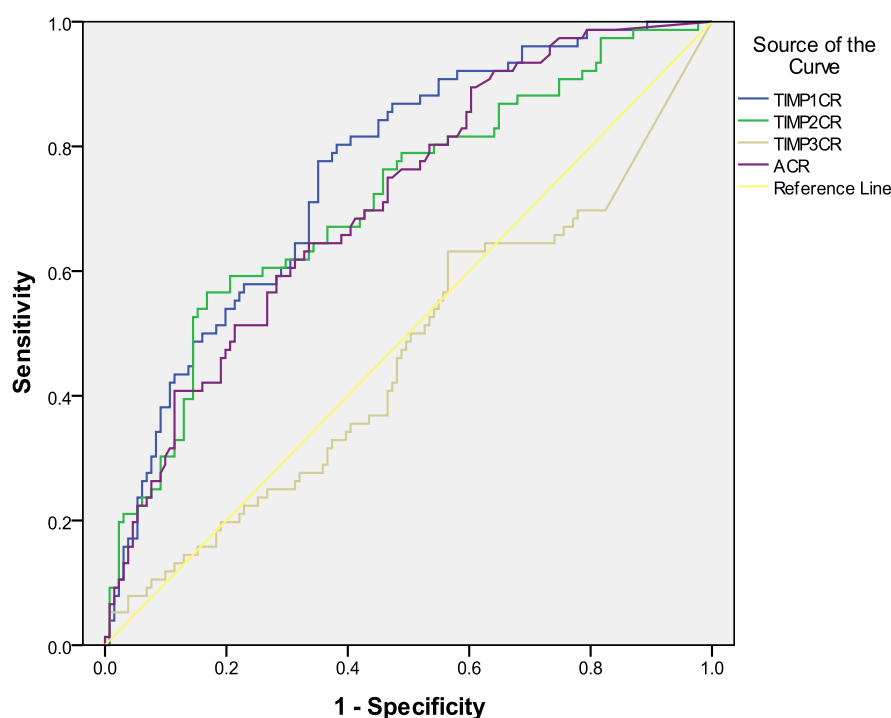


Figure 8.19: Scatter plots showing the TIMP1:CR (A), TIMP2:CR (B) and TIMP3:CR (C) in healthy volunteers compared to CKD patients ranked according to rate of disease progression. Y axis is plotted in log 10 scale in graphs A and B. Statistical significance is shown by One Way ANOVA with Bonferroni post test: NS= not statistically significant, * $p < 0.05$, ** $p < 0.01$, *** $p < 0.001$.

8.4.7. Determination of the predictive potential of urine TIMPs 1, 2 and 3 for rate of disease progression by Receiver Operating Characteristic curve analysis

To examine if MMP inhibitors TIMPs 1, 2 and 3 were a better predictor of progressive CKD than albuminuria we performed a ROC curve analysis of these biomarkers corrected to a creatinine ratio. Using this approach we observed that TIMP1CR presented the highest prediction rate at 75.7%, compared to 71.2% for both TIMP2CR and ACR. TIMP3:CR at only 46.6% was not a good predictor (figure 8.20).

Figure 8.20: TIMPs 1, 2 and 3 ability to predict CKD progression by ROC curve analysis



Area Under the Curve

Test Result Variable(s)	Area	Std. Error ^a	Asymptotic Sig. ^b	Asymptotic 95% Confidence Interval	
				Lower Bound	Upper Bound
TIMP1CR	.757	.034	.000	.691	.823
TIMP2CR	.712	.038	.000	.639	.786
TIMP3CR	.466	.043	.414	.382	.549
ACR	.712	.036	.000	.641	.783

Figure 8.20: The TIMP1CR, TIMP2CR and TIMP3CR ROC curves with sensitivity (probability of correctly identifying a positive finding) plotted in the Y axis and 1-specificity (false positives) in the x axis. TIMP1CR presented a higher area under the curve (75.7%) and therefore a higher accuracy of CKD progression prediction when compared to all other biomarkers; ACR (71.2%), TIMP2CR (also 71.2%) and TIMP3CR (46.6%). a = under the nonparametric assumption, b = null hypothesis: true area = 0.5.

8.5. Discussion

Matrix metalloproteinase activity can be measured in human urine from patients with different types of CKD. The level of MMP activity in the urine is not consistent with that reported in the kidneys in that while urine MMP activity is elevated in CKD, the levels in the kidney fall almost certainly due to the over expression of TIMPs (Johnson *et al.* 2002). The urine activity level of MMPs is highest in non-progressive patients which had over 7 times more than healthy volunteers. Similar levels were found in progressive patients. However, significantly lower MMP activity was observed in patients with rapid loss of kidney function which may have prognostic value in detecting such group of patients. Very similar results were reported in a recent publication just in diabetic kidney disease (Altemtam *et al.* 2012) suggesting this is a robust finding. This raises a series of questions – why the disconnection with the levels in the kidney and how is the overall MMP activity achieved?

To address the first of these, then perhaps there is not such a difference as the data may initially suggest. The elevated MMP activity in patients with stable CKD is certainly different to previous tissue studies where MMP activity in renal tissue is all put lost in the fibrotic process; at least in animal model studies (ref). However in the study here in those patients with more aggressive disease progression we also see a loss of activity mirroring what we “anticipate” in the renal tissue. Thus the disconnect between tissue and urine activity mainly sits in those patients with no progressive or slightly progressive CKD – which could be an artefact of that most of the studies of MMP activity come from animal models where by default rapidly progressing disease has been induced (Ahmed *et al.* 2007) and thus the MMP activity in stable CKD would never be observed in animal models. What is clear is that progressive patient have less MMP activity which may underlie the progression.

With regard to the second point, then in progressive patients MMP-2 and MMP-9 are elevated in rapidly progressing patients urine, but TIMP-1 is massively elevated in the same cohort and thus it seems logical (notwithstanding all MMP and TIMP have not been evaluated) that this massive TIMP-1 level is what blocks activity in the rapidly progressing group despite the clear elevations in TIMPs.

One could further speculate that CKD progression is slowed by elevated MMP activity arresting scar tissue accumulation in stable patients and that its only when that activity becomes compromised CKD enters a more progressive stage. This could further be supported by our previous results shown in experimental renal scarring (chapter 5).

Hypertensive patients presented the highest levels of MMP activity when compared to other CKD aetiologies. This represented a 10 fold increase when compared to healthy control subjects, but although more elevated, did not differ statistically from other group of CKD patients. DKD patients represented the second group with largest increase in MMP activity levels (7 fold increase). This agrees with previously reported results shown by our group (Altemtam *et al.* 2012). ADPKD patients represented the only group in this cohort which did not show significant increased mean levels of MMP activity. This might be due to the large spread of CKD stages within this group (from 1 to 5) or indeed, on some aspect of the pathology of the disease itself.

Although the activity of metalloproteinases was elevated in CKD, the quantity of MMPs 1, 2 and 9 detected in the urine was not high quantity which possibly indicates that other MMPs were also present that were not measured by ELISA. Urine MMP-1 was undetected in 94.86% of human CKD urines, whilst MMP-2 and MMP-9 were detected in approximately 88% and 95% of CKD samples respectively. As MMP-1 levels were uncountable in urine, we hypothesised that it could be mostly bound to TIMP-1. Therefore, we performed an additional analysis of MMP-1 complexed to TIMP-1, but this proved to be difficult as only 34.25% had detectable urine levels. MMP-2 corrected to a creatinine ratio was 2.4 fold higher in CKD patients when compared to healthy volunteers and once again Hypertensive patients showed the largest increase. Similarly, MMP-9: Creatinine ratio was massively increased in CKD patients (9 fold increase) where patients with HTN and CIN presented the highest significant increases of the molecule. Although rapidly progressing patients had higher amounts of the metalloproteinases 2 and 9 in the urine, the overall activity of these enzymes was drastically reduced.

There was an increase in both tissue inhibitor of metalloproteinase 1 and 2 in the urine of CKD patients. However, there was no difference between the urine levels of TIMP-3 in CKD and control subjects. Similar results in mRNA levels of TIMP-3 were previously showed in experimental animals (Johnson *et al.* 2002). Interestingly, ADPKD patients presented the highest amount of TIMP-3 present in the urine, but this difference was not statically relevant. Thus, it corroborated with the results showed in the previous chapter (TG2 and ϵ (γ glutamyl) lysine measurement) and supports the presupposition that ADPKD progression is more linked to other pathways involved in scaring process such as an increase in cyst size and kidney volume, development of hypertension and PKD-1 gene mutations.

Chapter 9

General Discussion

9.1. Summary analysis

A summary of the mean concentrations of all biomarkers studied in the human CKD cohort and presented in this thesis is displayed in table 9.1

Table 9.1: Summary of human ECM biomarkers data

	Control (n=33)	all CKD (n=292)	DKD (n=91)	CGN (n=66)	HTN (n=53)	ARVD (n=29)	CIN (n=15)	ADPKD (n=13)	Others (n=25)
TG2 pg/ml	94.18 ± 19.99	3346 ± 758.5 p<0.001	6071 ± 1989 p=0.0034	2157 ± 451.8 p<0.0001	2700 ± 1397 p=0.0167	914.2 ± 298.9 p=0.0106	2070 ± 912.9 p=0.0483	787.1 ± 561.9 p=0.2435	1064 ± 434.7 p=0.0382
XL nmols/mg protein	0.1945 ± 0.025	1.304 ± 0.075 p<0.001	1.317 ± 0.1644 p<0.0001	1.305 ± 0.1284 p<0.0001	1.425 ± 0.2173 p<0.0001	1.120 ± 0.1475 p<0.0001	1.324 ± 0.3021 p=0.0047	0.7210 ± 0.2033 p=0.0611	1.512 ± 0.2751 p=0.0006
TG2 BLOOD pg/ml	523.9 ± 107.3	3994 ± 358.8 P<0.0001	3831 ± 5513 P<0.0001	4704 ± 931.3 P=0.0002	3722 ± 692.2 p=0.0001	3085 ± 1133 P=0.0591	7300 ± 2813 P=0.0738	3468 ± 2580 P=0.3371	2934 ± 803.3 P=0.0207
MMP activity Δ FI / hr	0.4997 ± 0.076	2.376 ± 0.191 p<0.0001	2.407 ± 0.3090 p<0.0001	1.769 ± 0.309 p=0.0002	3.305 ± 0.6553 p=0.0001	1.589 ± 0.2957 p=0.0013	2.340 ± 0.8308 p=0.0443	1.361 ± 0.4767 p=0.1065	3.303 ± 0.8071 p=0.0026
MMP-1	undetec table	undetec table in 277 patients							
MMP-2 pg/ml*	919 ± 160	1341 ± 136 p=0.0481	1107 ± 210 p=0.4770	2114 ± 477 p=0.0209	1446 ± 292 p=0.1178	957 ± 244 p=0.8966	949 ± 324 p=0.9339	1082 ± 340 p = 0.6695	1272 ± 413 p=0.4333
MMP-9	327 ± 107	1354 ± 116 p<0.0001	1243 ± 237 p=0.0008	1119 ± 215 p=0.0016	1356 ± 273 p=0.0010	1612 ± 383 p=0.0033	1601 ± 453 p=0.0167	1864 ± 568 p=0.0211	1437 ± 373 p=0.0094
TIMP-1	186.84 ± 37.25	2383 ± 206.3 p<0.0001	2740.9 ± 361.8 p<0.0001	2832.7 ± 544.6 p<0.0001	2080.8 ± 417.9 p<0.0001	2127.3 ± 491.4 p=0.0005	2477.2 ± 1592.0 p=0.1759	863.15 ± 230.5 p=0.0139	1518 ± 190.6 p=0.0005
MMP- 1/TIMP-1 complex	Undetec table	Undetec table							
TIMP-2	2725.5 ± 363.11	2857 ± 363.1 p=0.7516	3060.0 ± 370.17 p=0.5208	3583.3 ± 439.02 p=0.1370	2852.6 ± 447.26 p=0.8262	1963.51 ± 483.57 p=0.2158	2756.29 ± 1201.53 p=0.9809	1798.14 ± 397.24 p=0.0957	1885.12 ± 292.72 p=0.0799
TIMP-3	302.35 ± 86.35	199.5 ± 16.71 p=0.2532	202.87 ± 23.51 p=0.1970	239.04 ± 66.63 p=0.4919	184.18 ± 23.93 p=0.1519	202.57 ± 31.65 p=0.2056	158.35 ± 28.01 p=0.0881	242.43 ± 111.47 p=5560	119.38 ± 25.52 p=0.0322

* Bellow detectable levels in 2 controls and 37 CKD patients

The Albumin: Creatinine ratio (ACR) was significantly elevated in overall CKD patients when compared to healthy volunteers. However, it failed to show differences between patients with rapid progression and those with progressive disease (figures 9.1-A and B).

Figure 9.1: Albuminuria vs. CKD progression

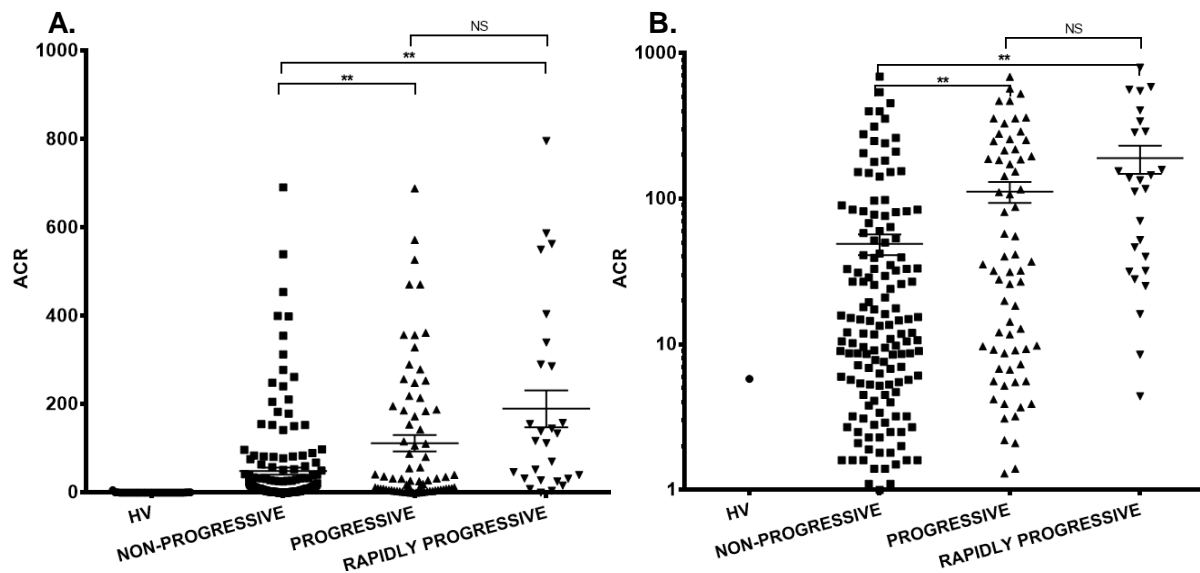


Figure 9.1: Albuminuria was measured in spot human urine samples by ELISA and adjusted to a creatinine ratio (ACR). **(A)** ACR according to CKD progression and **(B)** with X axis in log scale to better visualise the spread of the data.

Receiver Operating Characteristic (ROC) curve analysis of ACR and all urinary ECM biomarkers used in this study is shown in table 9.2.

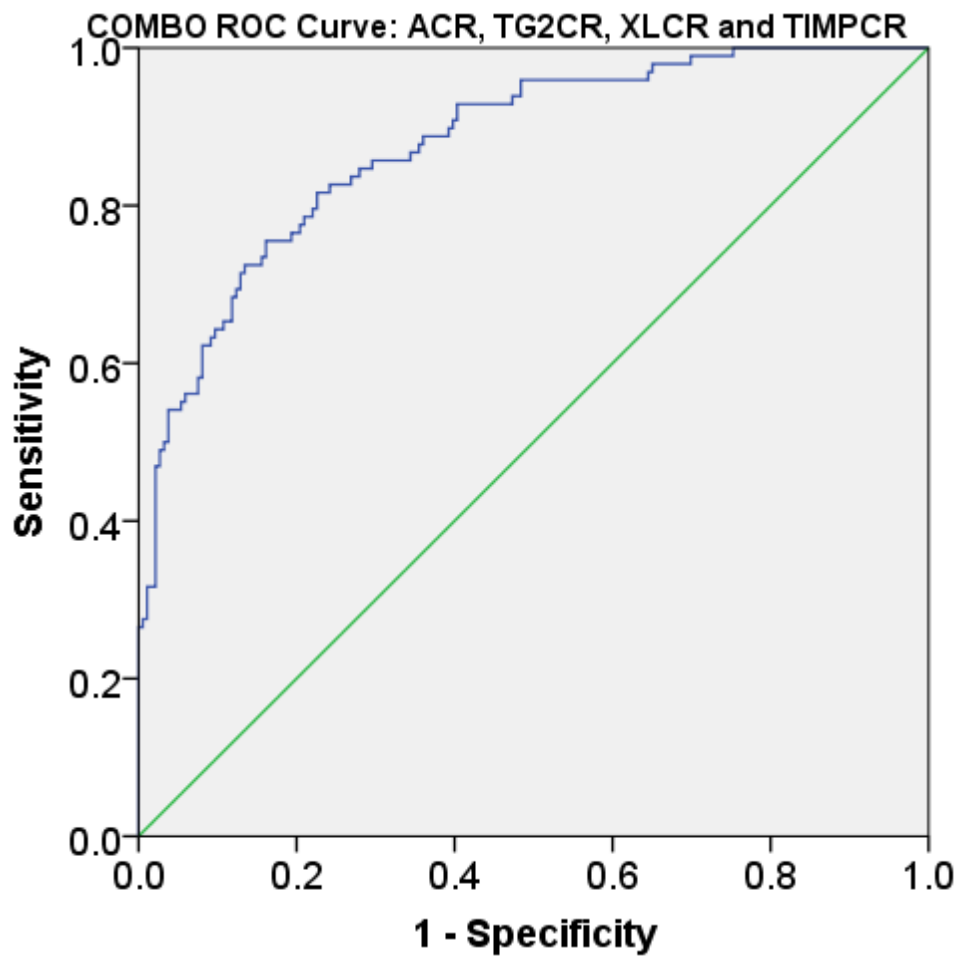
ROC curve analysis demonstrated that the TG2/CR ratio (86.4%) and TIMP1/CR ratio (75.7%) are better predictors of patients with progressive CKD than ACR (73.5%). The ROC curve analysis of ϵ (γ -glutamyl) lysine / CR ratio (73.3%) and TIMP2/ CR ratio (71.2%) presented similar levels of accuracy of prediction as ACR, whereas all other candidates were inferior to ACR. Measurement of MMP-1 activity had a remarkable predictive value in detecting rapid progressive patients, as very low levels were found in this subgroup of patients. A combo ROC curve analysis using TG2CR, XLCR, TIMP1CR and ACR as prognostic tools of CKD progression generated a remarkable 87.7% risk prediction (figure 9.2).

Table 9.2: ROC AUC values of ACR and Urinary ECM biomarkers

	Healthy Volunteers	CKD patients	p value	ROC AUC (%)
ACR	0.3061 ± 0.1787	80.49 ± 8.635	p<0.0001	73.5
TG2CR	9.72 ± 1.92	599.4 ±118.9	p<0.001	86.4
XLCR	0.0222 ± 0.004	0.2796 ± 0.0285	p<0.001	73.3
TIMP1CR	19.05 ± 3.475	426.1 ± 41.96	p<0.0001	75.7
TIMP2CR	259.9 ± 28.64	513.6 ± 44.69	p<0.0001	71.2
TIMP3CR	33.38 ± 7.675	38.90 ± 3.403	p=0.5150	46.6
MMP1CR	Undetectable	Undetectable in 94.86% patients	n/a	n/a
MMP2CR	118.6 ± 27.45	285.3 ± 31.48	p=0.0001	53.2
MMP9CR	34.67 ± 14.05	312.0 ± 40.71	p<0.0001	58.3
MMP1TIMP1 complex/Cr	Undetectable	Undetectable	n/a	n/a
MMPactivityCR	0.0741 ± 0.019	0.5394 ± 0.058	p<0.001	*68.3

*ROC AUC calculated in rapid progressive patients (eGFR decline > 5ml/min/1.73m²)

Figure 9.2: ACR, TG2CR, XLCR and TIMP1CR combo ROC curve



Area Under the Curve

Test Result Variable(s): Predicted probability

Area	Std. Error ^a	Asymptotic Sig. ^b	Asymptotic 95% Confidence Interval	
			Lower Bound	Upper Bound
.877	.021	.000	.836	.918

a. Under the nonparametric assumption

b. Null hypothesis: true area = 0.5

9.2. General discussion

The overall aim of this study was to determine if ECM proteins and related processing enzymes could be used as urine biomarkers of kidney fibrosis. To do this, we initially used archive urine samples from three different animal models of renal scarring: the 5/6th Subtotal nephrectomy, the UNx STZ model of diabetic nephropathy and the Fisher to Lewis model of chronic allograft nephropathy. In total, 153 urine samples from the above animal models were screened for 10 different potential biomarkers: TG2, ϵ (γ -glutamyl) lysine, hydroxyproline, Metalloproteinases 1, 2 and 9, TIMPs 1, 2 and 3, and PAI-1. Following establishment and optimization of urine assays for determination of such molecules, measurements were undertaken in 292 CKD patients, having 33 healthy volunteers and 19 patients with diabetes mellitus without laboratorial and clinical evidence of kidney dysfunction, as control groups. In addition to the above molecules, human patients were also screened for serum TG2, TIMP-1/MMP-1 complex and total MMP activity.

Numerous studies have demonstrated that TG2, ϵ (γ glutamyl) lysine, collagens and other ECM related molecules can be detected in kidney tissue from either animals (Norman *et al.* 1995, Johnson *et al.* 1997, Johnson *et al.* 2002, Ahmed *et al.* 2007) or humans (El Nahas *et al.* 2004, Thrailkill *et al.* 2009, Altemtam *et al.* 2012). Nonetheless, few studies have been performed in urine, which could represent an optimal non-invasive way to assess ECM regulation and consequently disease stage and progression. The few studies to date have been positive showing a positive correlation between tissue levels of ECM molecules and scarring histology. This study has assessed the predictive value of ECM in urine through RO-AUC curve analysis based on progression 3 years post sampling.

In this study, we used three animal models of CKD as their mechanisms of disease progression could be translated into human pathology. In the SNx model, a reduction in the number of functioning nephrons followed by glomerular and hemodynamic adaptive changes take place which leads to the development of hyperfiltration, proteinuria and systemic hypertension. The Streptozocin model of DN causes Type I diabetes by the administration of streptozotocin; an agent that promotes pancreatic β cell failure. Whilst the pathogenesis of CAN model involves the development of immune reaction (acute rejection, alloantibody, allorecognition) and existence of non-immune risk factors like the presence of ischaemia-reperfusion injury. Nonetheless, all three models are characterised by progressive loss of renal tissue and ECM deposition, culminating in kidney fibrosis and failure. Although these rodent models offer a good insight into human kidney disease manifestation, there are also

some disadvantages and limitations to these experiments such as the limited amount of experimental material produced, inter-animal variation and not an exact replication of the human pathophysiology of the disease (lack of vascular damage and some other morphological and histological changes). Other model that could have been useful to reproduce kidney injury due to interstitial fibrosis, the ureteral obstruction with reversal of obstruction, can cause ischaemia and consequently decrease in kidney function. However, this model is better associated with the development of AKI rather than CKD and may also prevent the collection of urine samples at early stages of the disease as there is a natural development of anuria as a consequence of the ligation of the ureters.

Initial results from our animal data suggested that TG2 and its crosslink product ϵ (γ -glutamyl) lysine could have value as urine biomarkers of CKD as levels were significantly increased earlier in all animal models and also correlated well with disease progression in SNx and CAN. However, in the DN study, no changes were detected by 8 months, with an increased level only achieved when its concentration was converted to a creatinine ratio or expressed per total amount excreted in 24 hours. This could be due the large amounts of diluted urine produced by diabetic animals.

It is known that the majority of patients with DKD typically progress with increased excretion of albumin and gradual decline in GFR until ESRD occurs (Ayodele *et al.* 2004, Chang 2008, Jefferson *et al.* 2008, Woredekal 2008). This albuminuria can vary from small amounts (30 to 300 mg/24h – Microalbuminuria) up to larger amounts (>300mg/24h – Macroalbuminuria). Concentrations given by the AAA are related to the amount of that amino acid or di amino acid present in 10 mg of urine protein (amount used to digest), therefore the expression of ϵ (γ -glutamyl) lysine related to this amount of protein digested might not represent an ideal way to express it as in diseased urines most of the protein load would be due to the increased presence of albumin and not collagen, fibronectin or other proteins of interest that could be crosslinked in the ECM. To investigate if albumin could be crosslinked by TG2, in chapter 7, an *in vitro* experiment testing different ECM substrates was conducted. This revealed little crosslinking of albumin and could justify the decrease in measured ϵ (γ -glutamyl) lysine levels in late DN. To minimise the effect of increased albuminuria steps could be added to remove albumin from samples. Application of albumin depletion methods could potentially improve ϵ (γ glutamyl) lysine detection as albuminuria impedes equivalent analysis of those molecules in diseased samples where a high abundance of albumin has more influence than control samples where potentially there is a lower abundance of albumin as a fraction of the total

protein load. However, albumin depletion is costly and certainly not a flawless technique, and so could potentially remove proteins of interest from samples.

In chapter 5, MMPs 1 and 9 as well as TIMPs 1, 2 and 3 and PAI-1 were measured in urines. MMPs 1, 2, 3, 8, 9 as well as TIMPs 1, 2, 3 have been shown to have significant renal expression (Engelmyer *et al.* 1995, Lenz *et al.* 2000). Confirming published data in renal tissues from the same animals used in this study (Johnson *et al.* 2002), urine measurements of MMP-1 were significantly increased in diseased animals. On the other hand, MMP-9 excretion was undetectable on all control samples and it had a steady, but not significant rise on SNx and Diabetic animals even when correcting by creatinine. A comparison of urine levels of MMP inhibitors showed that TIMP-1 was the most attractive biomarker and this substantiates the published tissue findings. TIMP-1 levels were highly increased as early as 7 days post subtotal nephrectomy and from 4 months post STZ injection. Similar findings were observed in relation to TIMP-2 excretion when corrected to a creatinine ratio. However, TIMP-3 levels were no different from diseased to controls in SNx, once again confirming previously published data from our group. Interestingly, urine TIMP-3 levels were quite significantly elevated in DN from 4 months after induction. In the CAN study, no difference was found in terms of TIMP-1 excretion between L-L isografts and F-L Allografts. However, the TIMP2/CR ratio was significantly increased as early as 8 weeks post transplantation up to 33 weeks of the study. Urine PAI-1 concentration was elevated only at early stages of the disease in SNx and highly increased at all time points in the UNx STZ model of Diabetic nephropathy. Such results ratify literature findings in which PAI-1 was shown to be highly expressed in fibrotic kidneys promoting migration of macrophages and myofibroblasts through interactions with uPA receptor, LDL receptor-associated protein-1 and leukocytes (Eddy 2009).

The third part of this study is concerned with the measurement of Hydroxyproline (chapter 6). Hydroxyproline is a major component of collagen and is found in few proteins other than collagen (e.g. elastin). It has been widely reported in histopathological studies that development of scarring is strongly associated with increased synthesis and deposition of particularly fibrillar collagens with collagen acting as a key component of scar tissue.

To date, there are surprisingly few studies correlating the use of urinary collagen as a possible marker of kidney scarring given its role in kidney fibrosis. Urinary amino terminal peptide of procollagen III (PIIINP) was positively correlated to interstitial fibrosis in humans, although it was not correlated to increased serum creatinine (Soylemezoglu *et al.* 1997). The urinary carboxy terminal fragment of type IV procollagen was found increased in Minimal Change disease, but again it was not correlated to increased serum creatinine and neither to CrCl or

other nephropathies (Keller *et al.* 1992). Irrespective of the limitations of these early studies of urine collagen in CKD, we hypothesised that measurement of urinary Hydroxyproline could be used as an useful non-invasive indirect indicator of total collagen, suppressing the need of processing fragments of individual collagens.

Initial assessment of Hydroxyproline showed no difference in both SNx and DN groups at later stages of the disease when expressed per mg of protein. Thus, urine excretion of hydroxyproline was not increased as a percentage of the total proteinuria. Such results could be due to an artefact, failure of analysis or be an authentic decrease in collagen excretion as disease progresses. There is also the possibility that hydroxyproline could be extensively crosslinked in the ECM and therefore excretion in the urine could be reduced. However, when corrected to a creatinine ratio, hydroxyproline excretion was markedly increased in the SNx and DN during all time points of both studies indicating that pathological changes in the kidney were being carried through to the urine.

In chapter 7, the epidemiological data from our cohort of 292 CKD patients as well as the measurements of TG2 and its crosslink ϵ (γ glutamyl) lysine is presented.

According to a wide range of adult population screening studies, overall CKD prevalence is estimated to be around 10% in the general population, with community prevalence screening ranging from 0.8% to 42.6% depending of the country of data collection (systematic review from (McCullough *et al.* 2012). Studies showed that the prevalence of community CKD in the USA is hardly detectable under the age of 60 (2-3%), over the age of 60 it is >30% and over 70 years, it is almost 40%, therefore this is a disease mostly diagnosed in elderly people which could suggest an overestimation in the number of CKD cases. However, there are several issues in the CKD screening programs; for instance, equating isolated microalbuminuria or microscopic haematuria to CKD (which per se defines CKD stages 1 and 2), the use of single collection and testing of samples during screening (which cannot guarantee the chronic status) and the use of imprecise formulas to calculate eGFR (for example, the MDRD formula is not applicable to general population and it uses creatinine which has large variability). In addition, there is a pathophysiological decline in kidney function of 0.79 to 1.2ml/min/year (average 1ml/min/year from around 40 years onward) and this is due to a normal shrinkage of kidneys with age (around 60% size at 60 years old), arteriosclerosis, vascular damage, reduction in effective renal plasma flow and hypoperfusion leading to ischaemia and the presence of risk factors such as hypertension.

Although communities studies show that around 10% of the general population has CKD, only 0.2% will progress to ESRD and this is specially present in people aged above 60 years (with

up to 30-40% of subjects at this age group having a low GFR). The Baltimore longitudinal study on aging had a 5 years observational period and showed three patterns of CKD progression: stable, with ageing subjects without co-morbidity with normal renal function; decline, subjects with co-morbidities such as CVD, HTN and DM, decline of eGFR (CrCl) between 1 to 1.5ml/min/1.73m²/year and fast decline, people with overt proteinuria, rCKD, DN, Nephrotic syndrome – CGN - eGFR decline above 5ml/min/1.73m²/year. Predictors of CKD development included the presence of Atherosclerosis with internal carotid intima media thickness more than 1.8cm, Coronary Heart disease (CHD), Stroke and Heart Failure. The outcomes of this large study showed that the risk of death from the underlying problem (i.e.; CVD) is higher than reaching ESRD. In addition, the Oregon study (n=27,988 people, (Keith *et al.* 2004)) confirmed that the risk of progression to ESRD in the elderly population is lower than the risk of death from CVD. However, on younger individuals with rCKD, there is a higher risk of reaching ESRD than death and the progression of CKD is mainly due to the presence of hypertension and proteinuria.

Early studies (Mitch *et al.*, 1976) believed that CKD progression complied with a linear slope of decline. However, later studies showed that some individuals decline in a linear fashion, some do not even have a decline and remain stable and majority which have a decline of kidney function over time do not present it in a linear way. This may be due to the presence of acute or chronic insults and improvement in the slope can be due to improvement in blood pressure control, reduction on proteinuria/albuminuria and improvement of other risk factors of progression or removal of the insulting agent (for example, NSAIDs or other nephrotoxic drugs / herbs).

Risk models of CKD progression (Cheugui and Kengne, 2012) recommended that new biomarkers should be compared or added to previously established biomarkers such as severity of hypertension, severity of proteinuria, level of kidney function impairment at presentation in order to provide a more precise accuracy of progression to ESRD. Previous studies have showed that Albumin predicts CKD progression by 60%, whereas HTN predicts 70% (guidelines 2002). So far hypertension is the single most important factor for CKD progression. Patients with uncontrolled HTN will progress fast and that is why the KDIGO 2012 supported an aim of BP < 130/80mmHg in DN and heavy proteinuric states and bellow 140/90mmHg in others etiologies.

With the above in mind, in the human section of this study, the aim was to recruit a significant cohort size which could be reflective of the general CKD population. Our study consisted of a prospective observational cohort of 292 CKD adult patients from stages 1 to 5 over a period

of 3 years. 19 patients with diabetes mellitus without any evidence of kidney dysfunction and 33 adult healthy volunteers were also recruited to this study. From those 292 CKD patients, 91 had diabetic kidney disease, 66 chronic glomerulonephritis, 53 hypertensive nephrosclerosis, 29 atherosclerotic renovascular disease, 15 chronic interstitial nephritis and 13 had ADPKD. 25 patients presented other causes of CKD such as Multiple Myeloma, amyloidosis, idiopathic thrombocytopenic purpura, Henoch Schölein purpura, monoclonal gammopathy of undetermined significance (MGUS), microscopic polyarteritis, familial renal disease, medullary sponge kidneys, sarcoidosis, lupus nephritis, HIV-associated nephritis, Tacrolimus toxicity and renal cell carcinoma. From this total, 41 patients were recruited at the time of renal biopsy.

Majority of the CKD population in this study was formed by caucasians (90.41%), males (61.31%), above the age of 65 years old (61.9%). Hypertension was the most common comorbidity within this group. In addition, most patients were either at CKD stage 3 (38.36%) or stage 4 (45.21%) at time of recruitment, and 108 patients were classified as progressors (rate of eGFR decline > -2 ml/min/1.73m²/year) throughout the study. Such outcomes represented a good reflection of what is commonly found in an average nephrology outpatients clinic.

Urine TG2 and its crosslink ϵ (γ -glutamyl) lysine were significantly elevated in CKD patients. TG2 concentration was over 35 fold higher in patients with all CKD causes (n=292) when compared to healthy volunteers (n=33). When corrected to a creatinine ratio, TG2 levels became around 60 times greater than controls. In the same manner, ϵ (γ -glutamyl) lysine was significantly elevated in CKD individuals, with a 6.7 fold rise in its excretion when compared to healthy volunteers. DKD subjects presented the highest levels of urine TG2 when compared to all other groups, with nearly double the values found in the general CKD population. This was also significantly elevated when compared to patients presenting Diabetes Mellitus (n=19) without CKD ($p < 0.0001$). The only group of patients without significantly elevated urine TG2 was ADPKD, the only group without rapidly progressive patients.

Likewise, ϵ (γ -glutamyl) lysine: creatinine was also substantially increased in all etiologies, excluding ADPKD and CIN, where a wide spread of values were observed. This could be due to a higher presence of patients at early stages of the disease in both groups and also to the prevalence of non-progressive cases. Alternatively, in ADPKD patients, this could be due to peculiarities of this disease which progression is more dependent on known risk factors such as PKD-1 gene mutation, hypertension (Schrier 2015), total kidney volume (Corradi *et al.* 2015) and urine copeptin levels (Nakajima *et al.* 2015).

While TG2: Creatinine ratio was elevated in progressive and rapidly progressive CKD, this was not reflected in terms of ϵ (γ -glutamyl) lysine excretion, where only rapid progressive patients displayed significant urine levels of the molecule. This suggests either a limitation in the types of proteins crosslinked to the ECM or that there is a need for more advanced kidney dysfunction to be translated into increased ϵ (γ -glutamyl) lysine excretion. To our knowledge, this is the first study to analyse human urine levels of both TG2 and ϵ (γ -glutamyl) lysine. Thus, no comparisons could be made with published data. An analogy could be traced with a previous study done by our group, in which the expression of TG2 and its crosslink product were significantly elevated in renal biopsies from CKD patients (Johnson *et al.* 2003). However, this study was done by immunofluorescence analysis and therefore, is not a quantitative method which could enable direct comparisons. Similar findings were also found in another work published by our group, where measurements in diabetic kidney disease patients showed tissue levels of TG2 much higher than ϵ (γ glutamyl) lysine (El Nahas *et al.* 2004). Nevertheless, such findings could also be attributed to higher affinity for the TG2 antibody rather than ϵ (γ glutamyl) lysine.

Measurement of circulating levels of TG2 provided valuable insight about how TG2 could be passing into urine. Serum levels of TG2 were five times higher than those found in the urine, suggesting a possible filtration mechanism of this molecule. The absence of correlation between urine TG2 and proteinuria also implied that increased TG2 excretion in the urine was not simply about raised proteinuria per se generating higher urine levels.

In chapter 8, we were able to measure the Matrix Metalloproteinase activity in human urine. Urine concentrations of MMP-1, 2, 9, MMP-1/TIMP-1 complex, as well as TIMPs 1, 2 and 3 were also quantified. MMP activity levels were not consistent with that reported in the kidneys where low levels were observed, mostly caused by an over expression of TIMPs (Johnson *et al.* 2002). Instead, our study showed elevated MMP activity in CKD urine, with non-progressive patients presenting over 7 times more than healthy volunteers. Progressive patients also presented significant higher urine MMP activity. However, patients presenting with rapid loss of kidney function had significant lower MMP activity and this could be used as an important tool for detecting such group of patients. The addition of the specific MMP inhibitor 1,10 phenanthroline to reactions largely implies that the proteolysis against the protein substrates occurs as a consequence of the gelatinase (MMPs 2 and 9) activity as this inhibitor presents minimal activity against serine proteases. A recent publication just in diabetic kidney disease (Altemtam *et al.* 2012) showed very similar findings, suggesting this is a robust

outcome. Thus, it seems that there is an up-regulation of MMP activity in non-progressive and stable patients, with a decrease of its levels as disease progresses.

Despite the increase in MMP activity in CKD, the quantity of MMPs 1 and 2 detected in the urine was not high. This suggests that other MMPs such as MMP-7 and MMP-13 could also be present and were not measured by ELISA. Urine MMP-1 was undetected in 94.86% of human CKD urines, whilst MMP-2 and MMP-9 were detected in approximately 88% and 95% of CKD samples respectively. As MMP-1 levels were below detection limits in urine, we hypothesised that it could be mostly bound to TIMP-1. For this reason, we performed an additional analysis of MMP-1 complexed to TIMP-1, but only 34.25% had detectable urine levels. MMP-2 corrected to a creatinine ratio was 2.4 fold higher in CKD patients when compared to healthy volunteers. Interestingly, MMP-9 urine levels were the highest among all MMPs evaluated in this study, presenting a 9 fold increased in CKD patients. This contrasted with our animal data, where high levels of MMP-1 were found and MMP-9 was hardly detectable. Also, MMP-9 levels in renal tissue are much lower than MMP-1 and 2 (Ahmed *et al.* 2012), however increased tissue levels were also found in diabetic individuals (Tashiro *et al.* 2004).

Tissue inhibitor of metalloproteinase 1 and 2 were significantly elevated in the urine of CKD patients. However, there was no difference between the urine levels of TIMP-3 in CKD and control subjects. Similar finding have been observed before. TIMP-1 levels in urine were significant higher in CKD patients (n=54) and also correlated with Tenascin levels (Horstrup *et al.* 2002).

Receiver Operating Characteristic (ROC) curve analysis was used to evaluate the accuracy of prediction of CKD progression in all biomarkers tested (table 9.2). Overall, ACR confirmed to be a valuable marker of disease progression as it presented 73.5% of accuracy in predicting the rate of annual eGFR decline. In the literature, ROC analysis of ACR ranged from 64% (Altemtam *et al.* 2012) to 71.5% (n= 1808, however, this was a retrospective study) (Methven *et al.*). Amongst all molecules evaluated by ROC curve analysis in our study, TG2/CR ratio showed the highest power of prediction. TG2/CR rate gave an impressive 86.4% accuracy in predicting CKD progression in a spot urine. This data suggests that TG2/CR ration could be a better prognostic tool than the currently used standard method (ACR). Measurement of urine TG2 was performed through a fast, reliable and non-invasive method which could easily be applied to clinical practice. Other good predictors of CKD progression were TIMP-1, which detected 75.7% of cases, and XLCR with a 73.3% prediction. All other markers were inferior

to ACR in detecting CKD progression. Combining TG2CR, ACR, TIMP1CR and XLCR as prognostic tools of CKD progression generated a remarkable 87.7% risk prediction by ROC-AUC analysis (figure 9.1).

In conclusion, our study has made novel observations on biomarkers of kidney fibrosis. This is the first to present urine measurements of TG2 and its crosslink ϵ (γ -glutamyl) lysine in a CKD cohort. The data presented in this thesis has shown significant increases of these molecules as well as TIMPs 1 and 2 and MMP activity in human urine. However, this study also has some limitations as the small number of subjects in some groups such as ADPKD and CIN. Although, the smaller proportion of these individuals mimics real findings in an average renal outpatient's clinic and in the national registry. We also acknowledge the small proportion of individuals at CKD stages 1 and 5. Once again, this is a reflexion of what is found in a routine clinical scenario. Nevertheless, our findings have potential implications for the clinical care of CKD patients as a combination of conventional (ACR) and novel biomarkers (TG2CR, TIMP-1CR and ϵ (γ -glutamyl) lysine levels) may represent a potential way of better detecting individuals which will progress from CKD to ESRD and this could enable prevention and possibly targeted therapeutic intervention.

References

- (1999). "X. The economic cost of ESRD and Medicare spending for alternative modalities of treatment." Am J Kidney Dis **34**(2 Suppl 1): S124-139.
- (2002). "K/DOQI clinical practice guidelines for chronic kidney disease: evaluation, classification, and stratification." Am J Kidney Dis **39**(2 Suppl 1): S1-266.
- (2008).
- (SLANH), L. A. S. o. N. a. H. e. (2012). SLANH Report 2012.
- Abbate, M., C. Zoja, et al. (2002). "Transforming growth factor-beta1 is up-regulated by podocytes in response to excess intraglomerular passage of proteins: a central pathway in progressive glomerulosclerosis." Am J Pathol. **161**(6): 2179-2193.
- Abdelhafiz, A. H., E. Tan, et al. (2008). "The epidemic challenge of chronic kidney disease in older patients." Postgrad Med **120**(4): 87-94.
- Adams, L. G., D. J. Polzin, et al. (1994). "Influence of dietary protein/calorie intake on renal morphology and function in cats with 5/6 nephrectomy." Lab Invest **70**(3): 347-357.
- Adamson, A., K. Ghoreschi, et al. (2013). "Tissue inhibitor of metalloproteinase 1 is preferentially expressed in Th1 and Th17 T-helper cell subsets and is a direct STAT target gene." PLoS One **8**(3): e59367.
- Adema, A. Y., M. H. de Borst, et al. (2013). "Dietary and Pharmacological Modification of Fibroblast Growth Factor-23 in Chronic Kidney Disease." J Ren Nutr.
- Adler, S. (2006). "Renal disease: environment, race, or genes?" Ethn Dis **16**(2 Suppl 2): S2-35-39.
- Aeschlimann, D., O. Kaupp, et al. (1995). "Transglutaminase-catalyzed matrix cross-linking in differentiating cartilage: identification of osteonectin as a major glutaminy substrate." J Cell Biol **129**(3): 881-892.
- Aeschlimann, D., M. Paulsson, et al. (1992). "Identification of Gln726 in nidogen as the amine acceptor in transglutaminase-catalyzed cross-linking of laminin-nidogen complexes." J Biol Chem **267**(16): 11316-11321.
- Aeschlimann, D. and V. Thomazy (2000). "Protein crosslinking in assembly and remodelling of extracellular matrices: the role of transglutaminases." Connect Tissue Res **41**(1): 1-27.
- Agarwal, R. (1993). "Creatinine clearance with cimetidine for measurement of GFR." Lancet **341**(8838): 188.
- Ahmed, A. K., A. M. El Nahas, et al. (2012). "Changes in matrix metalloproteinases and their inhibitors in kidney transplant recipients." Exp Clin Transplant **10**(4): 332-343.
- Ahmed, A. K., J. L. Haylor, et al. (2007). "Localization of matrix metalloproteinases and their inhibitors in experimental progressive kidney scarring." Kidney Int **71**(8): 755-763.
- Ahmed, A. K., N. S. Kamath, et al. (2010). "The impact of stopping inhibitors of the renin-angiotensin system in patients with advanced chronic kidney disease." Nephrol Dial Transplant **25**(12): 3977-3982.
- Ahonen, M., A. H. Baker, et al. (1998). "Adenovirus-mediated gene delivery of tissue inhibitor of metalloproteinases-3 inhibits invasion and induces apoptosis in melanoma cells." Cancer Res **58**(11): 2310-2315.
- Akalin, E., R. Dinavahi, et al. (2007). "Transplant glomerulopathy may occur in the absence of donor-specific antibody and C4d staining." Clin J Am Soc Nephrol **2**(6): 1261-1267.
- Akimov, S. S. and A. M. Belkin (2001). "Cell-surface transglutaminase promotes fibronectin assembly via interaction with the gelatin-binding domain of fibronectin: a role in TGFbeta-dependent matrix deposition." J Cell Sci **114**(Pt 16): 2989-3000.
- Almaani, N., L. Liu, et al. (2011). "Identical glycine substitution mutations in type VII collagen may underlie both dominant and recessive forms of dystrophic epidermolysis bullosa." Acta Derm Venereol **91**(3): 262-266.
- Altemtam, N., M. E. Nahas, et al. (2012). "Urinary matrix metalloproteinase activity in diabetic kidney disease: a potential marker of disease progression." Nephron Extra **2**: 219-232.
- Amour, A., C. G. Knight, et al. (2000). "The in vitro activity of ADAM-10 is inhibited by TIMP-1 and TIMP-3." FEBS Lett **473**(3): 275-279.

- Andersen, M. J. and R. Agarwal (2005). "Etiology and management of hypertension in chronic kidney disease." Med Clin North Am **89**(3): 525-547.
- Anderson, S., J. B. Halter, et al. (2009). "Prediction, progression, and outcomes of chronic kidney disease in older adults." J Am Soc Nephrol **20**(6): 1199-1209.
- Ando, R., S. Ueda, et al. (2013). "Involvement of advanced glycation end product-induced asymmetric dimethylarginine generation in endothelial dysfunction." Diab Vasc Dis Res **10**(5): 436-441.
- Andringa, G., K. Y. Lam, et al. (2004). "Tissue transglutaminase catalyzes the formation of alpha-synuclein crosslinks in Parkinson's disease." FASEB J **18**(7): 932-934.
- Antonyak, M. A., J. M. Jansen, et al. (2006). "Two isoforms of tissue transglutaminase mediate opposing cellular fates." Proc Natl Acad Sci U S A **103**(49): 18609-18614.
- Arthur, M. J. (2000). "Fibrogenesis II. Metalloproteinases and their inhibitors in liver fibrosis." Am J Physiol Gastrointest Liver Physiol **279**(2): G245-249.
- Asao, R., K. Asanuma, et al. (2012). "Relationships between levels of urinary podocalyxin, number of urinary podocytes, and histologic injury in adult patients with IgA nephropathy." Clin J Am Soc Nephrol **7**(9): 1385-1393.
- Astedt, B., C. Lindoff, et al. (1998). "Significance of the plasminogen activator inhibitor of placental type (PAI-2) in pregnancy." Semin Thromb Hemost **24**(5): 431-435.
- Avery, N. C. and A. J. Bailey (2006). "The effects of the Maillard reaction on the physical properties and cell interactions of collagen." Pathol Biol (Paris) **54**(7): 387-395.
- Avorn, J., W. C. Winkelmayr, et al. (2002). "Delayed nephrologist referral and inadequate vascular access in patients with advanced chronic kidney failure." J Clin Epidemiol **55**(7): 711-716.
- Baek, K. J., S. Kang, et al. (2001). "Phospholipase Cdelta1 is a guanine nucleotide exchanging factor for transglutaminase II (Galpha h) and promotes alpha 1B-adrenoreceptor-mediated GTP binding and intracellular calcium release." J Biol Chem **276**(8): 5591-5597.
- Baker, A. H., D. R. Edwards, et al. (2002). "Metalloproteinase inhibitors: biological actions and therapeutic opportunities." J Cell Sci **115**(Pt 19): 3719-3727.
- Baldassarre, M. E., A. Laneve, et al. (2012). "Usefulness of tissue transglutaminase type 2 antibodies in early pregnancy." Immunopharmacol Immunotoxicol **34**(6): 932-936.
- Baldwin, D., Jr., M. Prince, et al. (1980). "Regulation of insulin receptors: evidence for involvement of an endocytotic internalization pathway." Proc Natl Acad Sci U S A **77**(10): 5975-5978.
- Bao, Y. S., L. T. Song, et al. (2013). "Epidemiology and risk factors for chronic kidney disease in patients with ischaemic stroke." Eur J Clin Invest **43**(8): 829-835.
- Baricos, W. H., S. L. Cortez, et al. (1995). "ECM degradation by cultured human mesangial cells is mediated by a PA/plasmin/MMP-2 cascade." Kidney Int **47**(4): 1039-1047.
- Barri, Y. M. (2008). "Hypertension and kidney disease: a deadly connection." Curr Hypertens Rep **10**(1): 39-45.
- Barsigian, C., A. M. Stern, et al. (1991). "Tissue (type II) transglutaminase covalently incorporates itself, fibrinogen, or fibronectin into high molecular weight complexes on the extracellular surface of isolated hepatocytes. Use of 2-[(2-oxopropyl)thio]imidazolium derivatives as cellular transglutaminase inactivators." J Biol Chem **266**(33): 22501-22509.
- Baylis, C. (2012). "Nitric oxide synthase derangements and hypertension in kidney disease." Curr Opin Nephrol Hypertens **21**(1): 1-6.
- Bechtel, W., S. McGoohan, et al. (2010). "Methylation determines fibroblast activation and fibrogenesis in the kidney." Nat Med **16**(5): 544-550.
- Bello, A. K., J. Peters, et al. (2008). "Socioeconomic status and chronic kidney disease at presentation to a renal service in the United Kingdom." Clin J Am Soc Nephrol **3**(5): 1316-1323.

- Ben-Dov, I. Z., H. Galitzer, et al. (2007). "The parathyroid is a target organ for FGF23 in rats." J Clin Invest **117**(12): 4003-4008.
- Bernassola, F., M. Federici, et al. (2002). "Role of transglutaminase 2 in glucose tolerance: knockout mice studies and a putative mutation in a MODY patient." FASEB J **16**(11): 1371-1378.
- Bertini, E. and G. Pepe (2002). "Collagen type VI and related disorders: Bethlem myopathy and Ullrich scleroatonic muscular dystrophy." Eur J Paediatr Neurol **6**(4): 193-198.
- Bhavsar, N. A., L. J. Appel, et al. (2011). "Comparison of measured GFR, serum creatinine, cystatin C, and beta-trace protein to predict ESRD in African Americans with hypertensive CKD." Am J Kidney Dis **58**(6): 886-893.
- Bigg, H. F., Y. E. Shi, et al. (1997). "Specific, high affinity binding of tissue inhibitor of metalloproteinases-4 (TIMP-4) to the COOH-terminal hemopexin-like domain of human gelatinase A. TIMP-4 binds progelatinase A and the COOH-terminal domain in a similar manner to TIMP-2." J Biol Chem **272**(24): 15496-15500.
- Bode, W., C. Fernandez-Catalan, et al. (1999). "Structural properties of matrix metalloproteinases." Cell Mol Life Sci **55**(4): 639-652.
- Bolignano, D., G. Coppolino, et al. (2007). "Neutrophil gelatinase-associated lipocalin in patients with autosomal-dominant polycystic kidney disease." Am J Nephrol **27**(4): 373-378.
- Bolignano, D., V. Donato, et al. (2008). "Neutrophil gelatinase-associated lipocalin (NGAL) as a marker of kidney damage." Am J Kidney Dis **52**(3): 595-605.
- Bolignano, D., A. Lacquaniti, et al. (2009). "Neutrophil gelatinase-associated lipocalin (NGAL) and progression of chronic kidney disease." Clin J Am Soc Nephrol **4**(2): 337-344.
- Bonventre, J. V. (2008). "Kidney Injury Molecule-1 (KIM-1): a specific and sensitive biomarker of kidney injury." Scand J Clin Lab Invest Suppl **241**: 78-83.
- Boor, P. and J. Floege (2011). "Chronic kidney disease growth factors in renal fibrosis." Clin Exp Pharmacol Physiol **38**(7): 441-450.
- Bornstein, P. (2009). "Matricellular proteins: an overview." J Cell Commun Signal **3**(3-4): 163-165.
- Borth, W., V. Chang, et al. (1991). "Lipoprotein (a) is a substrate for factor XIIIa and tissue transglutaminase." J Biol Chem **266**(27): 18149-18153.
- Bourboulia, D. and W. G. Stetler-Stevenson (2010). "Matrix metalloproteinases (MMPs) and tissue inhibitors of metalloproteinases (TIMPs): Positive and negative regulators in tumor cell adhesion." Semin Cancer Biol **20**(3): 161-168.
- Bourgoignie, J. J., G. Gavellas, et al. (1994). "Effect of protein diets on the renal function of baboons (*Papio hamadryas*) with remnant kidneys: a 5-year follow-up." Am J Kidney Dis **23**(2): 199-204.
- Boutaud, A., D. B. Borza, et al. (2000). "Type IV collagen of the glomerular basement membrane. Evidence that the chain specificity of network assembly is encoded by the noncollagenous NC1 domains." J Biol Chem **275**(39): 30716-30724.
- Boyera, N., I. Galey, et al. (1998). "Effect of vitamin C and its derivatives on collagen synthesis and cross-linking by normal human fibroblasts." Int J Cosmet Sci **20**(3): 151-158.
- Brenner, B. M., M. E. Cooper, et al. (2000). "The losartan renal protection study--rationale, study design and baseline characteristics of RENAAL (Reduction of Endpoints in NIDDM with the Angiotensin II Antagonist Losartan)." J Renin Angiotensin Aldosterone Syst **1**(4): 328-335.
- Brenner, B. M., M. E. Cooper, et al. (2001). "Effects of losartan on renal and cardiovascular outcomes in patients with type 2 diabetes and nephropathy." N Engl J Med **345**(12): 861-869.
- Brew, K. and H. Nagase (2010). "The tissue inhibitors of metalloproteinases (TIMPs): an ancient family with structural and functional diversity." Biochim Biophys Acta **1803**(1): 55-71.

- Brodeur, A. C., D. A. Wirth, et al. (2007). "Type I collagen glomerulopathy: postnatal collagen deposition follows glomerular maturation." Kidney Int **71**(10): 985-993.
- Brosius, F. C., 3rd, C. E. Alpers, et al. (2009). "Mouse models of diabetic nephropathy." J Am Soc Nephrol **20**(12): 2503-2512.
- Brown, K. D. (2013). "Transglutaminase 2 and NF-kappaB: an odd couple that shapes breast cancer phenotype." Breast Cancer Res Treat **137**(2): 329-336.
- Brown, S. A. (2013). "Renal pathophysiology: lessons learned from the canine remnant kidney model." J Vet Emerg Crit Care (San Antonio) **23**(2): 115-121.
- Bungay, P. J., J. M. Potter, et al. (1984). "The inhibition of glucose-stimulated insulin secretion by primary amines. A role for transglutaminase in the secretory mechanism." Biochem J **219**(3): 819-827.
- Byrne, C., J. Nedelman, et al. (1994). "Race, socioeconomic status, and the development of end-stage renal disease." Am J Kidney Dis **23**(1): 16-22.
- Cacciamani, T., S. Virgili, et al. (2002). "Specific methylation of the CpG-rich domains in the promoter of the human tissue transglutaminase gene." Gene **297**(1-2): 103-112.
- Cai, L., J. Rubin, et al. (2010). "The origin of multiple molecular forms in urine of HNL/NGAL." Clin J Am Soc Nephrol **5**(12): 2229-2235.
- Candi, E., E. Tarcsa, et al. (1998). "A highly conserved lysine residue on the head domain of type II keratins is essential for the attachment of keratin intermediate filaments to the cornified cell envelope through isopeptide crosslinking by transglutaminases." Proc Natl Acad Sci U S A **95**(5): 2067-2072.
- Cao, L., M. Shao, et al. (2012). "Tissue transglutaminase links TGF-beta, epithelial to mesenchymal transition and a stem cell phenotype in ovarian cancer." Oncogene **31**(20): 2521-2534.
- Caron, A., R. R. Desrosiers, et al. (2005). "Ischemia-reperfusion injury stimulates gelatinase expression and activity in kidney glomeruli." Can J Physiol Pharmacol **83**(3): 287-300.
- Carracedo, J., P. Buendia, et al. (2012). "Klotho modulates the stress response in human senescent endothelial cells." Mech Ageing Dev **133**(11-12): 647-654.
- Carrero, J. J. (2010). "Gender differences in chronic kidney disease: underpinnings and therapeutic implications." Kidney Blood Press Res **33**(5): 383-392.
- Cass, A., J. Cunningham, et al. (2001). "Social disadvantage and variation in the incidence of end-stage renal disease in Australian capital cities." Aust N Z J Public Health **25**(4): 322-326.
- Catania, J. M., G. Chen, et al. (2007). "Role of matrix metalloproteinases in renal pathophysiology." Am J Physiol Renal Physiol **292**(3): F905-911.
- Caterina, J. J., S. Yamada, et al. (2000). "Inactivating mutation of the mouse tissue inhibitor of metalloproteinases-2(Timp-2) gene alters proMMP-2 activation." J Biol Chem **275**(34): 26416-26422.
- Chakraborti, S., M. Mandal, et al. (2003). "Regulation of matrix metalloproteinases: an overview." Mol Cell Biochem **253**(1-2): 269-285.
- Chakraborty, S., S. Kaur, et al. (2012). "The multifaceted roles of neutrophil gelatinase associated lipocalin (NGAL) in inflammation and cancer." Biochim Biophys Acta **1826**(1): 129-169.
- Chen, J. S. and K. Mehta (1999). "Tissue transglutaminase: an enzyme with a split personality." Int J Biochem Cell Biol **31**(8): 817-836.
- Chen, S., S. W. Hong, et al. (2001). "The key role of the transforming growth factor-beta system in the pathogenesis of diabetic nephropathy." Ren Fail **23**(3-4): 471-481.
- Chen, W., H. Wang, et al. (2009). "Prevalence and risk factors associated with chronic kidney disease in an adult population from southern China." Nephrol Dial Transplant **24**(4): 1205-1212.
- Chiocca, E. A., P. J. Davies, et al. (1988). "The molecular basis of retinoic acid action. Transcriptional regulation of tissue transglutaminase gene expression in macrophages." J Biol Chem **263**(23): 11584-11589.

- Chou, C. Y., A. J. Streets, et al. (2011). "A crucial sequence for transglutaminase type 2 extracellular trafficking in renal tubular epithelial cells lies in its N-terminal beta-sandwich domain." *J Biol Chem* **286**(31): 27825-27835.
- Chue, C. D., J. N. Townsend, et al. (2013). "Cardiovascular effects of sevelamer in stage 3 CKD." *J Am Soc Nephrol* **24**(5): 842-852.
- Cignarelli, M., O. Lamacchia, et al. (2008). "Cigarette smoking and kidney dysfunction in diabetes mellitus." *J Nephrol* **21**(2): 180-189.
- Clark, I. M., T. E. Swingle, et al. (2008). "The regulation of matrix metalloproteinases and their inhibitors." *Int J Biochem Cell Biol* **40**(6-7): 1362-1378.
- Clarke, D. D., A. Neidle, et al. (1957). "Metabolic activity of protein amide groups." *Arch Biochem Biophys* **71**(1): 277-279.
- Coimbra, T. M., J. Carvalho, et al. (1996). "Transforming growth factor-beta production during the development of renal fibrosis in rats with subtotal renal ablation." *Int J Exp Pathol* **77**(4): 167-173.
- Collighan, R. J. and M. Griffin (2009). "Transglutaminase 2 cross-linking of matrix proteins: biological significance and medical applications." *Amino Acids* **36**(4): 659-670.
- Collighan, R. J. and M. Griffin (2009). "Transglutaminase 2 cross-linking of matrix proteins: biological significance and medical applications." *Amino Acids* **36**(4): 659-670.
- Coresh, J., B. C. Astor, et al. (2003). "Prevalence of chronic kidney disease and decreased kidney function in the adult US population: Third National Health and Nutrition Examination Survey." *Am J Kidney Dis* **41**(1): 1-12.
- Cowland, J. B. and N. Borregaard (1997). "Molecular characterization and pattern of tissue expression of the gene for neutrophil gelatinase-associated lipocalin from humans." *Genomics* **45**(1): 17-23.
- Cozzolino, M., G. Gentile, et al. (2013). "Blood Pressure, Proteinuria, and Phosphate as Risk Factors for Progressive Kidney Disease: A Hypothesis." *Am J Kidney Dis*.
- Cravedi, P. and G. Remuzzi (2013). "Pathophysiology of proteinuria and its value as an outcome measure in CKD." *Br J Clin Pharmacol*.
- Cruz, M. C., C. Andrade, et al. (2011). "Quality of life in patients with chronic kidney disease." *Clinics (Sao Paulo)* **66**(6): 991-995.
- Datta, S., M. A. Antonyak, et al. (2007). "GTP-binding-defective forms of tissue transglutaminase trigger cell death." *Biochemistry* **46**(51): 14819-14829.
- Davey, A., M. F. Elias, et al. (2013). "Decline in renal functioning is associated with longitudinal decline in global cognitive functioning, abstract reasoning and verbal memory." *Nephrol Dial Transplant* **28**(7): 1810-1819.
- De Broe, M. E. (2012). "Chinese herbs nephropathy and Balkan endemic nephropathy: toward a single entity, aristolochic acid nephropathy." *Kidney Int* **81**(6): 513-515.
- De Muro, P., R. Faedda, et al. (2004). "Urinary transforming growth factor-beta 1 in various types of nephropathy." *Pharmacol Res* **49**(3): 293-298.
- De Vivo, G. and V. Gentile (2008). "Transglutaminase-Catalyzed Post-Translational Modifications of Proteins in the Nervous System and their Possible Involvement in Neurodegenerative Diseases." *CNS Neurol Disord Drug Targets* **7**(4): 370-375.
- de Zeeuw, D. (2004). "Should albuminuria be a therapeutic target in patients with hypertension and diabetes?" *Am J Hypertens* **17**(11 Pt 2): 11S-15S; quiz A12-14.
- de Zeeuw, D., G. Remuzzi, et al. (2004). "Albuminuria, a therapeutic target for cardiovascular protection in type 2 diabetic patients with nephropathy." *Circulation* **110**(8): 921-927.
- de Zeeuw, D., G. Remuzzi, et al. (2004). "Proteinuria, a target for renoprotection in patients with type 2 diabetic nephropathy: lessons from RENAAL." *Kidney Int* **65**(6): 2309-2320.
- Delanaye, P., E. Cavalier, et al. (2008). "Reproducibility of GFR measured by chromium-51-EDTA and iohexol." *Nephrol Dial Transplant* **23**(12): 4077-4078; author reply 4078.
- Devarajan, P. (2007). "Emerging biomarkers of acute kidney injury." *Contrib Nephrol* **156**: 203-212.

- Devarajan, P. (2008). "Neutrophil gelatinase-associated lipocalin (NGAL): a new marker of kidney disease." Scand J Clin Lab Invest Suppl **241**: 89-94.
- Dhanaraj, V., Q. Z. Ye, et al. (1996). "X-ray structure of a hydroxamate inhibitor complex of stromelysin catalytic domain and its comparison with members of the zinc metalloproteinase superfamily." Structure **4**(4): 375-386.
- Dharnidharka, V. R., C. Kwon, et al. (2002). "Serum cystatin C is superior to serum creatinine as a marker of kidney function: a meta-analysis." Am J Kidney Dis **40**(2): 221-226.
- Di Giacomo, G., A. Lentini, et al. (2009). "In vivo evaluation of type 2 transglutaminase contribution to the metastasis formation in melanoma." Amino Acids **36**(4): 717-724.
- Dieterich, W., T. Ehnis, et al. (1997). "Identification of tissue transglutaminase as the autoantigen of celiac disease." Nat Med **3**(7): 797-801.
- Ding, H., Y. He, et al. (2007). "Urinary neutrophil gelatinase-associated lipocalin (NGAL) is an early biomarker for renal tubulointerstitial injury in IgA nephropathy." Clin Immunol **123**(2): 227-234.
- Dobashi, K., B. Ghosh, et al. (2000). "Kidney ischemia-reperfusion: modulation of antioxidant defenses." Mol Cell Biochem **205**(1-2): 1-11.
- Donadio, C. (2010). "Serum and urinary markers of early impairment of GFR in chronic kidney disease patients: diagnostic accuracy of urinary beta-trace protein." Am J Physiol Renal Physiol **299**(6): F1407-1423.
- Douthwaite, J. A., T. S. Johnson, et al. (1999). "Effects of transforming growth factor-beta1 on renal extracellular matrix components and their regulating proteins." J Am Soc Nephrol **10**(10): 2109-2119.
- Dressler, G. R. (2008). "Epigenetics, development, and the kidney." J Am Soc Nephrol **19**(11): 2060-2067.
- Duan, S. B., G. L. Liu, et al. (2013). "Urinary KIM-1, IL-18 and Cys-c as early predictive biomarkers in gadolinium-based contrast-induced nephropathy in the elderly patients." Clin Nephrol **80**(11): 349-354.
- Dupuis, M., A. Levy, et al. (2004). "Functional coupling of rat myometrial alpha 1-adrenergic receptors to Gh alpha/tissue transglutaminase 2 during pregnancy." J Biol Chem **279**(18): 19257-19263.
- Duymelinck, C., J. T. Deng, et al. (1998). "Inhibition of the matrix metalloproteinase system in a rat model of chronic cyclosporine nephropathy." Kidney Int **54**(3): 804-818.
- Eddy, A. A. (2000). "Molecular basis of renal fibrosis." Pediatr Nephrol **15**(3-4): 290-301.
- Eddy, A. A. (2009). "Serine proteases, inhibitors and receptors in renal fibrosis." Thromb Haemost **101**(4): 656-664.
- Egeblad, M. and Z. Werb (2002). "New functions for the matrix metalloproteinases in cancer progression." Nat Rev Cancer **2**(3): 161-174.
- Eikmans, M., D. H. Ijpelaar, et al. (2004). "The use of extracellular matrix probes and extracellular matrix-related probes for assessing diagnosis and prognosis in renal diseases." Curr Opin Nephrol Hypertens **13**(6): 641-647.
- el Nahas, A. M. (1995). "Pathways to renal fibrosis." Exp Nephrol **3**(2): 71-75.
- El Nahas, A. M., H. Abo-Zenah, et al. (2004). "Elevated epsilon-(gamma-glutamyl)lysine in human diabetic nephropathy results from increased expression and cellular release of tissue transglutaminase." Nephron Clin Pract **97**(3): c108-117.
- El Nahas, A. M., Barsoum R., Dirks JH, Remuzzi G. (2005). Kidney Diseases in the Developing World and Ethnic Minorities. New York, Taylor and Francis.
- el Nahas, A. M. and G. A. Coles (1997). "Progressive renal failure." J R Coll Physicians Lond **31**(1): 27-31.
- El Nahas, M. (2005). "The global challenge of chronic kidney disease." Kidney Int **68**(6): 2918-2929.
- Erickson, K. F., J. Lea, et al. (2013). "Interaction between GFR and risk factors for morbidity and mortality in African Americans with CKD." Clin J Am Soc Nephrol **8**(1): 75-81.

- Eriksen, B. O. and O. C. Ingebretsen (2006). "The progression of chronic kidney disease: a 10-year population-based study of the effects of gender and age." *Kidney Int* **69**(2): 375-382.
- Ermolli, M., M. Schumacher, et al. (2003). "Differential expression of MMP-2/MMP-9 and potential benefit of an MMP inhibitor in experimental acute kidney allograft rejection." *Transpl Immunol* **11**(2): 137-145.
- Esposito, C. and I. Caputo (2005). "Mammalian transglutaminases." *FEBS Journal* **272**(3): 615-631.
- Esposito, C. and I. Caputo (2005). "Mammalian transglutaminases. Identification of substrates as a key to physiological function and physiopathological relevance." *FEBS J* **272**(3): 615-631.
- Esposito, C., I. Caputo, et al. (2005). "Tissue transglutaminase and celiac disease." *Prog Exp Tumor Res* **38**: 158-173.
- Esposito, C., M. Marra, et al. (2003). "Ubiquitination of tissue transglutaminase is modulated by interferon alpha in human lung cancer cells." *Biochem J* **370**(Pt 1): 205-212.
- Eyre, D. R. and J. J. Wu (2005). Collagen cross-links. *Collagen: Primer in Structure, Processing and Assembly*. J. Brinckmann, H. Notbohm and P. K. Muller. Berlin, Springer-Verlag Berlin. **247**: 207-229.
- Facchiano, A. and F. Facchiano (2009). "Transglutaminases and their substrates in biology and human diseases: 50 years of growing." *Amino Acids* **36**(4): 599-614.
- Facchiano, F., A. Facchiano, et al. (2006). "The role of transglutaminase-2 and its substrates in human diseases." *Front Biosci* **11**: 1758-1773.
- Fagerudd, J. A., P. H. Groop, et al. (1997). "Urinary excretion of TGF-beta 1, PDGF-BB and fibronectin in insulin-dependent diabetes mellitus patients." *Kidney Int Suppl* **63**: S195-197.
- Falasca, L., V. Iadevaia, et al. (2005). "Transglutaminase type II is a key element in the regulation of the anti-inflammatory response elicited by apoptotic cell engulfment." *J Immunol* **174**(11): 7330-7340.
- Fassett, R. G., S. K. Venuthurupalli, et al. (2011). "Biomarkers in chronic kidney disease: a review." *Kidney Int* **80**(8): 806-821.
- Faul, C., A. P. Amaral, et al. (2011). "FGF23 induces left ventricular hypertrophy." *J Clin Invest* **121**(11): 4393-4408.
- Faulkner, J. L., L. M. Szykalski, et al. (2005). "Origin of interstitial fibroblasts in an accelerated model of angiotensin II-induced renal fibrosis." *Am J Pathol* **167**(5): 1193-1205.
- Fesus, L. and M. Piacentini (2002). "Transglutaminase 2: an enigmatic enzyme with diverse functions." *Trends Biochem Sci* **27**(10): 534-539.
- Fesus, L. and Z. Szondy (2005). "Transglutaminase 2 in the balance of cell death and survival." *FEBS Lett* **579**(15): 3297-3302.
- Filler, G., R. A. Berard, et al. (2013). "ACE levels may affect cystatin C measurements." *Clin Biochem*.
- Filler, G., A. Bokenkamp, et al. (2005). "Cystatin C as a marker of GFR--history, indications, and future research." *Clin Biochem* **38**(1): 1-8.
- Filler, G., A. Yasin, et al. (2013). "Methods of assessing renal function." *Pediatr Nephrol*.
- Fingleton, B., T. Vargo-Gogola, et al. (2001). "Matrilysin [MMP-7] expression selects for cells with reduced sensitivity to apoptosis." *Neoplasia* **3**(6): 459-468.
- Fisher, M., R. A. Jones, et al. (2009). "Modulation of tissue transglutaminase in tubular epithelial cells alters extracellular matrix levels: a potential mechanism of tissue scarring." *Matrix Biol* **28**(1): 20-31.
- Fleckenstein, B., S. W. Qiao, et al. (2004). "Molecular characterization of covalent complexes between tissue transglutaminase and gliadin peptides." *J Biol Chem* **279**(17): 17607-17616.

- Fliser, D., B. Kollerits, et al. (2007). "Fibroblast growth factor 23 (FGF23) predicts progression of chronic kidney disease: the Mild to Moderate Kidney Disease (MMKD) Study." J Am Soc Nephrol **18**(9): 2600-2608.
- Floege, J., Johnson R.J., Feehally J., Ed. (2013). Comprehensive Clinical Nephrology.
- Flower, D. R., A. C. North, et al. (1991). "Mouse oncogene protein 24p3 is a member of the lipocalin protein family." Biochem Biophys Res Commun **180**(1): 69-74.
- Fored, C. M., E. Ejerblad, et al. (2003). "Socio-economic status and chronic renal failure: a population-based case-control study in Sweden." Nephrol Dial Transplant **18**(1): 82-88.
- Foster, M. C., S. J. Hwang, et al. (2007). "Cross-classification of microalbuminuria and reduced glomerular filtration rate: associations between cardiovascular disease risk factors and clinical outcomes." Arch Intern Med **167**(13): 1386-1392.
- Fowlkes, J. L., K. M. Thrailkill, et al. (1995). "Matrix metalloproteinases as insulin-like growth factor binding protein-degrading proteinases." Prog Growth Factor Res **6**(2-4): 255-263.
- Fox, C. S., M. G. Larson, et al. (2005). "Glycemic status and development of kidney disease: the Framingham Heart Study." Diabetes Care **28**(10): 2436-2440.
- Fraj, B. M. (2011). "Activation of tissue transglutaminase by removal of carboxyl-terminal peptides." J Cell Biochem **112**(11): 3469-3481.
- Frantz, C., K. M. Stewart, et al. (2010). "The extracellular matrix at a glance." J Cell Sci **123**(Pt 24): 4195-4200.
- Freedman, B. I., J. M. Soucie, et al. (1997). "Family history of end-stage renal disease among incident dialysis patients." J Am Soc Nephrol **8**(12): 1942-1945.
- Frennby, B. and G. Sterner (2002). "Contrast media as markers of GFR." Eur Radiol **12**(2): 475-484.
- Friedl, A., S. P. Stoesz, et al. (1999). "Neutrophil gelatinase-associated lipocalin in normal and neoplastic human tissues. Cell type-specific pattern of expression." Histochem J **31**(7): 433-441.
- Gajko-Galicka, A. (2002). "Mutations in type I collagen genes resulting in osteogenesis imperfecta in humans." Acta Biochim Pol **49**(2): 433-441.
- Galis, Z. S. and J. J. Khatri (2002). "Matrix metalloproteinases in vascular remodeling and atherogenesis: the good, the bad, and the ugly." Circ Res **90**(3): 251-262.
- Garg, A. X., P. G. Blake, et al. (2001). "Association between renal insufficiency and malnutrition in older adults: results from the NHANES III." Kidney Int **60**(5): 1867-1874.
- Gasson, J. C., D. W. Golde, et al. (1985). "Molecular characterization and expression of the gene encoding human erythroid-potentiating activity." Nature **315**(6022): 768-771.
- Gava, A. L., F. P. Freitas, et al. (2012). "Effects of 5/6 nephrectomy on renal function and blood pressure in mice." Int J Physiol Pathophysiol Pharmacol **4**(3): 167-173.
- Gelse, K., E. Poschl, et al. (2003). "Collagens--structure, function, and biosynthesis." Adv Drug Deliv Rev **55**(12): 1531-1546.
- Gharagozlian, S., K. Svennevig, et al. (2009). "Matrix metalloproteinases in subjects with type 1 diabetes." BMC Clin Pathol **9**: 7.
- Ghosh, A. K. and D. E. Vaughan (2012). "PAI-1 in tissue fibrosis." J Cell Physiol **227**(2): 493-507.
- Gomez, D. E., D. F. Alonso, et al. (1997). "Tissue inhibitors of metalloproteinases: structure, regulation and biological functions." Eur J Cell Biol **74**(2): 111-122.
- Gomis-Ruth, F. X., U. Gohlke, et al. (1996). "The helping hand of collagenase-3 (MMP-13): 2.7 Å crystal structure of its C-terminal haemopexin-like domain." J Mol Biol **264**(3): 556-566.
- Gordon, M. K. and R. A. Hahn (2010). "Collagens." Cell Tissue Res **339**(1): 247-257.
- Gorres, K. L. and R. T. Raines (2010). "Prolyl 4-hydroxylase." Crit Rev Biochem Mol Biol **45**(2): 106-124.

- Goumenos, D. S., B. Kavar, et al. (2009). "Early histological changes in the kidney of people with morbid obesity." Nephrol Dial Transplant **24**(12): 3732-3738.
- Grantham, J. J. (1996). "The etiology, pathogenesis, and treatment of autosomal dominant polycystic kidney disease: recent advances." Am J Kidney Dis **28**(6): 788-803.
- Grenard, P., S. Bresson-Hadni, et al. (2001). "Transglutaminase-mediated cross-linking is involved in the stabilization of extracellular matrix in human liver fibrosis." J Hepatol **35**(3): 367-375.
- Gretz N, W. R., Strauch M, Ed. (1993). Experimental and Genetic Rat Models of Chronic Renal Failure, Karger pp1-28.
- Griffin, K. A., H. Kramer, et al. (2008). "Adverse renal consequences of obesity." Am J Physiol Renal Physiol **294**(4): F685-696.
- Gundemir, S., G. Colak, et al. (2012). "Transglutaminase 2: a molecular Swiss army knife." Biochim Biophys Acta **1823**(2): 406-419.
- Gutierrez, O. M., J. L. Januzzi, et al. (2009). "Fibroblast growth factor 23 and left ventricular hypertrophy in chronic kidney disease." Circulation **119**(19): 2545-2552.
- Gutierrez, O. M., M. Mannstadt, et al. (2008). "Fibroblast growth factor 23 and mortality among patients undergoing hemodialysis." N Engl J Med **359**(6): 584-592.
- Ha, H. and H. B. Lee (2003). "Reactive oxygen species and matrix remodeling in diabetic kidney." J Am Soc Nephrol **14**(8 Suppl 3): S246-249.
- Haas, T. L., S. J. Davis, et al. (1998). "Three-dimensional type I collagen lattices induce coordinate expression of matrix metalloproteinases MT1-MMP and MMP-2 in microvascular endothelial cells." J Biol Chem **273**(6): 3604-3610.
- Hallan, S. I., E. Ritz, et al. (2009). "Combining GFR and albuminuria to classify CKD improves prediction of ESRD." J Am Soc Nephrol **20**(5): 1069-1077.
- Hamel, B. C., G. Pals, et al. (1998). "Ehlers-Danlos syndrome and type III collagen abnormalities: a variable clinical spectrum." Clin Genet **53**(6): 440-446.
- Hamze, A. B., S. Wei, et al. (2007). "Constraining specificity in the N-domain of tissue inhibitor of metalloproteinases-1; gelatinase-selective inhibitors." Protein Sci **16**(9): 1905-1913.
- Han, B.-G., J.-W. Cho, et al. (2010). "Crystal structure of human transglutaminase 2 in complex with adenosine triphosphate." International Journal of Biological Macromolecules **47**(2): 190-195.
- Han, W. K., V. Bailly, et al. (2002). "Kidney Injury Molecule-1 (KIM-1): a novel biomarker for human renal proximal tubule injury." Kidney Int **62**(1): 237-244.
- Hanai, K., T. Babazono, et al. (2009). "Asymmetric dimethylarginine is closely associated with the development and progression of nephropathy in patients with type 2 diabetes." Nephrol Dial Transplant **24**(6): 1884-1888.
- Handsley, M. M. and D. R. Edwards (2005). "Metalloproteinases and their inhibitors in tumor angiogenesis." Int J Cancer **115**(6): 849-860.
- Hara, M., K. Yamagata, et al. (2012). "Urinary podocalyxin is an early marker for podocyte injury in patients with diabetes: establishment of a highly sensitive ELISA to detect urinary podocalyxin." Diabetologia **55**(11): 2913-2919.
- Haroon, Z. A., J. M. Hettasch, et al. (1999). "Tissue transglutaminase is expressed, active, and directly involved in rat dermal wound healing and angiogenesis." FASEB J **13**(13): 1787-1795.
- Haroon, Z. A., T. S. Lai, et al. (1999). "Tissue transglutaminase is expressed as a host response to tumor invasion and inhibits tumor growth." Lab Invest **79**(12): 1679-1686.
- Haroun, M. K., B. G. Jaar, et al. (2003). "Risk factors for chronic kidney disease: a prospective study of 23,534 men and women in Washington County, Maryland." J Am Soc Nephrol **14**(11): 2934-2941.
- Harrison, C. A., C. M. Layton, et al. (2007). "Transglutaminase inhibitors induce hyperproliferation and parakeratosis in tissue-engineered skin." Br J Dermatol **156**(2): 247-257.

- Hasegawa, G., M. Suwa, et al. (2003). "A novel function of tissue-type transglutaminase: protein disulphide isomerase." *Biochem J* **373**(Pt 3): 793-803.
- He, J., Y. Xu, et al. (2013). "Role of the endothelial-to-mesenchymal transition in renal fibrosis of chronic kidney disease." *Clin Exp Nephrol* **17**(4): 488-497.
- He, R., J. Shen, et al. (2013). "High cystatin C levels predict severe retinopathy in type 2 diabetes patients." *Eur J Epidemiol*.
- Hemdahl, A. L., A. Gabrielsen, et al. (2006). "Expression of neutrophil gelatinase-associated lipocalin in atherosclerosis and myocardial infarction." *Arterioscler Thromb Vasc Biol* **26**(1): 136-142.
- Herbach, N., I. Schairer, et al. (2009). "Diabetic kidney lesions of GIPRdn transgenic mice: podocyte hypertrophy and thickening of the GBM precede glomerular hypertrophy and glomerulosclerosis." *Am J Physiol Renal Physiol* **296**(4): F819-829.
- Herget-Rosenthal, S., F. Pietruck, et al. (2005). "Serum cystatin C--a superior marker of rapidly reduced glomerular filtration after uninephrectomy in kidney donors compared to creatinine." *Clin Nephrol* **64**(1): 41-46.
- Hewitson, T. D. (2012). "Fibrosis in the kidney: is a problem shared a problem halved?" *Fibrogenesis Tissue Repair* **5 Suppl 1**: S14.
- Hibbs, M. S., J. R. Hoidal, et al. (1987). "Expression of a metalloproteinase that degrades native type V collagen and denatured collagens by cultured human alveolar macrophages." *J Clin Invest* **80**(6): 1644-1650.
- Hilbrands, L. B., J. F. Wetzels, et al. (1993). "Creatinine clearance with cimetidine for measurement of GFR." *Lancet* **341**(8838): 187-188.
- Hodgkins, K. S. and H. W. Schnaper (2012). "Tubulointerstitial injury and the progression of chronic kidney disease." *Pediatr Nephrol* **27**(6): 901-909.
- Hoegy, S. E., H. R. Oh, et al. (2001). "Tissue inhibitor of metalloproteinases-2 (TIMP-2) suppresses TKR-growth factor signaling independent of metalloproteinase inhibition." *J Biol Chem* **276**(5): 3203-3214.
- Honkanen, E., A. M. Teppo, et al. (1997). "Urinary transforming growth factor-beta 1 in membranous glomerulonephritis." *Nephrol Dial Transplant* **12**(12): 2562-2568.
- Horstrup, J. H., M. Gehrmann, et al. (2002). "Elevation of serum and urine levels of TIMP-1 and tenascin in patients with renal disease." *Nephrol Dial Transplant* **17**(6): 1005-1013.
- Horton, W. A., D. Campbell, et al. (1989). "Type II collagen screening in the human chondrodysplasias." *Am J Med Genet* **34**(4): 579-583.
- Hossain, P., B. Kavar, et al. (2007). "Obesity and diabetes in the developing world--a growing challenge." *N Engl J Med* **356**(3): 213-215.
- Hosseini, F., F. Kasraei, et al. (2009). "High prevalence of chronic kidney disease in Iran: a large population-based study." *BMC Public Health* **9**: 44.
- Hostetter, T. H., J. L. Olson, et al. (2001). "Hyperfiltration in remnant nephrons: a potentially adverse response to renal ablation." *J Am Soc Nephrol* **12**(6): 1315-1325.
- Houston, J., K. Smith, et al. (2013). "Associations of dietary phosphorus intake, urinary phosphate excretion, and fibroblast growth factor 23 with vascular stiffness in chronic kidney disease." *J Ren Nutr* **23**(1): 12-20.
- Hsieh, P. F., S. F. Liu, et al. (2012). "The role of IL-7 in renal proximal tubule epithelial cells fibrosis." *Mol Immunol* **50**(1-2): 74-82.
- Hsu, C. C., W. H. Kao, et al. (2005). "Apolipoprotein E and progression of chronic kidney disease." *Jama* **293**(23): 2892-2899.
- Hsu, H. J. and M. S. Wu (2009). "Fibroblast growth factor 23: a possible cause of left ventricular hypertrophy in hemodialysis patients." *Am J Med Sci* **337**(2): 116-122.
- Huang, L., J. L. Haylor, et al. (2010). "Do changes in transglutaminase activity alter latent transforming growth factor beta activation in experimental diabetic nephropathy?" *Nephrol Dial Transplant* **25**(12): 3897-3910.
- Huang, L., J. L. Haylor, et al. (2009). "Transglutaminase inhibition ameliorates experimental diabetic nephropathy." *Kidney Int* **76**(4): 383-394.

- Hudkins, K. L., W. Pichaiwong, et al. (2010). "BTBR Ob/Ob mutant mice model progressive diabetic nephropathy." J Am Soc Nephrol **21**(9): 1533-1542.
- Hudson, B. G., S. T. Reeders, et al. (1993). "Type IV collagen: structure, gene organization, and role in human diseases. Molecular basis of Goodpasture and Alport syndromes and diffuse leiomyomatosis." J Biol Chem **268**(35): 26033-26036.
- Huxley, R., A. Neil, et al. (2002). "Unravelling the fetal origins hypothesis: is there really an inverse association between birthweight and subsequent blood pressure?" Lancet **360**(9334): 659-665.
- Iismaa, S. E., B. M. Mearns, et al. (2009). "Transglutaminases and disease: lessons from genetically engineered mouse models and inherited disorders." Physiol Rev **89**(3): 991-1023.
- Iismaa, S. E., M. J. Wu, et al. (2000). "GTP binding and signaling by Gh/transglutaminase II involves distinct residues in a unique GTP-binding pocket." J Biol Chem **275**(24): 18259-18265.
- Im, M. J. and R. M. Graham (1990). "A novel guanine nucleotide-binding protein coupled to the alpha 1-adrenergic receptor. I. Identification by photolabeling or membrane and ternary complex preparation." J Biol Chem **265**(31): 18944-18951.
- Imai, E., M. Horio, et al. (2009). "Prevalence of chronic kidney disease in the Japanese general population." Clin Exp Nephrol **13**(6): 621-630.
- Inenaga, T., E. Nishida, et al. (2002). "Renal function tests on diabetes-induced and non-induced APA hamsters." Exp Anim **51**(5): 437-445.
- Inker, L. A., C. H. Schmid, et al. (2012). "Estimating glomerular filtration rate from serum creatinine and cystatin C." N Engl J Med **367**(1): 20-29.
- Inker, L. A., C. Wyatt, et al. (2012). "Performance of creatinine and cystatin C GFR estimating equations in an HIV-positive population on antiretrovirals." J Acquir Immune Defic Syndr **61**(3): 302-309.
- Isakova, T., O. M. Gutierrez, et al. (2011). "Pilot study of dietary phosphorus restriction and phosphorus binders to target fibroblast growth factor 23 in patients with chronic kidney disease." Nephrol Dial Transplant **26**(2): 584-591.
- Isakova, T., H. Xie, et al. (2011). "Fibroblast growth factor 23 and risks of mortality and end-stage renal disease in patients with chronic kidney disease." Jama **305**(23): 2432-2439.
- Ito, S. (2012). "Cardiorenal connection in chronic kidney disease." Clin Exp Nephrol **16**(1): 8-16.
- Ixkes, M. C., M. G. Koopman, et al. (1997). "Cimetidine improves GFR-estimation by the Cockcroft and Gault formula." Clin Nephrol **47**(4): 229-236.
- Iyer, R. P., N. L. Patterson, et al. (2012). "The history of matrix metalloproteinases: milestones, myths, and misperceptions." Am J Physiol Heart Circ Physiol **303**(8): H919-930.
- J Feehaly, J. F., R J Johnson (2007). Comprehensive Clinical Nephrology, Elsevier.
- Jackson, G. C., D. Marcus-Soekarman, et al. (2010). "Type IX collagen gene mutations can result in multiple epiphyseal dysplasia that is associated with osteochondritis dissecans and a mild myopathy." Am J Med Genet A **152A**(4): 863-869.
- Jang, G. Y., J. H. Jeon, et al. (2010). "Transglutaminase 2 suppresses apoptosis by modulating caspase 3 and NF-kappaB activity in hypoxic tumor cells." Oncogene **29**(3): 356-367.
- Jarvelainen, H., A. Sainio, et al. (2009). "Extracellular matrix molecules: potential targets in pharmacotherapy." Pharmacol Rev **61**(2): 198-223.
- Jeitner, T. M., W. R. Matson, et al. (2008). "Increased levels of gamma-glutamylamines in Huntington disease CSF." J Neurochem **106**(1): 37-44.
- Jeitner, T. M., N. A. Muma, et al. (2009). "Transglutaminase activation in neurodegenerative diseases." Future Neurol **4**(4): 449-467.

- Jensen, P. H., E. S. Sorensen, et al. (1995). "Residues in the synuclein consensus motif of the alpha-synuclein fragment, NAC, participate in transglutaminase-catalysed cross-linking to Alzheimer-disease amyloid beta A4 peptide." Biochem J **310 (Pt 1)**: 91-94.
- Jha, V., A. Y. Wang, et al. (2012). "The impact of CKD identification in large countries: the burden of illness." Nephrol Dial Transplant **27 Suppl 3**: iii32-38.
- Jimbo, R., F. Kawakami-Mori, et al. (2013). "Fibroblast growth factor 23 accelerates phosphate-induced vascular calcification in the absence of Klotho deficiency." Kidney Int.
- John, G. B., C. Y. Cheng, et al. (2011). "Role of Klotho in aging, phosphate metabolism, and CKD." Am J Kidney Dis **58(1)**: 127-134.
- Johnson, T. S., A. F. El-Koraie, et al. (2003). "Tissue transglutaminase and the progression of human renal scarring." J Am Soc Nephrol **14(8)**: 2052-2062.
- Johnson, T. S., M. Fisher, et al. (2007). "Transglutaminase inhibition reduces fibrosis and preserves function in experimental chronic kidney disease." J Am Soc Nephrol **18(12)**: 3078-3088.
- Johnson, T. S., M. Griffin, et al. (1997). "The role of transglutaminase in the rat subtotal nephrectomy model of renal fibrosis." J Clin Invest **99(12)**: 2950-2960.
- Johnson, T. S., J. L. Haylor, et al. (2002). "Matrix metalloproteinases and their inhibitors in experimental renal scarring." Exp Nephrol **10(3)**: 182-195.
- Johnson, T. S., C. I. Scholfield, et al. (1998). "Induction of tissue transglutaminase by dexamethasone: its correlation to receptor number and transglutaminase-mediated cell death in a series of malignant hamster fibrosarcomas." Biochem J **331 (Pt 1)**: 105-112.
- Jones, C., P. Roderick, et al. (2006). "Decline in kidney function before and after nephrology referral and the effect on survival in moderate to advanced chronic kidney disease." Nephrol Dial Transplant **21(8)**: 2133-2143.
- Jones, R. A., P. Kotsakis, et al. (2006). "Matrix changes induced by transglutaminase 2 lead to inhibition of angiogenesis and tumor growth." Cell Death Differ **13(9)**: 1442-1453.
- Joo, K. W., S. Kim, et al. (2013). "Dipeptidyl peptidase IV inhibitor attenuates kidney injury in rat remnant kidney." BMC Nephrol **14**: 98.
- Joosten, S. A., C. van Kooten, et al. (2004). "The pathobiology of chronic allograft nephropathy: immune-mediated damage and accelerated aging." Kidney Int **65(5)**: 1556-1559.
- Junaid, A., M. E. Rosenberg, et al. (1997). "Interaction of angiotensin II and TGF-beta 1 in the rat remnant kidney." J Am Soc Nephrol **8(11)**: 1732-1738.
- Juppner, H. (2011). "Phosphate and FGF-23." Kidney Int Suppl(121): S24-27.
- Kachra, Z., E. Beaulieu, et al. (1999). "Expression of matrix metalloproteinases and their inhibitors in human brain tumors." Clin Exp Metastasis **17(7)**: 555-566.
- Kadler, K. E., C. Baldock, et al. (2007). "Collagens at a glance." J Cell Sci **120(Pt 12)**: 1955-1958.
- Kagan, H. M. (2000). "Intra- and extracellular enzymes of collagen biosynthesis as biological and chemical targets in the control of fibrosis." Acta Trop **77(1)**: 147-152.
- Kahlem, P., H. Green, et al. (1998). "Transglutaminase action imitates Huntington's disease: selective polymerization of Huntingtin containing expanded polyglutamine." Mol Cell **1(4)**: 595-601.
- Kaneko, T., A. Shimizu, et al. (2012). "Role of matrix metalloproteinase-2 in recovery after tubular damage in acute kidney injury in mice." Nephron Exp Nephrol **122(1-2)**: 23-35.
- Kang, S. K., K. S. Yi, et al. (2004). "Alpha1B-adrenoceptor signaling and cell motility: GTPase function of Gh/transglutaminase 2 inhibits cell migration through interaction with cytoplasmic tail of integrin alpha subunits." J Biol Chem **279(35)**: 36593-36600.
- Kanno, K., H. Kawachi, et al. (2003). "Urinary sediment podocalyxin in children with glomerular diseases." Nephron Clin Pract **95(3)**: c91-99.
- Kashtan, C. E. (1993). "Alport Syndrome and Thin Basement Membrane Nephropathy."

- Kawar, B., A. K. Bello, et al. (2009). "High prevalence of microalbuminuria in the overweight and obese population: data from a UK population screening programme." Nephron Clin Pract **112**(3): c205-212.
- Kawasaki, Y. (2011). "Mechanism of onset and exacerbation of chronic glomerulonephritis and its treatment." Pediatr Int **53**(6): 795-806.
- Kazmi, W. H., G. T. Obrador, et al. (2004). "Late nephrology referral and mortality among patients with end-stage renal disease: a propensity score analysis." Nephrol Dial Transplant **19**(7): 1808-1814.
- KDIGO, K. D. I. G. O. (2012). "KDIGO 2012 Clinical Practice Guideline for the Evaluation and Management of Chronic Kidney Disease." Official Journal of the International Society of Nephrology **Volume 3**(Issue 1): 1-163.
- Kendrick, J., A. K. Cheung, et al. (2011). "FGF-23 associates with death, cardiovascular events, and initiation of chronic dialysis." J Am Soc Nephrol **22**(10): 1913-1922.
- Kim, K. H., Y. Kim, et al. (2003). "A re-evaluation of the renal ablation model of progressive renal disease in rats." J Nephrol **16**(2): 196-202.
- Kim, S. H., J. Turnbull, et al. (2011). "Extracellular matrix and cell signalling: the dynamic cooperation of integrin, proteoglycan and growth factor receptor." J Endocrinol **209**(2): 139-151.
- Kim, S. I., H. J. Na, et al. (2012). "Autophagy promotes intracellular degradation of type I collagen induced by transforming growth factor (TGF)-beta1." J Biol Chem **287**(15): 11677-11688.
- Kiraly, R., E. Csoz, et al. (2009). "Functional significance of five noncanonical Ca²⁺-binding sites of human transglutaminase 2 characterized by site-directed mutagenesis." FEBS J **276**(23): 7083-7096.
- Kiraly, R., M. Demyeny, et al. (2011). "Protein transamidation by transglutaminase 2 in cells: a disputed Ca²⁺-dependent action of a multifunctional protein." FEBS J **278**(24): 4717-4739.
- Kirkpantur, A., M. Balci, et al. (2011). "Serum fibroblast growth factor-23 (FGF-23) levels are independently associated with left ventricular mass and myocardial performance index in maintenance haemodialysis patients." Nephrol Dial Transplant **26**(4): 1346-1354.
- Kjeldsen, L., A. H. Johnsen, et al. (1993). "Isolation and primary structure of NGAL, a novel protein associated with human neutrophil gelatinase." J Biol Chem **268**(14): 10425-10432.
- Klag, M. J., P. K. Whelton, et al. (1996). "Blood pressure and end-stage renal disease in men." N Engl J Med **334**(1): 13-18.
- Klahr, S. and J. Morrissey (2003). "Progression of chronic renal disease." Am J Kidney Dis **41**(3 Suppl 1): S3-7.
- Klein, T. and R. Bischoff (2011). "Physiology and pathophysiology of matrix metalloproteinases." Amino Acids **41**(2): 271-290.
- Knowlden, J., J. Martin, et al. (1995). "Metalloproteinase generation by human glomerular epithelial cells." Kidney Int. **47**(6): 1682-1689.
- Knowlden, J., J. Martin, et al. (1995). "Metalloproteinase generation by human glomerular epithelial cells." Kidney Int **47**(6): 1682-1689.
- Komaba, H. and M. Fukagawa (2009). "FGF23: a key player in mineral and bone disorder in CKD." Nefrologia **29**(5): 392-396.
- Kong, L. L., H. Wu, et al. (2013). "Advances in murine models of diabetic nephropathy." J Diabetes Res **2013**: 797548.
- Kontinen, Y. T., M. Ainola, et al. (1999). "Analysis of 16 different matrix metalloproteinases (MMP-1 to MMP-20) in the synovial membrane: different profiles in trauma and rheumatoid arthritis." Ann Rheum Dis **58**(11): 691-697.
- Kopple, J. D., R. Berg, et al. (1989). "Nutritional status of patients with different levels of chronic renal insufficiency. Modification of Diet in Renal Disease (MDRD) Study Group." Kidney Int Suppl **27**: S184-194.

- Kotsakis, P. and M. Griffin (2007). "Tissue transglutaminase in tumour progression: friend or foe?" Amino Acids **33**(2): 373-384.
- Kotsakis, P., Z. Wang, et al. (2011). "The role of tissue transglutaminase (TG2) in regulating the tumour progression of the mouse colon carcinoma CT26." Amino Acids **41**(4): 909-921.
- Kovesdy, C. P. and L. D. Quarles (2013). "Fibroblast growth factor-23: what we know, what we don't know, and what we need to know." Nephrol Dial Transplant.
- Kovesdy, C. P. and L. D. Quarles (2013). "The Role of Fibroblast Growth Factor-23 in Cardiorenal Syndrome." Nephron Clin Pract **123**(3-4): 194-201.
- Krajisnik, T., P. Bjorklund, et al. (2007). "Fibroblast growth factor-23 regulates parathyroid hormone and 1alpha-hydroxylase expression in cultured bovine parathyroid cells." J Endocrinol **195**(1): 125-131.
- Kramer, B. K. and F. Schweda (1997). "Ramipril in non-diabetic renal failure (REIN study). Ramipril Efficiency in Nephropathy study." Lancet **350**(9079): 736; author reply 736-737.
- Kramer, H. (2006). "Obesity and chronic kidney disease." Contrib Nephrol **151**: 1-18.
- Kren, S. and T. H. Hostetter (1999). "The course of the remnant kidney model in mice." Kidney Int **56**(1): 333-337.
- Kuhlmann MK, K. A., Wittwer W, Horl WH (2007). "Malnutrition in Chronic Renal Failure " Nephrol Dial Transplant **22**(Suppl 3): iii3-iii9.
- Kuivaniemi, H., G. Tromp, et al. (1991). "Mutations in collagen genes: causes of rare and some common diseases in humans." FASEB J **5**(7): 2052-2060.
- Kumar, S. and K. Mehta (2013). "Tissue transglutaminase, inflammation, and cancer: how intimate is the relationship?" Amino Acids **44**(1): 81-88.
- Kunugi, S., A. Shimizu, et al. (2011). "Inhibition of matrix metalloproteinases reduces ischemia-reperfusion acute kidney injury." Lab Invest **91**(2): 170-180.
- Lai, T. S., A. Bielawska, et al. (1997). "Sphingosylphosphocholine reduces the calcium ion requirement for activating tissue transglutaminase." J Biol Chem **272**(26): 16295-16300.
- Lai, T. S., A. Hausladen, et al. (2001). "Calcium regulates S-nitrosylation, denitrosylation, and activity of tissue transglutaminase." Biochemistry **40**(16): 4904-4910.
- Lai, T. S., Y. Liu, et al. (2007). "Identification of two GTP-independent alternatively spliced forms of tissue transglutaminase in human leukocytes, vascular smooth muscle, and endothelial cells." FASEB J **21**(14): 4131-4143.
- Lai, Y. D., X. D. Ma, et al. (2010). "[Modulation of histone acetylation and induction of apoptosis in SMMC-7721 cells by phenylhexyl isothiocyanate]." Zhonghua Zhong Liu Za Zhi **32**(11): 804-807.
- Lam, S., R. N. van der Geest, et al. (2004). "Secretion of collagen type IV by human renal fibroblasts is increased by high glucose via a TGF-beta-independent pathway." Nephrol Dial Transplant **19**(7): 1694-1701.
- Lambert, E., E. Dasse, et al. (2004). "TIMPs as multifacial proteins." Crit Rev Oncol Hematol **49**(3): 187-198.
- Lasagni, L. and P. Romagnani (2010). "Glomerular epithelial stem cells: the good, the bad, and the ugly." J Am Soc Nephrol **21**(10): 1612-1619.
- Lauhio, A., T. Sorsa, et al. (2008). "Urinary matrix metalloproteinase -8, -9, -14 and their regulators (TRY-1, TRY-2, TATI) in patients with diabetic nephropathy." Ann Med **40**(4): 312-320.
- Lee, K. H., N. Lee, et al. (2003). "Calreticulin inhibits the MEK1,2-ERK1,2 pathway in alpha 1-adrenergic receptor/Gh-stimulated hypertrophy of neonatal rat cardiomyocytes." J Steroid Biochem Mol Biol **84**(1): 101-107.
- Legrand, C., M. Polette, et al. (2001). "uPA/Plasmin System-Mediated MMP-9 Activation Is Implicated in Bronchial Epithelial Cell Migration." Experimental Cell Research **264**(2): 326-336.

- Lemaitre, V. and J. D'Armiento (2006). "Matrix metalloproteinases in development and disease." Birth Defects Res C Embryo Today **78**(1): 1-10.
- Lemley, K. V. (2007). "An introduction to biomarkers: applications to chronic kidney disease." Pediatr Nephrol **22**(11): 1849-1859.
- Lenz, O., S. J. Elliot, et al. (2000). "Matrix metalloproteinases in renal development and disease." J Am Soc Nephrol **11**(3): 574-581.
- Lenzen, S. (2008). "The mechanisms of alloxan- and streptozotocin-induced diabetes." Diabetologia **51**(2): 216-226.
- Levin, A. (2001). "Identification of patients and risk factors in chronic kidney disease--evaluating risk factors and therapeutic strategies." Nephrol Dial Transplant **16 Suppl 7**: 57-60.
- Lewis, E. J., L. G. Hunsicker, et al. (2001). "Renoprotective effect of the angiotensin-receptor antagonist irbesartan in patients with nephropathy due to type 2 diabetes." N Engl J Med **345**(12): 851-860.
- Li, Z., M. P. Clarke, et al. (2005). "TIMP3 mutation in Sorsby's fundus dystrophy: molecular insights." Expert Rev Mol Med **7**(24): 1-15.
- Liabeuf, S., H. Okazaki, et al. (2013). "Vascular calcification in chronic kidney disease: are biomarkers useful for probing the pathobiology and the health risks of this process in the clinical scenario?" Nephrol Dial Transplant.
- Lim, A. I., S. C. Tang, et al. (2013). "Kidney injury molecule-1: more than just an injury marker of tubular epithelial cells?" J Cell Physiol **228**(5): 917-924.
- Lim, R., N. Ahmed, et al. (2007). "Neutrophil gelatinase-associated lipocalin (NGAL) an early-screening biomarker for ovarian cancer: NGAL is associated with epidermal growth factor-induced epithelio-mesenchymal transition." Int J Cancer **120**(11): 2426-2434.
- Lindsay, M. A., P. J. Bungay, et al. (1990). "Transglutaminase involvement in the secretion of insulin from electroporated rat islets of Langerhans." Biosci Rep **10**(6): 557-561.
- Ling, W., N. Zhaohui, et al. (2008). "Urinary IL-18 and NGAL as early predictive biomarkers in contrast-induced nephropathy after coronary angiography." Nephron Clin Pract **108**(3): c176-181.
- Liu, C. K., A. Lyass, et al. (2013). "Chronic Kidney Disease Defined by Cystatin C Predicts Mobility Disability and Changes in Gait Speed: The Framingham Offspring Study." J Gerontol A Biol Sci Med Sci.
- Liu, J., D. Wang, et al. (2013). "H NMR-based metabolomic analysis of serum and urine in a nonhuman primate model of diabetic nephropathy." Mol Biosyst.
- Liu, Q., J. Ryon, et al. (1997). "Uterocalin: a mouse acute phase protein expressed in the uterus around birth." Mol Reprod Dev **46**(4): 507-514.
- Liu, S., R. A. Cerione, et al. (2002). "Structural basis for the guanine nucleotide-binding activity of tissue transglutaminase and its regulation of transamidation activity." Proc Natl Acad Sci U S A **99**(5): 2743-2747.
- Liu, S., W. Tang, et al. (2006). "Fibroblast growth factor 23 is a counter-regulatory phosphaturic hormone for vitamin D." J Am Soc Nephrol **17**(5): 1305-1315.
- Liu, T., A. E. Tee, et al. (2007). "Activation of tissue transglutaminase transcription by histone deacetylase inhibition as a therapeutic approach for Myc oncogenesis." Proc Natl Acad Sci U S A **104**(47): 18682-18687.
- Liu, Y. (2006). "Renal fibrosis: new insights into the pathogenesis and therapeutics." Kidney Int **69**(2): 213-217.
- Liu, Y. (2010). "New insights into epithelial-mesenchymal transition in kidney fibrosis." J Am Soc Nephrol **21**(2): 212-222.
- Liu, Y. (2011). "Cellular and molecular mechanisms of renal fibrosis." Nat Rev Nephrol **7**(12): 684-696.
- Liu, Y., W. Guo, et al. (2013). "Urinary Interleukin 18 for Detection of Acute Kidney Injury: A Meta-analysis." Am J Kidney Dis.

- Locatelli, F., B. Canaud, et al. (2003). "Oxidative stress in end-stage renal disease: an emerging threat to patient outcome." Nephrol Dial Transplant **18**(7): 1272-1280.
- Loechel, F., J. W. Fox, et al. (2000). "ADAM 12-S Cleaves IGFBP-3 and IGFBP-5 and Is Inhibited by TIMP-3." Biochemical and Biophysical Research Communications **278**(3): 511-515.
- Lopes, J., E. Adiguzel, et al. (2013). "Type VIII collagen mediates vessel wall remodeling after arterial injury and fibrous cap formation in atherosclerosis." Am J Pathol **182**(6): 2241-2253.
- Lopez-Hernandez, F. J. and J. M. Lopez-Novoa (2012). "Role of TGF-beta in chronic kidney disease: an integration of tubular, glomerular and vascular effects." Cell Tissue Res **347**(1): 141-154.
- Lorand, L. and R. M. Graham (2003). "Transglutaminases: crosslinking enzymes with pleiotropic functions." Nat Rev Mol Cell Biol **4**(2): 140-156.
- Lovelock, J. D., A. H. Baker, et al. (2005). "Heterogeneous effects of tissue inhibitors of matrix metalloproteinases on cardiac fibroblasts." Am J Physiol Heart Circ Physiol **288**(2): H461-468.
- Lu, S. and P. J. Davies (1997). "Regulation of the expression of the tissue transglutaminase gene by DNA methylation." Proc Natl Acad Sci U S A **94**(9): 4692-4697.
- Lugon, J. R. (2009). "End-stage renal disease and chronic kidney disease in Brazil." Ethn Dis **19**(1 Suppl 1): S1-7-9.
- Lukasz, A., J. Beneke, et al. (2013). "Serum neutrophil gelatinase-associated lipocalin (NGAL) in patients with Shiga toxin mediated haemolytic uraemic syndrome (STEC-HUS)." Thromb Haemost **111**(2).
- Lutz, J., K. Risch, et al. (2006). "Angiotensin type 1 and type 2 receptor blockade in chronic allograft nephropathy." Kidney Int **70**(6): 1080-1088.
- Madero, M., M. J. Sarnak, et al. (2006). "Serum cystatin C as a marker of glomerular filtration rate." Curr Opin Nephrol Hypertens **15**(6): 610-616.
- Maheswaran, R., N. Payne, et al. (2003). "Socioeconomic deprivation, travel distance, and renal replacement therapy in the Trent Region, United Kingdom 2000: an ecological study." J Epidemiol Community Health **57**(7): 523-524.
- Malorni, W., M. G. Farrace, et al. (2009). "The adenine nucleotide translocator 1 acts as a type 2 transglutaminase substrate: implications for mitochondrial-dependent apoptosis." Cell Death Differ **16**(11): 1480-1492.
- Malyszko, J., J. S. Malyszko, et al. (2009). "Neutrophil gelatinase-associated lipocalin is a new and sensitive marker of kidney function in chronic kidney disease patients and renal allograft recipients." Transplant Proc **41**(1): 158-161.
- Mangala, L. S., B. Arun, et al. (2005). "Tissue transglutaminase-induced alterations in extracellular matrix inhibit tumor invasion." Mol Cancer **4**: 33.
- Mangala, L. S. and K. Mehta (2005). "Tissue transglutaminase (TG2) in cancer biology." Prog Exp Tumor Res **38**: 125-138.
- Manicone, A. M. and J. K. McGuire (2008). "Matrix metalloproteinases as modulators of inflammation." Semin Cell Dev Biol **19**(1): 34-41.
- Mariani, P., F. Carsughi, et al. (2000). "Ligand-induced conformational changes in tissue transglutaminase: Monte Carlo analysis of small-angle scattering data." Biophys J **78**(6): 3240-3251.
- Martin, A., G. Romito, et al. (2006). "Transglutaminase-catalyzed reactions responsible for the pathogenesis of celiac disease and neurodegenerative diseases: from basic biochemistry to clinic." Curr Med Chem **13**(16): 1895-1902.
- Martin, J., J. Knowlden, et al. (1994). "Identification and independent regulation of human mesangial cell metalloproteinases." Kidney Int **46**(3): 877-885.
- Martin, J., J. Knowlden, et al. (1994). "Identification and independent regulation of human mesangial cell metalloproteinases." Kidney Int **46**(3): 877-885.

- Martins, D., N. Tareen, et al. (2006). "The association of poverty with the prevalence of albuminuria: data from the Third National Health and Nutrition Examination Survey (NHANES III)." Am J Kidney Dis **47**(6): 965-971.
- Massova, I., L. P. Kotra, et al. (1998). "Matrix metalloproteinases: structures, evolution, and diversification." FASEB J **12**(12): 1075-1095.
- Mastroberardino, P. G., M. G. Farrace, et al. (2006). "'Tissue' transglutaminase contributes to the formation of disulphide bridges in proteins of mitochondrial respiratory complexes." Biochim Biophys Acta **1757**(9-10): 1357-1365.
- Mastroberardino, P. G., C. Iannicola, et al. (2002). "'Tissue' transglutaminase ablation reduces neuronal death and prolongs survival in a mouse model of Huntington's disease." Cell Death Differ **9**(9): 873-880.
- Matrisian, L. M. (1990). "Metalloproteinases and their inhibitors in matrix remodeling." Trends Genet **6**(4): 121-125.
- McClellan, W. M. and W. D. Flanders (2003). "Risk factors for progressive chronic kidney disease." J Am Soc Nephrol **14**(7 Suppl 2): S65-70.
- McCullough, K., P. Sharma, et al. (2012). "Measuring the population burden of chronic kidney disease: a systematic literature review of the estimated prevalence of impaired kidney function." Nephrol Dial Transplant **27**(5): 1812-1821.
- McLennan, S. V., D. K. Yue, et al. (1998). "Effect of glucose on matrix metalloproteinase activity in mesangial cells." Nephron **79**(3): 293-298.
- Mehta, K. (1994). "High levels of transglutaminase expression in doxorubicin-resistant human breast carcinoma cells." Int J Cancer **58**(3): 400-406.
- Mehta, K., J. Fok, et al. (2004). "Prognostic significance of tissue transglutaminase in drug resistant and metastatic breast cancer." Clin Cancer Res **10**(23): 8068-8076.
- Mehul, B., S. Bawumia, et al. (1995). "Cross-linking of galectin 3, a galactose-binding protein of mammalian cells, by tissue-type transglutaminase." FEBS Lett **360**(2): 160-164.
- Meng, Q., V. Malinovskii, et al. (1999). "Residue 2 of TIMP-1 is a major determinant of affinity and specificity for matrix metalloproteinases but effects of substitutions do not correlate with those of the corresponding P1' residue of substrate." J Biol Chem **274**(15): 10184-10189.
- Meran, S. and R. Steadman (2011). "Fibroblasts and myofibroblasts in renal fibrosis." Int J Exp Pathol **92**(3): 158-167.
- Merkin, S. S. (2008). "Exploring the pathways between socioeconomic status and ESRD." Am J Kidney Dis **51**(4): 539-541.
- Middleton, R. J., R. N. Foley, et al. (2006). "The unrecognized prevalence of chronic kidney disease in diabetes." Nephrol Dial Transplant **21**(1): 88-92.
- Mishra, S., G. Melino, et al. (2007). "Transglutaminase 2 kinase activity facilitates protein kinase A-induced phosphorylation of retinoblastoma protein." J Biol Chem **282**(25): 18108-18115.
- Mishra, S. and L. J. Murphy (2004). "Tissue transglutaminase has intrinsic kinase activity: identification of transglutaminase 2 as an insulin-like growth factor-binding protein-3 kinase." J Biol Chem **279**(23): 23863-23868.
- Mishra, S. and L. J. Murphy (2006). "The p53 oncoprotein is a substrate for tissue transglutaminase kinase activity." Biochem Biophys Res Commun **339**(2): 726-730.
- Mishra, S. and L. J. Murphy (2006-B). "Phosphorylation of transglutaminase 2 by PKA at Ser216 creates 14-3-3 binding sites." Biochem Biophys Res Commun **347**(4): 1166-1170.
- Mishra, S., A. Saleh, et al. (2006-A). "Phosphorylation of histones by tissue transglutaminase." J Biol Chem **281**(9): 5532-5538.
- Miyauchi, K., Y. Takiyama, et al. (2009). "Upregulated IL-18 expression in type 2 diabetic subjects with nephropathy: TGF-beta1 enhanced IL-18 expression in human renal proximal tubular epithelial cells." Diabetes Res Clin Pract **83**(2): 190-199.

- Miyazaki, M., T. Nishino, et al. (2003). "Regulation of renal extracellular matrix metabolism." Contrib Nephrol **139**: 141-155.
- Mochizuki, S., M. Shimoda, et al. (2004). "ADAM28 is activated by MMP-7 (matrilysin-1) and cleaves insulin-like growth factor binding protein-3." Biochem Biophys Res Commun **315**(1): 79-84.
- Mohan, R., W. B. Rinehart, et al. (1998). "Gelatinase B/lacZ transgenic mice, a model for mapping gelatinase B expression during developmental and injury-related tissue remodeling." J Biol Chem **273**(40): 25903-25914.
- Molven, A., U. Rishaug, et al. (2002). "Hunting for a hypoglycemia gene: severe neonatal hypoglycemia in a consanguineous family." Am J Med Genet **113**(1): 40-46.
- Monea, S., K. Lehti, et al. (2002). "Plasmin activates pro-matrix metalloproteinase-2 with a membrane-type 1 matrix metalloproteinase-dependent mechanism." J Cell Physiol **192**(2): 160-170.
- Moore, C. S. and S. J. Crocker (2012). "An alternate perspective on the roles of TIMPs and MMPs in pathology." Am J Pathol **180**(1): 12-16.
- Morales, J. M. (2005). "Immunosuppressive treatment and progression of histologic lesions in kidney allografts." Kidney Int Suppl(99): S124-130.
- Morgunova, E., A. Tuuttila, et al. (2002). "Structural insight into the complex formation of latent matrix metalloproteinase 2 with tissue inhibitor of metalloproteinase 2." Proc Natl Acad Sci U S A **99**(11): 7414-7419.
- Muma, N. A. (2007). "Transglutaminase is linked to neurodegenerative diseases." J Neuropathol Exp Neurol **66**(4): 258-263.
- Muntner, P., J. He, et al. (2005). "Traditional and nontraditional risk factors predict coronary heart disease in chronic kidney disease: results from the atherosclerosis risk in communities study." J Am Soc Nephrol **16**(2): 529-538.
- Muntner, P., S. E. Judd, et al. (2013). "Cardiovascular Risk Factors in CKD Associate with Both ESRD and Mortality." J Am Soc Nephrol.
- Murphy, G., A. Houbrechts, et al. (1991). "The N-terminal domain of tissue inhibitor of metalloproteinases retains metalloproteinase inhibitory activity." Biochemistry **30**(33): 8097-8102.
- Murphy, G. and H. Nagase (2008). "Progress in matrix metalloproteinase research." Mol Aspects Med **29**(5): 290-308.
- Murphy, G., J. J. Reynolds, et al. (1982). "Partial purification of collagenase and gelatinase from human polymorphonuclear leucocytes. Analysis of their actions on soluble and insoluble collagens." Biochem J **203**(1): 209-221.
- Murthy, S. N., S. Iismaa, et al. (2002). "Conserved tryptophan in the core domain of transglutaminase is essential for catalytic activity." Proc Natl Acad Sci U S A **99**(5): 2738-2742.
- Murthy, S. N., J. H. Wilson, et al. (1998). "Cross-linking sites of the human tau protein, probed by reactions with human transglutaminase." J Neurochem **71**(6): 2607-2614.
- Murthy, S. N., J. H. Wilson, et al. (2000). "Transglutaminase-catalyzed crosslinking of the Aalpha and gamma constituent chains in fibrinogen." Proc Natl Acad Sci U S A **97**(1): 44-48.
- Mussap, M., M. Dalla Vestra, et al. (2002). "Cystatin C is a more sensitive marker than creatinine for the estimation of GFR in type 2 diabetic patients." Kidney Int **61**(4): 1453-1461.
- Myllyla, R., K. Majamaa, et al. (1984). "Ascorbate is consumed stoichiometrically in the uncoupled reactions catalyzed by prolyl 4-hydroxylase and lysyl hydroxylase." J Biol Chem **259**(9): 5403-5405.
- Nagase, H. and J. F. Woessner, Jr. (1999). "Matrix metalloproteinases." J Biol Chem **274**(31): 21491-21494.
- Nagy, L., M. Saydak, et al. (1996). "Identification and characterization of a versatile retinoid response element (retinoic acid receptor response element-retinoid X receptor

- response element) in the mouse tissue transglutaminase gene promoter." J Biol Chem **271**(8): 4355-4365.
- Nahas, A. M. E. (2000). Mechanisms and Clinical Management of Chronic Renal Failure, Oxford University Press.
- Nakaoka, H., D. M. Perez, et al. (1994). "Gh: a GTP-binding protein with transglutaminase activity and receptor signaling function." Science **264**(5165): 1593-1596.
- Nankivell, B. J., C. A. Fenton-Lee, et al. (2001). "Effect of histological damage on long-term kidney transplant outcome." Transplantation **71**(4): 515-523.
- Nath, K. A. (1998). "The tubulointerstitium in progressive renal disease." Kidney International **54**(3): 992-994.
- Nefrologia, S. B. d. (2011). Censo de dialise 2011 SBN. Sao Paulo.
- Nesheim, M. (2003). "Thrombin and fibrinolysis." Chest **124**(3 Suppl): 33S-39S.
- Nestor Schor, H. A. (2004). Nefrologia. Sao Paulo, Manole.
- Neugarten, J. and L. Golestaneh (2013). "Gender and the Prevalence and Progression of Renal Disease." Advances in Chronic Kidney Disease **20**(5): 390-395.
- Newman, D. J., H. Thakkar, et al. (1994). "Serum cystatin C: a replacement for creatinine as a biochemical marker of GFR." Kidney Int Suppl **47**: S20-21.
- Nickolas, T. L., J. Barasch, et al. (2008). "Biomarkers in acute and chronic kidney disease." Curr Opin Nephrol Hypertens **17**(2): 127-132.
- Norman, J. T., L. Gatti, et al. (1995). "Matrix metalloproteinases and tissue inhibitor of matrix metalloproteinases expression by tubular epithelia and interstitial fibroblasts in the normal kidney and in fibrosis." Exp Nephrol **3**(2): 88-89.
- Norris, K. C. and L. Y. Agodoa (2005). "Unraveling the racial disparities associated with kidney disease." Kidney Int **68**(3): 914-924.
- Nurminskaya, M. V. and A. M. Belkin (2012). "Cellular functions of tissue transglutaminase." Int Rev Cell Mol Biol **294**: 1-97.
- Oberg, B. P., E. McMenamin, et al. (2004). "Increased prevalence of oxidant stress and inflammation in patients with moderate to severe chronic kidney disease." Kidney Int **65**(3): 1009-1016.
- Obermuller, N., N. Morente, et al. (2001). "A possible role for metalloproteinases in renal cyst development." Am J Physiol Renal Physiol **280**(3): F540-550.
- Oh, J., R. Takahashi, et al. (2001). "The membrane-anchored MMP inhibitor RECK is a key regulator of extracellular matrix integrity and angiogenesis." Cell **107**(6): 789-800.
- Oikonen, M., M. Wendelin-Saarenhovi, et al. (2012). "Tissue inhibitor of matrix metalloproteinases 4 (TIMP4) in a population of young adults: relations to cardiovascular risk markers and carotid artery intima-media thickness. The Cardiovascular Risk in Young Finns Study." Scand J Clin Lab Invest **72**(7): 540-546.
- Okuda, S., L. R. Languino, et al. (1990). "Elevated expression of transforming growth factor-beta and proteoglycan production in experimental glomerulonephritis. Possible role in expansion of the mesangial extracellular matrix." J Clin Invest **86**(2): 453-462.
- Olauson, H. and T. E. Larsson (2013). "FGF23 and Klotho in chronic kidney disease." Curr Opin Nephrol Hypertens **22**(4): 397-404.
- Oliveira, M. B., J. E. Romao, Jr., et al. (2005). "End-stage renal disease in Brazil: epidemiology, prevention, and treatment." Kidney Int Suppl(97): S82-86.
- Oliveira, R. B., A. L. Cancela, et al. (2010). "Early control of PTH and FGF23 in normophosphatemic CKD patients: a new target in CKD-MBD therapy?" Clin J Am Soc Nephrol **5**(2): 286-291.
- Oliverio, S., A. Amendola, et al. (1997). "Tissue transglutaminase-dependent posttranslational modification of the retinoblastoma gene product in promonocytic cells undergoing apoptosis." Mol Cell Biol **17**(10): 6040-6048.
- Olsen, K. C., R. E. Sapinoro, et al. (2011). "Transglutaminase 2 and Its Role in Pulmonary Fibrosis." American Journal of Respiratory and Critical Care Medicine **184**(6): 699-707.

- Olson, T. M., S. Hirohata, et al. (1998). "Cloning of the Human Tissue Inhibitor of Metalloproteinase-4 Gene (TIMP4) and Localization of the TIMP4 and Timp4 Genes to Human Chromosome 3p25 and Mouse Chromosome 6, Respectively." Genomics **51**(1): 148-151.
- Orth, S. R. (2000). "Smoking--a risk factor for progression of renal disease." Kidney Blood Press Res **23**(3-5): 202-204.
- Orth, S. R. (2004). "Effects of smoking on systemic and intrarenal hemodynamics: influence on renal function." J Am Soc Nephrol **15 Suppl 1**: S58-63.
- Orth, S. R. and S. I. Hallan (2008). "Smoking: a risk factor for progression of chronic kidney disease and for cardiovascular morbidity and mortality in renal patients--absence of evidence or evidence of absence?" Clin J Am Soc Nephrol **3**(1): 226-236.
- Orth, S. R., E. Ritz, et al. (1997). "The renal risks of smoking." Kidney Int **51**(6): 1669-1677.
- Osenkowski, P., M. Toth, et al. (2004). "Processing, shedding, and endocytosis of membrane type 1-matrix metalloproteinase (MT1-MMP)." J Cell Physiol **200**(1): 2-10.
- Othman, M., B. Kawar, et al. (2009). "Influence of obesity on progression of non-diabetic chronic kidney disease: a retrospective cohort study." Nephron Clin Pract **113**(1): c16-23.
- Ozden, F., C. Saygin, et al. (2013). "Expression of MMP-1, MMP-9 and TIMP-2 in prostate carcinoma and their influence on prognosis and survival." J Cancer Res Clin Oncol **139**(8): 1373-1382.
- Page-McCaw, A., A. J. Ewald, et al. (2007). "Matrix metalloproteinases and the regulation of tissue remodelling." Nat Rev Mol Cell Biol **8**(3): 221-233.
- Palmer, S., M. Vecchio, et al. (2013). "Prevalence of depression in chronic kidney disease: systematic review and meta-analysis of observational studies." Kidney Int **84**(1): 179-191.
- Parikh, C. R., A. Jani, et al. (2004). "Urinary interleukin-18 is a marker of human acute tubular necrosis." Am J Kidney Dis **43**(3): 405-414.
- Park, E. S., J. H. Won, et al. (1998). "Phospholipase C-delta1 and oxytocin receptor signalling: evidence of its role as an effector." Biochem J **331 (Pt 1)**: 283-289.
- Parving, H. H., B. M. Brenner, et al. (2012). "Cardiorenal end points in a trial of aliskiren for type 2 diabetes." N Engl J Med **367**(23): 2204-2213.
- Patari, A., C. Forsblom, et al. (2003). "Nephropathy in diabetic nephropathy of type 1 diabetes." Diabetes **52**(12): 2969-2974.
- Pavik, I., P. Jaeger, et al. (2013). "Secreted Klotho and FGF23 in chronic kidney disease Stage 1 to 5: a sequence suggested from a cross-sectional study." Nephrol Dial Transplant **28**(2): 352-359.
- Payne, R. B. (1993). "Creatinine clearance with cimetidine for measurement of GFR." Lancet **341**(8838): 187.
- Peng, X., Y. Zhang, et al. (1999). "Interaction of tissue transglutaminase with nuclear transport protein importin-alpha3." FEBS Lett **446**(1): 35-39.
- Perico, N., I. Codreanu, et al. (2005). "Prevention of progression and remission/regression strategies for chronic renal diseases: can we do better now than five years ago?" Kidney Int Suppl(98): S21-24.
- Peters, H. P., F. Waanders, et al. (2011). "High urinary excretion of kidney injury molecule-1 is an independent predictor of end-stage renal disease in patients with IgA nephropathy." Nephrol Dial Transplant **26**(11): 3581-3588.
- Peterson, J. C., S. Adler, et al. (1995). "Blood pressure control, proteinuria, and the progression of renal disease. The Modification of Diet in Renal Disease Study." Ann Intern Med **123**(10): 754-762.
- Piecha, G., A. Wiecek, et al. (2012). "Epidemiology and optimal management in patients with renal artery stenosis." J Nephrol **25**(6): 872-878.
- Pietschmann, P., U. Foger-Samwald, et al. (2013). "The role of cathepsins in osteoimmunology." Crit Rev Eukaryot Gene Expr **23**(1): 11-26.

- Pinkas, D. M., P. Strop, et al. (2007). "Transglutaminase 2 undergoes a large conformational change upon activation." *PLoS Biol* **5**(12): e327.
- Piredda, L., M. G. Farrace, et al. (1999). "Identification of 'tissue' transglutaminase binding proteins in neural cells committed to apoptosis." *FASEB J* **13**(2): 355-364.
- Platt, R., M. H. Roscoe, et al. (1952). "Experimental renal failure." *Clin Sci (Lond)* **11**(3): 217-231.
- Pope, F. M. and A. C. Nicholls (1987). "Molecular abnormalities of collagen in human disease." *Arch Dis Child* **62**(5): 523-528.
- Prockop, D. J. and K. I. Kivirikko (1995). "Collagens: molecular biology, diseases, and potentials for therapy." *Annu Rev Biochem* **64**: 403-434.
- Qi, J. H., Q. Ebrahim, et al. (2003). "A novel function for tissue inhibitor of metalloproteinases-3 (TIMP3): inhibition of angiogenesis by blockage of VEGF binding to VEGF receptor-2." *Nat Med* **9**(4): 407-415.
- Quarles, L. D. (2012). "Role of FGF23 in vitamin D and phosphate metabolism: implications in chronic kidney disease." *Exp Cell Res* **318**(9): 1040-1048.
- Ran, L. Y., H. N. Su, et al. (2013). "Structural and mechanistic insights into collagen degradation by a bacterial collagenolytic serine protease in the subtilisin family." *Mol Microbiol*.
- Rasmussen, L. K., E. S. Sorensen, et al. (1994). "Identification of glutamine and lysine residues in Alzheimer amyloid beta A4 peptide responsible for transglutaminase-catalysed homopolymerization and cross-linking to alpha 2M receptor." *FEBS Lett* **338**(2): 161-166.
- Rawal, N., R. Rajpurohit, et al. (1995). "Structural specificity of substrate for S-adenosylmethionine:protein arginine N-methyltransferases." *Biochim Biophys Acta* **1248**(1): 11-18.
- Registry, E.-E. (2012). ERA-EDTA Annual Report 2010. *Academic Medical Center, Department of Medical Informatics*. Amsterdam, The Netherlands, 2012.
- Registry, U. R. (2012). The Renal Association UK Renal Registry. *The fifteen annual report*. Bristol, UK.
- Remacle, A., K. McCarthy, et al. (2000). "High levels of TIMP-2 correlate with adverse prognosis in breast cancer." *Int J Cancer* **89**(2): 118-121.
- Remuzzi, G., A. Benigni, et al. (2006). "Mechanisms of progression and regression of renal lesions of chronic nephropathies and diabetes." *J Clin Invest* **116**(2): 288-296.
- Remuzzi, G. and T. Bertani (1998). "Pathophysiology of progressive nephropathies." *N Engl J Med* **339**(20): 1448-1456.
- Reponen, P., C. Sahlberg, et al. (1994). "High expression of 92-kD type IV collagenase (gelatinase B) in the osteoclast lineage during mouse development." *J Cell Biol* **124**(6): 1091-1102.
- Report, A. R. (2012). The 35th Annual ANZDATA Report 2012. Adelaide, South Australia, ANZDATA Registry.
- Rerolle, J. P., A. Hertig, et al. (2000). "Plasminogen activator inhibitor type 1 is a potential target in renal fibrogenesis." *Kidney Int* **58**(5): 1841-1850.
- Ricard-Blum, S. (2011). "The collagen family." *Cold Spring Harb Perspect Biol* **3**(1): a004978.
- Ritchie, H., L. C. Lawrie, et al. (2000). "Cross-linking of plasminogen activator inhibitor 2 and alpha 2-antiplasmin to fibrin(ogen)." *J Biol Chem* **275**(32): 24915-24920.
- Ritz, E. and S. R. Orth (2000). "Adverse effect of smoking on the renal outcome of patients with primary hypertension." *Am J Kidney Dis* **35**(4): 767-769.
- Robitaille, K., A. Daviau, et al. (2004). "Tissue transglutaminase triggers oligomerization and activation of dual leucine zipper-bearing kinase in calphostin C-treated cells to facilitate apoptosis." *Cell Death Differ* **11**(5): 542-549.
- Rodolfo, C., E. Mormone, et al. (2004). "Tissue transglutaminase is a multifunctional BH3-only protein." *J Biol Chem* **279**(52): 54783-54792.

- Rodrigo, E., M. Lopez-Hoyos, et al. (2000). "Circulating levels of matrix metalloproteinases MMP-3 and MMP-2 in renal transplant recipients with chronic transplant nephropathy." Nephrol Dial Transplant **15**(12): 2041-2045.
- Rodriguez, D., C. J. Morrison, et al. (2010). "Matrix metalloproteinases: what do they not do? New substrates and biological roles identified by murine models and proteomics." Biochim Biophys Acta **1803**(1): 39-54.
- Romanic, A. M., C. L. Burns-Kurtis, et al. (2001). "Upregulated expression of human membrane type-5 matrix metalloproteinase in kidneys from diabetic patients." Am J Physiol Renal Physiol **281**(2): F309-317.
- Ruggenenti, P., P. Cravedi, et al. (2012). "Mechanisms and treatment of CKD." J Am Soc Nephrol **23**(12): 1917-1928.
- Ruggenenti, P., A. Perna, et al. (1998). "Urinary protein excretion rate is the best independent predictor of ESRF in non-diabetic proteinuric chronic nephropathies. "Gruppo Italiano di Studi Epidemiologici in Nefrologia" (GISEN)." Kidney Int **53**(5): 1209-1216.
- Rule, A. D., K. R. Bailey, et al. (2013). "Estimating the glomerular filtration rate from serum creatinine is better than from cystatin C for evaluating risk factors associated with chronic kidney disease." Kidney Int **83**(6): 1169-1176.
- Rydlova, M., L. Holubec, Jr., et al. (2008). "Biological activity and clinical implications of the matrix metalloproteinases." Anticancer Res **28**(2B): 1389-1397.
- Sakai, K., W. H. Busby, Jr., et al. (2001). "Tissue transglutaminase facilitates the polymerization of insulin-like growth factor-binding protein-1 (IGFBP-1) and leads to loss of IGFBP-1's ability to inhibit insulin-like growth factor-I-stimulated protein synthesis." J Biol Chem **276**(12): 8740-8745.
- Sanders, J. S., H. van Goor, et al. (2004). "Renal expression of matrix metalloproteinases in human ANCA-associated glomerulonephritis." Nephrol Dial Transplant **19**(6): 1412-1419.
- Santhanam, L., E. C. Tuday, et al. (2010). "Decreased S-nitrosylation of tissue transglutaminase contributes to age-related increases in vascular stiffness." Circ Res **107**(1): 117-125.
- Santos, L. S., E. W. Chin, et al. (2006). "Surgical reduction of the renal mass in rats: morphologic and functional analysis on the remnant kidney." Acta Cir Bras **21**(4): 252-257.
- Sato, H., M. Iwano, et al. (1998). "Increased excretion of urinary transforming growth factor beta 1 in patients with diabetic nephropathy." Am J Nephrol **18**(6): 490-494.
- Satpathy, M., M. Shao, et al. (2009). "Tissue transglutaminase regulates matrix metalloproteinase-2 in ovarian cancer by modulating cAMP-response element-binding protein activity." J Biol Chem **284**(23): 15390-15399.
- Satriano, J., K. Sharma, et al. (2013). "Induction of AMPK activity corrects early pathophysiological alterations in the subtotal nephrectomy model of chronic kidney disease." Am J Physiol Renal Physiol **305**(5): F727-733.
- Scarpellini, A., R. Germack, et al. (2009). "Heparan sulfate proteoglycans are receptors for the cell-surface trafficking and biological activity of transglutaminase-2." J Biol Chem **284**(27): 18411-18423.
- Schieppati, A. and G. Remuzzi (2005). "Chronic renal diseases as a public health problem: epidemiology, social, and economic implications." Kidney Int Suppl(98): S7-S10.
- Schilcher, G., W. Ribitsch, et al. (2011). "Early detection and intervention using neutrophil gelatinase-associated lipocalin (NGAL) may improve renal outcome of acute contrast media induced nephropathy: a randomized controlled trial in patients undergoing intra-arterial angiography (ANTI-CIN Study)." BMC Nephrol **12**: 39.
- Schlondorff, D. O. (2008). "Overview of factors contributing to the pathophysiology of progressive renal disease." Kidney International **74**(7): 860-866.
- Schmid, A. W., E. Condemi, et al. (2011). "Tissue transglutaminase-mediated glutamine deamidation of beta-amyloid peptide increases peptide solubility, whereas enzymatic

- cross-linking and peptide fragmentation may serve as molecular triggers for rapid peptide aggregation." *J Biol Chem* **286**(14): 12172-12188.
- Schmidt, G., J. Selzer, et al. (1998). "The Rho-deamidating cytotoxic necrotizing factor 1 from *Escherichia coli* possesses transglutaminase activity. Cysteine 866 and histidine 881 are essential for enzyme activity." *J Biol Chem* **273**(22): 13669-13674.
- Schmitt, R., S. Coca, et al. (2008). "Recovery of kidney function after acute kidney injury in the elderly: a systematic review and meta-analysis." *Am J Kidney Dis* **52**(2): 262-271.
- Schmitt, R., A. Marlier, et al. (2008). "Zag expression during aging suppresses proliferation after kidney injury." *J Am Soc Nephrol* **19**(12): 2375-2383.
- Schnackenberg, L. K., J. Sun, et al. (2012). "Metabolomics evaluation of hydroxyproline as a potential marker of melamine and cyanuric acid nephrotoxicity in male and female Fischer F344 rats." *Food Chem Toxicol* **50**(11): 3978-3983.
- Schoenwaelder, S. M., S. C. Hughan, et al. (2002). "RhoA sustains integrin alpha IIb beta 3 adhesion contacts under high shear." *J Biol Chem* **277**(17): 14738-14746.
- Schrier, R. W., Ed. (2003). *Renal and Electrolyte disorders*. Philadelphia, USA, Lippincott Williams & Wilkins.
- Schrier, R. W. (2005). *Manual of Nephrology*, Lippincott Williams & Wilkins.
- Selkoe, D. J., C. Abraham, et al. (1982). "Brain transglutaminase: in vitro crosslinking of human neurofilament proteins into insoluble polymers." *Proc Natl Acad Sci U S A* **79**(19): 6070-6074.
- Sesso Rde, C., A. A. Lopes, et al. (2012). "[Chronic dialysis in Brazil: report of the Brazilian dialysis census, 2011]." *J Bras Nefrol* **34**(3): 272-277.
- Shah, S. V. (2004). "Oxidants and iron in chronic kidney disease." *Kidney Int Suppl.*(91): S50-55.
- Shan, L., O. Molberg, et al. (2002). "Structural basis for gluten intolerance in celiac sprue." *Science* **297**(5590): 2275-2279.
- Sharifipour, F., A. Zeraati, et al. (2013). "Association of urinary lipocalin-2 with lupus nephritis." *Iran J Basic Med Sci* **16**(9): 1011-1015.
- Shigemura, M., S. Konno, et al. (2012). "Impact of asthmatic control status on serum cystatin C concentrations." *Clin Chem Lab Med* **50**(8): 1367-1371.
- Shiiki, H., T. Nishino, et al. (1996). "Clinical and morphological predictors of renal outcome in adult patients with focal and segmental glomerulosclerosis (FSGS)." *Clin Nephrol* **46**(6): 362-368.
- Shimada, T., M. Kakitani, et al. (2004). "Targeted ablation of Fgf23 demonstrates an essential physiological role of FGF23 in phosphate and vitamin D metabolism." *J Clin Invest* **113**(4): 561-568.
- Shiraki-lida, T., H. Aizawa, et al. (1998). "Structure of the mouse klotho gene and its two transcripts encoding membrane and secreted protein." *FEBS Lett* **424**(1-2): 6-10.
- Shlipak, M. G., L. F. Fried, et al. (2005). "Cardiovascular mortality risk in chronic kidney disease: comparison of traditional and novel risk factors." *Jama* **293**(14): 1737-1745.
- Shoulders, M. D. and R. T. Raines (2009). "Collagen structure and stability." *Annu Rev Biochem* **78**: 929-958.
- Shweke, N., N. Boulos, et al. (2008). "Tissue transglutaminase contributes to interstitial renal fibrosis by favoring accumulation of fibrillar collagen through TGF-beta activation and cell infiltration." *Am J Pathol* **173**(3): 631-642.
- Siegel, M., P. Strnad, et al. (2008). "Extracellular transglutaminase 2 is catalytically inactive, but is transiently activated upon tissue injury." *PLoS One* **3**(3): e1861.
- Silbiger, S. and J. Neugarten (2008). "Gender and human chronic renal disease." *Gender Medicine* **5**, Supplement 1(0): S3-S10.
- Silbiger, S. R. (2011). "Raging hormones: gender and renal disease." *Kidney Int* **79**(4): 382-384.

- Singh, A. K., Y. M. Farag, et al. (2013). "Epidemiology and risk factors of chronic kidney disease in India - results from the SEEK (Screening and early evaluation of kidney disease) study." *BMC Nephrol* **14**(1): 114.
- Singh, U. S., M. T. Kunar, et al. (2001). "Role of transglutaminase II in retinoic acid-induced activation of RhoA-associated kinase-2." *EMBO J* **20**(10): 2413-2423.
- Singh, U. S., J. Pan, et al. (2003). "Tissue transglutaminase mediates activation of RhoA and MAP kinase pathways during retinoic acid-induced neuronal differentiation of SH-SY5Y cells." *J Biol Chem* **278**(1): 391-399.
- Singhal, P. C., S. Sagar, et al. (1996). "Simulated glomerular pressure modulates mesangial cell 72 kDa metalloproteinase activity." *Connect Tissue Res* **33**(4): 257-263.
- Sjoberg, J. S. and S. Bulterijs (2009). "Characteristics, formation, and pathophysiology of glucosepane: a major protein cross-link." *Rejuvenation Res* **12**(2): 137-148.
- Skill, N. J., M. Griffin, et al. (2001). "Increases in renal epsilon-(gamma-glutamyl)-lysine crosslinks result from compartment-specific changes in tissue transglutaminase in early experimental diabetic nephropathy: pathologic implications." *Lab Invest* **81**(5): 705-716.
- Skill, N. J., T. S. Johnson, et al. (2004). "Inhibition of transglutaminase activity reduces extracellular matrix accumulation induced by high glucose levels in proximal tubular epithelial cells." *J Biol Chem* **279**(46): 47754-47762.
- Smith, M. R., H. Kung, et al. (1997). "TIMP-3 induces cell death by stabilizing TNF-alpha receptors on the surface of human colon carcinoma cells." *Cytokine* **9**(10): 770-780.
- Soler, M. J., M. Riera, et al. (2012). "New experimental models of diabetic nephropathy in mice models of type 2 diabetes: efforts to replicate human nephropathy." *Exp Diabetes Res* **2012**: 616313.
- Sollid, L. M. (2002). "Celiac disease: dissecting a complex inflammatory disorder." *Nat Rev Immunol* **2**(9): 647-655.
- Sollid, L. M. and B. Jabri (2005). "Is celiac disease an autoimmune disorder?" *Curr Opin Immunol* **17**(6): 595-600.
- Solomon, R. J., R. Mehran, et al. (2009). "Contrast-induced nephropathy and long-term adverse events: cause and effect?" *Clin J Am Soc Nephrol* **4**(7): 1162-1169.
- Song, F., K. Wisithphrom, et al. (2006). "Matrix metalloproteinase dependent and independent collagen degradation." *Front Biosci* **11**: 3100-3120.
- Soylemezoglu, O., G. Wild, et al. (1997). "Urinary and serum type III collagen: markers of renal fibrosis." *Nephrol Dial Transplant* **12**(9): 1883-1889.
- Spanaus, K. S., B. Kollerits, et al. (2010). "Serum creatinine, cystatin C, and beta-trace protein in diagnostic staging and predicting progression of primary nondiabetic chronic kidney disease." *Clin Chem* **56**(5): 740-749.
- Srivastava, S. P., D. Koya, et al. (2013). "MicroRNAs in Kidney Fibrosis and Diabetic Nephropathy: Roles on EMT and EndMT." *Biomed Res Int* **2013**: 125469.
- SRR (2009). Singapore Renal Registry. Ministry of Health, Singapore, National Registry of Diseases Office.
- Stamnaes, J., D. M. Pinkas, et al. (2010). "Redox regulation of transglutaminase 2 activity." *J Biol Chem* **285**(33): 25402-25409.
- Staruschenko, A., O. Palygin, et al. (2013). "Epidermal growth factors in the kidney and relationship to hypertension." *Am J Physiol Renal Physiol* **305**(1): F12-20.
- Stetler-Stevenson, W. G. (2008). "Tissue inhibitors of metalloproteinases in cell signaling: metalloproteinase-independent biological activities." *Sci Signal* **1**(27): re6.
- Stetler-Stevenson, W. G., N. Bersch, et al. (1992). "Tissue inhibitor of metalloproteinase-2 (TIMP-2) has erythroid-potentiating activity." *FEBS Lett* **296**(2): 231-234.
- Stoesz, S. P., A. Friedl, et al. (1998). "Heterogeneous expression of the lipocalin NGAL in primary breast cancers." *Int J Cancer* **79**(6): 565-572.

- Stringer, S., P. Sharma, et al. (2013). "The natural history of, and risk factors for, progressive Chronic Kidney Disease (CKD): the Renal Impairment in Secondary care (RIISC) study; rationale and protocol." BMC Nephrol **14**: 95.
- System, U. S. R. D. (2012). *USRDS 2012 Annual Data Report: Atlas of Chronic Kidney Disease and End-Stage Renal Disease in the United States*. M. Bethesda, National Institute of Health, National Institute of Diabetes and Digestive and Kidney Diseases.
- Tampe, B. and M. Zeisberg (2013). "Contribution of genetics and epigenetics to progression of kidney fibrosis." Nephrol Dial Transplant.
- Tanaka, T. and M. Nangaku (2010). "The role of hypoxia, increased oxygen consumption, and hypoxia-inducible factor-1 alpha in progression of chronic kidney disease." Curr Opin Nephrol Hypertens **19**(1): 43-50.
- Tarver-Carr, M. E., N. R. Powe, et al. (2002). "Excess risk of chronic kidney disease among African-American versus white subjects in the United States: a population-based study of potential explanatory factors." J Am Soc Nephrol **13**(9): 2363-2370.
- Tashiro, K., I. Koyanagi, et al. (2004). "Levels of urinary matrix metalloproteinase-9 (MMP-9) and renal injuries in patients with type 2 diabetic nephropathy." J Clin Lab Anal **18**(3): 206-210.
- Tee, A. E., G. M. Marshall, et al. (2010). "Opposing effects of two tissue transglutaminase protein isoforms in neuroblastoma cell differentiation." J Biol Chem **285**(6): 3561-3567.
- Telci, D., R. J. Collighan, et al. (2009). "Increased TG2 expression can result in induction of transforming growth factor beta1, causing increased synthesis and deposition of matrix proteins, which can be regulated by nitric oxide." J Biol Chem **284**(43): 29547-29558.
- Telci, D. and M. Griffin (2006). "Tissue transglutaminase (TG2)--a wound response enzyme." Front Biosci **11**: 867-882.
- Tervaert, T. W., A. L. Mooyaart, et al. (2010). "Pathologic classification of diabetic nephropathy." J Am Soc Nephrol **21**(4): 556-563.
- Thamer, M., S. C. Henderson, et al. (1999). "Unequal access to cadaveric kidney transplantation in California based on insurance status." Health Serv Res **34**(4): 879-900.
- Thompson, R. W. and W. C. Parks (1996). "Role of matrix metalloproteinases in abdominal aortic aneurysms." Ann N Y Acad Sci **800**: 157-174.
- Thraillkill, K. M., R. Clay Bunn, et al. (2009). "Matrix metalloproteinases: their potential role in the pathogenesis of diabetic nephropathy." Endocrine **35**(1): 1-10.
- Tonelli, M., N. Wiebe, et al. (2006). "Chronic kidney disease and mortality risk: a systematic review." J Am Soc Nephrol **17**(7): 2034-2047.
- Tozawa, M., K. Iseki, et al. (2003). "Blood pressure predicts risk of developing end-stage renal disease in men and women." Hypertension **41**(6): 1341-1345.
- Tracy, R. P., A. M. Arnold, et al. (1999). "The relationship of fibrinogen and factors VII and VIII to incident cardiovascular disease and death in the elderly: results from the cardiovascular health study." Arterioscler Thromb Vasc Biol **19**(7): 1776-1783.
- Traub, S. J., J. A. Kellum, et al. (2013). "Risk factors for radiocontrast nephropathy after emergency department contrast-enhanced computerized tomography." Acad Emerg Med **20**(1): 40-45.
- Turgut, F., M. Kanbay, et al. (2007). "Risk factors affecting the incidence of chronic kidney disease." Kidney Int **71**(10): 1076; author reply 1076.
- Ueda, S., S. I. Yamagishi, et al. (2013). "Role of asymmetric dimethylarginine in cardiorenal syndrome." Curr Pharm Des.
- Umar, S., F. Malavasi, et al. (1996). "Post-translational modification of CD38 protein into a high molecular weight form alters its catalytic properties." J Biol Chem **271**(27): 15922-15927.
- Urbschat, A., N. Obermuller, et al. (2011). "Biomarkers of kidney injury." Biomarkers **16 Suppl 1**: S22-30.

- Usui, T., J. Takagi, et al. (1993). "Propolypeptide of von Willebrand factor serves as a substrate for factor XIIIa and is cross-linked to laminin." J Biol Chem **268**(17): 12311-12316.
- Vader, L. W., A. de Ru, et al. (2002). "Specificity of tissue transglutaminase explains cereal toxicity in celiac disease." J Exp Med **195**(5): 643-649.
- Vaidya, V. S., J. S. Ozer, et al. (2010). "Kidney injury molecule-1 outperforms traditional biomarkers of kidney injury in preclinical biomarker qualification studies." Nat Biotechnol **28**(5): 478-485.
- van den Brule, F. A., F. T. Liu, et al. (1998). "Transglutaminase-mediated oligomerization of galectin-3 modulates human melanoma cell interactions with laminin." Cell Adhes Commun **5**(6): 425-435.
- van der Velde, M., K. Matsushita, et al. (2011). "Lower estimated glomerular filtration rate and higher albuminuria are associated with all-cause and cardiovascular mortality. A collaborative meta-analysis of high-risk population cohorts." Kidney Int **79**(12): 1341-1352.
- van der Zijl, N. J., R. Hanemaaijer, et al. (2010). "Urinary matrix metalloproteinase-8 and -9 activities in type 2 diabetic subjects: A marker of incipient diabetic nephropathy?" Clin Biochem **43**(7-8): 635-639.
- Van Herck, J. L., D. M. Schrijvers, et al. (2010). "Transglutaminase 2 deficiency decreases plaque fibrosis and increases plaque inflammation in apolipoprotein-E-deficient mice." J Vasc Res **47**(3): 231-240.
- van Koppen, A., M. C. Verhaar, et al. (2013). "5/6th nephrectomy in combination with high salt diet and nitric oxide synthase inhibition to induce chronic kidney disease in the Lewis rat." J Vis Exp(77): e50398.
- van Timmeren, M. M., V. S. Vaidya, et al. (2007). "High urinary excretion of kidney injury molecule-1 is an independent predictor of graft loss in renal transplant recipients." Transplantation **84**(12): 1625-1630.
- van Timmeren, M. M., M. C. van den Heuvel, et al. (2007). "Tubular kidney injury molecule-1 (KIM-1) in human renal disease." J Pathol **212**(2): 209-217.
- Vanacore, R., A. J. Ham, et al. (2009). "A sulfilimine bond identified in collagen IV." Science **325**(5945): 1230-1234.
- Vanhoutte, D. and S. Heymans (2010). "TIMPs and cardiac remodeling: 'Embracing the MMP-independent-side of the family'." J Mol Cell Cardiol **48**(3): 445-453.
- Vanhoutte, D., M. Schellings, et al. (2006). "Relevance of matrix metalloproteinases and their inhibitors after myocardial infarction: a temporal and spatial window." Cardiovasc Res **69**(3): 604-613.
- Varghese, S. (2006). "Matrix metalloproteinases and their inhibitors in bone: an overview of regulation and functions." Front Biosci **11**: 2949-2966.
- Vass, D. G., B. Shrestha, et al. (2012). "Inflammatory lymphangiogenesis in a rat transplant model of interstitial fibrosis and tubular atrophy." Transpl Int **25**(7): 792-800.
- Vempati, P., E. D. Karagiannis, et al. (2007). "A biochemical model of matrix metalloproteinase 9 activation and inhibition." J Biol Chem **282**(52): 37585-37596.
- Verderio, E. and A. Scarpellini (2010). "Significance of the syndecan-4-transglutaminase-2 interaction." ScientificWorldJournal **10**: 1073-1077.
- Verderio, E. A., T. Johnson, et al. (2004). "Tissue transglutaminase in normal and abnormal wound healing: review article." Amino Acids **26**(4): 387-404.
- Verderio, E. A., T. S. Johnson, et al. (2005). "Transglutaminases in wound healing and inflammation." Prog Exp Tumor Res **38**: 89-114.
- Verderio, E. A., D. Telci, et al. (2003). "A novel RGD-independent cell adhesion pathway mediated by fibronectin-bound tissue transglutaminase rescues cells from anoikis." J Biol Chem **278**(43): 42604-42614.
- Verma, A., S. Guha, et al. (2008). "Therapeutic significance of elevated tissue transglutaminase expression in pancreatic cancer." Clin Cancer Res **14**(8): 2476-2483.

- Vervloet, M. G., F. J. van Ittersum, et al. (2011). "Effects of dietary phosphate and calcium intake on fibroblast growth factor-23." *Clin J Am Soc Nephrol* **6**(2): 383-389.
- Vervloet, M. G., A. D. van Zuilen, et al. (2012). "Fibroblast growth factor 23 is associated with proteinuria and smoking in chronic kidney disease: an analysis of the MASTERPLAN cohort." *BMC Nephrol* **13**: 20.
- Veza, R., A. Habib, et al. (1999). "Differential signaling by the thromboxane receptor isoforms via the novel GTP-binding protein, Gh." *J Biol Chem* **274**(18): 12774-12779.
- Viau, A., K. El Karoui, et al. (2010). "Lipocalin 2 is essential for chronic kidney disease progression in mice and humans." *J Clin Invest* **120**(11): 4065-4076.
- Visse, R. and H. Nagase (2003). "Matrix metalloproteinases and tissue inhibitors of metalloproteinases: structure, function, and biochemistry." *Circ Res* **92**(8): 827-839.
- Vivekanandan-Giri, A., J. L. Slocum, et al. (2011). "Urine glycoprotein profile reveals novel markers for chronic kidney disease." *Int J Proteomics* **2011**: 214715.
- Vives-Pi, M., S. Takasawa, et al. (2013). "Biomarkers for diagnosis and monitoring of celiac disease." *J Clin Gastroenterol* **47**(4): 308-313.
- Wang, G., F. M. Lai, et al. (2008). "Urinary messenger RNA expression of podocyte-associated molecules in patients with diabetic nephropathy treated by angiotensin-converting enzyme inhibitor and angiotensin receptor blocker." *Eur J Endocrinol* **158**(3): 317-322.
- Wang, G., F. M. Lai, et al. (2007). "Messenger RNA expression of podocyte-associated molecules in urinary sediment of patients with lupus nephritis." *J Rheumatol* **34**(12): 2358-2364.
- Wang, Z. and M. Griffin (2012). "TG2, a novel extracellular protein with multiple functions." *Amino Acids* **42**(2-3): 939-949.
- Wang, Z., R. Juttermann, et al. (2000). "TIMP-2 is required for efficient activation of proMMP-2 in vivo." *J Biol Chem* **275**(34): 26411-26415.
- Ward, M. M. (2008). "Socioeconomic status and the incidence of ESRD." *Am J Kidney Dis* **51**(4): 563-572.
- Watson, B., Jr., M. A. Khan, et al. (2001). "Mitochondrial DNA mutations in black Americans with hypertension-associated end-stage renal disease." *Am J Kidney Dis* **38**(3): 529-536.
- Weber, T. J., S. Liu, et al. (2003). "Serum FGF23 levels in normal and disordered phosphorus homeostasis." *J Bone Miner Res* **18**(7): 1227-1234.
- Weiner, D. E. (2007). "Causes and consequences of chronic kidney disease: implications for managed health care." *J Manag Care Pharm* **13**(3 Suppl): S1-9.
- Whaley-Connell, A. T., J. R. Sowers, et al. (2008). "Diabetes mellitus in CKD: Kidney Early Evaluation Program (KEEP) and National Health and Nutrition and Examination Survey (NHANES) 1999-2004." *Am J Kidney Dis* **51**(4 Suppl 2): S21-29.
- Wilhelm, S. M., I. E. Collier, et al. (1989). "SV40-transformed human lung fibroblasts secrete a 92-kDa type IV collagenase which is identical to that secreted by normal human macrophages." *J Biol Chem* **264**(29): 17213-17221.
- Will, H., S. J. Atkinson, et al. (1996). "The soluble catalytic domain of membrane type 1 matrix metalloproteinase cleaves the propeptide of progelatinase A and initiates autoproteolytic activation. Regulation by TIMP-2 and TIMP-3." *J Biol Chem* **271**(29): 17119-17123.
- Witko-Sarsat, V., M. Friedlander, et al. (1996). "Advanced oxidation protein products as a novel marker of oxidative stress in uremia." *Kidney Int* **49**(5): 1304-1313.
- Woelfle, J. V., R. E. Brenner, et al. (2011). "Schmid-type metaphyseal chondrodysplasia as the result of a collagen type X defect due to a novel COL10A1 nonsense mutation: A case report of a novel COL10A1 mutation." *J Orthop Sci* **16**(2): 245-249.
- Woo, K. T., Y. K. Lau, et al. (1991). "Pattern of proteinuria in IgA nephritis by SDS-PAGE: clinical significance." *Clin Nephrol* **36**(1): 6-11.

- Wright, J. T., Jr., G. Bakris, et al. (2002). "Effect of blood pressure lowering and antihypertensive drug class on progression of hypertensive kidney disease: results from the AASK trial." Jama **288**(19): 2421-2431.
- Wu, C. F., W. C. Chiang, et al. (2013). "Transforming growth factor beta-1 stimulates profibrotic epithelial signaling to activate pericyte-myofibroblast transition in obstructive kidney fibrosis." Am J Pathol **182**(1): 118-131.
- Wu, J., S. L. Liu, et al. (2000). "Roles of tissue transglutaminase in ethanol-induced inhibition of hepatocyte proliferation and alpha 1-adrenergic signal transduction." J Biol Chem **275**(29): 22213-22219.
- Wu, J. J., M. A. Weis, et al. (2009). "Differences in chain usage and cross-linking specificities of cartilage type V/XI collagen isoforms with age and tissue." J Biol Chem **284**(9): 5539-5545.
- Wu, J. J., M. A. Weis, et al. (2010). "Type III collagen, a fibril network modifier in articular cartilage." J Biol Chem **285**(24): 18537-18544.
- Xu, S. Y., M. Carlson, et al. (1994). "Purification and characterization of a human neutrophil lipocalin (HNL) from the secondary granules of human neutrophils." Scand J Clin Lab Invest **54**(5): 365-376.
- Yamagata, K., K. Ishida, et al. (2007). "Risk factors for chronic kidney disease in a community-based population: a 10-year follow-up study." Kidney Int **71**(2): 159-166.
- Yan, Q., W. Sui, et al. (2012). "Expression of MMP-2 and TIMP-1 in renal tissue of patients with chronic active antibody-mediated renal graft rejection." Diagn Pathol **7**: 141.
- Yang, H. and A. B. Fogo (2010). "Cell senescence in the aging kidney." J Am Soc Nephrol **21**(9): 1436-1439.
- Yang, J., J. Chen, et al. (2012). "Effect of interleukin 6 deficiency on renal interstitial fibrosis." PLoS One **7**(12): e52415.
- Yazawa, N., K. Kikuchi, et al. (2000). "Serum levels of tissue inhibitor of metalloproteinases 2 in patients with systemic sclerosis." J Am Acad Dermatol **42**(1 Pt 1): 70-75.
- Ye, Y., X. Gai, et al. (2013). "Impact of thyroid function on serum cystatin C and estimated glomerular filtration rate: a cross-sectional study." Endocr Pract **19**(3): 397-403.
- Yoshioka, K., T. Takemura, et al. (1989). "Glomerular localization of type III collagen in human kidney disease." Kidney Int **35**(5): 1203-1211.
- Yoshioka, K., M. Tohda, et al. (1990). "Distribution of type I collagen in human kidney diseases in comparison with type III collagen." J Pathol **162**(2): 141-148.
- Young-Min, S. A., C. Beeton, et al. (2001). "Serum TIMP-1, TIMP-2, and MMP-1 in patients with systemic sclerosis, primary Raynaud's phenomenon, and in normal controls." Ann Rheum Dis **60**(9): 846-851.
- Young, E. W., E. A. Mauger, et al. (1994). "Socioeconomic status and end-stage renal disease in the United States." Kidney Int **45**(3): 907-911.
- Yu, D., A. Petermann, et al. (2005). "Urinary podocyte loss is a more specific marker of ongoing glomerular damage than proteinuria." J Am Soc Nephrol **16**(6): 1733-1741.
- Yu, W. H., S. Yu, et al. (2000). "TIMP-3 binds to sulfated glycosaminoglycans of the extracellular matrix." J Biol Chem **275**(40): 31226-31232.
- Yuan, L., M. Siegel, et al. (2007). "Transglutaminase 2 inhibitor, KCC009, disrupts fibronectin assembly in the extracellular matrix and sensitizes orthotopic glioblastomas to chemotherapy." Oncogene **26**(18): 2563-2573.
- Yusuf, S., K. K. Teo, et al. (2008). "Telmisartan, ramipril, or both in patients at high risk for vascular events." N Engl J Med **358**(15): 1547-1559.
- Zainelli, G. M., C. A. Ross, et al. (2004). "Calmodulin regulates transglutaminase 2 cross-linking of huntingtin." J Neurosci **24**(8): 1954-1961.
- Zebrowska, A., J. Narbutt, et al. (2005). "The imbalance between metalloproteinases and their tissue inhibitors is involved in the pathogenesis of dermatitis herpetiformis." Mediators Inflamm **2005**(6): 373-379.

- Zeisberg, M., G. Bonner, et al. (2001). "Renal fibrosis: collagen composition and assembly regulates epithelial-mesenchymal transdifferentiation." Am J Pathol **159**(4): 1313-1321.
- Zeisberg, M. and E. G. Neilson (2010). "Mechanisms of tubulointerstitial fibrosis." J Am Soc Nephrol **21**(11): 1819-1834.
- Zemskov, E. A., I. Mikhailenko, et al. (2011). "Unconventional secretion of tissue transglutaminase involves phospholipid-dependent delivery into recycling endosomes." PLoS One **6**(4): e19414.
- Zhao, H. J., S. Wang, et al. (2006). "Endothelial nitric oxide synthase deficiency produces accelerated nephropathy in diabetic mice." J Am Soc Nephrol **17**(10): 2664-2669.
- Zheng, M., L. L. Lv, et al. (2011). "Urinary podocyte-associated mRNA profile in various stages of diabetic nephropathy." PLoS One **6**(5): e20431.
- Zoccali, C., M. I. Yilmaz, et al. (2013). "FGF23: a mature renal and cardiovascular risk factor?" Blood Purif **36**(1): 52-57.
- Zoccali, C., M. I. Yilmaz, et al. (2013). "FGF23: A Mature Renal and Cardiovascular Risk Factor?" Blood Purif **36**(1): 52-57.
- Zou, J., F. Zhu, et al. (2004). "Catalytic activity of human ADAM33." J Biol Chem **279**(11): 9818-9830.

Appendix

10.1. 5/6th Subtotalnephrectomy study

Assessment of renal function and damage in the SNx Model

Table 10.1: SNx study renal function data

Experimental Group	Number of animals	Proteinuria (mg/24h)	Ur. Creatinine (μ mol/L)	CrCl (ml/min)	24h urine volume (ml)
SNC 1 week	3	68.32 \pm 9.5	16759 \pm 1191	1.16 \pm 0.67	3.48 \pm 0.92
SNX 1 week	3	128.31 \pm 0.5 *	4051.33 \pm 138 *	0.61 \pm 0.35 *	20.86 \pm 1.51 **
SNC 1 month	3	118.7 \pm 27.1	15899.33 \pm 212	1.32 \pm 0.29	4.52 \pm 0.92
SNX 1 month	3	299.94 \pm 77.9 *	3787.33 \pm 607 *	0.97 \pm 0.11 *	28 \pm 6.03 **
SNC 3 months	11	143.05 \pm 15.9	13443.58 \pm 1239	1.94 \pm 0.19	9.42 \pm 0.95
SNX 3 months	7	574.94 \pm 53.3 **	2379.86 \pm 312 *	0.32 \pm 0.18 **	38.79 \pm 2.25 **
NTU C7 1 week	3	109.45 \pm 17.5	6947 \pm 276	0.54 \pm 0.31	27.27 \pm 2.89
NTU C56 1 week	3	136.89 \pm 8.1	7109.67 \pm 248	0.63 \pm 0.36	25.74 \pm 0.92
NTU C7 1 month	3	168.58 \pm 21.1 ^a	7061.66 \pm 213	0.76 \pm 0.06	29.67 \pm 0.33
NTU C56 1 month	3	148.59 \pm 7.9 ^a	6516.33 \pm 318	0.86 \pm 0.13	21.57 \pm 1.39
NTU C7 3 months	4	259.67 \pm 46.3 ^a	5638.25 \pm 319	0.86 \pm 0.05 ^a	39.5 \pm 2.77
NTU C56 3 months	4	214.38 \pm 11.2 ^a	5749.25 \pm 627	0.93 \pm 0.10 ^b	35.61 \pm 6.76

Table 10.1: Renal function was assessed in sham-operated (SNC), diseased (SNx) and SNx rats treated with TG inhibitors (NTU C7 and NTU C56) at 7, 28 and 84 days post SNx. Total urine volume, proteinuria and creatinine levels were assessed. Serum and urine creatinine was measured and used to calculate creatinine clearance. Data represents mean value \pm SEM. * = $p < 0.05$, ** = $p < 0.01$, *** = $p < 0.001$ between SNx and normal urine, a = $p < 0.05$, b = $p < 0.01$, c = $p < 0.001$ between either NTU C7 or NTU C56 and untreated SNx, 2 way ANOVA, with Bonferroni post test.

Total proteinuria and albuminuria

Protein excretion (figure 10.1-A) steadily increased in the SNx animals throughout the time course showing 1.8, 2.5 and 4.2 fold increase at day 7, 28 and 84 respectively ($p < 0.05$, 2 way ANOVA, with Bonferroni post test) when compared to sham-operated controls. Protein excretion in sham operated rats ranged 68.32-143.09mg/24hours throughout the study. Rats treated with two different TG2 inhibitors also showed significant increase on proteinuria levels at 7 days post SNx; NTU C7 (109.45 \pm 17.5mg/24h) and NTU C56 (136.89 \pm 8.1mg/24h) compared to SNC ($p < 0.05$, 2 way ANOVA, with Bonferroni post test). By 28 days post surgery, protein excretion reached a plateau on both treated groups; NTU C7 (168.58 \pm 21.1mg/24h) and NTU C56 (148.59 \pm 7.9mg/24h). There was no statistical significance on the average protein excretion between the two treatment groups and SNC at 28 and 84 days post surgery. Albuminuria (figure 10.1-B) followed a similar pattern to total protein excretion, with SNx animals having a progressive increase. At 7 days post Subtotalnephrectomy, albuminuria levels were an average 27.85 \pm 9.0mg/24h in SNx animals, this was increased by 1.7 and 10.5 fold at day 28 and 84 respectively ($p < 0.05$ and $p < 0.001$, 2 way ANOVA, with Bonferroni post test) compared to SNC. NTU C7 and NTU C56 displayed a similar trend on albuminuria

excretion through the study time course. At day 84, NTU C7 and NTU C56 had significant lower excretion of albuminuria when compared to SNx animals ($p < 0.05$ and $p < 0.01$, 2 way ANOVA, with Bonferroni post test).

Urine creatinine and creatinine clearance

Urinary creatinine was significantly higher in Sham-operated rats compared to SNx, NTU C7 and NTU C56 treated SNx rats at all time points ($p < 0.05$, 2 way ANOVA, with Bonferroni post test). Creatinine Clearance (CrCl), which is a measure for approximating the GFR, ranged from 1.16-1.94ml/min in SNc animals (figure 11.1-C). Renal function of SNx animals was 50% lower than SNc at day 7 due to loss of the renal mass. In response to compensatory renal growth, there was a slight elevation of CrCl by day 28 before a fall to 16.5% of control levels at day 84 ($p < 0.01$, 2 way ANOVA) due to disease progression.

Creatinine Clearance of NTU C7 and NTU C56 was 46% and 54% of SNc levels respectively at day 7, due to the reduction on renal mass. Then, CrCl of both groups progressively increased throughout the time course. By day 84, there was a significant improvement on renal function of both groups. At this time point, CrCl was significantly higher at NTU C7 and NTU C56 treated animals ($p < 0.05$ and $p < 0.01$, 2 way ANOVA, with Bonferroni post test) when compared to SNx.

Figure 10.1: Assessment of kidney function and damage in the SNx Model

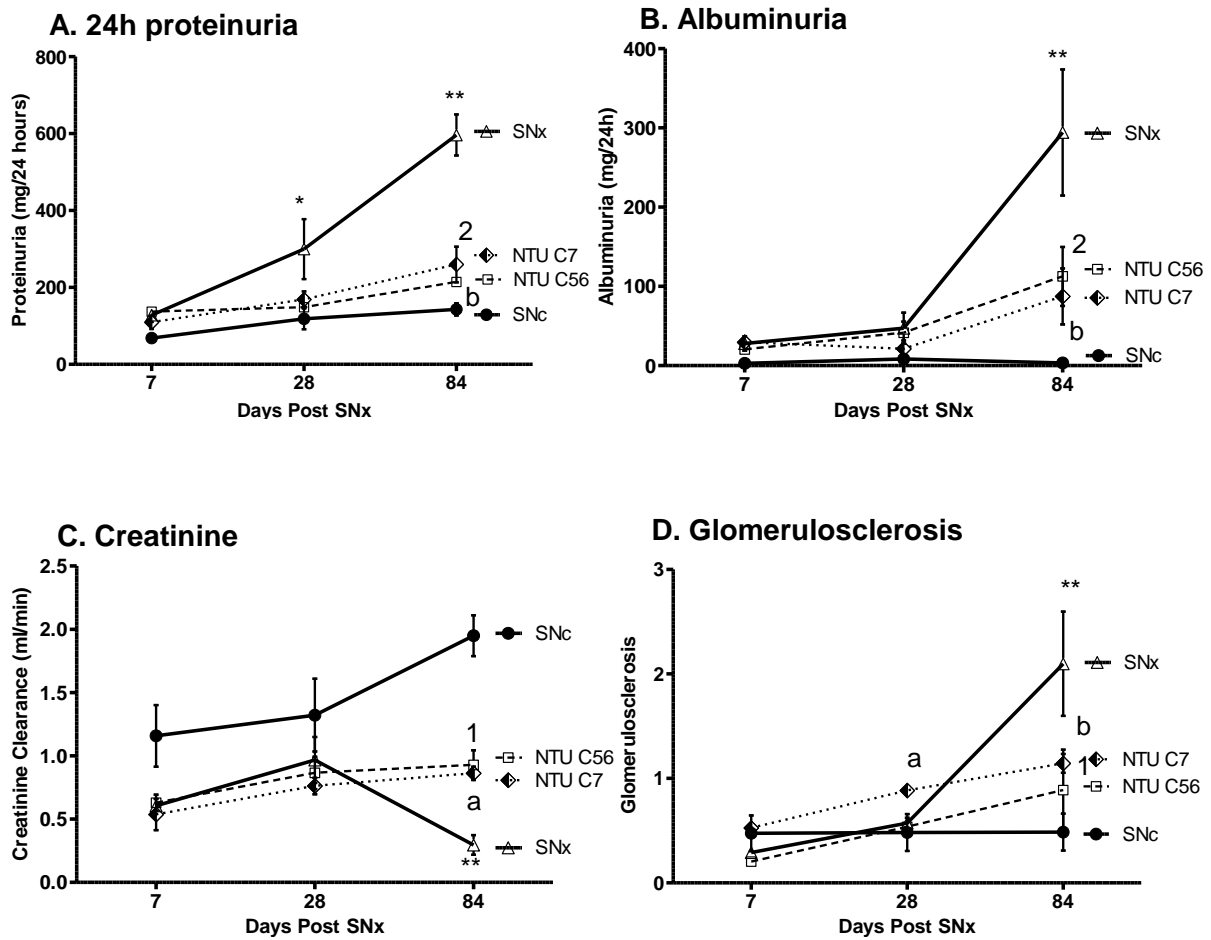


Figure 10.1: (A) 24h Proteinuria and (B) albuminuria were used to assess Glomerular damage in all groups at 7, 28 and 84 days post SNx. The first was assessed by using the Lowry assay and the second by a commercial ELISA kit. Kidney function and fibrosis were evaluated by creatinine clearance (C) and the degree of glomerulosclerosis (D) assessed in Masson's Trichrome stained sections respectively. Data represents mean values \pm SEM. * $p < 0.05$, ** = $p < 0.01$, SNx to sham group, a = $p < 0.05$, b = $p < 0.01$, between NTU C7 and SNx and 1 = $p < 0.05$, 2 = $p < 0.01$, between NTU C56 and SNx.

10.2. Diabetic Nephropathy study

Assessment of renal function and damage in the UNx STZ model of DN

Table 10.2: UNx STZ model of DN renal function data

Experimental Group	Number of animals	Proteinuria (mg/24h)	Ser. Creatinine ($\mu\text{mol/L}$)	CrCl (ml/min)	Glycaemia (mmol/L)
Control 1 month	4	76.45 \pm 11.81	44.90 \pm 5266	0.92 \pm 0.12	4.81 \pm 0.09
DN 1 month	3	151.25 \pm 31.53	49.03 \pm 2738	1.28 \pm 0.12	12.43 \pm 0.68 *
Control 4 months	3	74.69 \pm 7.89	35.62 \pm 1001	1.57 \pm 0.29	4.83 \pm 0.23
DN 4 months	7	379.13 \pm 46.63 **	76.16 \pm 373	1.97 \pm 0.36	22.61 \pm 1.62 *
Control 8 months	3	77.09 \pm 5.86	33.75 \pm 513	1.83 \pm 0.24	4.92 \pm 0.03
DN 8 months	5	853.15 \pm 180.67 *	216.50 \pm 212	1.21 \pm 0.33 *	22.51 \pm 1.41 *

Table 10.2: Average proteinuria, serum Creatinine, Creatinine Clearance and glycaemia on Controls and DN samples after 1, 4 and 8 months post DN induction. Data represents mean value \pm SEM. *= $p < 0.05$, **= $p < 0.01$, ***= $p < 0.001$ between DN and sham operated rats

Total proteinuria

Protein excretion was used as a measure of glomerular damage and leakage (figure 10.2-A). Sham operated animals never exceeded 99.2mg/24hrs proteinuria throughout the study. Diabetic animals showed a steady increase in protein excretion, reaching significance by 4 months with a level of 379.1 \pm 46.63mg/24hrs ($p = 0.0033$). By 8 months, protein excretion reached an average of 853.2 \pm 180.7mg/24hrs ($p = 0.0181$).

Glycaemia

At 1 month post STZ administration, blood glucose concentration was 2.5 fold higher than controls with average levels of 12.43 \pm 0.68mmol/L ($p < 0.05$, figure 10.2-B). Glycaemia was significantly increased in diabetic rats being 22.61 \pm 1.62mmol/L at 4 months and 22.50 \pm 1.41mmol/L at 8 months ($p < 0.05$ at both time points).

Serum creatinine and creatinine clearance

There was no difference in the serum creatinine concentration between diabetic and sham operated rats at 1 month post STZ administration. Serum creatinine was significantly higher in DN rats compared to controls at 4 and 8 months (2.1 and 6.4 fold increase respectively) ($p < 0.05$, 2 way ANOVA, with Bonferroni post test).

Measurement of kidney function by creatinine clearance showed a 1.3 and 1.4 fold increase at 1 and 4 months post STZ injection on diabetic animals compared to controls. This prompt

rise in CrCl on diseased animals was associated with the typical glomerular hyperfiltration that occurs in the initial stages of Diabetic Nephropathy. As result of the elevation of glucose levels, it is expected that a 25 to 50 percent increase in the GFR will occur. By 8 months, CrCl was 34% lower in diabetic rats ($p < 0.05$), confirming disease progression (figure 10.2-D).

Figure 10.2: Assessment of kidney function and damage in the UNx STZ model of DN

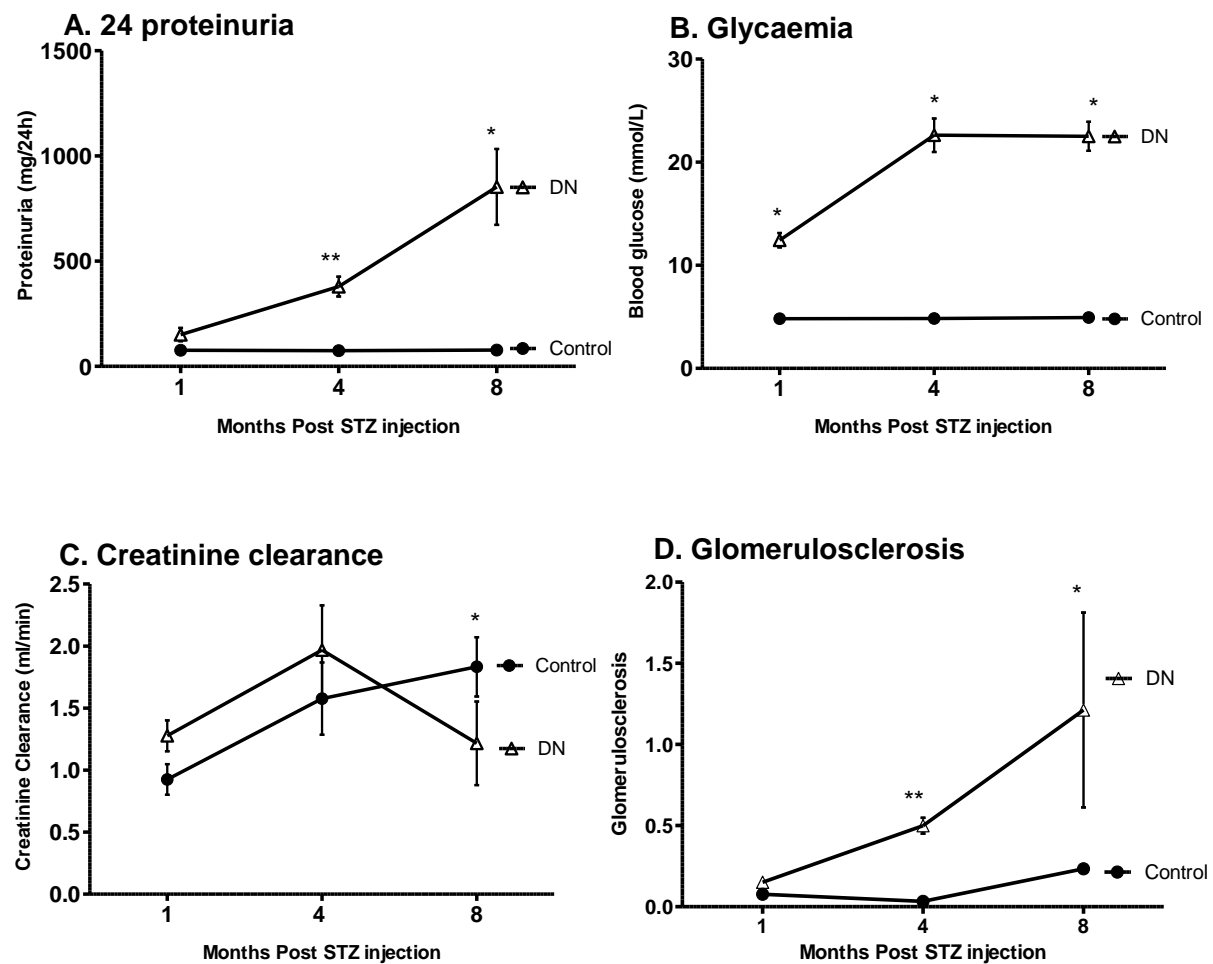


Figure 10.2: (A) 24h Proteinuria was used to assess glomerular damage in all groups at 1, 4 and 8 months post STZ injection using the Lowry assay. **(B)** Average blood glucose. Kidney function and fibrosis were evaluated by creatinine clearance **(C)** and the degree of glomerulosclerosis **(D)** assessed in Masson's Trichrome stained sections respectively. Data represents mean values \pm SEM. * $p < 0.05$, ** $p < 0.01$, to sham group using 2 way ANOVA, with Bonferroni post test

10.3. Chronic Allograft Nephropathy study

Assessment of renal function and damage in the in the Fisher to Lewis transplant model of CAN

Table 10.3: Fisher to Lewis transplant model of CAN renal function data

Experimental Group	Number of animals	Proteinuria (mg/24h)	Ur. Creatinine ($\mu\text{mol/L}$)	CrCl (ml/min)	24h urine vol (ml)
Isograft 2 weeks	5	15.32 \pm 1.38	5240 \pm 787	0.97 \pm 0.17	14.40 \pm 2.62
Allograft 2 weeks	7	19.36 \pm 1.42	3600 \pm 604	0.57 \pm 0.08	19.80 \pm 3.14
Isograft 8 weeks	5	16.60 \pm 4.04	7040 \pm 997	1.25 \pm 0.14	11.22 \pm 1.11
Allograft 8 weeks	7	29.65 \pm 8.26	4657 \pm 836	1.03 \pm 0.09	22.57 \pm 4.34
Isograft 17 weeks	5	19.70 \pm 7.33	6025 \pm 495	1.43 \pm 0.11	8.80 \pm 1.69
Allograft 17 weeks	7	44.67 \pm 13.62	5671 \pm 1042	1.12 \pm 0.18	22.38 \pm 3.89
Isograft 24 weeks	5	28.00 \pm 14.41	6775 \pm 1122	1.48 \pm 0.14	15.12 \pm 3.54
Allograft 24 weeks	7	74.54 \pm 22.13 *	5683 \pm 1156	0.99 \pm 0.21 *	19.67 \pm 2.86
Isograft 33 weeks	5	14.87 \pm 2.69	8000 \pm 901	1.63 \pm 0.18	11.00 \pm 1.52
Allograft 33 weeks	7	133.07 \pm 34.73 **	5280 \pm 1220	0.88 \pm 0.21 *	22.60 \pm 6.49
Isograft 52 weeks	5	18.16 \pm 2.36	10133 \pm 721	1.57 \pm 0.19	11.23 \pm 0.76
Allograft 52 weeks	7	282.59 \pm 77.44 ***	4080 \pm 1332	0.62 \pm 0.17 *	28.00 \pm 6.79

Table 10.3: Average proteinuria, urinary Creatinine, Creatinine Clearance and total volume of urine in 24 hours on Isografts and Allografts samples after 2, 8, 17, 24, 33 and 52 weeks post kidney transplantation. Data represents mean value \pm SEM. *= p<0.05, **=p<0.01, ***= p<0.001 between F-L Allografts and L-L Isografts.

Total proteinuria

Urinary protein excretion at 2 weeks was similar between L-L isografts and F-L allografts (15.32 \pm 1.38 vs. 19.36 \pm 1.42mg/24h). L-L isografts showed a consistent pattern of urinary protein excretion during the study. In contrast, F-L allografts had a significant increase in urinary protein excretion over the 52 week observation period (figure 10.4-A). At termination, F-L allografts average proteinuria was 15 fold higher than the L-L isografts (18.16 \pm 2.36 vs. 282.59 \pm 77.44mg/24h, p<0.001).

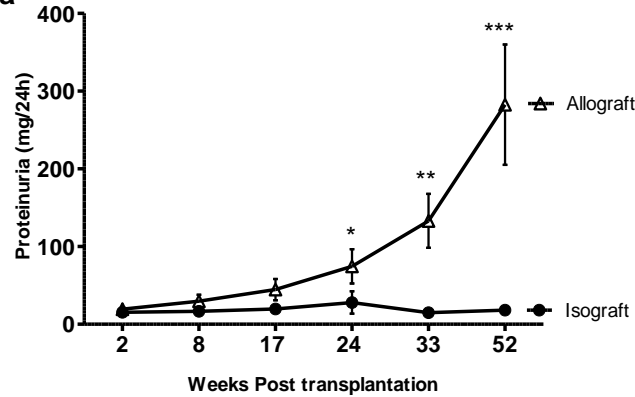
Urine creatinine and creatinine clearance

Two weeks post transplantation, creatinine clearance was raised in both L-L isograft and F-L allograft groups (0.97 \pm 0.17 and 0.57 \pm 0.08ml/min, respectively). This rise was supported up to 17 weeks by the right kidney, at which point it was removed to allow functional monitoring of the transplanted kidney. Over the 17-52 week period, CrCl was stable in the L-L isograft but declined progressively in the F-L allograft together with an elevation in the serum creatinine (figure 10.4-B). At termination, creatinine clearance was significantly lower (1.57 \pm 0.19 vs.

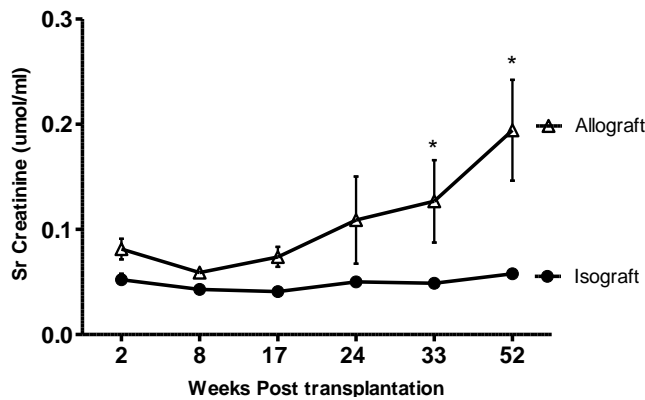
0.62 ± 0.17 ml/min, p<0.05) and serum creatinine significantly higher (0.058 ± 0.005 vs. 0.194 ± 0.048 μmol/ml, p<0.05) in the F-L allograft than the L-L isograft group (figure 10.4-C).

Figure 10.2: Assessment of kidney function and damage in the Fisher to Lewis transplant model of CAN

A. 24h proteinuria



B. Serum creatinine



C. Creatinine

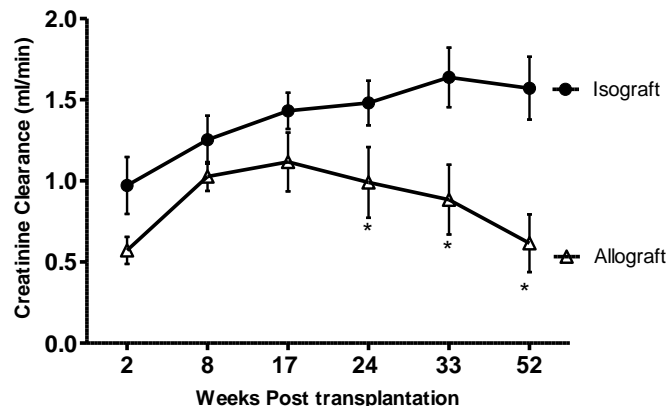


Figure 10.4: Serial measurements of (A) 24h urine protein (B) serum creatinine and creatinine clearance (C) are compared for the L-L isograft (n=5) and the F-L allograft (n=7) over 52 weeks. Results were expressed as mean values ± SEM, * p<0.05, ** p<0.01, *** p<0.001, 2 way ANOVA, with Bonferroni post test.

Centre Number:
Study Number:
Patient Identification number for this study:

Title of Project: Study of the natural history of diabetic & non-diabetic chronic kidney disease).

Name of Researchers:

1. Professor A.M.El Nahas, PhD, FRCP
2. Professor Tim Johnson, PhD BSc
3. Dr Bisher Kawar, PhD, FRCP,
4. Dr Michelle DaSilva-Lodge, MBChB, MmedSci
5. Dr Tajdida Magayr, MBChB
6. Dr Zainal Abedin, MBChB, MmedSci
7. Professor Albert Ong PhD FRCP

Please initial box

1. I confirm that I have read and understand the information sheet dated (Version.....) for the above study and have had the opportunity to ask questions.
2. I understand that my participation is voluntary and that I am free to withdraw at any time, without giving any reason and without my medical care or legal rights being affected.
3. I understand that relevant sections of my medical records/data collected during the study may be looked at by individuals from the University of Sheffield, from regulatory authorities or from the NHS Trust, where it is relevant to my taking part in this research. I give permission for these individuals to have access to my records
4. I agree to take part in the above study.
5. I agree for the samples taken to be used in future research

Name of Patient	Date	Signature
-----------------	------	-----------

Name of Person taking consent (If different from researcher)	Date	Signature
---	------	-----------

Researcher	Date	Signature
------------	------	-----------

When completed, 1 copy for the patient; 1 copy for the study site file; Original form to be kept in medical notes

Centre Number:
Study Number:
Patient Identification number for this study:

Title of Project: Study of the natural history of diabetic & non-diabetic chronic kidney disease).

Name of Researchers:

1. Professor A.M.El Nahas, PhD, FRCP
2. Professor Tim Johnson, PhD BSc
3. Dr Bisher Kawar, PhD, FRCP,
4. Dr Michelle DaSilva-Lodge, MBChB, MmedSci
5. Dr Tajdida Magayr, MBChB
6. Dr Zainal Abedin, MBChB, MmedSci
7. Professor Albert Ong PhD FRCP

Please initial box

1. I confirm that I have read and understand the information sheet dated (Version.....) for the above study and have had the opportunity to ask questions.
2. I understand that my participation is voluntary and that I am free to withdraw at any time, without giving any reason and without my medical care or legal rights being affected.
3. I understand that relevant sections of my medical records/data collected during the study may be looked at by individuals from the University of Sheffield, from regulatory authorities or from the NHS Trust, where it is relevant to my taking part in this research. I give permission for these individuals to have access to my records
4. I agree to take part in the above study.
5. I agree for the samples taken to be used in future research

Name of Patient	Date	Signature
-----------------	------	-----------

Name of Person taking consent (If different from researcher)	Date	Signature
---	------	-----------

Researcher	Date	Signature
------------	------	-----------

When completed, 1 copy for the patient; 1 copy for the study site file; Original form to be kept in medical notes

Centre Number:
Study Number:
Patient Identification number for this study:

Title of Project: Study of the natural history of diabetic & non-diabetic chronic kidney disease).

Name of Researchers:

1. Professor A.M.El Nahas, PhD, FRCP
2. Professor Tim Johnson, PhD BSc
3. Dr Bisher Kawar, PhD, FRCP,
4. Dr Michelle DaSilva-Lodge, MBChB, MmedSci
5. Dr Tajdida Magayr, MBChB
6. Dr Zainal Abedin, MBChB, MmedSci
7. Professor Albert Ong PhD FRCP

Please initial box

1. I confirm that I have read and understand the information sheet dated (Version.....) for the above study and have had the opportunity to ask questions.
2. I understand that my participation is voluntary and that I am free to withdraw at any time, without giving any reason and without my medical care or legal rights being affected.
3. I understand that relevant sections of my medical records/data collected during the study may be looked at by individuals from the University of Sheffield, from regulatory authorities or from the NHS Trust, where it is relevant to my taking part in this research. I give permission for these individuals to have access to my records
4. I agree to take part in the above study.
5. I agree for the samples taken to be used in future research

Name of Patient	Date	Signature
-----------------	------	-----------

Name of Person taking consent (If different from researcher)	Date	Signature
--	------	-----------

Researcher	Date	Signature
------------	------	-----------

When completed, 1 copy for the patient; 1 copy for the study site file; Original form to be kept in medical notes

Version 3, 10th July 2013

1. Study title: Study of the natural history of diabetic & non-diabetic chronic kidney disease.

2. Invitation paragraph

You are being invited to take part in a research study. Before you decide it is important for you to understand why the research is being done and what it will involve. Please **take time** to read the following information carefully and **discuss it** with others if you wish. **Ask us** if there is anything that is not clear or if you would like more information. Take time to decide (**up to 2 hours**) whether or not you wish to take part.

Thank you for reading this.

3. What is the purpose of the study?

This is an educational research study aims to **collect blood and urine samples** from patients who have **Chronic Kidney Disease** (CKD) and are investigated and followed up at the Sheffield Kidney Institute (SKI). The blood and urine collected will allow us to **study** proteins patterns that may reflect the severity of kidney damage and predict the progression of the kidney disease and its fate. Proteins identified in such a way will be studied in relation to patient's existing kidney damage (histology), function and its progression. This may in turn **identify** predictors of the future course of the kidney function. We will continue to **follow you** up at the outpatient clinic and monitor your kidney function and compare it with the proteins we would have found in the urine or blood.

4. Why have I been chosen?

We intend to study patients with CKD attending the outpatient clinic at the Sheffield Kidney Institute but also those admitted to the Sheffield Kidney Institute for a kidney biopsy. This will allow us to compare the nature of the proteins found in their blood and urine with the degree of damage noted on the kidney biopsy. It is hoped that such an approach can give in the long term more information on the degree of kidney damage by analysing blood and urine sample that reflect the severity of the damage.

5. Do I have to take part?

No, it is **up to you** to decide whether or not to take part. If you do decide to take part you will be given this **information sheet** to keep and be asked to sign a **consent form**. You can take the necessary time (**up to 2 hours**) to read this information sheet, discuss it with friends and relatives if you deem appropriate before you make your mind up about your involvement in this study. If you decide to take part you are still **free to withdraw** at any time and without giving

giving a reason. A decision to withdraw at any time, or a decision not to take part, **will not** affect the standard of care you receive.

6. What will happen to me if I take part?

If you decide to take part, we will ask you to **donate** a blood and urine specimen when you come to the hospital to have your kidney biopsy; the blood sample will consist of around **10 mls of blood**, which is equivalent to **two teaspoonfuls**. The urine specimen will consist of a spot urine specimen like to one you give every time you attend the outpatient clinic which is equivalent to **200 mls** (20 teaspoonfuls or half a cup in size). No additional biopsy will be taken as the one being taken for clinical purposes is suitable. We will request access to the pathology report of your biopsy, and where possible acquire an image of the biopsy slide that we can use for computer based analysis. The socio-economic data will also be gathered at the start of the study; this refers to some information relating to where you live, your education, employment as well as income. This information is **optional** as you do not have to provide it to be involved in this educational research project. With your **permission**, your GP (General Practitioner) will be informed of your participation in this study if you consent to take part. All blood and urine samples taken from you in relation to this research project will be **analysed and stored** for up to 8 years after which the study will be completed and all samples taken from you **destroyed**. However the urine and blood samples we collect are extremely valuable to us and would be extremely useful both in the extension of this current study as well as in future biomarker and pathology studies on kidney disease. On the consent form you will be given the option to donate the samples we take for future research projects.

7. What are the alternatives for diagnosis or treatment?

The current way of define the severity of kidney damage is by taking a piece of the kidney (biopsy) and examining it under the microscope. It is hoped that by identifying blood or urine markers that can accurately reflect the severity of kidney damage we may, in the long term, be able to replace many kidney biopsies with urine measurements.

8. What are the side effects of any treatment received when taking part?

No **side effects** are expected from donating an additional blood and urine specimens when you attend the outpatient clinic. No additional biopsy will be taken and thus there is no additional discomfort or risk.

9. What are the possible disadvantages and risks of taking part?

The minor disadvantage of having to give one more blood and urine specimen when you attend the Sheffield Kidney Institute to have your kidney biopsy.

10. What are the possible benefits of taking part?

If we can manage to find proteins/markers in the blood or urine of kidney patients that accurately reflect the severity of their kidney damage; this may one day reduce the need to bring patients into hospital for biopsies.

11. What if new information becomes available?

Any additional research-derived information that becomes available will help us in our focus on proteins that may be of **relevance** to your own kidney condition or stage of progression. We will also keep you personally informed of any new discoveries and findings.

12. What happens when the research study stops?

After we take your blood and urine sample we will undergo **a lengthy analysis** and examine our results in the light of your own clinical data derived from the routine tests we undertake

After we take your blood and urine sample we will undergo **a lengthy analysis** and examine our results in the light of your own clinical data derived from the routine tests we undertake every time you come to the clinic. When the research is completed we hope to **identify** new markers for kidney disease and their outcome and **disseminate** this knowledge through scientific publications.

13. What if something goes wrong?

It is **extremely unlikely** that anything can go wrong in providing an additional blood or urine sample along with all those you provide routinely during your hospitalisation.

14. Will my taking part in this study be kept confidential?

All information which is collected about you during the course of the research will be kept **strictly confidential**. Any information about you which leaves the hospital/surgery will have your name and address **removed** so that you cannot be recognised from it.

15. What will happen to the results of the research study?

Once the study is completed and the data analysed, we intend to **disseminate** the results obtained through scientific publications, seminars and conferences. The study will also form the basis for the award of a higher degree by the University of Sheffield. However; **under no circumstances** will you be identified in any way in the process. We will also provide all our participants with a summary of our key findings for their own records.

16. Who is organising and funding the research?

The research is **organised** by the Sheffield Kidney Institute and funding is provided by the Sheffield Kidney institute and the research fees (bench fees) provided by postgraduate students undertaking this research.

17. Who has reviewed the study?

This study has been **reviewed** by the relevant experts in the field through the Sheffield Teach Hospitals Trust' Research Department and The Bradford Research Ethics Committee.

18. Contact for Further Information

For any more information concerning this study please contact:

Professor Tim Johnson, Academic Nephrology Unit, The Medical School, University of Sheffield, Beech hill Road, Sheffield S10 2RZ. T.johnson@sheffield.ac.uk, 0114 2712842

Thank you very much for taking time to read this information sheet.

If you choose to participate in this study, you will be given **a copy** of the patient information sheet and **a signed consent form** to take home with you and keep for future reference.

(Form to be on headed paper)

T S Johnson BSc PhD
Professor of Kidney Science
Sheffield Kidney Institute

University of Sheffield
Medical School
Sheffield, S10 2RZ, UK

Direct line: 0114 2712842
Direct fax: 0114 2431575
Email: t.johnson@sheffield.ac.uk

Version 3, 10th July 2013

1. Study title: Study of the natural history of diabetic & non-diabetic chronic kidney disease).

2. Invitation paragraph

You are being invited to take part in a research study. Before you decide it is important for you to understand why the research is being done and what it will involve. Please take time to read the following information carefully and discuss it with others if you wish. Ask us if there is anything that is not clear or if you would like more information. Take time to decide whether or not you wish to take part.

Thank you for reading this.

3. What is the purpose of the study?

This is an educational research study aimed to collect blood and urine samples from patients who have **chronic kidney disease (CKD)** and are followed up at the Sheffield Kidney institute (SKI). This will involve patients whose own kidneys are affected. The blood and urine collected will allow us to study proteins patterns that may predict the progression of the kidney disease and its fate. Proteins identified in such a way will be studied in relation to patient's kidney function and its progression. This may in turn identify predictors of the future course of the kidney function and thus allow better treatment. We will continue to follow you up at the outpatient clinic and monitor your kidney function and compare it with the proteins we have found in the urine or blood.

4. Why have I been chosen?

We intend to study a sample of **patients with various types kidney disease** and are followed up at the Sheffield Kidney Institute outpatients' clinics, who have either stable or declining kidney function. This will allow us to compare the protein patterns in blood and urine and match them against the patient's kidney function and rate of progression of their kidney condition.

5. Do I have to take part?

No, it is up to you to decide whether or not to take part. If you do decide to take part you will be given this information sheet to keep and be asked to sign a consent form. You can take the necessary time (up to 4 weeks) to read this information sheet, discuss it with friends and relatives if you deem appropriate before you make your mind up about your involvement in this study. However, if after thorough explanation of the study and adequate time (up to 30 minutes) for you to read the patient information sheet (PIS), you are happy to participate, you will be asked to sign the consent form. If you decide to take part you are still free to withdraw at any

at any time and without giving a reason. A decision to withdraw at any time, or a decision not to take part, will not affect the standard of care you receive.

6. What will happen to me if I take part?

If you decide to take part, we will ask when you attend the outpatient clinic for your routine visits to donate a blood and urine specimen once a year for 5 years (the duration of the study; a total of 6 samples, one at the beginning of the study, the second after 1 year, the third after 2 years etc). This will ensure that the levels of these markers in individuals with diabetes are not variable with time. The blood sample will be equivalent to 10 mls (two teaspoonfuls in size); whereas urine sample will be equivalent to 200 mls (20 teaspoonfuls or half a cup in size). The socio-economic data will also be gathered at the start of the study; this refers to some information relating to where you live, your education, employment as well as income. This information is optional as you do not have to provide it to be involved in this educational research project. With your permission, your GP (General Practitioner) will be informed of your participation in this study if you consent to take part. All blood and urine samples taken from you in relation to this research project will be analysed and stored for up to 8 years after which the study will be completed and all samples taken from you destroyed. However the urine and blood samples we collect are extremely valuable to us and would be extremely useful both in the extension of this current study as well as in future biomarker and pathology studies on kidney disease. On the consent form you will be given the option to donate the samples we take for future research projects.

7. What are the alternatives for diagnosis or treatment?

The Current alternative predictors of the outcome of your condition (involvement of kidneys by diabetes) include the quality of your diabetes (blood sugar) control if you are diabetic, your blood pressure control as well as the degree/level of protein in your urine. However, these are not fully predictive of the outcome of kidney disease in people with kidney disease and we are seeking better and novel alternatives.

8. What are the side effects of any treatment received when taking part?

No side effects are expected from donating an additional blood and urine specimens when you attend the outpatient clinic.

9. What are the possible disadvantages and risks of taking part?

The minor disadvantage of having to give one more blood and urine specimen when you attend your routine outpatient appointments.

10. What are the possible benefits of taking part?

Indirect benefits in the long term if we manage to identify markers in your blood or urine that will predict the outcome of kidney function and the natural history of kidney conditions such as yours.

11. What if new information becomes available?

Any additional research-derived information that becomes available will help us in our focus on proteins that may be of relevance in your own kidney condition or stage of progression. We will also keep you personally informed of any new discoveries and findings.

12. What happens when the research study stops?

After we take your blood and urine sample we will undergo a lengthy analysis and examine our results in the light of your own clinical data derived from the routine tests we undertake

every time you come to the clinic. When the research is completed we hope to identify new markers for kidney disease and their outcome and disseminate this knowledge through scientific publications.

13. What if something goes wrong?

It is extremely unlikely that anything can go wrong in providing an additional blood or urine sample along with all those you provide routinely at every outpatient visit

If you are harmed by taking part in this research project, there are no special compensation arrangements. If you are harmed due to someone's negligence, then you may have grounds for a legal action but you may have to pay for it. Regardless of this, if you wish to complain, or have any concerns about any aspect of the way you have been approached or treated during the course of this study, the normal National Health Service complaints mechanisms should be available to you.

If you have any complaints or concerns relating to the above study please contact: Dr Mike Richmond, Medical Director, Sheffield Teaching Hospitals NHS Foundation Trust, 8 Beech Hill Road, Sheffield S10 2SB (Tel: 0114 271 2923).

14. Will my taking part in this study be kept confidential?

All information which is collected about you during the course of the research will be kept strictly confidential. Any information about you which leaves the hospital/surgery will have your name and address removed so that you cannot be recognised from it.

15. What will happen to the results of the research study?

Once the study is completed and the data analysed, we intend to disseminate the results obtained through scientific publications, seminars and conferences. The study will also form the basis for the award of a higher degree by the University of Sheffield. However; under no circumstances will you be identified in any way in the process. We will also provide all our participants with a summary of our key findings for their own records.

16. Who is organising and funding the research?

The research is organised by the Sheffield Kidney Institute and funding is provided by the Sheffield Kidney institute and the research fees (bench fees) provided by postgraduate research students who will undertake this research.

17. Who has reviewed the study?

This study has been reviewed by the relevant experts in the field through the Sheffield Teaching Hospitals Trust' Research Department and Bradford Research Ethics Committee.

18. Contact for Further Information

For any more information concerning this study please contact:

For any more information concerning this study please contact:

Professor Tim Johnson, Academic Nephrology Unit, The Medical School, University of Sheffield, Beech hill Road, Sheffield S10 2RZ. T.johnson@sheffield.ac.uk, 0114 2712842

Thank you very much for taking time to read this information sheet.

If you choose to participate in this study, you will be given a copy of the patient information sheet and a signed consent form to take home with you and keep for future reference.

(Form to be on headed paper)

T S Johnson BSc PhD
Professor of Kidney Science
Sheffield Kidney Institute

University of Sheffield
Medical School
Sheffield, S10 2RZ, UK

Direct line: 0114 2712842
Direct fax: 0114 2431575
Email: t.johnson@sheffield.ac.uk

Version 3, 10th July 2013

1. Study title: Study of the natural history of diabetic & non-diabetic chronic kidney disease).

2. Invitation paragraph

You are being invited to take part in a research study. Before you decide it is important for you to understand why the research is being done and what it will involve. Please take time to read the following information carefully and discuss it with others if you wish. Ask us if there is anything that is not clear or if you would like more information. Take time to decide whether or not you wish to take part.

Thank you for reading this.

3. What is the purpose of the study?

This is an educational research study aimed to collect blood and urine samples from patients who have chronic kidney disease (CKD) and are followed up at the Sheffield Kidney institute (SKI). This will involve patients whose own kidneys are affected. We would like to be able to better understand why kidney disease develops and develop new tests to monitor its development. To do this we intend to follow a group of patients with chronic kidney disease for 5 years. We also need to be able to compare their course with that of **a small group of healthy individuals like you who don't have diabetes or suffering from any form of kidney disease.**

4. Why have I been chosen?

Basically, we would like to measure some blood and urine substances that may explain why some patients do well in the long term without any damage while others have ongoing problems with their kidneys. We also need to know what the level of these substances is in **normal healthy individuals.** For that, we would require a blood and urine sample from you once a year. This will allow us to compare the protein patterns in blood and urine and match them against the patient's kidney function and rate of progression.

5. Do I have to take part?

No, it is up to you to decide whether or not to take part. You can take the necessary time (up to 4 weeks) to read this information sheet, discuss it with friends and relatives if you deem appropriate before you make your mind up about your involvement in this study. However, if after thorough explanation of the study and adequate time (up to 30 minutes) for you to read the patient information sheet (PIS), you are happy to participate, you will be asked to sign the consent form. If you do decide to take part you will be given this information sheet to keep

and be asked to sign a consent form. If you decide to take part you are still free to withdraw at any time and without giving a reason

6. What will happen to me if I take part?

If you decide to take part, we will ask you to donate a blood and urine specimen once a year for 5 years (the duration of the study; a total of 5 samples, one at the beginning of the study, the second after 1 year, the third after 2 years etc..). This will ensure that the levels of these markers in normal healthy volunteers are not variable with time. The blood sample will consist of around 10 mls of blood, which is equivalent to two teaspoons; whereas urine sample will be equivalent to 200 mls (40 teaspoonfuls or half a cup in size).

All blood and urine samples taken from you in relation to this research project will be analysed and stored for up to 8 years after which the study will be completed and all samples destroyed. However the urine and blood samples we collect are extremely valuable to us and would be extremely useful both in the extension of this current study as well as in future biomarker and pathology studies on kidney disease. On the consent form you will be given the option to donate the samples we take for future research projects.

7. What are the side effects of any treatment received when taking part?

No side effects are expected from donating blood and urine specimens once a year.

8. What are the possible disadvantages and risks of taking part?

The minor disadvantage of having to give one blood sample and urine specimen once a year.

9. What are the possible benefits of taking part?

There will be no benefit to you personally, but we hope to identify markers in blood and urine that will predict the outcome of kidney function.

10. What if new information becomes available?

We will keep you personally informed of any new discoveries and findings.

11. What happens when the research study stops?

After we take your blood and urine sample we will undergo a lengthy analysis and examine our results in the light of your own clinical data. When the research is completed we hope to identify new markers for kidney disease and their outcome and disseminate this knowledge through scientific publications.

12. What if something goes wrong?

It is extremely unlikely that anything can go wrong in providing blood or urine sample. If you are harmed by taking part in this research project, there are no special compensation arrangements. If you are harmed due to someone's negligence, then you may have grounds for a legal action but you may have to pay for it. Regardless of this, if you wish to complain, or have any concerns about any aspect of the way you have been approached or treated during the course of this study, the normal National Health Service complaints mechanisms should be available to you.

If you have any concerns or complaints relating to the above study please contact: Dr Mike Richmond, Medical Director, Sheffield Teaching Hospitals NHS Foundation Trust, 8 Beech Hill Road, Sheffield S10 2SB (Tel: 0114 271 2923).

13. Will my taking part in this study be kept confidential?

All information which is collected about you during the course of the research will be kept strictly confidential. Any information about you which leaves the hospital/surgery will have your name and address removed so that you cannot be recognised from it.

14. What will happen to the results of the research study?

Once the study is completed and the data analysed, we intend to disseminate the results obtained through scientific publications, seminars and conferences. The study will also form the basis for the award of a higher degree by the University of Sheffield. However; under no circumstances will you be identified in any way in the process. We will also provide all our participants with a key summary of our findings for their own records. We hold regular open meetings where all those involved in a given research projects are invited to share with them the outcome of the research.

15. Who is organising and funding the research?

The research is organised by the Sheffield Kidney Institute and Academic nephrology Unit and the University of Sheffield. Funding is provided by the Sheffield Kidney Institute and the research fees (bench fees) provided by postgraduate students who will undertake this research.

16. Who has reviewed the study?

This study has been reviewed by the relevant experts in the field through the Sheffield Teaching Hospitals Trust' Research Department and Bradford Research Ethics Committee.

19. Contact for Further Information

For any more information concerning this study please contact:

Professor Tim Johnson, Academic Nephrology Unit, The Medical School, University of Sheffield, Beech hill Road, Sheffield S10 2RZ. T.johnson@sheffield.ac.uk, 0114 2712842

Thank you very much for taking time to read this information sheet.

If you choose to participate in this study, you will be given a copy of the patient information sheet and a signed consent form to take home with you and keep for future reference

(Form to be on headed paper)